



## **Appendix B**

# **Ramboll Geophysical Data Report: Salinas Valley Deep Aquifers AEM Survey Geophysical Report**

Intended for  
**Montgomery and Associates**

Document type  
**Data Report**

Date  
**July 2023**

# Salinas Valley Deep Aquifers AEM Survey Data Report



# Salinas Valley Deep Aquifers AEM Survey Data Report

Project name **Salinas Deep Aquifers AEM Study**  
Project no. **1690025794**  
Recipient **Montgomery and Associates**  
Document type **Report**  
Version **3**  
Date **July 28, 2023**

Description **This data report describes the acquisition, processing, inversion, and analysis of the AEM dataset acquired in the Salinas Valley to better understand the Deep Aquifers in the region. The report also provides a description of the existing well and AEM data compiled along the planned flight lines and its integration into the analysis.**

Ramboll  
2200 Powell Street  
Suite 700  
Emeryville, CA 94608  
USA

<https://ramboll.com>

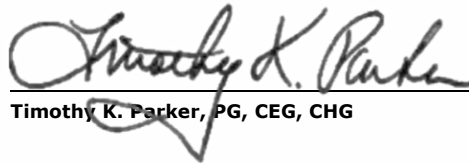


7/28/2023

---

Ian Gottschalk, PhD

Date



7/28/2023

---

Timothy K. Parker, PG, CEG, CHG

Date

# Contents

List of Abbreviations and Acronyms	iv
Project Team	iv
1. Introduction	1
2. Existing Data Compilation	3
2.1 Datasets	3
2.1.1 Deep Aquifers Study Phase 1 Borehole Dataset and Resistivity Logs	3
2.1.2 2021 and 2022 DWR Statewide AEM Surveys	4
2.1.3 2017 and 2019 Coastal Salinas Valley AEM Surveys	5
2.1.4 Digitized Borehole Geophysical Logs	6
2.2 Lithology Data Processing	7
2.3 Borehole Resistivity Logs	9
2.4 Existing AEM Data	9
3. Deep Aquifers AEM Survey	10
3.1 AEM Method	10
3.1.1 AEM Principles	10
3.1.2 Rock-Physics Relationship	12
3.1.3 Resistivity Color Scale	13
3.2 AEM Survey Flight Line Planning	13
3.3 AEM Survey Equipment and Instrumentation	14
3.4 AEM Survey Operation	15
3.4.1 Landing Zones	15
3.4.2 AEM Data Acquisition	15
3.4.3 Reference Lines	17
4. AEM Data Processing and Inversion	18
4.1 Data Processing	19
4.2 Inversion	20
4.2.1 Inversion Scheme	21
4.2.2 Depth of Investigation	21
5. Survey and Interpretation Results	22
5.1 Deep Aquifers Study Phase 1 Borehole Data	22
5.2 AEM Data	25
5.2.1 Resistivity Cross-sections	25
5.2.2 Mean Resistivity Maps	28
5.2.3 Comparison of Lithology and Resistivity from AEM Data	31
5.3 Delineation of Continuous Conductor	36
5.4 Deep Conductor	48
6. Summary and Conclusions	49
6.1 Recommended Future Work	49
7. Deliverables	50
8. References	53

## Figures

Figure 1-1 Survey area and planned flight lines for the Deep Aquifers survey	2
Figure 2-1 Existing data used from the Deep Aquifers Study Phase 1 Borehole Dataset and Resistivity Logs	4
Figure 2-2 Existing data used from the DWR Statewide AEM Surveys	5
Figure 2-3 Flight lines from the coastal Salinas Valley AEM surveys	6
Figure 2-4 Borehole resistivity logs digitized as part of this project	7
Figure 2-5 Histogram of borehole depth from analyzed well completion reports	8
Figure 3-1 AEM Survey Schematic	11
Figure 3-2 Example of a single sounding of acquired AEM data and the resulting resistivity model	12
Figure 3-3 General relationship between resistivity and subsurface materials	13
Figure 3-4 The resistivity color scale used in this study for presentation of all resistivity AEM results in this report	13
Figure 3-5 AEM Equipment and instrumentation configuration	15
Figure 3-6 Photos of the AEM system in operation in the Salinas Valley for the Deep Aquifers Study	16
Figure 3-7 Map showing the planned and flown AEM flight lines	17
Figure 3-8 Reference flight line	18
Figure 4-1 Map showing the retained and removed AEM data	20
Figure 4-2 Depth of investigation histogram	21
Figure 5-1 Interpreted depth of the top and bottom of the 400-FDA from the Deep Aquifers Study Phase 1 Borehole Dataset	23
Figure 5-2 Depth of the 400-FDA interpreted from borehole data as a function of distance.	24
Figure 5-3 Resistivity along Section 101600	26
Figure 5-4 Resistivity along Section 100300	27
Figure 5-5 Resistivity along Section 100200	28
Figure 5-6 Mean resistivity plan-view map in the depth interval 5 to 15 m (16 to 49 ft) bgs	29
Figure 5-7 Mean resistivity plan-view map in the elevation interval of -150 to -100 m (-492 to -328 ft) amsl	30
Figure 5-8 Mean resistivity plan-view map in the elevation interval of -250 to -200 m (-820 to -656 ft) amsl	31
Figure 5-9 Mean resistivity plan-view map in the elevation interval of -350 to -300 m (-1148 to -984 ft) amsl	31
Figure 5-10 Distribution of AEM resistivity values compared to lithology from boreholes within 300 m	33
Figure 5-11 Distribution of AEM resistivity values within 300 m of boreholes with interpretations of the 400-FDA	35
Figure 5-12 Annotated resistivity along Section 200400	37
Figure 5-13 Annotated resistivity along Section 101600	38
Figure 5-14 Annotated resistivity along Section 100600	39
Figure 5-15 Series of cross-sections across the survey area oriented northeast to southwest	41
Figure 5-16 Series of cross-sections across the survey area oriented across the basin southwest to northeast	42

Figure 5-17 Series of cross-sections oriented across the basin southwest to northeast from the northernmost and southernmost parts of the survey area	43
Figure 5-18 Interpreted depth of the top and bottom of the 400-FDA and the continuous conductor	45
Figure 5-19 Depth of the continuous conductor, interpreted from AEM data, shown as a function of distance.	47

## Tables

Table 2-1 Mapping from the lithology descriptors used in the DWR AEM Surveys lithology data to the lithology descriptors used in this project	9
Table 2-2 Existing AEM datasets	10
Table 7-1 Structure of the project digital delivery folder.	51

## Appendices

### **Appendix 1**

Borehole Geophysical Data

### **Appendix 2**

SkyTEM Data Report

### **Appendix 3**

AEM Inversion Cross-sectional Results

### **Appendix 4**

AEM Inversion Mean Resistivity Maps

## List of Abbreviations and Acronyms

<b>400-FDA</b>	400 Foot/Deep Aquitard
<b>AEM</b>	Airborne Electromagnetic
<b>amsl</b>	Above mean sea level
<b>bgs</b>	Below ground surface
<b>DEM</b>	Digital elevation model
<b>DGPS</b>	Differential global positioning system
<b>DMS</b>	Data management system
<b>DOI</b>	Depth of Investigation
<b>DWR</b>	Department of Water Resources
<b>ft</b>	Foot
<b>GIS</b>	Geographic Information System
<b>km</b>	Kilometer
<b>L</b>	Liter
<b>LAS</b>	Log-ASCII Standard
<b>m</b>	Meter
<b>M&amp;A</b>	Montgomery and Associates
<b>SCI</b>	Spatially constrained inversion
<b>SGMA</b>	Sustainable Groundwater Management Act
<b>TEM</b>	Time-domain (or Transient) Electromagnetics
<b>TEM</b>	Time-domain electromagnetic

## Project Team

The project team for the Salinas Deep Aquifers AEM Survey includes:

- **Ramboll** – responsible for coordination of the contractors and acquisition of AEM data, borehole data compilation, interpretation, and reporting and quality control of deliverables.
- **Geophysical Imaging Partners** – conducted daily quality control of the data during the flight operation, data processing and inversion, interpretation support, and assisted in report preparation.
- **SkyTEM** – responsible for the final planning and execution of the AEM survey.
- **Eclogite** – digitized a set of geophysical logs.

## 1. Introduction

In March 2023, Ramboll carried out a geophysical airborne electromagnetic (AEM) survey in Monterey County, California to support analysis by Montgomery and Associates (M&A) of the Deep Aquifers in the northern Salinas Valley. An important step in understanding the Deep Aquifers, expected to be encountered 750 ft or more below ground surface (bgs), is defining the overlying 400-Foot/Deep Aquitard (400-FDA). Data from AEM surveys contain information that can be used to identify clay-rich sediment, such as composes the 400-FDA. However, while multiple AEM surveys have been flown previously in the northern Salinas Valley, the depth of the 400-FDA is often below the depth at which these existing data provide useful information, and the paths along which AEM data were acquired southeast of Salinas have a wide lateral separation. The AEM survey conducted by Ramboll used a more powerful AEM system, which can image the subsurface to greater depths, and was designed to provide additional data coverage, especially south of Salinas. The central objective of the AEM survey was to determine the geometry of a continuous feature in the geophysical data with the depth and character expected of the 400-FDA.

The AEM method is a geophysical technique that measures the electrical resistivity of the subsurface from an airborne platform. The AEM system used in this survey includes a large hexagonal frame containing the geophysical equipment suspended by cable beneath a helicopter about 100 feet above the ground surface along a defined flight path. During the survey, the system sends a weak, pulsed electromagnetic signal that, in most alluvial subsurface environments, can penetrate hundreds of meters into the subsurface. The returning signal is measured by receivers in the frame as a voltage timeseries. The resulting data provide a measurement of the electrical resistivity of the subsurface with depth, which can be related to material properties of the subsurface such as groundwater salinity, sediment type, and degree of water saturation. The AEM system in this survey was customized to extend the depth of penetration beyond that of typical AEM surveys, with the goal of obtaining information relevant to the understanding of the Deep Aquifers.

The planned flight lines for the AEM survey are shown as black lines Figure 1-1. Most of the survey was conducted in the 180/400 Foot Aquifer, East Side Aquifer, and Forebay Aquifer Groundwater Subbasins, with some of the survey overlapping the Monterey, Langley Area, and Seaside Groundwater Subbasins. The survey flight lines have a high degree of overlap with the extent of the Phase 1 400-FDA (blue polygon), as determined by M&A in their Deep Aquifers Study (Montgomery & Associates, 2022). The survey flight lines largely avoid the coastal Salinas Valley where the depth to which the AEM method can obtain useful information is reduced due to elevated chloride concentrations, which have been recorded in the 180-Foot Aquifer (orange polygon) and the 400-Foot Aquifer (not pictured).

This report presents the methodology, results, and analysis related to the acquired AEM data and integration of the existing data from the survey area. The report describes the following topics:

- compilation of existing borehole and existing AEM data
- operation of the AEM survey
- processing and inversion of the AEM data
- analysis and results of the existing data and newly acquired AEM data
- contents of the deliverables attached to this report.

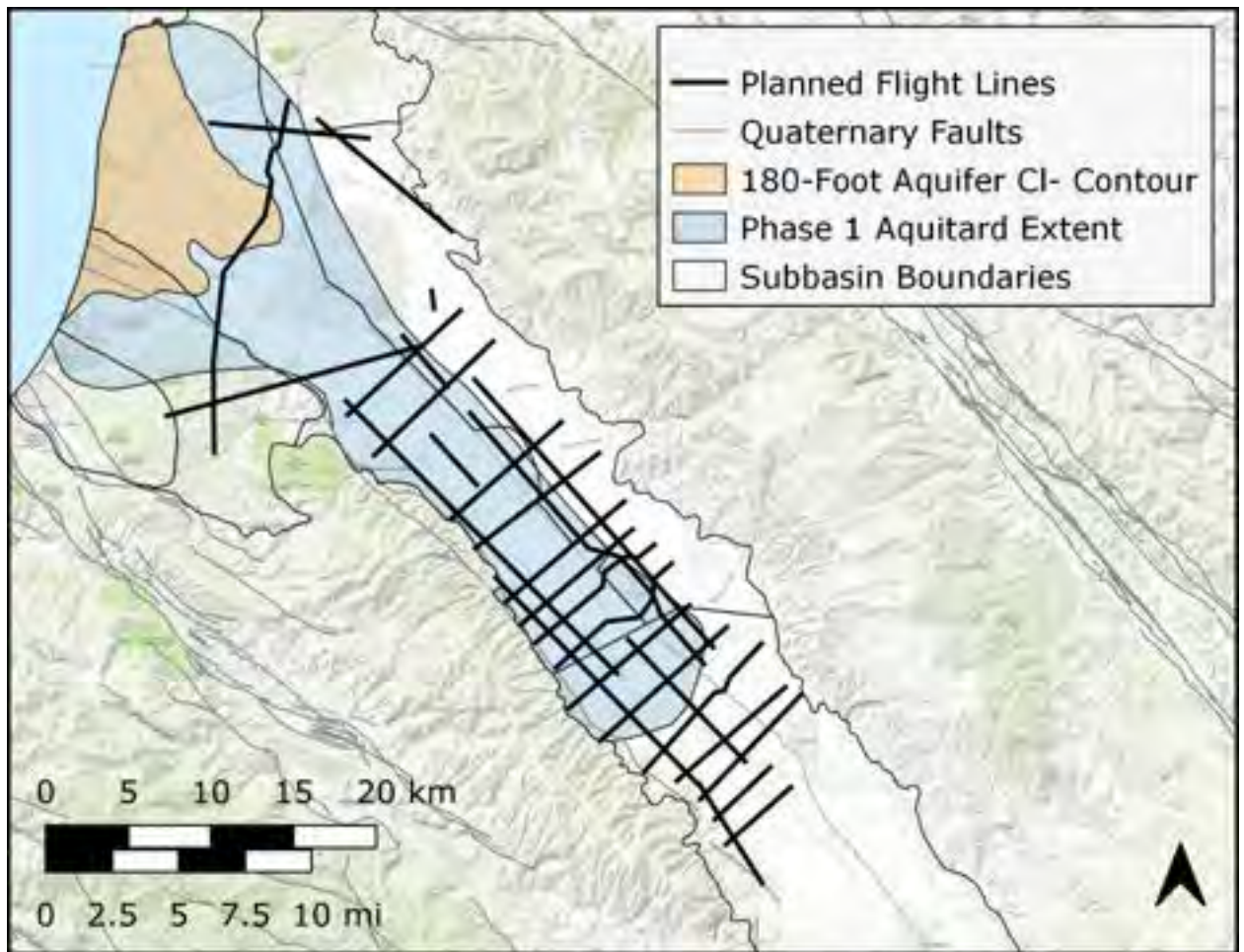


Figure 1-1 Survey area and planned flight lines for the Deep Aquifers survey.

## 2. Existing Data Compilation

Independent datasets, including borehole lithology, borehole resistivity, and pre-existing geophysical data, are of critical value to the interpretation and corroboration of AEM data. As part of this project, existing data were compiled to support the analysis of the newly acquired AEM data. The goal of the data compilation was to assemble data that could contribute independent information on the subsurface resistivity structure, especially at depth. The data types compiled were lithology and resistivity data from boreholes, and resistivity estimates from other AEM surveys.

This section provides a description of the existing data compilation process. The compiled data are provided as deliverables (see Section 7 for format). A graphical display of the borehole geophysical data is presented in Appendix 1.

Data from boreholes within 5 km of the planned AEM flight lines were integrated into the analysis and interpretation. The data were processed and integrated into a data management system (DMS) for this project. All coordinates were transformed into NAD 83 California Albers projection (EPSG 3310).

### 2.1 Datasets

The existing data in used in this project were compiled from four sources and are outlined in the following four sections.

#### 2.1.1 *Deep Aquifers Study Phase 1 Borehole Dataset and Resistivity Logs*

A lithology dataset, compiled by M&A for the Deep Aquifers Study Phase 1, was made available for analysis in this project. The dataset includes lithology, screen interval information, and interpretations of the top and bottom of the 400-FDA from the deep boreholes in the survey area. Additionally, a set of borehole resistivity logs were made available, sourced from multiple datasets.

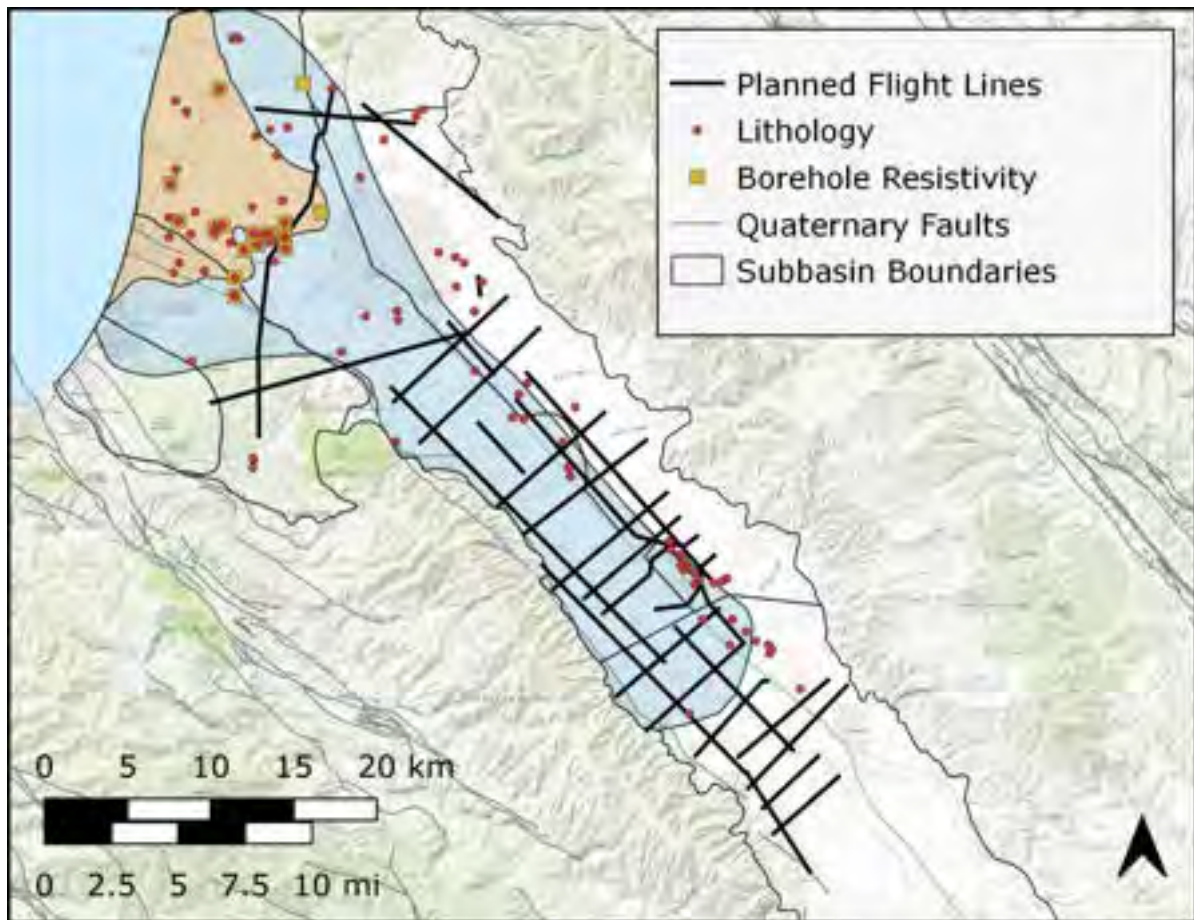


**Figure 2-1 Existing data used from the Deep Aquifers Study Phase 1 Borehole Dataset and Resistivity Logs.**

### 2.1.2 2021 and 2022 DWR Statewide AEM Surveys

The California Department of Water Resources (DWR) is conducting a series of AEM surveys in groundwater basins across California to improve the understanding of groundwater aquifer structure in support of the implementation of the Sustainable Groundwater Management Act. The AEM surveys include the compilation of existing borehole data, namely lithology, borehole resistivity, water quality, and water level data. The data were compiled from wells along the planned flight lines before they were flown.

The DWR Statewide AEM Surveys intersecting the survey area for the current project come from Survey Area 1, completed in August 2021, which mainly covers the Salinas Valley east of Salinas south to Paso Robles Area Groundwater Subbasin, and Survey Area 8, completed in November 2022 and covers the coastal Salinas Valley south, west, and north of Salinas. The flight lines corresponding to Survey Areas 1 and 8 are shown in Figure 2-2.

Borehole lithology and geophysical data from the DWR Statewide AEM Surveys were also compiled for use in this project; the locations of these borehole data are shown in Figure 2-2. All borehole data compiled come only from Survey Area 1, since the borehole data compiled for Survey Area 8 have not been published yet.

All AEM and compiled borehole data from the DWR Statewide AEM Surveys are publicly accessible and are hosted, along with reports detailing existing data compilation, the AEM surveys, data

processing, inversion, and further products, at the following website:  
<https://data.cnra.ca.gov/dataset/aem>.

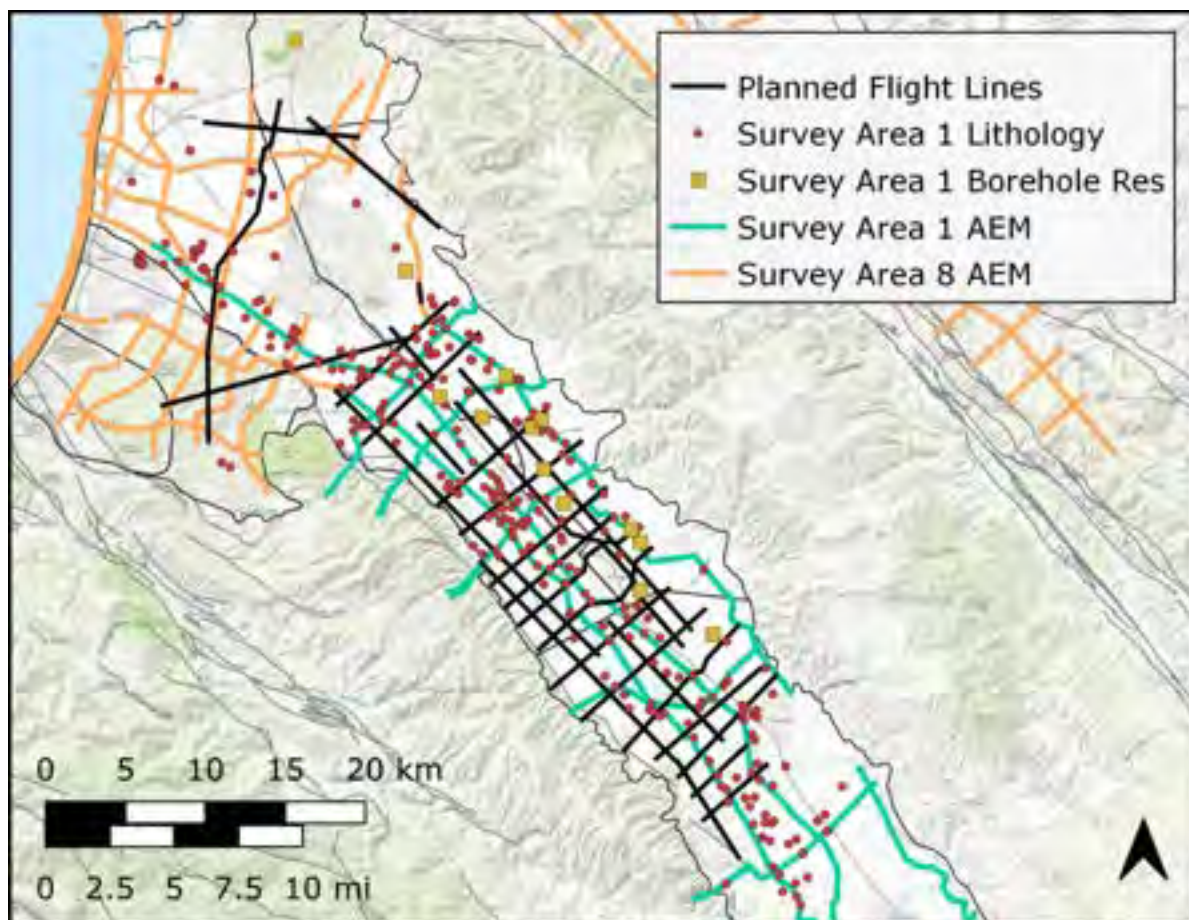


**Figure 2-2 Existing data used from the DWR Statewide AEM Surveys. Survey Area 8 borehole data are not yet available.**

### 2.1.3 2017 and 2019 Coastal Salinas Valley AEM Surveys

Two previous AEM surveys were flown in the coastal Salinas Valley, extending from the coast to the city of Salinas, shown in Figure 2-3. The two surveys, conducted in 2017 and 2019, contain nearly identical flight paths, although the 2019 survey lines (grey in Figure 2-3) extend farther south into the Seaside Groundwater Subbasin than do the survey lines from 2017 (blue lines in Figure 2-3). The AEM system used in the 2019 survey is the SkyTEM 312 system, which is the same as used in the DWR Statewide AEM Surveys. The 2017 survey used a SkyTEM 304 system, which, as compared to the SkyTEM 312 system, has a smaller magnetic moment and thus a shallower average depth of investigation. The acquisition and interpretation of the 2017 dataset is detailed in Gottschalk et al. (2020) and in the following report: [http://svbgsa.org/wp-content/uploads/2020/09/Stanford-AGF\\_2017-AEM-Study-Report\\_Final.pdf](http://svbgsa.org/wp-content/uploads/2020/09/Stanford-AGF_2017-AEM-Study-Report_Final.pdf), and the results of the 2019 dataset can be found in the following appendix: <http://svbgsa.org/wp-content/uploads/2020/09/3.-Appendix-1-2D-Profiles-2019-Rho-CLconc-Lith-ELogs-Comparison.pdf>

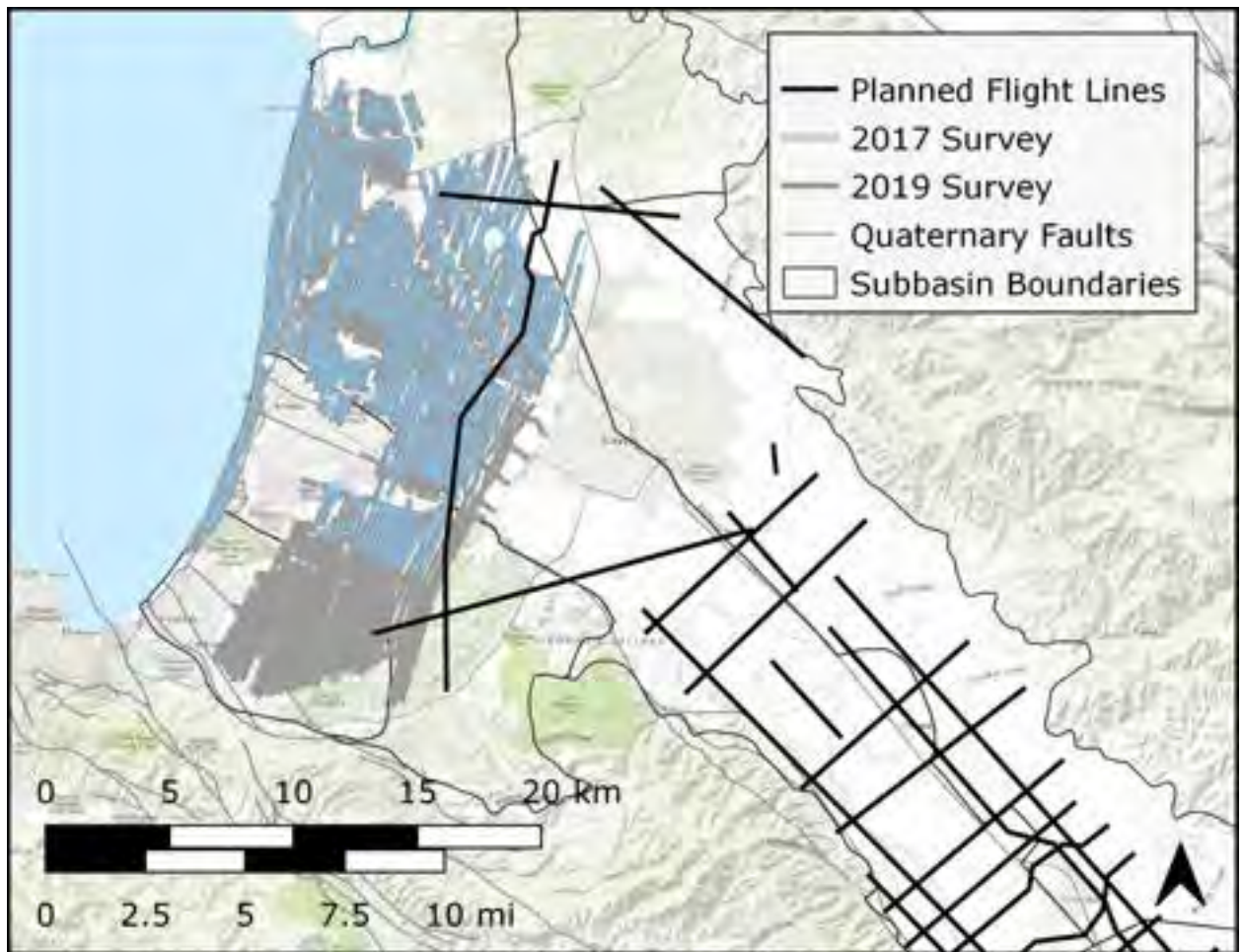


**Figure 2-3 Flight lines from the coastal Salinas Valley AEM surveys.**

#### *2.1.4 Digitized Borehole Geophysical Logs*

A set of 18 borehole resistivity logs were digitized to support this project. The locations of the selected resistivity logs were near planned flight lines and correspond to areas of higher uncertainty about the 400-FDA, and areas without nearby borehole resistivity data. The resistivity logs were selected from well completion reports in the form of scanned PDF documents. The scanned documents were converted to the tabulated, Log ASCII Standard (LAS) format. Figure 2-4 shows the locations of the digitized borehole resistivity logs.

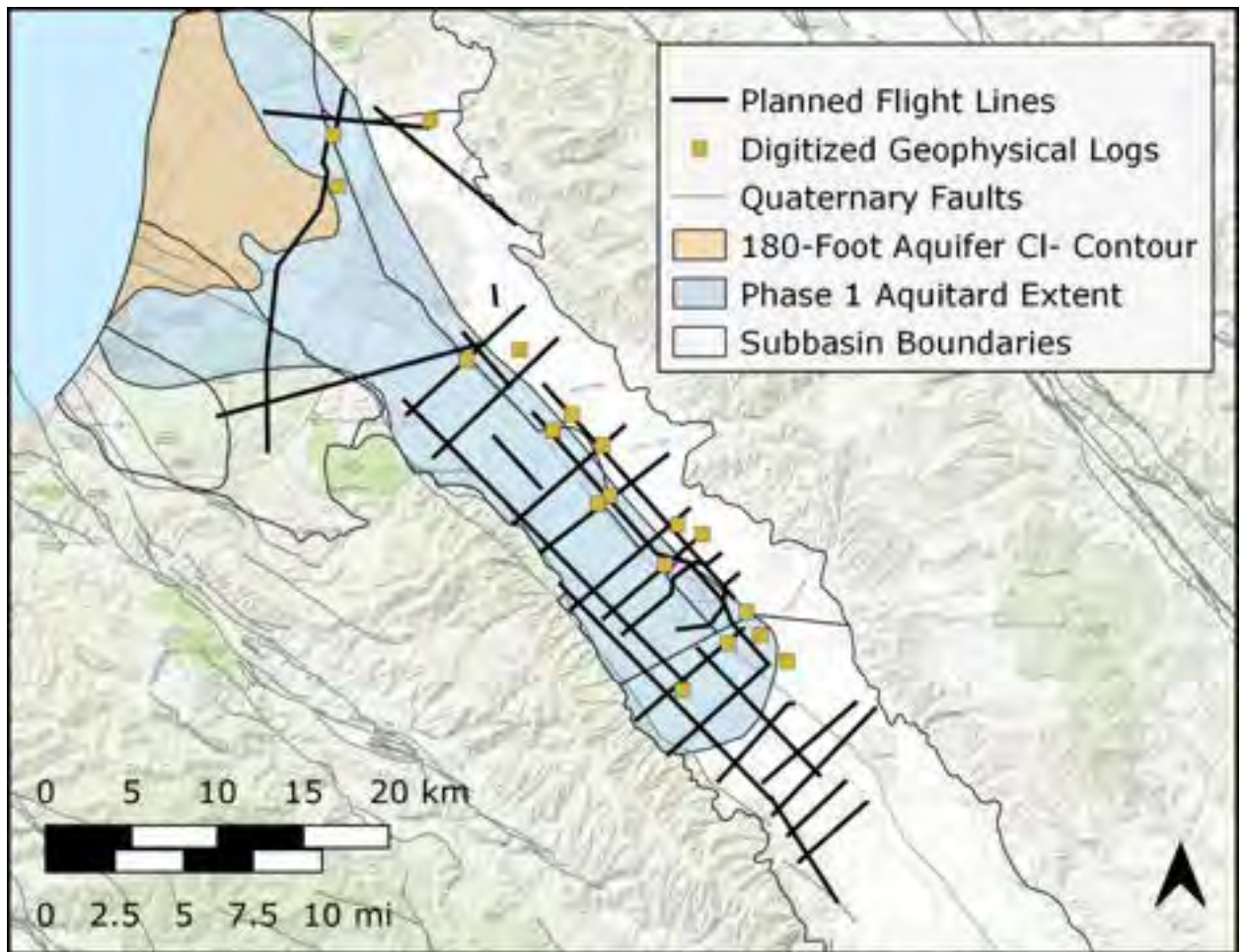
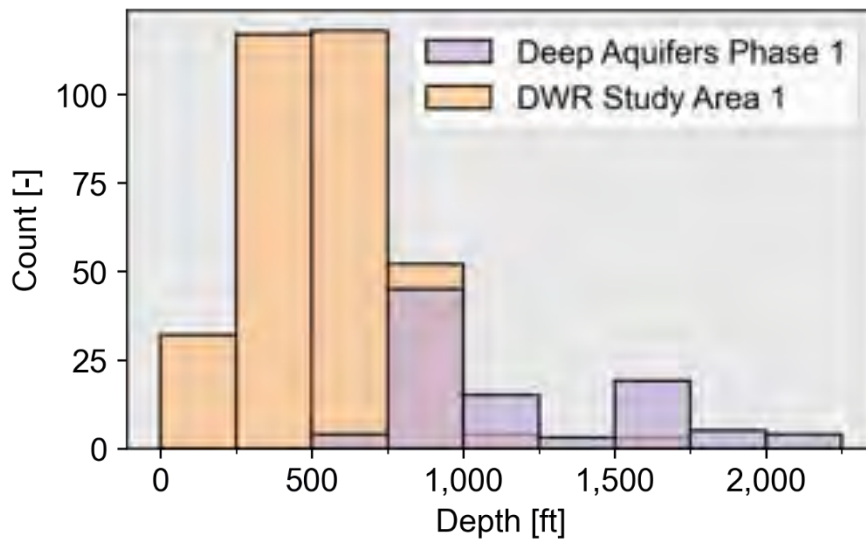


Figure 2-4 Borehole resistivity logs digitized as part of this project.

## 2.2 Lithology Data Processing

Lithology data were available from the Deep Aquifers Study Phase 1 Borehole Dataset and from Survey Area 1 of the DWR Statewide AEM Surveys. The lithology data from each dataset were processed to merge the two datasets for the current project. Figure 2-5 shows the distribution of borehole depths from the two datasets. Many more boreholes are available from the DWR AEM Surveys dataset; however, almost all boreholes are shallower than those in the Deep Aquifers Study Phase 1 Borehole Dataset.



**Figure 2-5 Histogram of borehole depth from analyzed well completion reports.**

A final list of lithology descriptors was established for all lithology data analyzed in support of locating the 400-FDA. The final list contains the descriptors from the Deep Aquifers Study Phase 1 Borehole Dataset and two additional descriptors from the DWR Statewide AEM Surveys. The final list is shown below:

- clay
- clay and
- not clay
- soil
- rock
- unknown

The lithology descriptors in the Deep Aquifers Study Phase 1 Borehole Dataset begin at approximately 450 ft bgs and continue to the bottom of each borehole. Lithology data are grouped into five descriptors: “clay”, “clay and”, “not clay”, and “rock”; the definition of each descriptor can be found in Montgomery & Associates (2022). For each borehole, the shallowest lithology interval, corresponding to shallow depths where the lithology descriptors were not logged, was set to “unknown”.

Lithology data from boreholes in the DWR Statewide AEM Surveys, which span a much larger area than the current survey, were included for consideration if within 5 km of the planned flight lines for the current AEM survey. The lithology data include both a lithology description transcribed from the well completion report and multiple sets of categorized descriptors. The “texture refined” descriptor set focuses on the lithology texture and contains a similar degree of specificity as they were mapped onto the descriptors used in this project. Table 2-1 shows the mapping of each category.

Lithology intervals described as “rock” with an original transcription containing the word “shale” were reclassified if the interval was considered not to refer to consolidated rock (shale), but rather to compacted sediment (clay). Of the evaluated intervals, 11 were reclassified to “clay”, 2 to “not clay”, and 3 to “clay and”. This change was made to accommodate various historical descriptions that may not be accurate when viewed in the light of updated data and improved geologic knowledge of the area.

**Table 2-1 Mapping from the lithology descriptors used in the DWR AEM Surveys lithology data to the lithology descriptors used in this project. \*Each descriptor containing the word “shale” and classified as “rock” was evaluated as to whether it corresponded to consolidated rock or clay.**

<b>DWR AEM Surveys descriptor</b>	<b>Reclassified descriptor</b>
fine	clay
fine with coarse	clay and
coarse with fine	not clay
coarse	not clay
soil	soil
unknown	unknown
rock	rock*

The lithology data from multiple boreholes in the DWR Statewide AEM Surveys dataset appeared to be duplicated in the Deep Aquifers Study Phase 1 Borehole Dataset. Although the naming convention is not the same between the datasets, potential duplicates were identified by the proximity between recorded borehole positions (less than 5 m apart) and an identical or near-identical depth discretization and description of the lithology intervals. For each potential duplicate, the lithology intervals from the Deep Aquifers Study Phase 1 Borehole Dataset were given preference.

**2.3 Borehole Resistivity Logs**

Borehole resistivity logs were available from three datasets: the Deep Aquifers Phase 1 Borehole Dataset and Resistivity Logs, Survey Area 1 of the DWR AEM Statewide Surveys, and the Digitized Borehole Geophysical Logs. The logs from each dataset were available in a LAS or similar text format. In the case that the log did not conform to the LAS format, slight modifications were made to get the file into the standard format.

**2.4 Existing AEM Data**

AEM data from four previous surveys were available in the survey area, listed in Table 2-2. The surveys come from two datasets: the DWR Statewide AEM Surveys and the Coastal Salinas Valley AEM Surveys. The two AEM datasets from the DWR Statewide AEM Surveys were used for further analysis in the project because each dataset covers a complementary area and overlaps the survey area. Of the two datasets from the Coastal Salinas Valley AEM Surveys dataset, only the 2019 dataset was used for further analysis in this project. This decision was made because little additional value was expected from using the 2017 dataset in addition to the 2019 dataset: the flightline coverage of both datasets is very similar (see Figure 2-3), the 2017 dataset is older than the 2019 dataset, and the same equipment was used in the 2019 dataset and in the DWR Statewide AEM Survey Areas 1 and 8.

The resistivity values resulting from inversion were imported into the Aarhus Workbench software for analysis.

**Table 2-2 Existing AEM datasets.**

<b>AEM Dataset</b>	<b>Survey</b>	<b>AEM System</b>	<b>Region</b>	<b>Used in analysis</b>
DWR Statewide AEM Surveys	Survey Area 1	SkyTEM 312	Salinas Valley and Paso Robles Basins	Yes
	Survey Area 8	SkyTEM 312	Coastal Monterey Bay	Yes
Coastal Salinas Valley AEM Surveys	2017 Survey	SkyTEM 304	Coastal Salinas Valley	No
	2019 Survey	SkyTEM 312	Coastal Salinas Valley	Yes

### 3. Deep Aquifers AEM Survey

This section provides a description of the methodology used for the AEM data acquisition, survey objectives, and procedures taken for flight planning. A more detailed description of the survey and SkyTEM system specifications can be found in Appendix 2.

#### 3.1 AEM Method

##### 3.1.1 AEM Principles

The AEM method deploys the time-domain electromagnetic (TEM) method on an airborne platform. The TEM method is based on the principle of inducing electrical currents into the subsurface and receiving Earth’s response over a short period of time. During each transient measurement, direct current is conveyed through the transmitter loop, which, after a very short time, is abruptly turned off. This abrupt turn-off induces electrical currents (called eddy currents) in the subsurface that in return, generates secondary magnetic fields that decay with time. With depth, the area in which currents are induced expands, such that a larger region of the subsurface is sampled with depth. The decaying magnetic fields are measured using the receiver coils as a voltage timeseries, also referred to as a sounding. An optimization algorithm, called inversion, is then applied to the processed data to yield estimates of the subsurface resistivity structure, called resistivity models.

The TEM system can be deployed on the ground surface for stationary measurements or carried on moving platforms such as sleds, boats or, in the case of AEM, carried by a helicopter or airplane. Figure 3-1 provides an image of an AEM system operated by SkyTEM, similar to the one used in the current project.

An example of a single sounding of AEM data and a corresponding resistivity model of the subsurface is shown in Figure 3-2. During the inversion, the entire AEM dataset is inverted together and the resistivity model for each sounding is constrained. This is done by introducing a dependency in between models for neighboring soundings, as discussed in Section 4.2.

More information on the physical principles of the TEM method can be found in Ward and Hohmann (1988), Schamper et al. (2013), and in Appendix 2. A detailed description of the SkyTEM/AEM system used in this survey can be found in Section 3.2.1 and Appendix 2.

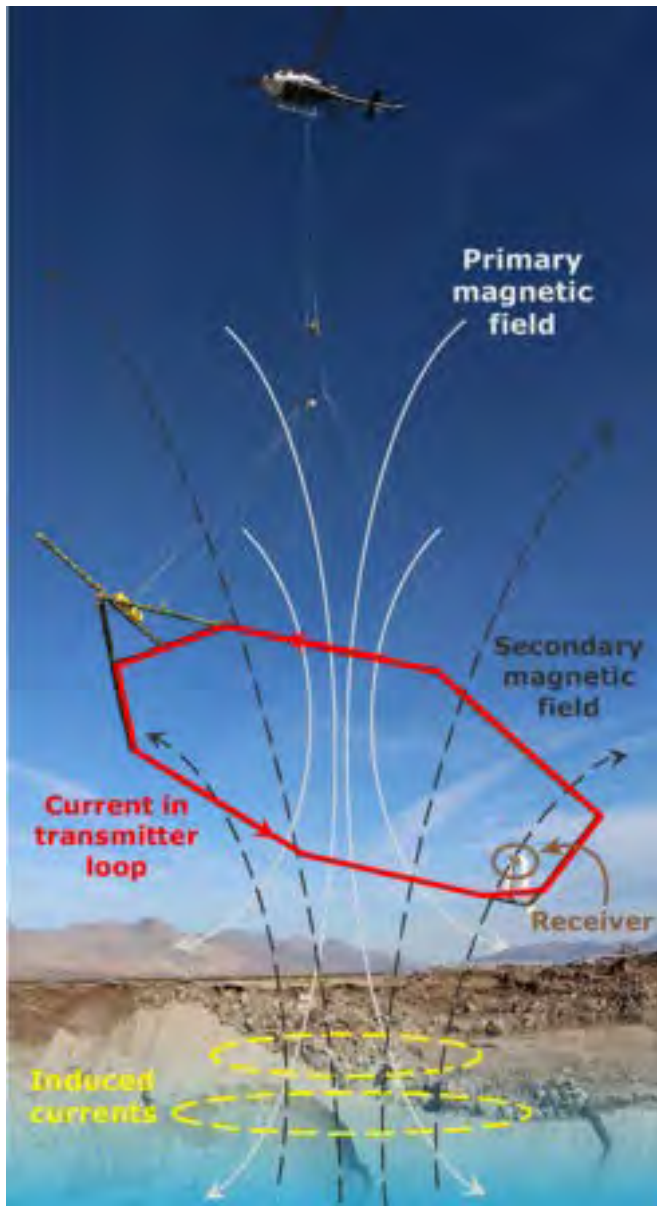
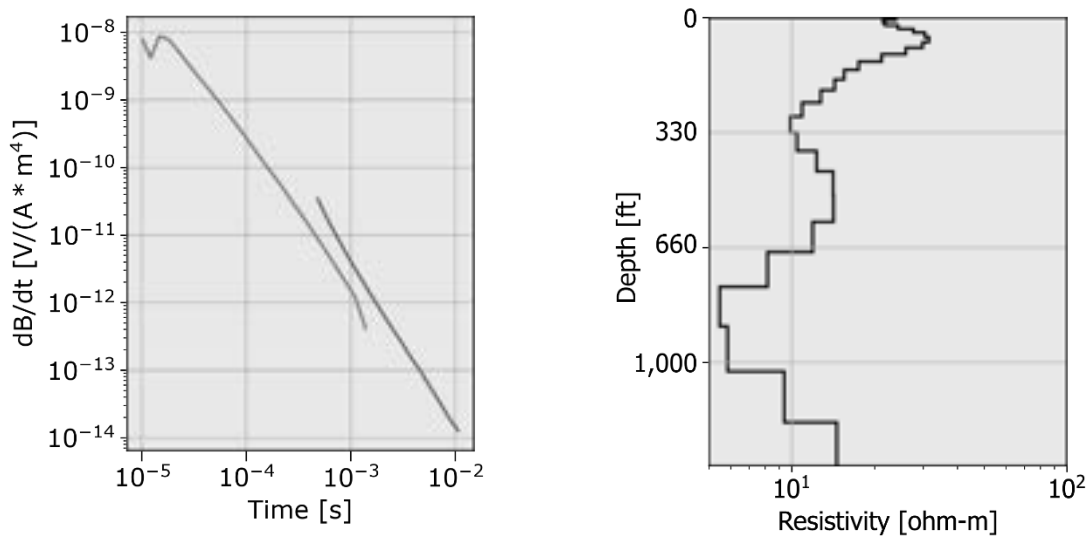


Figure 3-1 AEM Survey Schematic including the transmitter loop (current in red), the primary magnetic field (in grey), the induced subsurface currents (in yellow), and subsurface response (in dashed black lines) which is picked up by the system receiver (circled in brown).



**Figure 3-2 Example of a single sounding of acquired AEM data and the resulting resistivity model. Left: acquired AEM data (change in magnetic field as a function of time). Right: resulting resistivity model, showing the resistivity from the ground surface to a depth of 350 meters (1,150 feet).**

### 3.1.2 Rock-Physics Relationship

The resistivity values estimated using the AEM method provide value for groundwater management because of the relationship between electrical resistivity and subsurface properties of interest. These include the degree of saturation, groundwater salinity, and lithology. This relationship is known as the rock-physics relationship. Generally, resistivity will decrease with an increase in fine sediment, salinity, and saturation. The relationship between resistivity values, lithology, and salinity can be seen in Figure 3-3, where the resistivity range corresponding to gravel and sand is higher than that of glacial tills and higher still than that of clays. Similarly, saltwater has a much lower resistivity than does freshwater. Consolidated rocks such as granite will typically have very high resistivities. Shales, on the other hand, can take on a wide range of resistivity values. In this project, variations in water saturation are not considered since the deep subsurface considered for analysis is assumed to be below the water table.

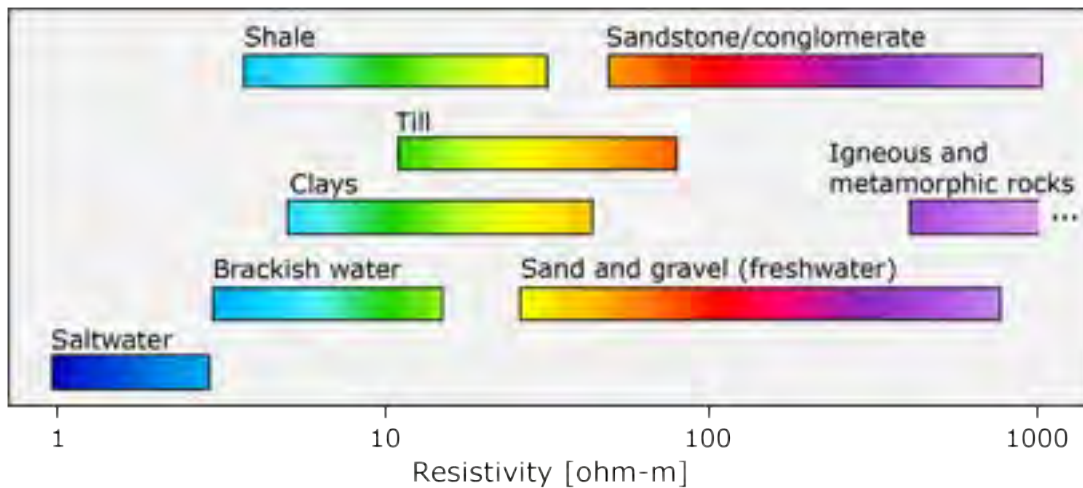


**Figure 3-3 General relationship between resistivity and subsurface materials: type of rock, sediments, and water salinity. Modified from Palacky (1987).**

### 3.1.3 Resistivity Color Scale

The wide range of resistivity values spanned by each bar in Figure 3-3 (most spanning over an order of magnitude) underscores the variable and site-specific nature of the relationship between resistivity and earth materials. Locally variable conditions can cause coarse sediments to have higher resistivity in some areas than in others, and mixtures of sediments (e.g., glacial till) result in resistivity values between those of coarse and fine. Thus, the choice of color scale for the presentation of all resistivity results should reflect the span of resistivity values found at the specific site.

For the resistivity values displayed in this report, a color scale was chosen with resistivity values ranging from 3-300 ohm-m to represent the resistivity variations seen in AEM data from the survey area. The color scale varies on a logarithmic scale, which is appropriate for visualizing the subsurface resistivity, which often varies over orders of magnitude (Figure 3-3).

The scale bar is shown in Figure 3-4.

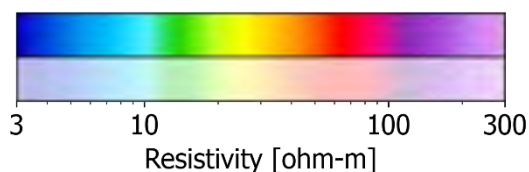


**Figure 3-4 The resistivity color scale used in this study for presentation of all resistivity AEM results in this report.**

## 3.2 AEM Survey Flight Line Planning

The flight lines for the AEM survey were preliminarily prepared by M&A working with Ramboll, considering the Phase 1 Extent of the 400-FDA and DWR Survey Area 1 flightlines. Ramboll, SkyTEM and Sinton Helicopters conducted a final review of the planned flight lines using aerial photos from Google Earth and aeronautical charts to identify possible safety considerations in relation to:

- Land use, including built up areas that would need to be avoided, and vineyards that contain metal in the trellises that interferes with the AEM signal

- Trees and forested areas that the pilot either would need to navigate around or climb in altitude while flying over
- Towers, power lines, and other infrastructure that the pilot either would need to navigate around or climb in altitude while flying over
- Major roads that the pilot would need to navigate around
- Restricted air space
- Restricted areas due to environmental sensitivities

Taking as input the preliminary flight lines, SkyTEM prepared a final flight line map (Figure 1-1), after conducting a safety review of the flight lines and landing zone bases (small airports) that were identified for survey logistics, equipment checks, data downloads, and fueling.

### **3.3 AEM Survey Equipment and Instrumentation**

The helicopter-borne SkyTEM 312HPM time-domain electromagnetic system was used during this survey. The AEM instrumentation consists of a transmitter loop, two receiver coils, two inclinometers, two altimeters, and two differential global positioning system (DGPS) units (for more information, see Appendix 2).

The AEM system is carried as a sling load, suspended 40 m (120 ft) beneath the helicopter and flown 30-50 m (98-164 ft) above the land surface (Figure 3-5) while flying at a ground speed of 60-80 kph (37-50mph). The system is designed for hydrogeological, environmental, and mineral investigations. The SkyTEM 312HPM system has a transmitter loop area of 342 m<sup>2</sup> (3,681 ft<sup>2</sup>) contained within a hexagonal frame suspended beneath the helicopter. The transmitter contains 12 turns making the effective area of loop 4,104 m<sup>2</sup> (44,172 ft<sup>2</sup>).

In addition to acquiring electromagnetic data, which provide information about the resistivity structure of the subsurface, the system also collects magnetic data that are primarily used for mapping magnetic anomalies, fractures, and faults. Auxiliary data are also recorded and include GPS data for positional accuracy, inclinometer data for the pitch and roll of the system, laser altimeter data for elevation, and video for a record of the ground surface along the flight path.

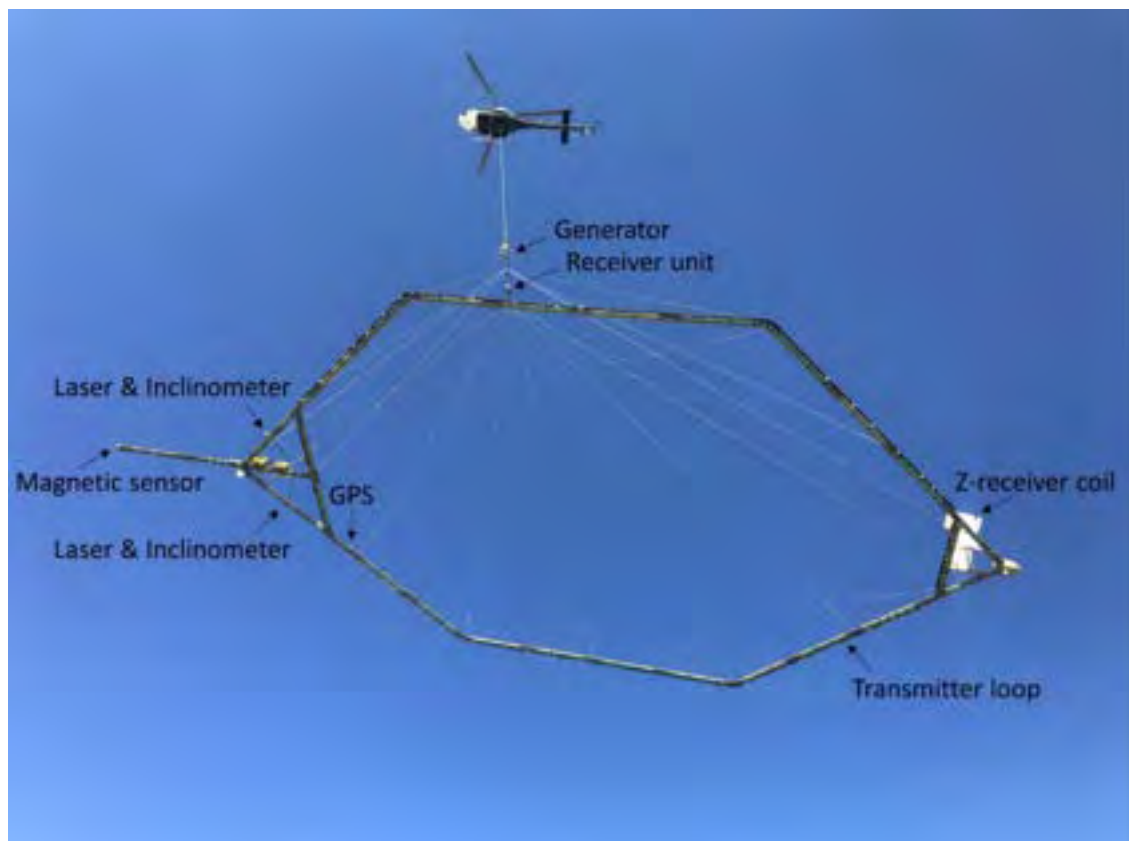


**Figure 3-5 AEM Equipment and instrumentation configuration.** The picture shows the helicopter towing the hexagonal transmitter loop. The front of the loop contains the GPS, laser, inclinometer, and magnetic sensor. At the back of the loop is the Z-receiver coil. Suspended between the transmitter loop and the helicopter are the generator and receiver unit.

### **3.4 AEM Survey Operation**

#### *3.4.1 Landing Zones*

The Salinas Municipal Airport was used as a base for the operation.

#### *3.4.2 AEM Data Acquisition*

The AEM survey was carried out between March 1-2, 2023. Data were acquired along a total of 300.3 line-km (186.6 line-miles). Figures of the AEM system during the survey are shown in Figure 3-6.



**Figure 3-6 Photos of the AEM system in operation in the Salinas Valley for the Deep Aquifers Study.**

Before, during and after the acquisition of the AEM data, several measures were taken to ensure that the AEM system functioned properly, and that the quality of the acquired data was acceptable. During the initial on-site SkyTEM system set-up phase, very high-altitude tests, waveform, configuration settings and null positions were checked in collaboration with SkyTEM. This was to ensure that the configuration and specifications were performing as agreed upon in the contract.

During the survey, SkyTEM provided daily updates, including a map of daily production, high altitude test, raw electromagnetic, magnetic, and reference line data, which was quality control checked. The quality of the data evaluated daily during the AEM survey was found to be acceptable.

Figure 3-7 shows the actual flown flight lines compared with the planned flight lines. The flown flight lines were in good agreement with the planned lines.

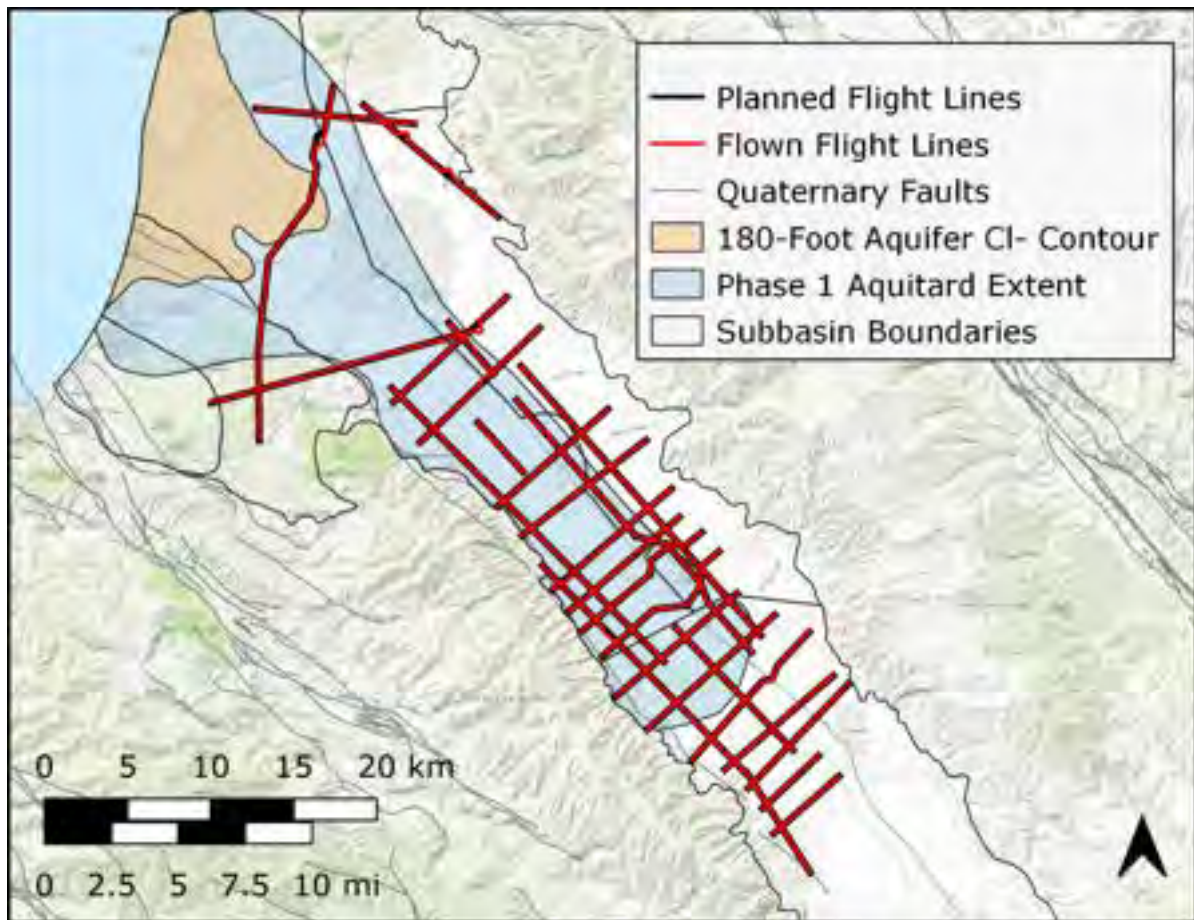


**Figure 3-7 Map showing the planned and flown AEM flight lines.**

### 3.4.3 Reference Lines

Reference lines are flight lines where AEM data are acquired multiple times throughout the survey. This is to ensure the reproducibility of the AEM system during the survey to validate instrument performance, to identify any potential drift and to document the stability of the data processing and inversion algorithms. The reference line was flown during each of the two production days, March 1-2, 2023, which resulted in a total of three repetitions of a flight line with a length of 1,000 m (3,300 ft) located east of the airport.

The AEM data acquired along the reference lines demonstrate that the AEM system was not affected by drift or instrumentation issues. It also showed that the processing and inversion schemes were consistent. Figure 3-8 offers a comparison between the AEM data from the current project and from a co-located flight line from Survey Area 8 in the DWR Statewide AEM Surveys.

The resistivity values result show excellent agreement, with the same resistivity structures present. The newly acquired AEM data offering information to a greater depth, indicated by the depth to which data are not greyed out. The results demonstrate that the data are highly repeatable. More information and the results of the reference lines can be found in Appendix 2.

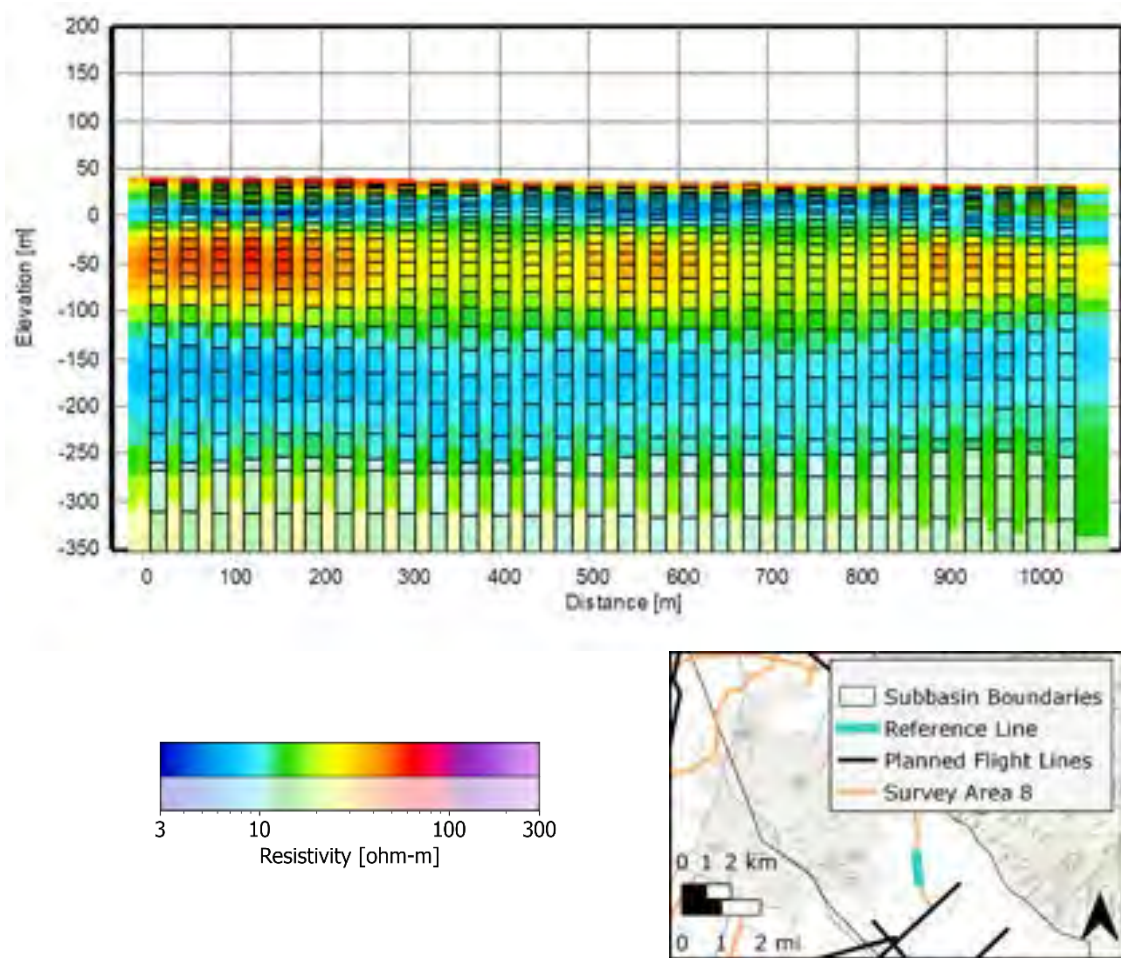


**Figure 3-8 Reference flight line. Resistivity values shown in the background come from the current project. The resistivity values in the foreground, outlined in black, come from Survey Area 8 of the DWR Statewide AEM Surveys.**

## 4. AEM Data Processing and Inversion

To obtain quantitative information on the subsurface resistivity from the raw AEM data, all the data acquired during the survey must go through the steps of processing and inversion. This includes the soundings and auxiliary data (location, flight height, angle of the transmitter tilt). Processing refers to actions that prepare the data for inversion, including the removal of noisy or coupled AEM data, and the application of averaging filters to the data. Filters are applied to obtain usable, noise-free data and optimize lateral resolution. Inversion refers to the numerical optimization algorithm that identifies the subsurface resistivity distribution that agrees with the AEM data.

All raw (electromagnetic & auxiliary) data are first checked for quality, then imported into the Aarhus Workbench software (<https://www.aarhusgeossoftware.dk/aarhus-workbench>) for data processing and inversion, which comprises the following steps:

1. Process auxiliary data (e.g., location, height)
2. Process AEM data automatically and manually
3. Run inversion on the AEM data

#### 4. Calculate the depth of investigation from AEM data

This section provides an overview of the processing and inversion.

##### **4.1 Data Processing**

The first data to be processed are the auxiliary data: these include pitch and roll (tilt) data, transmitter height data, and GPS data. The tilt and transmitter height data affect the raw AEM measurement and must be accounted for during the inversion, while the GPS data are needed to relate each measurement to its correct geographic position. To relate the resistivity models to the topography of the landscape, a terrain elevation was assigned to each electromagnetic sounding using a digital elevation model (DEM).

Next, the raw AEM data (voltage timeseries) are processed to prepare for inversion. The AEM system continuously makes electromagnetic measurements, which are averaged together every 1.2 seconds. The average ground speed of the helicopter during the survey was 43.2 miles per hour, resulting in one measurement every 76 ft (23 m) on average, or 70 measurements per mile (43 measurements per km). The AEM data processing comprises an automatic and a manual component. The automatic processing requires selection of appropriate filters and other parameters.

After automatic processing, the data are manually reviewed for noise, as well as interference from infrastructure, such as powerlines, pipes or vineyards. The distance of AEM data locations to human-made structures was considered, and portions of the dataset were selectively removed. The AEM data processing is an iterative process, which requires revisiting the data after each step, and again after provisional inversion results are visualized. The AEM data retained for inversion, along with the locations of infrastructure, are shown in Figure 4-1.

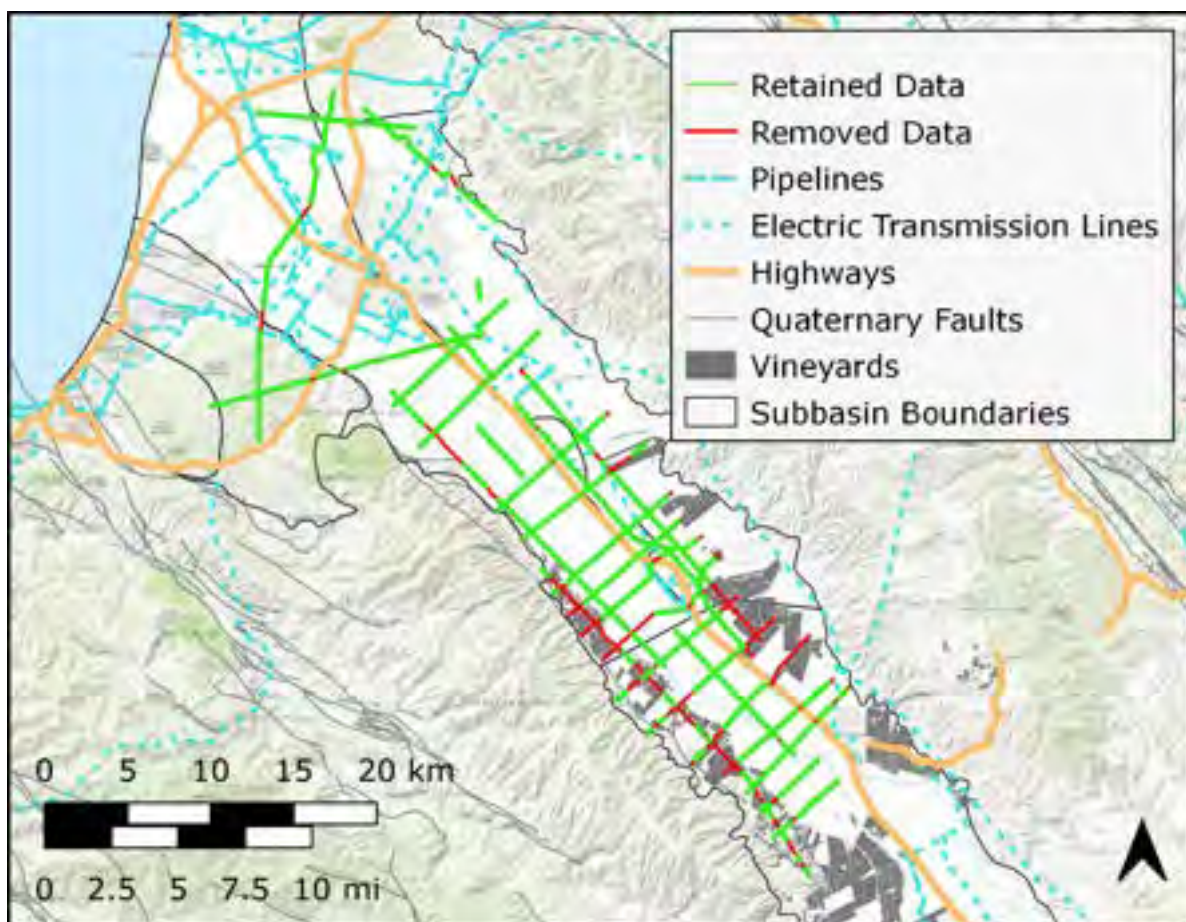


**Figure 4-1** Map showing the retained and removed AEM data. Retained data are shown in green, while the removed data are shown in red.

#### 4.2 Inversion

Once the auxiliary and AEM data were processed, the data were used to produce resistivity models through inversion. The inversion is an iterative optimization; the resistivity model at each location where AEM data were acquired (i.e., each sounding) along each flight line, is used to calculate synthetic AEM data. This synthetic AEM data are compared to the processed AEM data acquired during the survey. The misfit between the observed and synthetic data is used as a criterion to update the resistivity model, and the process is repeated. While minimizing the data misfit, the inversion allows nearby AEM data to be constrained vertically (i.e., between the resistivity values of adjacent layers) and horizontally (i.e., along and between flight lines) to allow the migration of information to nearby AEM data. Once the synthetic AEM data match the acquired AEM data within a specified tolerance, the resistivity model is considered final.

All AEM data are inverted simultaneously using the spatially constrained inversion (SCI) approach (Viezzoli et al., 2008), which accounts for all model parameters, AEM data and spatial constraints. The system setup information (AEM equipment metrics) is used during the inversion when calculating the synthetic AEM data. The inversion algorithm requires user input on specific values, including the depth discretization of the resistivity model (i.e., the estimate of the subsurface resistivity structure), the initial estimate of resistivity values, and horizontal and vertical constraints. Each value is selected based on the AEM system setup, depth interval of interest, and background geologic information of the study area. Multiple inversions may be run on the same dataset to find the optimal values for these input values. Typically, two to three inversions are run

on the dataset to 1) finalize the processing of the data (e.g., by removing noisy or coupled data that appear in the inversion result) and 2) obtain final input values for the inversion. Detailed information of the inversion approach can be found in Auken et al. (2015).

**4.2.1 Inversion Scheme**

Using the SCI approach, the AEM data were inverted in a smooth inversion scheme. In this scheme, many layers (in this project, 35 layers) are used in the model, where each layer thickness is larger than the layer above it. Each layer thickness remains fixed during iterations of the inversion, but the resistivity value of each layer is allowed to vary. Using spatial constraints, resistivity values are constrained to stay within a factor of neighboring resistivity values, resulting in smoothly varying resistivity-depth models.

**4.2.2 Depth of Investigation**

The resistivity values resulting from inversion were used to calculate the depth of investigation (DOI). The DOI is an estimate of the depth, below which there is an elevated uncertainty of resistivity values. For the AEM method, as for all diffusive geophysical methods, it is not possible to define an exact depth, below which there is no information on the resistivity structure. Thus, resistivity information below the DOI may still be useful. But interpretation of resistivity values below the DOI is cautioned.

The DOI is dependent on 1) the AEM data quality and 2) the subsurface resistivity structure. The DOI in this survey was maximized in two ways: first, by using the modified setup of the SkyTEM 312HPM system, high data quality was maintained until later times (corresponding to deeper subsurface information) in the AEM measurement, as compared to previous AEM surveys in the area; this results in a deeper DOI. Second, areas known to contain shallow, low-resistivity layers, such as areas containing thick conductive clays and saline water, were avoided, since these layers reduce the DOI due to the physics of the AEM measurement.

In this survey, the DOI was calculated using sensitivity information output from the inversion, following the approach presented by Christiansen et al. (2012). The resulting DOI varies throughout the survey area; a histogram of all DOI values can be seen in Figure 4-2. In the westernmost part of the survey area, south and west of Salinas and the areas close to the coast, the DOI is typically below 350-400 m (1,150-1,310 ft), while for the central and eastern parts of the survey area, the DOI is typically 400-600 m (1,310-1,970 ft). In a few locations, the DOI extends beyond 600 m (1,970 ft) in a few places.

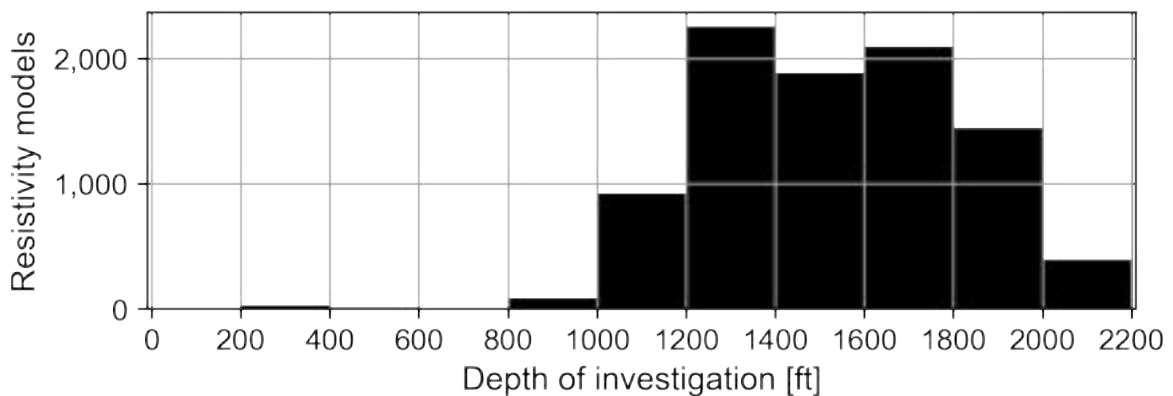


**Figure 4-2 Depth of investigation histogram for all resistivity models in the inversion. In most locations where AEM data were acquired, the DOI is between 1,000 and 2,000 ft (300 and 600 m).**

## 5. Survey and Interpretation Results

In this section, the results of the Deep Aquifers AEM survey and analysis of borehole data are presented. First, analysis of the borehole lithology and geophysical data is presented. Next, selected results of the AEM survey are shown, with additional results in Appendix 3 and 4.

It is important to underscore that, while the goal of this study is to improve the understanding of the Deep Aquifers and the overlying 400-FDA, AEM data are sensitive to variations in the subsurface resistivity (see Section 3.1) and cannot directly identify hydrogeologic units. Thus, the focus of the interpretation of the AEM resistivity results in this project is to identify, within the resistivity results, a continuous unit that corresponds to expected character and depth of the 400-FDA.

Within the survey area, the 400-FDA is expected to be a continuous unit that is more conductive than the overlying and underlying units (400-Foot Aquifer and Deep Aquifers, respectively). A resistivity decrease is expected compared to adjacent units because the 400-FDA contains an elevated percentage of clays. Furthermore, high TDS concentrations are not expected in the 400-FDA or adjacent units to confound the resistivity signal attributed to clay content. In this report, the identified unit is referred to as the "continuous conductor".

### 5.1 Deep Aquifers Study Phase 1 Borehole Data

The borehole data compiled from the Deep Aquifers Study Phase 1 include valuable interpreted depth intervals of the 400-FDA. The top and bottom of these intervals, shown as two maps in Figure 5-1, provide a starting point from which to understand the geometry of the 400-FDA. Figure 5-1a and Figure 5-1b show the interpreted depth to the top and bottom of the 400-FDA, respectively. Visibly, the top and bottom of the 400-FDA appear to shallow with distance away from the coast. A notable data gap is the lack of data points on the southeast side of the basin south of Salinas.

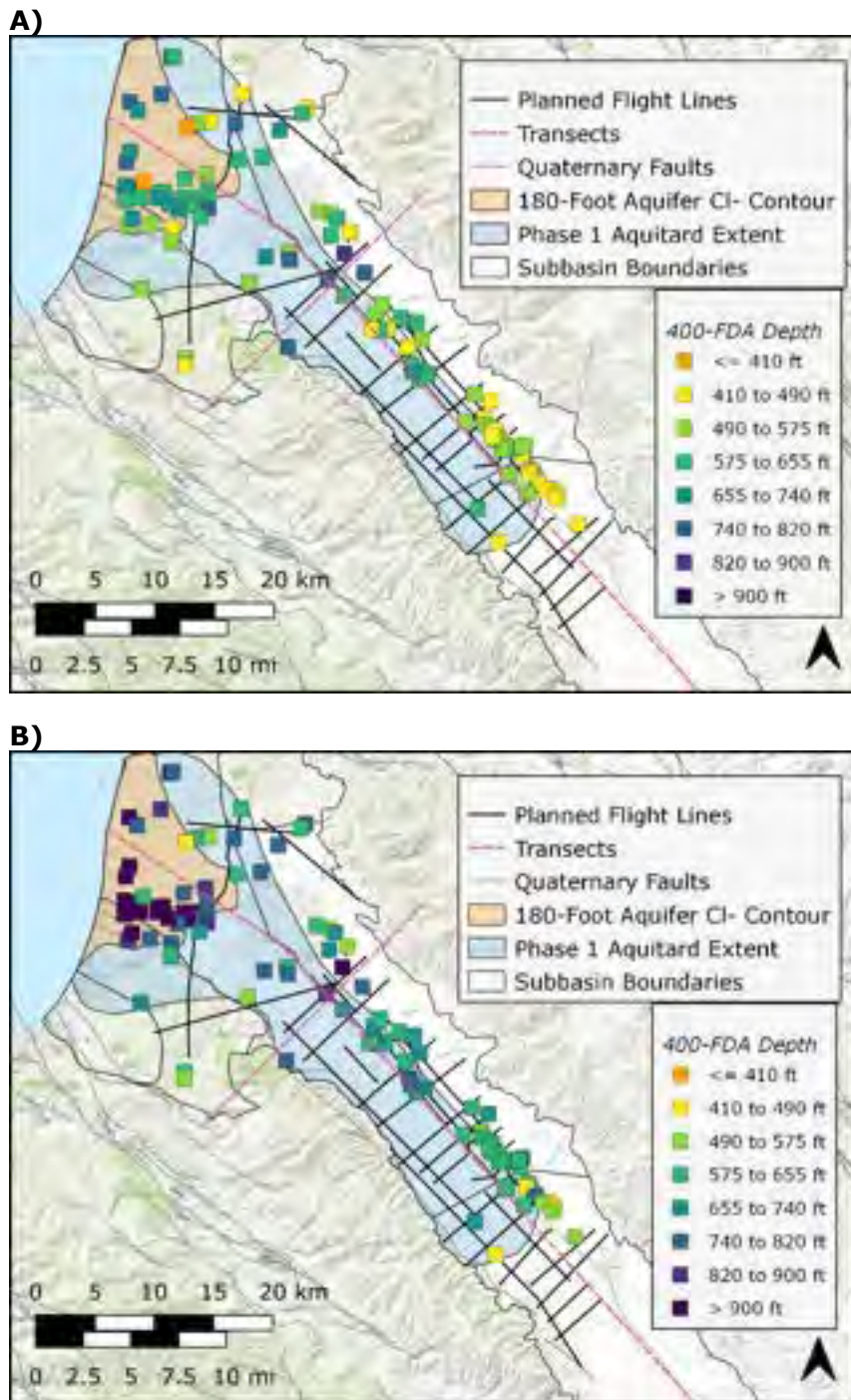


**Figure 5-1** Interpreted depth of the top and bottom of the 400-FDA from the Deep Aquifers Study Phase 1 Borehole Dataset. A) Depth to the top of the 400-FDA, B) Depth to the bottom of the 400-FDA.

Figure 5-2 plots the interpreted depths as a function of distance from the coast (Figure 5-2a) and across the Salinas Valley (Figure 5-2b), as defined by the pink transects shown in Figure 5-1. Each bar, showing the top and bottom of the 400-FDA, is colored by the subbasin corresponding to the measurement point. This view of the data shows a significant thinning of the 400-FDA with distance inland, indicated by the regression lines fitted to the top (dashed) and bottom (dotted) of the 400-FDA in Figure 5-2a. Moving across the Salinas Valley (Figure 5-2b), the interpreted

thickness of the 400-FDA increases upon crossing from the Monterey Subbasin to the 180/400 Foot Aquifer Subbasin. Once in the East Side Aquifer Subbasin and Forebay Aquifer Subbasin, the interpreted 400-FDA begins to thin again.

In both plots of Figure 5-2, a significant degree of variance can be seen along the x-axis. This variance is reflected in the maps of Figure 5-1, where significantly different interpreted depths of the 400-FDA can be found in nearby boreholes. These results suggest that some regional trends are present in the 400-FDA, but a high degree of local variability is expected.

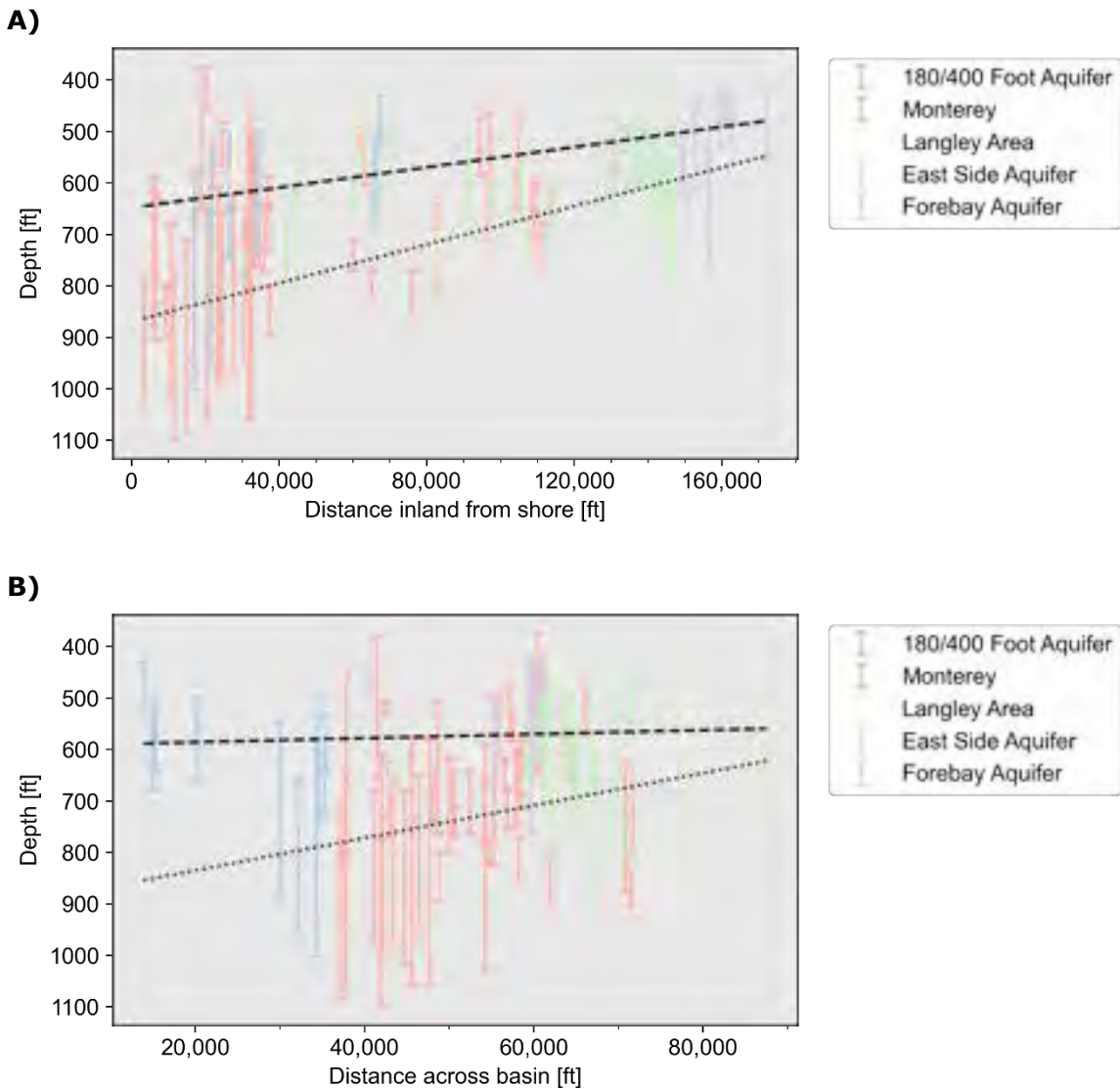


**Figure 5-2** Depth of the 400-FDA interpreted from borehole data as a function of distance. **A)** Distance inland from shore, **B)** distance across the Salinas Valley from SW to NE, as shown by the pink transect lines in Figure 5-1. The top and bottom of each bar indicates the depth to the top and bottom of the 400-FDA, respectively. Each bar is colored by the subbasin corresponding to the measurement location. The black dashed and dotted line, respectively, show the least squares regression line fit to the interpreted top and bottom of the 400-FDA.

## 5.2 AEM Data

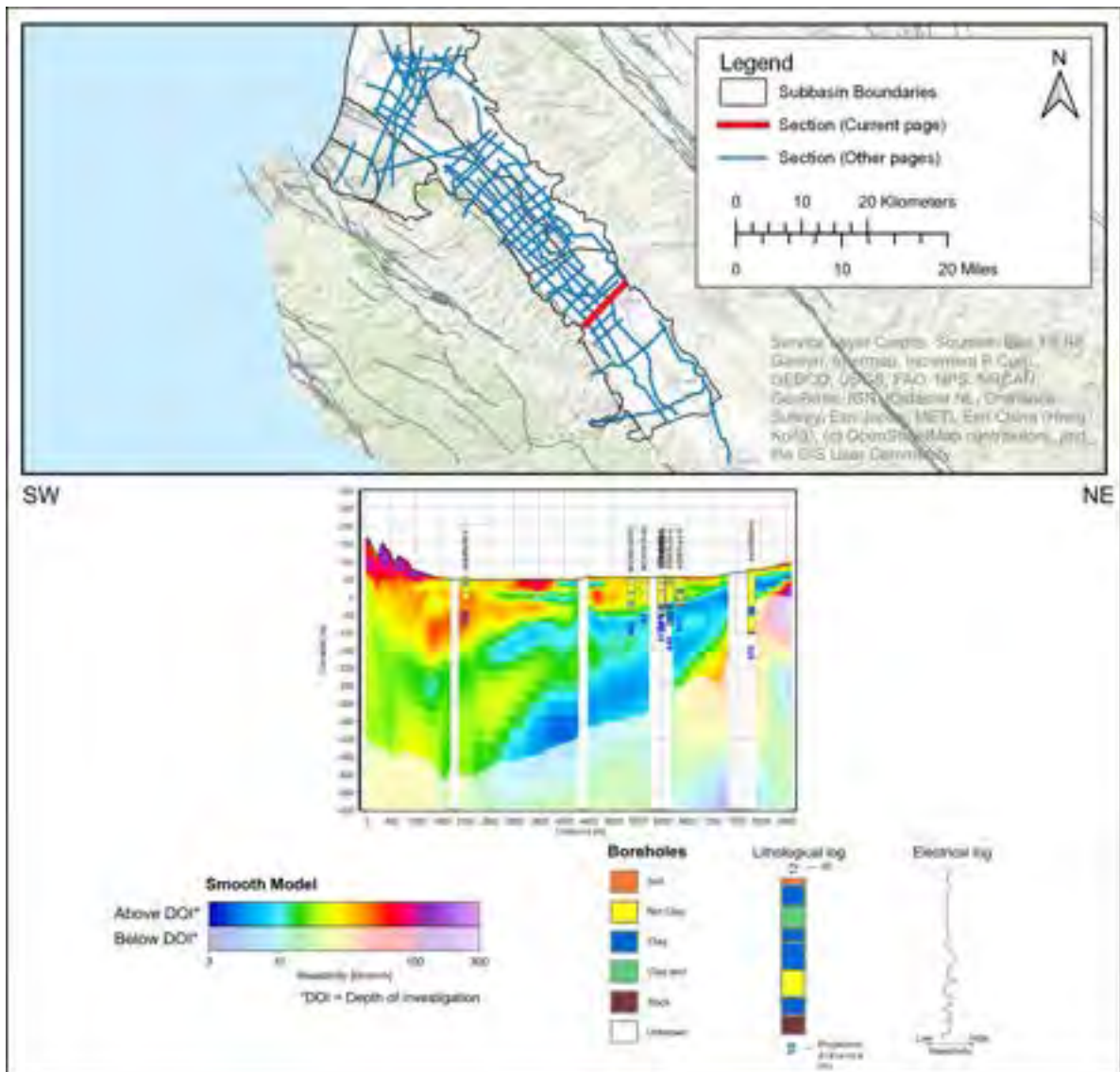
The inversion of the AEM data produces many 1D vertical estimates. The resistivity estimates can be stitched together to form 2D vertical sections or cut into depth or elevation slices to show the spatial distribution of mean resistivity across different depth or elevation intervals.

### 5.2.1 Resistivity Cross-sections

A total of 63 resistivity cross-sections were generated along the flight lines and show the resistivity distribution of the subsurface to depths of 1,000-2,000 ft (300-600 m) below ground surface. A selected set of cross-sections are shown in Figure 5-3 through Figure 5-5. All resistivity values are colored according to the color bar shown in Figure 3-4, showing low and high resistivity values in cool and warm colors, respectively. Resistivity values below the DOI are partially greyed out in each cross-section to reflect that the resistivity values are more uncertain. The sections are presented with the same horizontal and vertical scale. The x-axis shows distance along each flight line in meters, as constrained by the software used to render the cross-sections. Borehole lithology and resistivity data within 500 m of the transect defining each cross-section are also plotted on each section. Borehole lithology data from the Deep Aquifer Study Phase 1 contain lithology descriptors starting at 450 ft depth; above this depth, a white bar is shown, indicating no data. Section 5.3 includes additional cross-sections plotted with interpretive annotations. The entire set of sections are presented, along with existing data and interpretive annotations, in Appendix 3.

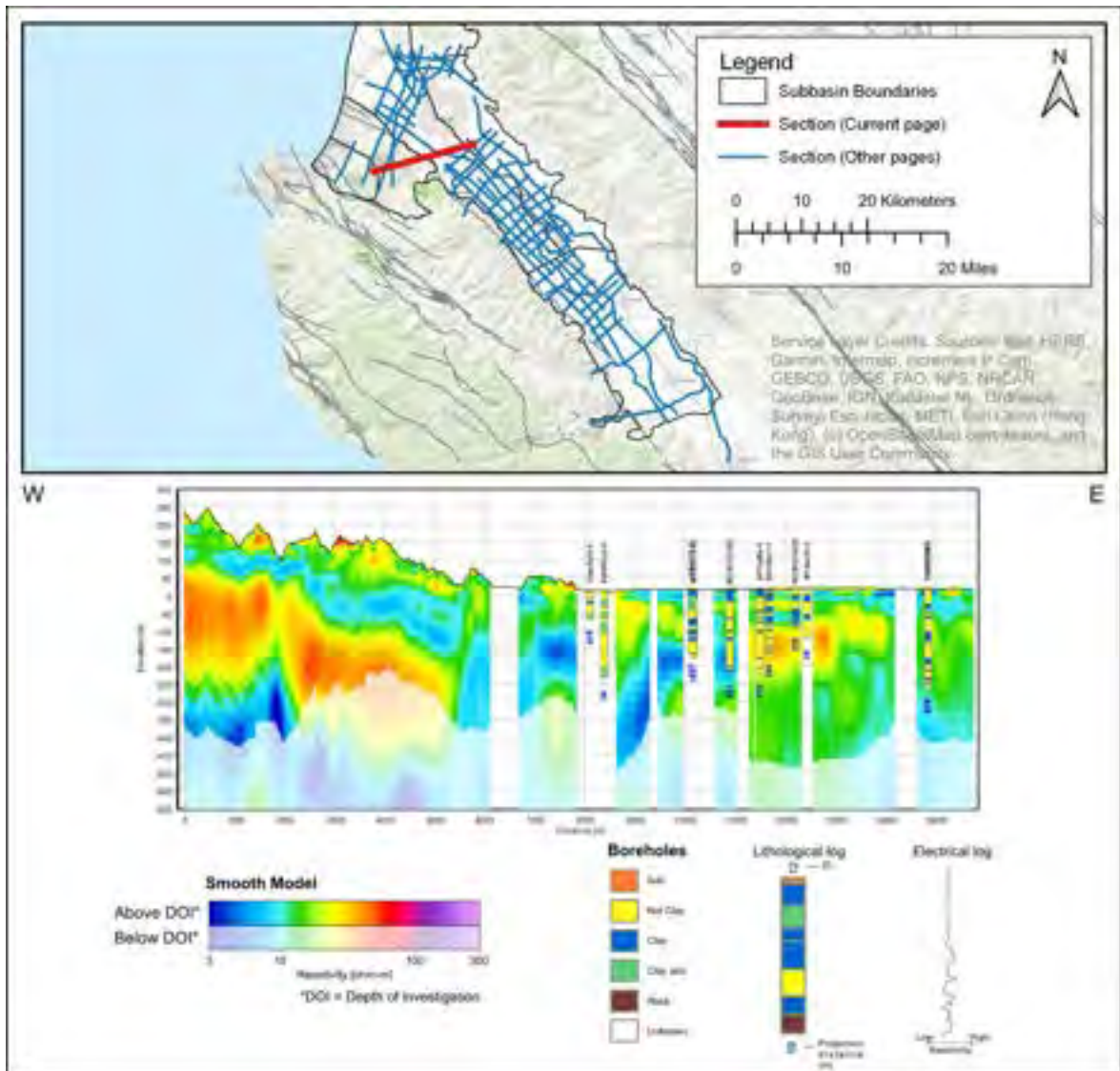
In Figure 5-3 through Figure 5-5, three vertical model-sections across the surveyed area are provided to illustrate the spatial variations with a focus on how generated resistivity models compare to borehole lithology and resistivity data. All the resistivity data demonstrate good near surface resolution with the SkyTEM 312HPM system, which has deeper penetration capability than the AEM systems used to produce the existing AEM data in the survey area. The near-surface resolution of the SkyTEM 312HPM system allows for additional use of the AEM data for identifying near-surface units, and for validation with previous AEM surveys (e.g. Figure 3-8).

Figure 5-3 shows a section spanning 8.5 km (5.3 mi) in the central part of the area. Several borehole logs are included with lithologies that generally agree with the resistivities. The resistivity data on the section shows varying resistivity layers in the basin, with the lowest resistivity layer (blue color) overlain by a moderate resistivity layer (yellow and green colors), overlain by a high resistivity layer (orange and red colors). In the right (eastern) portion of the section, a very high resistivity layer (purple color) forms the base of the sediments and is likely bedrock (undifferentiated igneous and metamorphic). The lithology data in the cross-section show almost all "not clay" intervals, with "clay" intervals near the bottom of some boreholes.



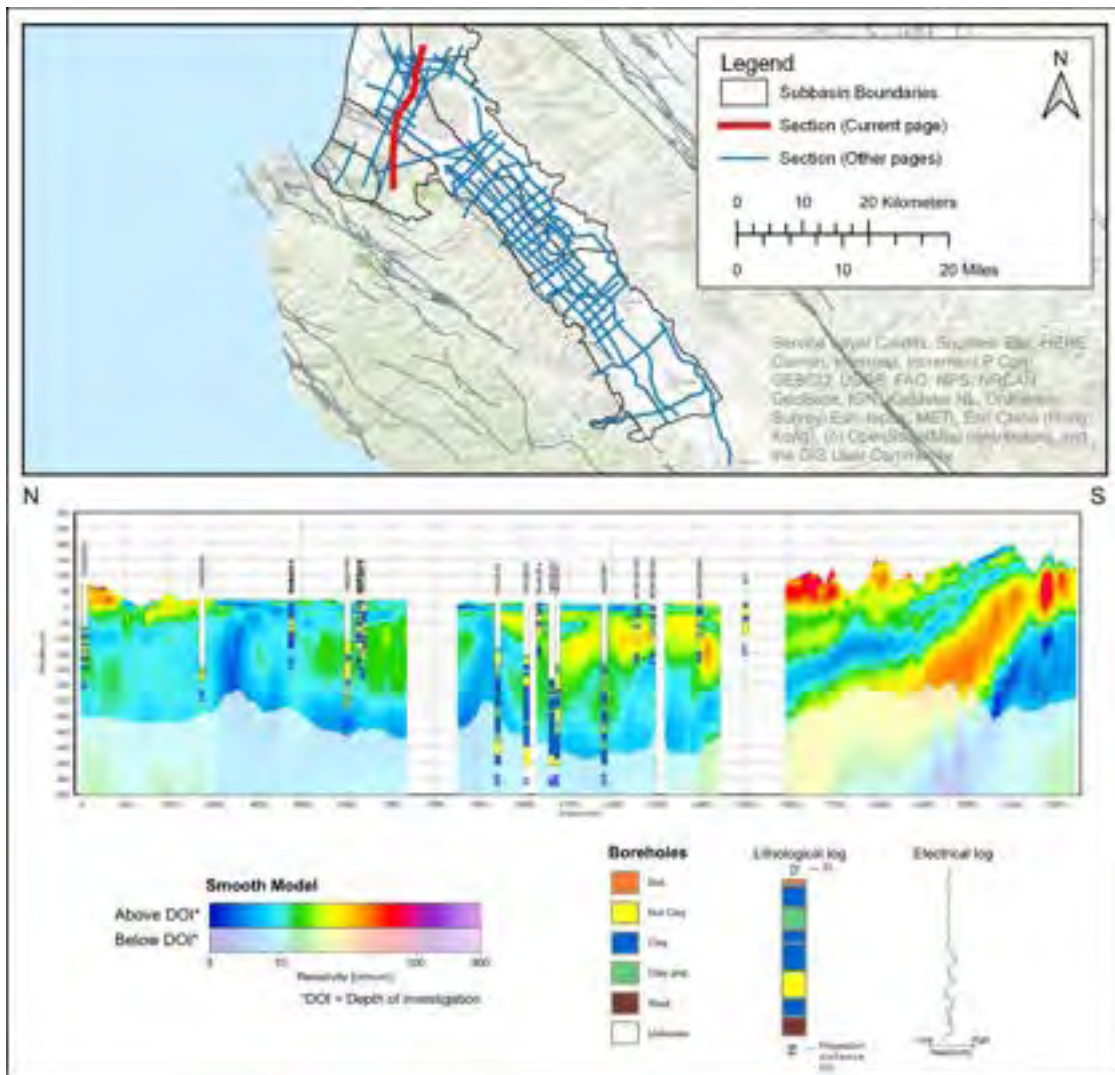
**Figure 5-3 Resistivity along Section 101600.** The section location is shown as the red line in the top panel, while the vertical resistivity section from northeast to southwest is provided in the bottom panel. Faded colors near the bottom of the cross-section represent resistivity values below the DOI. Borehole lithology data (colored columns) are projected onto the section.

Figure 5-4 shows a section spanning 16 km (9.9 mi) in the northern part of the survey area, including nearby borehole lithology logs projected onto the section. The resistivity values show various resistivity layers, with a low-resistivity layer (blue and green colors), overlain by a moderate resistivity layer (yellow and green colors), overlain by a low resistivity layer to the east. The lithology log from the well on the right (eastern) portion of the section shows alternating lithology and fits well with alternating resistivity layers seen on the section. In the western part of the section, a high resistivity region (red color) is present below the layers; this may be Salinian Block granitic rocks that have been reverse faulted against older sediments to the east. There also appears to be evidence of folding in the layers from the faulting. The Reliz Fault is mapped at 8 km along the section (<https://www.usgs.gov/programs/earthquake-hazards/faults>), corresponding to the area (6.7 to 9 km) where abrupt elevation shifts can be seen in the elevation of the top of the conductor between -100 to -200 m.



**Figure 5-4 Resistivity along Section 100300.** The section location is shown as the red line in the top panel, while the vertical resistivity section from northeast to southwest is provided in the bottom panel. Faded colors near the bottom of the cross-section represent resistivity values below the DOI. Borehole lithology data (colored columns) are projected onto the section. The Reliz Fault is mapped at 8 km along the section

Figure 5-5 shows a section spanning 22.5 km (14 mi) in the northern part of the survey area. Nearby borehole lithology logs are projected onto the section. A relatively uniform series of alternating high- and low-resistivity layers can be found on the left (south) side of the section, while the remaining portion of the section shows a complex distribution of resistivity, where resistivity values change over short lateral and vertical distances.



**Figure 5-5 Resistivity along Section 100200. The section location is shown as the red line in the top panel, while the vertical resistivity section from northeast to southwest is provided in the bottom panel. Faded colors near the bottom of the cross-section represent resistivity values below the DOI. Borehole lithology data (colored columns) are projected onto the section.**

### 5.2.2 Mean Resistivity Maps

Mean resistivity maps provide another visualization means to illustrate the variation in resistivity across the survey area. The maps can be shown as mean values over either depth or elevation intervals.

The mean resistivity values were calculated at each location where AEM data were retained for inversion, with the mean defined as the harmonic mean over the given vertical interval. Once calculated, each mean resistivity value was then estimated on a uniform grid using inverse distance interpolation with a node spacing of 40 m and search radius of 400 m.

Four representative plan-view maps of horizontal slices along the flight lines are displayed at different depth and elevation intervals in Figure 5-6 through Figure 5-9. These maps illustrate detailed structures and provide insight into variations across the surveyed area at each interval. A larger set of mean resistivity maps can be found in Appendix 4.

Figure 5-6 illustrates the mean resistivity over the depth interval 5-15 m (16-49 ft) bgs. Within this shallow depth interval, resistivity values vary over a short lateral distance; however, regional trends can be identified: extremely low resistivity values (dark blue colors) are found along the shore, corresponding to ocean water and saline groundwater. Low resistivity values are present in the northwestern part of the survey area (light blue colors) where the Salinas Valley Aquitard is expected. Moderate-to-high resistivity values (green, yellow, and orange colors) can be found throughout the rest of the survey area.

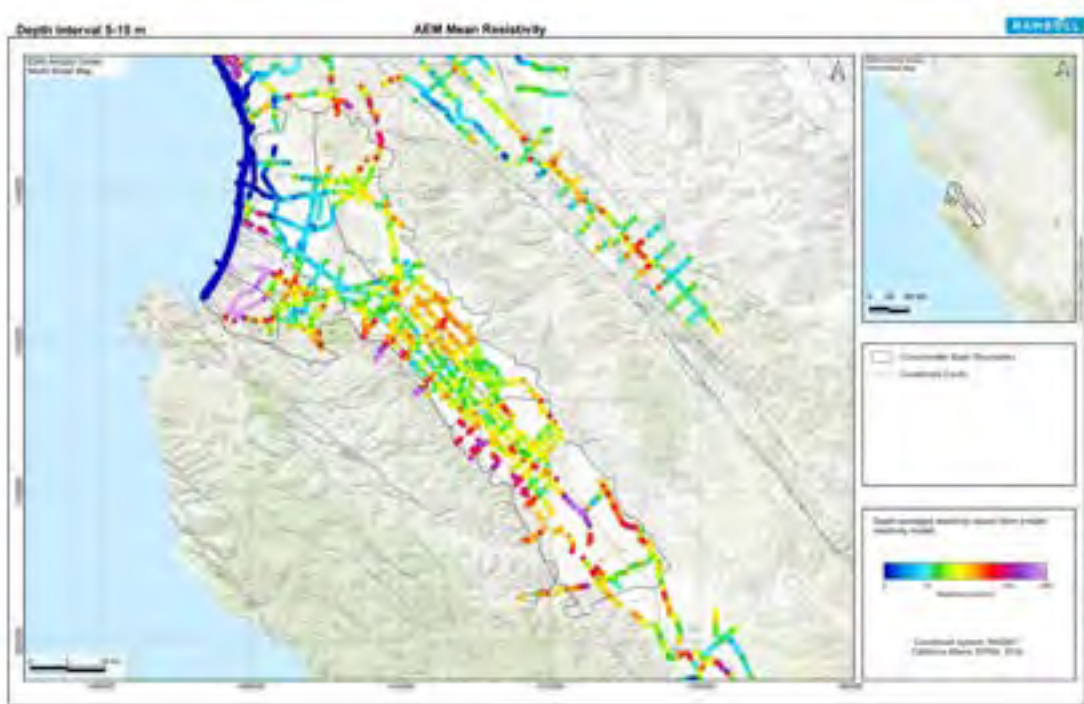


**Figure 5-6 Mean resistivity plan-view map in the depth interval 5 to 15 m (16 to 49 ft) bgs.**

Figure 5-7 shows the mean resistivity values in the elevation interval of -150 to -100 m (-492 to -328 ft) above mean sea level (amsl). At this elevation, south of Salinas, the southwest side of the basin has a high resistivity (red color), while the northeast side has a significantly lower resistivity (green and blue colors). The northern and southern side of the area have relatively low resistivity values. Very high resistivity values (purple color) emerge along the eastern edge of the survey area, corresponding to where bedrock is expected.

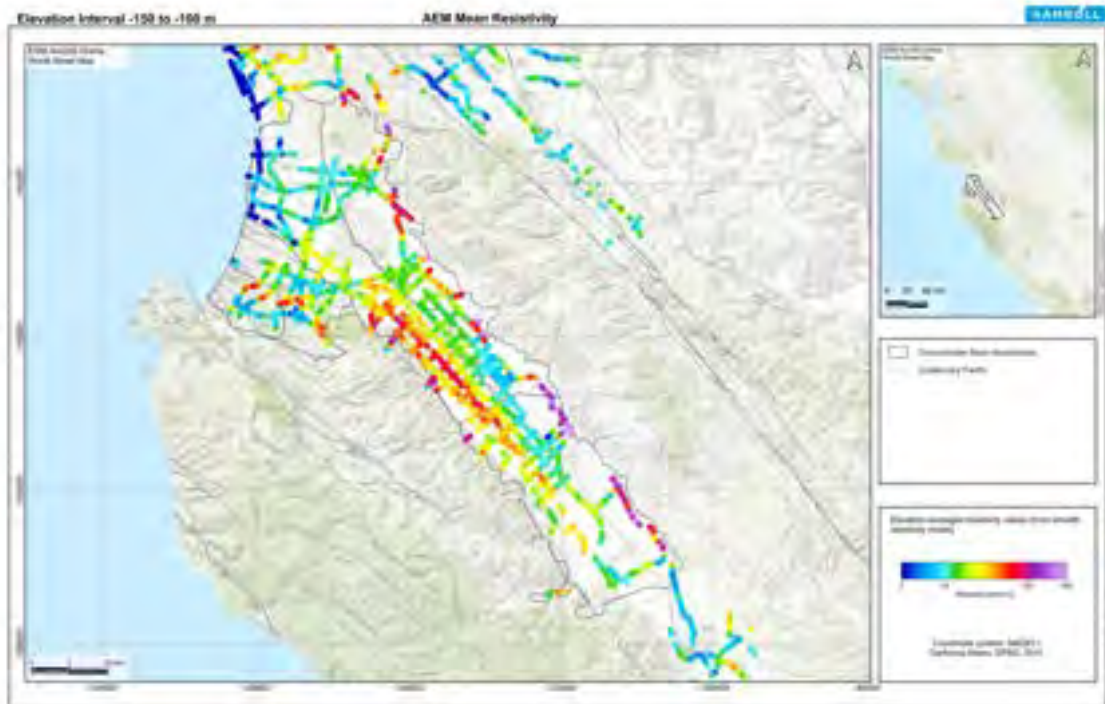
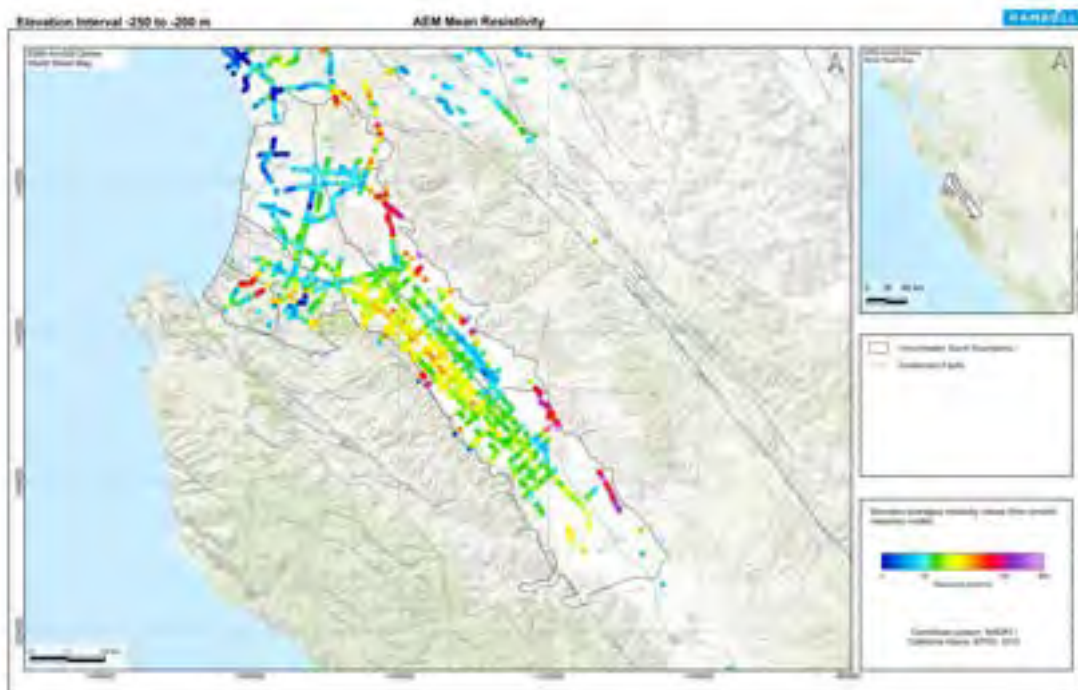


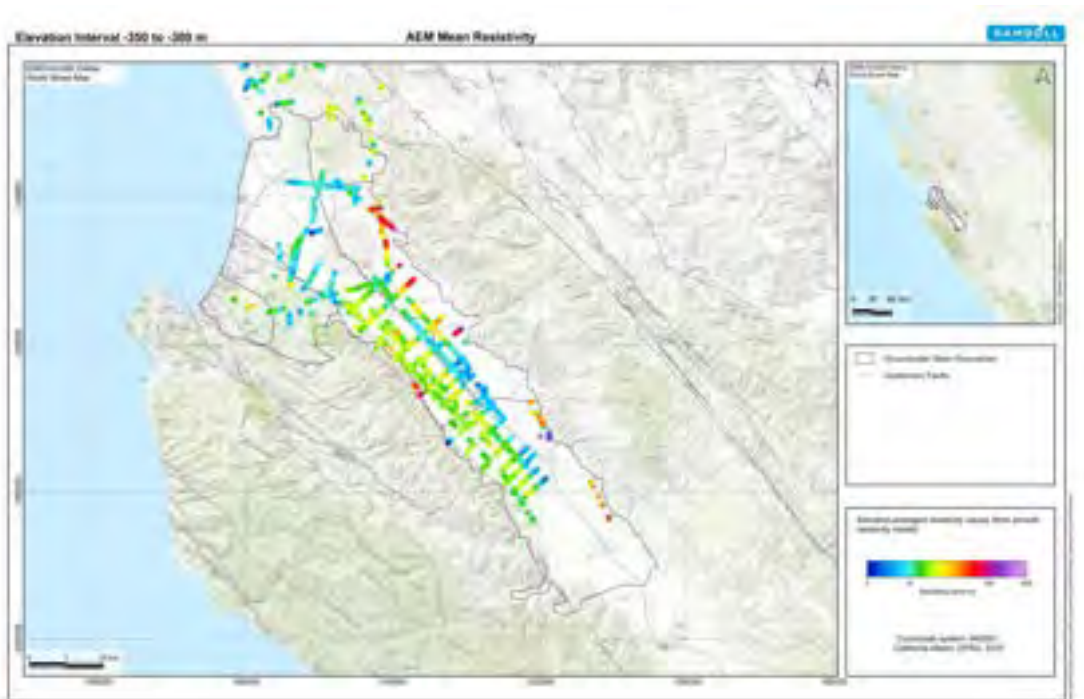
Figure 5-7 Mean resistivity plan-view map in the elevation interval of -150 to -100 m (-492 to -328 ft) amsl.

Figure 5-8 shows the mean resistivity values in the elevation interval -250 to -200 m (-820 to -656 ft) amsl. Low resistivity values are found in the areas north and west of Salinas, while south of Salinas, as in Figure 5-7, resistivity values are higher in the southwest than in the northeast. However, the resistivity values on both sides of the basin are lower than in Figure 5-7.



**Figure 5-8 Mean resistivity plan-view map in the elevation interval of -250 to -200 m (-820 to -656 ft) amsl.**

The data presented in Figure 5-9 illustrate the mean resistivity values within the elevation range of -350 to -300 m (-1,148 to -984 ft) amsl. Notably, a significant portion of the data in both the southern and northern regions fall below the DOI at this elevation and are therefore not displayed. South of Salinas, the trend of lower resistivity in the northeast side of the basin is still present at this elevation.



**Figure 5-9 Mean resistivity plan-view map in the elevation interval of -350 to -300 m (-1148 to -984 ft) amsl.**

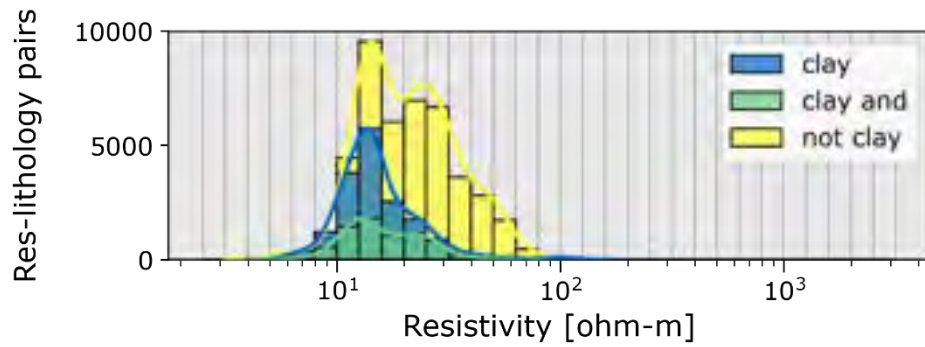
### 5.2.3 Comparison of Lithology and Resistivity from AEM Data

Nearby AEM and lithology data can provide a baseline understanding of the rock-physics relationship between resistivity and lithology. As can be seen in the cross-sections and mean resistivity maps above (Figure 5-3 through Figure 5-9), a significant degree of regional change is expected in the distribution of resistivity values and may be related to underlying changes in rock-physics relationship. In cases where this relationship varies within the study area, it can be challenging to produce quantitative metrics for the rock-physics relationship: statistical relationships built from data across the study area will tend to smear and obfuscate the underlying, local relationships.

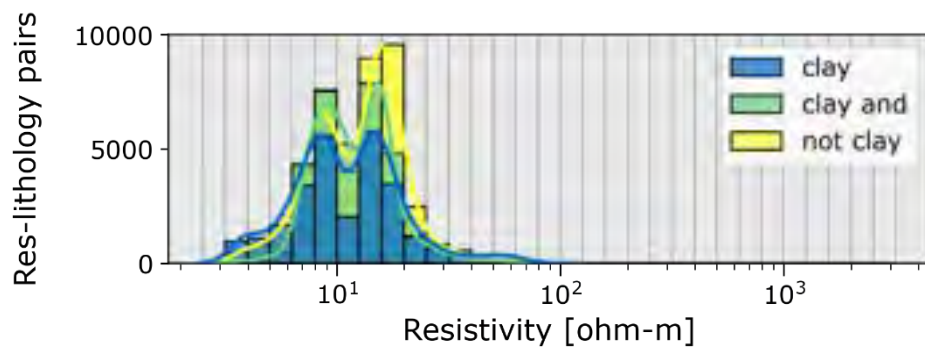
Figure 5-10 presents this relationship in the three subbasins where a significant amount of data are available: a) the 180/400 Foot Aquifer Subbasin, b) East Side Aquifer Subbasin, c) Forebay Aquifer Subbasin, and d) all available data. In each histogram, resistivity values from the newly acquired AEM data are paired with lithology descriptors from boreholes within 300 m. Every meter along the borehole, a sample is taken of the resistivity-lithology pair, generating tens of thousands of points. The histograms are shown colored by the lithology descriptor, and a line depicting the kernel density estimate is shown as a visual aid in case one histogram is partially hidden.

The results in Figure 5-10 show interesting differences in the relative amount of lithology descriptors and the shifting resistivity-lithology relationship between the different subbasins. In the 180/400-Foot Aquifer and Forebay Aquifer Subbasins, the “not clay” descriptor has an overlapping but distinguishable resistivity distribution from the “clay” and “clay and” descriptors. However, in the East Side Aquifer Subbasin, each distribution overlaps almost completely. Furthermore, the range of resistivity values in the Forebay Aquifer Subbasin compare more closely to the East Side Aquifer Subbasin (most data approximately 7 to 30 ohm-m) than to the 180-Foot Aquifer Subbasin, which has a higher average resistivity (most data approximately 10 to 70 ohm-m). Based on the data available, these figures suggest that a global relationship between resistivity and the defined sediment types (“clay”, “clay and”, and “not clay”) will be more readily identified within the Forebay Subbasin and the 180/400-Foot Subbasin than in the East Side Aquifer Subbasin.

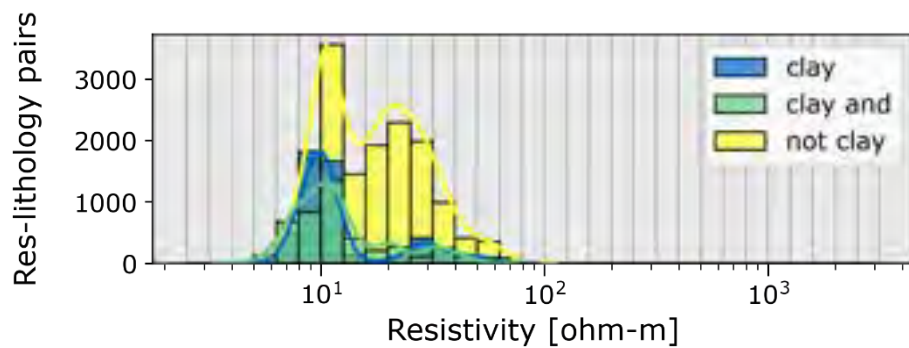
**A) 180/400 Foot Aquifer Subbasin**



**B) East Side Aquifer Subbasin**



**C) Forebay Aquifer Subbasin**



**D) All Data**

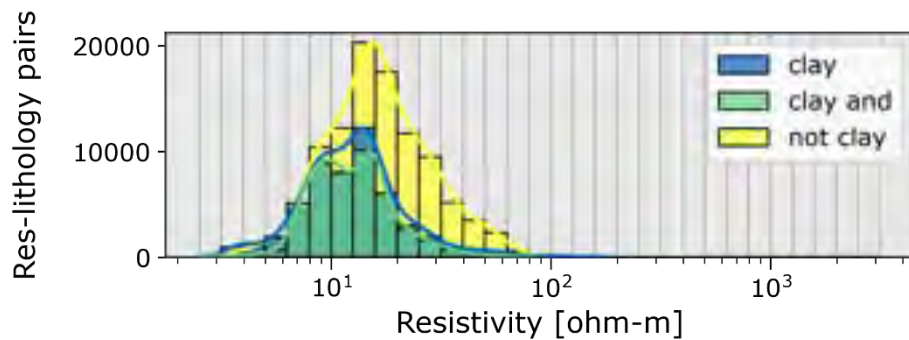


**Figure 5-10 Distribution of AEM resistivity values compared to lithology from boreholes within 300 m. The distributions are shown for A) the 180/400 Foot Aquifer Subbasin, B) the East Side Aquifer Subbasin, C) the Forebay Aquifer Subbasin, and D) all data.**

Another perspective on borehole and AEM data can be gained from the interpretations of the 400-FDA from the Deep Aquifers Study Phase 1 Borehole Dataset. The panels in Figure 5-11 contain a set of smoothed histograms, each of which show the distribution of resistivity values (x-axis) over a 50-foot elevation interval. Resistivity values are shown if they are within 1,000 ft (300 m) of a borehole with an interpretation of the 400-FDA. Values on the y-axis indicate the elevation interval as an offset from the interval interpreted as the 400-FDA from analysis of the Deep Aquifers Study Phase 1 Borehole Dataset: positive values indicate the offset above the top of the interval, and negative values indicate the offset below the bottom of the interval. At the zero value on the y-axis, the resistivity is averaged over the elevation interval corresponding to the interpretation of the 400-FDA (which may be more or less than 50 feet); this histogram is shown in blue to distinguish it from the rest in the series. The mean resistivity (taken on a logarithmic scale) is displayed as a line crossing each histogram. Only values above the DOI are used for calculation; thus, fewer data are generally available with increasing depth as more resistivity values fall below the DOI.

The distributions in the panels of Figure 5-11 share some general trends: the mean resistivity generally decreases with a decrease in offset, although at a modest rate. AEM data away from borehole data with interpretations of the 400-FDA show this trend of decreasing resistivity with depth as well (e.g., Figure 5-3). Furthermore, the resistivity values near the boreholes used in Figure 5-11 all fall within a relatively small range: approximately 3 to 30 ohm-m.

While some trends are shared across the subbasins represented in Figure 5-11, distinct differences can be seen as well. For the 180/400 Foot Aquifer Subbasin (Figure 5-11a), the resistivity distributions are generally monomodal, with not much of a shift in the distributions at zero offset (blue distribution), which corresponds to the elevation interval of the interpreted 400-FDA and has a mean resistivity of 11 ohm-m. These results suggest that, based on the borehole data available in the Deep Aquifers Study Phase 1 Borehole Dataset, correlating the interpreted 400-FDA to a shift in resistivity may prove challenging.

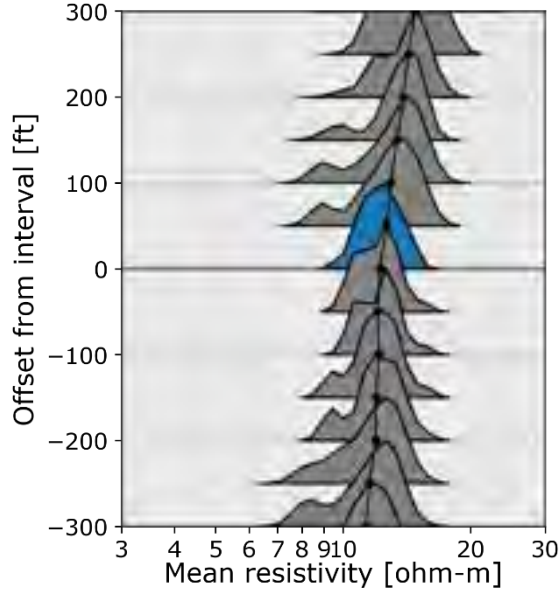
In the East Side Aquifer Subbasin (Figure 5-11b), the distributions are more complex, and are often bimodal and long tailed. A shift in character of the distributions can be seen around the zero offset, where distributions with a positive offset generally have a long, higher resistivity tail, and distributions with a negative offset have long, low-resistivity tails. Furthermore, the distributions shift from more bimodal to monomodal from positive to negative offset, respectively. The distribution with a zero offset has short tails and modes around 8 and 15 ohm-m, which are slightly more conductive than the modes of the distributions with positive offset. The shorter tails and well-defined modes suggest that borehole interpretations of the 400-FDA may be more easily correlated to the resistivity estimates from AEM data than in the 180/400 Foot Aquifer Subbasin.

Few borehole data with interpretations of the 400-FDA are present in the Forebay Aquifer Subbasin, which decreases confidence in the trends seen in Figure 5-11c. There appears to be a slight and gradual decrease in the resistivity value with a decreasing offset until the offset is zero. The mean resistivity of the interval associated with the 400-FDA is around 10 ohm-m.

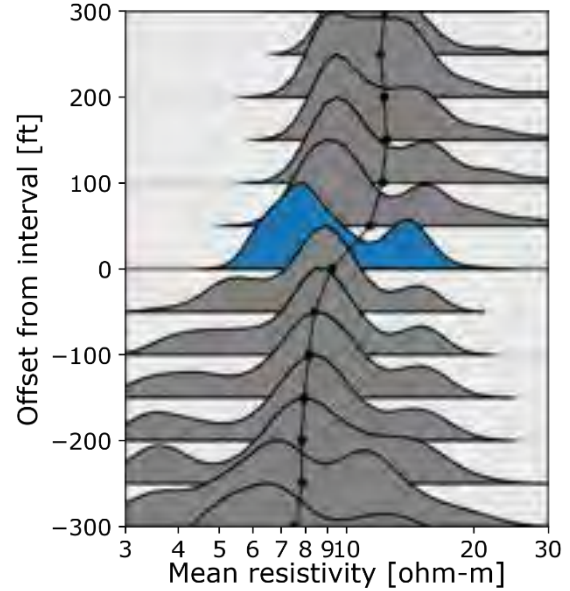
The 400-FDA is expected to be a generally continuous unit that is more conductive than the overlying and underlying units; however, the distributions in Figure 5-11 show only a slight correlation between the AEM resistivity values and the interpretations of the 400-FDA. This ostensibly modest correlation may be explained by a few potential underlying causes, including that the resistivity corresponding to the 400-FDA varies throughout each subbasin due to variability in sediment deposition (i.e., that the relationship is non-stationary, suggested by the bimodal zero-offset distribution in Figure 5-11b), that the interpretations of the 400-FDA do not

correspond closely to a continuous conductor in the region, or that not enough deep boreholes are available near AEM data to identify the underlying relationship.

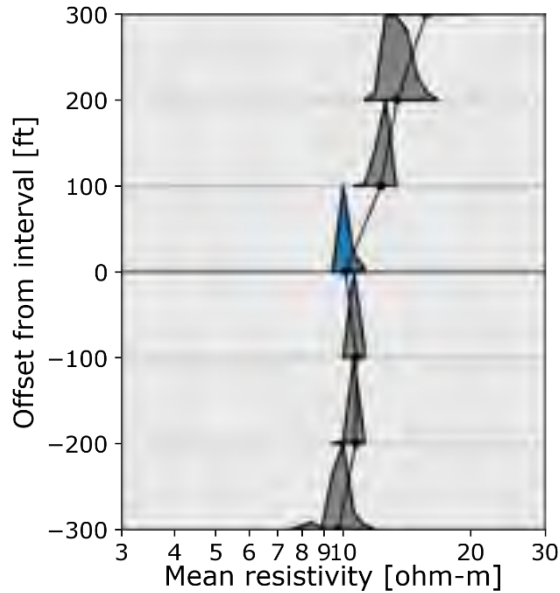
**A) 180/400 Foot Aquifer Subbasin**



**B) East Side Aquifer Subbasin**



**C) Forebay Aquifer Subbasin \***



**D) All Data**

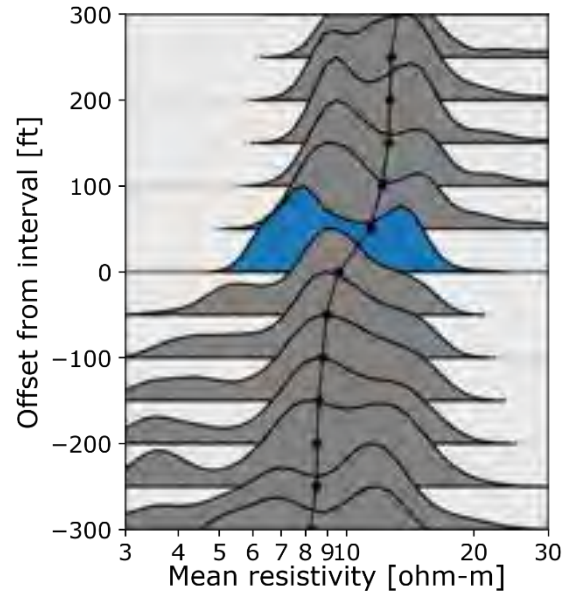


**Figure 5-11 Distribution of AEM resistivity values within 300 m of boreholes with interpretations of the 400-FDA. Each panel contains a set of smoothed histograms displaying the distribution of resistivity values over a 50-foot sliding elevation interval. The black line indicates the mean value for each distribution. Positive and negative y-values, respectively, indicate the number of feet the sliding window is offset above and below the interval interpreted as “aquitard” in the Deep Aquifers Study Phase 1 Borehole Dataset. An offset of zero corresponds to the data within the interval interpreted as “aquitard”, and the corresponding histogram is colored blue. The data are shown for A) the 180/400 Foot Aquifer Subbasin, B) the East Side Aquifer Subbasin, C) the Forebay Aquifer Subbasin, and D) all data. \*The size of the sliding window was increased to 100 feet to increase the amount of data.**

### 5.3 Delineation of Continuous Conductor

The goal of the Deep Aquifers AEM survey is to better understand the Deep Aquifers and the overlying 400-FDA using the resistivity values from AEM data. While the AEM data cannot directly confirm the presence of the 400-FDA, they can be used to identify continuous resistors and conductors in the survey area, which in turn, can be compared to auxiliary information to make a more informed interpretation of the 400-FDA. This section describes the interpretation of a continuous conductor that generally corresponds to the expected depth and location of the 400-FDA (referred to as the “continuous conductor”), as identified from the AEM resistivity values, in concert with borehole lithology data, borehole resistivity logs, and lithology interpretations from the Deep Aquifers Study Phase 1 Borehole Dataset. As discussed in Section 5.2.3, any continuous conductor identified from AEM data was not expected to correlate perfectly with existing interpretations of the 400-FDA; however, these interpretations offer a separate dataset to help guide the interpretations of AEM-derived resistivity cross-sections.

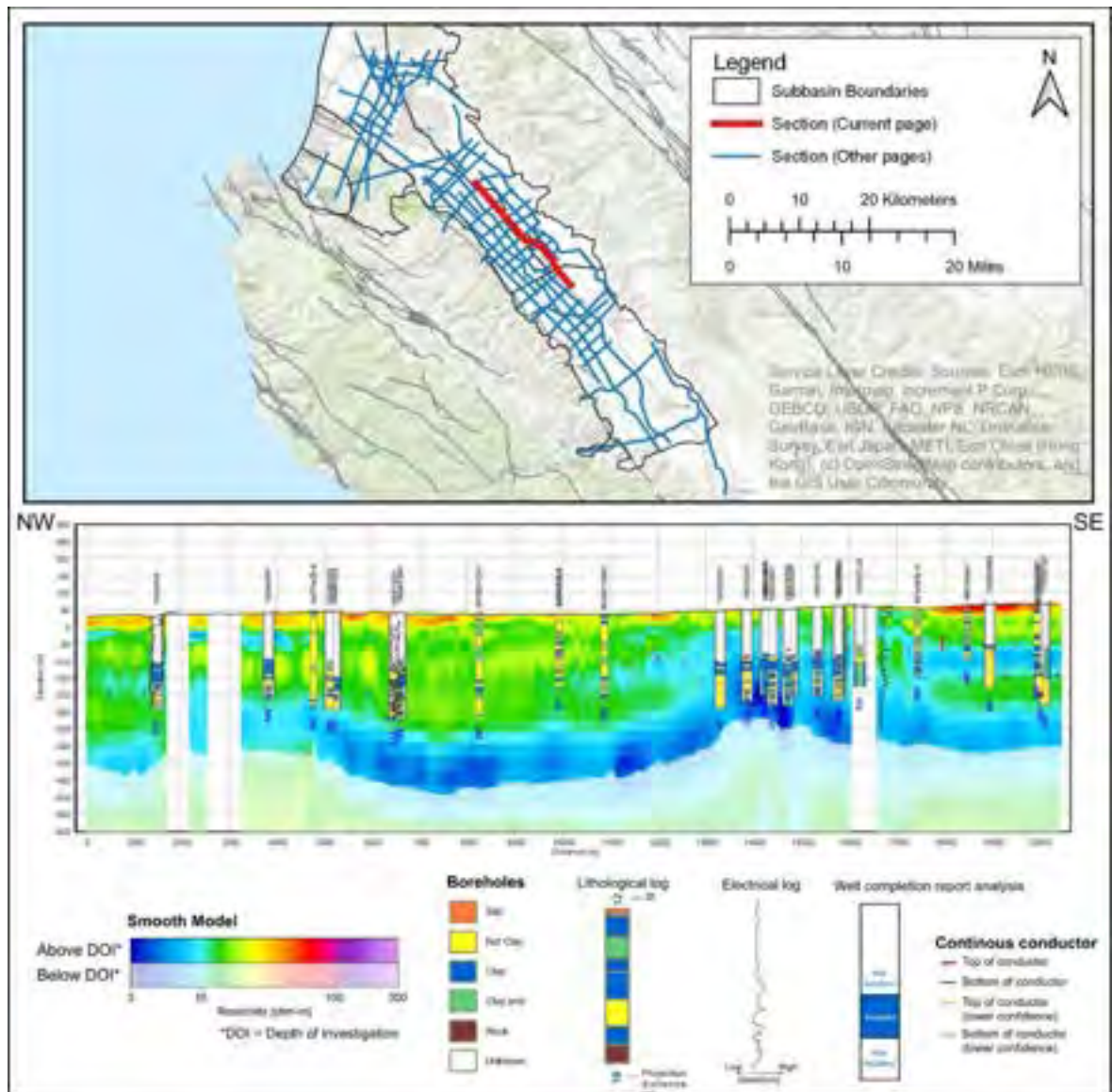
Points of interpretation were added to resistivity cross-sections from the AEM datasets considered for analysis (2019 coastal AEM dataset, DWR Survey Areas 1 and 8, Deep Aquifers AEM Survey) where the top or bottom of the continuous conductor was identified. In cases where the top or bottom of the continuous conductor was identified with lower confidence, the interpretive point was flagged as a lower confidence interpretation.

In this section, three cross-sections (Figure 5-12 through Figure 5-14) across the survey area are discussed. The entire set of annotated cross-sections are presented in Appendix 3. Each cross-section displays the following data:

- the resistivity data resulting from the inversion of AEM data (colored according to Figure 3-4);
- nearby lithology data, colored by lithology descriptor;
- nearby borehole resistivity data, displayed as a curve with depth;
- nearby interpreted intervals of the 400-FDA (shown in blue behind the lithology data) from the Deep Aquifers Study Phase 1 Borehole Dataset;
- points indicating the interpreted depth of the top and bottom (red and blue, respectively) of the continuous conductor corresponding to the depth of the 400-FDA.

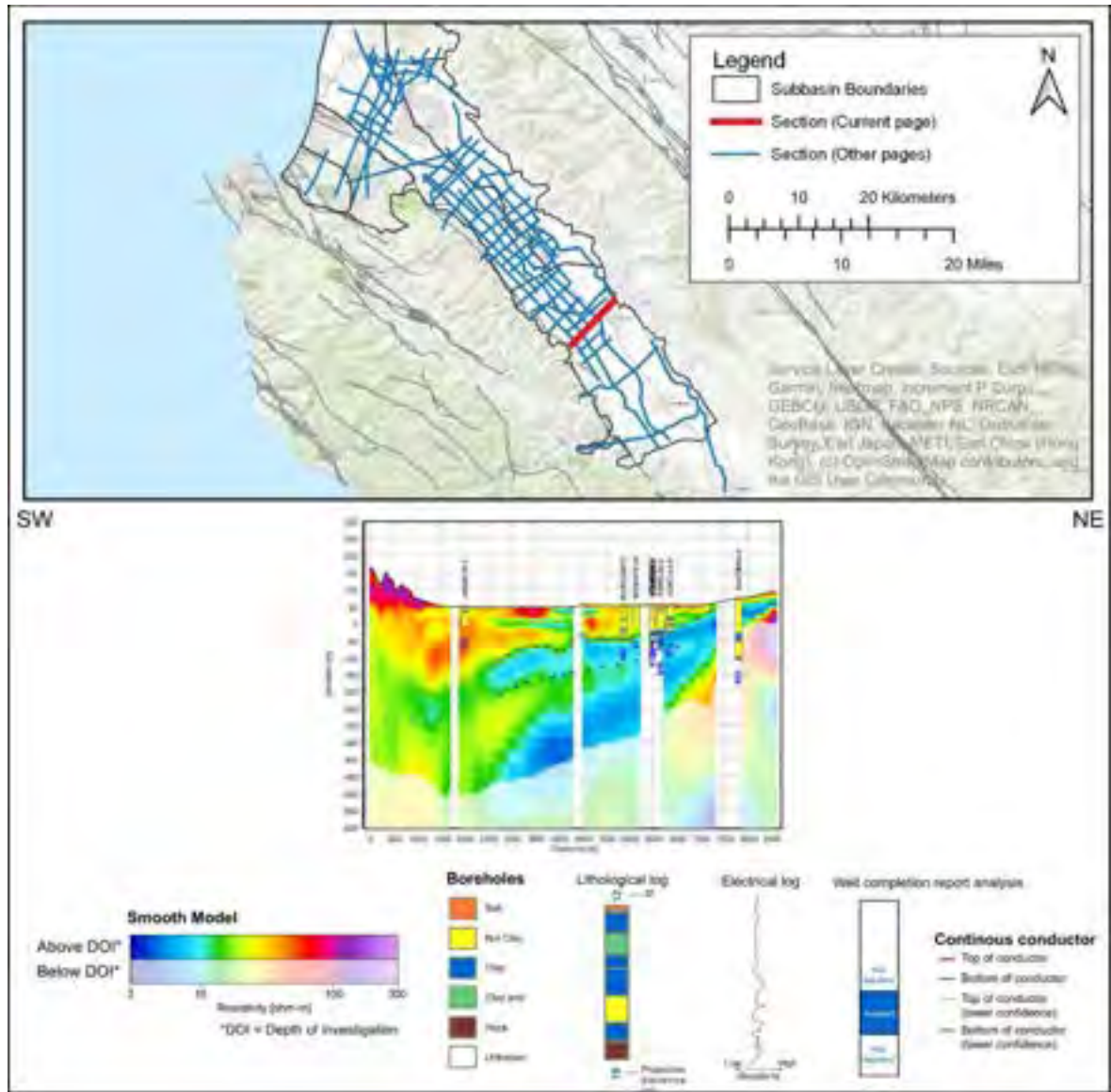
Figure 5-12 shows a section spanning 20.5 km (13.7 mi) in the central part of the area. On the right side of the cross-section (southeast), the continuous conductor (blue color) can be seen from around -50 to -150 m (-160 to -490 ft) amsl, dipping slowly toward the left (northwest). Moving toward the left side of the cross-section, the conductor becomes more muted in resistivity contrast (1.5-10 km) but becomes slightly more prominent on the left side of the cross-section.

On the left and right sides of the cross-section (0-1.5 km and 13-20 km distance), the continuous conductor identified with high confidence (red and dark blue dots) agrees with most of the interpretations of the 400-FDA, except for the borehole at 19 km along the cross-section, which identifies the entire continuous conductor as "not clay". In the middle of the section, the continuous conductor is identified with lower confidence (yellow and light blue dots).



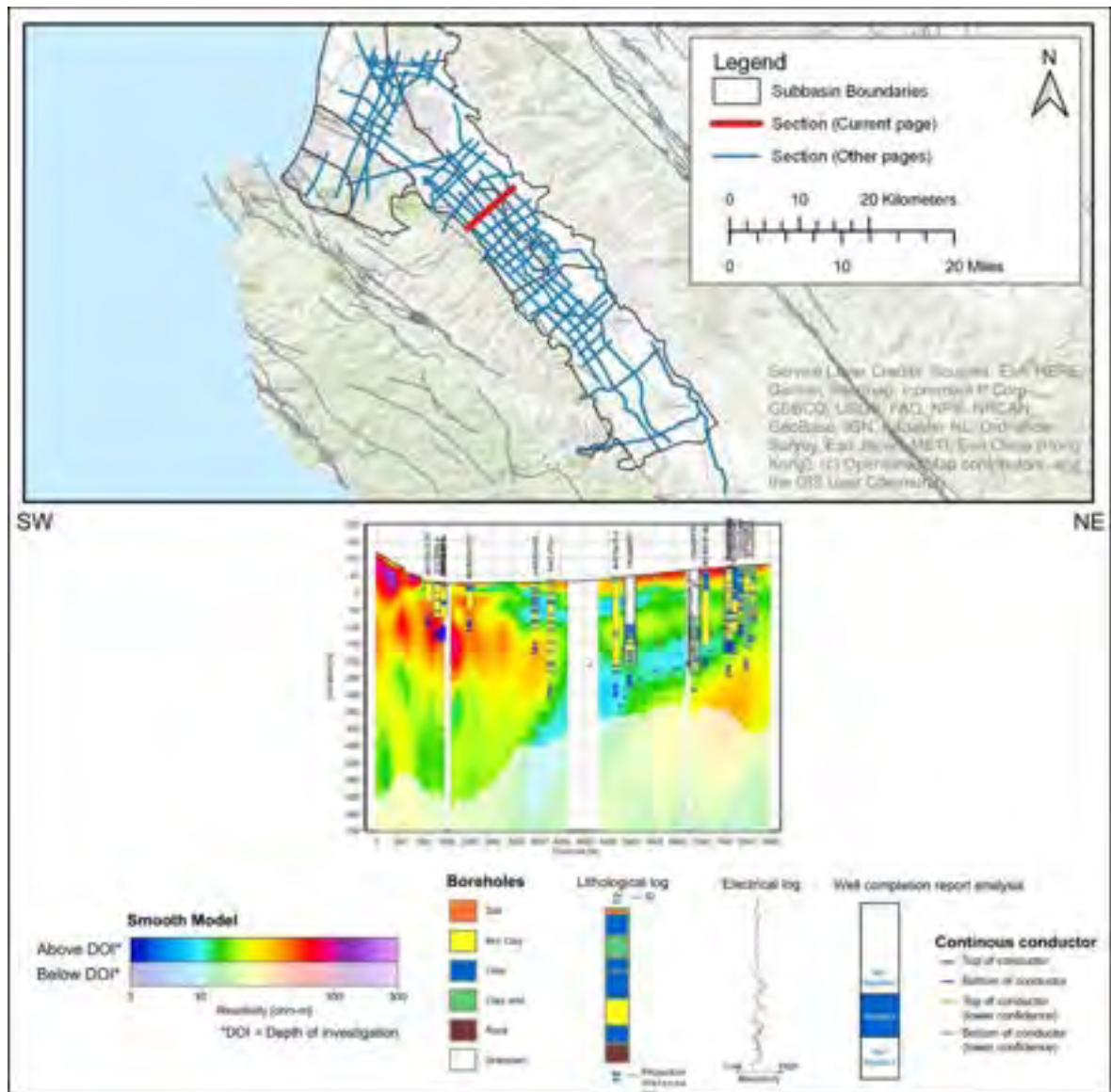
**Figure 5-12 Annotated resistivity along Section 200400.** The section location is shown as the red line in the top panel, while the vertical resistivity section from northwest to southeast is provided in the bottom panel. Faded colors near the bottom of the cross-section represent resistivity values below the DOI. Borehole lithology data (colored columns) are projected onto the section. Borehole intervals interpreted as the 400-FDA are shown behind the lithology data in blue. The top and bottom of the continuous conductor are shown as red and blue points, respectively.

Figure 5-13 shows a section spanning 8.5 km (5.3 mi) in the southern part of the area. A very distinct, continuous conductor can be seen overlying a region of high resistivity (likely bedrock) on the right side of the section and dipping toward the center of the basin. Left of 5.5 km along the cross-section, a deeper conductor appears to split off from the continuous conductor.



**Figure 5-13 Annotated resistivity along Section 101600. The section location is shown as the red line in the top panel, while the vertical resistivity section from southwest to northeast is provided in the bottom panel. Faded colors near the bottom of the cross-section represent resistivity values below the DOI. Borehole lithology data (colored columns) are projected onto the section. Borehole intervals interpreted as the 400-FDA are shown behind the lithology data in blue. The top and bottom of the continuous conductor are shown as red and blue points, respectively.**

Figure 5-14 shows a section spanning 8.5 km (5.3 mi) in the central part of the survey area. Here, similar patterns are seen as in Figure 5-13 but with resistivity variations of lower magnitude: the continuous conductor has a higher resistivity than in Figure 5-13. The resistivity structure and values on the left side of the cross-section (180/400 Foot Aquifer Subbasin) are distinctive from those on the right side of the cross-section (East Side Aquifer Subbasin), with resistivity values much higher in the 180/400 Foot Aquifer Subbasin, reflecting the distributions shown in Figure 5-10. The changing nature of the continuous conductor across the survey area underscores the need for closely spaced AEM flightlines (available in this area from the current survey and the DWR Survey Area 1 survey) to track spatially variable patterns with high confidence.



**Figure 5-14 Annotated resistivity along Section 100600.** The section location is shown as the red line in the top panel, while the vertical resistivity section from southwest to northeast is provided in the bottom panel. Faded colors near the bottom of the cross-section represent resistivity values below the DOI. Borehole lithology data (colored columns) are projected onto the section. Borehole intervals interpreted as the 400-FDA are shown behind the lithology data in blue. The top and bottom of the continuous conductor are shown as red and blue points, respectively.

Figure 5-15 through Figure 5-17 provide sequential views of selected resistivity cross-sections across the survey area that help to visualize the overall structure and trends in lithology across the basin. Figure 5-15 presents cross-sections oriented northwest-southeast from the northeast to southwest, while Figure 5-16 and Figure 5-17 display cross-sections oriented southwest-northeast from the northwest to the southeast. Several observations are clear from the sequential sections:

- Coarse-grained deposits tend to dominate the western portion of the basin, while the eastern portion of the basin tends to be finer-grained sediments overall, based on the higher resistivity values in the west (red-orange-yellow colors) as compared to the east (blue-green colors). The reds and purples along the basin boundary typically represent consolidated sediments and bedrock.
- Layering is evident in the resistivity profiles that generally dips downward to the basin center. The resistivity sections illustrating generally dipping alluvial layers and fluvial deposits and coarsening and fining lithology trends help provide more detail for the hydrogeologic conceptual model for the basin.
- The continuous conductor (light to dark blue) layers that may represent the 400-FDA are most obvious and thickest in the eastern part of the basin. These layers appear to coarsen toward the north, evidenced by higher resistivity, and then become finer once again.
- Salinas Lines DWR\_SA1103800\_1, DWR\_SA1103800\_2, and 200400 in the eastern portion of the basin display the deep blue continuous conductor as two distinct layers and join with the lower layer geometry, suggesting compressional folding as is common withing the Coast Ranges. The discontinuous and changing nature of the conductor is especially evident in Salinas Line 200400 starting in the center and moving to the left (north).
- In the northwest portion of the basin, Salinas Lines DWR\_SA1103305\_1, DWR\_SA1103305\_2, 200700, and DWR\_SA1103304 illustrate the extent of the 180-Foot Aquifer, 180-Foot Aquitard, 400-Foot Aquifer, and some areas where the aquifers may be interconnected, and the 180-Foot Aquitard seems to be absent. A low-resistivity region can be seen in the far lefthand side (northwest) of the cross-section, reflecting influence of high-salinity groundwater.
- In the northernmost southwest-northeast cross-sections (Figure 5-17), seawater intrusion is evident where there is a strong conductor (blue) present in the upper half of the cross-section. On the southwest side of the cross-sections, folding and faulting appear to be present, most prominent in Salinas Line 100300.
- In the southernmost southwest-northeast lines, the continuous conductor (blue) appears evident on the west and east sides of the basin.

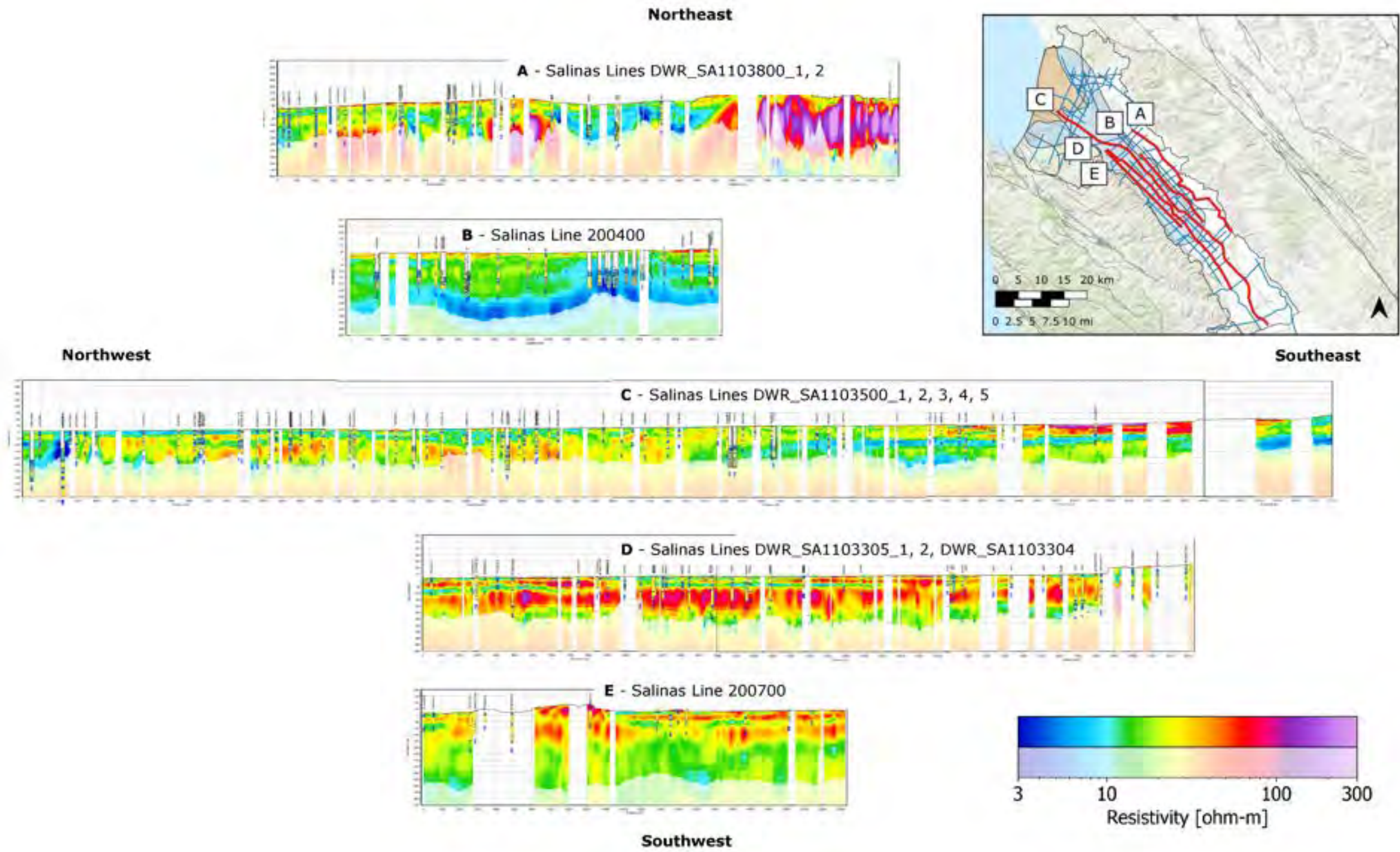


Figure 5-15 Series of cross-sections across the survey area oriented northeast to southwest. Cross-sections A, C, and D come from the DWR Statewide AEM Surveys, while cross-sections B and E come from the current survey. The name of each cross-section refers to the page name in Appendix 3. The dots shown in each cross-section are the interpretations of the top and bottom of the continuous conductor.

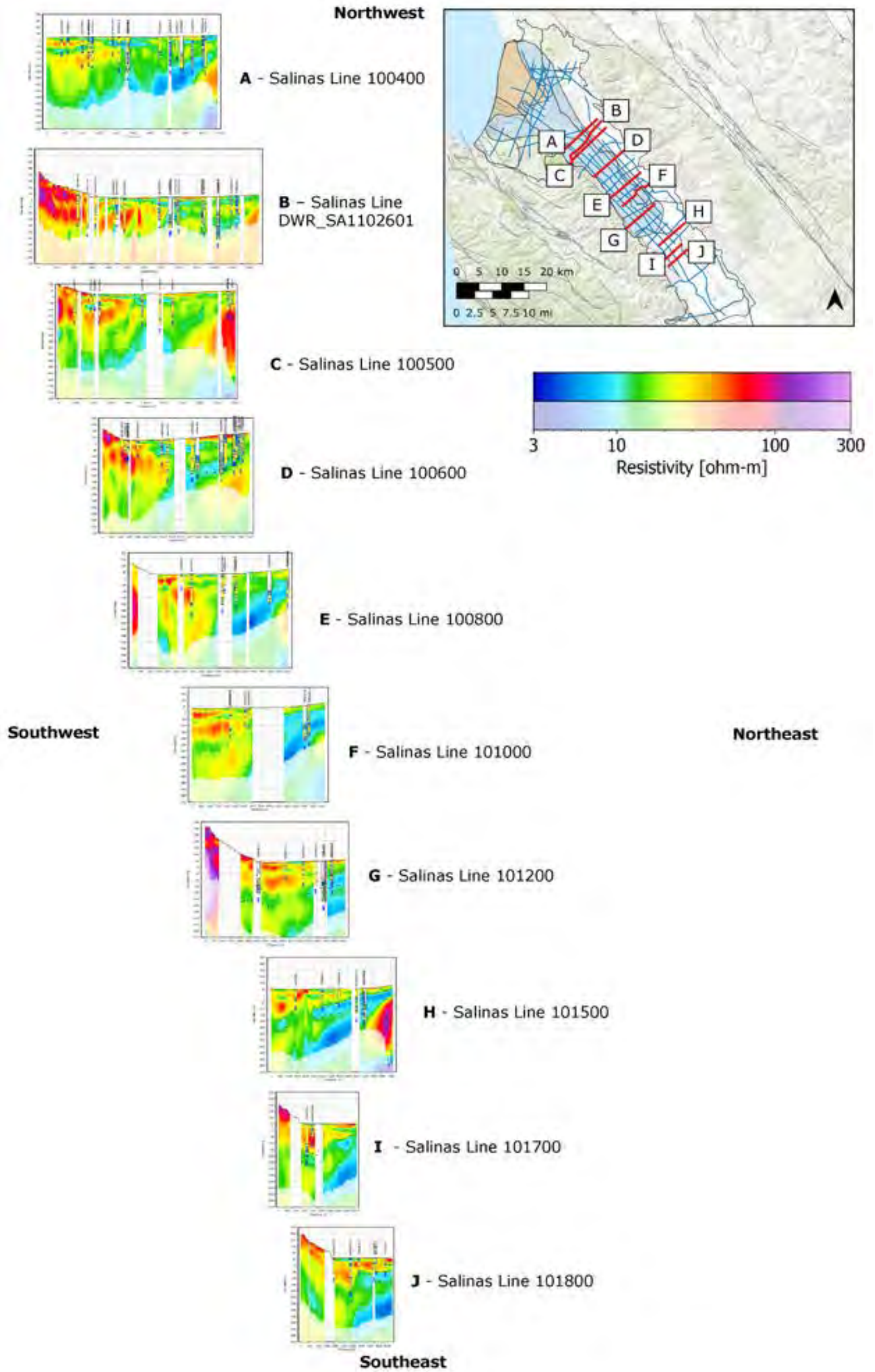


Figure 5-16 Series of cross-sections across the survey area oriented across the basin southwest to northeast. Cross-section B comes from the DWR Statewide AEM Surveys, while all other cross-sections come from the current survey. The name of each cross-section refers to the page name in Appendix 3. The dots shown in each cross-section are the interpretations of the top and bottom of the continuous conductor.

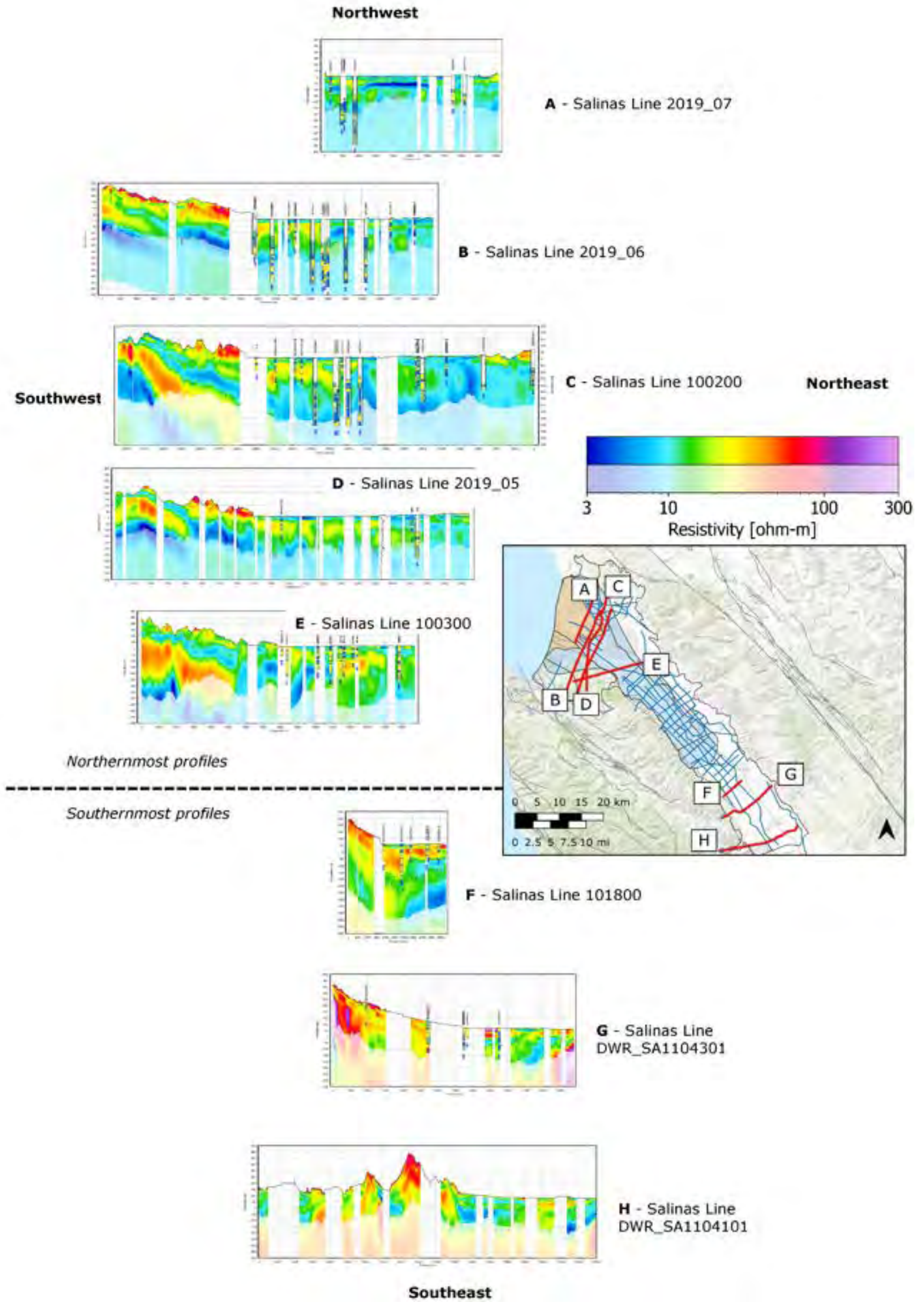


Figure 5-17 Series of cross-sections oriented across the basin southwest to northeast from the northernmost and southernmost parts of the survey area. Cross-sections A, B, and D come from the Coastal Salinas Valley AEM Surveys 2019 dataset, cross-sections G and H come from the DWR Statewide AEM Surveys, while all other cross-sections come from the current survey. The name of each cross-section refers to the page name in Appendix 3.

The interpreted depths of the continuous conductor are summarized as two maps in Figure 5-18. The interpreted depth to the top and bottom of the continuous conductor are shown as circles in Figure 5-18a and Figure 5-18b, respectively. Locations where the interpreted depth had lower confidence, shown as a smaller circle with a grey border, are more abundant for the bottom of the continuous conductor than for the top, largely because the depth of the bottom may be approaching the DOI. As in Figure 5-1, the interpreted depths to the 400-FDA from the Deep Aquifers Study Phase 1 Borehole Dataset are presented as large squares.

The maps in Figure 5-18 offer a wealth of information about the geometry of the continuous conductor, provided by the density and spatial continuity of data points. While borehole data are unevenly distributed across the survey area to identify the 400-FDA (see Figure 5-1), the AEM data could be used across the entire survey area to interpret the depth to the continuous conductor. Notably, the continuous conductor was mapped much farther south into the Salinas Valley than was suggested by the Phase 1 extent of the 400-FDA.

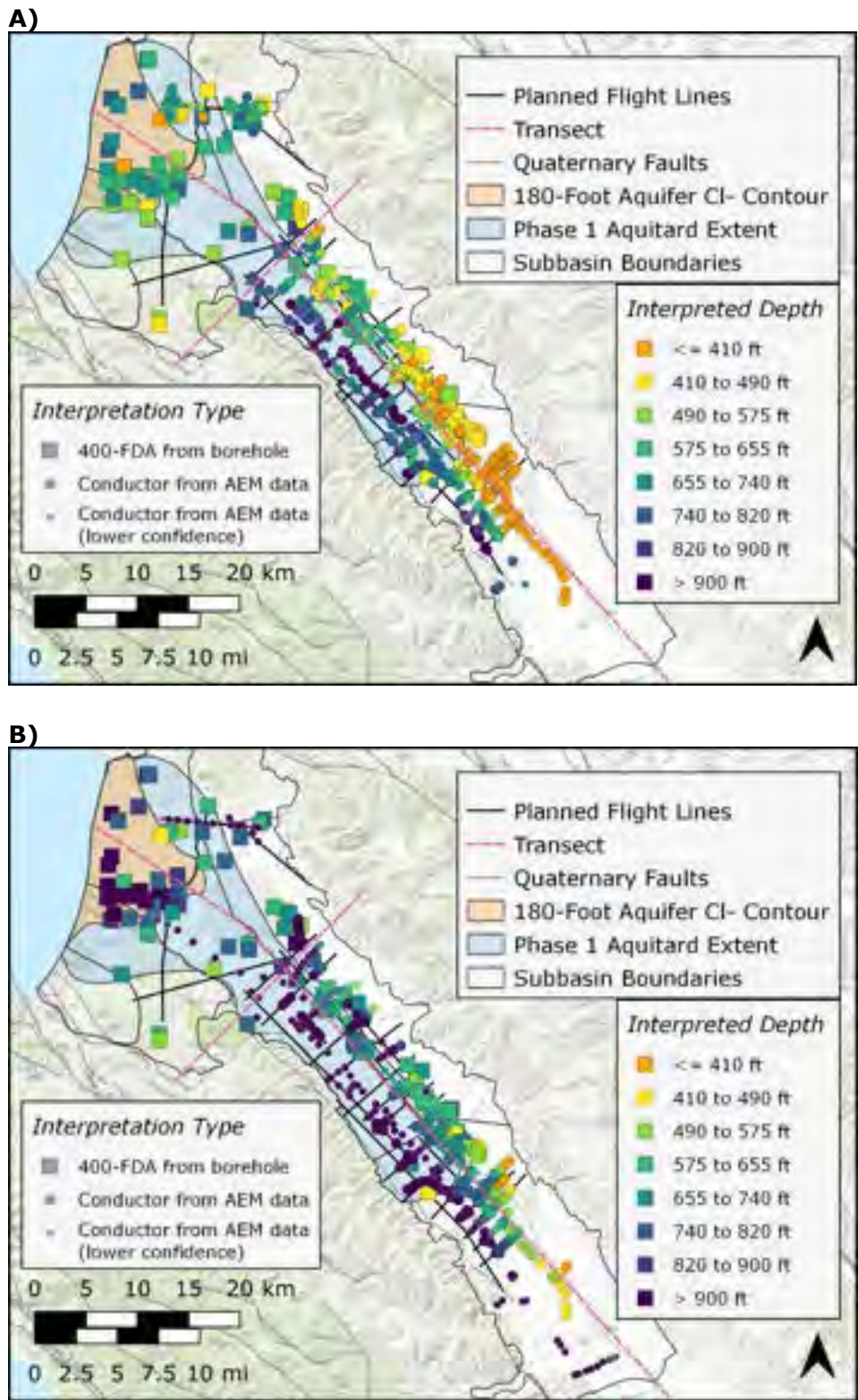
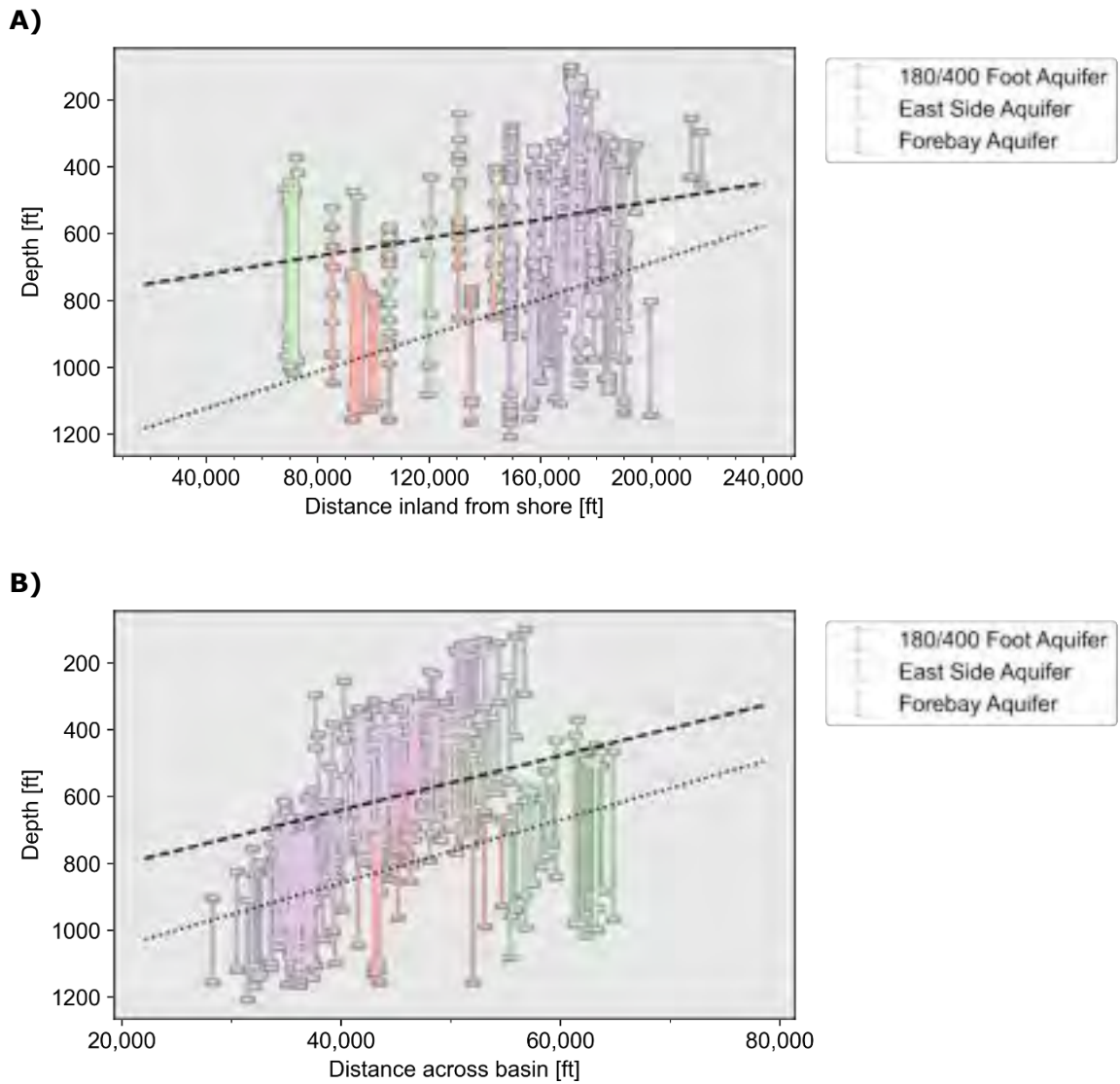


Figure 5-18 Interpreted depth of the top and bottom of the 400-FDA and the continuous conductor. Depth to the 400-FDA was interpreted from borehole data in the Deep Aquifers Study Phase 1 Borehole Dataset, while depth to the continuous conductor is interpreted from AEM data. A) Depth to the top of the 400-FDA and continuous conductor, B) Depth to the bottom of the 400-FDA and continuous conductor. Lower confidence interpretations from AEM data are shown as smaller dots with grey borders.

The interpreted depths of the conductor as a function of distance along the pink transect lines are provided in Figure 5-19. The tops and bottoms of the continuous conductor are shown connected by vertical bars. Although the tops and bottoms of the continuous conductor were interpreted independently, each interpreted top was linked to the closest interpreted bottom, within 500 ft. Depths interpreted with lower confidence are not shown.

As in the analysis of the Deep Aquifers Phase 1 Borehole Dataset (Figure 5-2), the regression line best fitting the depth to the top and bottom of the continuous conductor is shown as a dashed and dotted line, respectively. Figure 5-19a shows that the continuous conductor shallows and thins with distance inland, as shown similarly with the 400-FDA in the analysis of the Deep Aquifers Phase 1 Borehole Dataset, although the average depth of the continuous conductor is greater in Figure 5-19a than the average depth of the 400-FDA shown in Figure 5-2a.

Figure 5-19b shows the continuous conductor dipping toward the southwest. This dip is a strong and consistent trend across each of the subbasins displayed. In the analysis of the Deep Aquifers Phase 1 Borehole Dataset (Figure 5-2b), the depth of the 400-FDA was shown to thicken toward the southwest, and then shallow and thin in the Monterey Subbasin. In the case of Figure 5-19b, however, data come from farther inland, and no data are displayed from the Monterey Subbasin. In contrast, Figure 5-19b adds a wealth of information from the Forebay Aquifer Subbasin, and to a lesser degree the East Side Aquifer Subbasin. Because of the spatial continuity of the AEM data, there are rarely nearby interpretation points that vary significantly; however, because the AEM data extended much farther to the southwest side of the basin as well as higher into the foothills in the northeast, there is a much larger portion of the basin structure represented in the AEM data, leading to higher scatter within both Figure 5-19a and Figure 5-19b.



**Figure 5-19** Depth of the continuous conductor, interpreted from AEM data, shown as a function of distance.

**A)** Distance inland from shore, **B)** distance across the Salinas Valley from SW to NE, as shown by the pink transect lines in Figure 5-18 where circles and squares indicate the depth to the top and bottom of the continuous conductor, respectively. Each point is colored by the Subbasin corresponding to the measurement location. The black dashed and dotted line, respectively, show the least squares regression line fit to the interpreted top and bottom of the continuous conductor. Only points with high confidence are shown.

#### **5.4 Deep Conductor**

Presence of a deep, continuous conductor was noted in the AEM data at multiple locations, below the continuous conductor outlined in Section 5.3. Within the groundwater basin, this deeper conductor appears 100 m below the bottom of the continuous conductor delineated above. While not the focus of this project, this deep conductor is a regionally consistent and potentially geologically relevant feature that can be seen in many cross-sections.

The trend of the deep conductor in the direction of the Salinas Valley can be seen in Figure 5-12, where the deep conductor appears to dip regionally toward the coast with significant undulation along the cross-section distance.

Cross-sections E through J in Figure 5-16 show the regional change in this deep conductor moving from the north to the south of the survey area. Farther north (E), the continuous conductor is indistinguishable from a deeper conductor on the right side (northeast) of the cross-section. Moving south (G), there are two visibly separate conductors, which both appear to dip toward the basin center, although the deep conductor has a larger dip than the continuous conductor.

## 6. Summary and Conclusions

The Salinas Valley has been the location of multiple AEM surveys, with the current survey conducted with the goal of better understanding the Deep Aquifers, the top of which is defined by the presence of the 400-FDA. The SkyTEM 312HPM time-domain electromagnetic system was used for this survey and provided the ability for deeper penetration into the subsurface than did previous AEM surveys, offering information from the ground surface to a depth of between 1,000 and 2,000 ft (300 and 600 m). As a result, the AEM data could be used to successfully locate the top—and in many cases the bottom—of a continuous conductor at depth intervals corresponding to the current understanding of the 400-FDA. While some differences exist when comparing the continuous conductor as interpreted from AEM resistivity values, to the depth interval of the 400-FDA as interpreted from the Deep Aquifers Phase 1 Borehole Dataset, regional trends show a close correlation.

The results of the geophysical surveys in general confirm the working hydrogeologic conceptual model of finer grained alluvial plain deposits filling the eastern portion of the survey area of the Salinas Valley, and generally coarser grained fluvial and alluvial deposits in the western portion. Several southwest-northeast resistivity cross-sections across the survey area demonstrate this with the coarser deposits designated by red, orange, and yellow colors, and the finer grained green to blue with the blue generally indicative of clay aquitards, although increased salinity near the coast can lower the resistivity as well. Northwest-southeast resistivity cross-sections also demonstrate this trend in lithology. The newly acquired AEM data, in concert with existing data, show a consistent indication of faulting along the Reliz Fault, accompanying possible folding and warping of adjacent and underlying sediments.

The results in this report suggest a conductor across much of the study area corresponding to the depth at which the 400-FDA is expected. However, the interpreted conductor does not necessarily reflect variation in sediment provenance, which may have implications for the definition of the 400-FDA: resistivity values from AEM data can only distinguish between sediments insofar as a resistivity contrast is present. Additional data should be analyzed in combination with the AEM data to understand the relationship of the continuous conductor to the 400-FDA.

### 6.1 Recommended Future Work

The work completed in this project provides a strong foundation for integrating AEM and existing borehole data into a unified interpretation of the Deep Aquifers. To continue building on this work, we foremost recommend integrating AEM resistivity and supporting data into a three-dimensional geologic modeling and visualization platform. Because the analysis completed in this project relied on two-dimensional maps and cross-sections, additional cross checks and interpretation for regional and localized geologic trends and structure mapping can be achieved through three-dimensional analysis.

Furthermore, addressing the following data gaps would add additional clarity to the AEM data results:

- Mineralogy data could be helpful in further understanding the source and differentiating provenance of the 400-FDA
- Geophysical logging of cased holes could help reduce uncertainties and help quantify aquifer properties
- Identification and prioritization of key areas for an additional data collection next step based on combined geophysics and log data

## 7. Deliverables

The project deliverables consist of the following files:

1. **Raw AEM Data.** Raw data as extracted from the instrument, including:
  1. “.xyz” files – ASCII files with information about the geographical coordinates, transmitted current and many other supporting data.
  2. “.gex” and “.sr2” files – ASCII files containing the system description (geometry, waveform, filters etc.).
  3. “.alc” files – ASCII files describing the mapping from the “.xyz” file to the datatype used in the Aarhus Workbench software.
2. **AEM Database.** A Firebird database containing all raw data, processed data, and inversion results. The database is structured according to the Danish Geologic Survey “GERDA” format (<https://eng.geus.dk/products-services-facilities/data-and-maps/national-geophysical-database-gerda/>). The database can be opened with the Aarhus Workbench Viewer software package (<https://www.aarhusgeosoftware.dk/workbench-viewer>).
3. **Geospatial data (shapefile, grid, GeoTIFF).** ArcGIS shapefiles, grid files and/or geo-referenced TIF files including:
  1. Layout: Shapefiles (“.shp”) containing geographical information about the surveyed area, surveyed flight lines, retained flight lines after data processing, etc.
  2. Boreholes: Shapefile containing locations of the boreholes used in the project.
  3. Mean Resistivity Maps: Geo-referenced TIF files (“.tif”) illustrating plan-view maps of average resistivities within different elevation intervals that are presented in this report. Each file name includes information about the top and bottom of the interval.
  4. Resistivity Cross-Sections: Shapefiles (“.shp”) containing geographical information for the vertical sections presented in this report.
  5. 3D Resistivity Cross-Sections: Google Earth KMZ (“.kmz”) containing a 3D gridded representation of the AEM resistivity results.
  6. Interpretations: Shapefiles containing locations of interpretations of the top and bottom of the continuous conductor in the survey area.
4. **CSV Results.** Text files containing 3D results. Included files are the direct export from the Aarhus Workbench software (extension of “.xyz”) and set of files formatted for import into Leapfrog software (<https://www.seequent.com/products-solutions/leapfrog-geo/>, “.csv” extension).
  1. AEM: Resistivity values resulting from inversion.
  2. Interpretations: Locations of interpretations of the top and bottom of the continuous conductor in the survey area.
5. **Project Report.** The project report is delivered as a PDF document.
6. **Borehole Database.** Files containing the borehole data compiled for this project.
  1. Collar: CSV (“.csv”) containing high-level information for each borehole
  2. Interval: CSV (“.csv”) containing the depth interval information on lithology, screen intervals, and interpreted depths of the 400-FDA.
  3. LAS: Log-ASCII Standard (LAS) files containing borehole geophysical data.

The file structure of the deliverables is shown in Table 7-1. In each folder, a text file named “Readme.txt” describes detailed information of the files within the folder.

**Table 7-1 Structure of the project digital delivery folder.**

Parent Folder	Subfolder	Subfolder	Extension	Content
01_Raw_SkyTEM_Data	01_XYZ		.xyz	Raw data file
	02_GEX		.gex .sr2	System description
	03_ALC		.alc	Column mapping from xyz file
02_AEM_Database			.gdb	Firebird Database
03_GIS_Grid_GeoTIFF	01_Layout	01_Flightlines	.shp	General survey information
		02_Magnetics	.tif	Magnetics information
		03_Distance_Lines	.shp	Distance along and across basin
		04_DEM	.grd .tif	Elevation model
	02_Boreholes		.shp	Borehole locations
	03_Mean_Resistivity_Maps		.tif	Mean resistivity plan view maps
	04_CrossSections		.shp	Locations of the cross-sections
	05_CrossSections_3D		.kmz	3D representation of cross-sections
	06_Interpretations		.shp	Locations of interpretation points

**Table 7-1 Structure of the project digital delivery folder.**

Parent Folder	Subfolder	Subfolder	Extension	Content
04_CSV	01_AEM	Dataset	.xyz .csv	AEM resistivity values
	02_Interpretations		.xyz .csv	Interpretation locations
05_Report			.pdf	Project report
06_Borehole_Database	01_Collar		.xlsx	Borehole point information
	02_Interval		.xlsx	Lithology, interpreted aquitard, screen intervals
	02_LAS	Dataset	.las	Borehole geophysical data

## 8. References

Auken, E., A.V. Christiansen, C. Kirkegaard, G. Fiandaca, C. Schamper, A.A. Behroozmand, et al. 2015. An overview of a highly versatile forward and stable inverse algorithm for airborne, ground-based and borehole electromagnetic and electric data. *Explor. Geophys.* 46:223–235. doi: 10.1071/EG13097

Christiansen, A. V., and Auken, E., 2012, A global measure for depth of investigation: *Geophysics*, 77, WB171–WB177.

Gottschalk, I., Knight, R., Asch, T., Abraham, J. and Cannia, J., 2020. Using an airborne electromagnetic method to map saltwater intrusion in the northern Salinas Valley, California. *Geophysics*, 85(4), pp.B119-B131.

Palacky, G.J., 1987, Resistivity characteristics of geologic targets, in Nabighian, M.N., ed., *Electromagnetic methods in applied geophysics: Volume 1, theory*: Tulsa, Society of Exploration Geophysicists

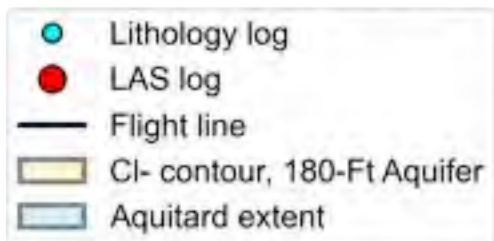
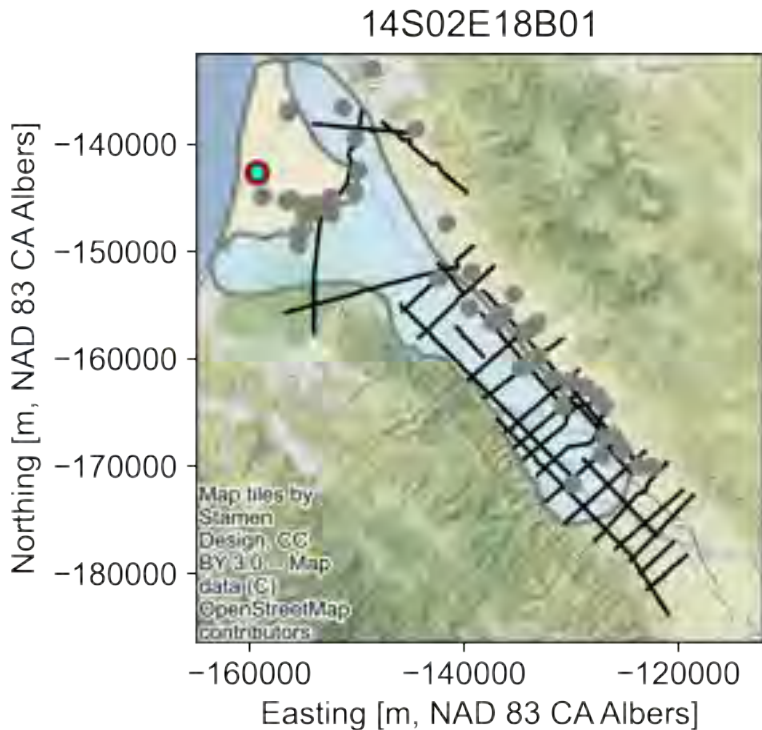
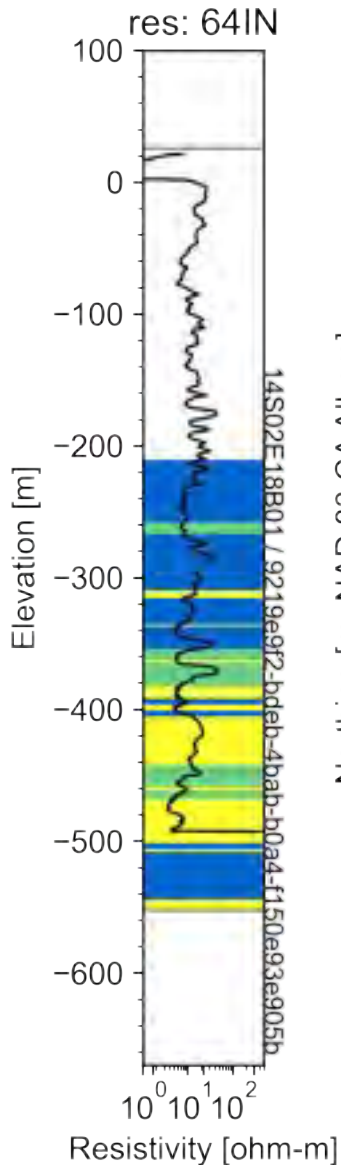
Schamper C., Pedersen, J., Auken, E., Christiansen, A., Vittecoq, B., Deparis, J., Jaouen, T., Lacquement, F., Nehlig, P., Perrin, J. and Reninger, P. (2013). Airborne Transient EM Methods and Their Applications for Coastal Groundwater Investigations. In: Wetzelhuetter C. (eds) *Groundwater in the Coastal Zones of Asia-Pacific*. Coastal Research Library, vol 7. Springer, Dordrecht.

Viezzoli, A., Christiansen, A. V., Auken, E., and Sørensen, K. I., 2008, Quasi-3D modeling of airborne TEM data by spatially constrained inversion: *Geophysics*, 73, F105–F113. doi:10.1190/1.2895521

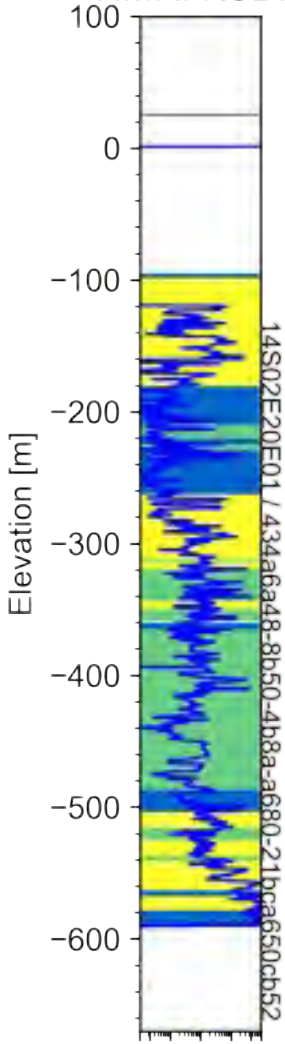
Ward SH, Hohmann GW (1988) *Electromagnetic theory for geophysical applications*. *Electromagnetic Methods in Applied Geophysics*, vol. 1, (ed MN Nabighian), pp 131–311, SEG publication.

# Appendices

## Appendix 1 Borehole Geophysical Data

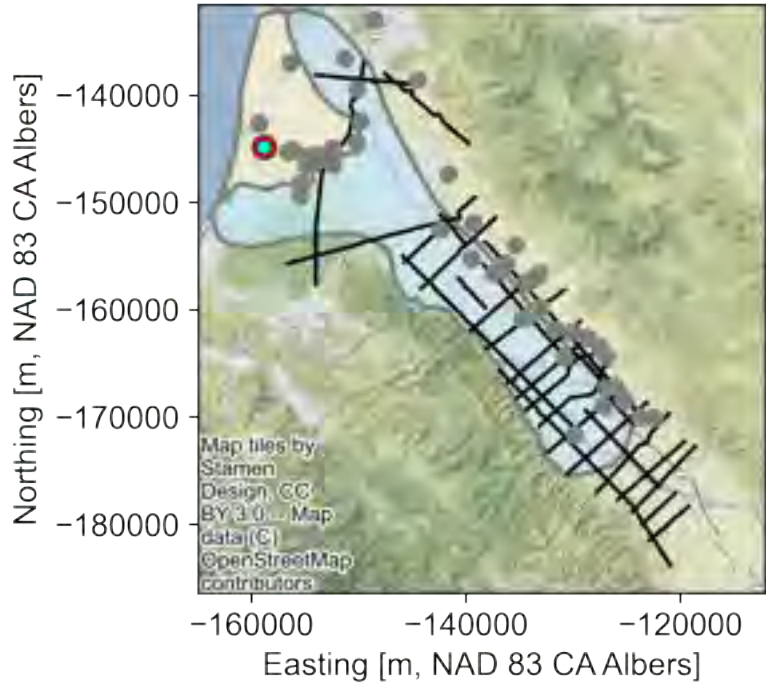


NMR: KSDR

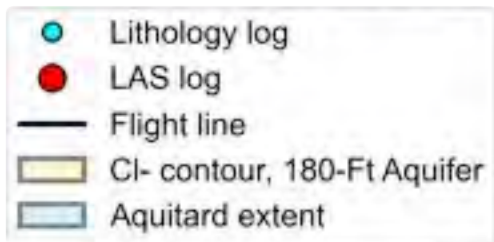
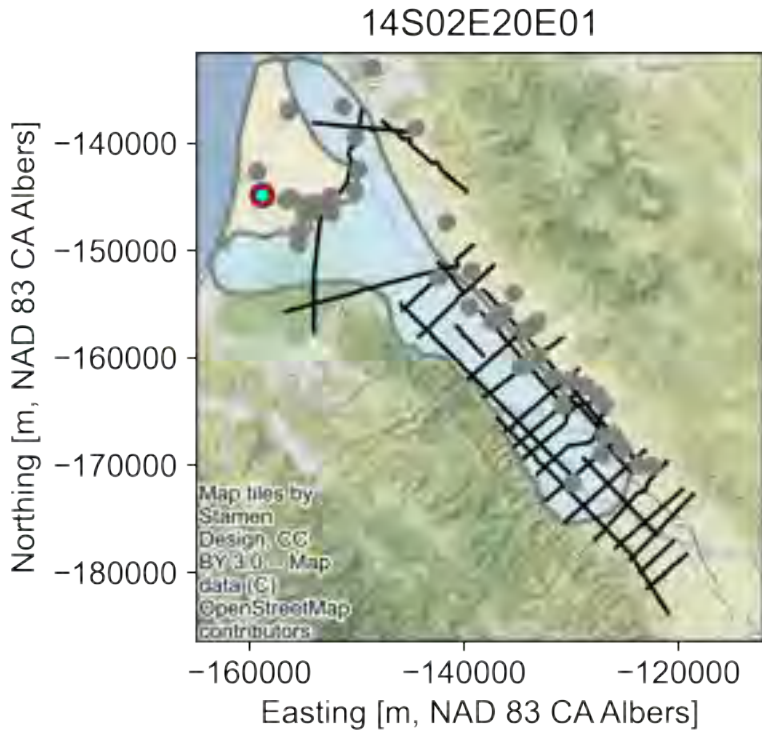
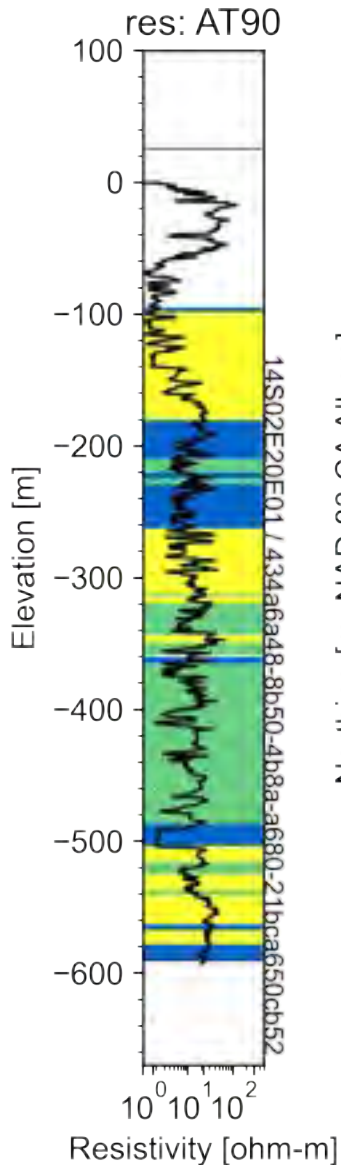


10<sup>-1</sup> 10<sup>0</sup> 10<sup>1</sup> 10<sup>2</sup> 10<sup>3</sup>  
KSDR [mD]

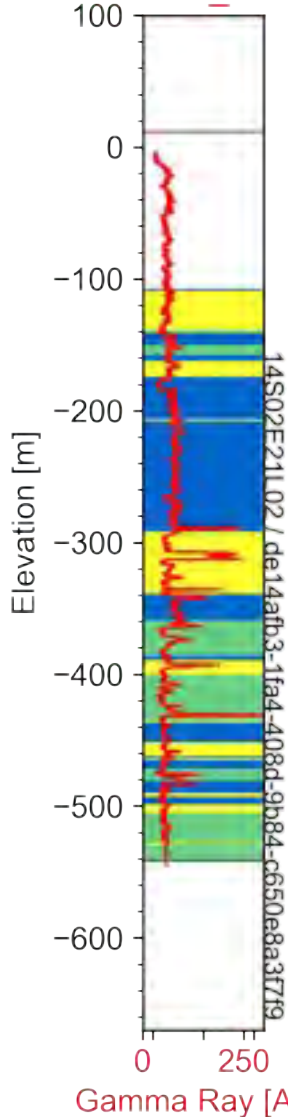
14S02E20E01



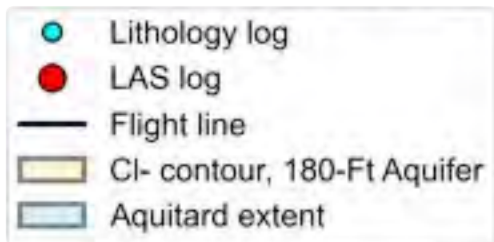
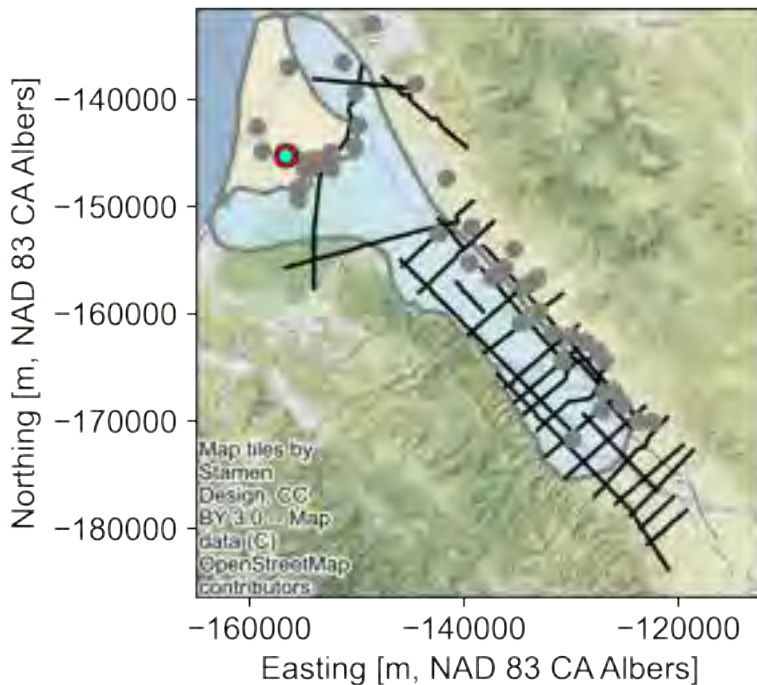
- Lithology log
- LAS log
- Flight line
- CI-contour, 180-Ft Aquifer
- Aquitard extent

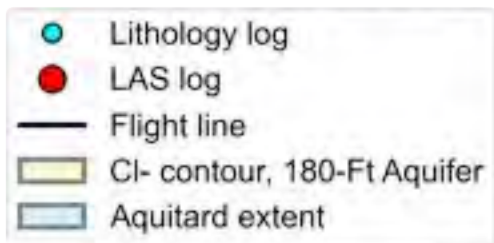
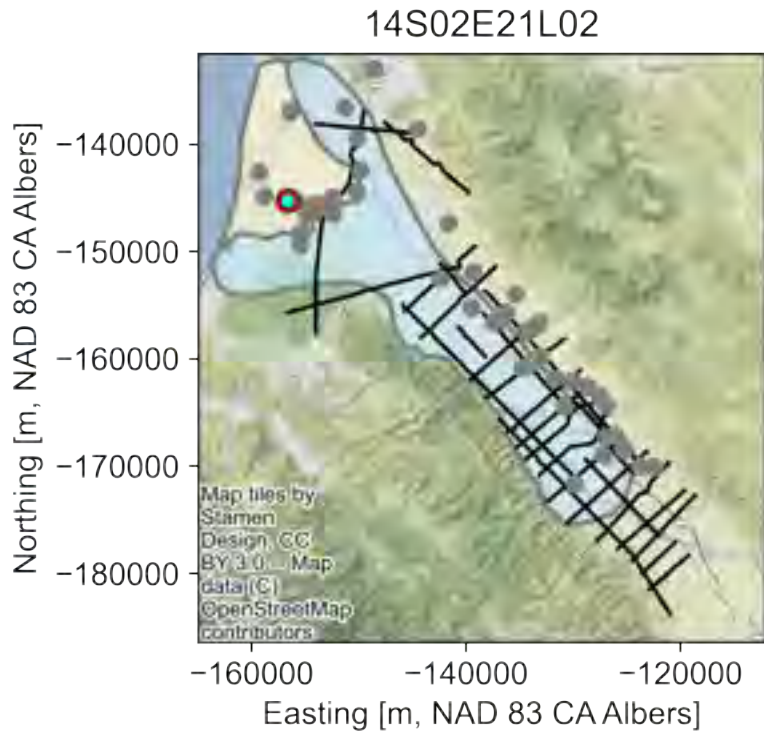
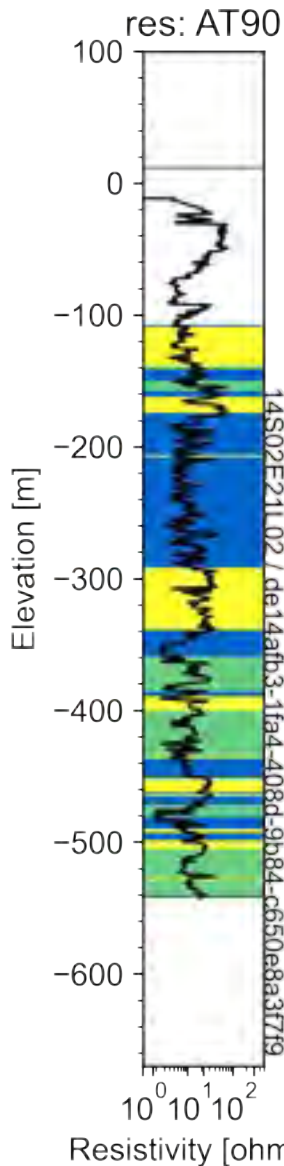


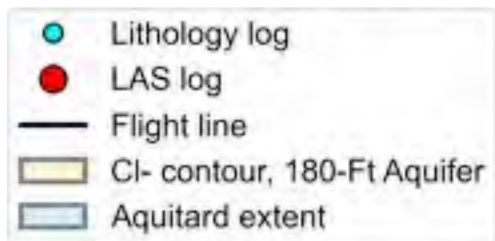
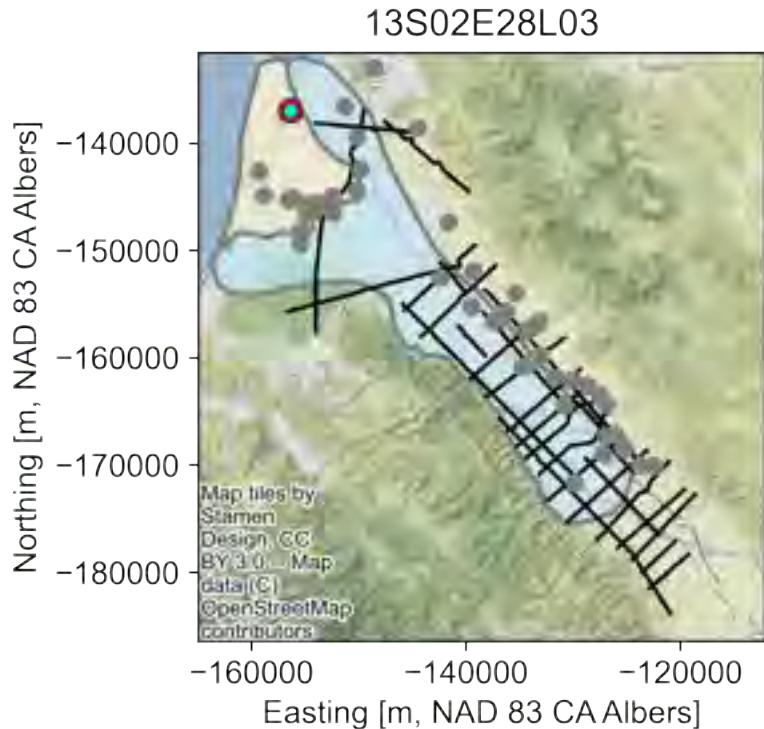
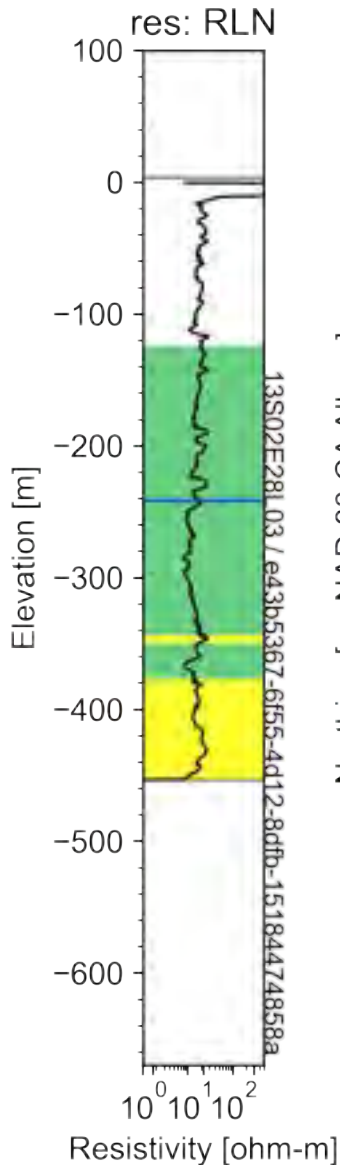
GR: GR\_EDTC



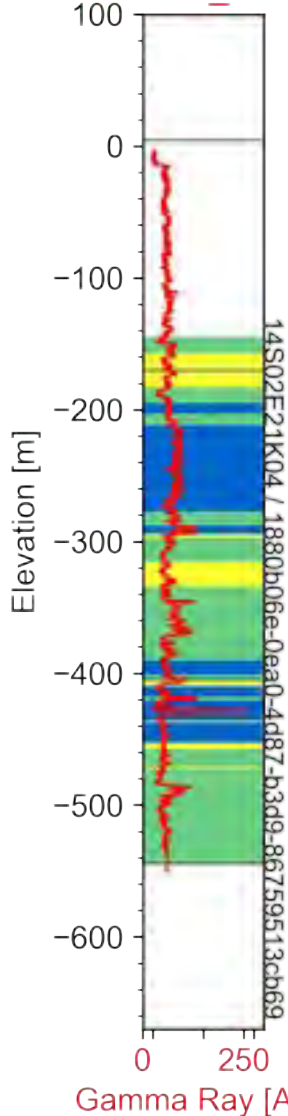
14S02E21L02



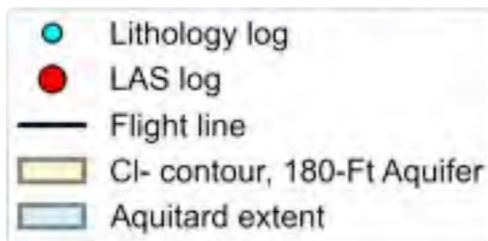
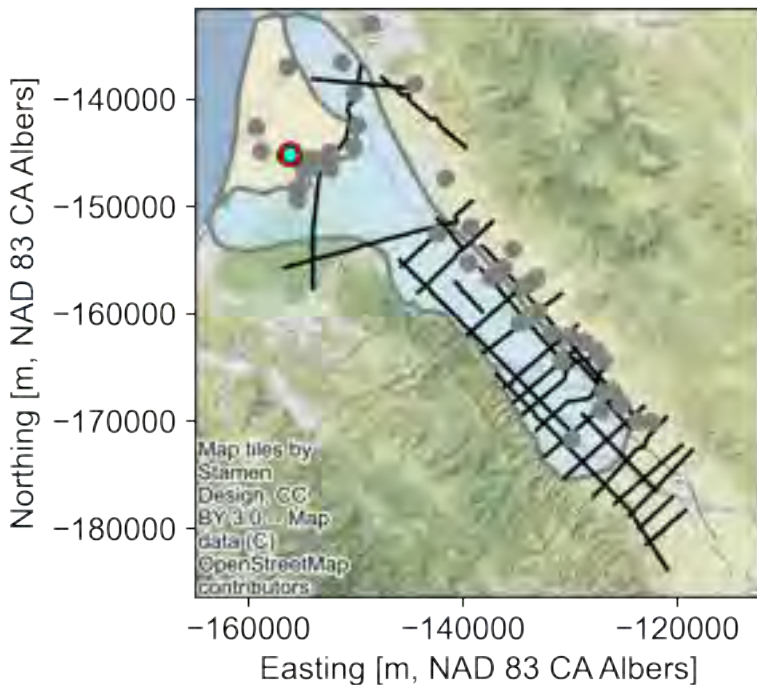




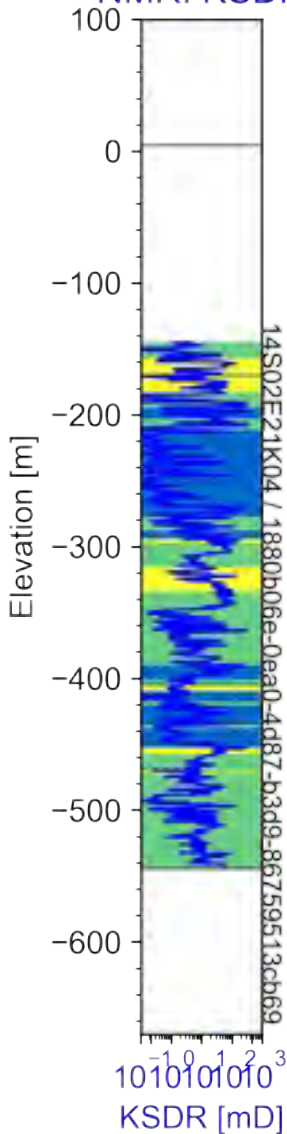
GR: GR\_EDTC



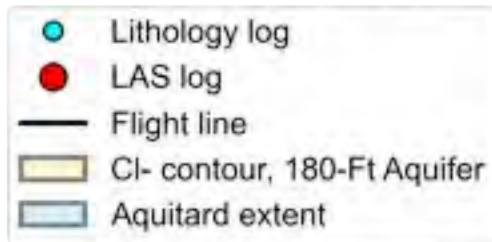
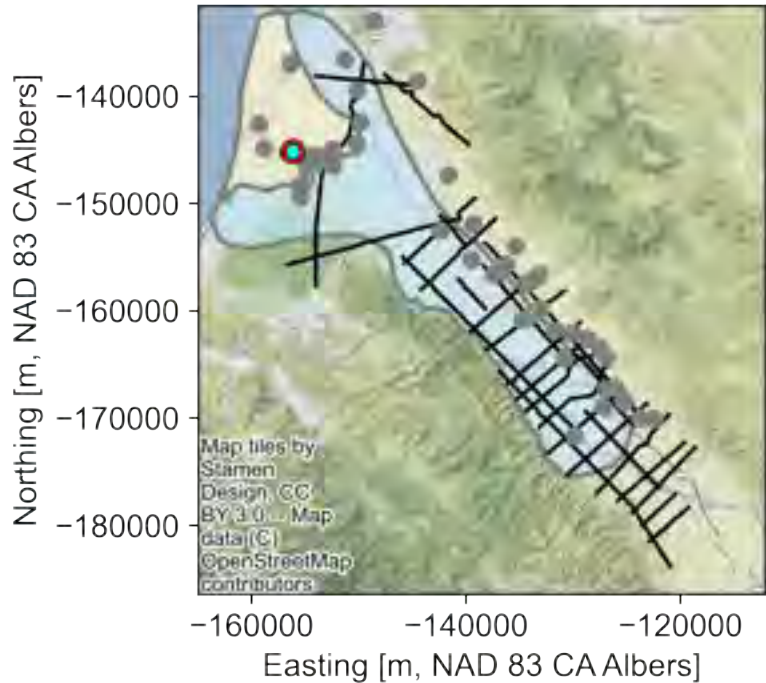
14S02E21K04

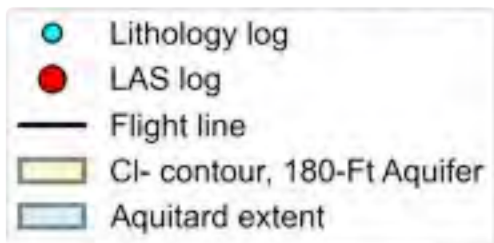
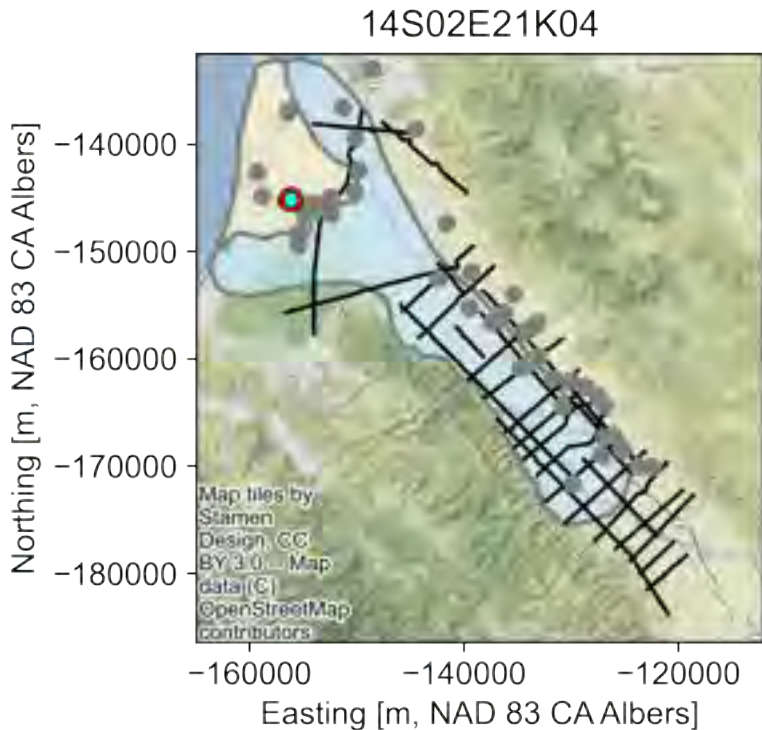
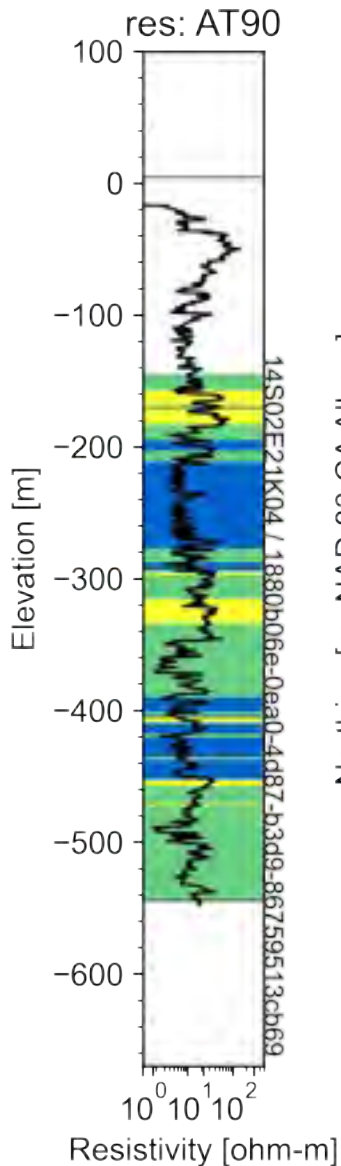


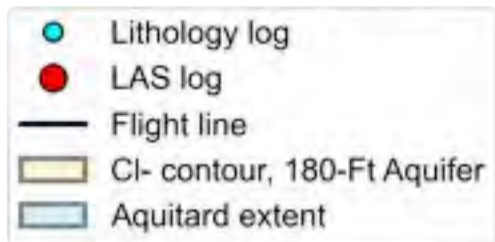
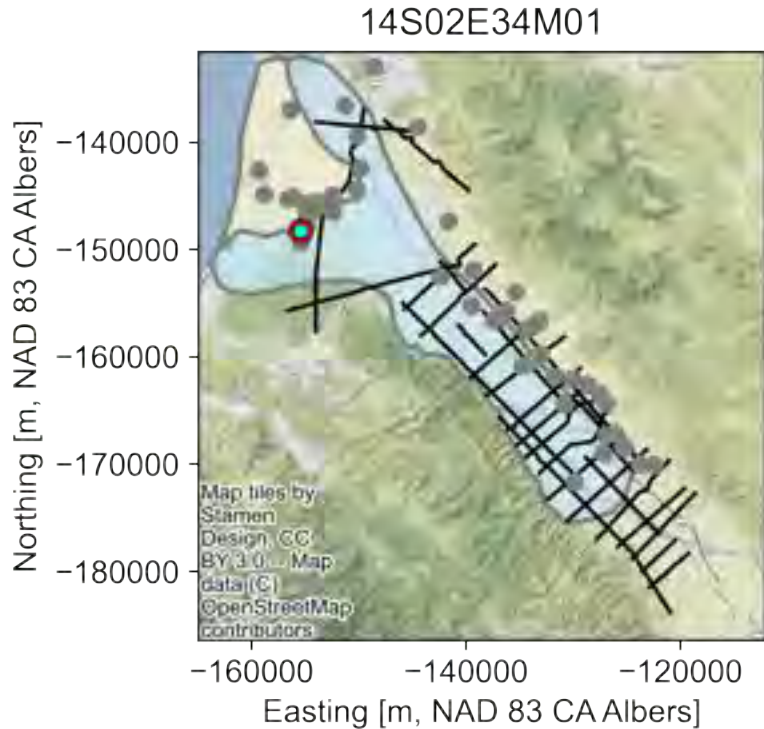
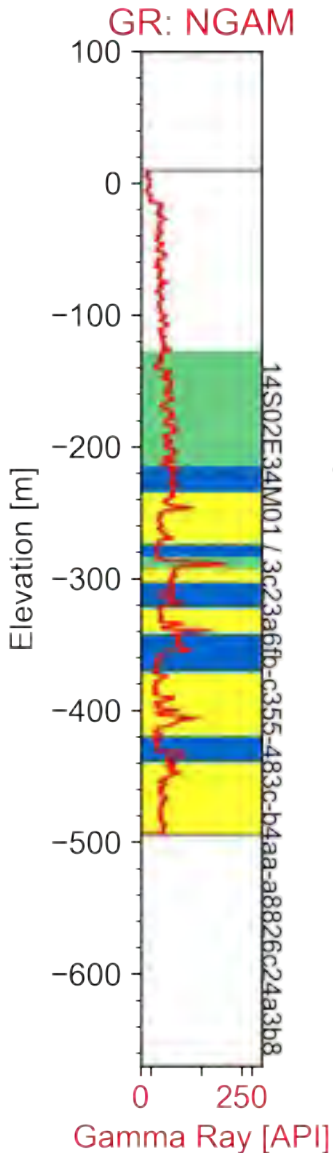
NMR: KSDR

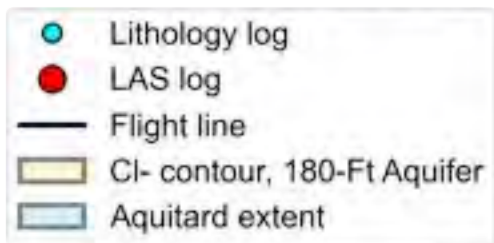
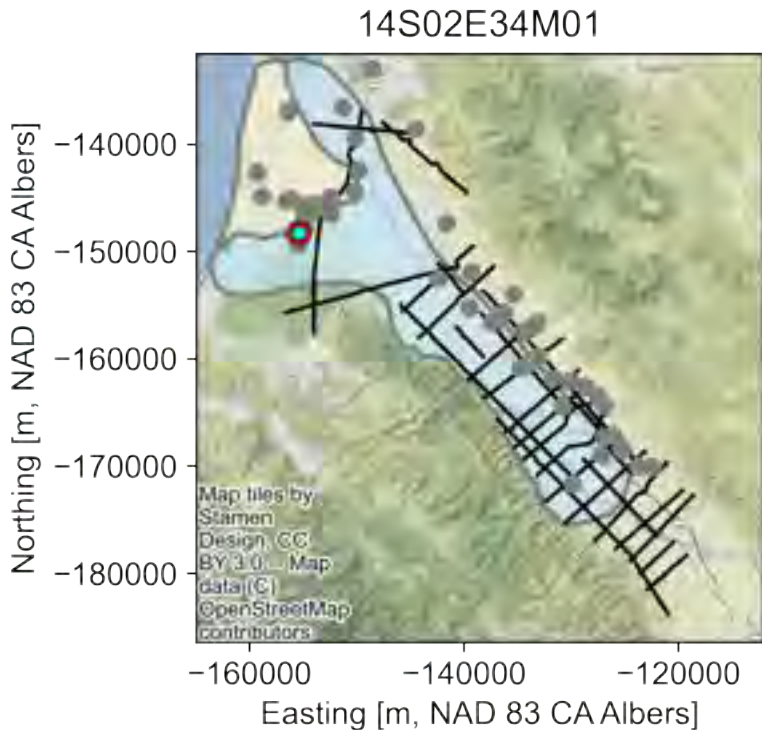
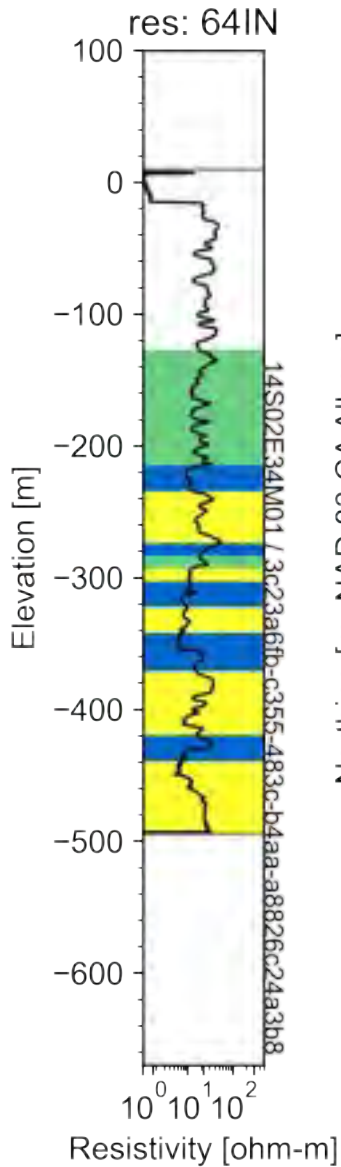


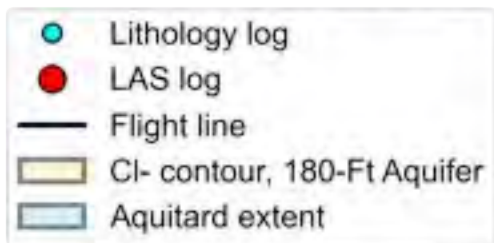
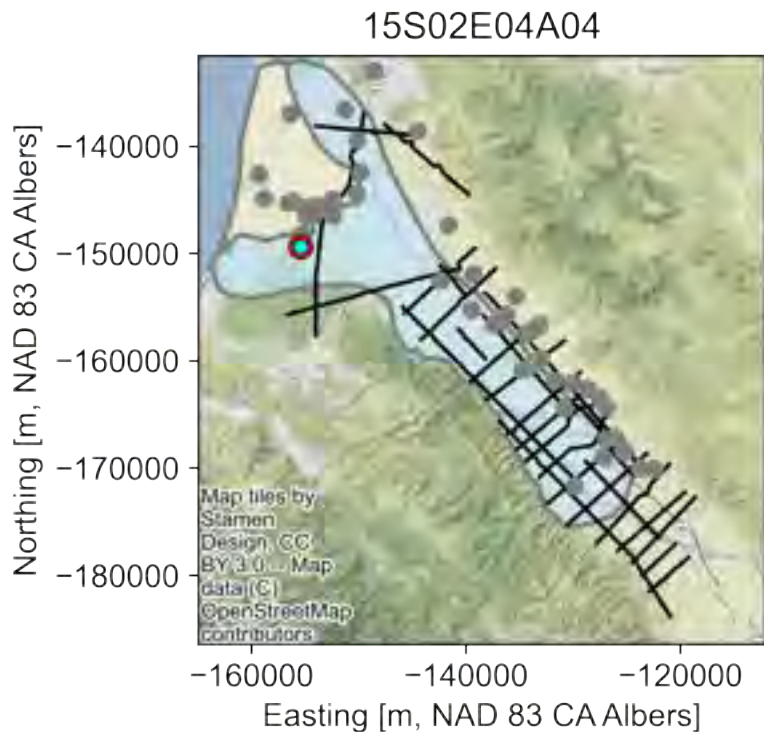
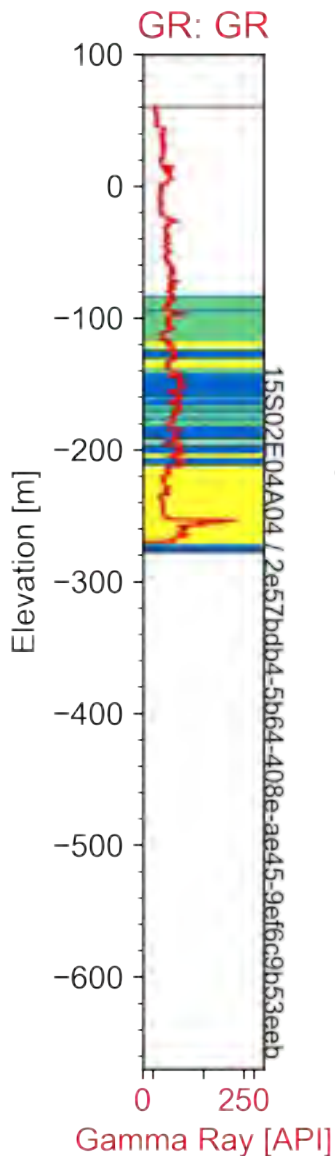
14S02E21K04

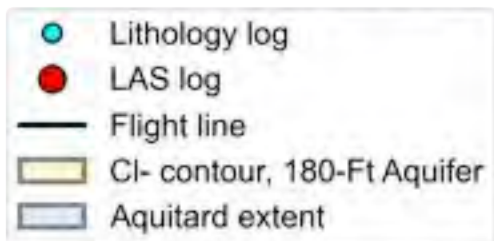
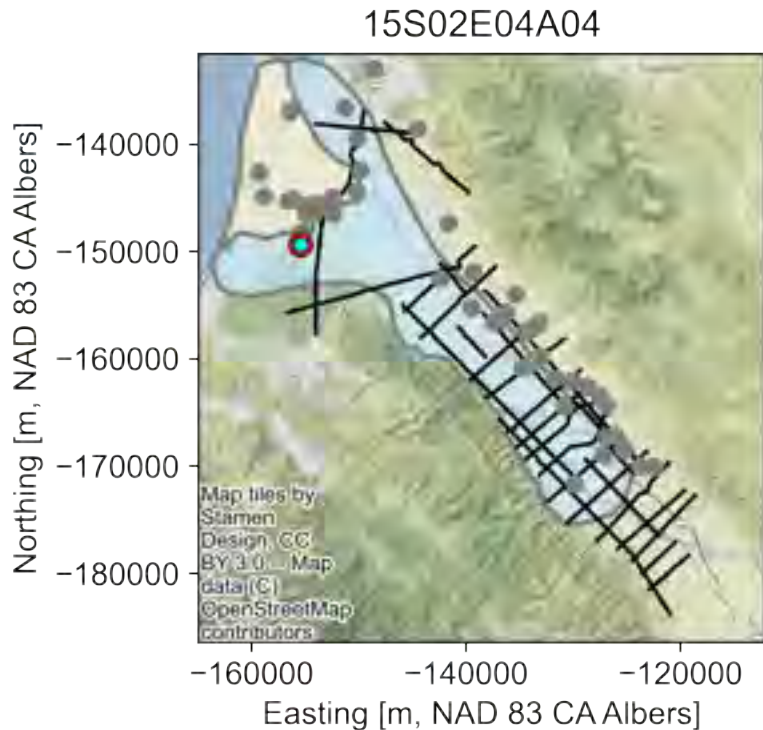
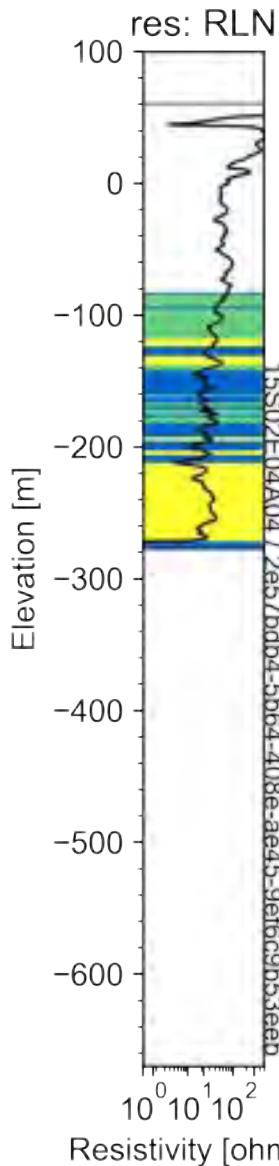


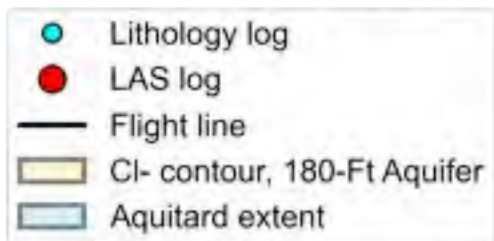
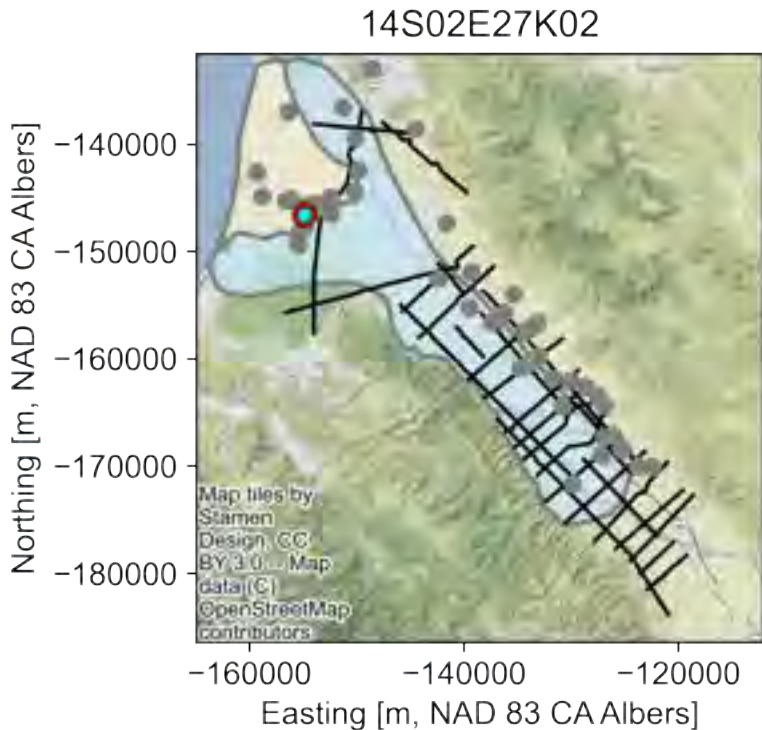
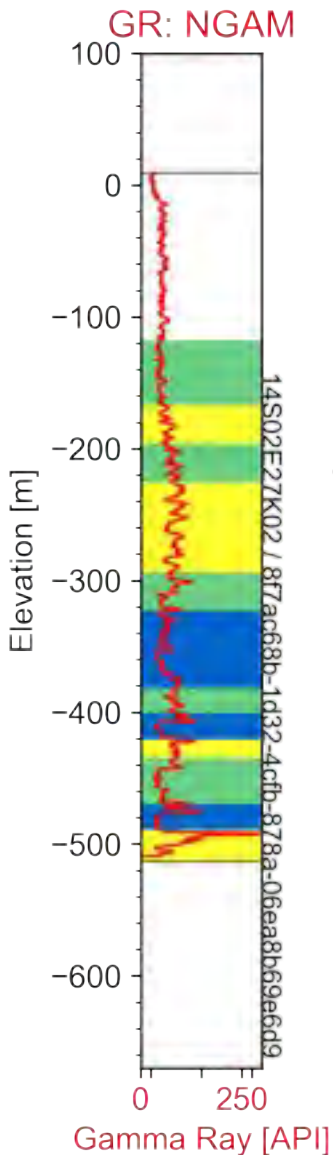


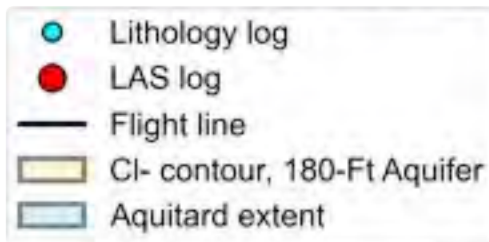
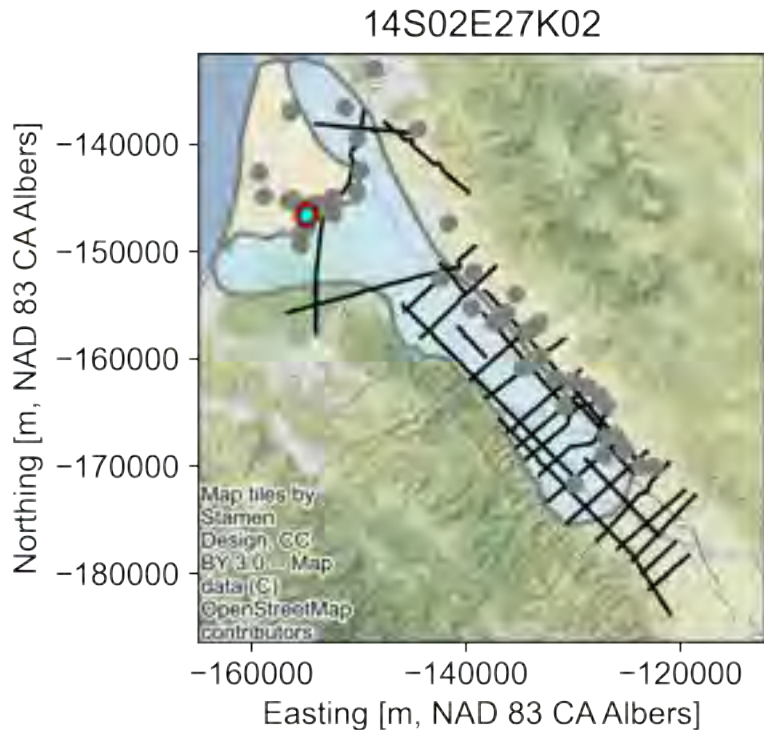
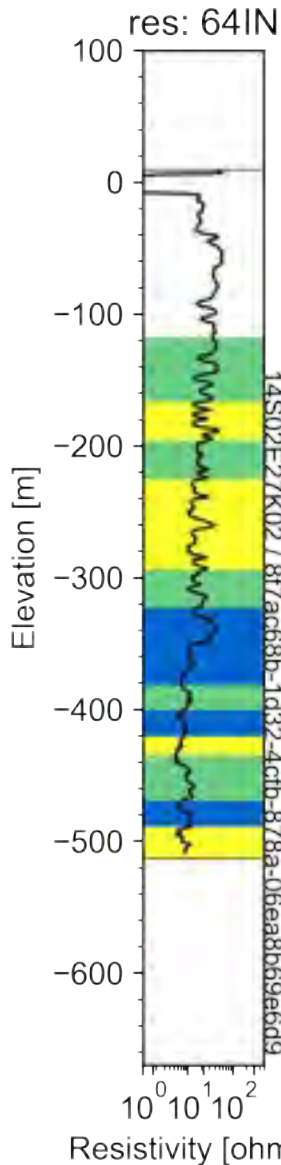


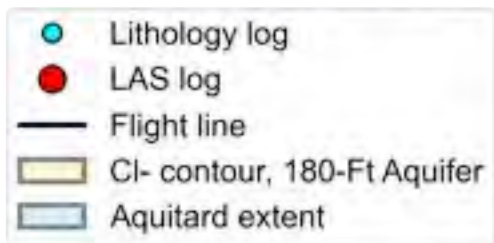
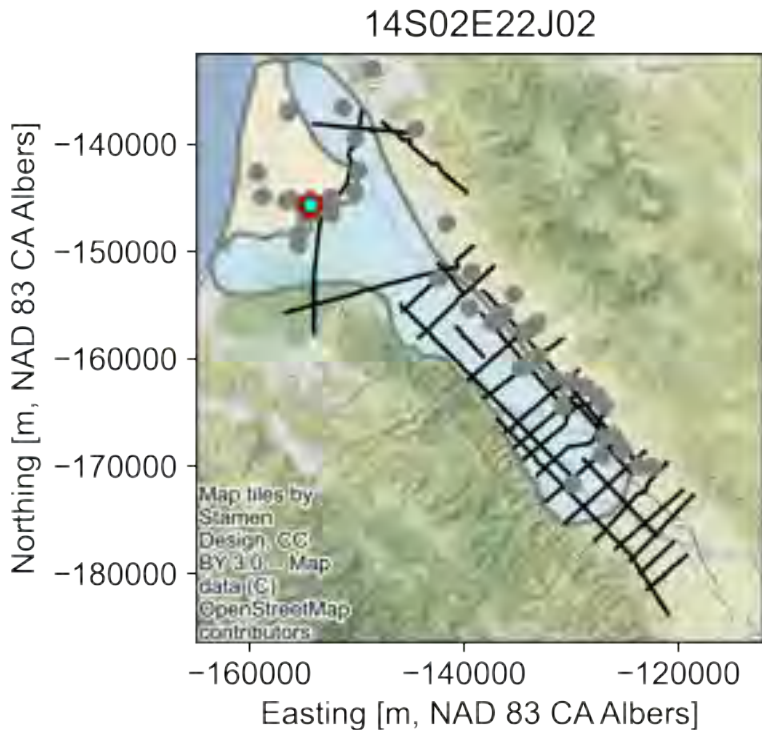
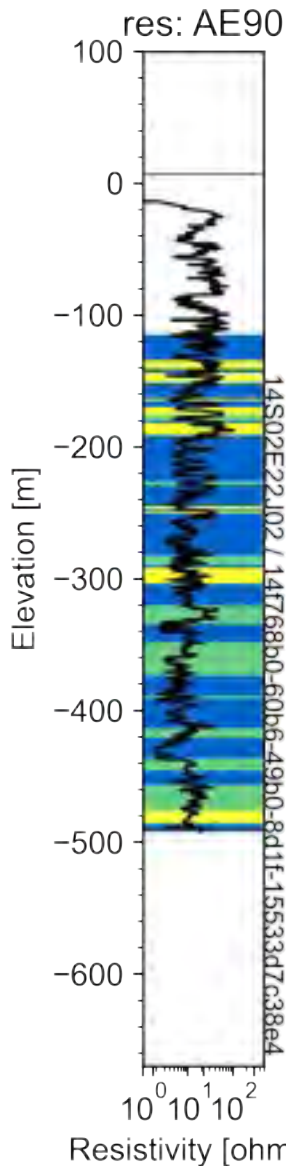


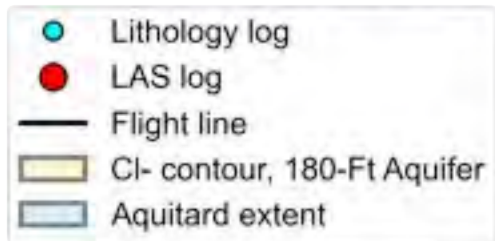
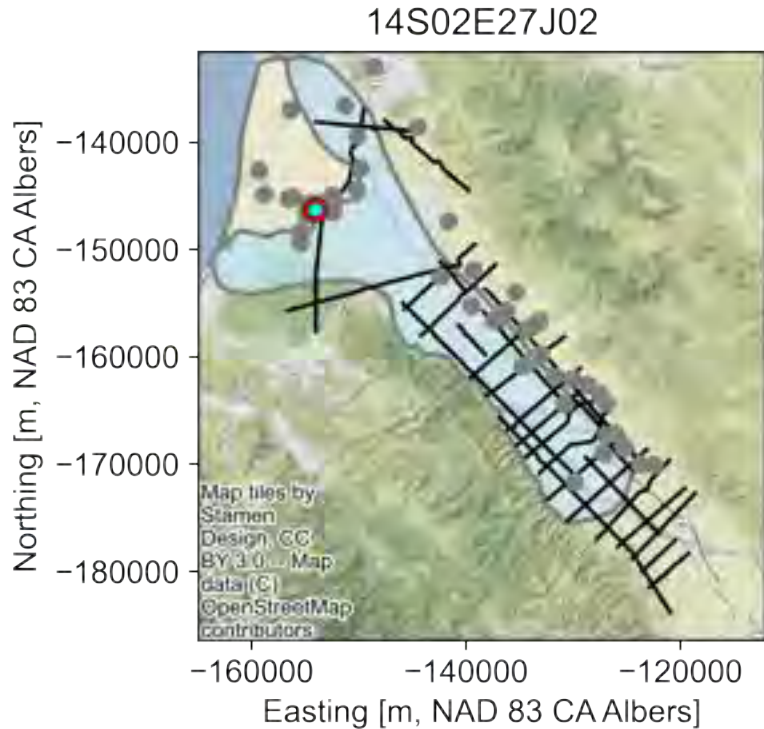
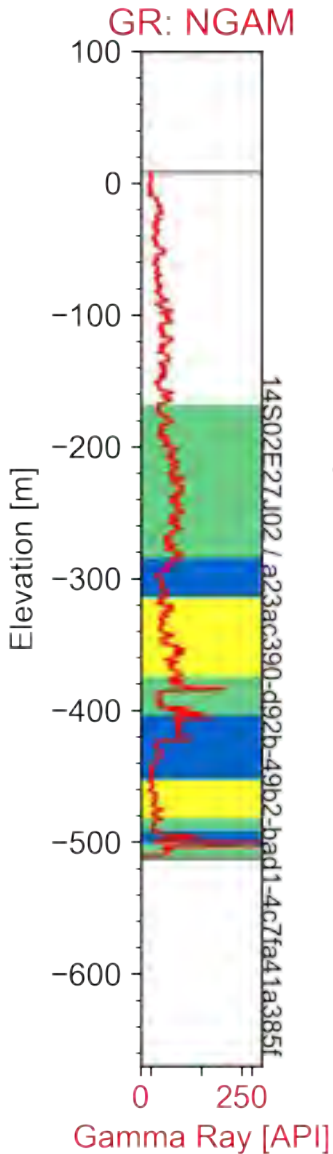


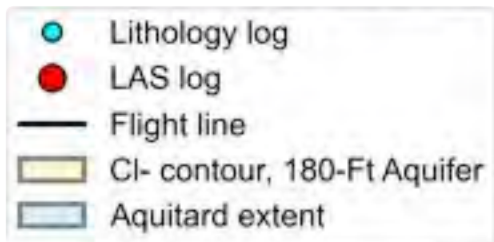
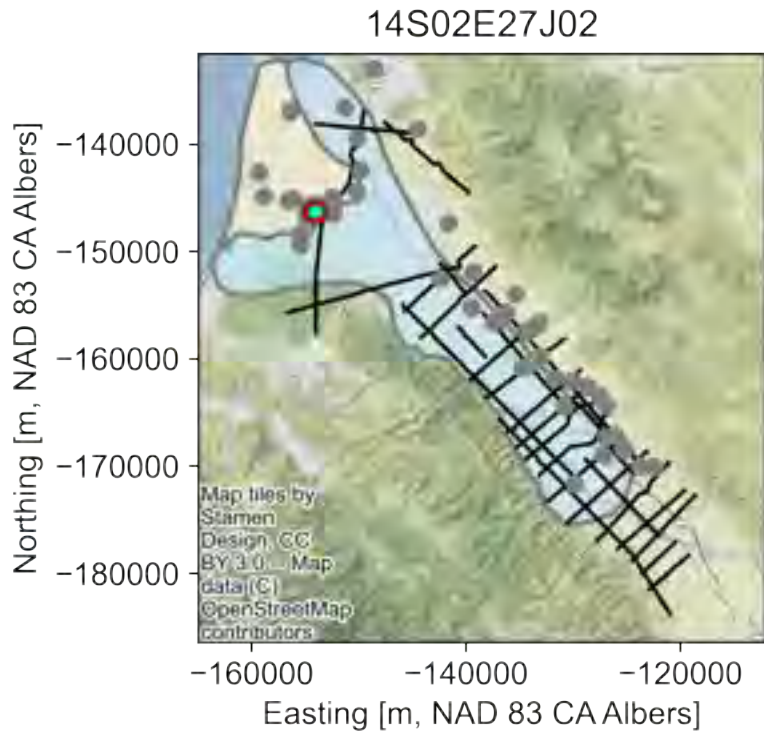
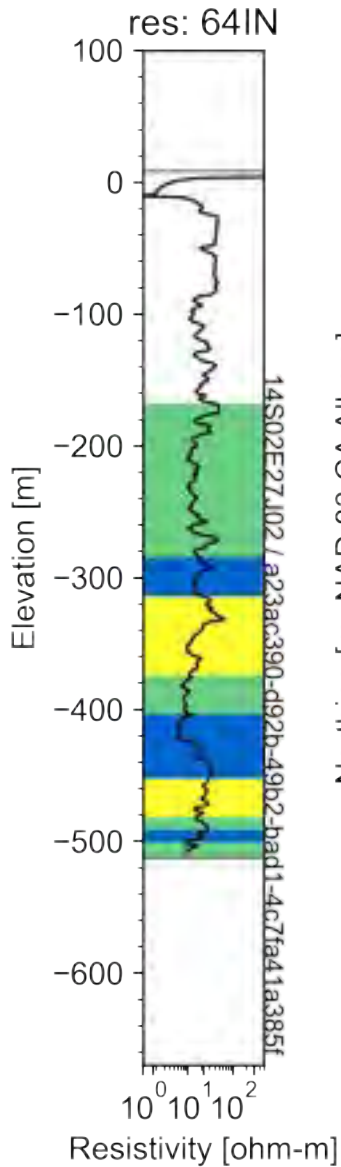


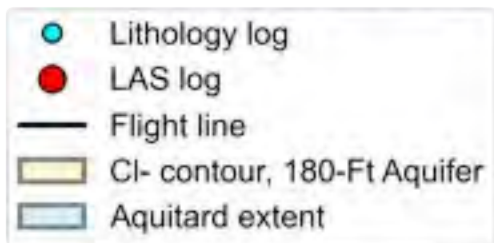
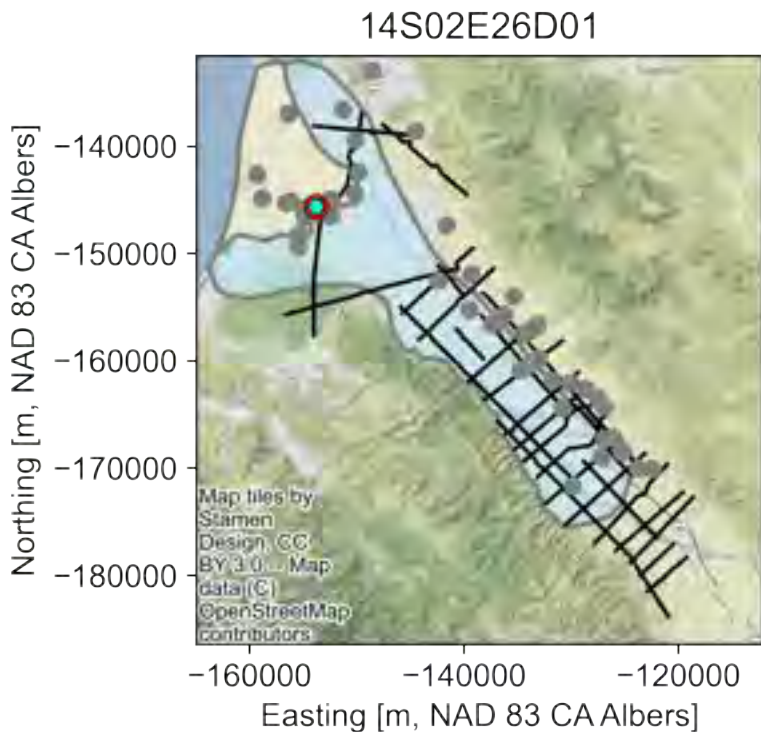
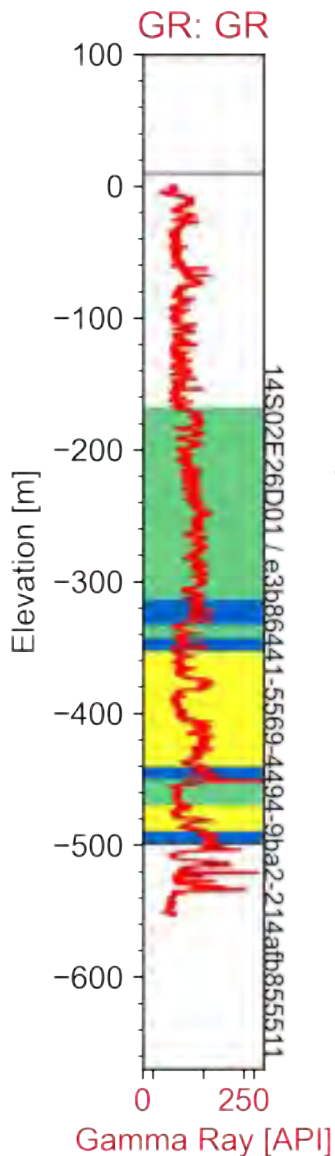


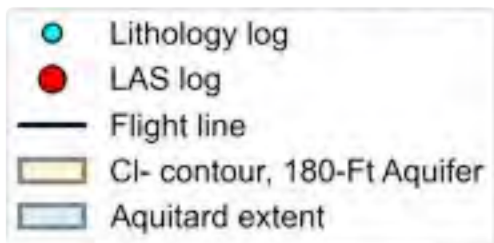
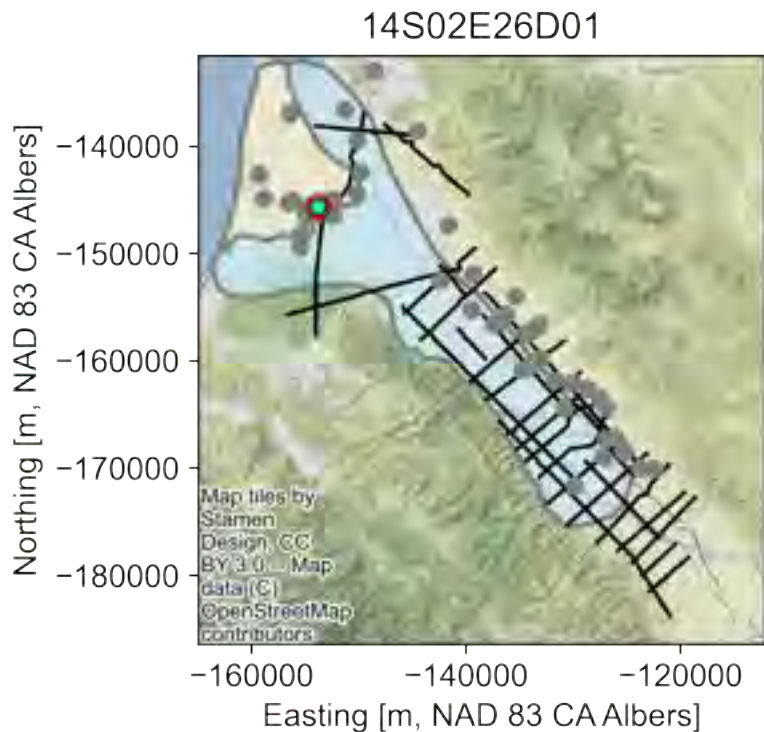
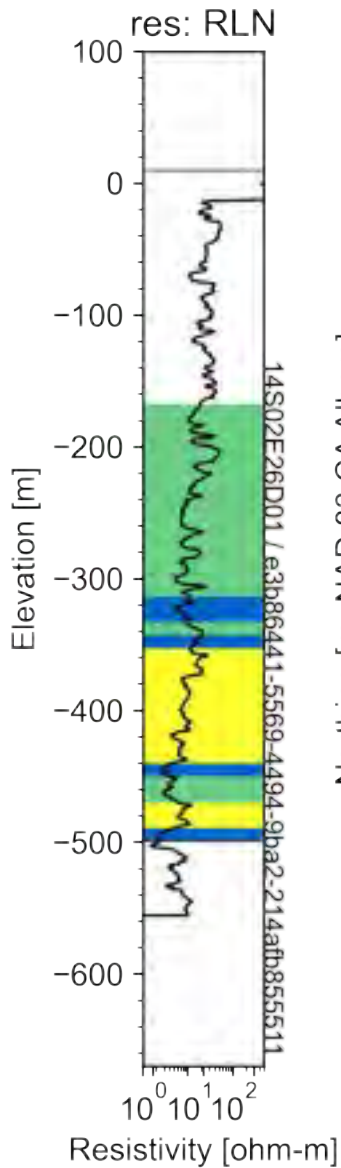


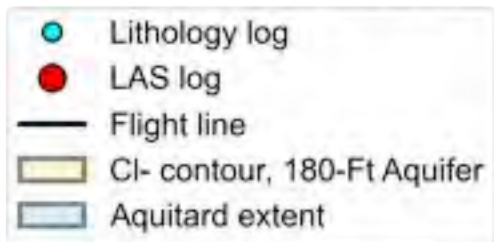
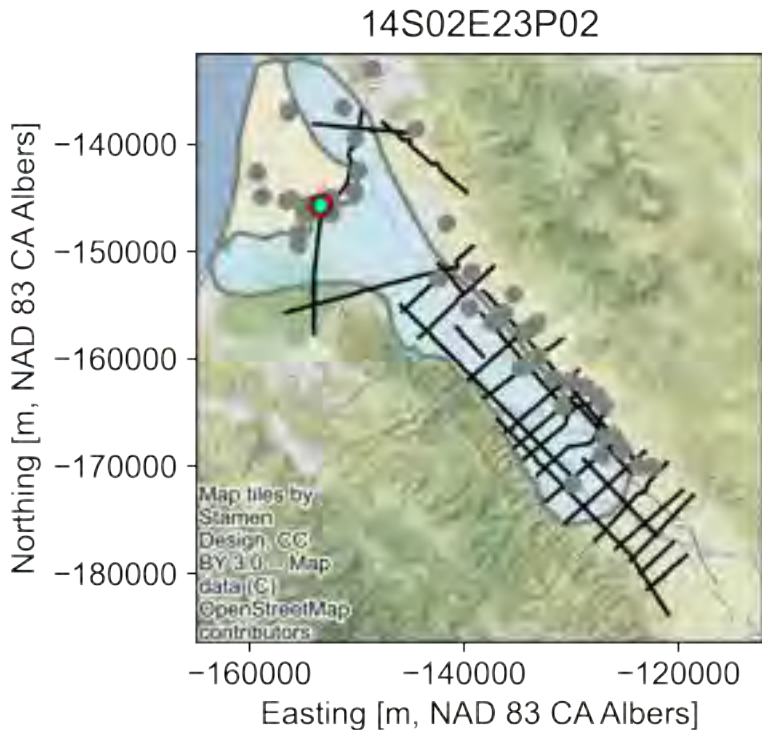
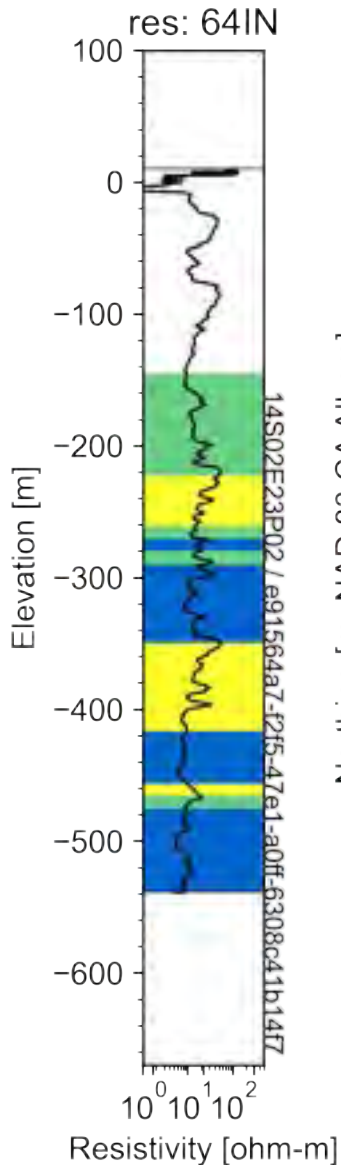


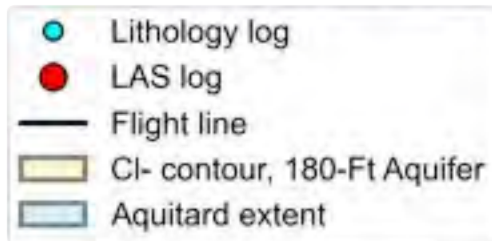
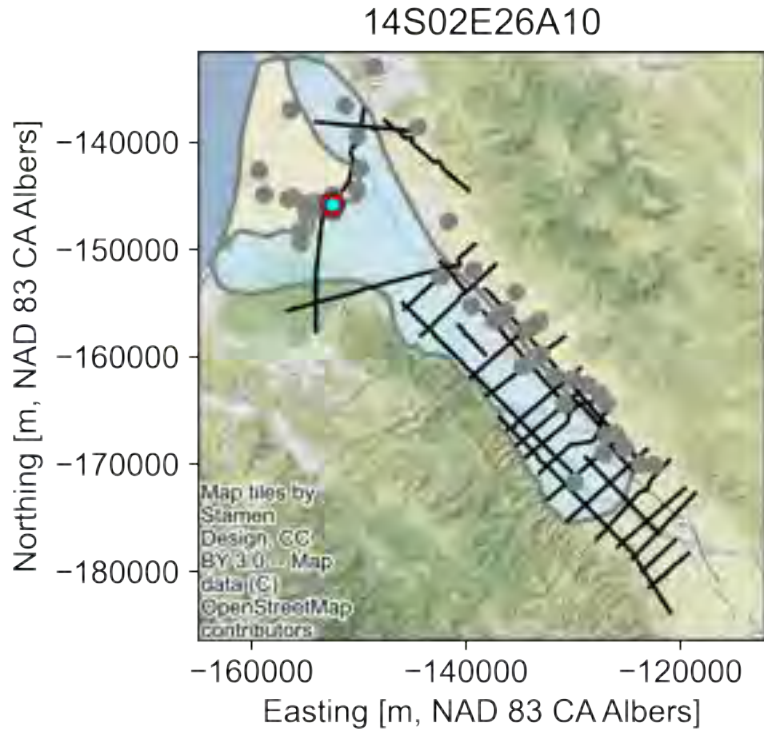
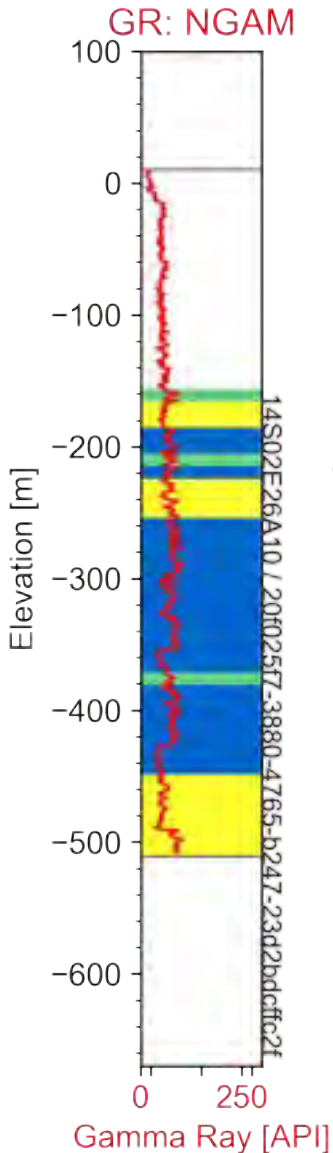


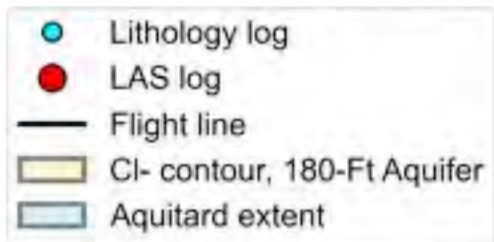
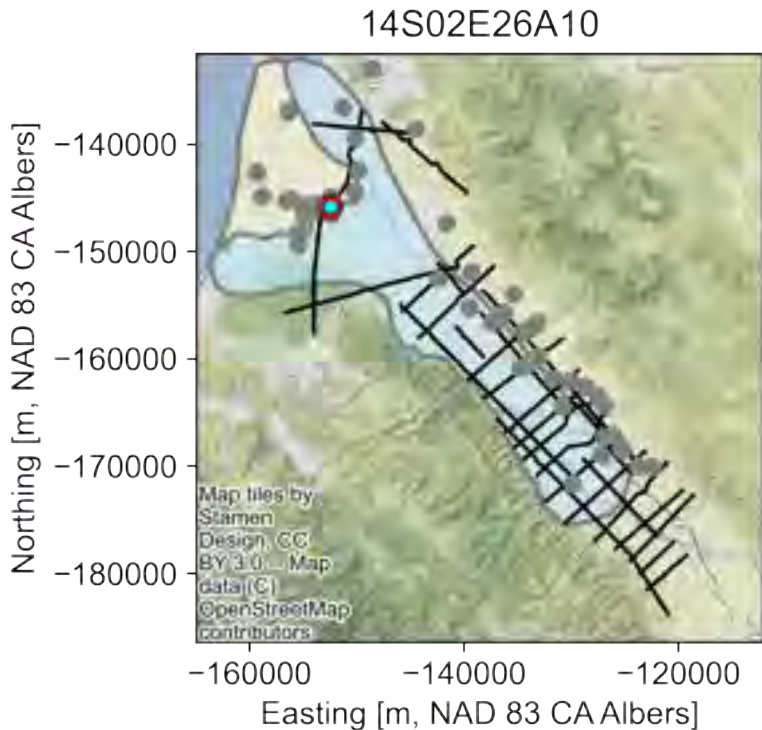
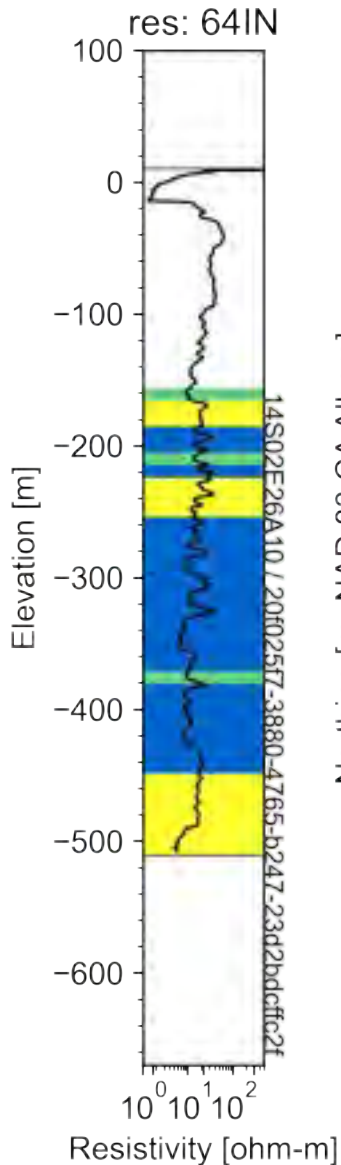


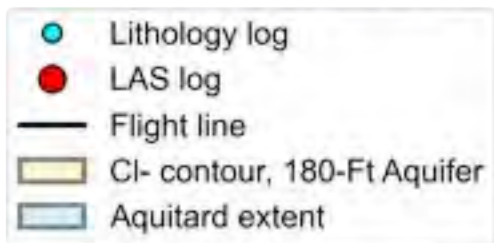
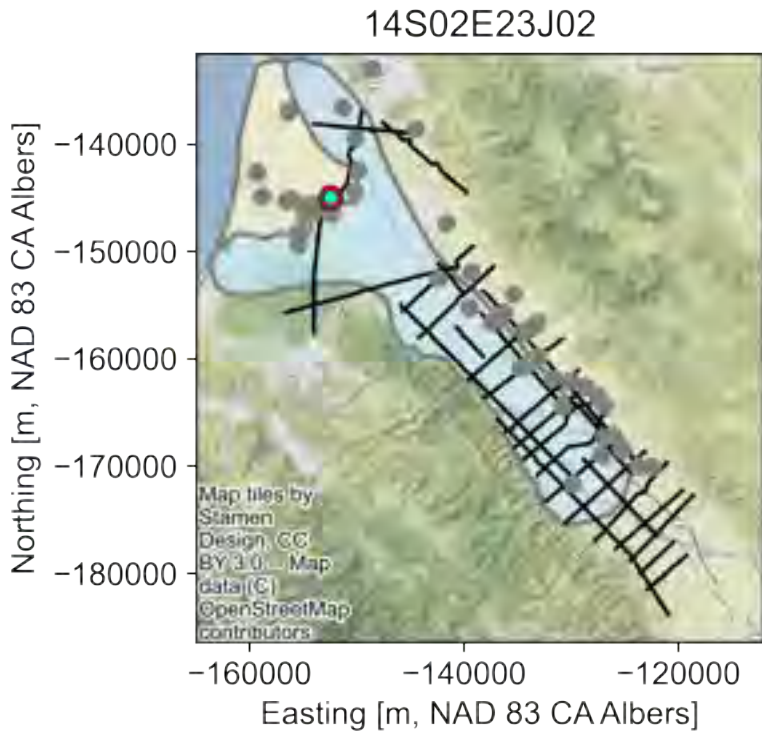
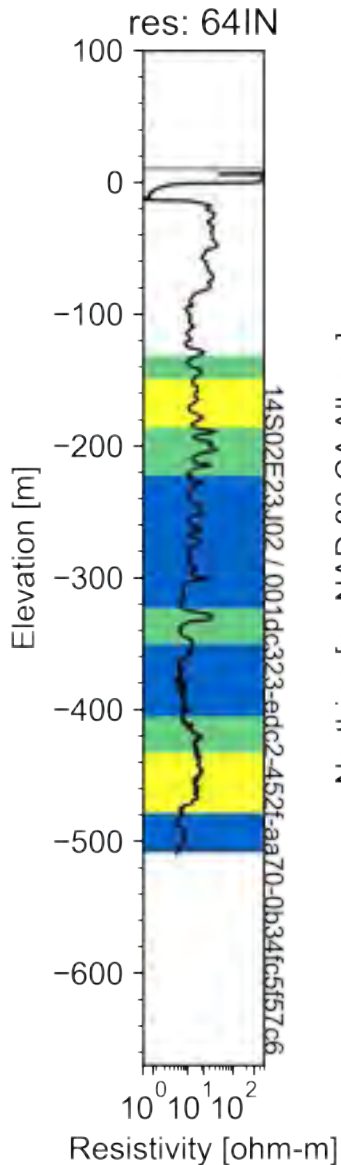


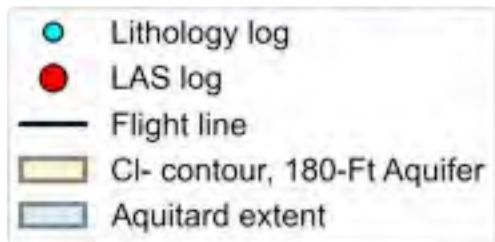
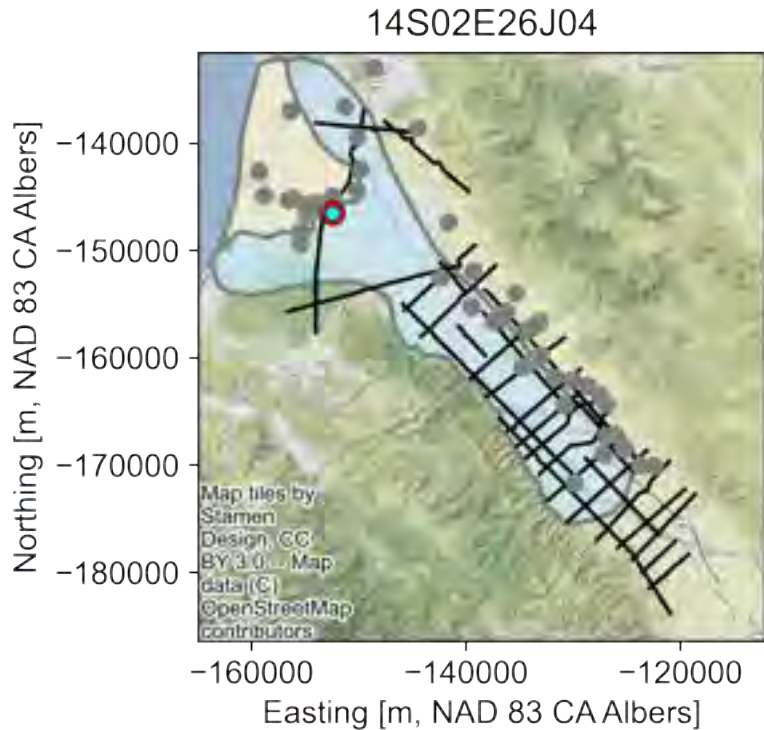
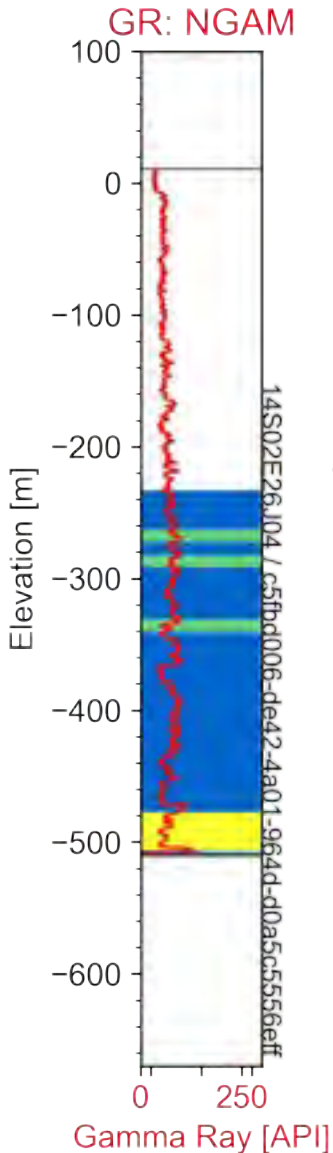


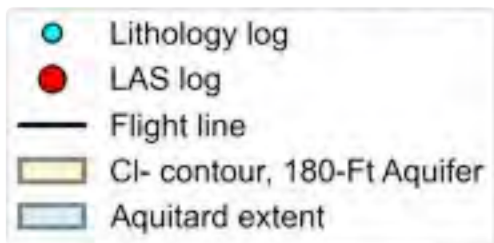
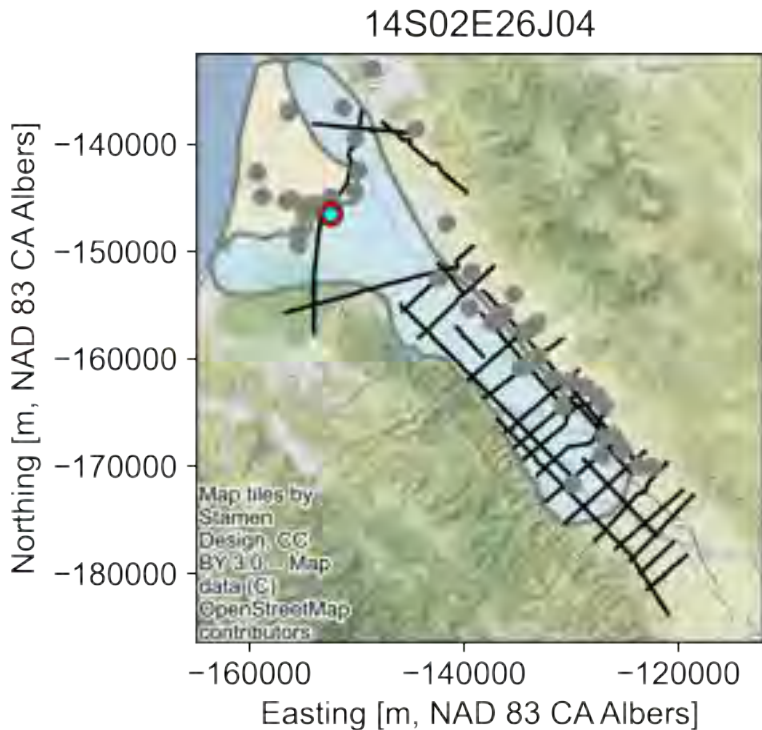
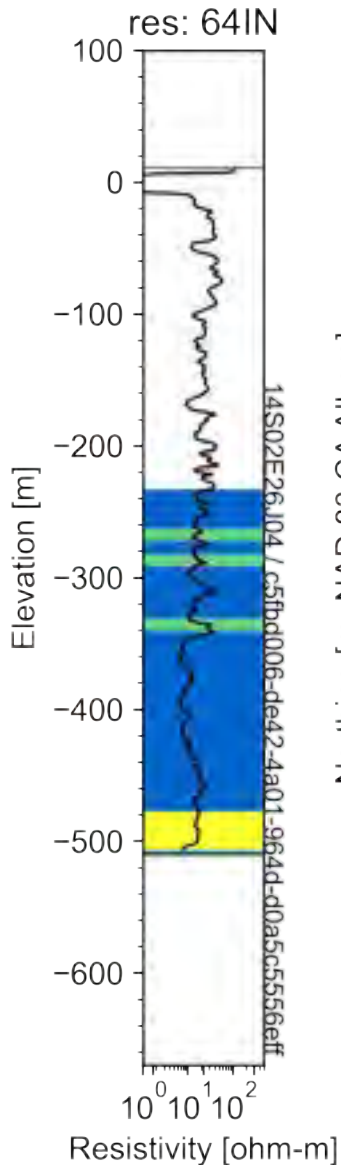


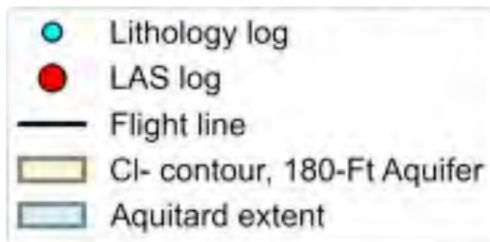
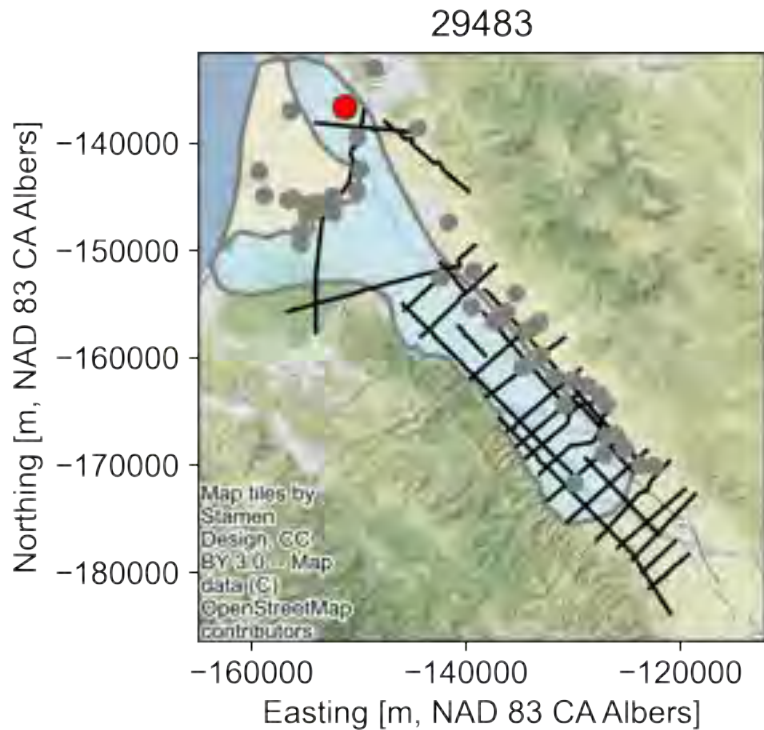
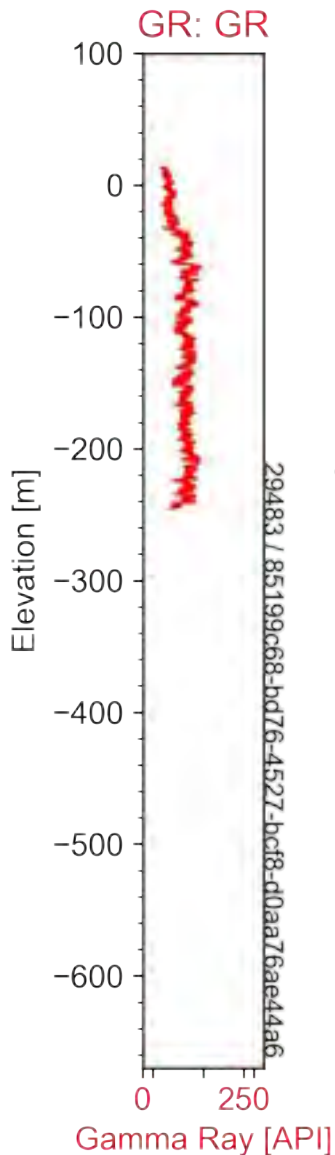


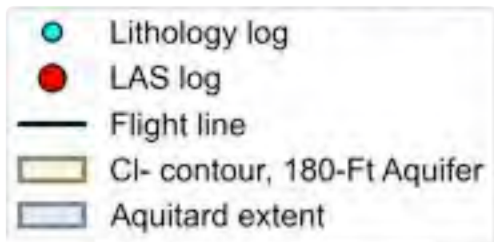
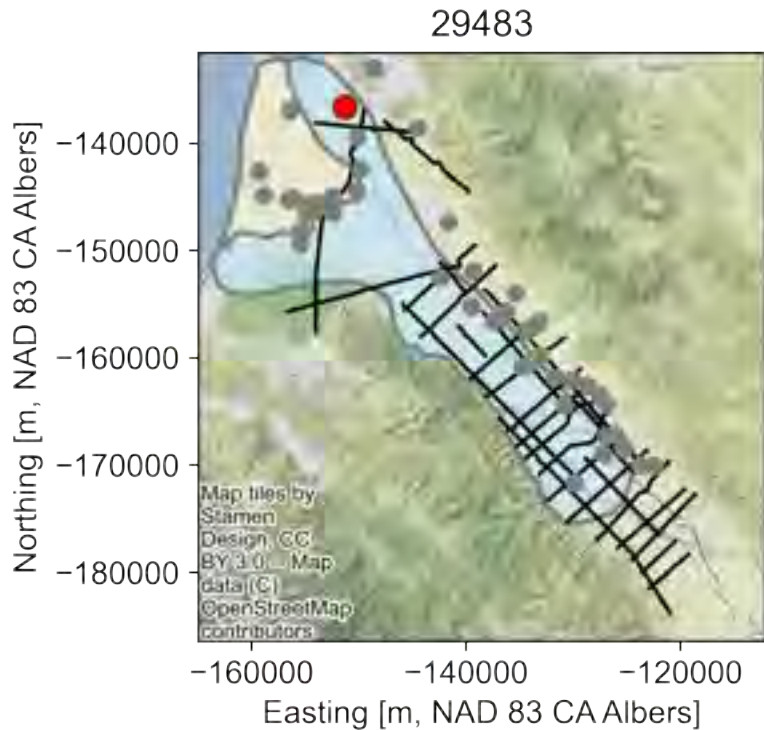
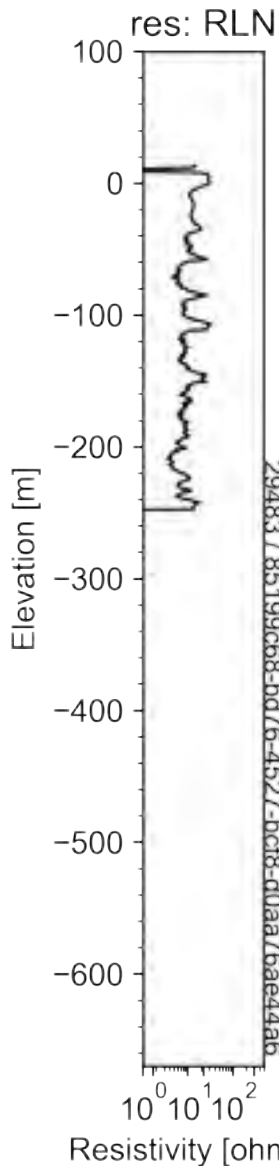


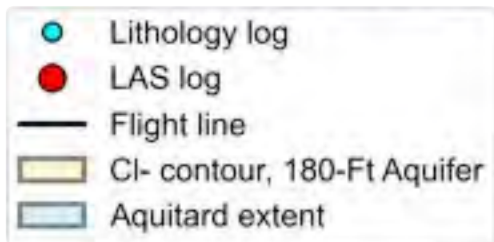
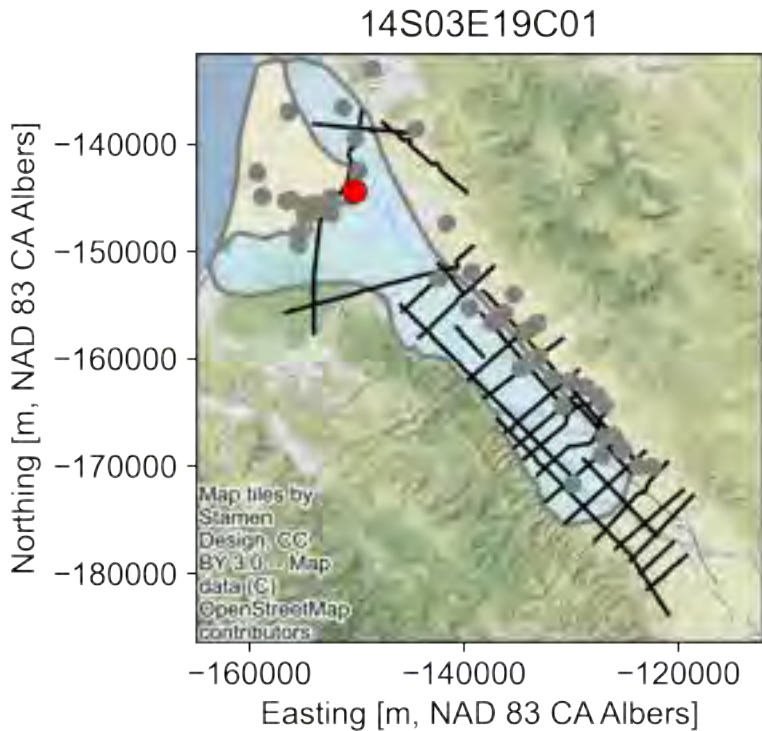
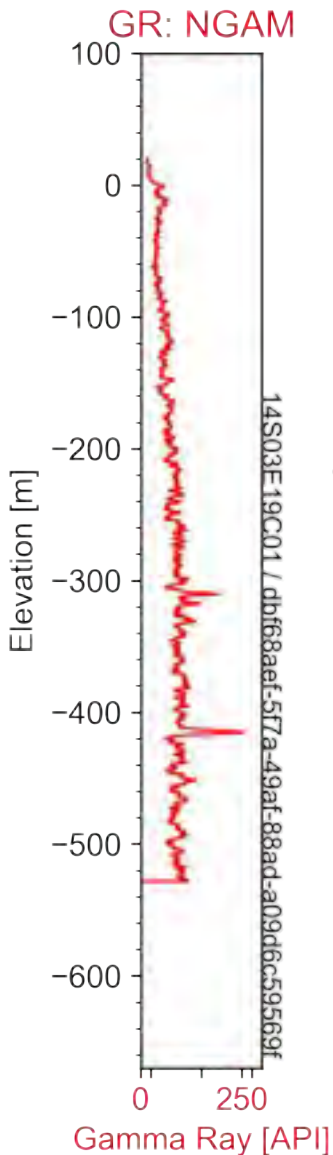


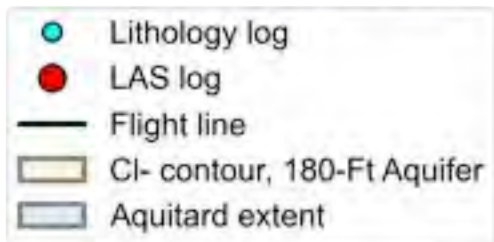
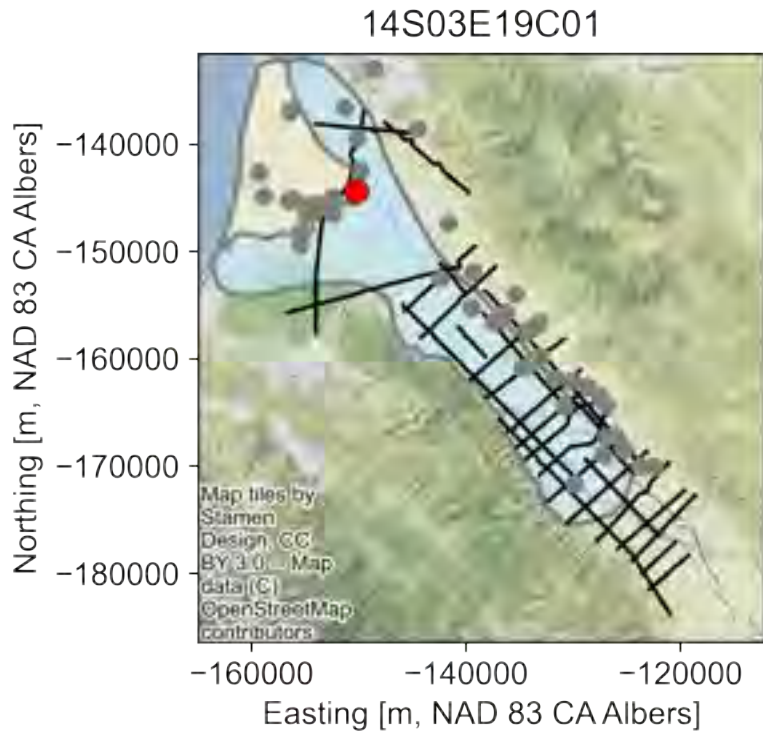
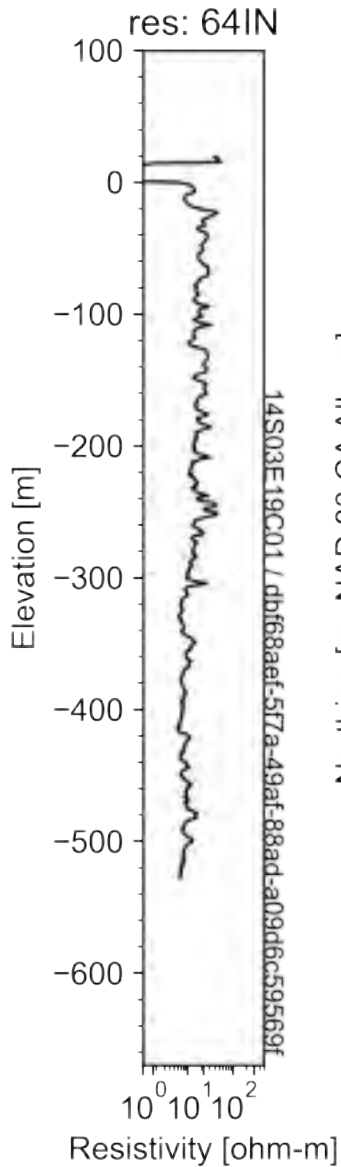


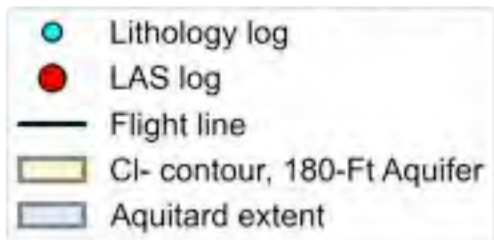
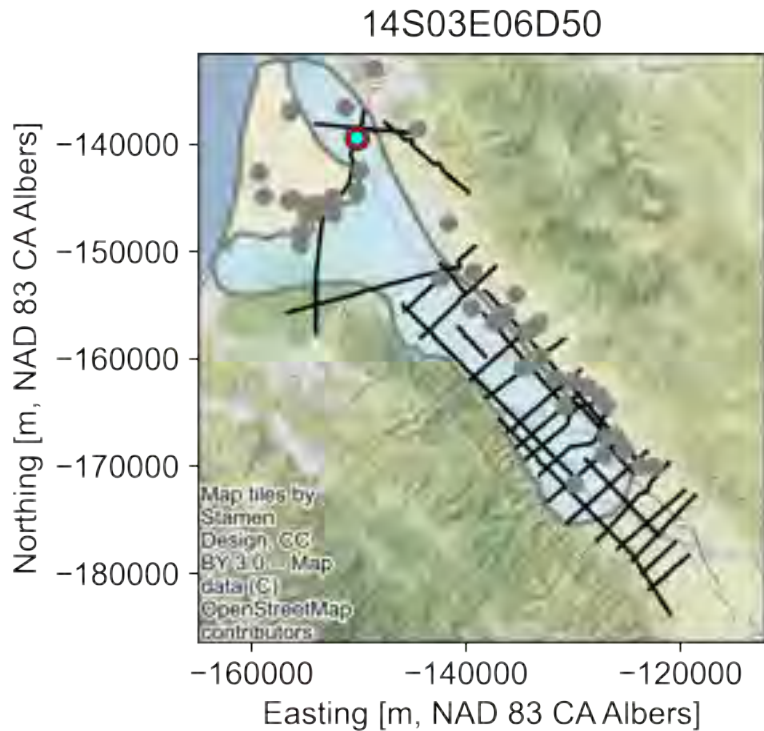
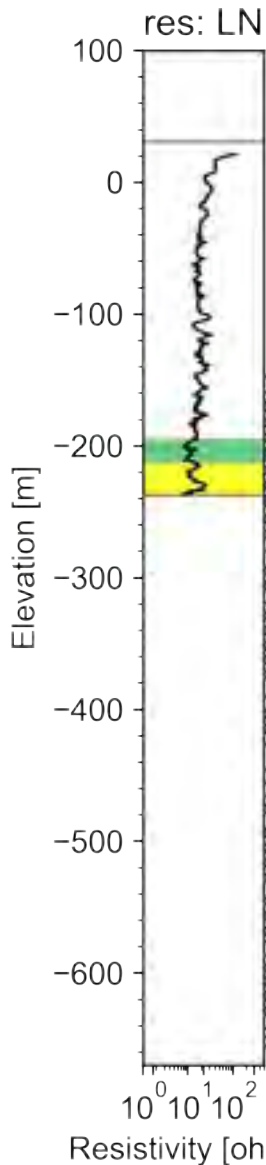


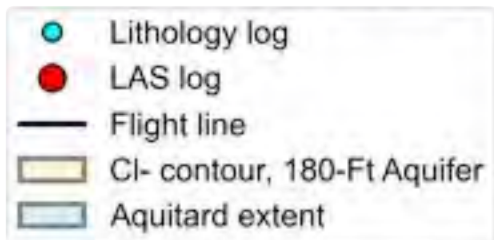
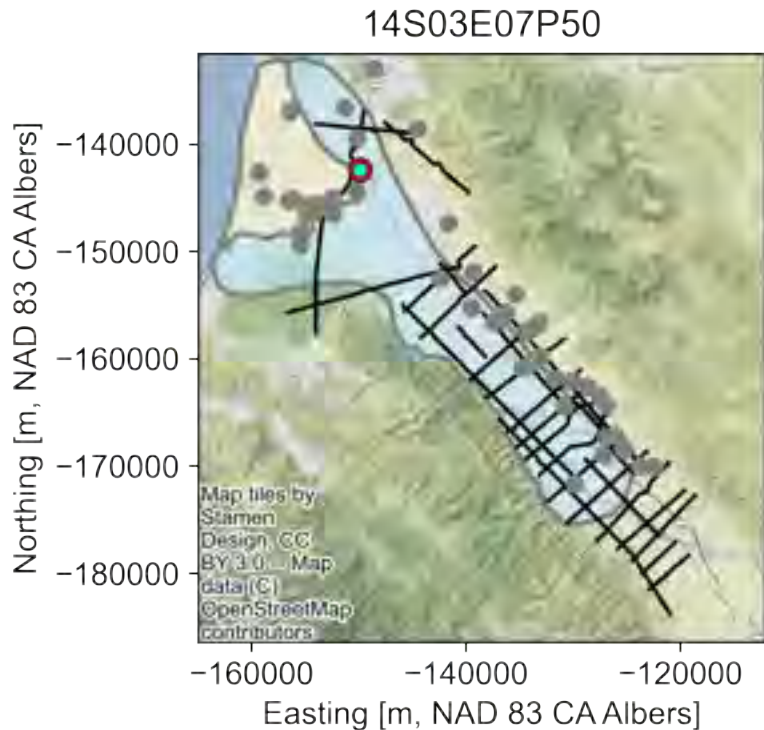
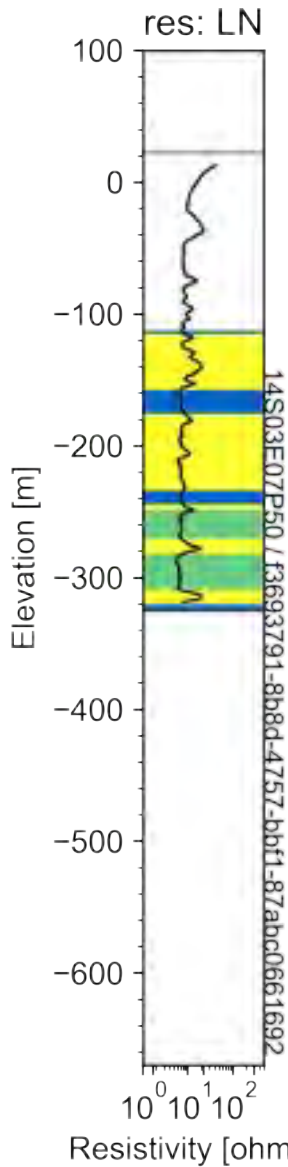


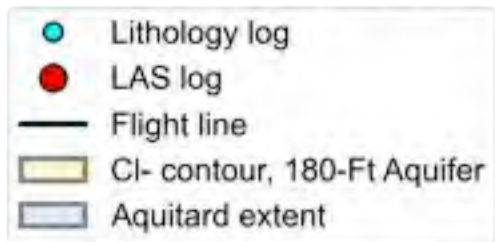
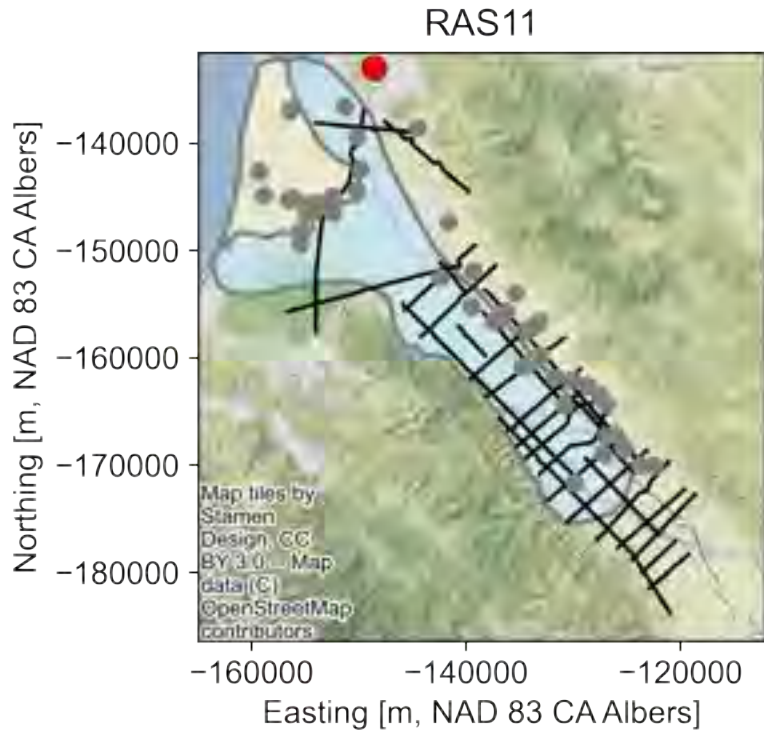
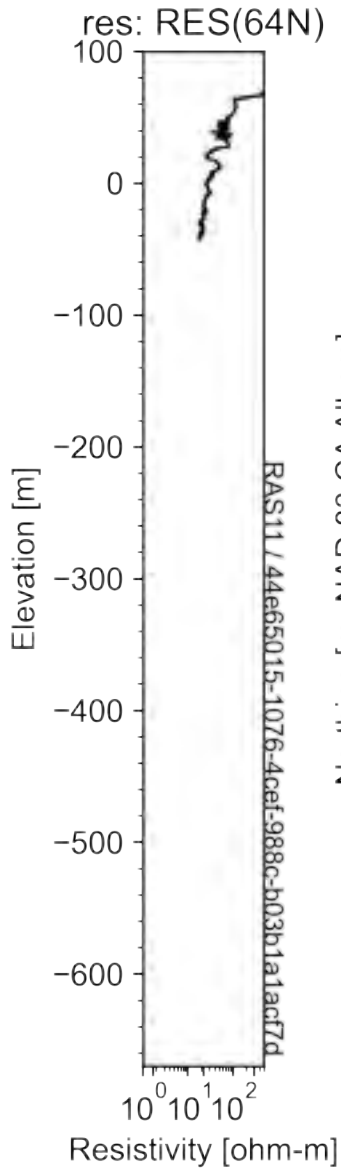


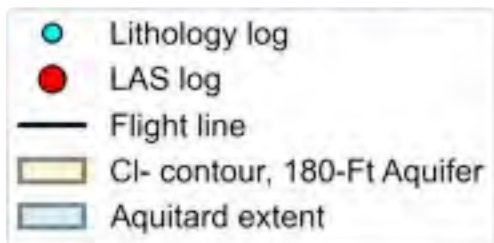
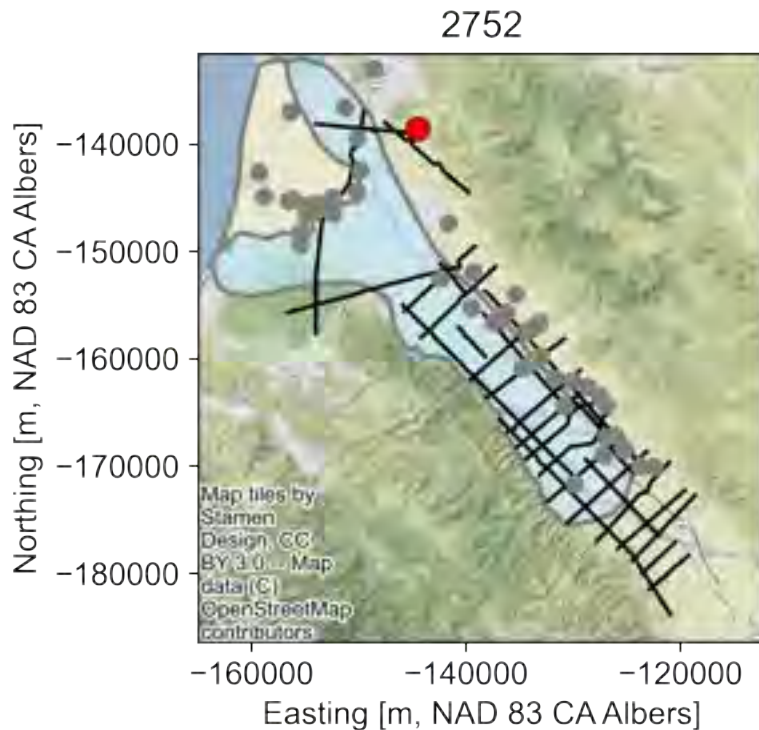
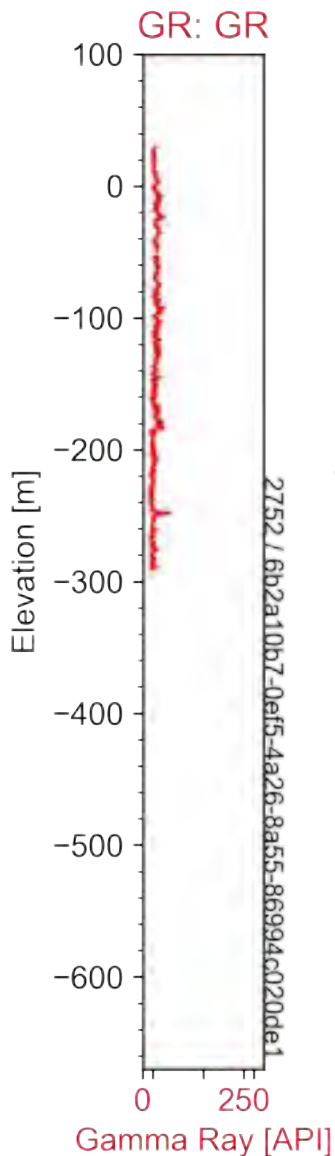


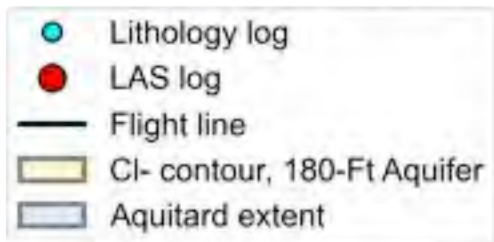
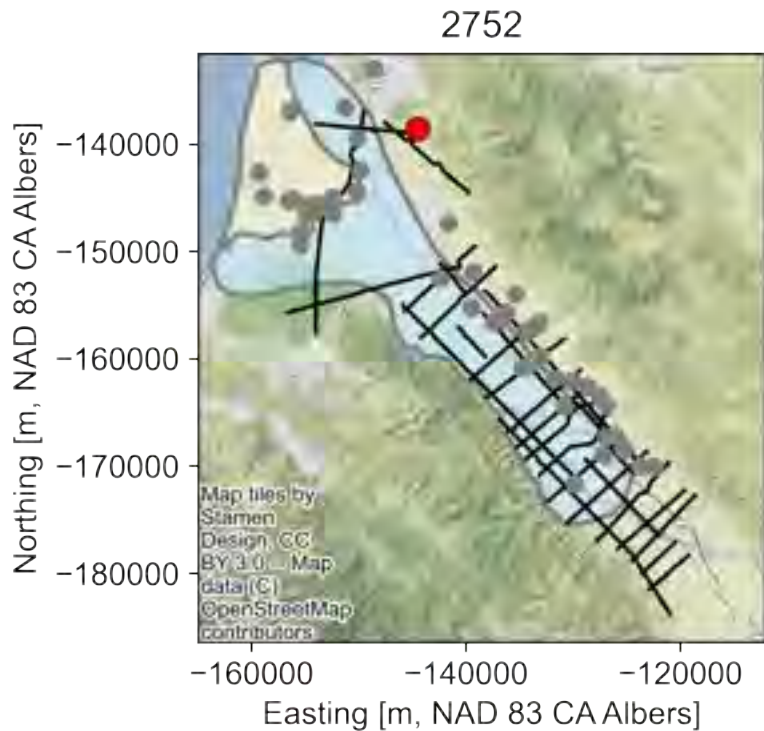
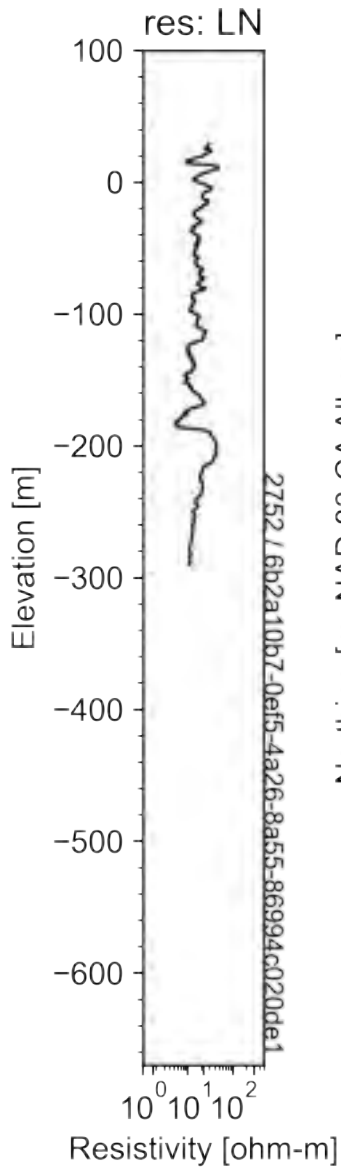


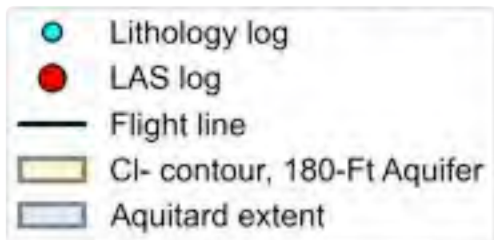
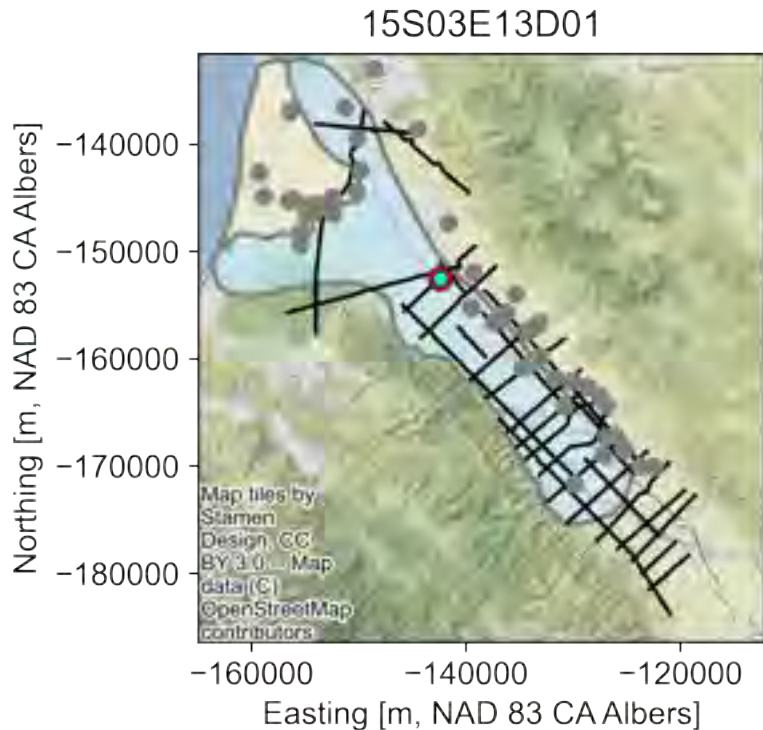
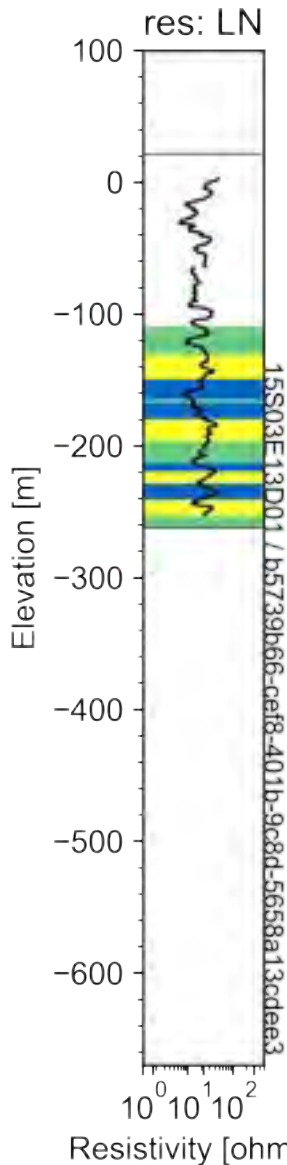


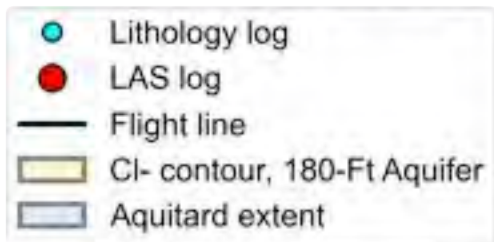
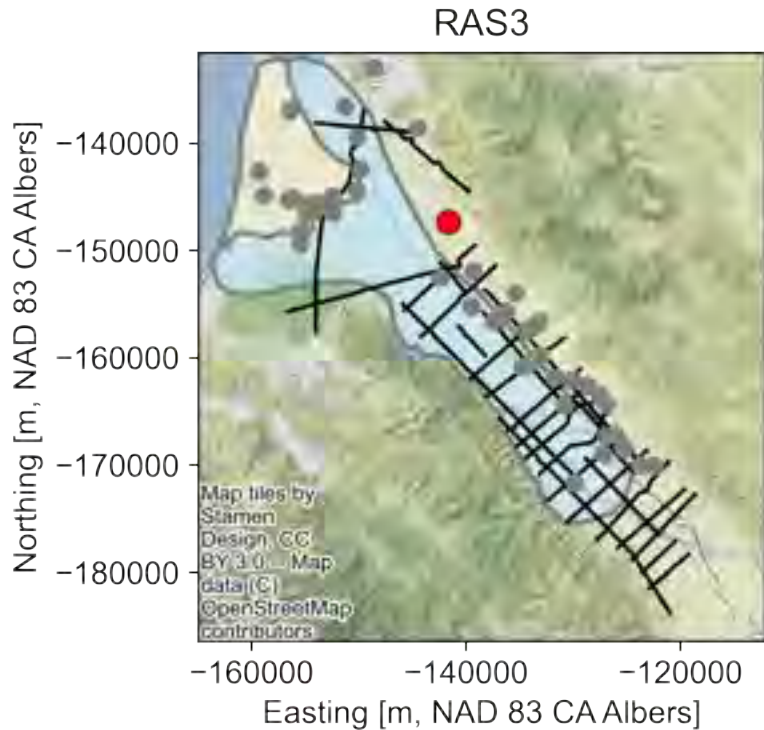
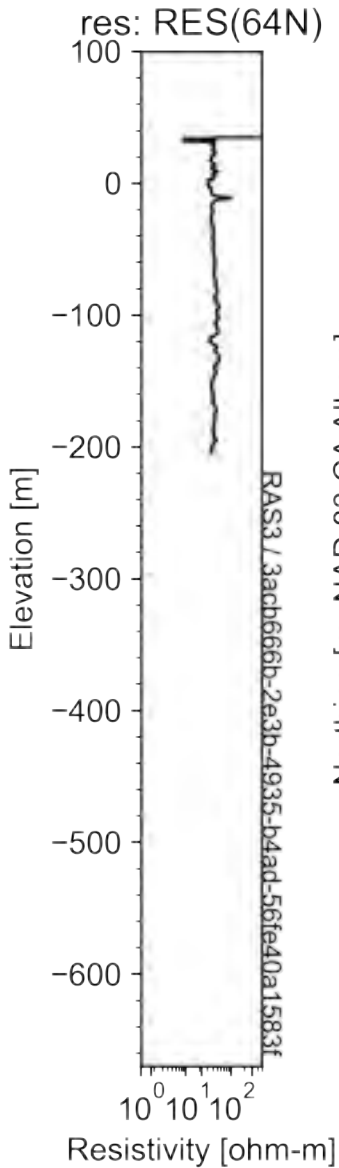


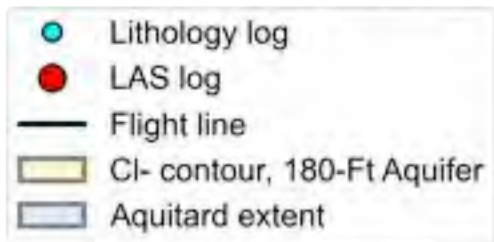
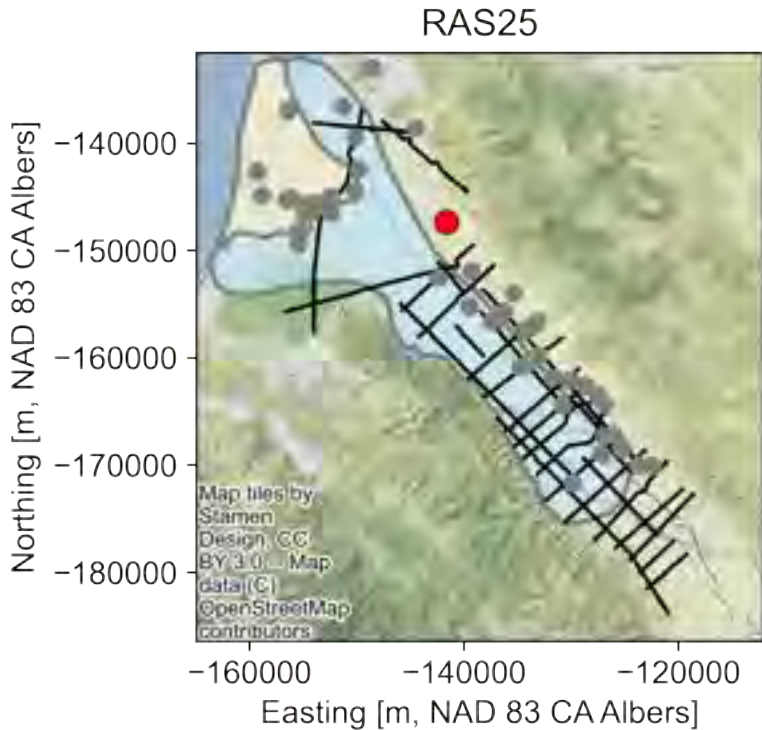
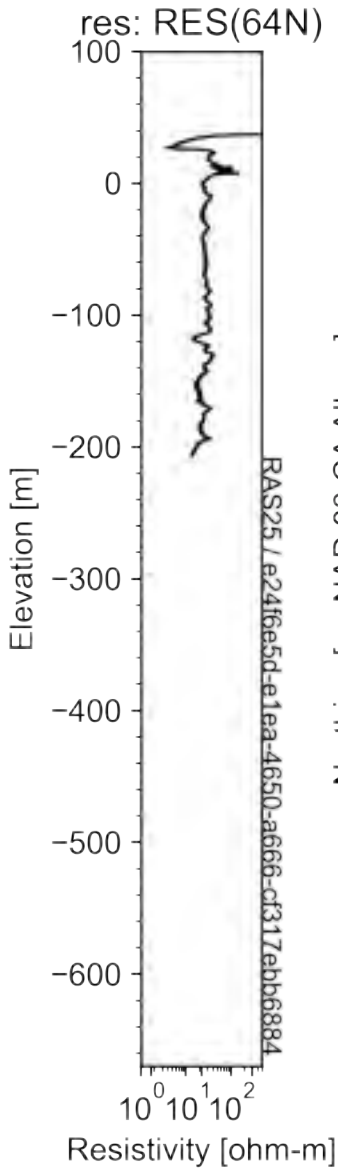


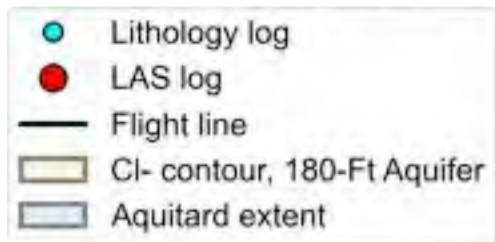
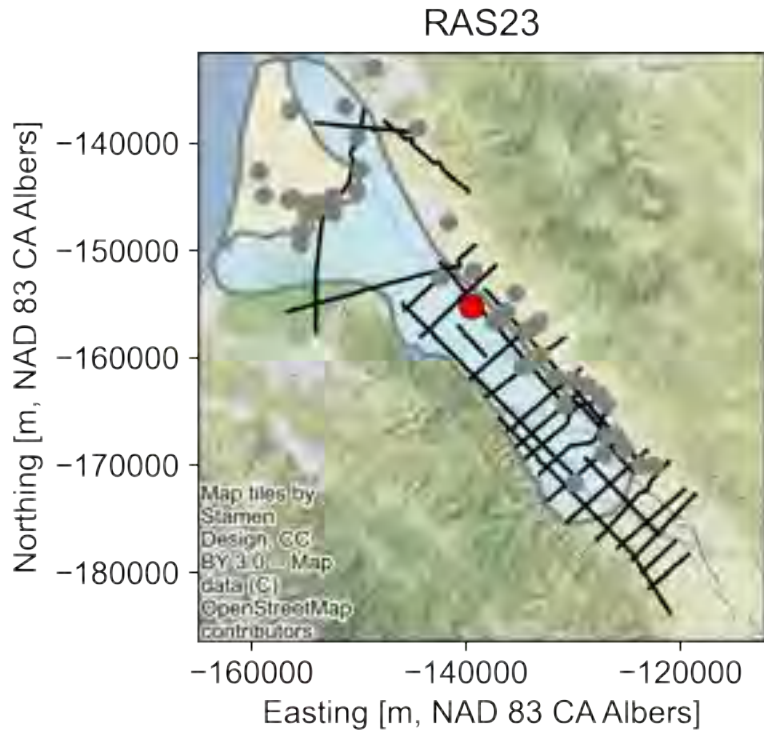
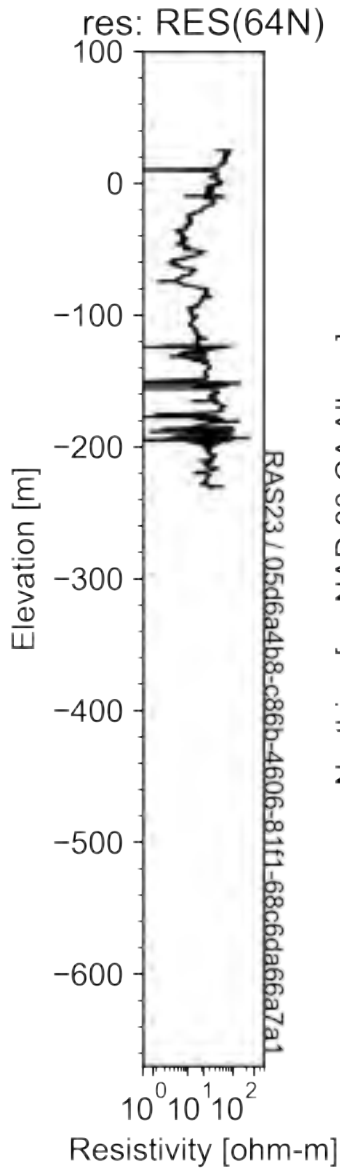


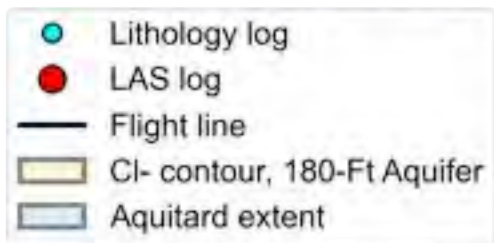
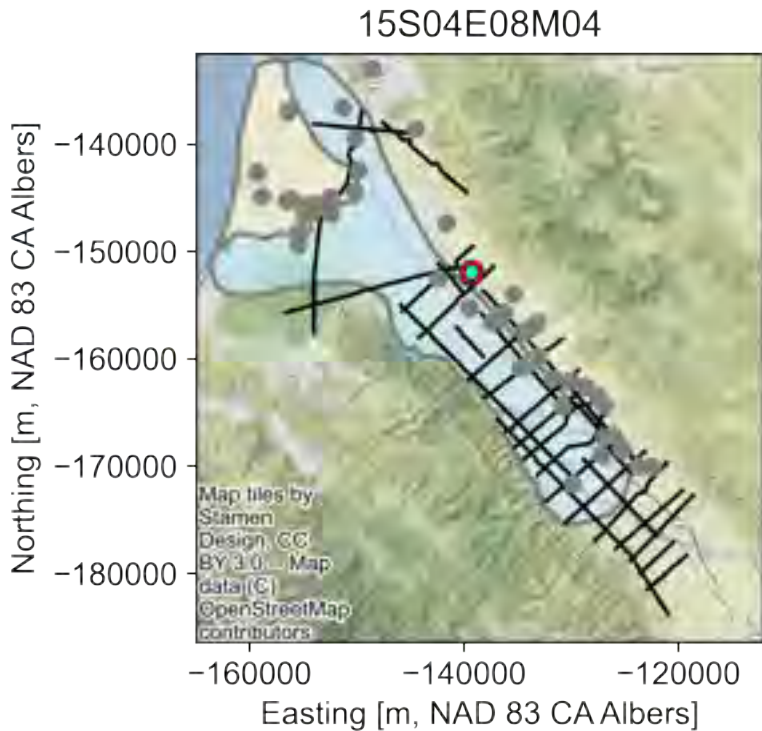
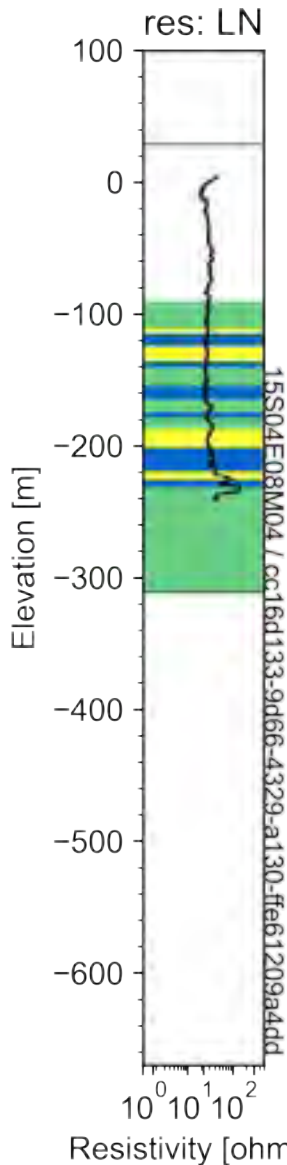


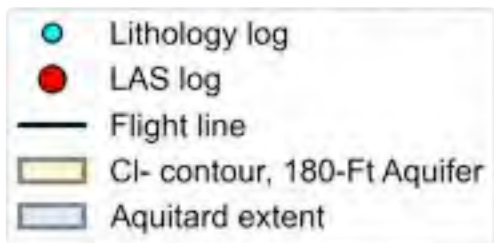
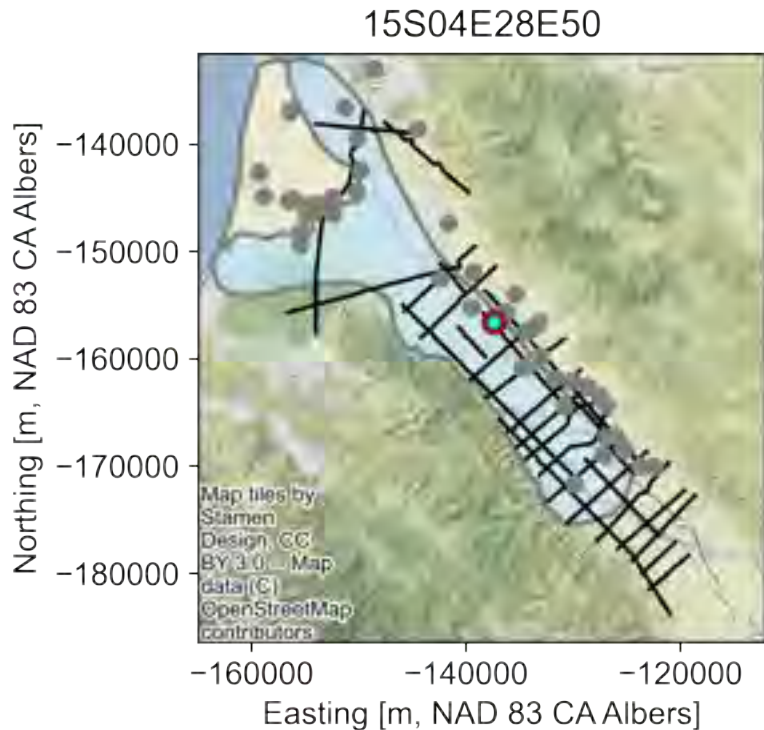
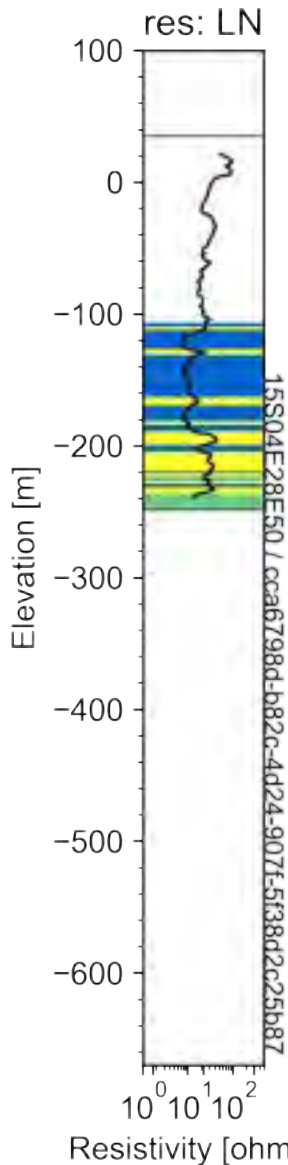


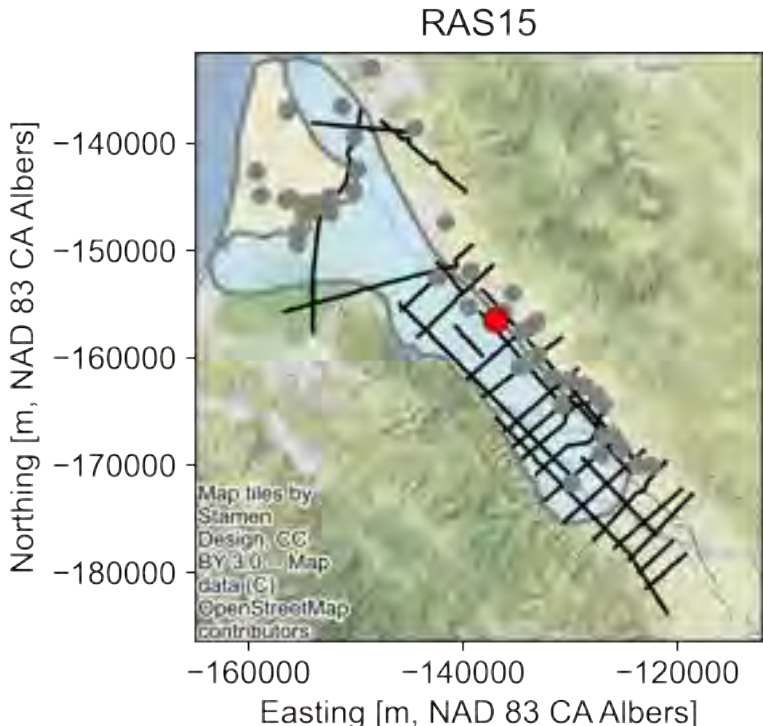
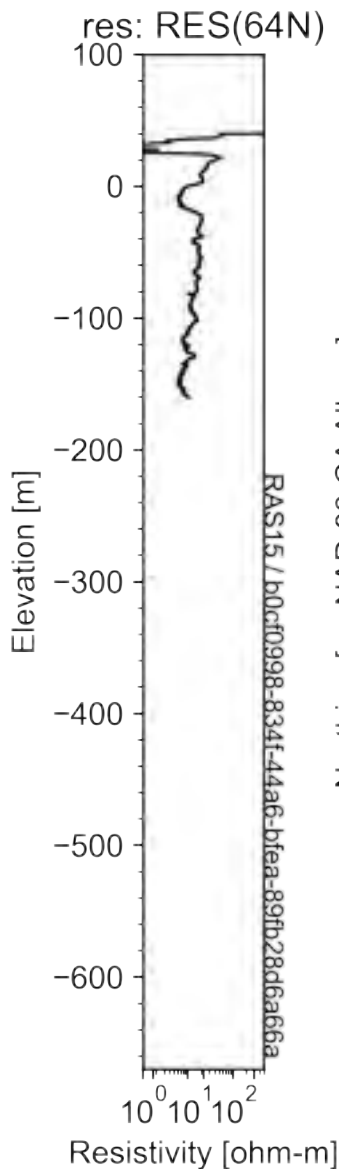




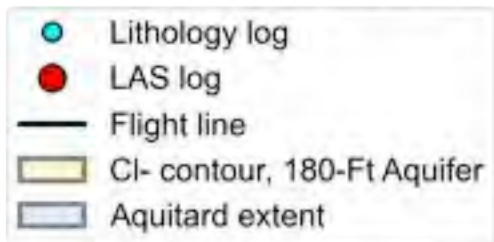
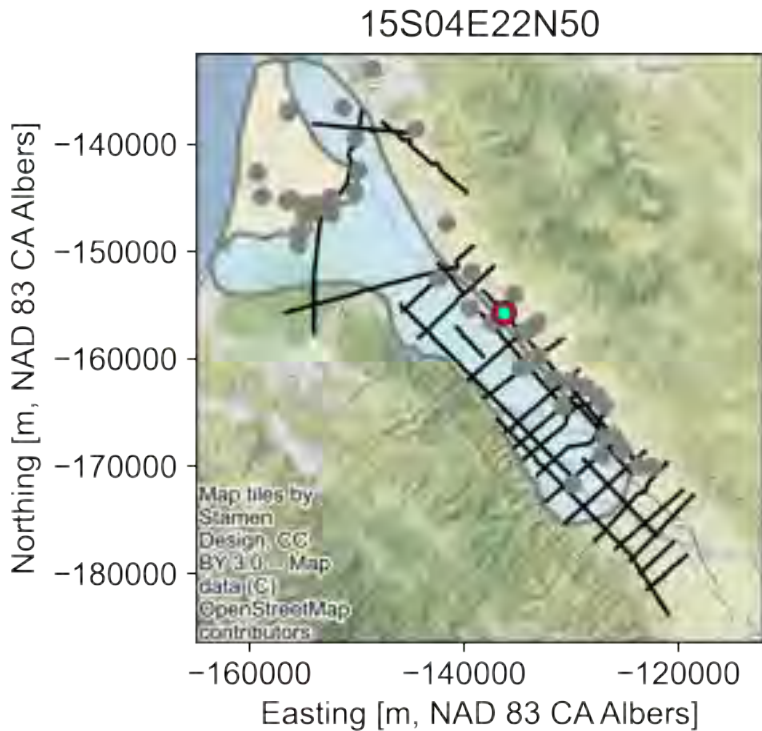
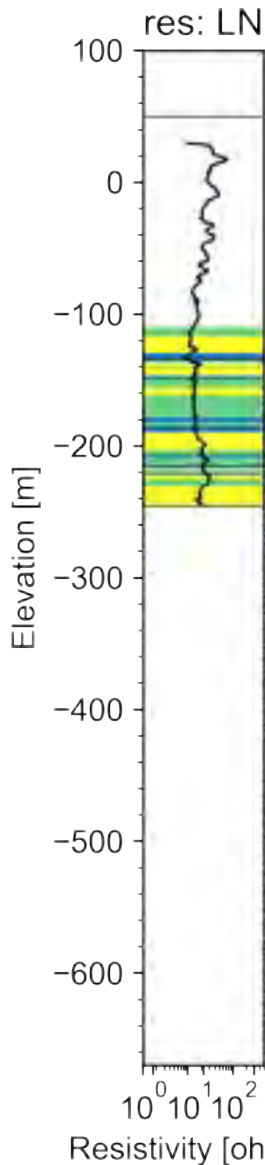


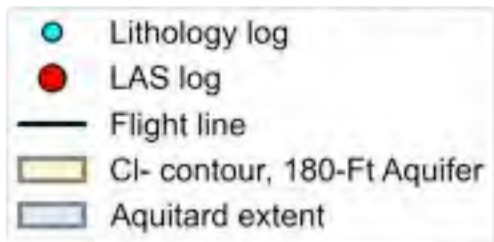
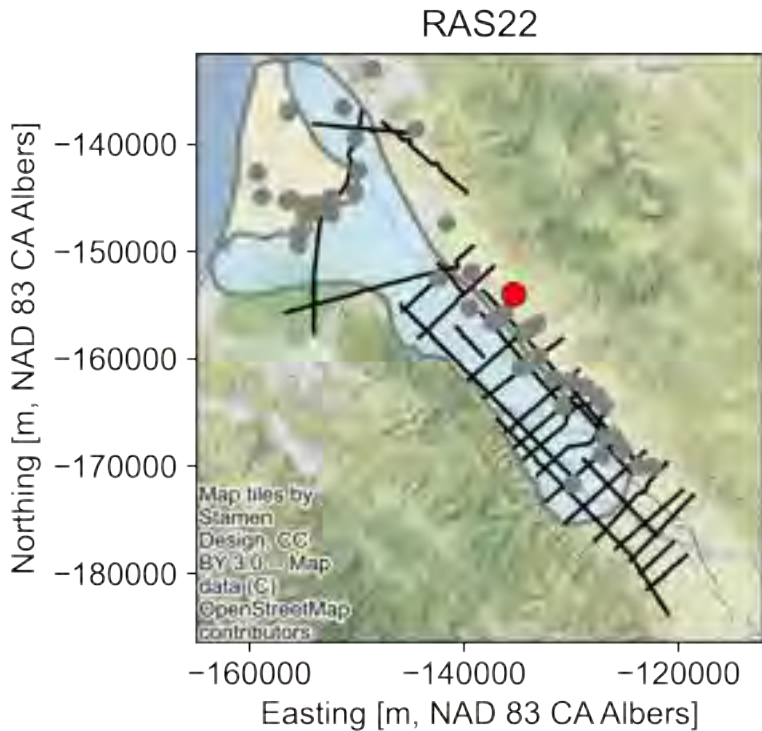
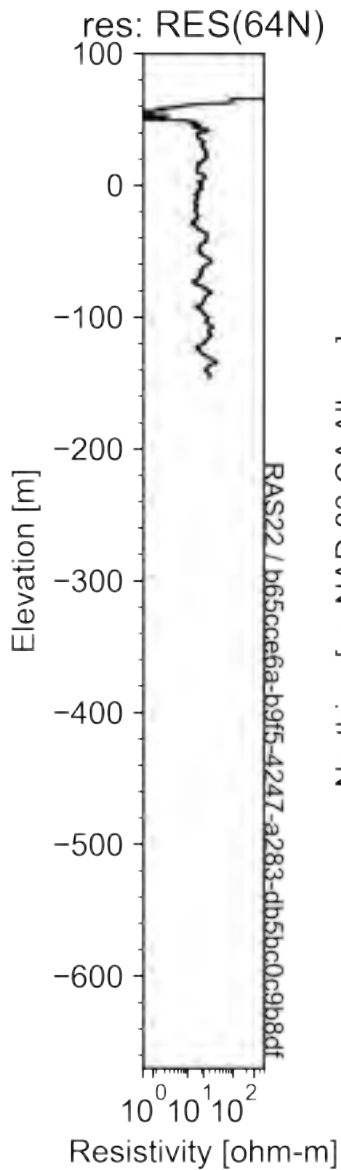


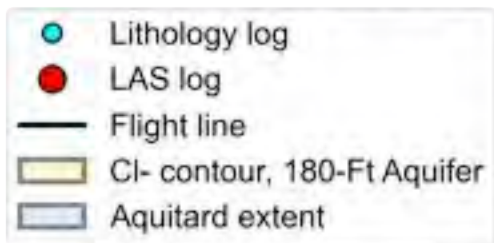
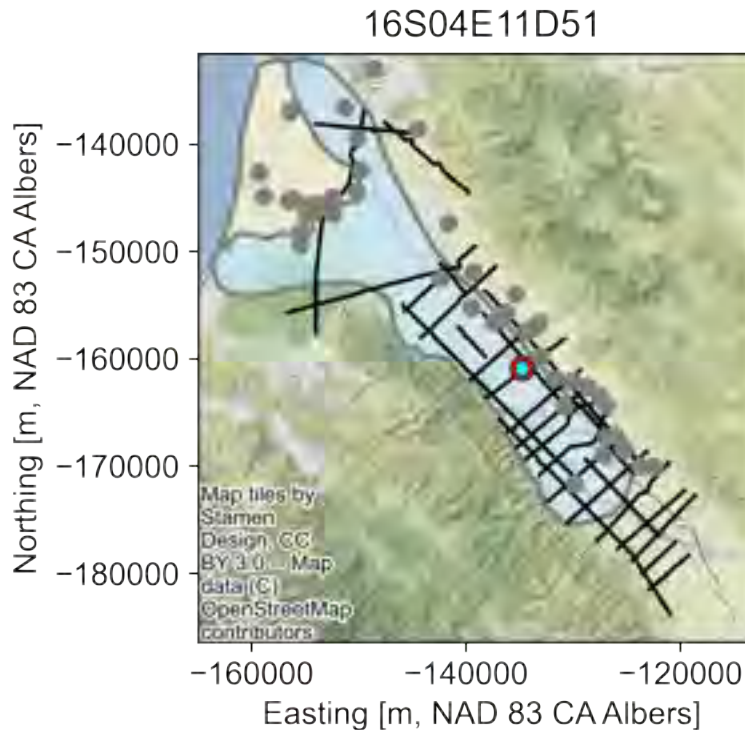
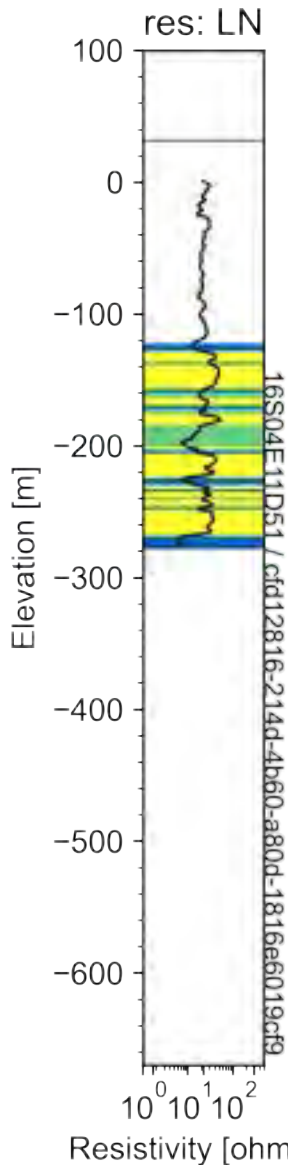


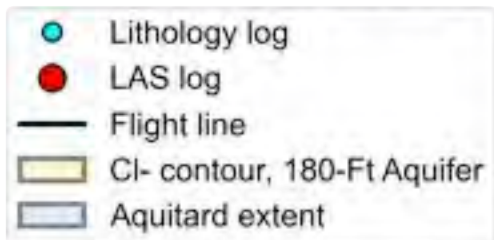
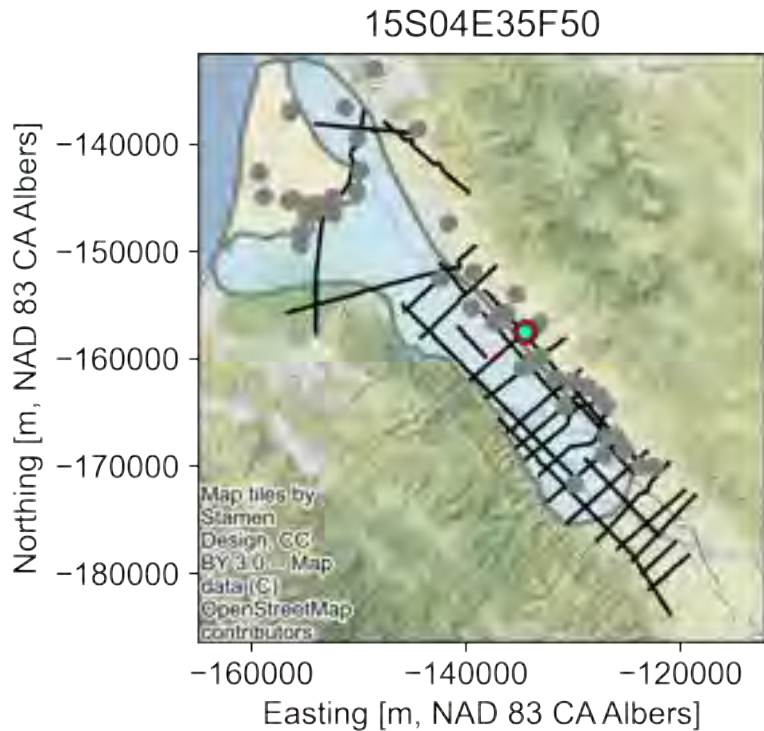
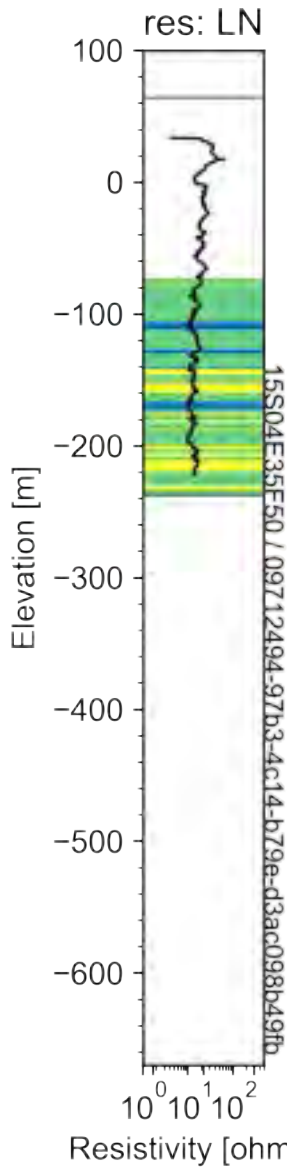


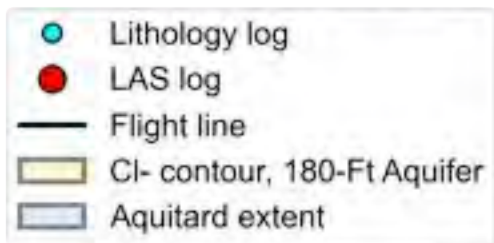
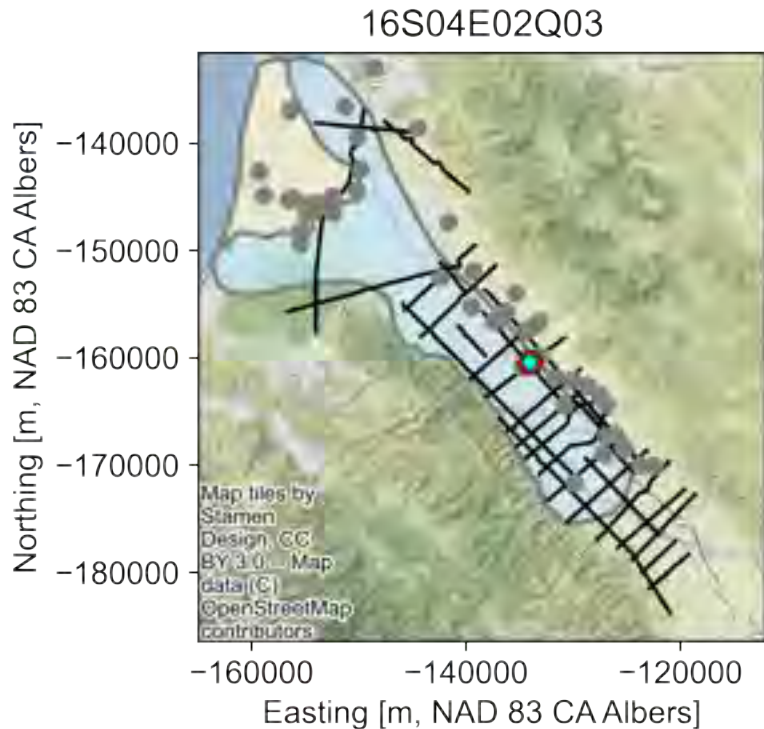
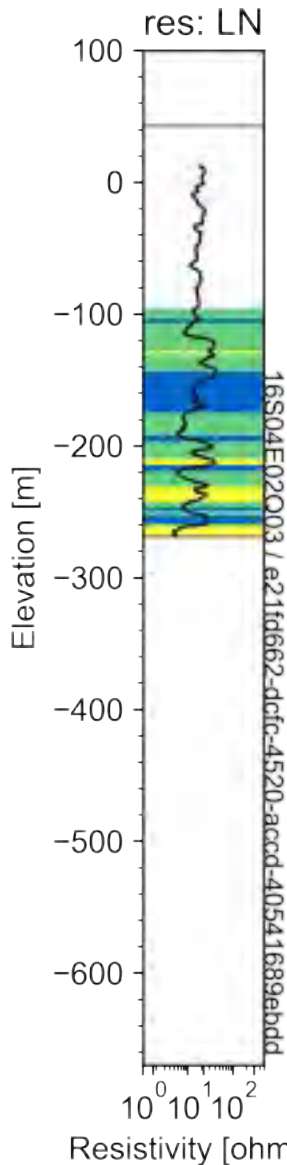
- Lithology log
- LAS log
- Flight line
- Cl- contour, 180-Ft Aquifer
- Aquitard extent

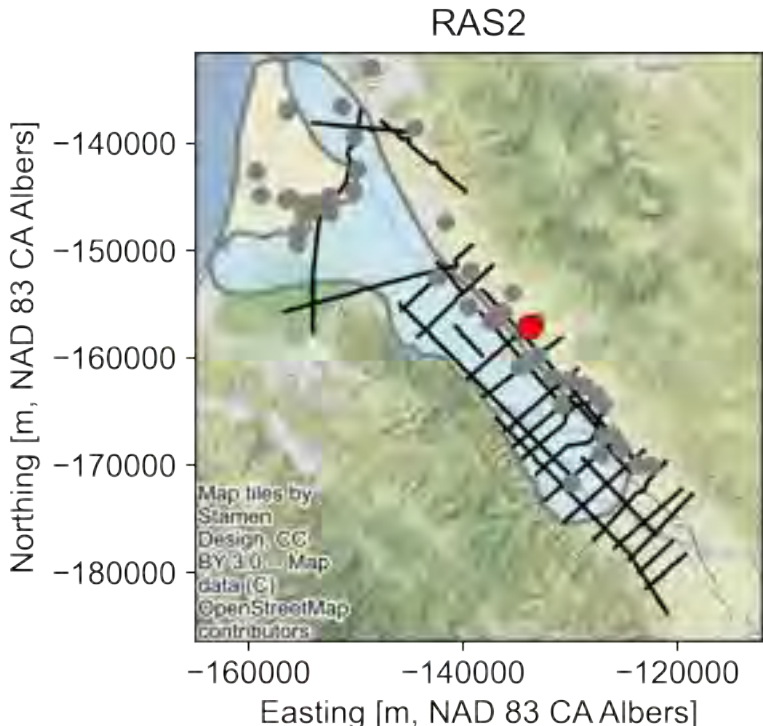
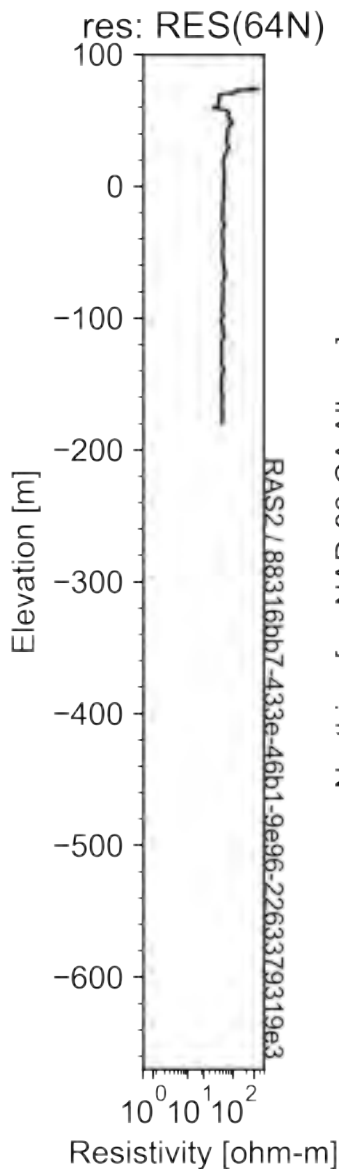




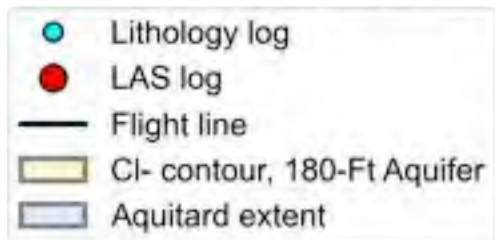
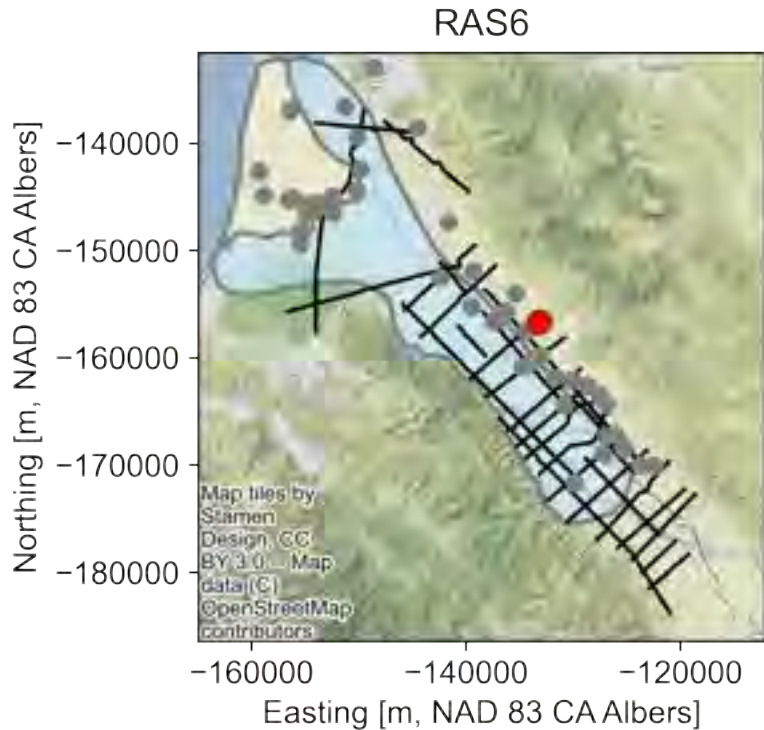
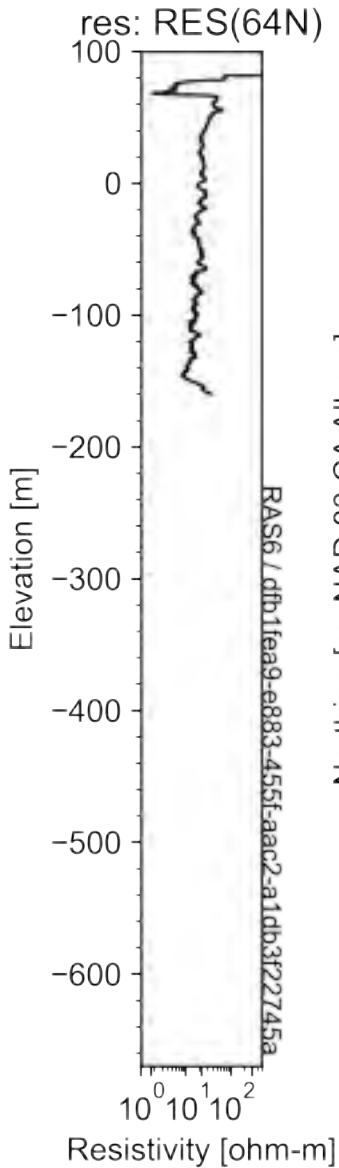


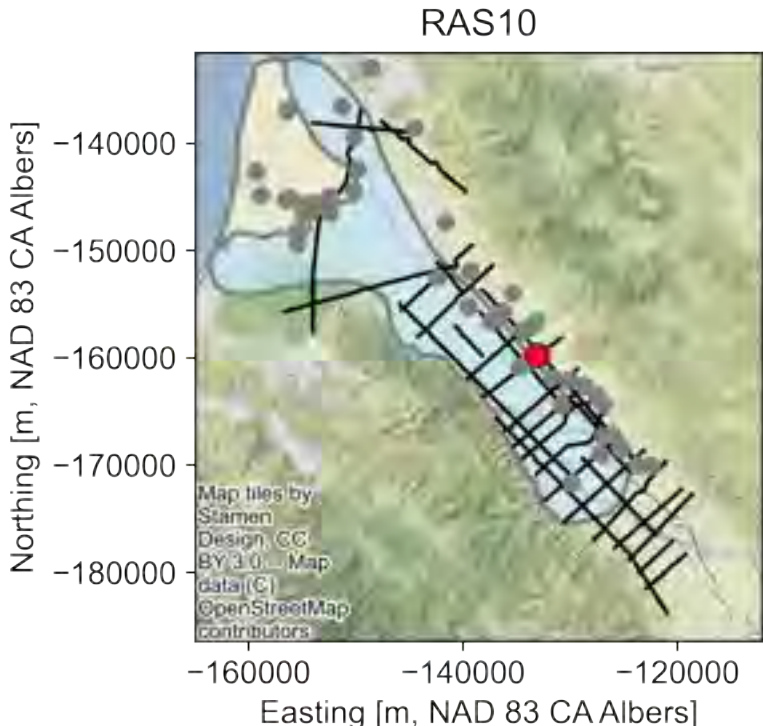
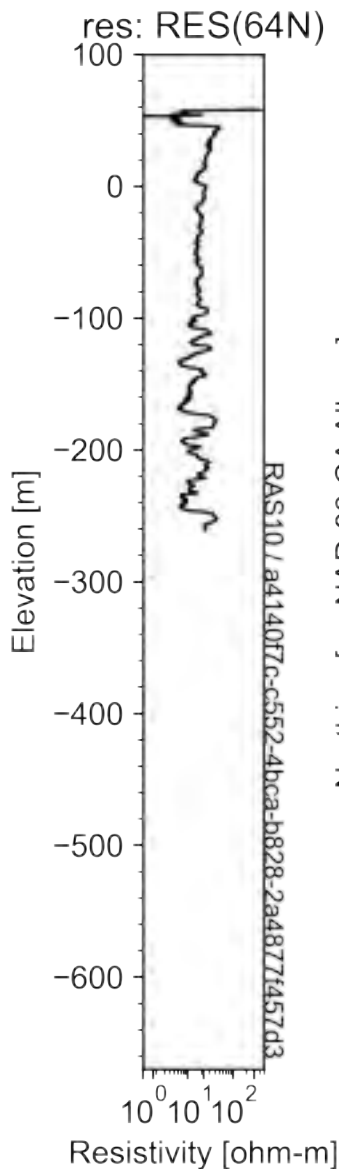




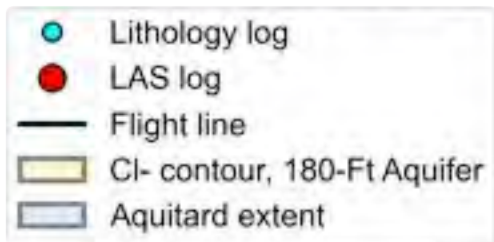
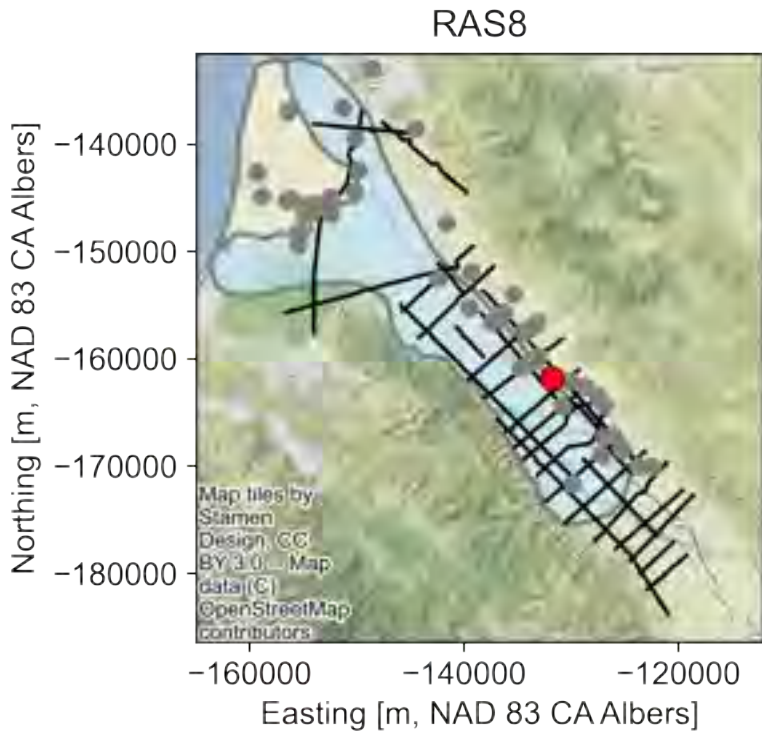
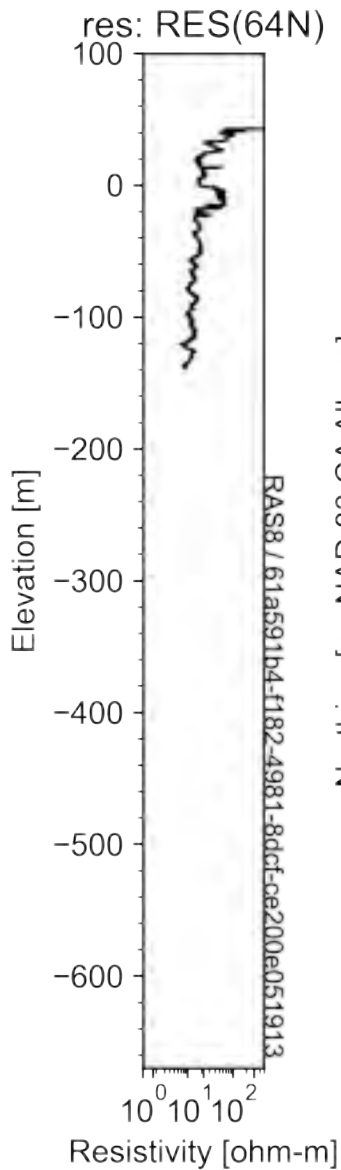


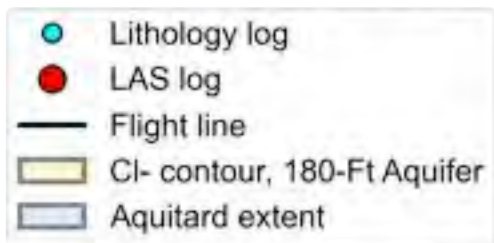
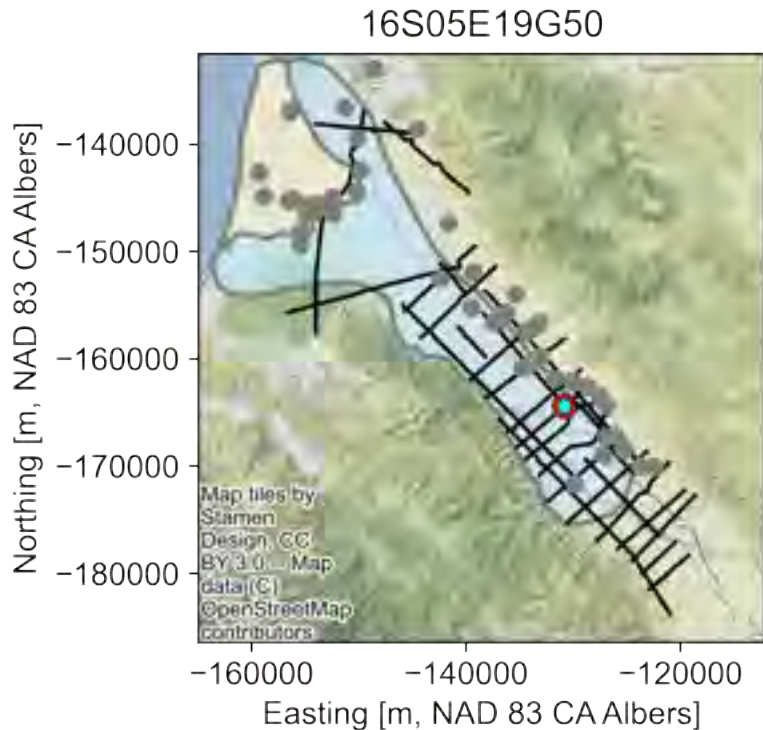
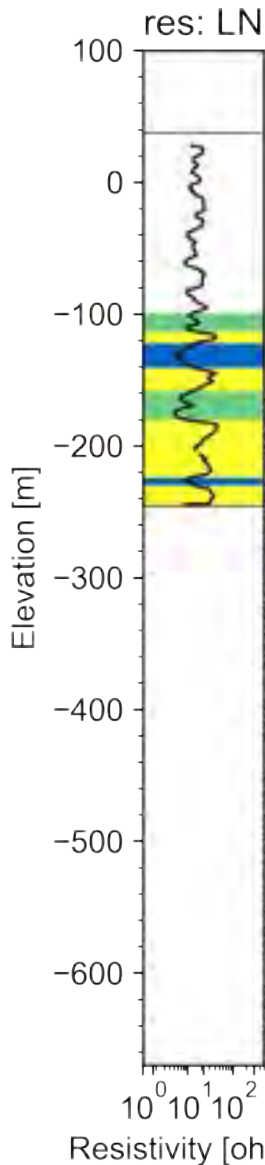
- Lithology log
- LAS log
- Flight line
- Cl- contour, 180-Ft Aquifer
- Aquitard extent

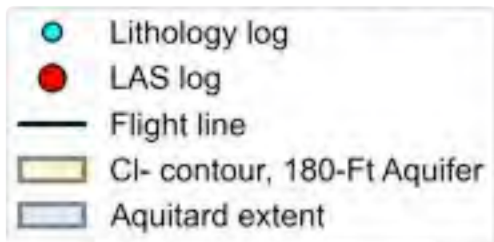
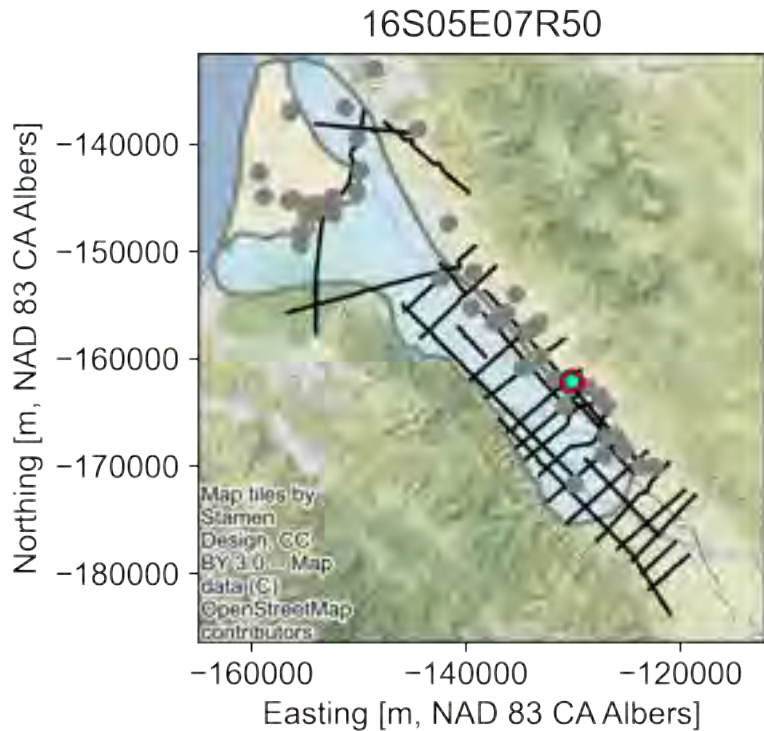
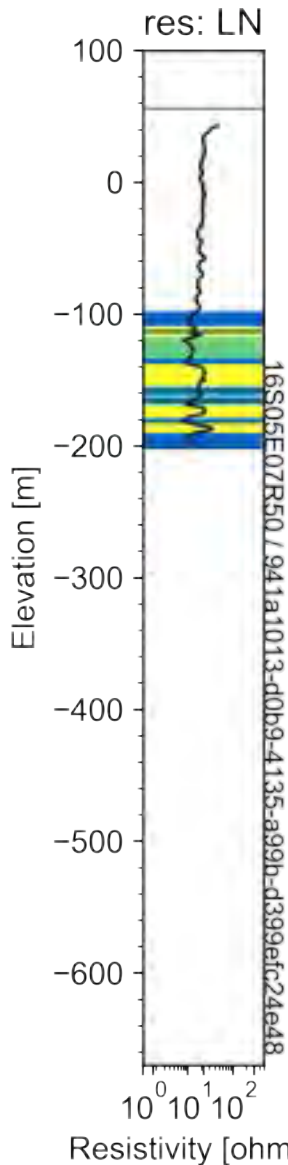


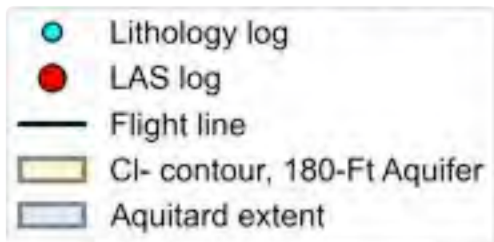
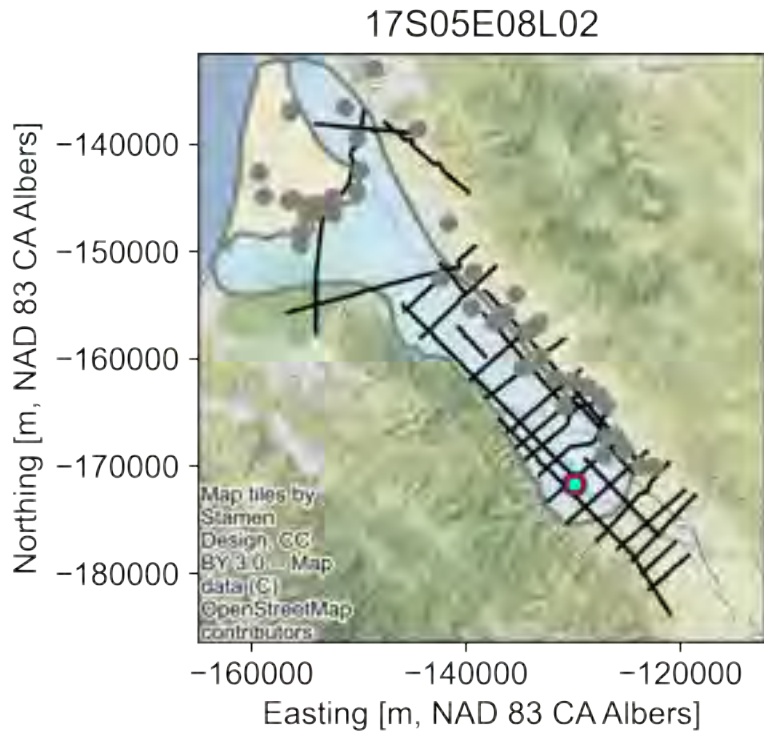
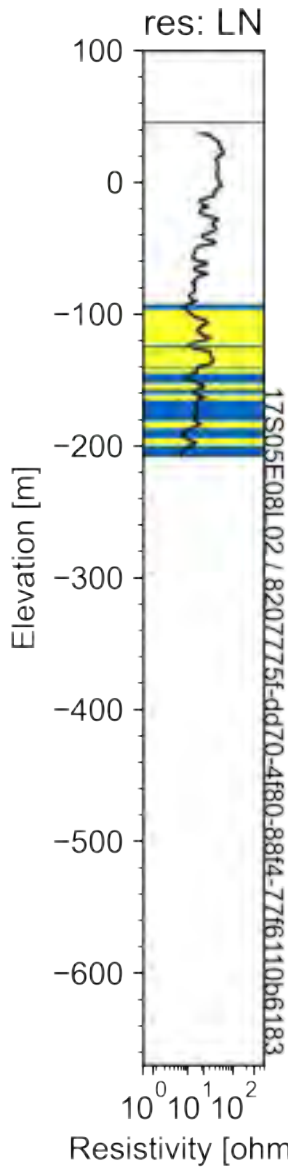


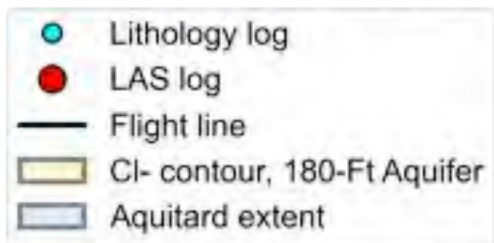
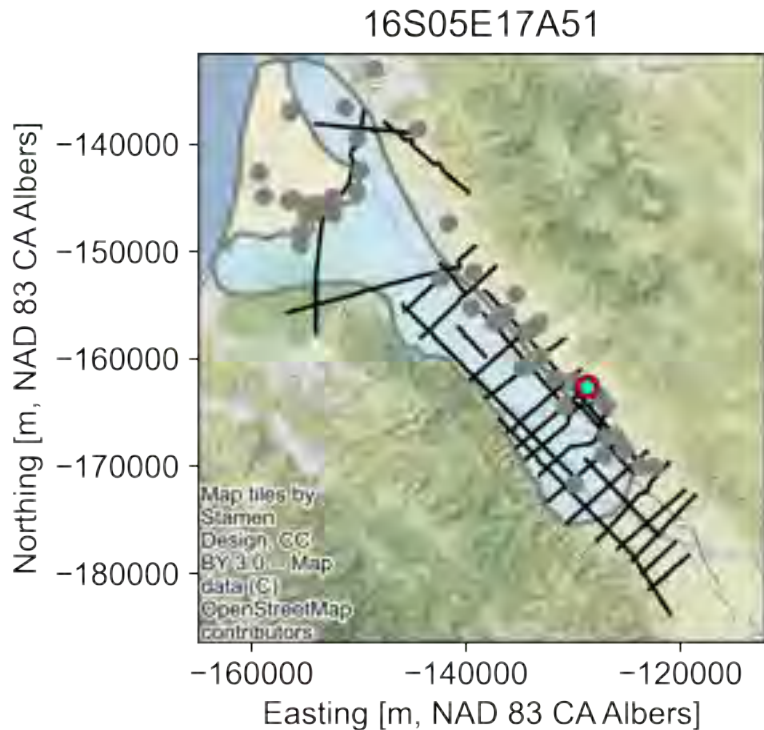
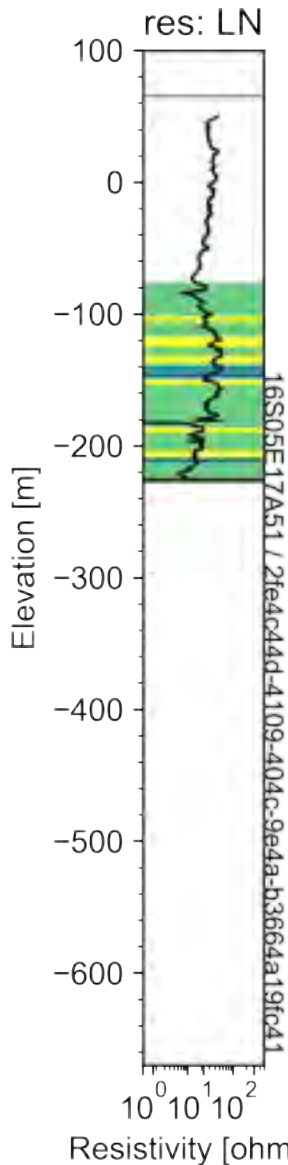
- Lithology log
- LAS log
- Flight line
- CI- contour, 180-Ft Aquifer
- Aquitard extent

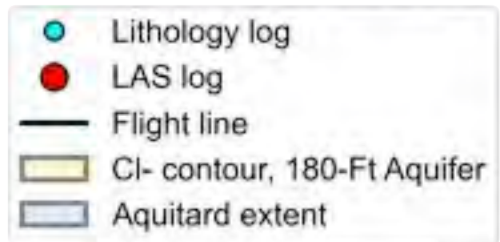
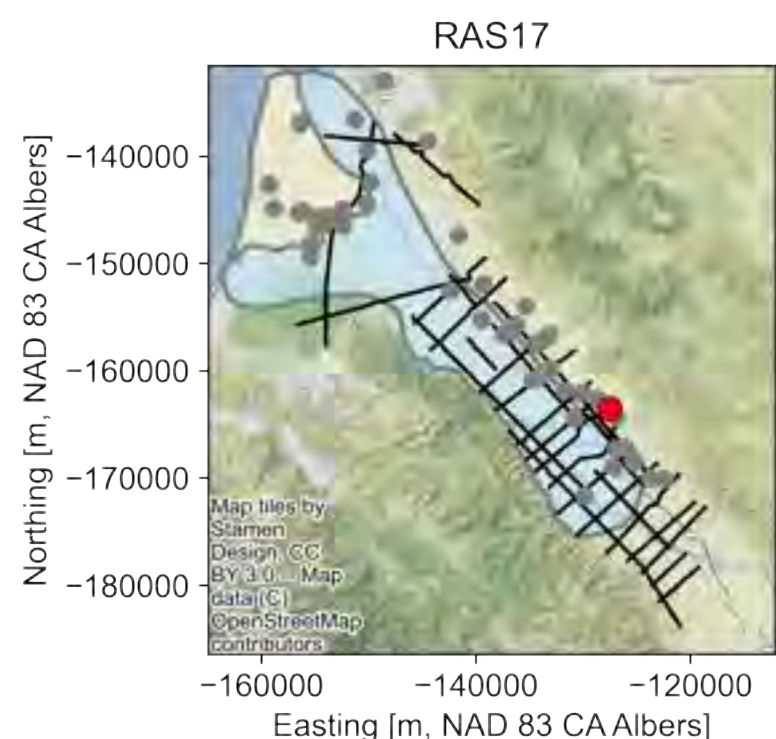
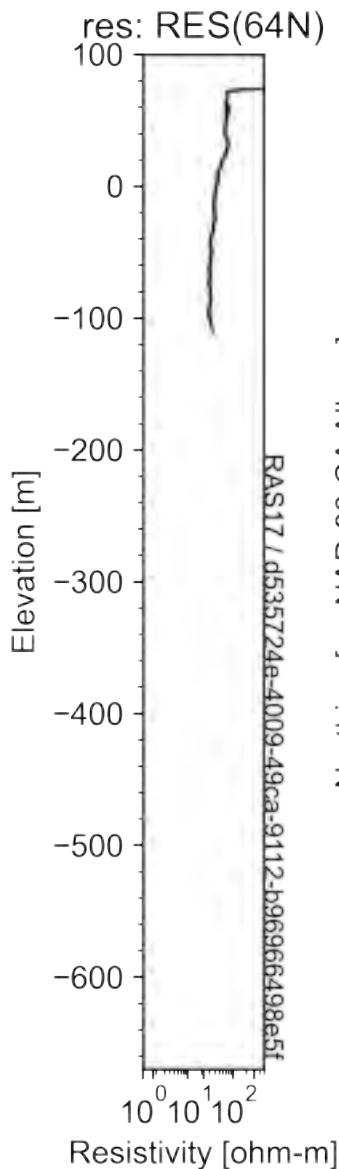


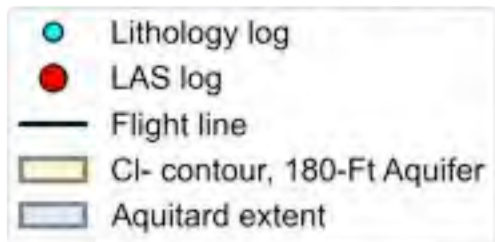
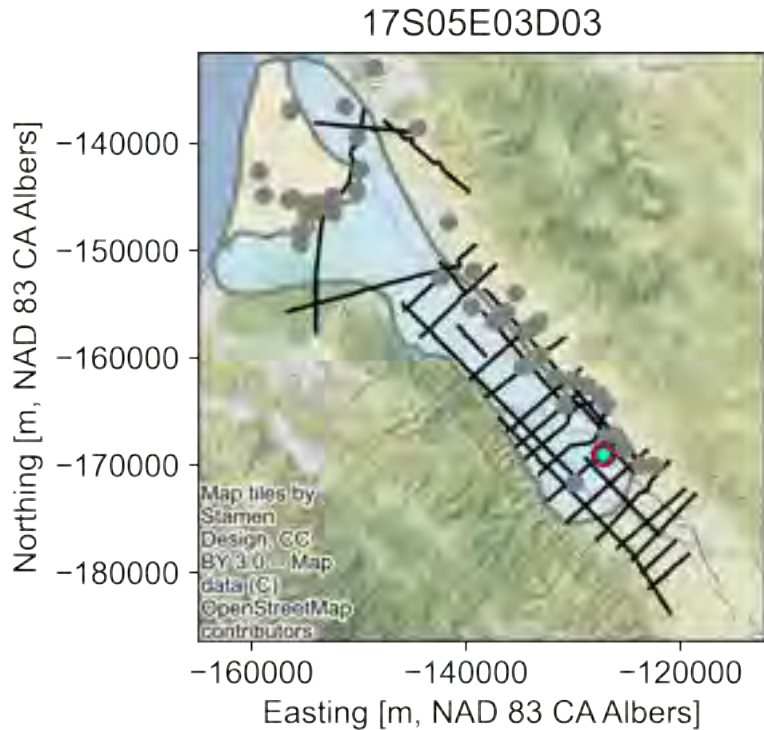
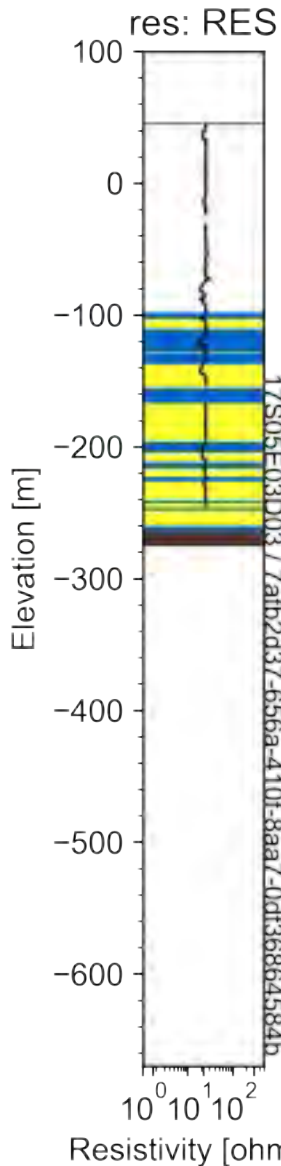


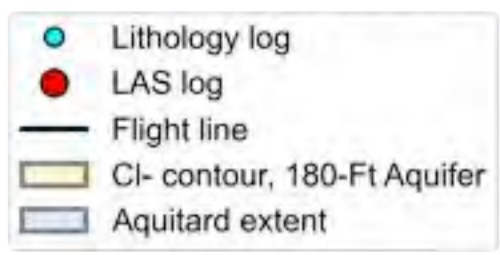
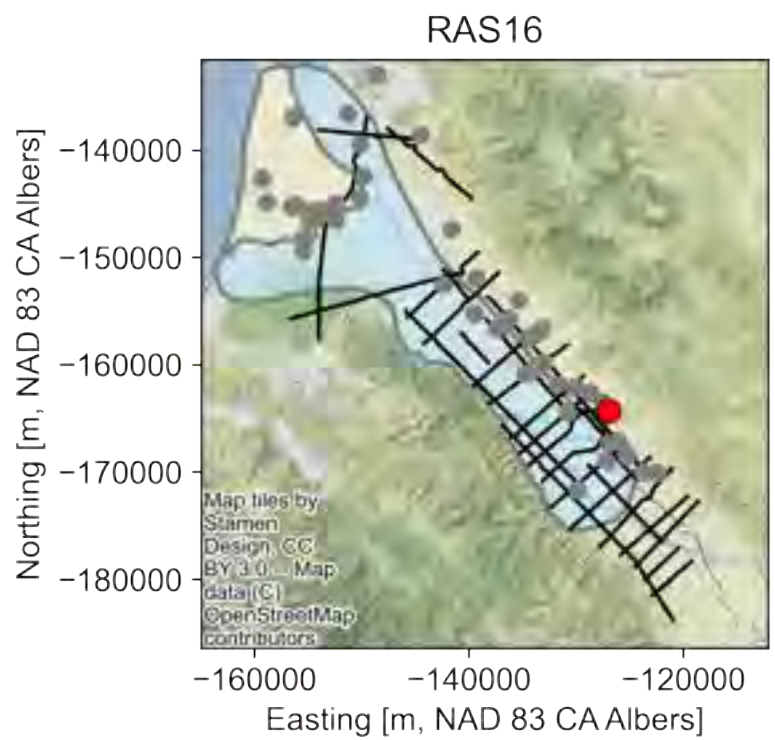
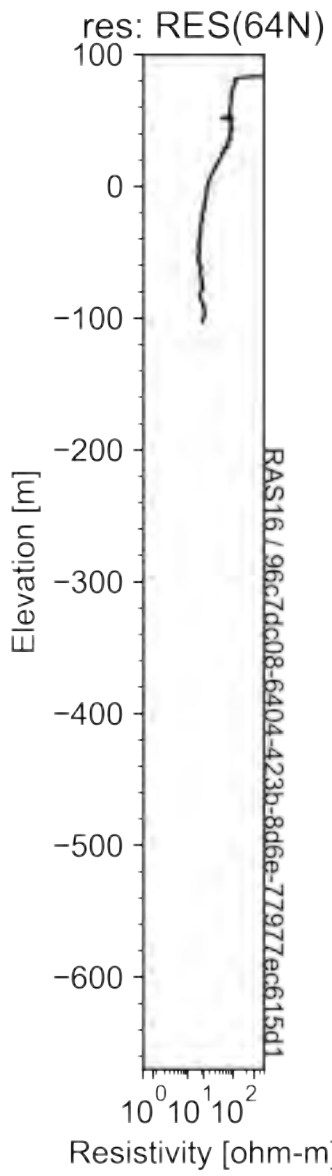


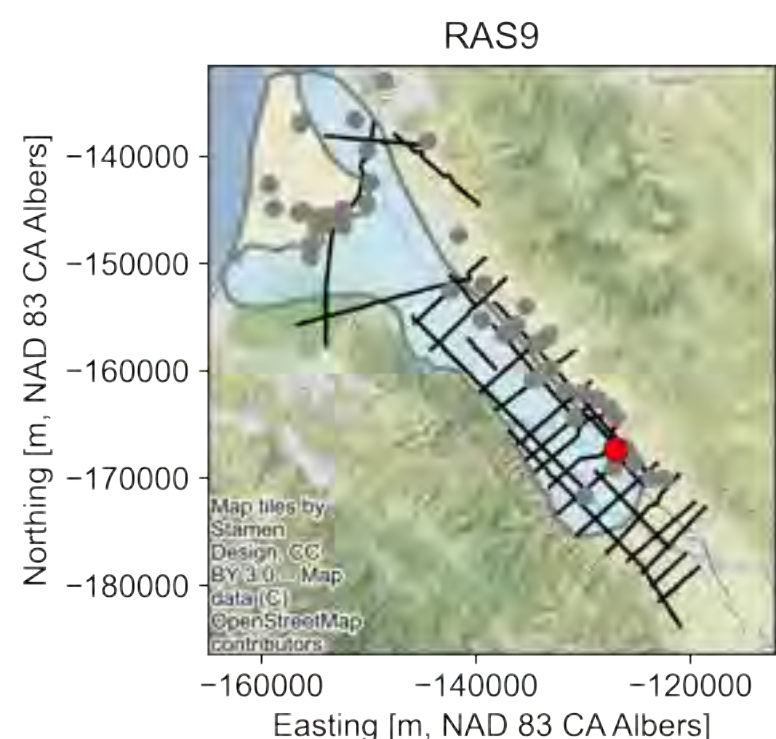
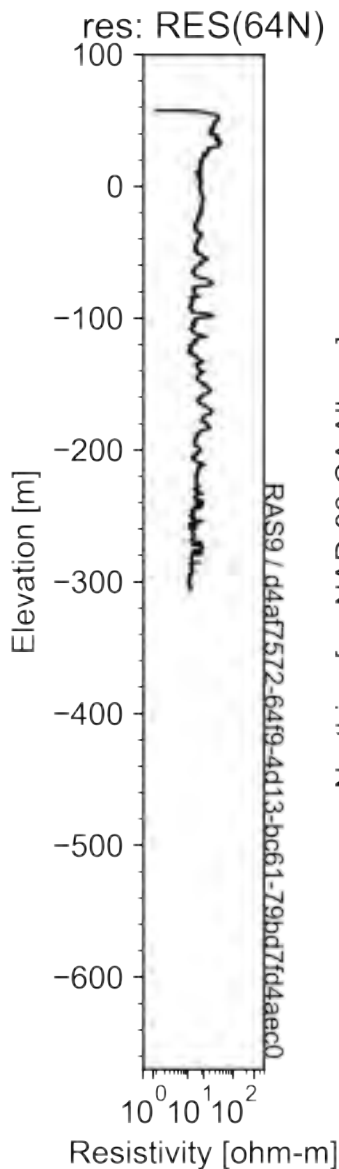




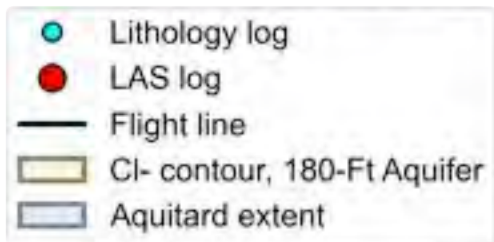
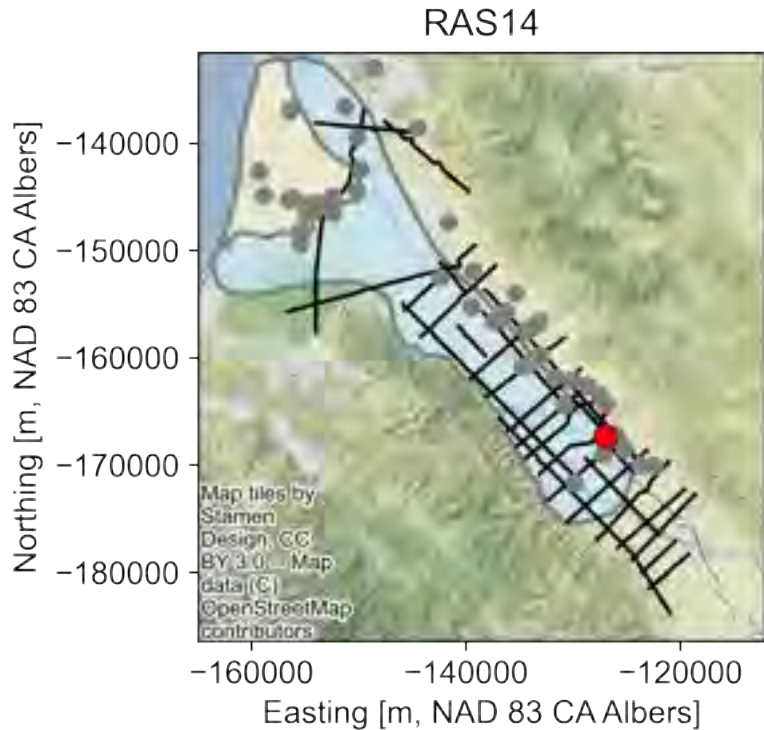
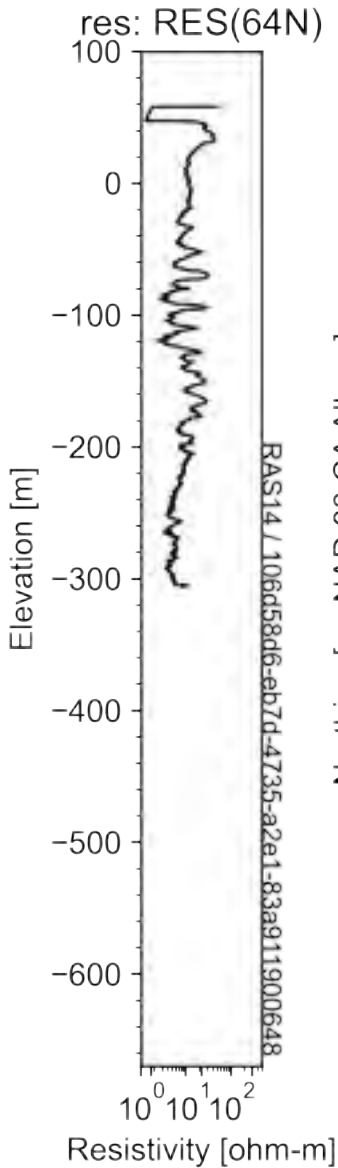


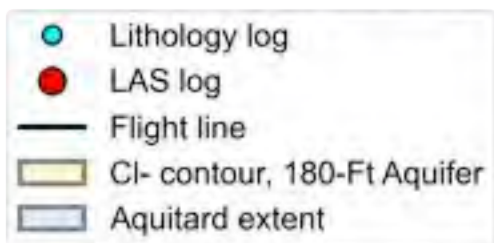
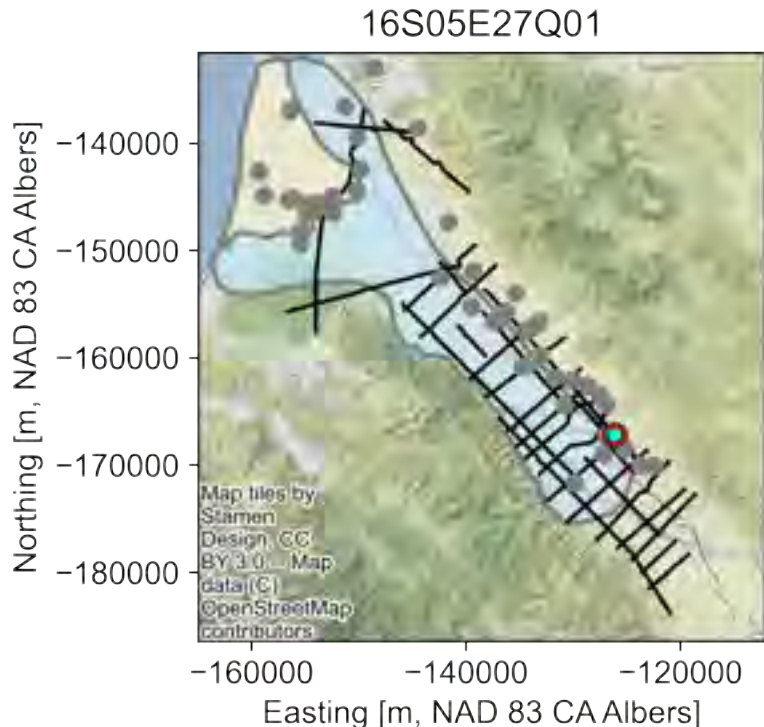
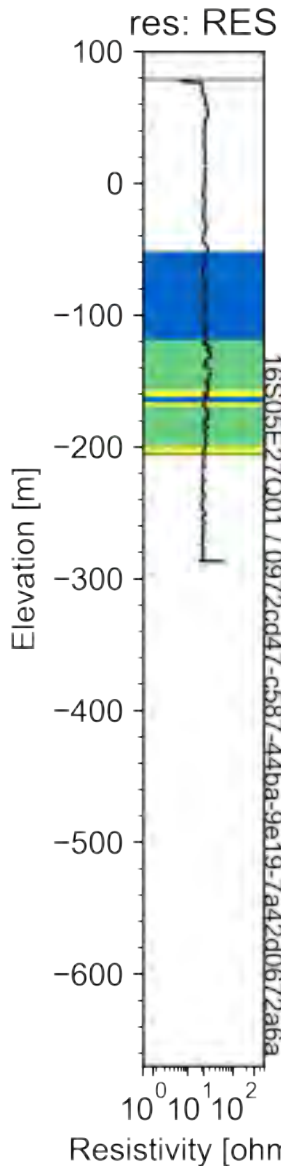


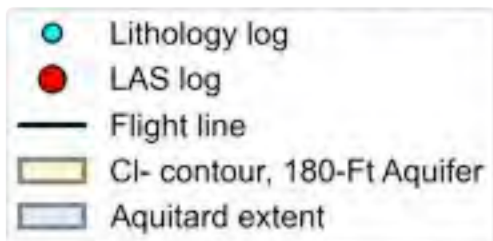
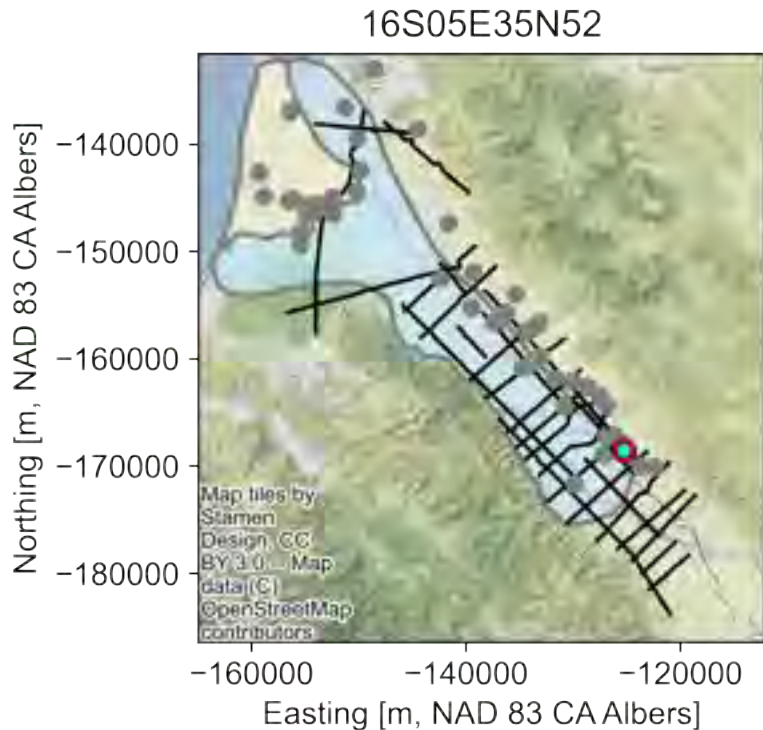
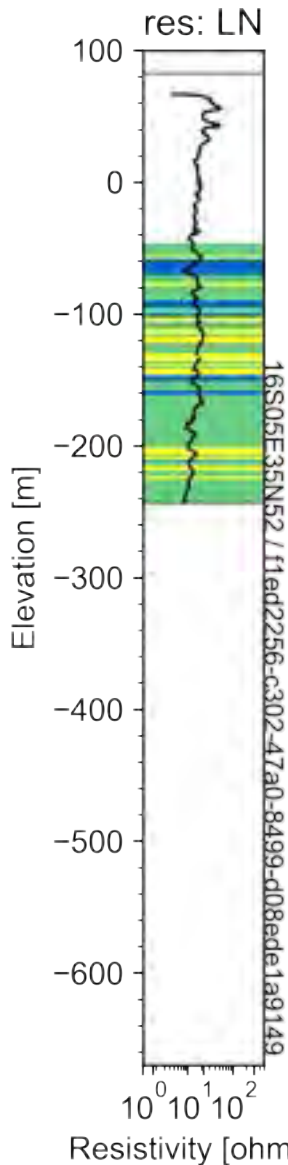


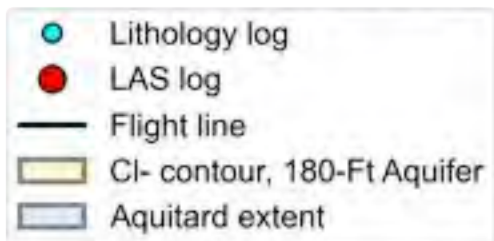
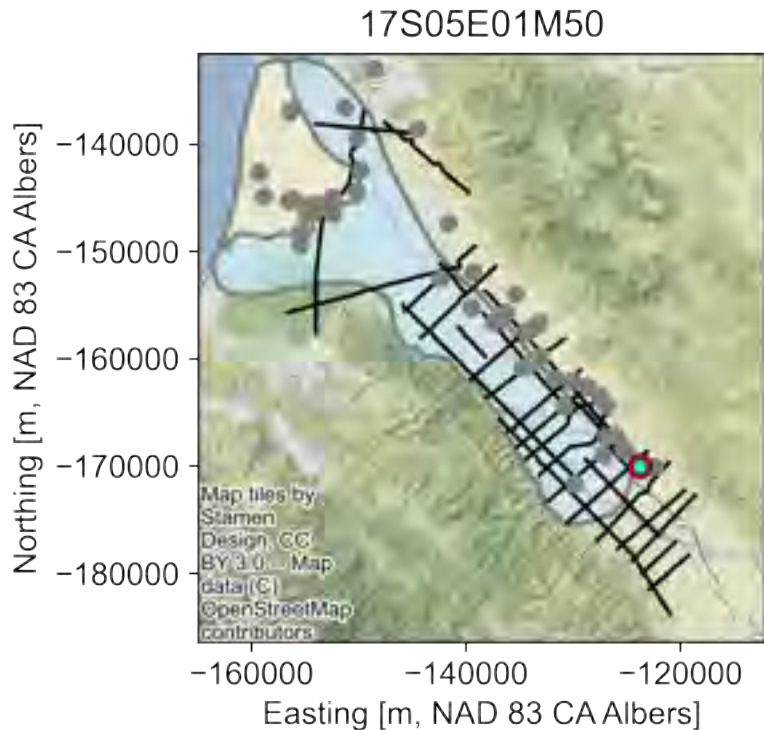
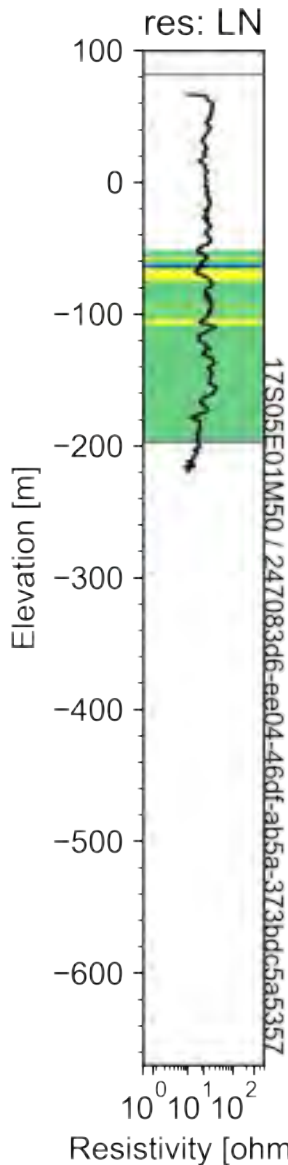


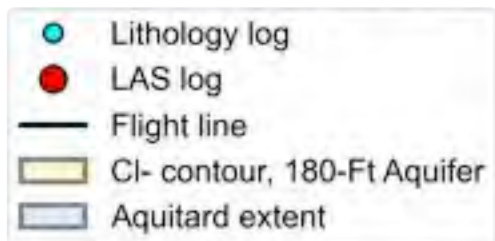
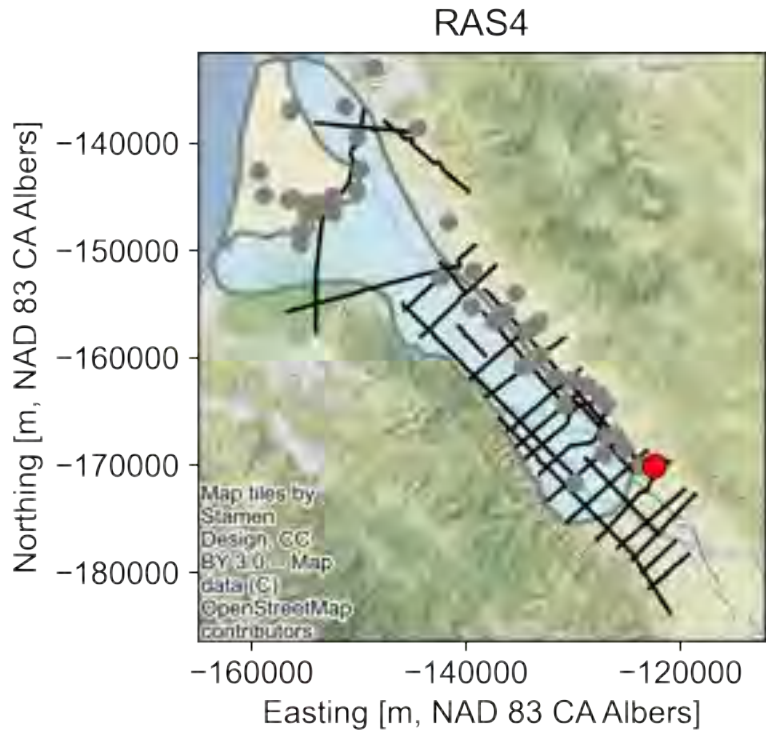
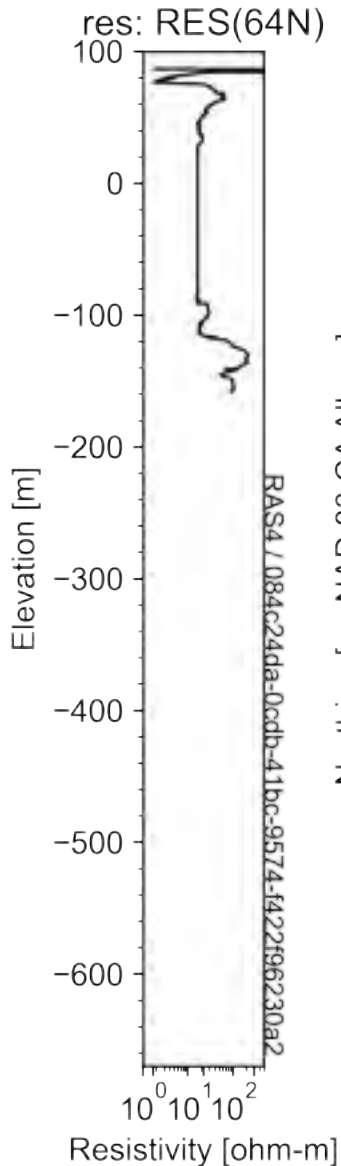
- Lithology log
- LAS log
- Flight line
- Cl- contour, 180-Ft Aquifer
- Aquitard extent











Appendix 2  
SkyTEM Data Report

# DATA REPORT

## SkyTEM Survey: Salinas, California

Client: Ramboll US Consulting, Inc

Date: March 2023



## Structure of the Digital Data Delivery catalogue

Folder	Sub folder	Sub folder	File format	Content
01_Data	01_GDB		.gdb (Geosoft database)	Data
	02_Workbench	01_XYZ 02_GEX 03_ALC	*.XYZ *.gex, *.SR2 *.ALC	EM and Auxiliary data files for Workbench processing
02_MapsGridsGIS	01_FlightPath 02_Grids 03_VD1_CSV		.shp .grd (Geosoft grids)  .csv .Tiff (GeoTiff)	Flown and planned lines. PLNI and Magnetic data (TMI, RMF, 1 <sup>st</sup> vertical derivative)
03_Report			.docx, .pdf	Data report

# Contents

Contents .....	3
Abbreviations Table .....	4
Executive Summary.....	5
Introduction .....	6
Survey outline .....	7
Line Numbering .....	7
Flight Parameters .....	10
Flight Reports.....	11
High Altitude Flights .....	11
Reference Lines .....	11
Instruments .....	12
Airborne unit.....	12
Instrument positions.....	13
Magnetometer airborne unit .....	15
Inclination .....	15
Altimeter.....	16
Ground base stations.....	17
DGPS base station .....	17
Magnetometer base station .....	17
Transmitter .....	18
Receiver system.....	19
Waveform .....	21
Data Acquisition .....	25
Gate times.....	26
Digital Data .....	30
Workbench Input File Description.....	32
Data processing .....	33
Auxiliary data .....	33
Magnetic data.....	37
EM data .....	42
B-field .....	43
Power Line Noise Intensity (PLNI) .....	43

## Abbreviations Table

$\mu$ s:	microsecond
A/Amp:	Ampere
Base Station:	ground monitoring station used to correct or verify data.
dB/dt:	change in amplitude of magnetic field over the time it takes to make that change.
C:	degrees Celsius
DGPS:	Differential Global Positioning System
EM:	Electromagnetic
Gate Time:	A small amount of time over which the amplitude of the decaying magnetic field is measured and output as a data channel.
GDB:	Geosoft database
GMT:	Greenwich Mean Time
GNSS:	Global Navigation Satellite System
HA:	High Altitude, a flying height such that the return ground EM signal is greatly reduced or eliminated.
HM:	High Moment EM dB/dt data
Hz:	Hertz
IGRF:	International Geomagnetic Reference Field
l-km:	Line kilometre
LM:	Low moment EM dB/dt data
Km	Kilometres
Kph:	Kilometres per hour
masl:	metres above sea level
m:	metre
NIA:	Strength of generated EM field, i.e. dipole moment. Where $I$ is the current in the transmitter, $A$ is the area of the transmitter and $N$ is the number of turns of wire
nT:	nano Tesla
PFC:	Primary Field Compensation
PLNI:	Power Line Noise Intensity
PPP:	Precise Point Positioning (GPS)
pV:	pico Volts
RX:	EM Receiver
TEM:	Time-domain (transient) Electromagnetic
TX:	EM Transmitter
UTC:	Coordinated Universal Time
UTM:	Universal Transverse Mercator coordinate system
V:	Volts
X data:	Measurement of the horizontal component of the secondary magnetic field
Z data:	Measurement of the vertical component of the secondary magnetic field
$\rho$ :	Resistivity
$\Omega$ :	Ohm

# Executive Summary

This report covers data acquisition, technical specifications, data processing and presentation of data results for the SkyTEM312HPM survey flown on March 1st to March 2nd, 2023 in the Salinas, California. The survey is comprised of 1 block with a total of 300.3 km planned flight lines.

All planned lines were covered during the survey, giving a total number of flown km for the entire work order as 300.3 km.

The SkyTEM312HPM collects time domain electromagnetic and magnetic data along with supporting navigation measurements.

All material is delivered digitally. The final product includes:

- Data report
- Data files (GDB and XYZ)
- Workbench input files
- Processed data in a Geosoft database
- Grids in Geosoft format

An overview of the digital data delivery can be seen on the inside of the front cover of this report.

## Introduction

The SkyTEM electromagnetic (EM) and magnetic survey described in this report was requested by Ramboll US Consulting, Inc and performed by SkyTEM Canada Inc using the SkyTEM312HPM system. Basic survey information and key personnel are listed in Table 1.

The report covers survey specifications, data acquisition, instrument specifications, data processing and various images of the system. The data delivery includes raw and processed electromagnetic data, magnetic data, positional data, and input files for Workbench software. The digital data delivery folder is described on the inside of the front cover of this report.

This report does not include any geological interpretations of the geophysical dataset.

<b>Ramboll US Consulting, Inc (Client)</b>	
Client Contact person	Mr Ian Gottschalk Email: IGOTTSCHALK@ramboll.com
<b>SkyTEM Canada Inc. (Contractor)</b>	
Contact person	Ms Mandy Long Email: mlo@skytem.com
Project Manager	Steve Startor Email: ssa@skytem.com
Field Crew	Mr Poul Mousten Sørensen Mr Dominic Leblanc Mr Louis-Philippe Chénard
<b>Helicopter operator</b>	Sinton Helicopter
Helicopter type	Eurocopter Astar 350 B3
Pilot	Mr Haydn Gaw Mr Scot Sinton
Data acquisition period	March 1st to March 2nd, 2023
Data processing and report	Mr Rasmus Teilmann

*Table 1 Key personnel and survey information.*

## Survey outline

The survey areas are positioned near Salinas, California, USA. The planned survey lines have an irregular layout of varying line spacing and direction. Flight line details for the survey are listed in Table 2 and Table 3. The survey was flown from March 1st to March 2nd, 2023.

The coordinate system NAD83 / California Albers (EPSG 3310) was used throughout this report, and in the data delivery.

Area name	Line spacing (m)	Line direction (deg)	Tie line spacing (m)	Flight lines (km)	Tie lines (km)	Total line kilometers (km)
Salinas	Varying	Varying	Varying	<b>300.3 km</b>	0	<b>300.3 km</b>
<b>Flown in total</b>						<b>300.3 km</b>

*Table 2 Survey line details.*

The survey area is comprised by 1 block with lines of different spacings and directions as shown in Figure 1.

The actual surveyed lines are shown in as red lines in Figure 2

## Line Numbering

The line numbering system uses the following six-digit convention:

- The first 6 digits represent the unique line number.
- Test lines begin with a 92 for reference lines and 93 for high altitude bias lines.

Area	Line numbering	Tie line numbering
Salinas SW-NE	100101 – 101801	N/A
Salinas NW-SE	200101 – 200901	N/A
Ref lines	920001 – 920003	N/A
High Altitude line	930002	N/A

*Table 3 Line numbering.*

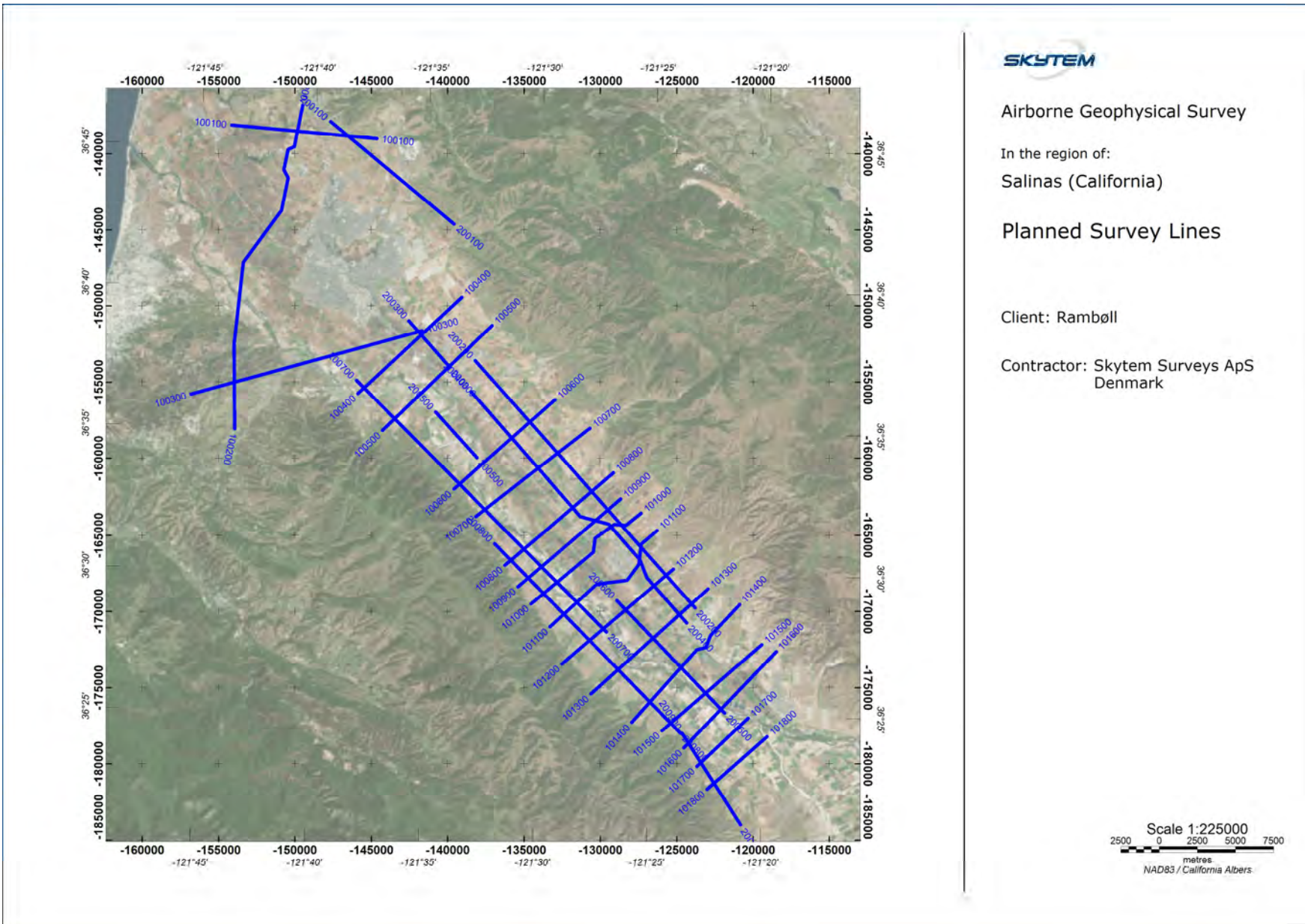
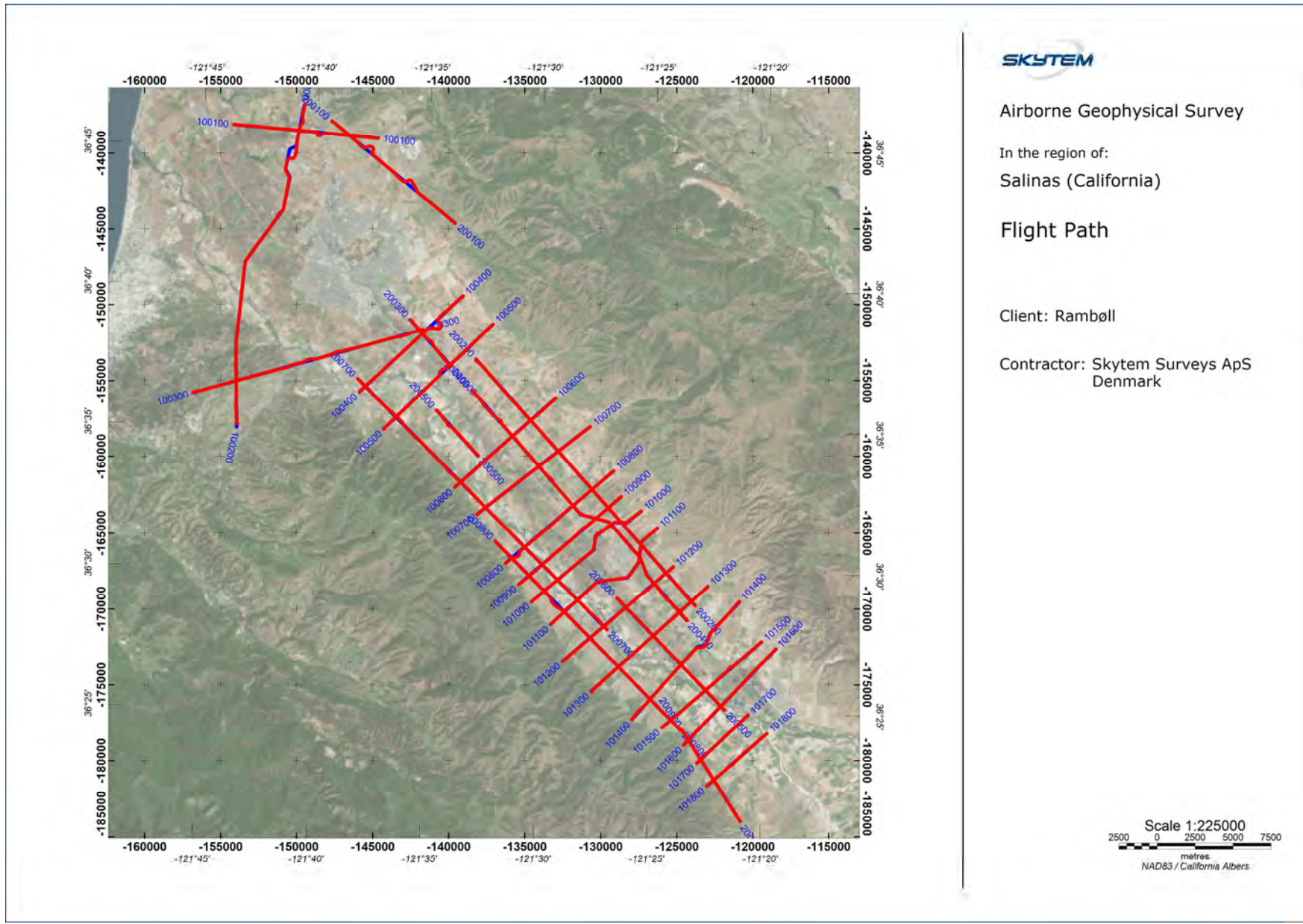


Figure 1. Planned lines (Blue).



Airborne Geophysical Survey

In the region of:  
Salinas (California)

Flight Path

Client: Rambøll

Contractor: Skytem Surveys ApS  
Denmark

Figure 2. Flown lines (Red) on top of planned lines (Blue)

## Flight Parameters

The nominal terrain clearance is 30 - 40 m, with a potential increase due to steep terrain, forests, power lines and any other obstacles or hazards on the ground. The safe flying height during the survey is always based on the pilot's assessment of risk and deviations from nominal values are at the discretion of the pilot.

The nominal production airspeed is 60 - 80 kph for a flat topography with no wind. This may vary in areas of rugged terrain and/or windy conditions.

Average values and standard deviations of survey flight parameters are found in Table 4.

Control parameter		Average Value	Standard Deviation
Ground speed*)		67.7 kph	14.7 kph
Processed height		38.1 m	13.5 m
Tilt angle	X	0.8 degrees	2.4 degrees
	Y	-0.3 degrees	1.1 degrees
Low Moment Current		6.0 A	0.03 A
High Moment Current		223.5 A	6.2 A

\*) Actual speed varies as a function of day and flight direction due to different wind directions and magnitude.

Table 4 Flight parameters for Salinas.

## Flight Reports

For each flight, a report with key information regarding the data acquisition is made in the field. Listed in the reports are details on the weather, special data parameters and other events which may influence data. Details of the reports are shown in Table 5 and Table 6.

Flight	Temperature (C)	Wind (m/s)	Visibility
20230221.01	-	-	-
20230222.01	-	-	-
20230222.02	8	5W	Excellent
20230225.01	8	5W	Excellent
20230227.01	-	-	-
20230301.01	5	2S	Excellent
20230302.01	5	2NW	Excellent
20230302.02	3	1E	Excellent

Table 5 Weather report.

Flight	Comments
20230221.01	400 m - Calibration flight
20230222.01	1000 m - Calibration flight
20230222.02	400 m - Calibration flight
20230225.01	Ferry to Salinas
20230227.01	1000 m and ref line
20230301.01	Production
20230302.01	Production
20230302.02	Production

Table 6 Flight report.

## High Altitude Flights

High altitude tests were flown at approximately 1000 m above terrain or high enough to negate the ground signal prior to production.

## Reference Lines

In conjunction with every production flight a reference line was flown of a minimum 1 km length. This was established to ensure repeatability of the SkyTEM system during the survey period.

## Instruments

This section provides an overview of airborne as well as ground base instruments.

### Airborne unit

The airborne instrumentation comprising a SkyTEM312HPM system includes a time domain electromagnetic system, a magnetic data acquisition system and an auxiliary data acquisition system containing two inclinometers, two altimeters and two DGPS'. All instruments are mounted on the frame which is suspended ~40 m below the helicopter. The generator used to power the transmitter is suspended between the frame and the helicopter approximately 20 m below the helicopter. A picture of the airborne SkyTEM312HPM unit is seen in Figure 3, and a sketch of the instrumentation is seen in Figure 4.



*Figure 3 SkyTEM312HPM Airborne unit.*

## Instrument positions

The instrumentation involves a time domain electromagnetic system, two inclinometers, two altimeters and two DGPS'.

The measurements were carried out, using a setup as described below.

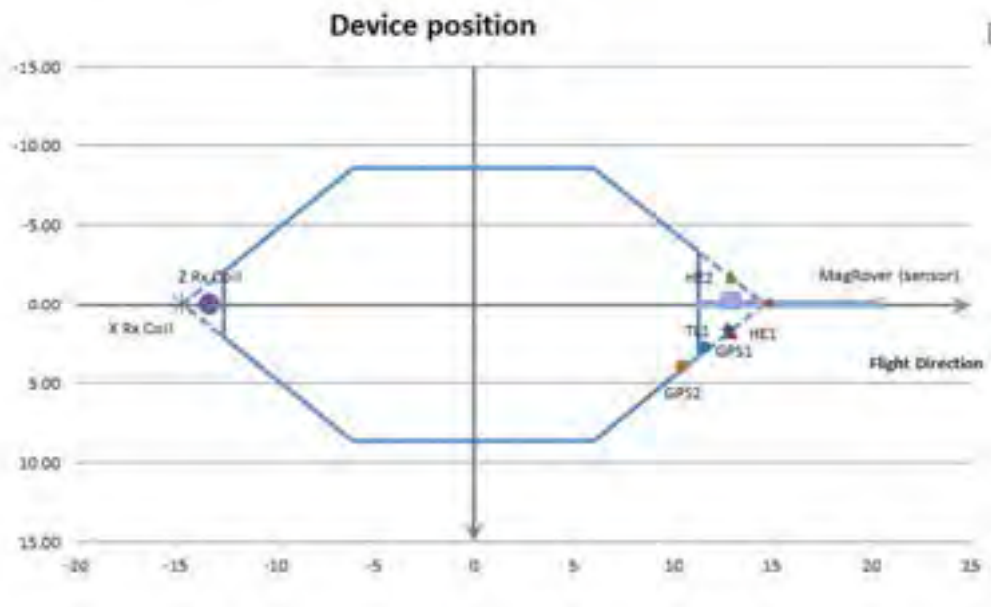


Figure 4 Sketch showing the frame and the position of the basic instruments. The blue line defines the transmitter loop. The horizontal plane is defined by  $(x, y)$ .

The location of instruments in respect to the frame shown in Figure 4 is given in  $(x, y, z)$  coordinates in Table 7 below.

$X$  and  $y$  define the horizontal plane.  $Z$  is perpendicular to  $(x, y)$ .  $X$  is positive in the flight direction,  $y$  is positive to the right of the flight direction, and  $z$  is positive downwards.

The generator used for powering of the transmitter is  $\sim 20$  m below the helicopter.

<b>Device</b>	<b>X</b>	<b>Y</b>	<b>Z</b>
DGPS1 (EM)	11.68	2.79	-0.16
DGPS2 (EM)	10.51	3.95	-0.16
HE1 (altim.)	12.94	1.79	-0.12
HE2 (altim.)	12.94	-1.79	-0.12
Inclinometer 1	12.79	1.64	-0.12
Inclinometer 2	12.79	1.64	-0.12
RX (Z Coil)	-13.65	0.00	-2.00
RX (X Coil)	-14.65	0.00	0.00
Mag sensor	20.50	0.00	-0.56

*Table 7 Position of instrumentation on the system frame.*

# Magnetometer airborne unit

Instrument type: Geometrics G822A sensor and Kroum KMAG4 counter.

The Geometrics G822A sensor and Kroum KMAG4 counter is a high sensitivity Cesium magnetometer. The basic of the sensor is a self-oscillating split-beam Cesium vapor (non-radioactive) Principle, which operates on principles similar to other alkali vapor magnetometers.

The sensitivity of the Geometrics G822A sensor and Kroum KMAG4 counter is stated as  $<0.0005 \text{ nT}/\sqrt{\text{Hz}}$  rms. Typically 0.002 nT P-P at a 0.1 second sample rate, combined with absolute accuracy of 3 nT over its full operating range.

The magnetometer is synchronized with the TEM system. When the TEM signal is on, the counter is closed. In the TEM off-time the magnetometer data is measured from 100 microseconds until the next TEM pulse is transmitted. The data are averaged and sampled as 30 Hz.

Parameter	Value
Sample frequency	30 Hz (in between each HM EM pulse)
Magnetometer on	HM Cycles
Magnetometer off	LM Cycles

Table 8 Airborne Magnetometer sampling

## Inclination

Instrument type: Bjerre Technology

The inclination of the frame is measured with 2 independent inclinometers. The x and y angles are measured 2 times per second in both directions. The inclinometers are placed on the frame as close to the z coil as possible, see Figure 4.

The angle data are stored as x, y readings. X is parallel to the flight direction and positive when the front of the frame is above horizontal. Y is perpendicular to the flight direction and negative when the right side of the frame is above horizontal.

The angle is checked and calibrated manually within 1.0 degree by use of a level meter.

# Altimeter

Instrument type: MDL ILM300R

Two independent laser units mounted on the frame measuring the distance from the frame to the ground, see Figure 4.

Each laser delivers 30 measurements per second and covers the interval from 0.2 m to approximately 200 m.

Dark surfaces including water surfaces will reduce the reflected signal. Consequently, it may occur that some measurements do not result in useful values.

The altimeter measurements are given in meters with two decimals. The uncertainty is 10 - 30 cm. The lasers are checked on a regular basis against well-defined targets.

<b>Laser parameters</b>	
Sample rate	30 Hz
Uncertainty	10 - 30 cm
Min/ max range	0.2 m / 200 m

*Table 9 Laser Altimeter Sample Rate*

# Ground base stations

The DGPS and magnetic base stations were positioned within the survey area.

## DGPS base station

DGPS base stations were placed at locations of maximum possible view to satellites and away from metallic objects that could influence the GPS antenna. The DGPS base stations were used as a back-up to the Precise Point Positioning (PPP) utilized on this project.

In the final PPP processing all data was processed without the use of GPS base stations.

## Magnetometer base station

Instrument type: GEM Proton.

The GEM Proton is a portable high-sensitivity precession magnetometer.

The GEM Proton is a secondary standard for measurement of the Earth’s magnetic field with 0.01 nT resolutions, and 1 nT absolute accuracy over its full temperature range. The base station data are sampled with 1 Hz frequency.

The base station magnetometer was placed in a location of low magnetic gradient.

Table 10 below shows the locations of the magnetic base station:

Magnetometer Base station	Period	Longitude	Latitude	Elevation
Salinas	20230301 – 20230302	-121.603432°	36.664833°	25 m

*Table 10 Location of the magnetic base station.*

# Transmitter

The time domain transmitter loop can be described as an octagon with the corners listed below:

X	Y
-12.64	-2.10
-6.14	-8.58
6.14	-8.58
11.41	-3.31
11.41	3.31
6.14	8.58
-6.14	8.58
-12.64	2.10

Table 11 Transmitter loop corner points

The total area of the transmitter coil defined by the corner points is 342 m<sup>2</sup> and 68.3 m in circumference.

The key parameters defining the transmitter set up listed in Table 12 and Table 13.

Parameter	Value
Number of transmitter turns	2
Transmitter area	342 m <sup>2</sup>
Peak current	6 amp
Peak moment	~4,000 NIA
Repetition frequency	15 Hz
On-time	1000 μs
Off-time	492 μs
Duty cycle	67 %
Wave form	Sinusoidal

Table 12 Low Moment

Parameter	Value
Number of transmitter turns	12
Transmitter area	342 m <sup>2</sup>
Peak current	225 Amp
Peak moment	~930,000 NIA
Repetition frequency	15 Hz
On-time	8000 μs
Off-time	25333.4 μs
Duty cycle	24 %
Wave form	Square

Table 13 High Moment

## Receiver system

The decay of the secondary magnetic field is measured using two independent active induction coils. The Z coil is the vertical component, and the X coil is the horizontal in-line component. Each coil has an effective receiver area of 100 m<sup>2</sup> (Z), 40 m<sup>2</sup> (x).

The receiver coils are placed in a null-position:

Z coil  $(x, y, z) = (-13.65 \text{ m}, 0.0 \text{ m}, -2.0 \text{ m})$

X coil  $(x, y, z) = (-14.65 \text{ m}, 0.0 \text{ m}, 0.0 \text{ m})$

In the null-position, the primary field is damped with a factor of 0.01 on HM and due to PFC correction it can be neglected on LM.



*Figure 5 Rudder containing the Z coil located in the top part of the tower.*

The key parameters defining the receiver set up listed in Table 14.

Receiver parameters		
Sample rate		All decays are measured
Number of output gates		40 (HM) and 22 (LM)
Receiver coil low pass filter		48.7 kHz (Z-coil) and 46.1 kHz (X-coil)
Receiver instrument low pass filter		1 MHz
Repetition frequency	LM	15 Hz
	HM	15 Hz
Front gate	LM	0.0 $\mu$ s
	HM	40 $\mu$ s

*Table 14 Receiver set-up*

A complete list describing gate open, close and centre times are listed in Table 19 and Table 20.

# Waveform

The waveforms for LM and HM are measured using a Rogowski coil on the SkyTEM312HPM system. An approximation to the measured waveform is applied in modelling of the EM data.

## **SkyTEM312HPM:**

Figure 6 and Figure 7 show the approximated up- and down ramp of the waveform.

Details are presented in Table 15 and Table 16.

Waveform tables are found in Table 17 and Table 18.

Parameter	Value
Base frequency (Multi moment)	15 Hz
Current range	6 amp

*Table 15: Waveform parameters for LM*

Parameter	Value
Base frequency (Multi moment)	15 Hz
Current range	225 Amp

*Table 16: Waveform parameters for HM*

The calibration parameters for the system are defined as:

## **SkyTEM312HPM:**

Low Moment

Shift factor: 1.0 (on the raw dB/dt data)

Time shift: 0.0 s

High Moment

Shift factor: 1.0 (on the raw dB/dt data)

Time shift: 0.0 s

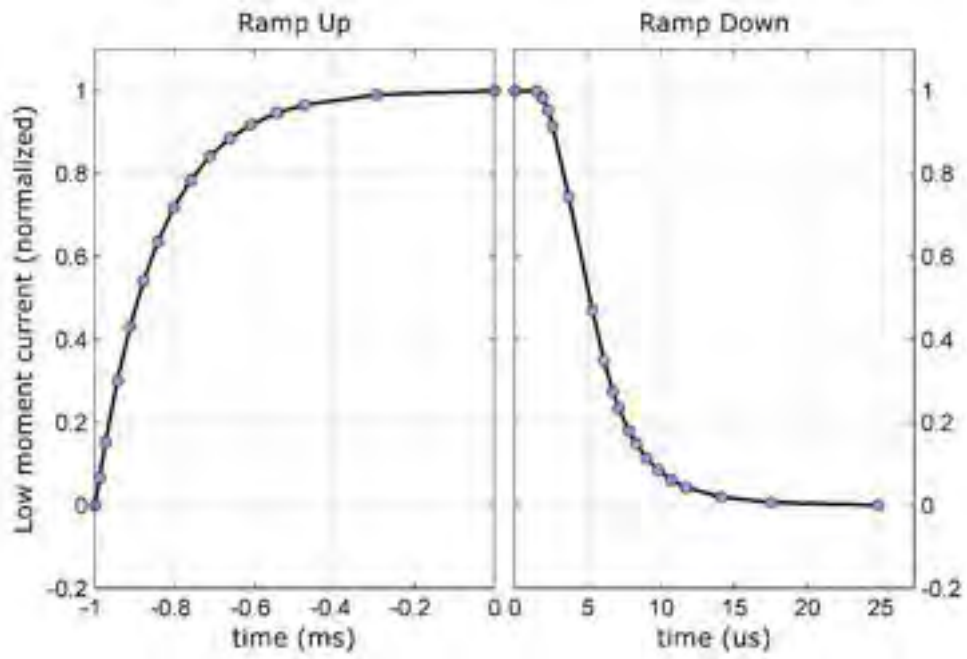


Figure 6. Ramp up and down for the LM waveform. The current is normalised.

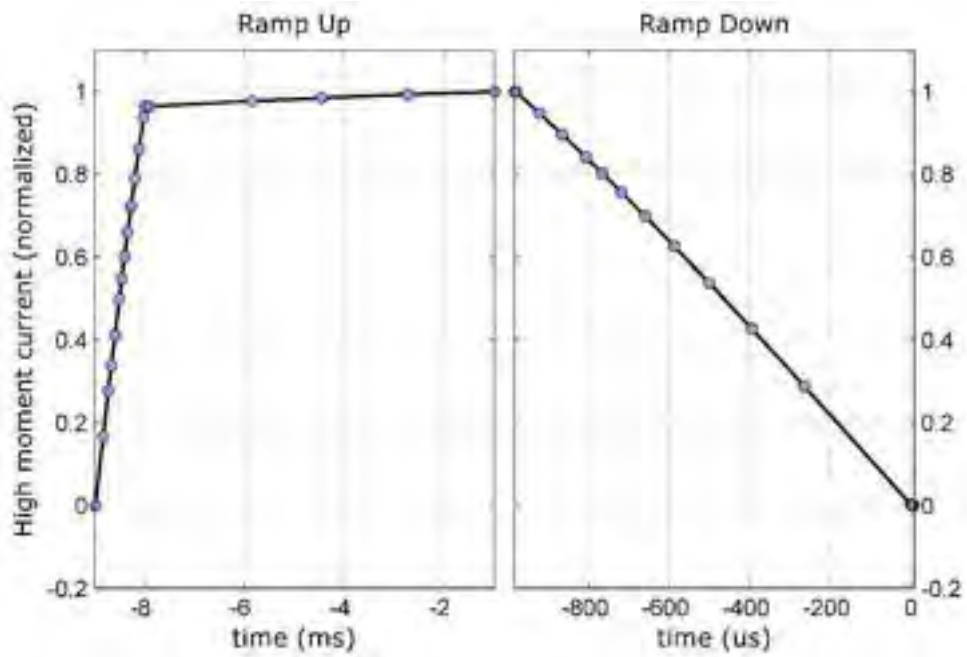


Figure 7. Ramp up and down for the HM waveform. The current is normalised.

Time [s]	Normalized current
-2.49000E-03	-0.00000E+00
-2.47920E-03	-3.32455E-02
-2.46440E-03	-7.63144E-02
-2.43460E-03	-1.50826E-01
-2.40290E-03	-2.15445E-01
-2.36910E-03	-2.71083E-01
-2.33360E-03	-3.17786E-01
-2.29360E-03	-3.59044E-01
-2.25160E-03	-3.92373E-01
-2.20280E-03	-4.21375E-01
-2.15330E-03	-4.42825E-01
-2.10090E-03	-4.59284E-01
-2.03610E-03	-4.73275E-01
-1.96590E-03	-4.83203E-01
-1.78510E-03	-4.95245E-01
-1.49200E-03	-5.00000E-01
-1.49050E-03	-4.99524E-01
-1.49010E-03	-4.91506E-01
-1.48970E-03	-4.76825E-01
-1.48940E-03	-4.57179E-01
-1.48830E-03	-3.72235E-01
-1.48670E-03	-2.35769E-01
-1.48590E-03	-1.74637E-01
-1.48530E-03	-1.37536E-01
-1.48490E-03	-1.17515E-01
-1.48420E-03	-8.94979E-02
-1.48370E-03	-7.41392E-02
-1.48300E-03	-5.68731E-02
-1.48220E-03	-4.24776E-02
-1.48130E-03	-3.07410E-02
-1.48030E-03	-2.16804E-02
-1.47790E-03	-9.82808E-03
-1.47450E-03	-3.52297E-03
-1.46720E-03	0.00000E+00
-9.98000E-04	0.00000E+00
-9.87200E-04	6.64910E-02
-9.72400E-04	1.52629E-01
-9.42600E-04	3.01653E-01
-9.10900E-04	4.30890E-01
-8.77100E-04	5.42165E-01
-8.41600E-04	6.35573E-01
-8.01600E-04	7.18088E-01
-7.59600E-04	7.84745E-01
-7.10800E-04	8.42750E-01
-6.61300E-04	8.85651E-01
-6.08900E-04	9.18568E-01
-5.44100E-04	9.46550E-01
-4.73900E-04	9.66407E-01
-2.93100E-04	9.90489E-01
0.00000E+00	1.00000E+00
1.50000E-06	9.99049E-01
1.90000E-06	9.83012E-01
2.30000E-06	9.53651E-01
2.60000E-06	9.14359E-01
3.70000E-06	7.44470E-01
5.30000E-06	4.71538E-01
6.10000E-06	3.49274E-01
6.70000E-06	2.75073E-01
7.10000E-06	2.35029E-01
7.80000E-06	1.78996E-01
8.30000E-06	1.48278E-01
9.00000E-06	1.13746E-01
9.80000E-06	8.49552E-02
1.07000E-05	6.14820E-02
1.17000E-05	4.33608E-02
1.41000E-05	1.96562E-02
1.75000E-05	7.04595E-03
2.48000E-05	0.00000E+00

Table 17: Normalized current waveform for LM

Time [s]	Normalized current
-4.23146E-02	-0.00000E+00
-4.21594E-02	-1.67413E-01
-4.20542E-02	-2.77595E-01
-4.19954E-02	-3.38342E-01
-4.19238E-02	-4.11322E-01
-4.18364E-02	-4.98688E-01
-4.17858E-02	-5.48290E-01
-4.17298E-02	-6.02257E-01
-4.16682E-02	-6.60403E-01
-4.16000E-02	-7.23165E-01
-4.15246E-02	-7.90421E-01
-4.14416E-02	-8.61658E-01
-4.13496E-02	-9.36920E-01
-4.13146E-02	-9.64139E-01
-4.12340E-02	-9.64146E-01
-3.91702E-02	-9.77312E-01
-3.77850E-02	-9.84994E-01
-3.60574E-02	-9.93202E-01
-3.43184E-02	-1.00000E+00
-3.43154E-02	-9.99783E-01
-3.42570E-02	-9.47956E-01
-3.42004E-02	-8.96622E-01
-3.41406E-02	-8.40997E-01
-3.41008E-02	-8.03225E-01
-3.40526E-02	-7.56728E-01
-3.39938E-02	-6.98961E-01
-3.39222E-02	-6.27208E-01
-3.38348E-02	-5.37775E-01
-3.37282E-02	-4.26420E-01
-3.35984E-02	-2.88324E-01
-3.33334E-02	-2.66916E-03
-3.33304E-02	-8.31366E-04
-3.33254E-02	-0.00000E+00
-8.98120E-03	0.00000E+00
-8.82600E-03	1.67413E-01
-8.72080E-03	2.77595E-01
-8.66200E-03	3.38342E-01
-8.59040E-03	4.11322E-01
-8.50300E-03	4.98688E-01
-8.45240E-03	5.48290E-01
-8.39640E-03	6.02257E-01
-8.33480E-03	6.60403E-01
-8.26660E-03	7.23165E-01
-8.19120E-03	7.90421E-01
-8.10820E-03	8.61658E-01
-8.01620E-03	9.36920E-01
-7.98120E-03	9.64139E-01
-7.90060E-03	9.64146E-01
-5.83680E-03	9.77312E-01
-4.45160E-03	9.84994E-01
-2.72400E-03	9.93202E-01
-9.85000E-04	1.00000E+00
-9.82000E-04	9.99783E-01
-9.23600E-04	9.47956E-01
-8.67000E-04	8.96622E-01
-8.07200E-04	8.40997E-01
-7.67400E-04	8.03225E-01
-7.19200E-04	7.56728E-01
-6.60400E-04	6.98961E-01
-5.88800E-04	6.27208E-01
-5.01400E-04	5.37775E-01
-3.94800E-04	4.26420E-01
-2.65000E-04	2.88324E-01
0.00000E+00	2.66916E-03
3.00000E-06	8.31366E-04
8.00000E-06	0.00000E+00

Table 18: Normalized current waveform for HM

## Data Acquisition

The SkyTEM312HPM system setup uses dual moment configuration containing a Low Moment (LM) with a peak moment of  $\sim 4,000$  NIA and a High Moment (HM) with a peak moment of  $\sim 930,000$  NIA.

A dual moment system provides a major advantage over single moment systems as it is possible to measure a wider range of time gates. In LM mode earlier time gates can be measured allowing for a more accurate near surface resolution while in the HM mode, measuring at later times, a deeper penetration into the ground can be achieved.

Data from two GPS receivers are recorded by the EM data acquisition system while a third GPS is recorded by the magnetic data acquisition system. The DGPS system is used for time stamping, positioning, and correlation of the EM and magnetic datasets. All recorded data are marked with a time stamp which is used to link the different data types. The GPS receivers on the frame are activated for Precise Point Positioning (PPP) processing, which allows for a precise processing of the GPS position without the need of a base station.

The time stamp is in UTC/GMT and the formats are either,

- Date and Time defined as; yyyy/mm/dd hh:mm:ss.sss  
or
- Datetime values defined as decimal days since 1900-01-01 and seconds of the day; dddd.ssssssss

## Gate times

The gate times for the SkyTEM312HPM system are found in the following tables.

Gate times for the Low moment gates are presented in Table 19. Gate 1 – 10 of the LM gates were corrected for the primary field allowing the use of earlier gates than otherwise possible and are represented by boxcar gates. Gate 11 to 22 are provided as tapered gate values, where the gate tapering results in improved suppression of high frequency noise in the data. The times refer to beginning of ramp down. The 2 latest LM gates are not as wide as the previous gates and can as a result appear noisier. They can be omitted in the workbench processing.

The High moment data are provided as tapered gate values, where the gate tapering results in improved suppression of high frequency noise in the data. The equivalent gate times of the tapered gates are presented in Table 9 for the SkyTEM312HPM. The times refer to the end of ramp.

The tapered gates constitute smooth weighing functions which are applied to the recorded dB/dt signals with overlap between neighbouring gates. The weighing functions used are B-splines of order 3, which means that they are piecewise polynomial functions of order 2. The B-spline has been chosen specifically for the purpose of weighing function due to its property of:

- being maximally smooth while being compact (resulting in superior low pass filtering qualities),
- in combination the set of gates ensure equal weighing of the entire sounding curve,
- being uniquely defined simply by the chosen set of gate transition times (also called knot points),
- associated expressions exist for its function moments and frequency transform

The tapered gates are generated with gate transition times/knot points located at the gate transitions of the box gates. This means that every tapered gate contains signal contributions from three neighbouring box gate intervals.

The B field channels represent the actual B field level at the given channel time. Channel times for system SkyTEM312HPM can be found in Table 21.

The earliest gates for HM are not used as these are in the transition zone and affected by the primary field of the transmitter.

The earliest gates for LM can be used carefully when linked with the system response (SR2)

Gate #	Gate Center (s)	Gate Open (s)	Gate Close (s)	Comment
1	1.50000E-06	0.00000E+00	3.00000E-06	LM (PFC - Box)
2	4.50000E-06	3.00000E-06	6.00000E-06	LM (PFC - Box)
3	7.70000E-06	6.00000E-06	9.40000E-06	LM (PFC - Box)
4	1.13000E-05	9.40000E-06	1.32000E-05	LM (PFC - Box)
5	1.53000E-05	1.32000E-05	1.74000E-05	LM (PFC - Box)
6	1.99000E-05	1.74000E-05	2.24000E-05	LM (PFC - Box)
7	2.53000E-05	2.24000E-05	2.82000E-05	LM (PFC - Box)
8	3.17000E-05	2.82000E-05	3.52000E-05	LM (PFC - Box)
9	3.94000E-05	3.52000E-05	4.36000E-05	LM (PFC - Box)
10	4.87000E-05	4.36000E-05	5.38000E-05	LM (PFC - Box)
11	6.11000E-05	5.48667E-05	6.73333E-05	LM
12	7.49500E-05	6.74167E-05	8.24833E-05	LM
13	9.17500E-05	8.25833E-05	1.00917E-04	LM
14	1.12250E-04	1.01083E-04	1.23417E-04	LM
15	1.37200E-04	1.23567E-04	1.50833E-04	LM
16	1.67600E-04	1.51000E-04	1.84200E-04	LM
17	2.04700E-04	1.84467E-04	2.24933E-04	LM
18	2.49900E-04	2.25233E-04	2.74567E-04	LM
19	3.05000E-04	2.74900E-04	3.35100E-04	LM
20	3.72250E-04	3.35550E-04	4.08950E-04	LM
21	4.27650E-04	4.00617E-04	4.54683E-04	LM (reduced width)
22	4.68450E-04	4.53317E-04	4.83583E-04	LM (reduced width)

Table 19. SkyTEM312HPM. LM merged gate times with respect to the beginning of ramp down.

Gate #	Gate Center (s)	Gate Open (s)	Gate Close (s)	Comment
1	1.50000E-06	0.00000E-00	3.00000E-06	Not used
2	4.60000E-06	3.03333E-06	6.16667E-06	Not used
3	7.90000E-06	6.20000E-06	9.60000E-06	Not used
4	1.15000E-05	9.60000E-06	1.34000E-05	Not used
5	1.56000E-05	1.34333E-05	1.77667E-05	Not used
6	2.03000E-05	1.78000E-05	2.28000E-05	Not used
7	2.58000E-05	2.28333E-05	2.87667E-05	Not used
8	3.23500E-05	2.88167E-05	3.58833E-05	Not used
9	4.02000E-05	3.59333E-05	4.44667E-05	Not used
10	4.96500E-05	4.45167E-05	5.47833E-05	Not used
11	6.11000E-05	5.48667E-05	6.73333E-05	Not used
12	7.49500E-05	6.74167E-05	8.24833E-05	HM
13	9.17500E-05	8.25833E-05	1.00917E-04	HM
14	1.12250E-04	1.01083E-04	1.23417E-04	HM
15	1.37200E-04	1.23567E-04	1.50833E-04	HM
16	1.67600E-04	1.51000E-04	1.84200E-04	HM
17	2.04700E-04	1.84467E-04	2.24933E-04	HM
18	2.49900E-04	2.25233E-04	2.74567E-04	HM
19	3.05000E-04	2.74900E-04	3.35100E-04	HM
20	3.72250E-04	3.35550E-04	4.08950E-04	HM
21	4.54300E-04	4.09500E-04	4.99100E-04	HM
22	5.54400E-04	4.99733E-04	6.09067E-04	HM
23	6.76550E-04	6.09850E-04	7.43250E-04	HM
24	8.25600E-04	7.44233E-04	9.06967E-04	HM
25	1.00745E-03	9.08150E-04	1.10675E-03	HM
26	1.22935E-03	1.10818E-03	1.35052E-03	HM
27	1.50010E-03	1.35227E-03	1.64793E-03	HM
28	1.83045E-03	1.65008E-03	2.01082E-03	HM
29	2.23355E-03	2.01345E-03	2.45365E-03	HM
30	2.72540E-03	2.45683E-03	2.99397E-03	HM
31	3.32555E-03	2.99785E-03	3.65325E-03	HM
32	4.05785E-03	3.65802E-03	4.45768E-03	HM
33	4.95140E-03	4.46350E-03	5.43930E-03	HM
34	6.04170E-03	5.44637E-03	6.63703E-03	HM
35	7.37210E-03	6.64567E-03	8.09853E-03	HM
36	8.99550E-03	8.10910E-03	9.88190E-03	HM
37	1.09764E-02	9.89475E-03	1.20580E-02	HM
38	1.33934E-02	1.20736E-02	1.47131E-02	HM
39	1.63105E-02	1.47216E-02	1.78994E-02	HM
40	1.86941E-02	1.75392E-02	1.98490E-02	HM (reduced width)

Table 20 SkyTEM312HPM: HM gate times referenced to the end of ramp down.

Channel number #	Channel time (s)	Comment
1	3.00000E-06	Not used
2	6.00000E-06	Not used
3	9.40000E-06	Not used
4	1.32000E-05	Not used
5	1.74000E-05	Not used
6	2.24000E-05	Not used
7	2.82000E-05	Not used
8	3.52000E-05	Not used
9	4.36000E-05	Not used
10	5.38000E-05	Not used
11	6.60000E-05	Not used
12	8.10000E-05	HM B-field
13	9.90000E-05	HM B-field
14	1.21000E-04	HM B-field
15	1.48000E-04	HM B-field
16	1.80800E-04	HM B-field
17	2.20600E-04	HM B-field
18	2.69400E-04	HM B-field
19	3.28800E-04	HM B-field
20	4.01200E-04	HM B-field
21	4.89600E-04	HM B-field
22	5.97600E-04	HM B-field
23	7.29200E-04	HM B-field
24	8.89800E-04	HM B-field
25	1.08580E-03	HM B-field
26	1.32500E-03	HM B-field
27	1.61680E-03	HM B-field
28	1.97280E-03	HM B-field
29	2.40720E-03	HM B-field
30	2.93740E-03	HM B-field
31	3.58420E-03	HM B-field
32	4.37340E-03	HM B-field
33	5.33640E-03	HM B-field
34	6.51160E-03	HM B-field
35	7.94540E-03	HM B-field
36	9.69500E-03	HM B-field
37	1.18300E-02	HM B-field
38	1.44350E-02	HM B-field
39	1.76134E-02	HM B-field
40	2.13634E-02	HM B-field

Table 21 SkyTEM312HPM HM B-field channel times are referenced to end of ramp down.

## Digital Data

The complete dataset of the SkyTEM survey is delivered as a Geosoft database (GDB) which can be used as input for further processing, gridding and as input to inversion and interpretation software. The channels of the GDB and xyz are described in Table 22.

### Channel description, Survey Data

Parameter	Explanation	Unit
Fid	Unique Fiducial number	seconds
Line	Line number	LLLLLL
Flight	Name of flight	yyyymmdd.ff
DateTime	DateTime format	Decimal days
Date	Date	Yyyy/mm/dd
Time	Time	HH:MM:SS.ss
AngleX	Angle in flight direction	Degrees
AngleY	Angle perpendicular to flight direction	Degrees
Height	Filtered transmitter terrain clearance	Meters
Height_Raw	Measured transmitter terrain clearance	Meters
Lon*	Latitude/Longitude, WGS84	Decimal degrees
Lat*	Latitude/Longitude, WGS84	Decimal degrees
E_NAD83*	NAD83 / California Albers	Meter
N_NAD83*	NAD83 / California Albers	Meter
DEM	Digital Elevation Model	Meters above sea level
Alt	DGPS Altitude	Meters above sea level
GdSpeed	Ground Speed	kph
LMcurrent	Current, low moment	Amps
HMcurrent	Current, high moment	Amps
LM_Z_dBdt[xx]**	Geosoft array channels normalized LM dB/dt Z-coil value. Voltage/(Tx moment*RX area), normalization includes the number of transmitter turns	pV/(m4*A)
HM_Z_dBdt[xx]**	Geosoft array channels normalized HM dB/dt Z-coil value. Voltage/(Tx moment*RX area), normalization includes the number of transmitter turns	pV/(m4*A)

Parameter	Explanation	Unit
HM_X_dBdt[xx]**	Geosoft array channels normalized dB/dt HM X-coil value. Voltage/(Tx moment*RX area), normalization includes the number of transmitter turns	pV/(m <sup>4</sup> *A)
HM_Z_B[xx]**	Geosoft array channels normalized HM Z B-field value. Voltage/(Tx moment*RX area), normalization includes the number of transmitter turns	fT/(m <sup>2</sup> *A)
HM_X_B[xx]**	Geosoft array channels normalized HM X B-field value. Voltage/(Tx moment*RX area), normalization includes the number of transmitter turns	fT/(m <sup>2</sup> *A)
PLNI	Powerline Noise intensity (60Hz)	PLNI
Bmag_Raw	Total Magnetic Intensity (1 Hz) Magnetic base station data	nT
Diurnal	Diurnal variation Magnetic base station data	nT
Mag_Raw	Total Magnetic Intensity Raw magnetic data	nT
Mag_Cor	Magnetic Intensity Filtered and diurnal corrected	nT
RMF	Residual magnetic Field Final Level and IGRF corrected data	nT
TMI	Total Magnetic Intensity IGRF recalculated	nT
RMF_1VD_calc	Calculated 1 <sup>st</sup> Vertical derivative of the RMF Channel	nT/m
RelUnc_LM_Z_dBdt_Merge[**]	Relative uncertainty of LM_Z	-
RelUnc_HM_Z_dBdt_Spline[**]	Relative uncertainty of HM_Z	-
RelUnc_HM_Z_dBdt_Spline[**]	Relative uncertainty of HM_X	-

Table 22 Channel description, survey data

\*) Data positions refer to the center of the frame.

\*\*\*) The first valid gates are: 2 (LM Z), 11 (HM Z), 11 (HM X).

## Workbench Input File Description

### **ASCII XYZ**

The GDB data is stored in 10 HZ and has been exported into XYZ files.

- One XYZ file maintain the 10 Hz sample rate.
- A decimated XYZ file in 1 Hz has been exported as well. It is suggested to import the 1 Hz XYZ file to Workbench for inverting the data.

### **Geometry file (GEX)**

The geometry file (GEX) contains information on the configuration of the SkyTEM system. This information is used during data processing and inversion in the Aarhus Workbench package. Two geometry files have been provided, one for use with the system response file, description below, and one for use without the system response file.

### **System Response file (GEX + SR2)**

The System Response file (SR2) contains information regarding the system response of the SkyTEM system and is derived from the high-altitude data. This information is used during data processing and inversion and allows for the use of very early time gate information during the inversion process. Should be used cautiously by advanced users.

### **ALC file**

An ALC file contains header information of the XYZ file. It is used to import XYZ files into Workbench.

## Data processing

This section covers processing of auxiliary, magnetic and EM data that were applied to the data to create the Geosoft databases.

In the processing procedure all devices (DGPS, Laser altimeters, inclinometers) are moved to the centre of the frame and corrected for the tilt of the frame hence all data positions refer to the center of the frame. Data is split at the beginning and end of each planned flight line, to create individual lines of data.

After initial filtering, all data are resampled to 10Hz.

### Gridding method and parameters

Grids generated with using the parameters in Table 23.

Area	Gridding algorithm	Gridding filter	Cell size	Blanking distance
Salinas	Minimum curvature	-	333 m	2000 m

Table 23 Geosoft gridding details.

## Auxiliary data

### Tilt processing

The X and Y angle processing involves manual and automated routines using a combination of the SkyTEM in-house software SkyLab and Geosoft.

The processing involves the following steps:

1. 3 sec box filter (SkyLab)
2. Low pass filtering of 3.0 sec. (Geosoft)

## **Height processing**

The height processing involves automated routines using a combination of the SkyTEM in-house software (HEfiltering and SkyLab) and Geosoft.

The processing involves the following steps:

1. Iterative weighted splines to remove low values to correct for the canopy effect (treetop filter) (HEfilter)
2. Final spline of remaining data (HEfilter)
3. Tilt correction (SkyLab)
4. Averaging of the two laser values (SkyLab)
5. Additional filters:
  - a. Low pass filter of 3.0 sec (Geosoft)

## **DGPS processing**

The DGPS has been PPP processed (Precise Point Positioning) using the Waypoint GrafNav Differential GPS processing tool. PPP processing involves utilizing corrections derived from GNSS satellite clock and orbit corrections. These corrections are provided by a 3<sup>rd</sup> party, NovAtel, and are employed in correcting the raw airborne GPS data to improve the accuracy of the positional data. The PPP solution should provide a better solution when the distance between the airborne GPS antennae and the base station GPS location becomes quite long.

The standard airborne settings have been used.

- Import of airborne files (Rover)
- Download precise ephemeris and almanac
- Precise Point Positioning processing
- Export solution as .txt file
- Convert .txt file to .sps

The DGPS.txt files are used as input to the SkyLab software assuring DGPS corrected data in the processed files.

The ground speed, altitude, latitude and longitude from the processed DGPS' are imported into Geosoft and merged into the final database, where the coordinates are converted into NAD83 / California Albers and a low pass filter of 3.0 sec is applied.

### **Digital elevation model**

A digital elevation model (DEM) has been calculated by subtracting the filtered laser altimeter data from the DGPS elevation. The vertical datum has been calculated to the EGM96 Datum. All steps related to the DEM are carried out Geosoft.

The processing of the final DEM involves the following steps:

- Filtering and processing of the laser altimeter height as described above
- DEM data received by subtraction of final filtered laser data from final processed DGPS altitude data

Figure 8 shows the DEM.

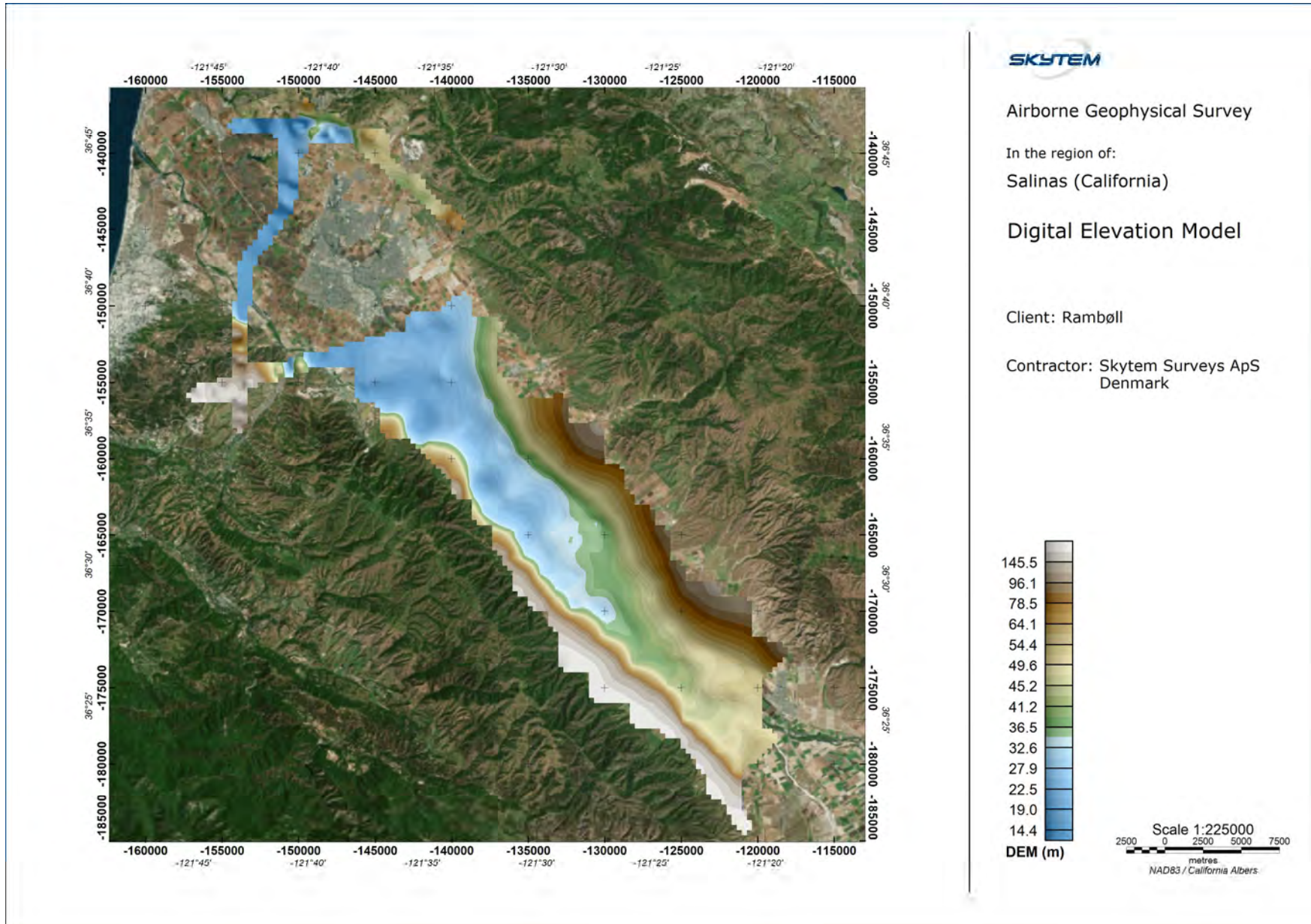


Figure 8. DEM.

## Magnetic data

Final processing of the magnetic data involves the application of traditional corrections to compensate for diurnal variation and heading effects prior to gridding. Geosoft magnetic data processing tools are applied as follows:

- Processing of static magnetic data acquired on magnetic base station
- Pre-processing of airborne magnetic data
  - Stacking of data to 10 Hz in SkyLab.
  - Moving positions to the center of the system in SkyLab.
  - Matlab Despiking
- Processing and filtering of airborne magnetic data
- Standard corrections to compensate the diurnal variation
- IGRF correction
- No levelling was applied due to the nature of the line layout
- Gridding

### **Processing of base station magnetic data**

The base station magnetometer data was merged into the base station Geosoft database daily for further processing.

The following filtering was applied:

- Fraser Low-pass filter (width 60 sec)
- Diurnal variations calculated by subtracting mean value according to the table below.
- Processed residual magnetic data from the magnetic base station representing short term variations was merged with the airborne magnetic data.
- Base stations were levelled each time location was changed.

Magnetometer Base station	Period	Mean diurnal
Salinas	20230301 – 20230302	47183.1 nT

## **Processing and Filtering of airborne magnetic data**

Airborne magnetic data is filtered and interpolated as follows:

- Matlab Despiking
  - The powerful EM system caused the mag sensor to be more sensitive to sensor orientation and variations in flight orientation. As a consequence more spikes than usual were introduced. A despiking routine in matlab was developed to preprocess the data before standard tools were applied.
  - Analysis showed that the positive EM pulses affected the data more and generated more spikes. It was decided to remove all data from the potentially affected pulses, so instead of 30 mag readings/second, we have 15 mag readings/sec and we are still able to process the mag data with acceptable result.
  - After this step traditional processing has been applied
- Adjustment of the data for the time lag between the GPS position and the position of the magnetic sensor
- Data resampling to 10 Hz (stacking)
- Nonlinear filtering (despiking in Geosoft)
- Manual despiking to remove spikes and spurious data
- Geosoft processing:
  - B-spline, smoothness 0.60, tension 0.0

## **Corrections to the magnetic data**

The following corrections are applied to the airborne magnetic data:

- Correction for diurnal variation using the digitally recorded ground base station magnetic values as described above
- Lag is negligible for the SkyTEM312HPM and no lag correction was applied
- Heading is negligible for the SkyTEM312HPM and no correction was applied
- IGRF correction

## **IGRF correction**

The International Geomagnetic Reference Field (IGRF) is a long-wavelength regional magnetic field calculated from permanent observatory data collected around the world. The IGRF is updated and determined by an international committee of geophysicists every 5 years. Secular variations in the Earth's magnetic field are incorporated into the determination of the IGRF.

The IGRF model is calculated before levelling using the following parameters:

IGRF model year: IGRF 13th generation

Date: variable according to date channel in database

Position: variable according to GPS WGS84 longitude and latitude

Elevation: variable according to magnetic sensor altitude derived from DGPS data

### **Residual Magnetic Field**

The outcome of processed magnetic data after all corrections and levelling is the Residual magnetic field (RMF). See Figure 9.

The magnetic data maps the distribution of magnetic minerals within the ground from surface to great depths. Under favorable geologic conditions, it can help map geological formations, faults and fractures within the earth. The data can also be used to identify metallic man-made objects either on surface or buried.



Airborne Geophysical Survey

In the region of:  
Salinas (California)

### Residual Magnetic Field

Client: Rambøll

Contractor: Skytem Surveys ApS  
Denmark

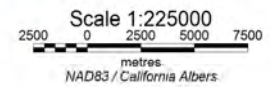
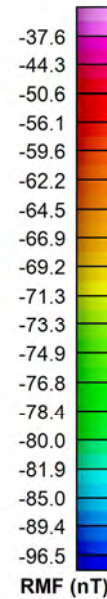
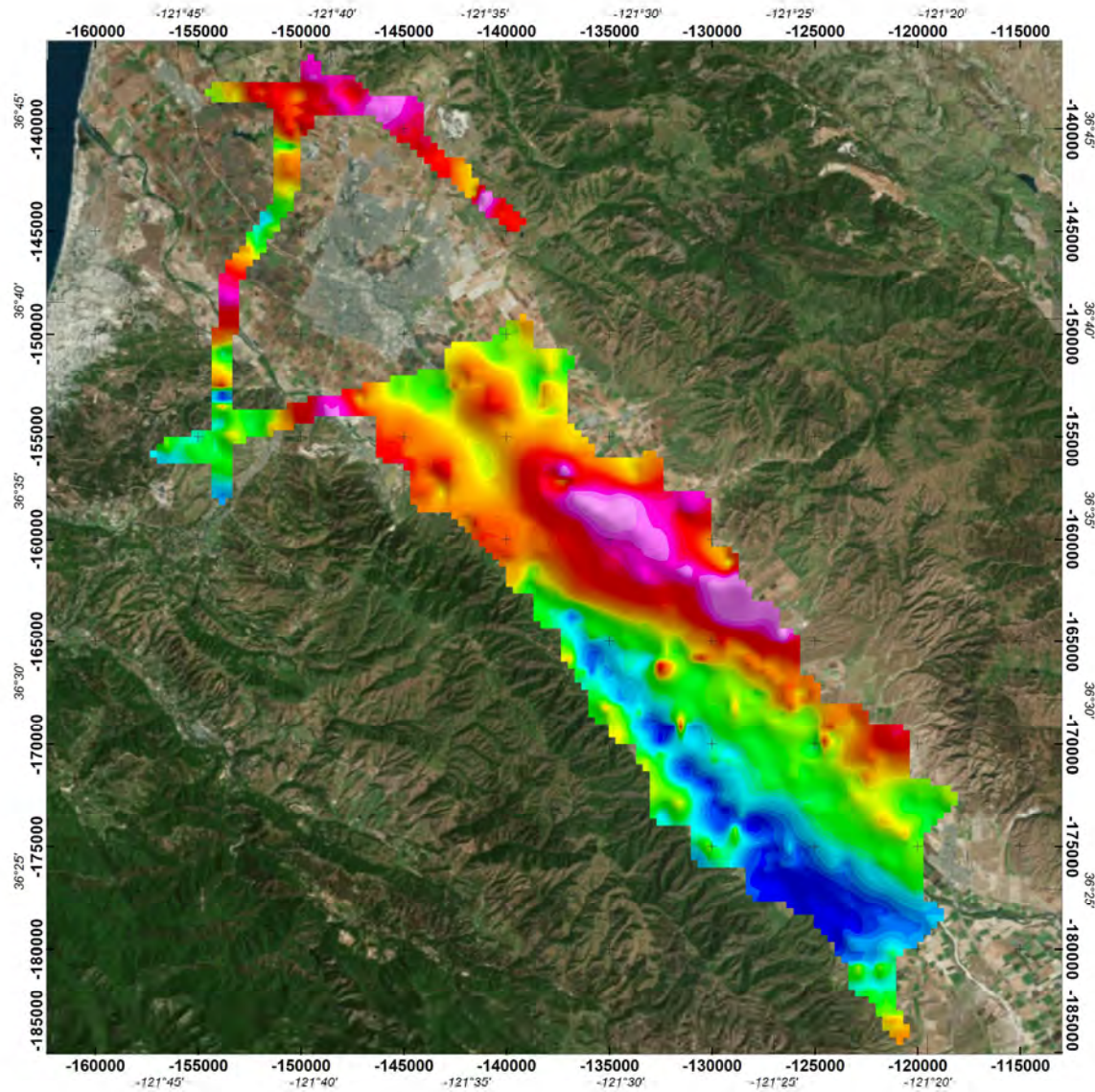


Figure 9. RMF of the entire survey area.

### **TMI recalculation**

The outcome of processed magnetic data after all corrections and levelling is the Residual magnetic field (RMF).

The RMF data is used to generate the Total Magnetic Intensity (TMI) grid by adding the IGRF data from a fixed date and altitude.

Date: 2023/03/01

Position: variable according to GPS WGS84 longitude and latitude

Elevation: 0 m

### **First Vertical Magnetic Derivative**

The first vertical derivative is a high pass filter which when applied to the gridded magnetic data enhances near surface magnetic responses while downplaying the longer wavelength response from deep seated sources. The first vertical magnetic derivative can be used to highlight the presence of faults, lineaments and near surface magnetic features. It can also be used to map metallic infrastructures either on surface or buried, if the source is large enough.

## EM data

This section covers processing of EM data and filtering of EM data.

### **Primary Field Compensation (PFC)**

The magnetic field coupling between the receiver coils and the transmitter loop is continuously hardware-monitored, providing a separate value for the magnetic field coupling during each transient sounding. These data are used for raw data correction in a separate post-processing step. The primary field compensation technique has proven stable and has routinely yielded a reduction of the primary field influence in very early time gates by a factor exceeding 50.

### **EM Filtering**

The data are normalized in respect to effective Rx coil area, Tx coil area, number of turns and current giving the unit [pV/(m<sup>4</sup>\*A)].

### **Pre-averaging steps**

Prior to applying standard averaging to the recorded data, the raw data are subjected to a few data processing steps:

- PFC correction of LM Z dBdt
- Outlier rejection filtering of the raw data, which reduces the influence from spherics and transient cultural noise. Outlier rejection has been performed on a gate-by-gate basis as a non-linear STD-estimate-scaled thresholding and interpolation process on minimally averaged EM data. The thresholding is a variant of the Median Absolute Deviation outlier detection method.
- Removal of constant system self-response (bias) on SkyTEM312HPM HM dBdt and B-field data
- Estimation of noise standard-deviation throughout the survey area on a gate-by-gate basis

The level of the constant system self-response (bias) is found in high altitude, where the recorded signal is free of signal from the ground. The self-response is approximated by fitting a sum of exponential functions to the sounding curves and subsequently the self-response is removed from data by subtracting the approximation.

### **Averaging approach**

The averaging approach comprises applying a tapered convolution filter to all gates, where the filter has a fixed duration independent of the gate number. The full width at half maximum of the applied filter is 2.0 s.

## B-field

The B-field data are recorded using the same induction coil receivers as are used for the dB/dt data. The receivers continuously monitor all B-field changes in their respective field component over the entire waveform (i.e. both during ON- and OFF time).

The continuous monitoring and the ability to integrate these changes allows for exact measured B-field response outputs.

Notice that the periodic and sign-alternating properties of the transmitted waveform permits the unique and accurate determination of the constant of integration.

## Power Line Noise Intensity (PLNI)

The PLNI is a powerful tool for identifying power line noise effect on EM and magnetic data. The PLNI monitor values are derived from a frequency analysis of the raw Z-component EM data. The Fourier transformation is evaluated at the local power transmission frequency yielding the amplitude spectral density of the power line noise.

CAUTION - When evaluating the PLNI values one should be aware of the following factors that may give rise to anomalous PLNI patterns unrelated to the actual power line noise level:

- Other noise sources than power line noise may contribute to the total noise spectral density in the data at the power transmission frequency. When power line noise is present it tends to dominate all such other noise sources.
- The presented PLNI values are not corrected for fly height or frame angles, which means that adjacent lines crossing the same power line may not exhibit the same values of PLNI.

Figure 10 shows the PLNI.

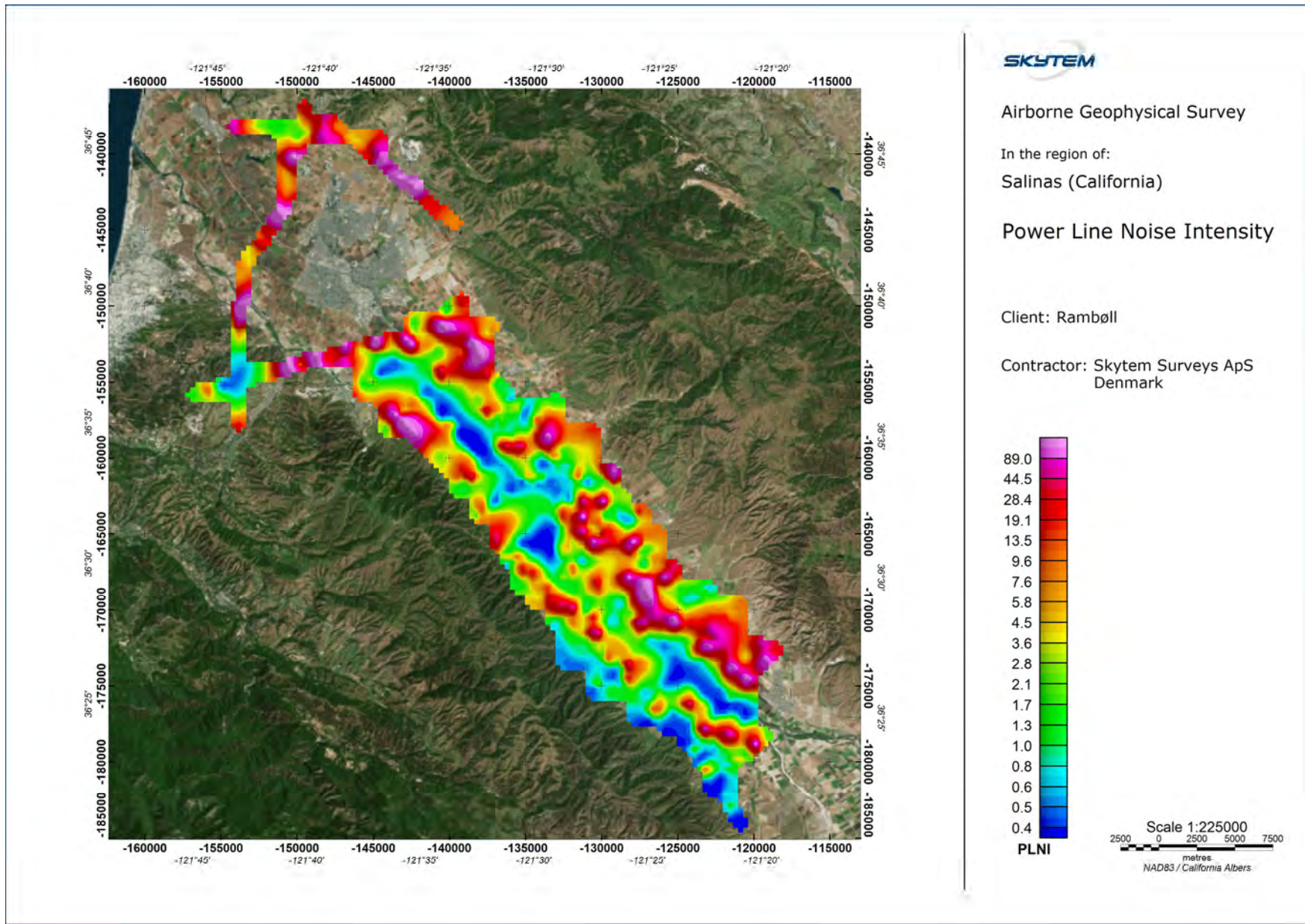
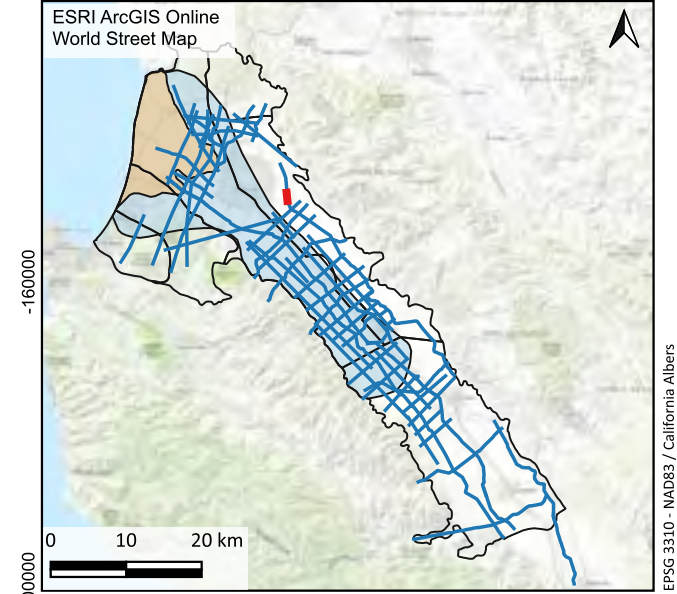
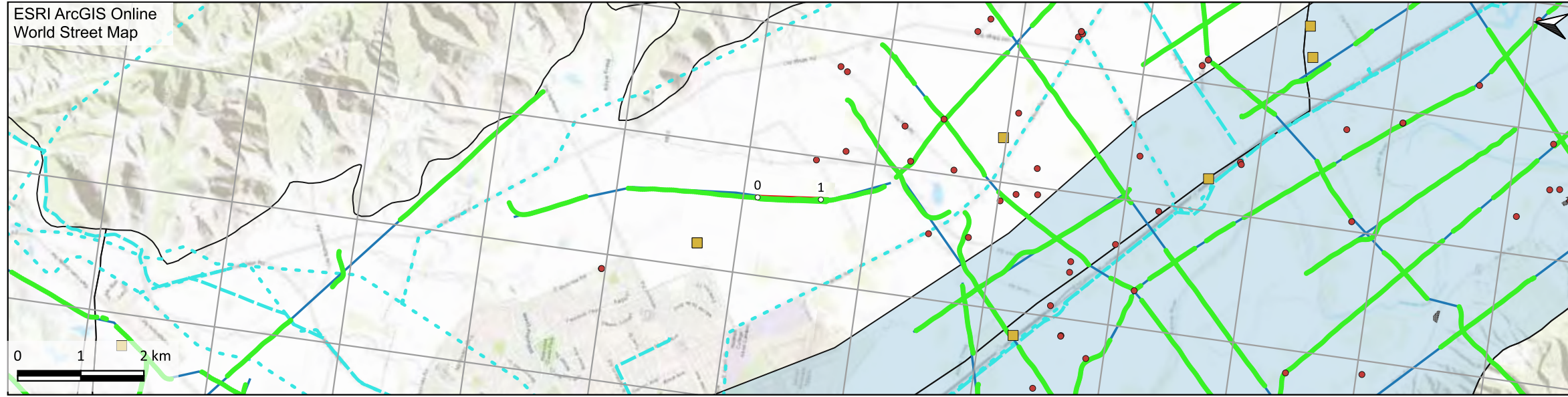


Figure 10. Power line noise intensity.

## Appendix 3

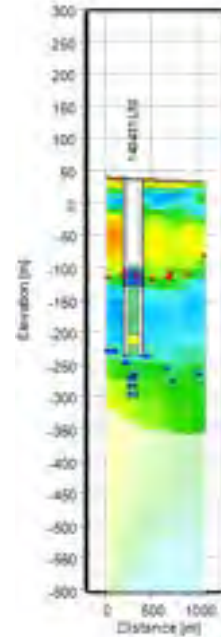
### AEM Inversion Cross-sectional Results



Legend for Maps

- Groundwater Basin Boundary (DWR - B118)
- Vineyards
- Phase 1 Aquitard Extent
- 180-Foot Aquifer CI- Contour
- Section (Current page)
- Section (Other pages)
- AEM data used for inversion**
  - Lithology logs
  - Resistivity logs
  - Electric transmission lines (CA State Geoportals, 2020)
  - Pipelines (AmeriGEOSS, 2022)

Smooth Model



Legend for Model Sections

**Resistivity: AEM inversion results**

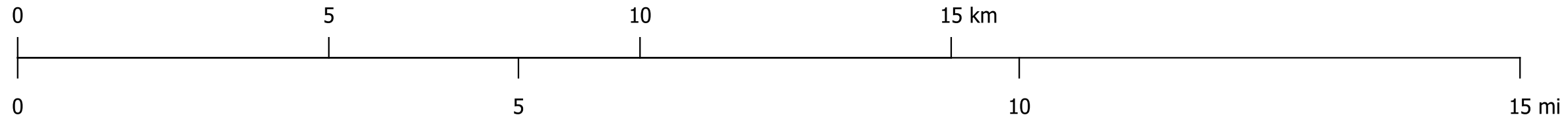
3      10      100      300  
Resistivity [ohm-m]

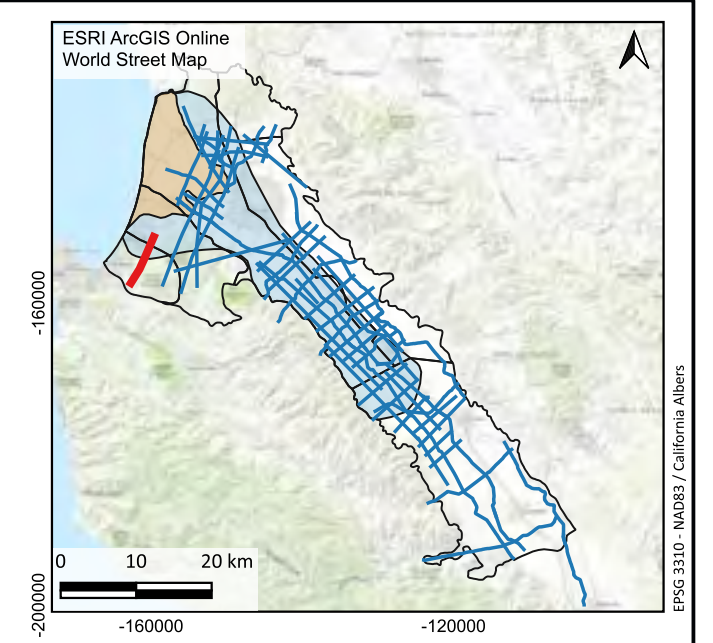
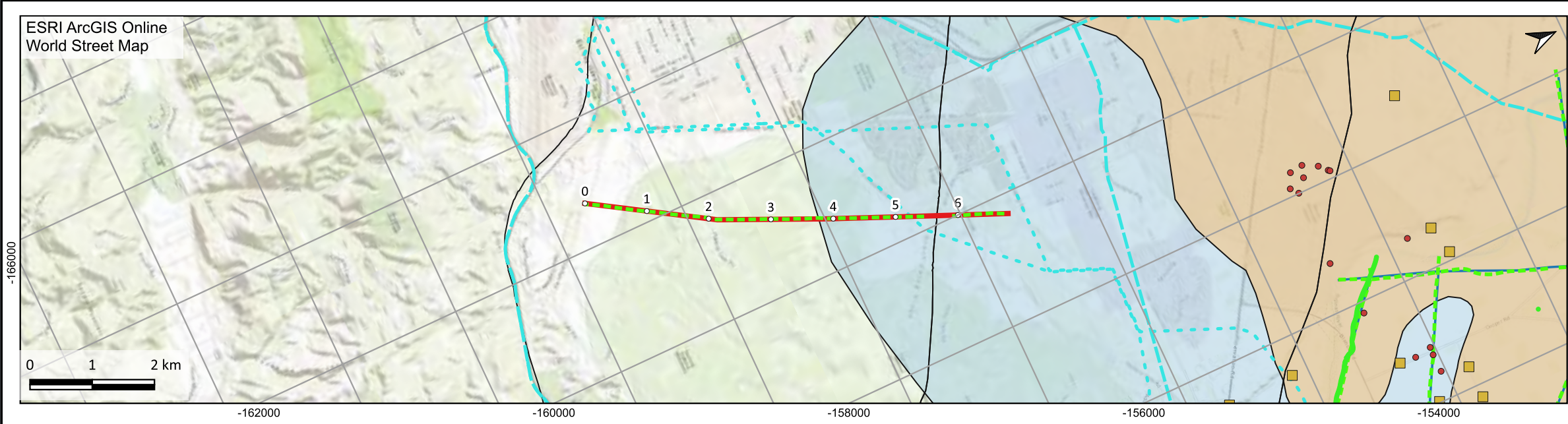
\*DOI = Depth of investigation

Lithology log	Resistivity log	Well completion report analysis
Sand		
Silt Clay		
Clay		
Clay shale		
Siltstone		
Limestone		

**Continuous conductor**

- Top of conductor
- Bottom of conductor
- Top of conductor (lower confidence)
- Bottom of conductor (lower confidence)



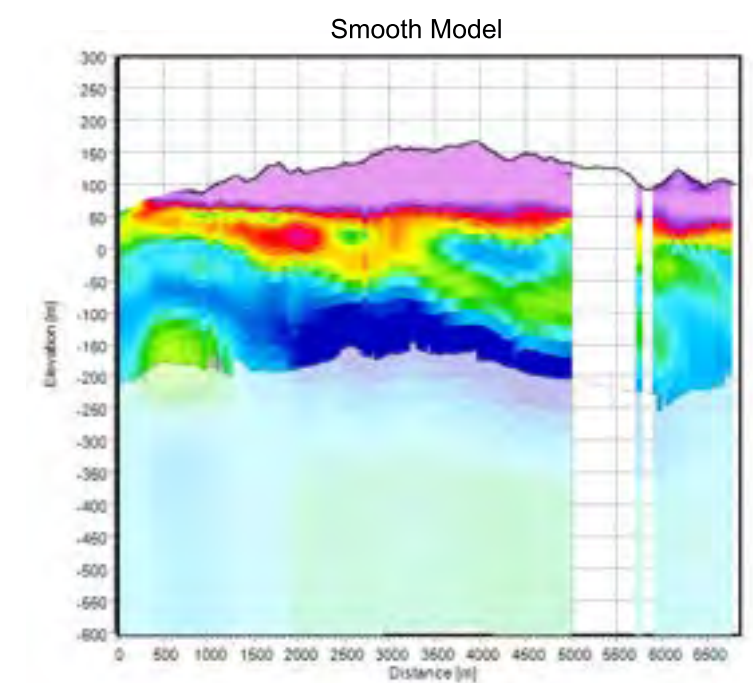


**Legend for Maps**

- Groundwater Basin Boundary (DWR - B118)
- Vineyards
- Phase 1 Aquitard Extent
- 180-Foot Aquifer CI- Contour
- Section (Current page)
- Section (Other pages)

**AEM data used for inversion**

- Lithology logs
- Resistivity logs
- Electric transmission lines (CA State Geoportal, 2020)
- Pipelines (AmeriGEOSS, 2022)



**Legend for Model Sections**

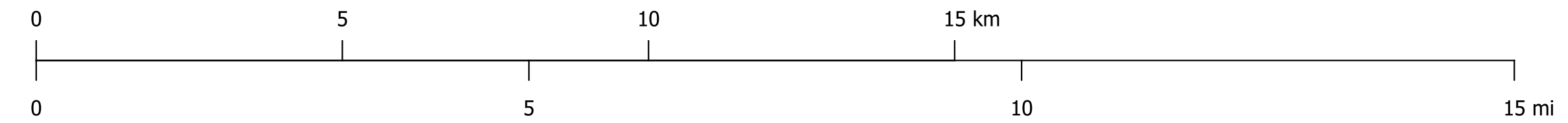
**Resistivity: AEM inversion results**

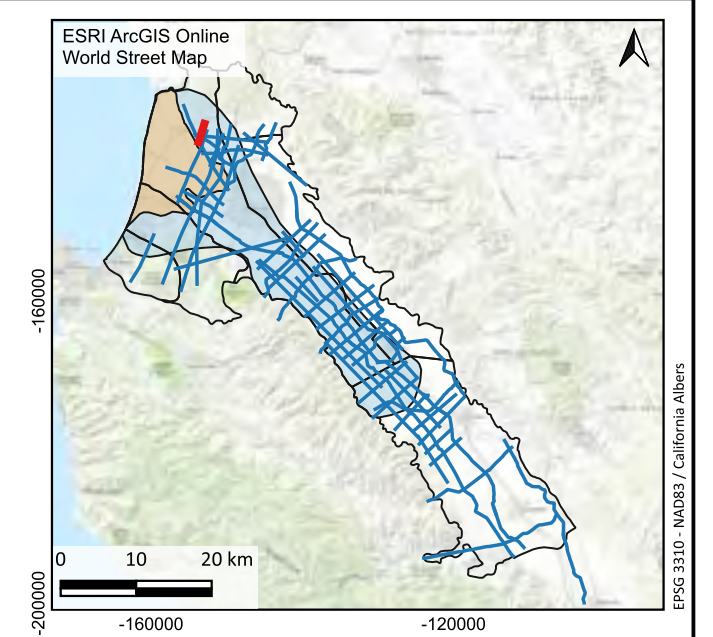
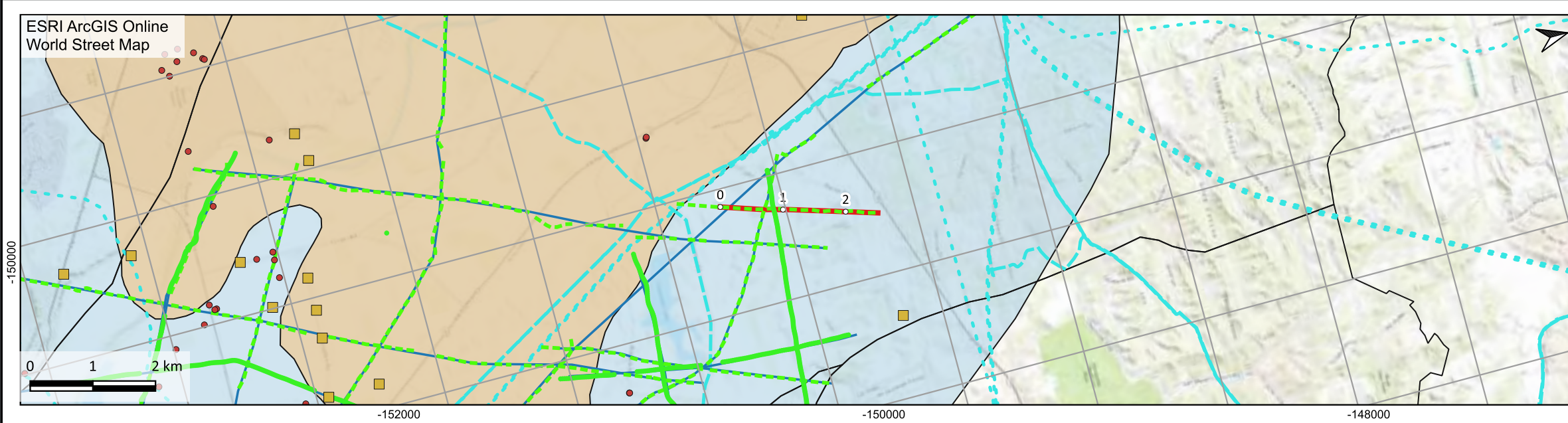
\*DOI = Depth of investigation

Lithology log	Resistivity log	Well completion report analysis
<ul style="list-style-type: none"> <li>Soil</li> <li>Fill Clay</li> <li>Clay</li> <li>Clay shale</li> <li>Sand</li> <li>Siltstone</li> </ul>		

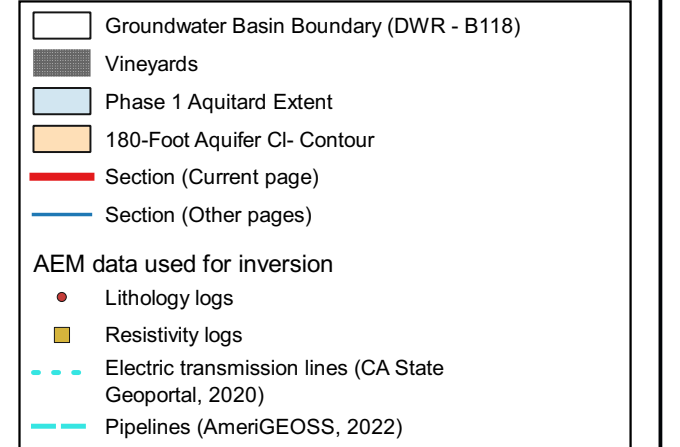
**Continuous conductor**

- Top of conductor
- Bottom of conductor
- Top of conductor (lower confidence)
- Bottom of conductor (lower confidence)

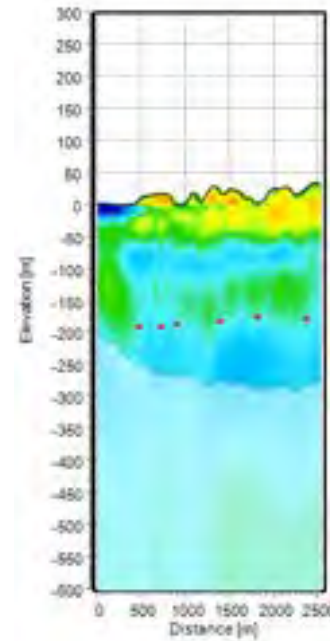




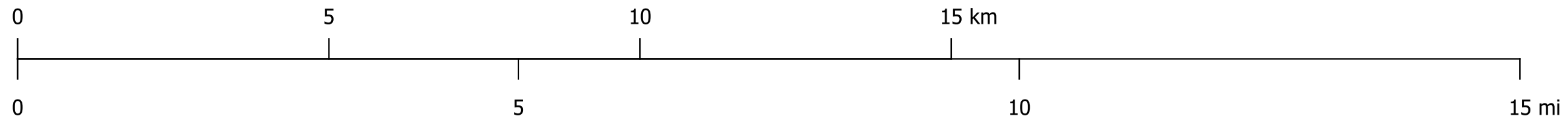
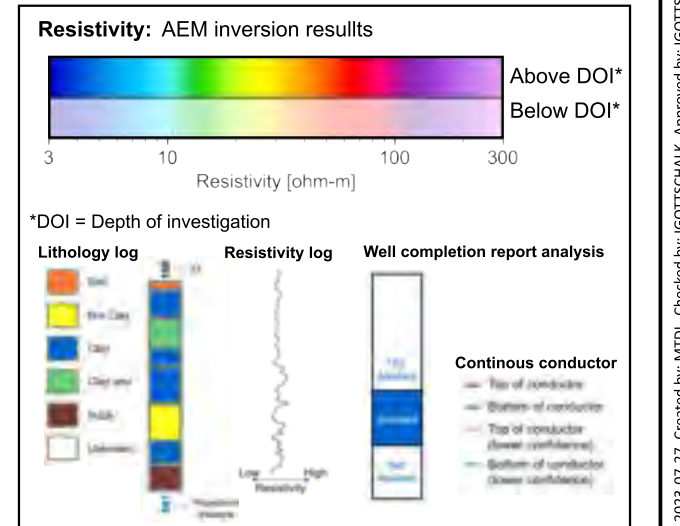
Legend for Maps

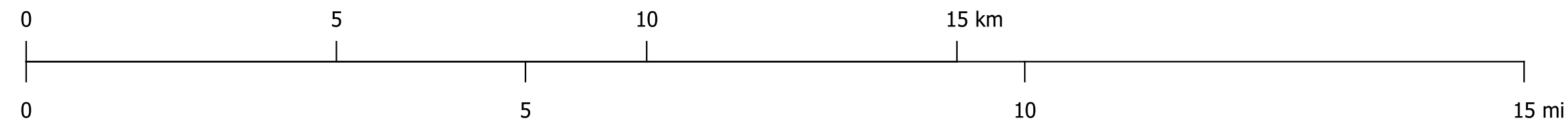
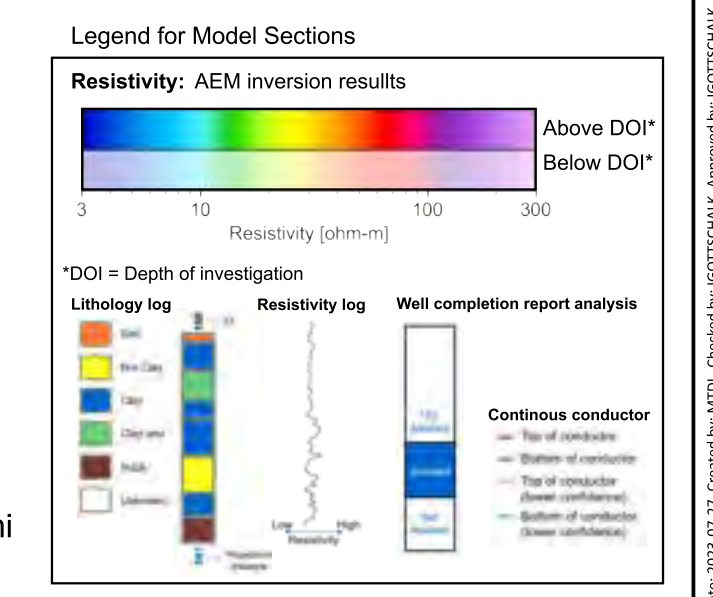
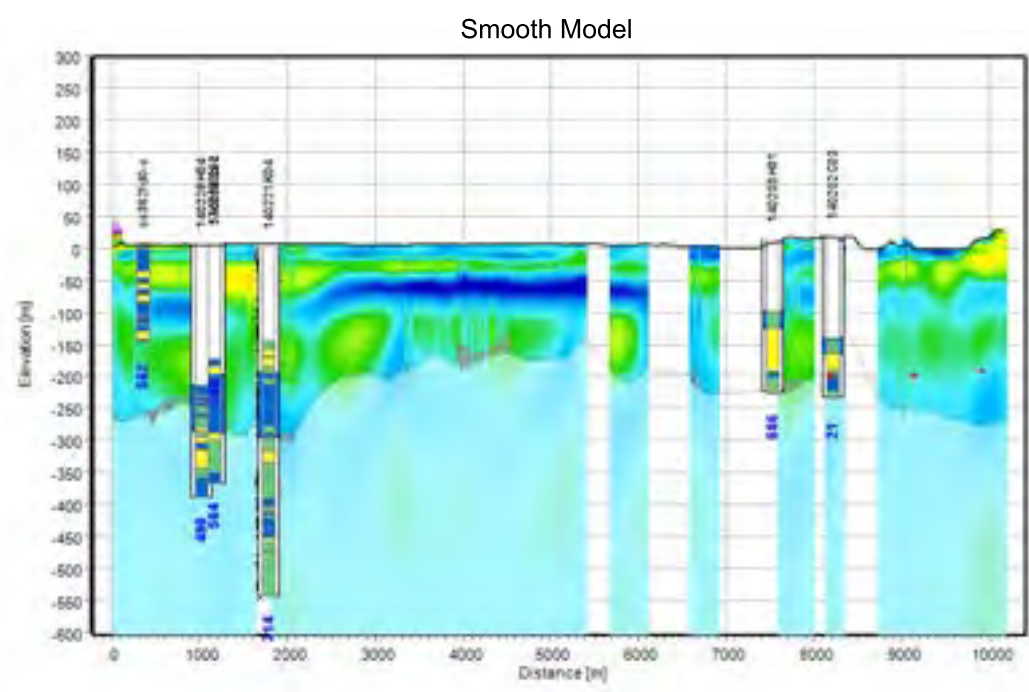
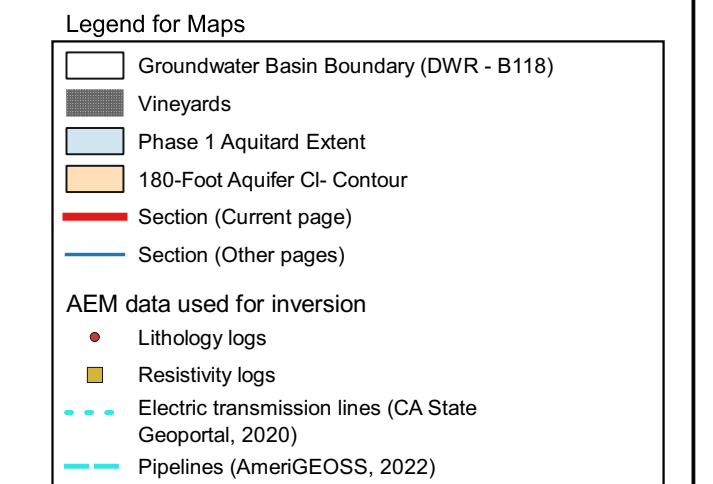
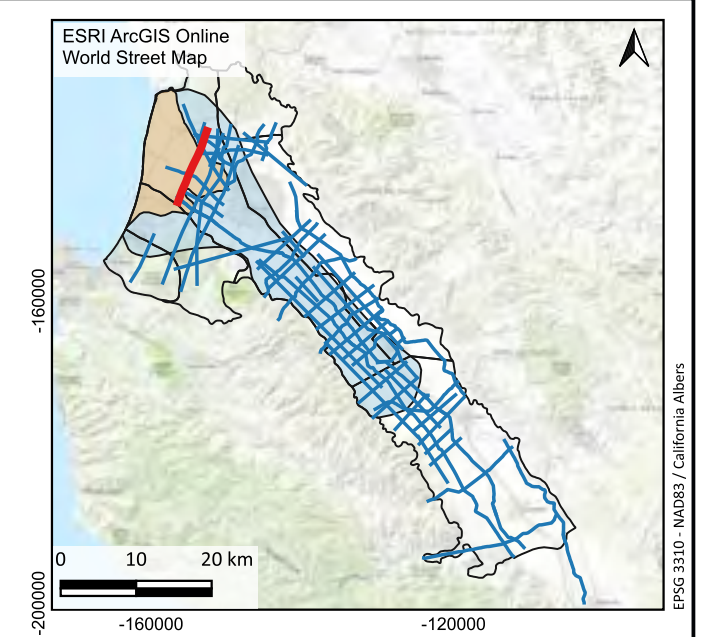
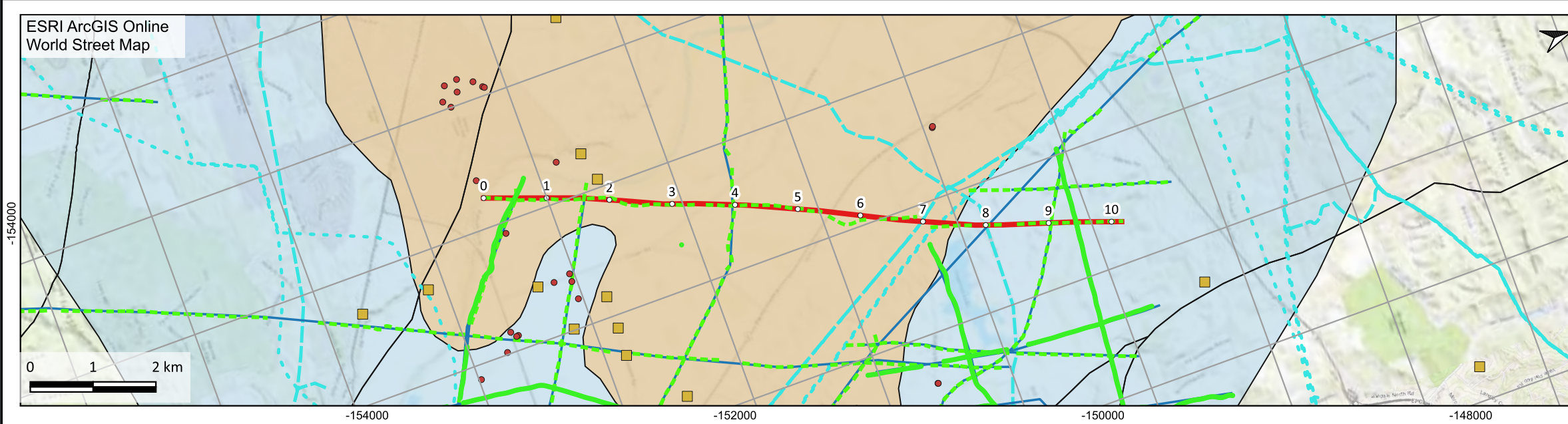


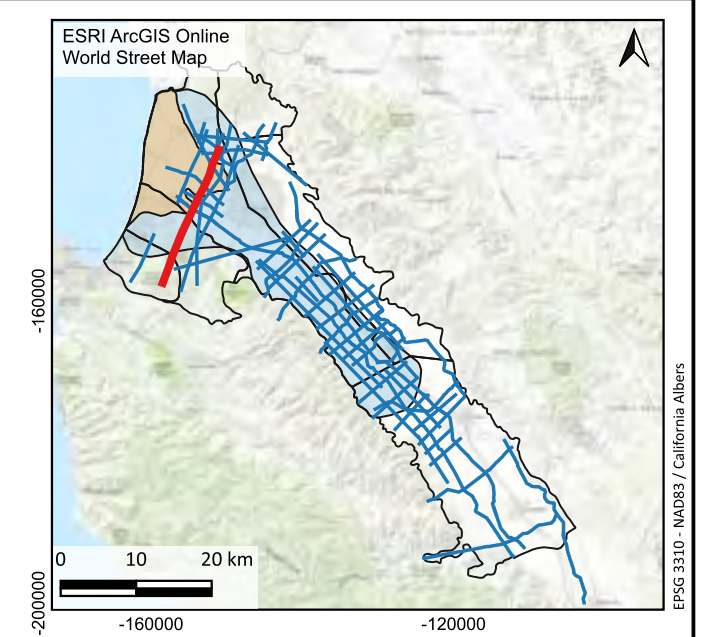
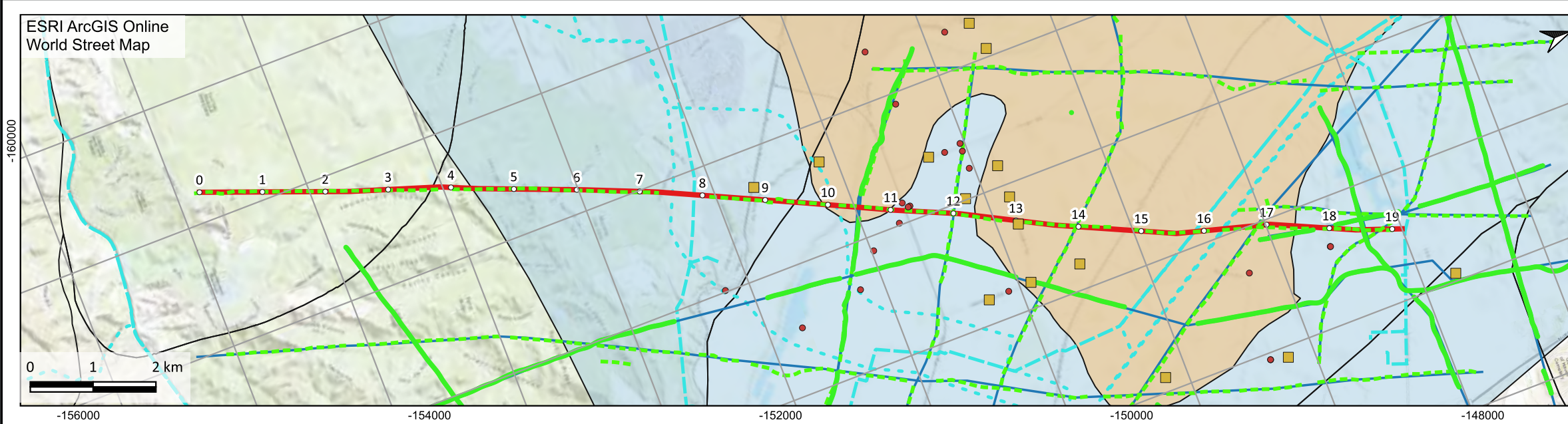
Smooth Model



Legend for Model Sections







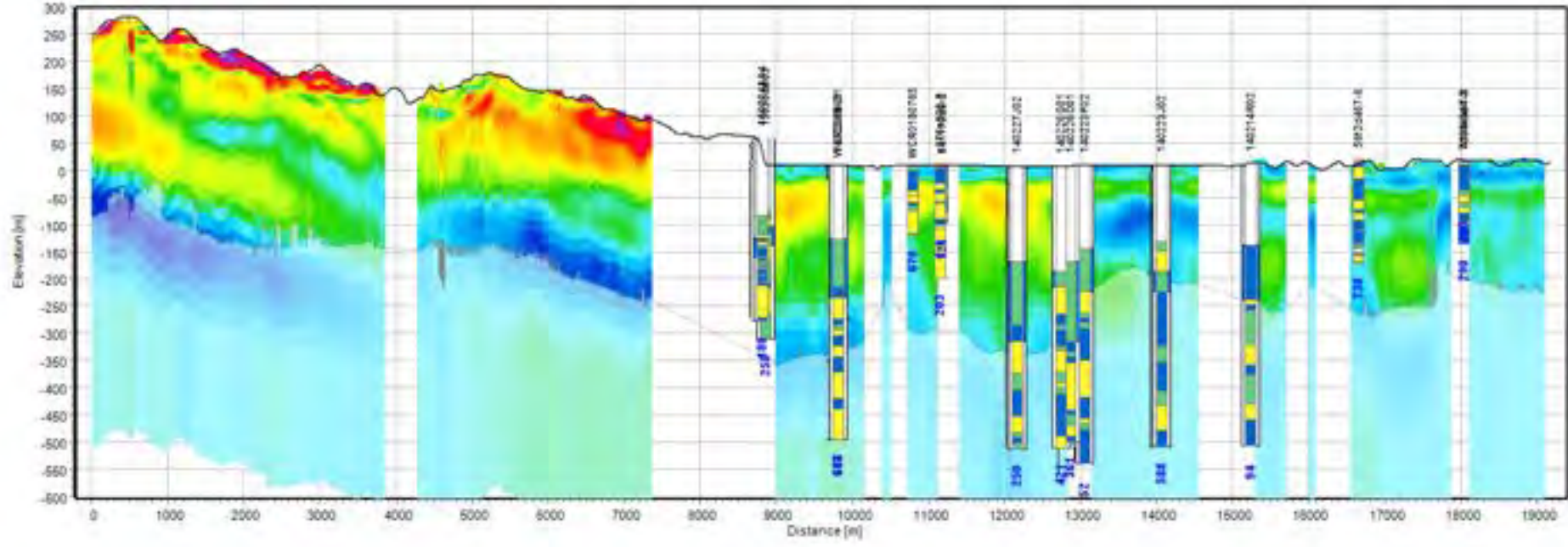
**Legend for Maps**

- Groundwater Basin Boundary (DWR - B118)
- Vineyards
- Phase 1 Aquitard Extent
- 180-Foot Aquifer CI- Contour
- Section (Current page)
- Section (Other pages)

**AEM data used for inversion**

- Lithology logs
- Resistivity logs
- Electric transmission lines (CA State Geoportals, 2020)
- Pipelines (AmeriGEOSS, 2022)

Smooth Model



**Legend for Model Sections**

**Resistivity: AEM inversion results**

Above DOI\*  
Below DOI\*

3 10 100 300  
Resistivity [ohm-m]

\*DOI = Depth of investigation

**Lithology log**

- Soil
- Fine Clay
- Clay
- Clay shale
- Silt
- Sandstone

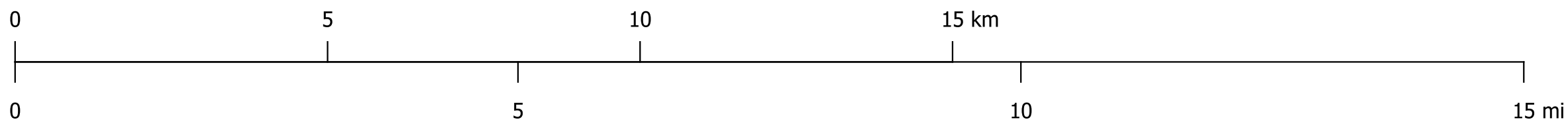
**Resistivity log**

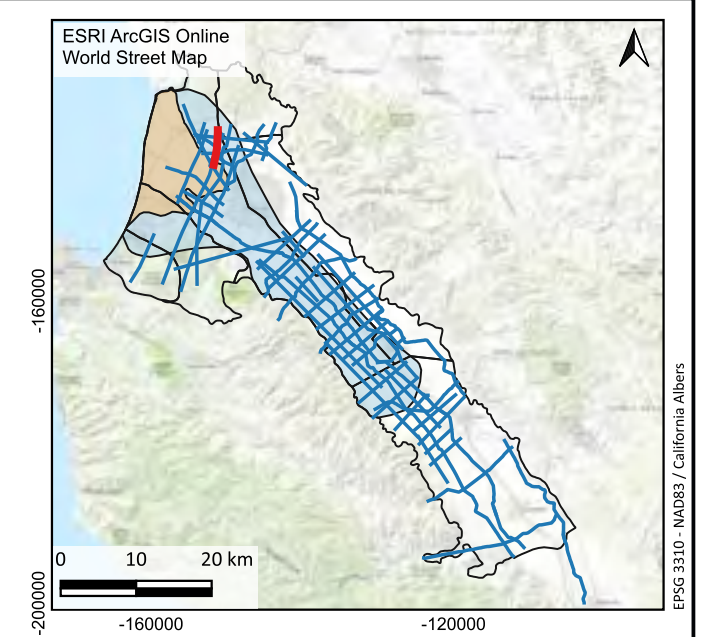
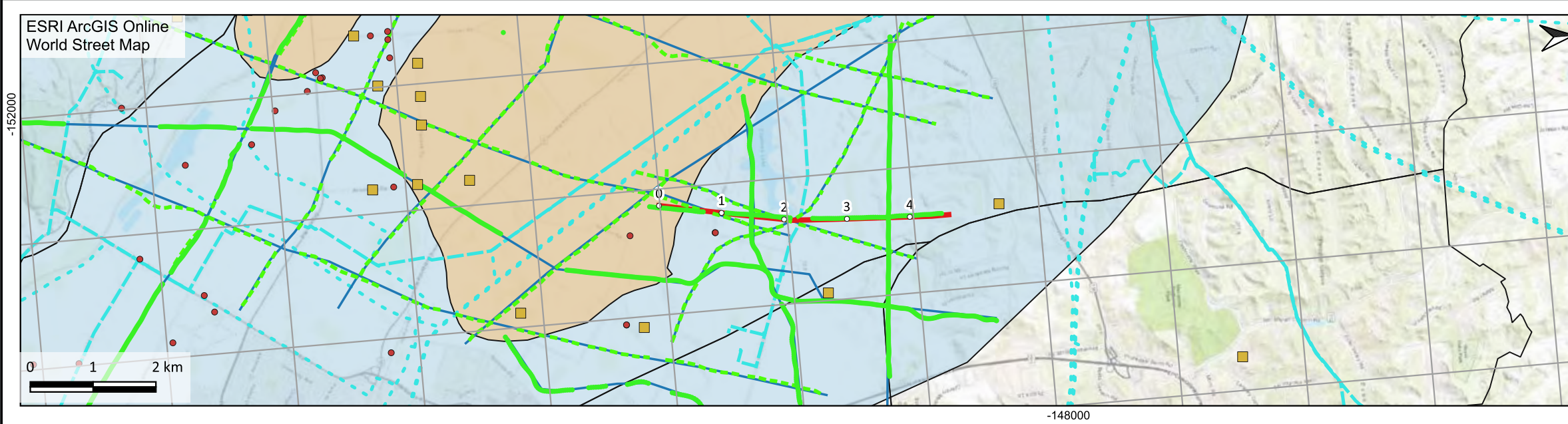
Low Resistivity High Resistivity

**Well completion report analysis**

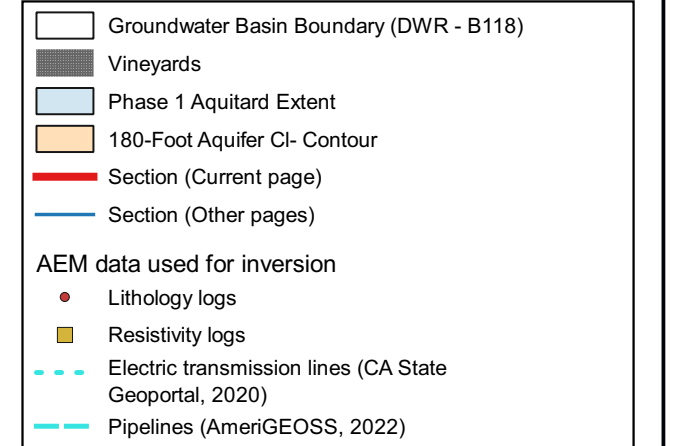
**Continuous conductor**

- Top of conductor
- Bottom of conductor
- Top of conductor (lower confidence)
- Bottom of conductor (lower confidence)

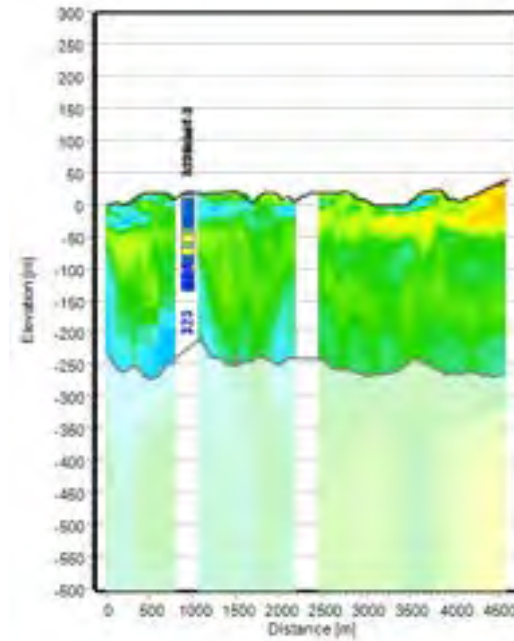




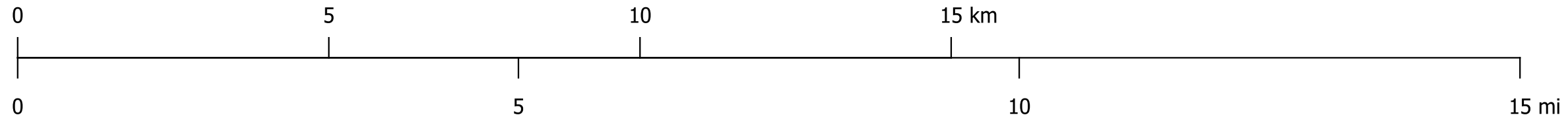
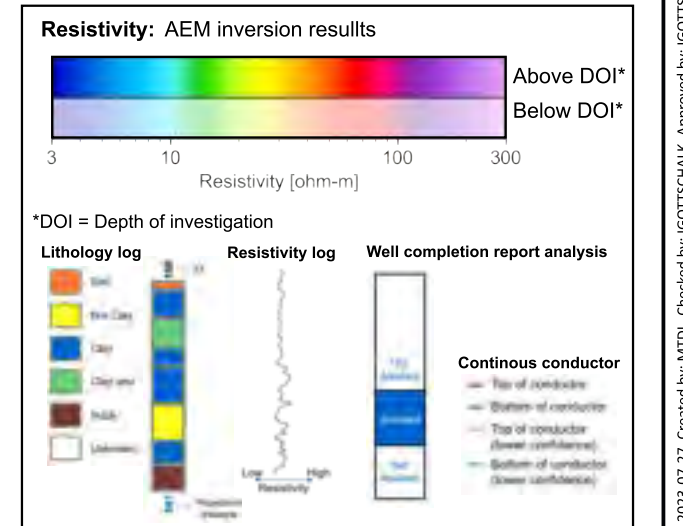
Legend for Maps

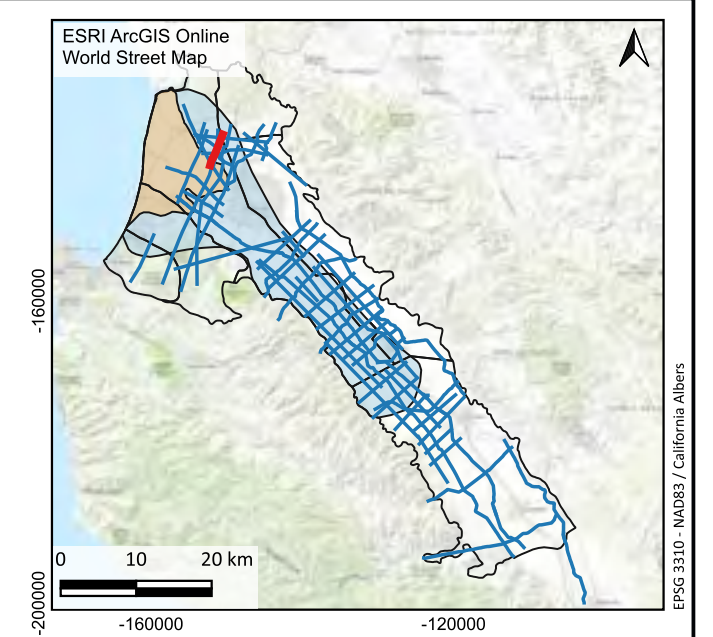
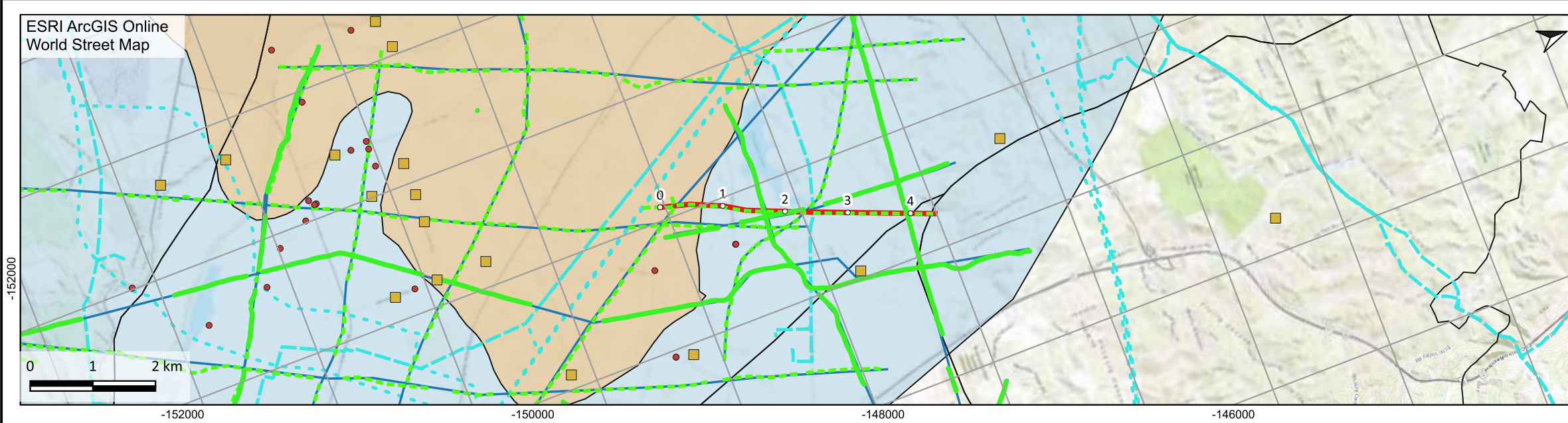


Smooth Model

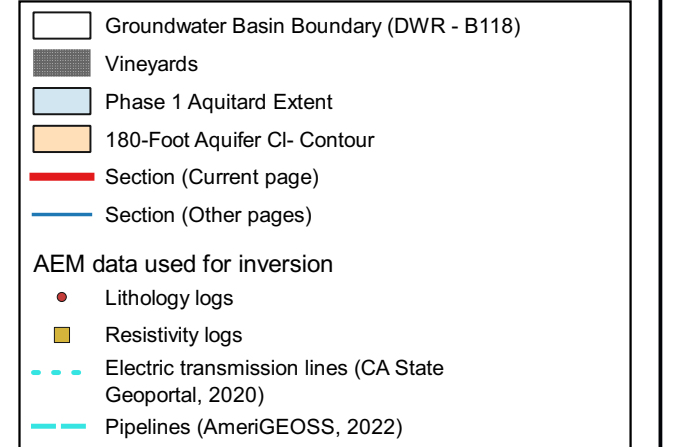


Legend for Model Sections

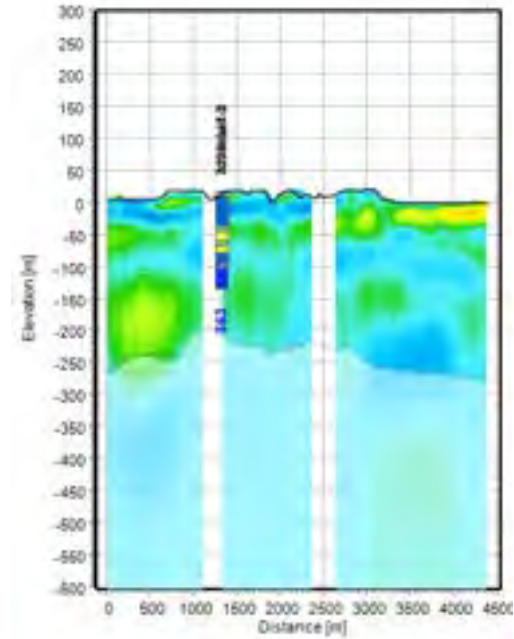




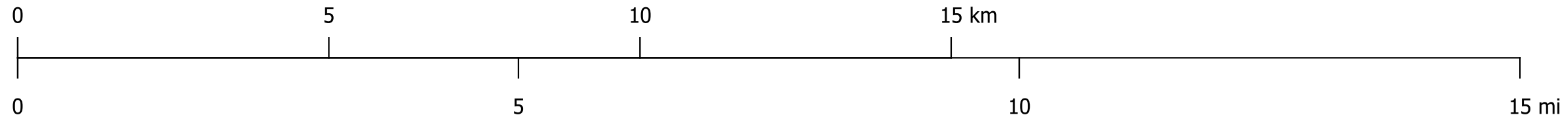
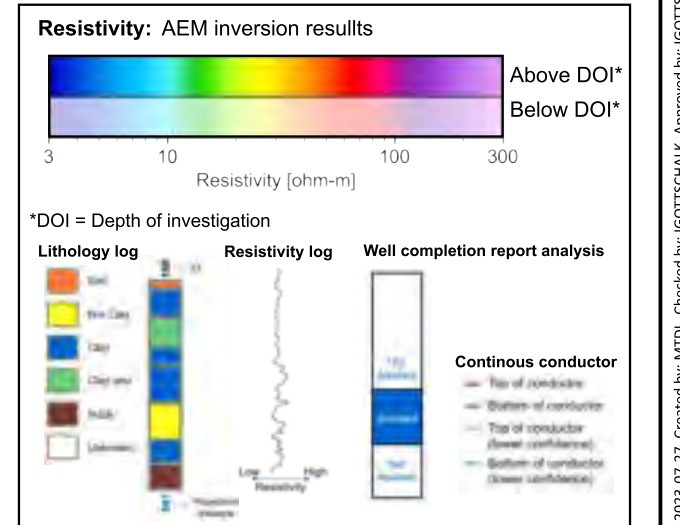
Legend for Maps

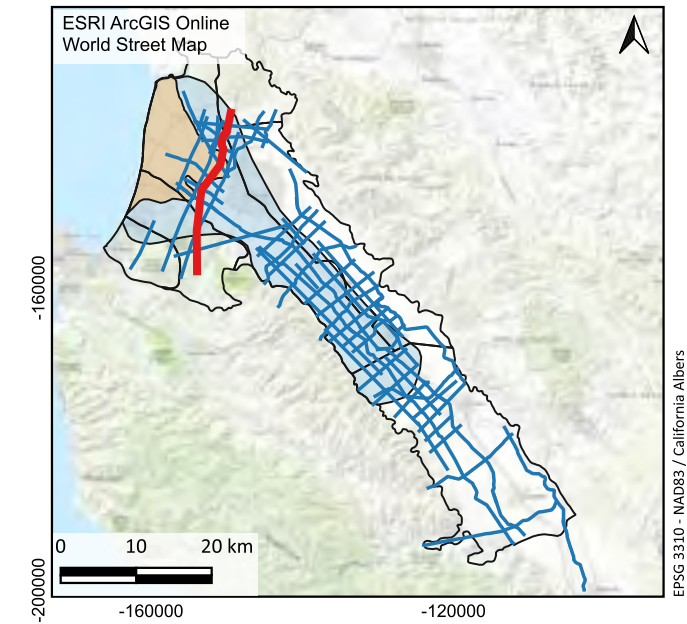
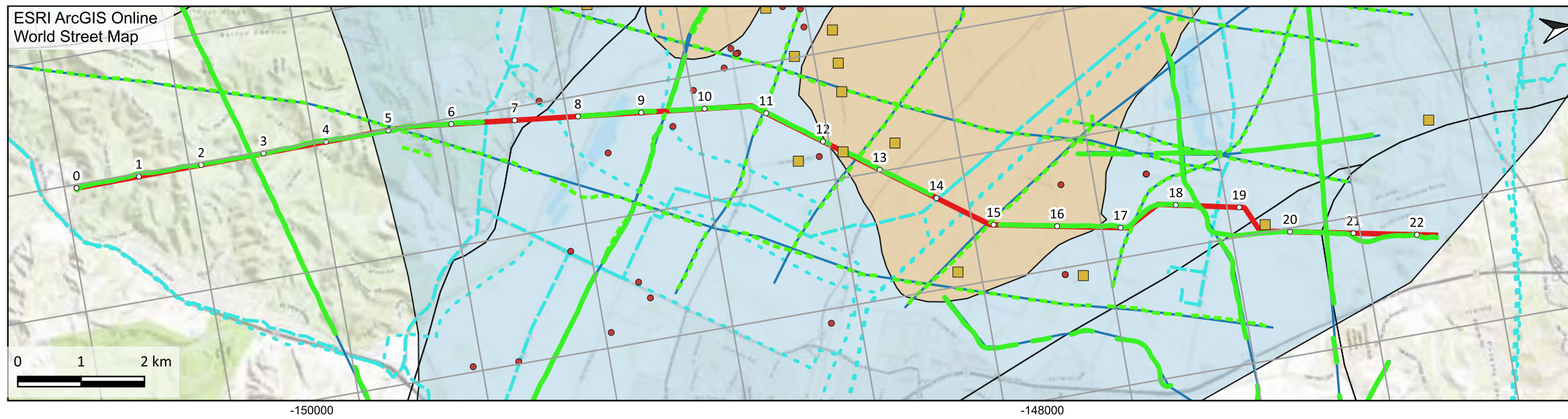


Smooth Model



Legend for Model Sections





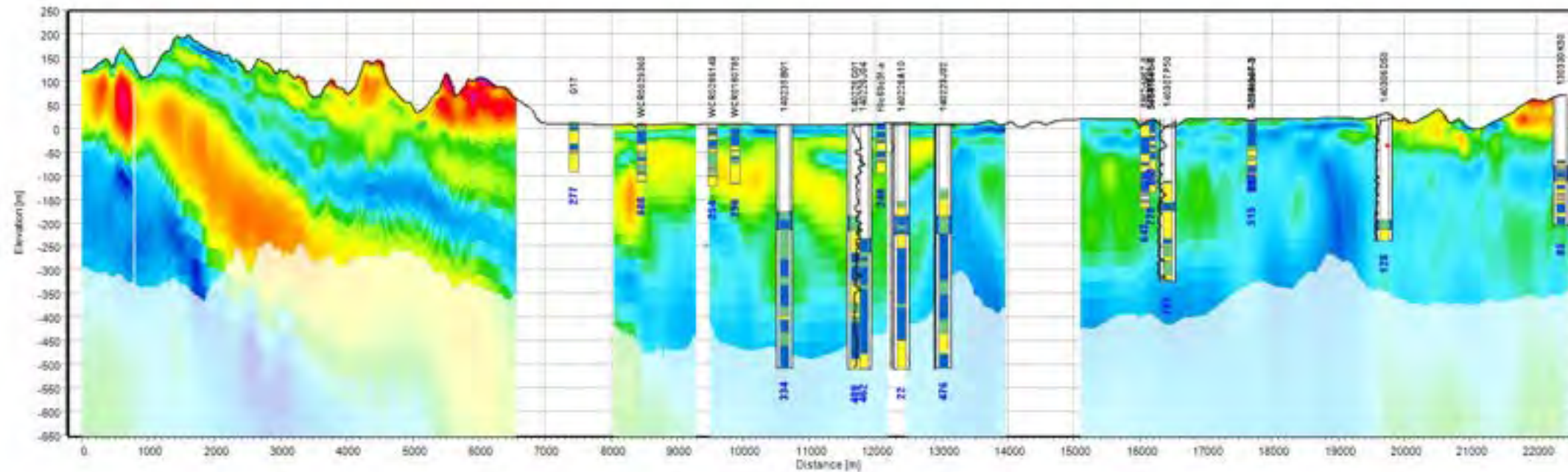
**Legend for Maps**

- Groundwater Basin Boundary (DWR - B118)
- Vineyards
- Phase 1 Aquitard Extent
- 180-Foot Aquifer CI- Contour
- Section (Current page)
- Section (Other pages)

**AEM data used for inversion**

- Lithology logs
- Resistivity logs
- Electric transmission lines (CA State Geoportals, 2020)
- Pipelines (AmeriGEOSS, 2022)

Smooth Model



**Legend for Model Sections**

**Resistivity: AEM inversion results**

Resistivity [ohm-m]

\*DOI = Depth of investigation

**Lithology log**

- Soil
- Fine Clay
- Clay
- Clay shale
- Silt
- Sandstone

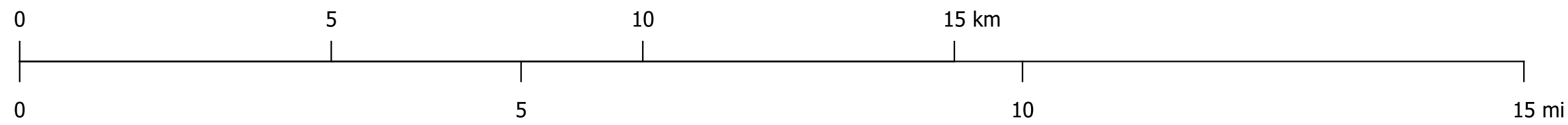
**Resistivity log**

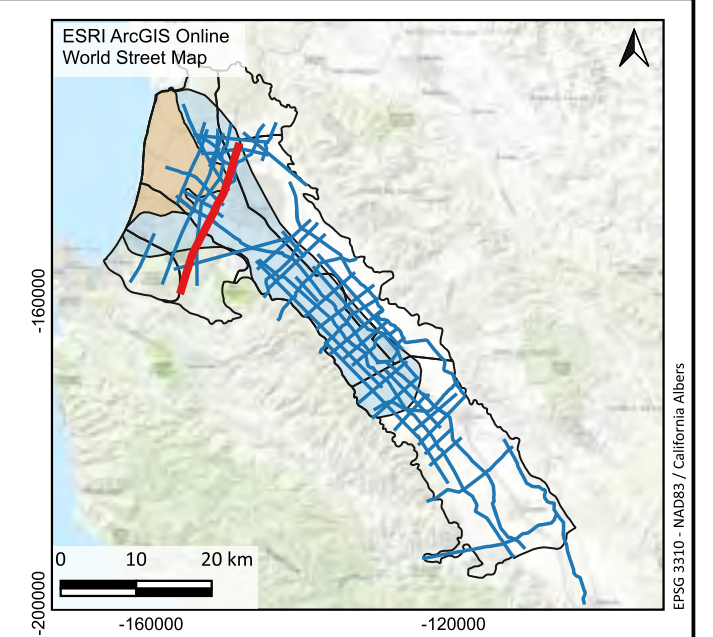
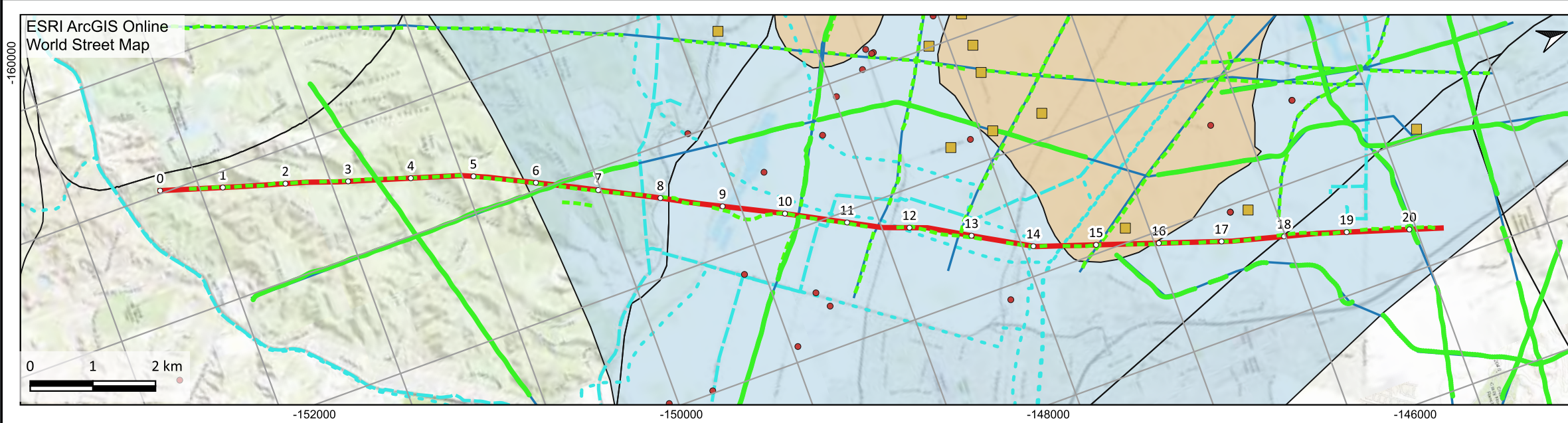
Log Resistivity

**Well completion report analysis**

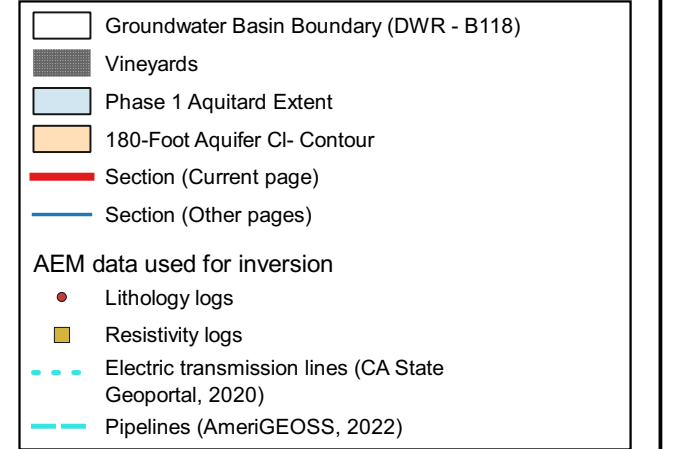
**Continuous conductor**

- Top of conductor
- Bottom of conductor
- Top of conductor (lower confidence)
- Bottom of conductor (lower confidence)

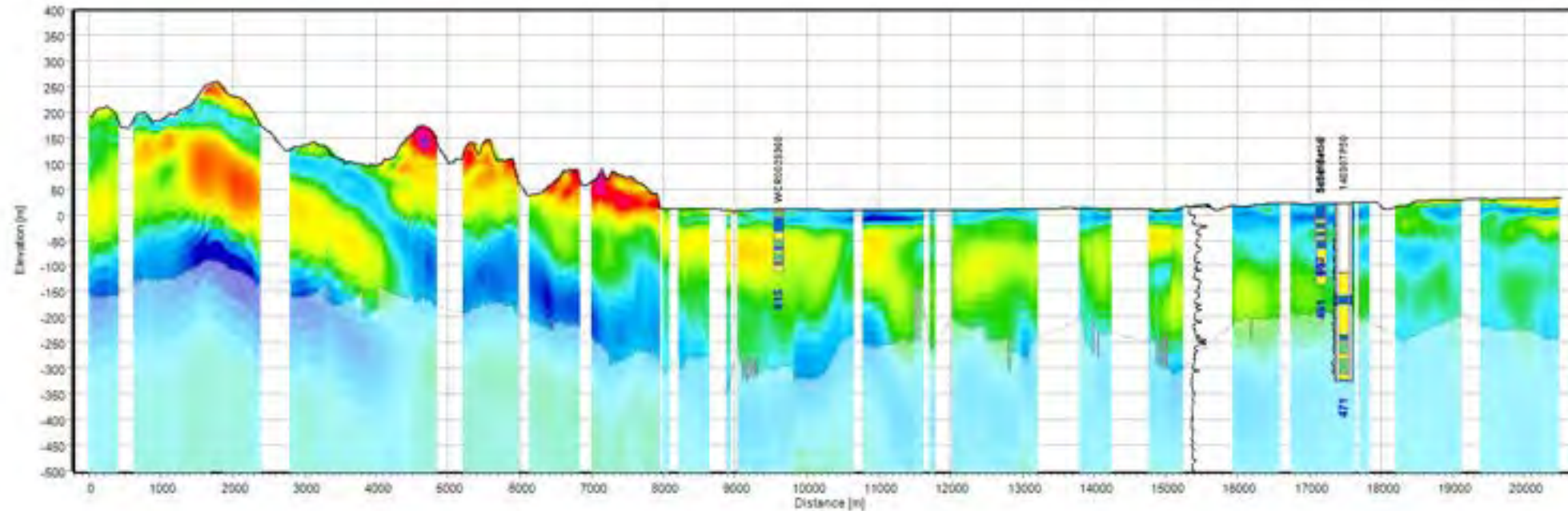




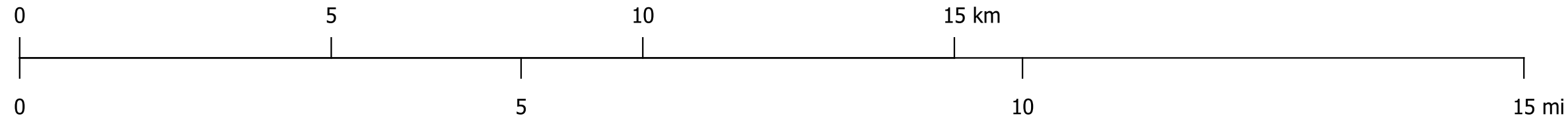
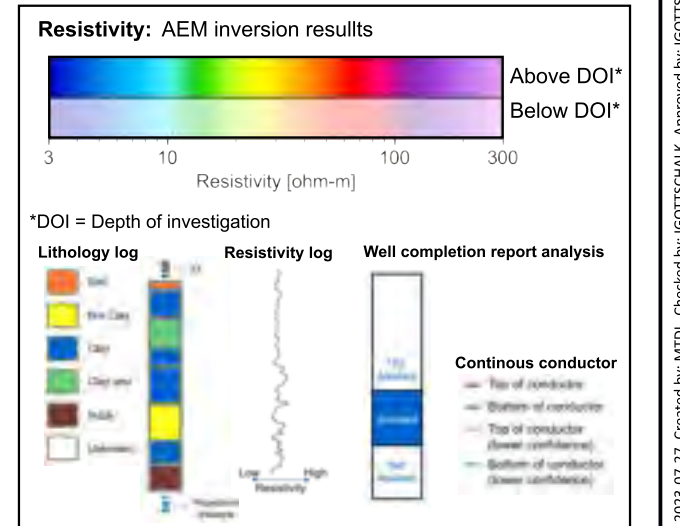
Legend for Maps

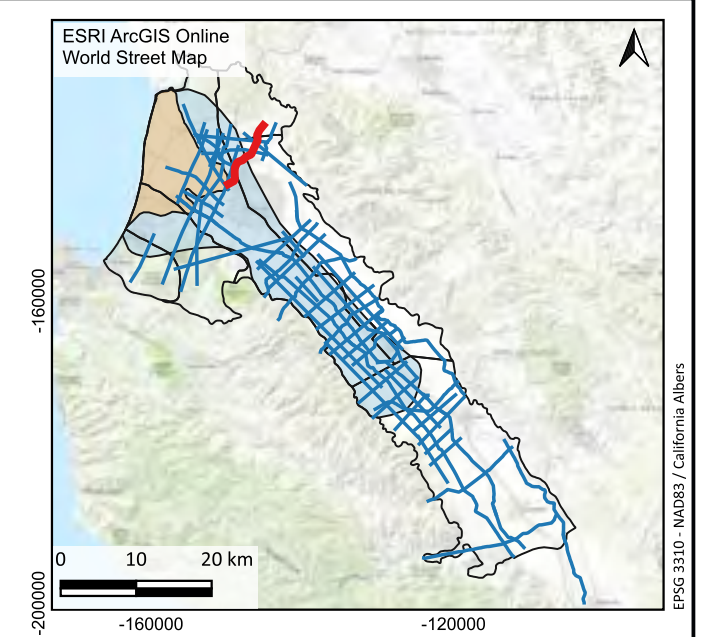
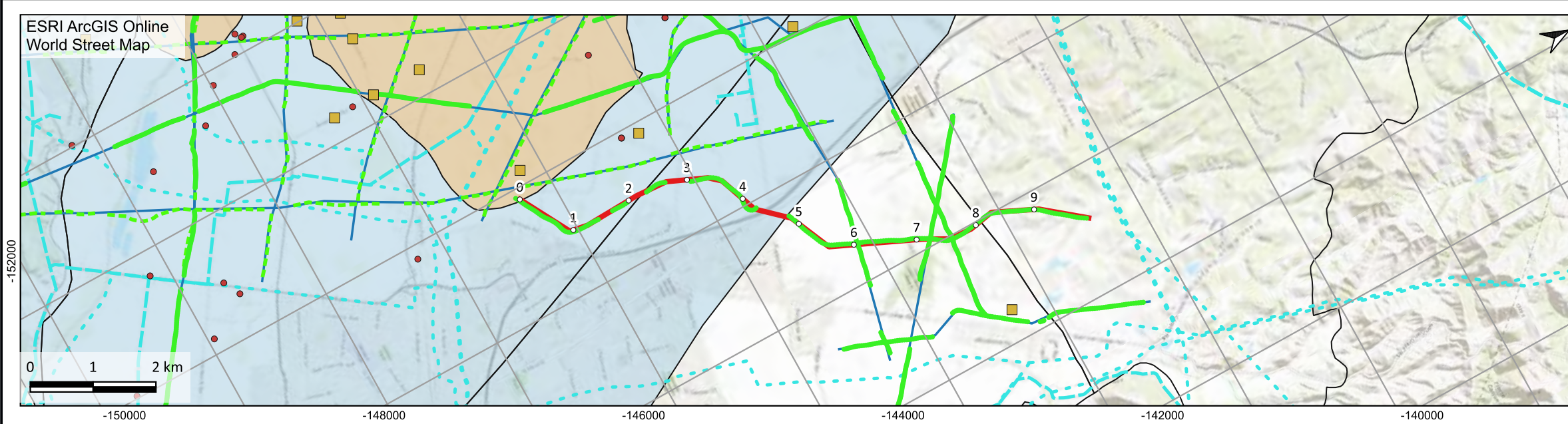


Smooth Model



Legend for Model Sections

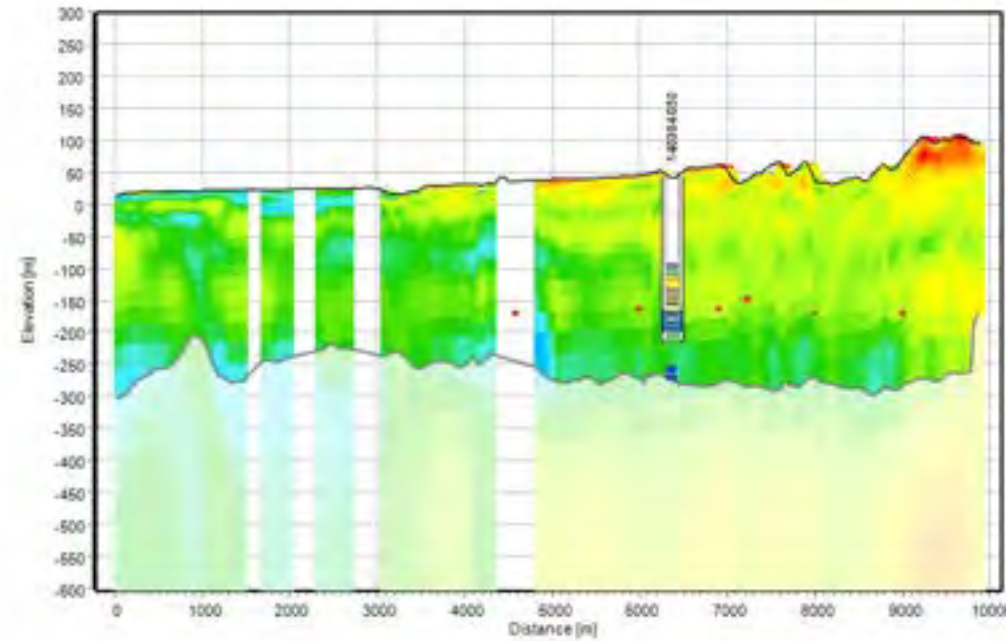




Legend for Maps

- Groundwater Basin Boundary (DWR - B118)
  - Vineyards
  - Phase 1 Aquitard Extent
  - 180-Foot Aquifer CI- Contour
  - Section (Current page)
  - Section (Other pages)
- AEM data used for inversion
- Lithology logs
  - Resistivity logs
  - Electric transmission lines (CA State Geoportal, 2020)
  - Pipelines (AmeriGEOSS, 2022)

Smooth Model



Legend for Model Sections

**Resistivity: AEM inversion results**

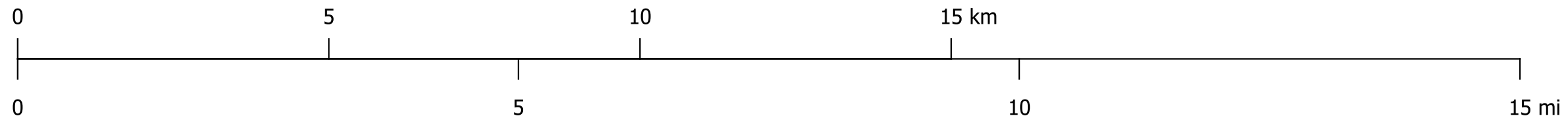
3 10 100 300  
Resistivity [ohm-m]

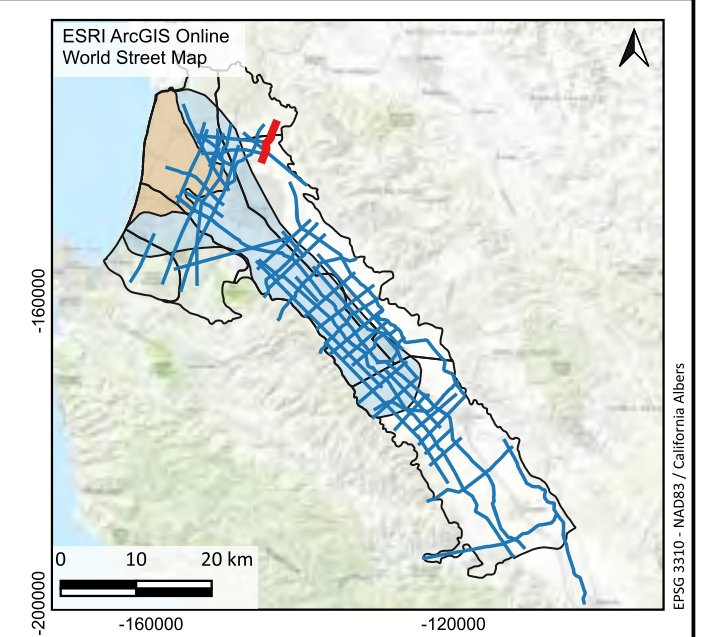
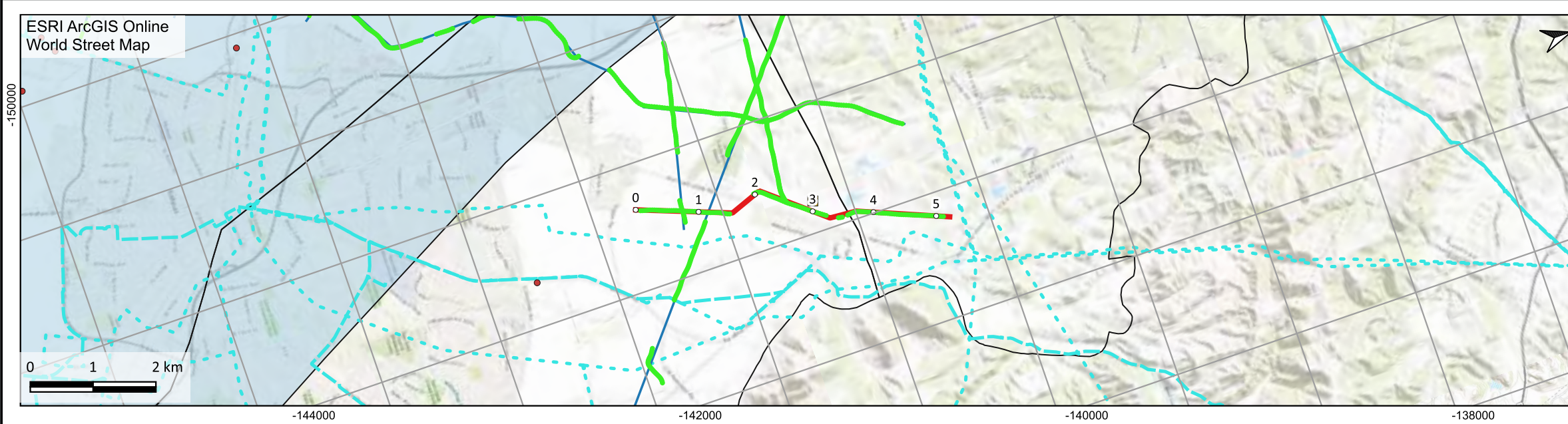
\*DOI = Depth of investigation

Lithology log	Resistivity log	Well completion report analysis
Sand		
Silt Clay		
Clay		
Clay shale		
Siltstone		
Limestone		

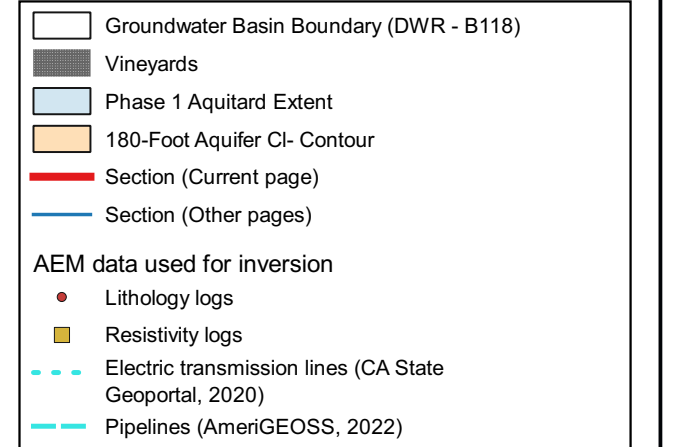
**Continuous conductor**

- Top of conductor
- Bottom of conductor
- Top of conductor (lower confidence)
- Bottom of conductor (lower confidence)

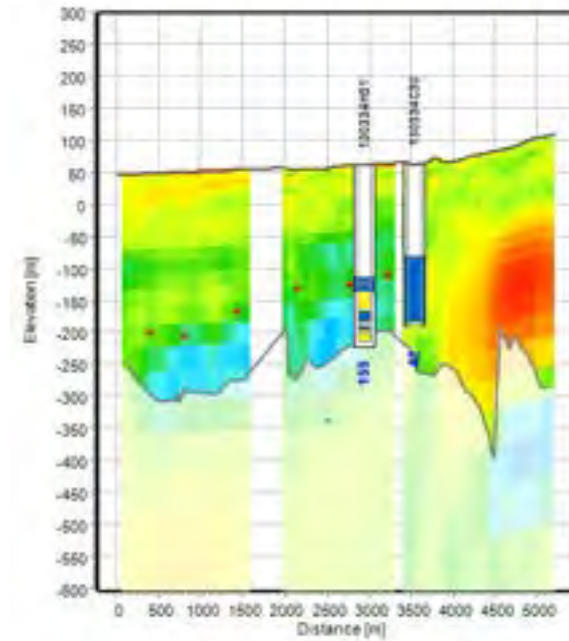




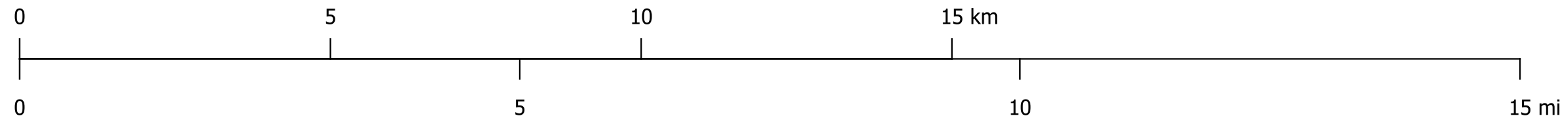
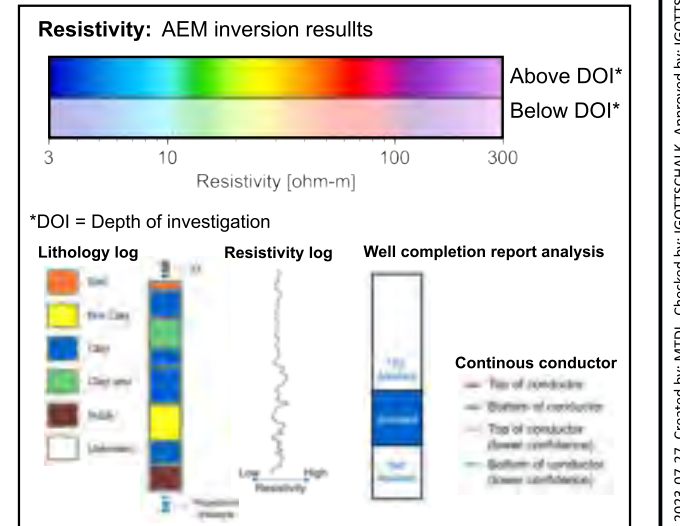
Legend for Maps

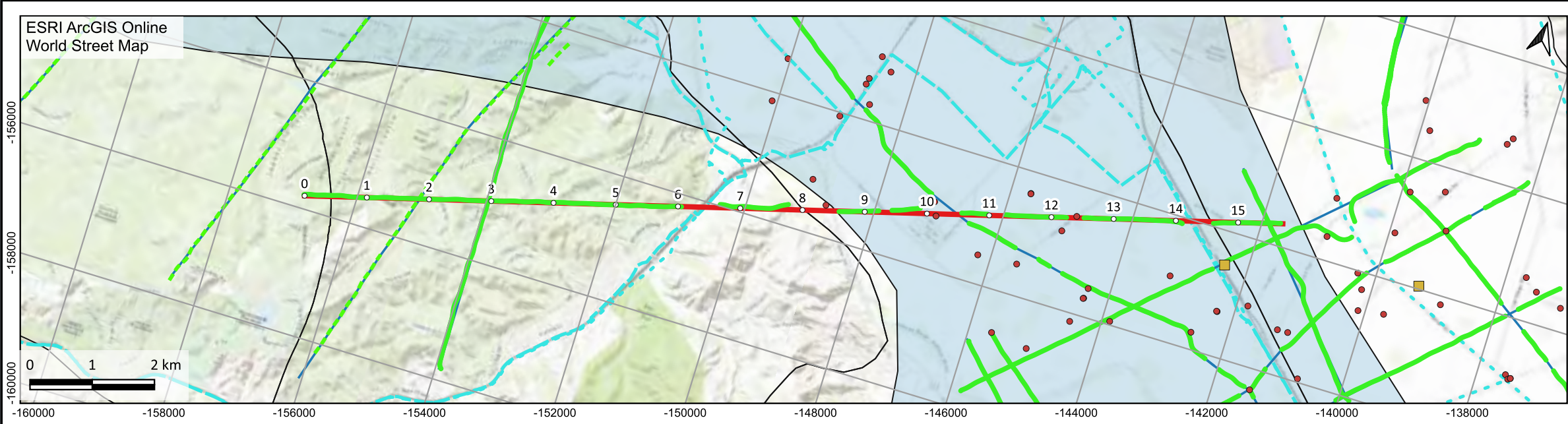


Smooth Model



Legend for Model Sections





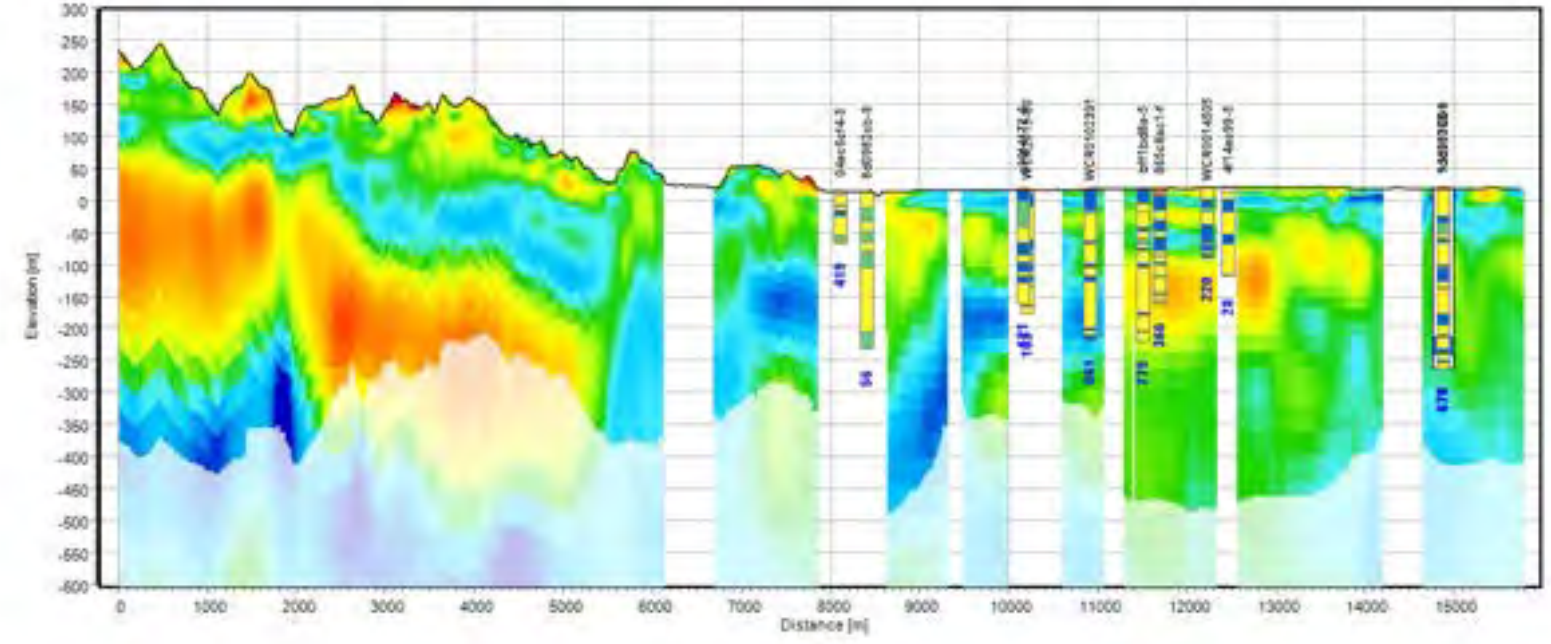
**Legend for Maps**

- Groundwater Basin Boundary (DWR - B118)
- Vineyards
- Phase 1 Aquitard Extent
- 180-Foot Aquifer CI- Contour
- Section (Current page)
- Section (Other pages)

**AEM data used for inversion**

- Lithology logs
- Resistivity logs
- Electric transmission lines (CA State Geoportal, 2020)
- Pipelines (AmeriGEOSS, 2022)

Smooth Model



**Legend for Model Sections**

**Resistivity: AEM inversion results**

3 10 100 300  
Resistivity [ohm-m]

\*DOI = Depth of investigation

**Lithology log**

- Soil
- Fine Clay
- Clay
- Clay shale
- Silt
- Sandstone

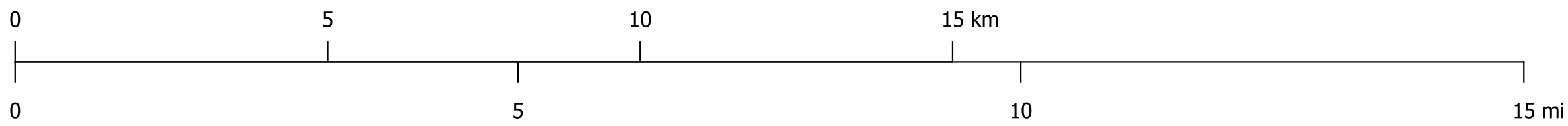
**Resistivity log**

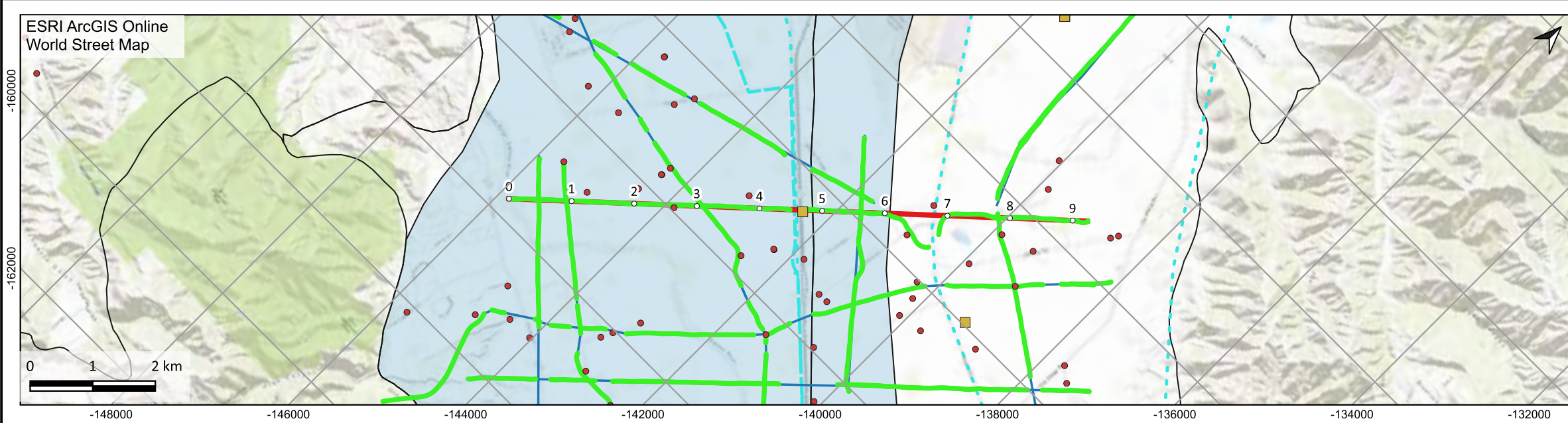
Log Resistivity High

**Well completion report analysis**

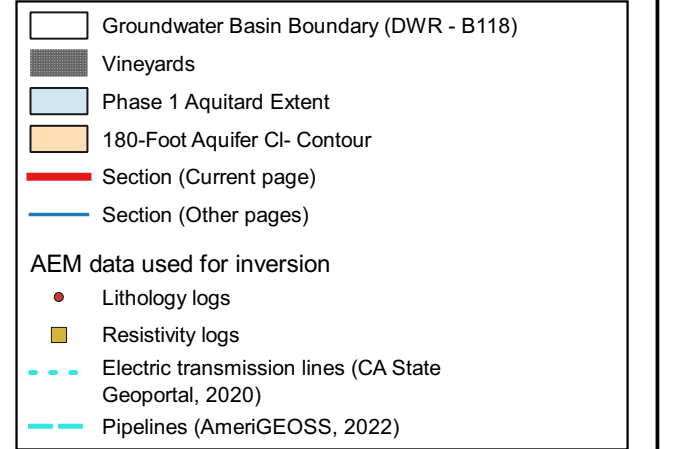
**Continuous conductor**

- Top of conductor
- Bottom of conductor
- Top of conductor (lower confidence)
- Bottom of conductor (lower confidence)

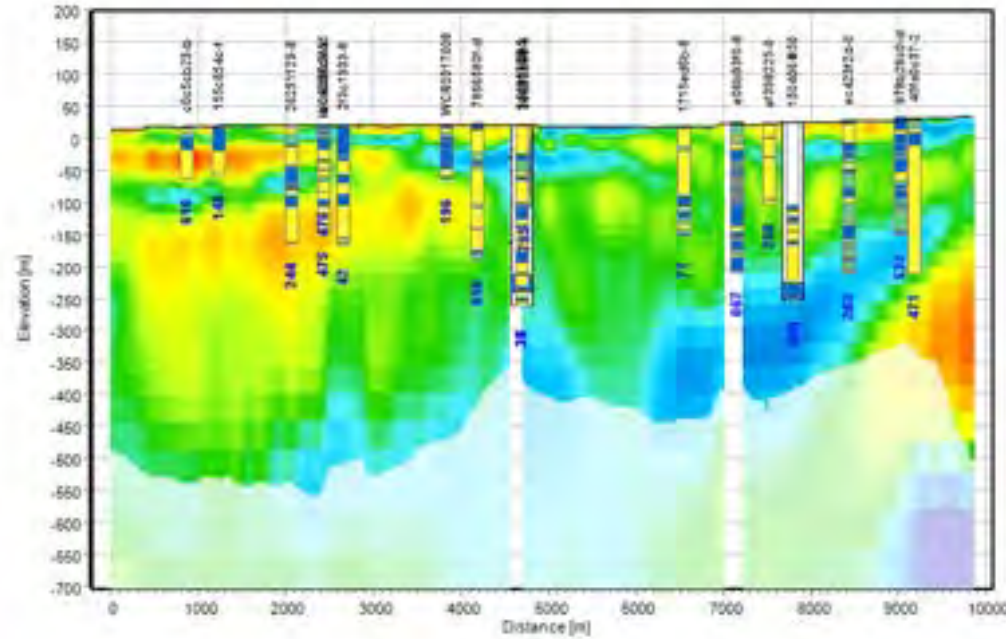




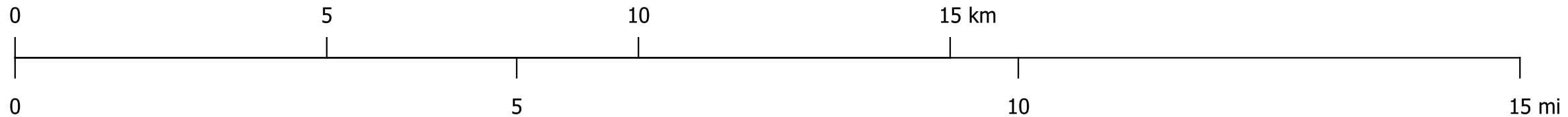
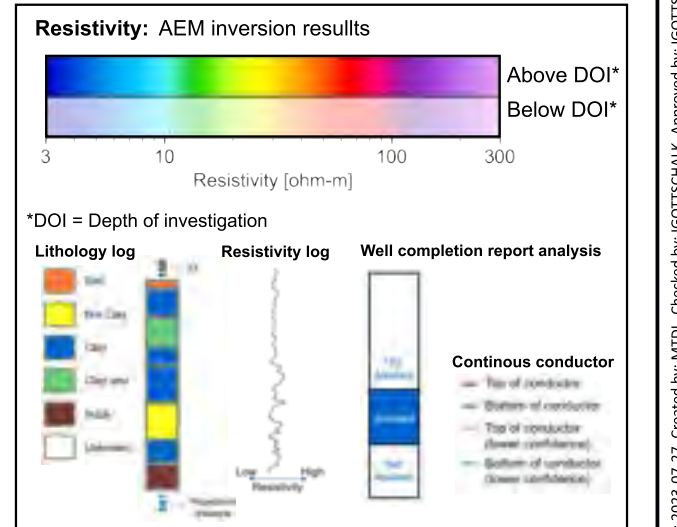
Legend for Maps

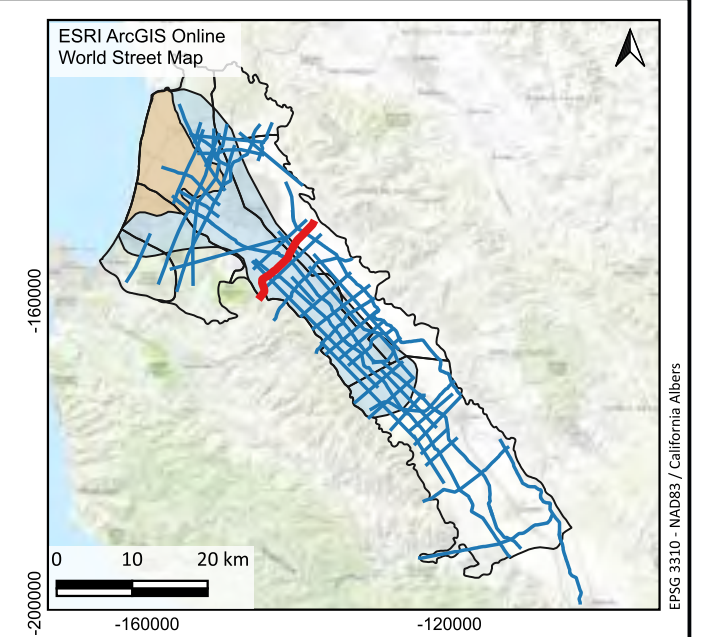
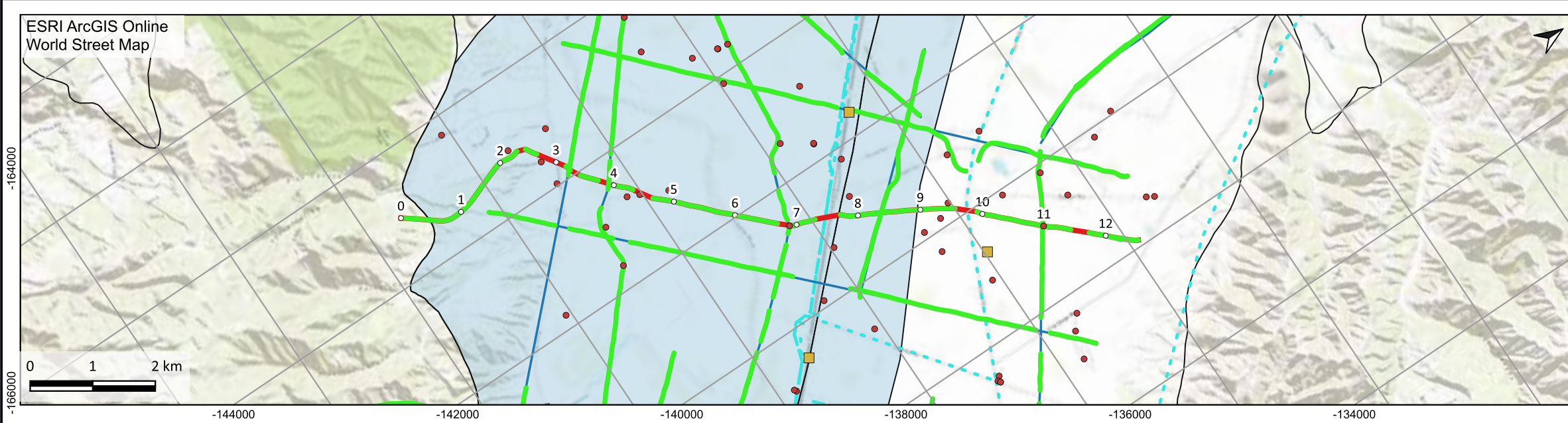


Smooth Model

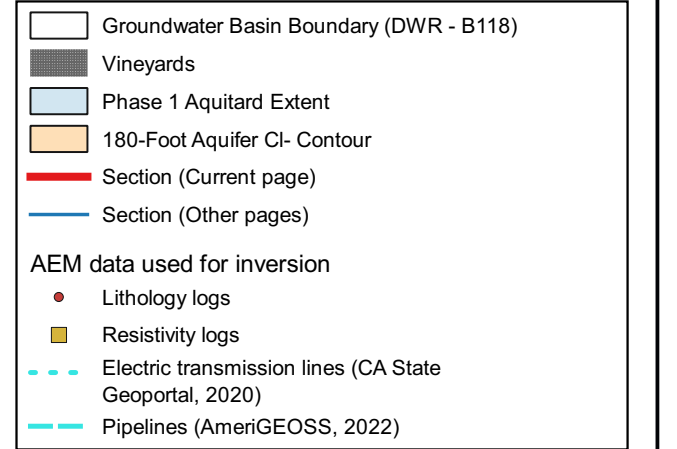


Legend for Model Sections

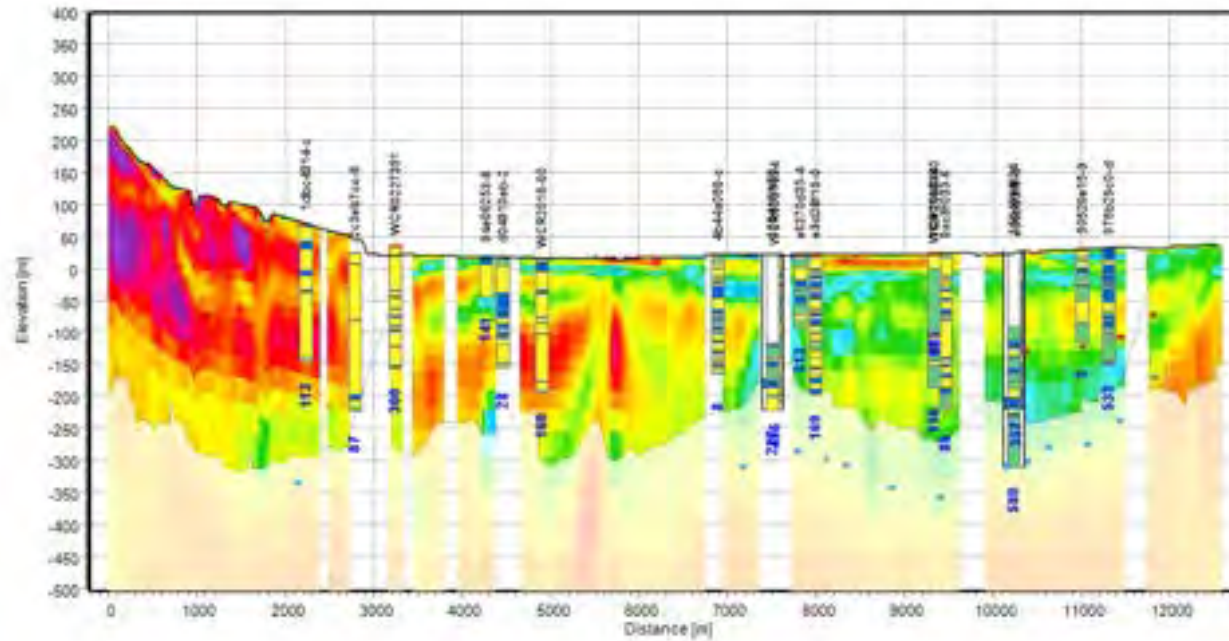




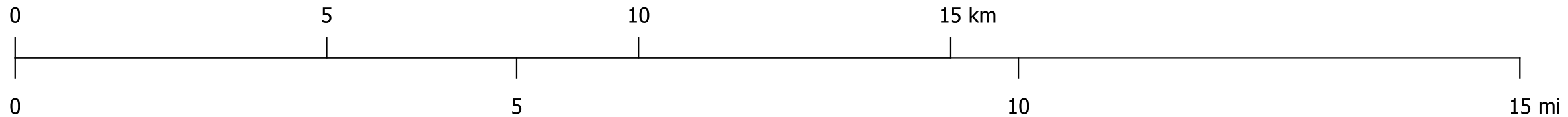
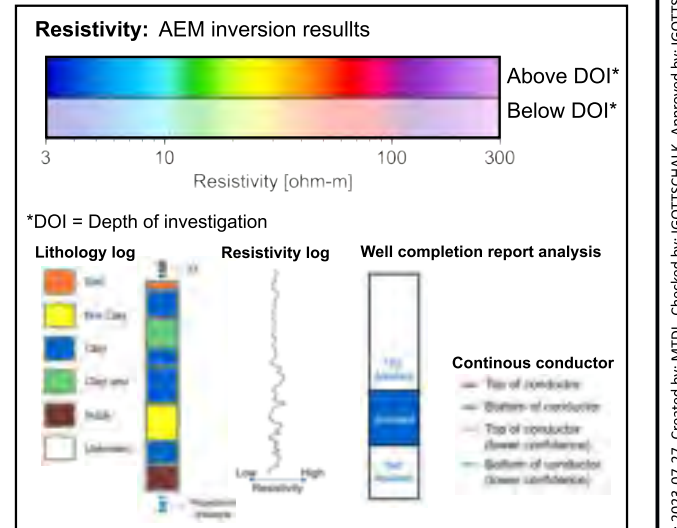
Legend for Maps

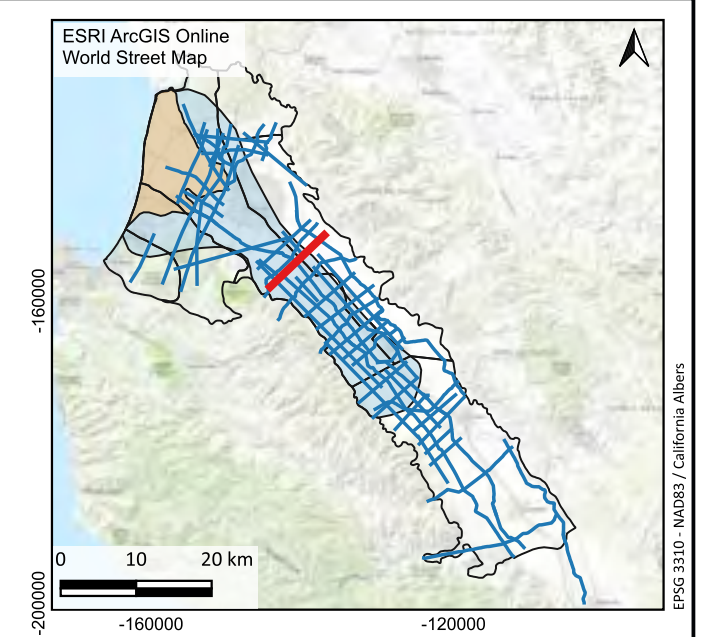
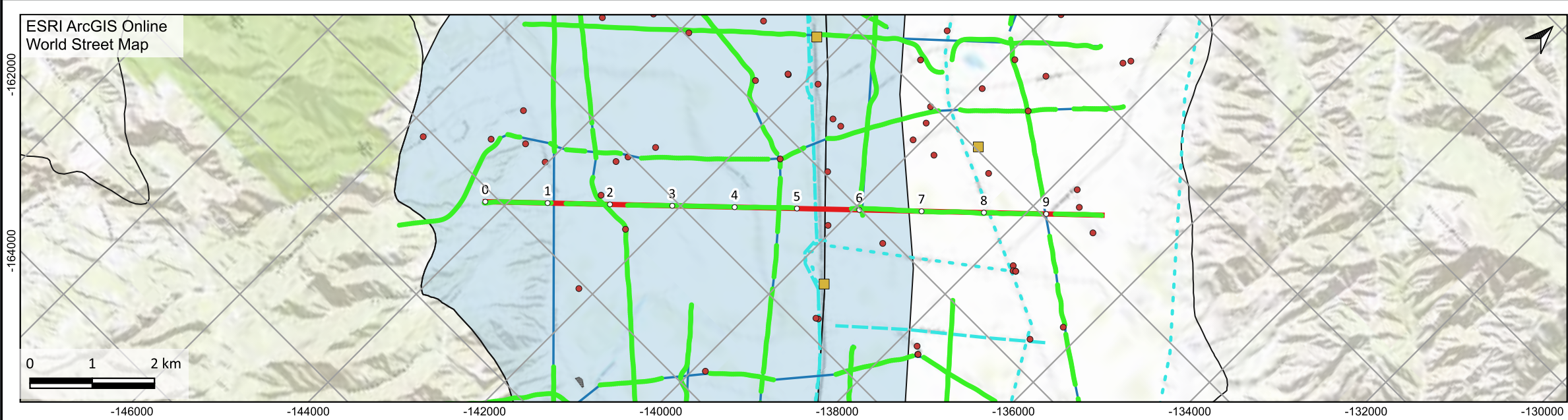


Smooth Model

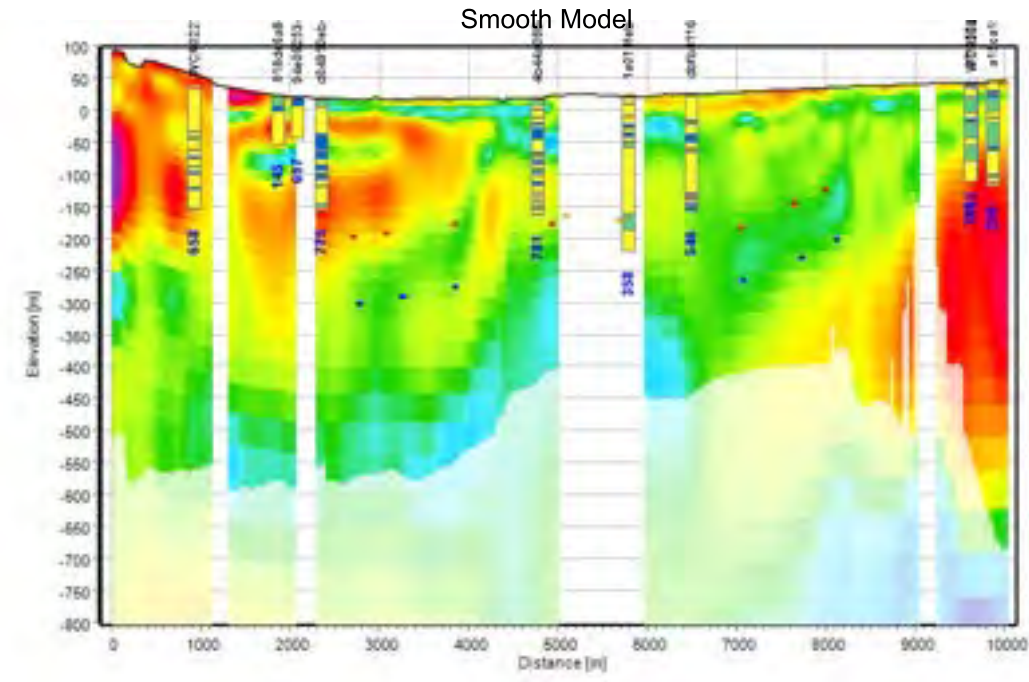
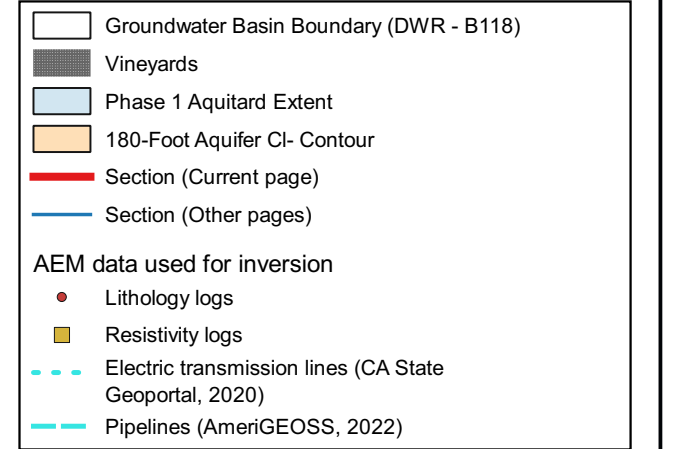


Legend for Model Sections

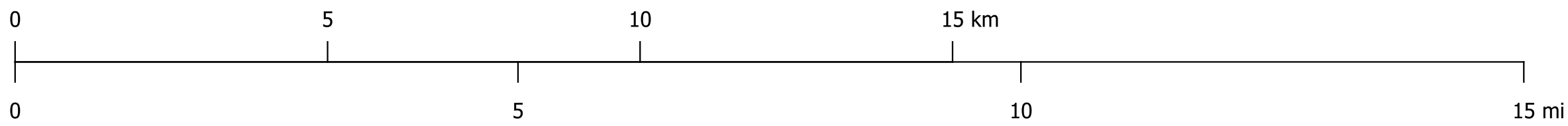
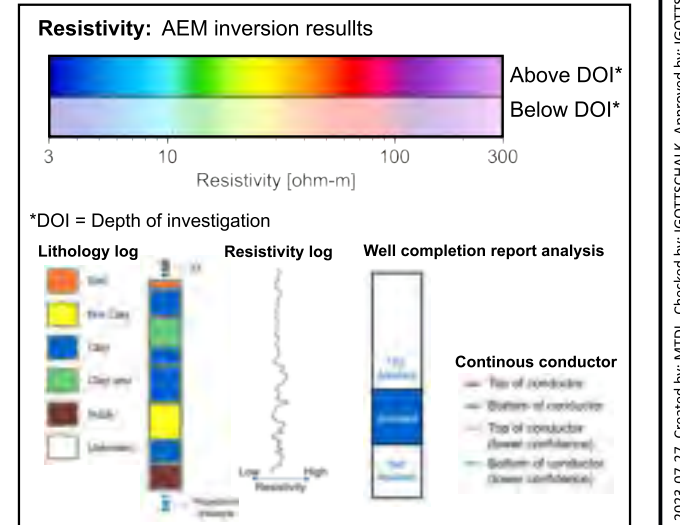


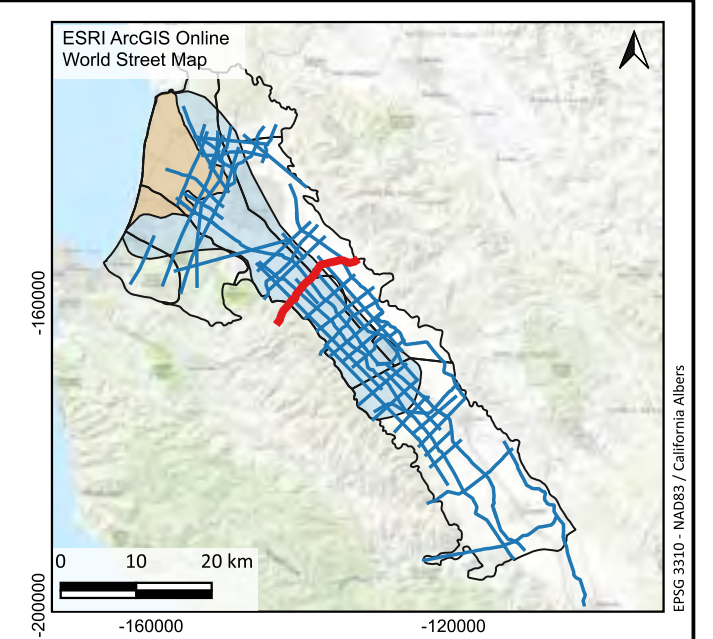
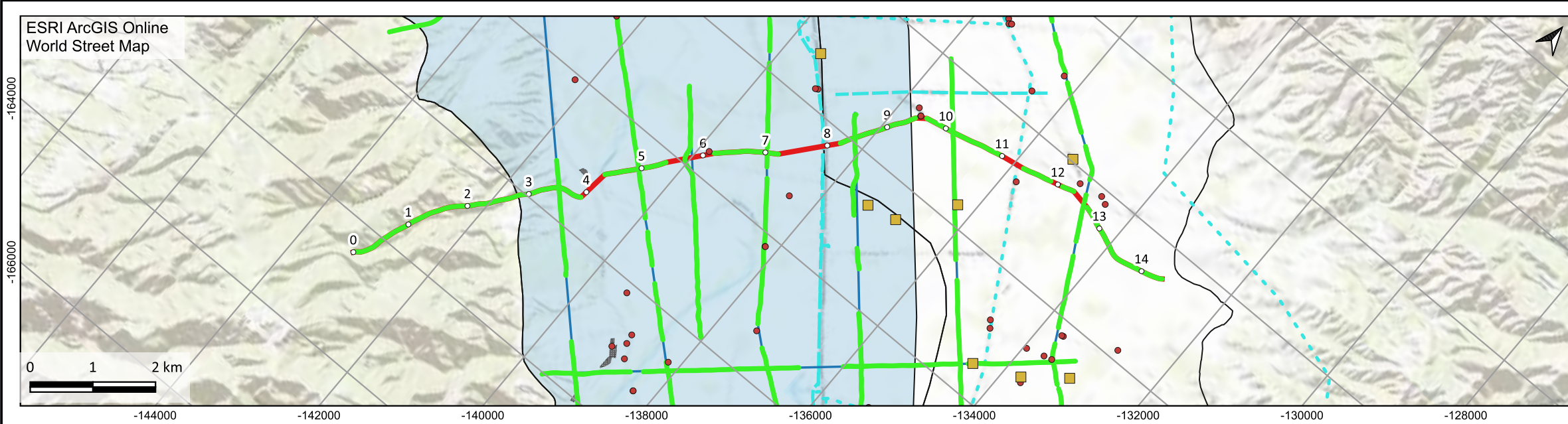


Legend for Maps



Legend for Model Sections



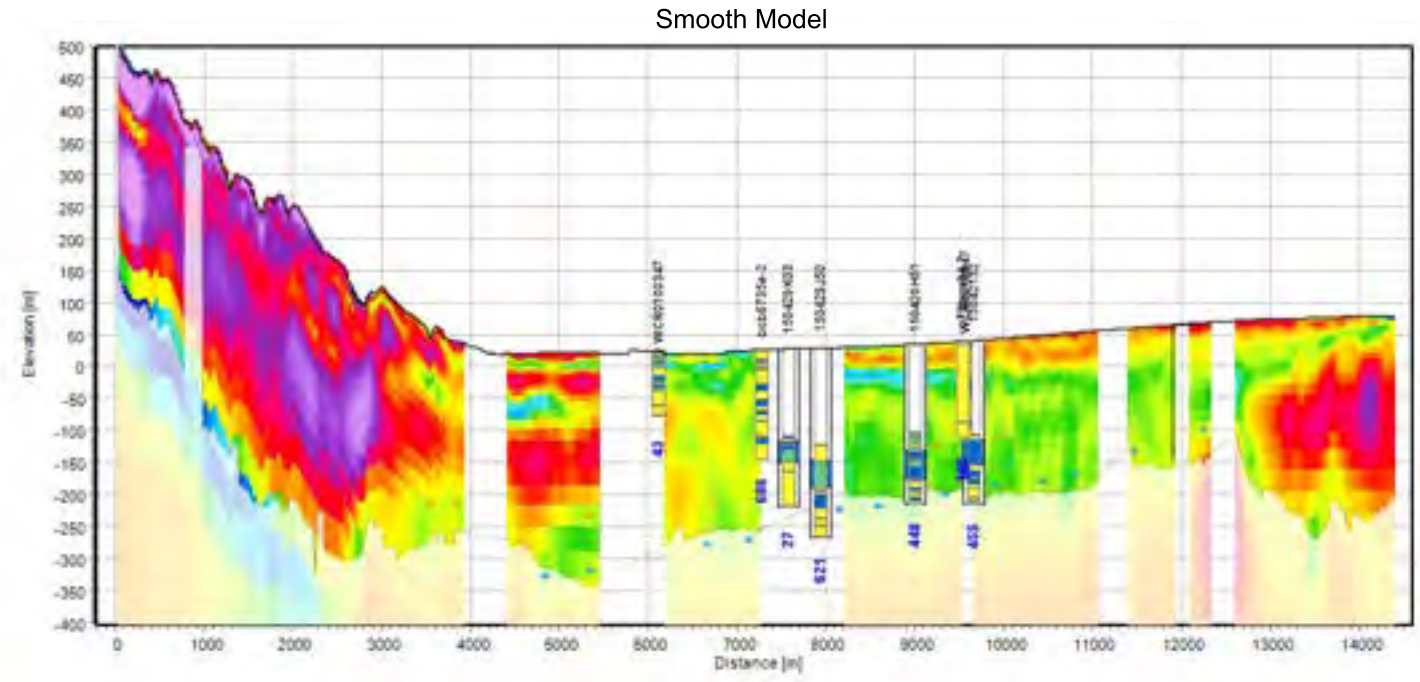


**Legend for Maps**

- Groundwater Basin Boundary (DWR - B118)
- Vineyards
- Phase 1 Aquitard Extent
- 180-Foot Aquifer CI- Contour
- Section (Current page)
- Section (Other pages)

**AEM data used for inversion**

- Lithology logs
- Resistivity logs
- Electric transmission lines (CA State Geoportal, 2020)
- Pipelines (AmeriGEOSS, 2022)



**Legend for Model Sections**

**Resistivity: AEM inversion results**

3 10 100 300  
Resistivity [ohm-m]

\*DOI = Depth of investigation

**Lithology log**

- Soil
- Fine Clay
- Clay
- Claystone
- Siltstone
- Limestone

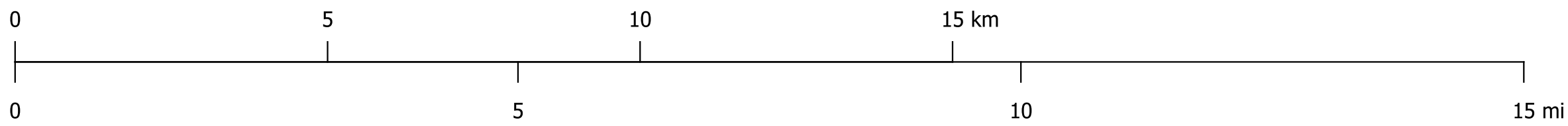
**Resistivity log**

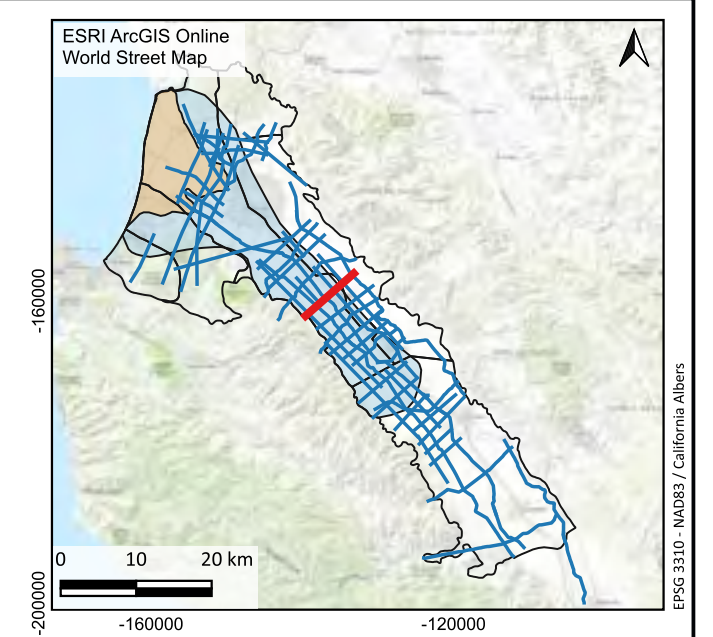
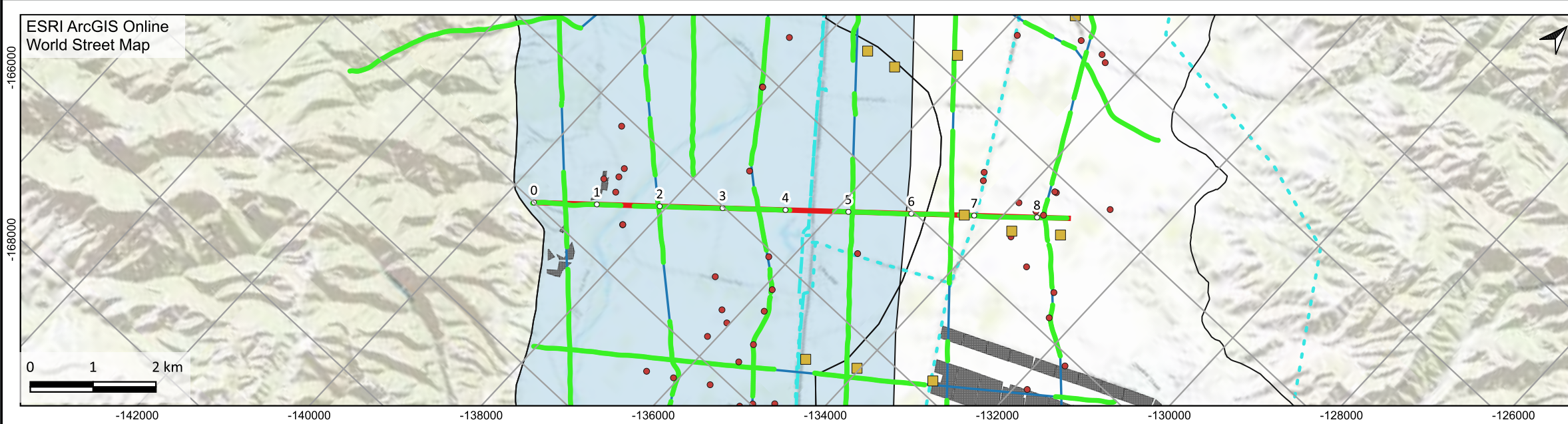
Log Resistivity

**Well completion report analysis**

**Continuous conductor**

- Top of conductor
- Bottom of conductor
- Top of conductor (lower confidence)
- Bottom of conductor (lower confidence)



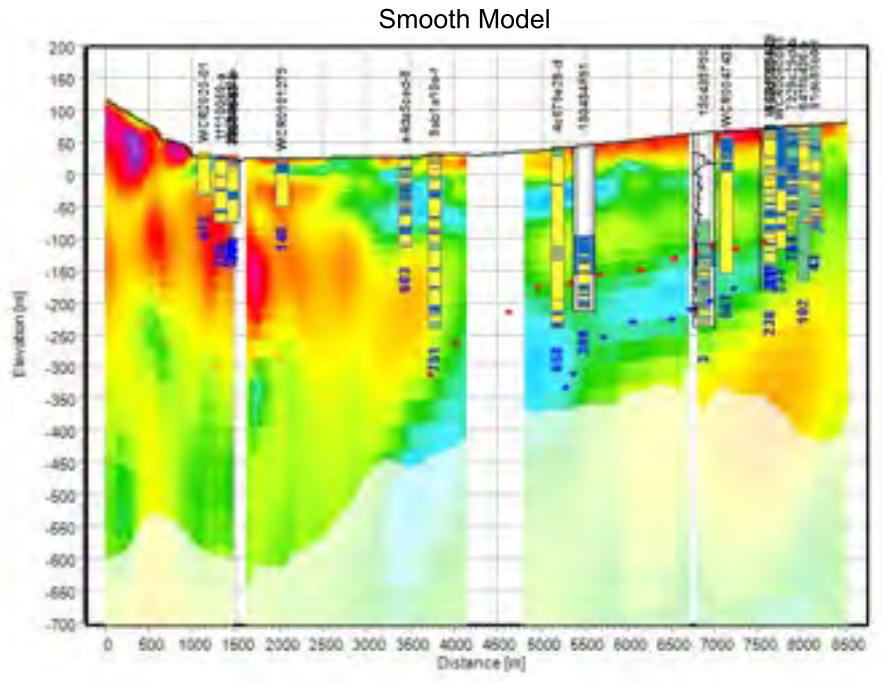


**Legend for Maps**

- Groundwater Basin Boundary (DWR - B118)
- Vineyards
- Phase 1 Aquitard Extent
- 180-Foot Aquifer CI- Contour
- Section (Current page)
- Section (Other pages)

**AEM data used for inversion**

- Lithology logs
- Resistivity logs
- Electric transmission lines (CA State Geoportal, 2020)
- Pipelines (AmeriGEOSS, 2022)

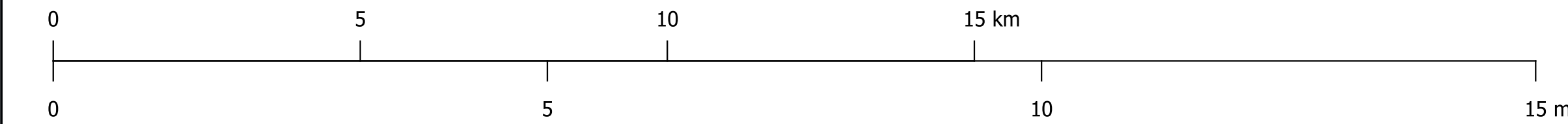


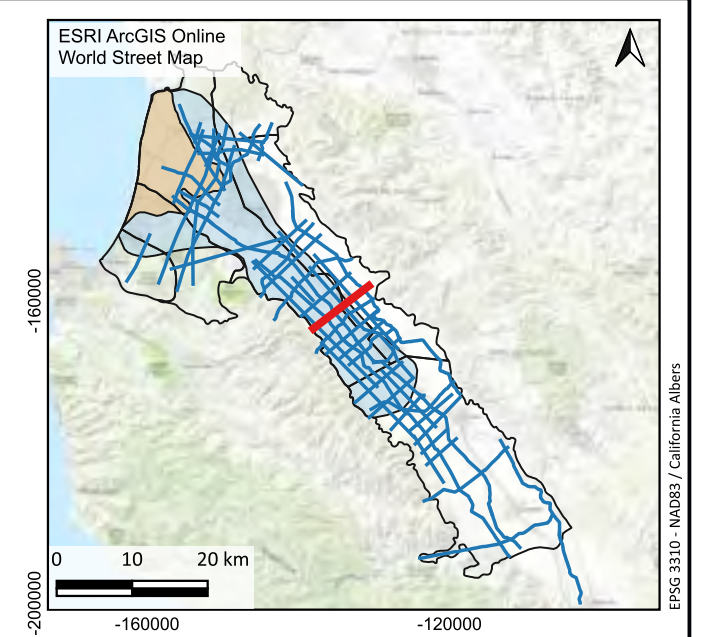
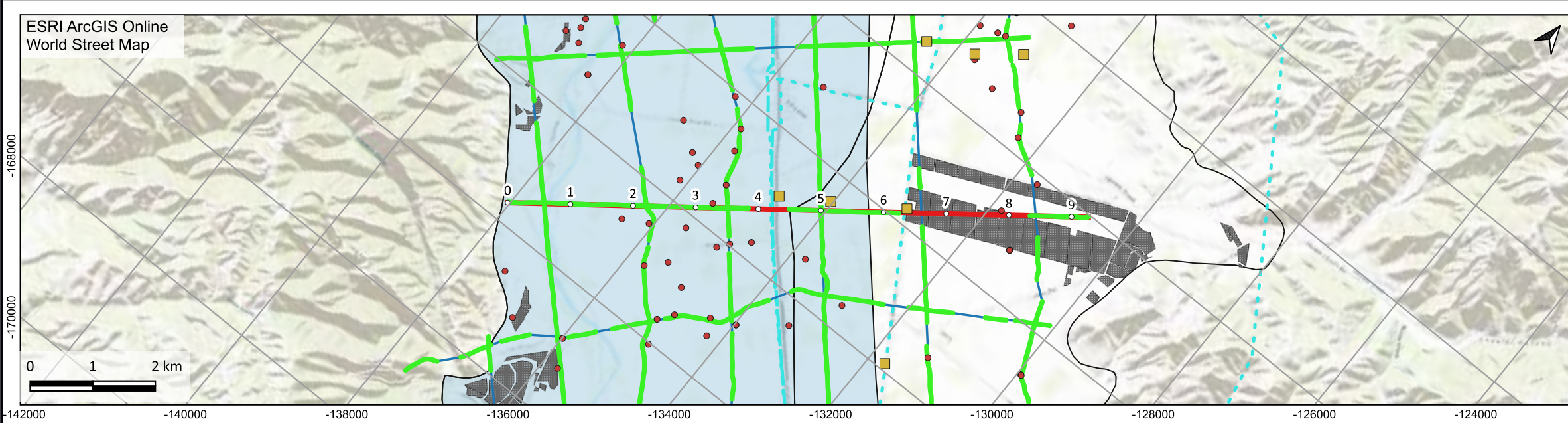
**Legend for Model Sections**

**Resistivity: AEM inversion results**

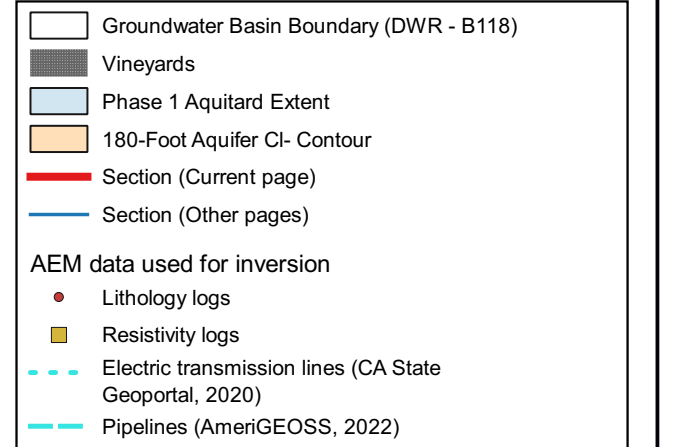
**\*DOI = Depth of investigation**

Lithology log	Resistivity log	Well completion report analysis
<ul style="list-style-type: none"> <li>Soil</li> <li>Fine Clay</li> <li>Clay</li> <li>Clay shale</li> <li>Sand</li> <li>Siltstone</li> </ul>		<ul style="list-style-type: none"> <li>Top of conductor</li> <li>Bottom of conductor</li> <li>Top of conductor (lower confidence)</li> <li>Bottom of conductor (lower confidence)</li> </ul>

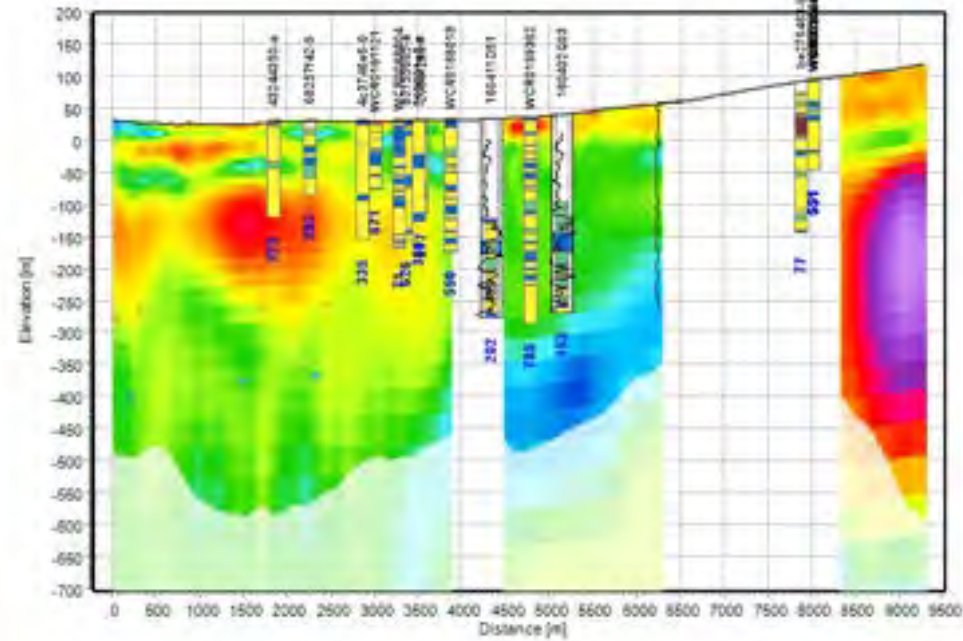




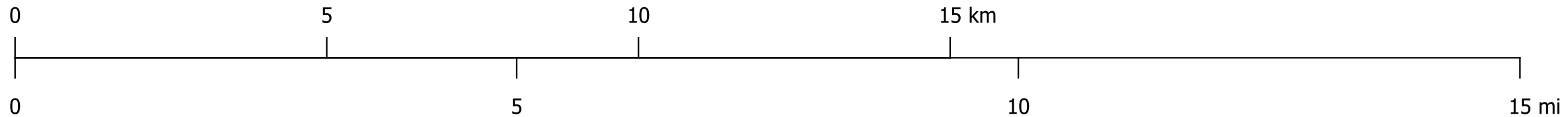
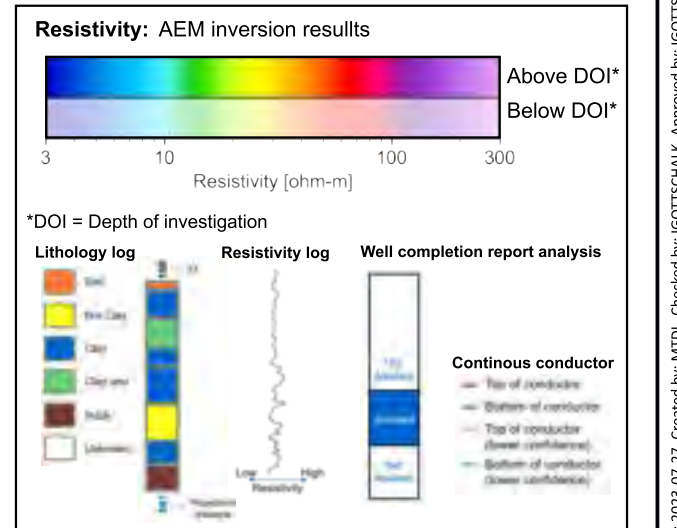
Legend for Maps

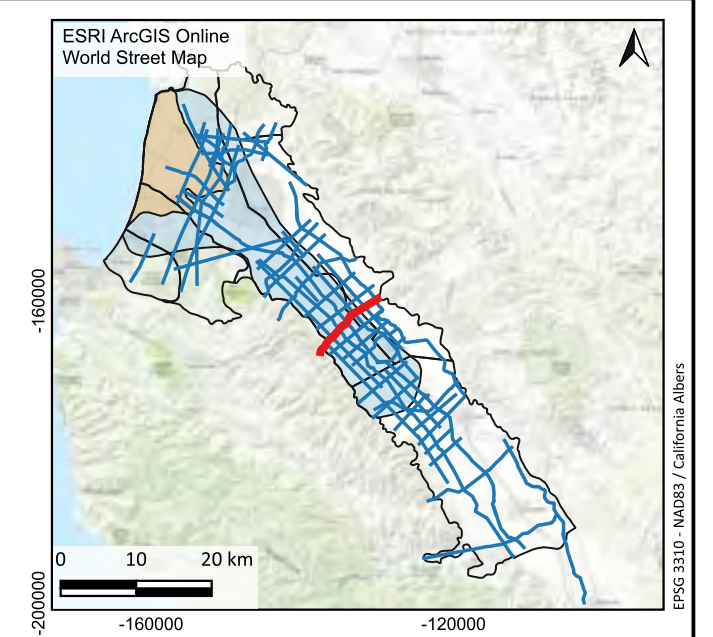
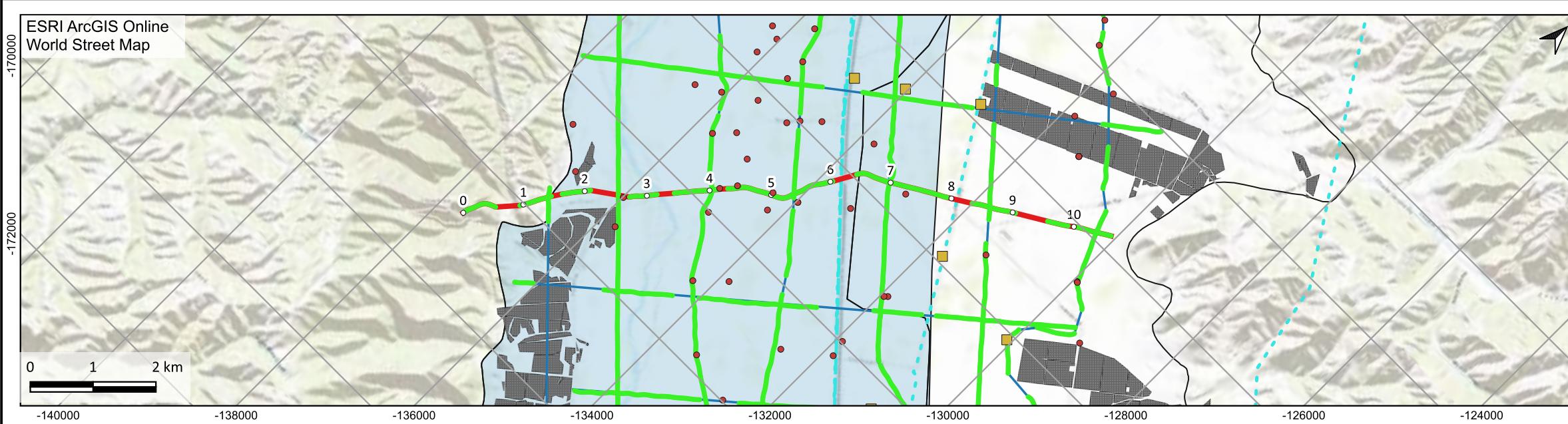


Smooth Model

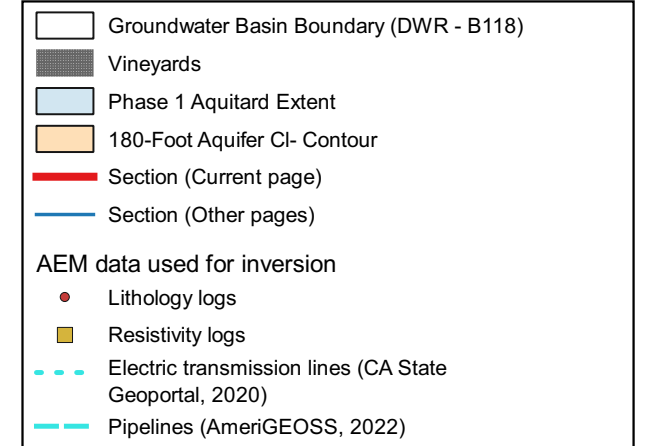


Legend for Model Sections

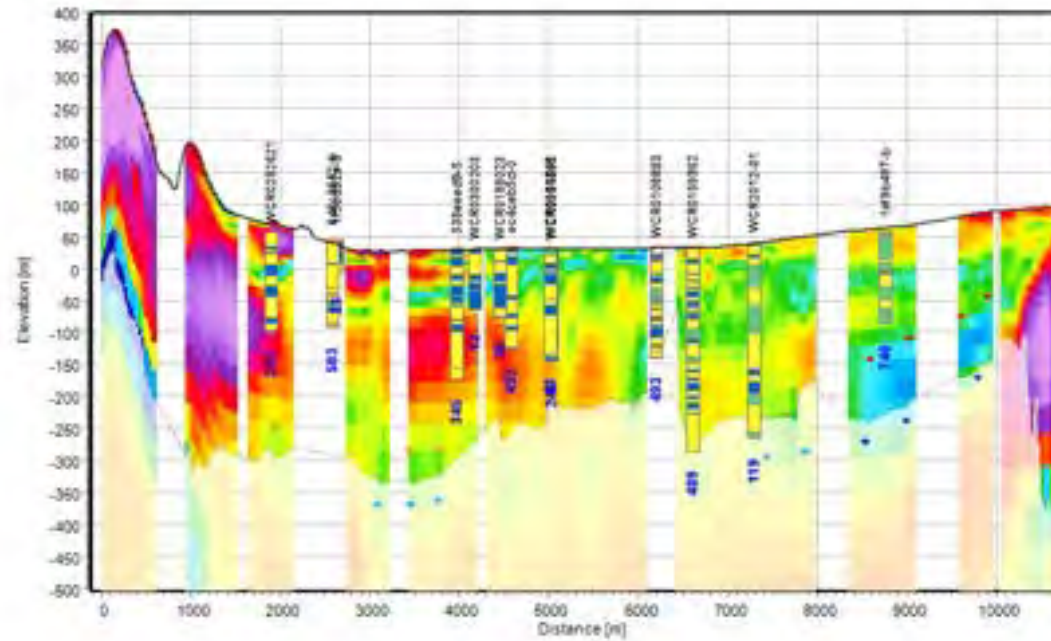




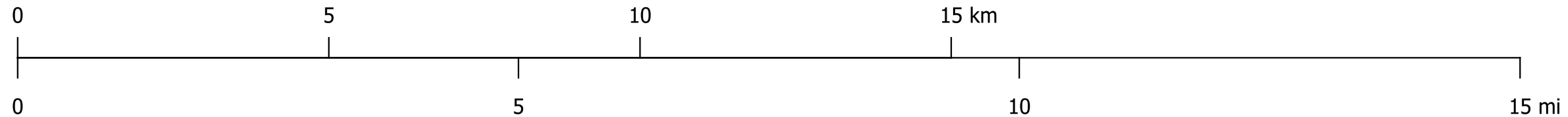
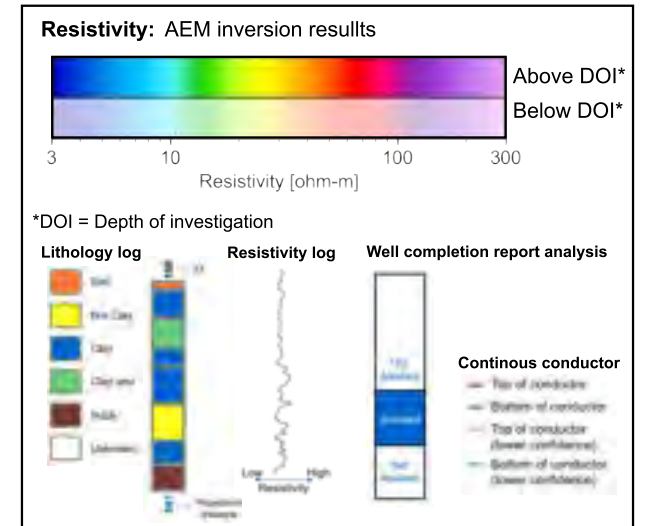
Legend for Maps

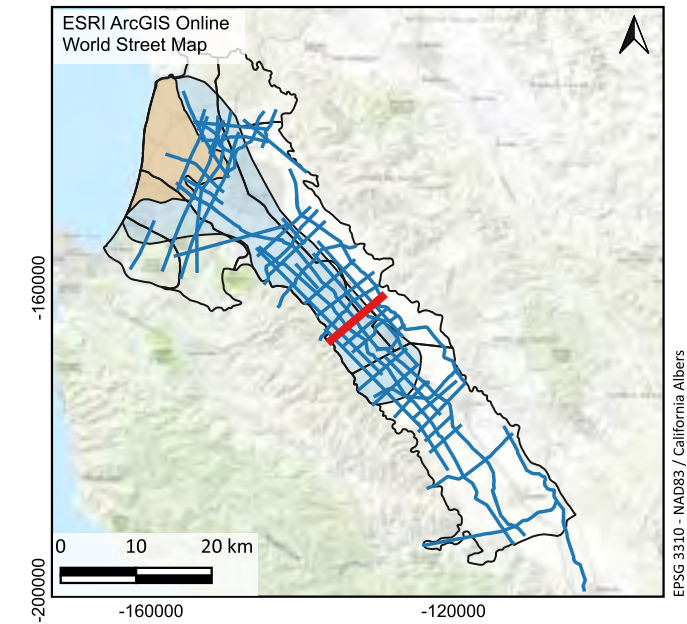
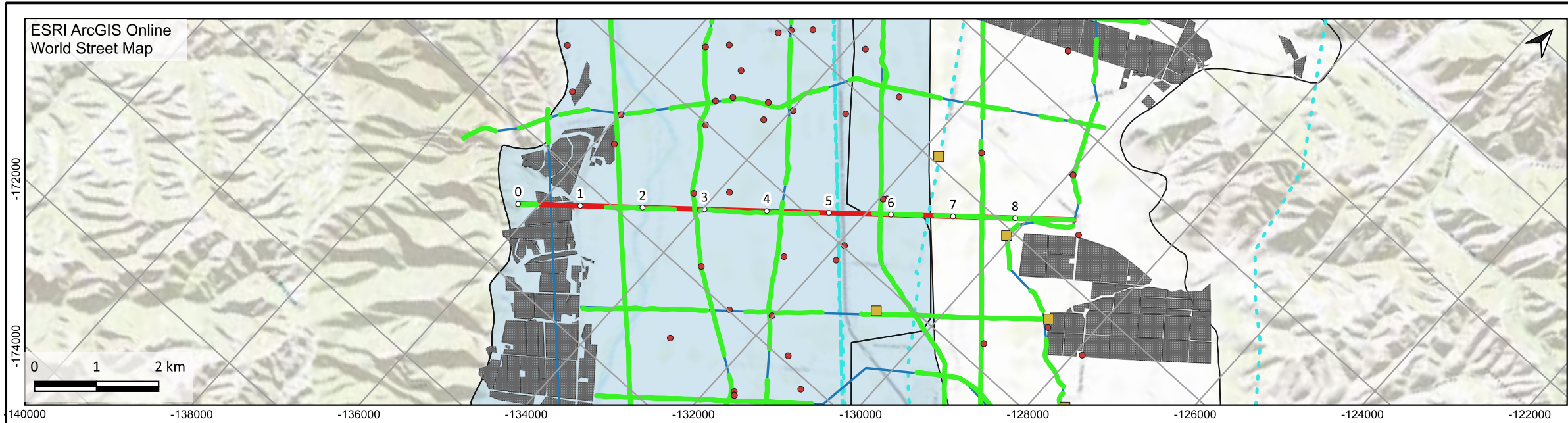


Smooth Model



Legend for Model Sections



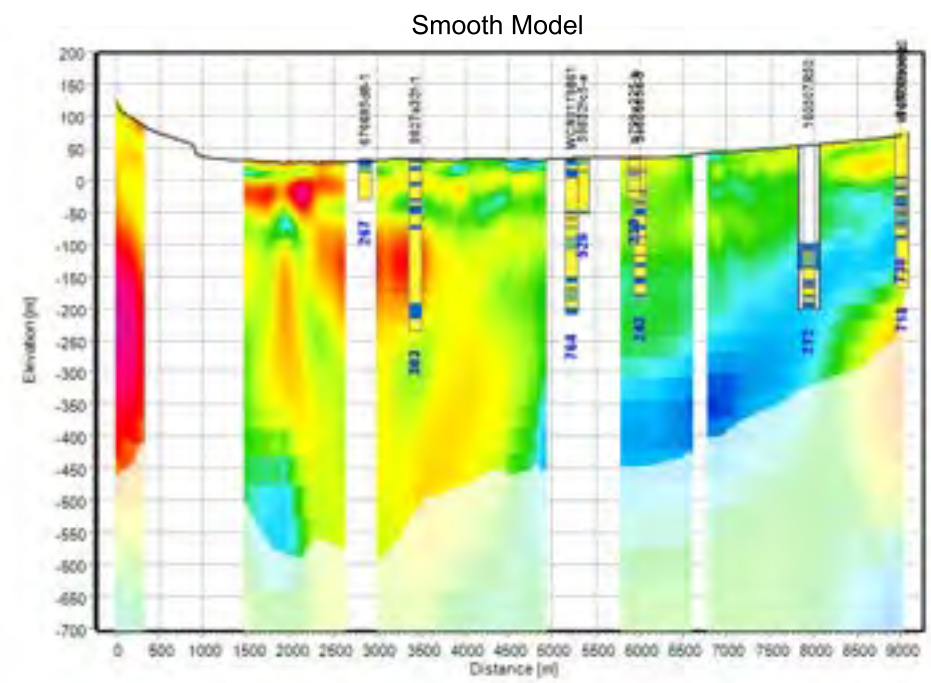


**Legend for Maps**

- Groundwater Basin Boundary (DWR - B118)
- Vineyards
- Phase 1 Aquitard Extent
- 180-Foot Aquifer CI- Contour
- Section (Current page)
- Section (Other pages)

**AEM data used for inversion**

- Lithology logs
- Resistivity logs
- Electric transmission lines (CA State Geoportal, 2020)
- Pipelines (AmeriGEOSS, 2022)



**Legend for Model Sections**

**Resistivity: AEM inversion results**

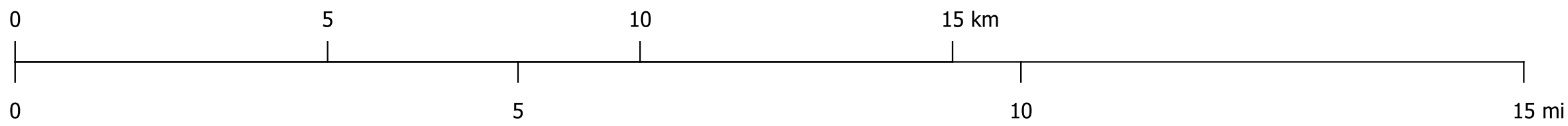
3      10      100      300  
Resistivity [ohm-m]

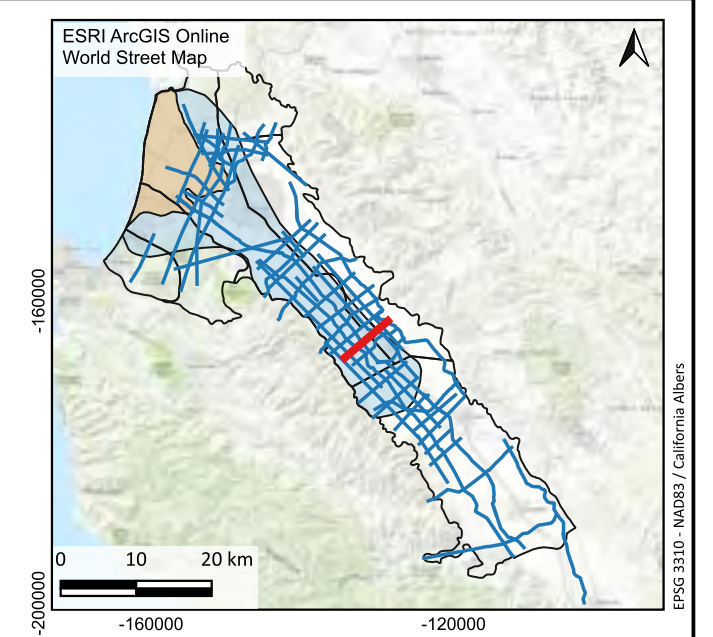
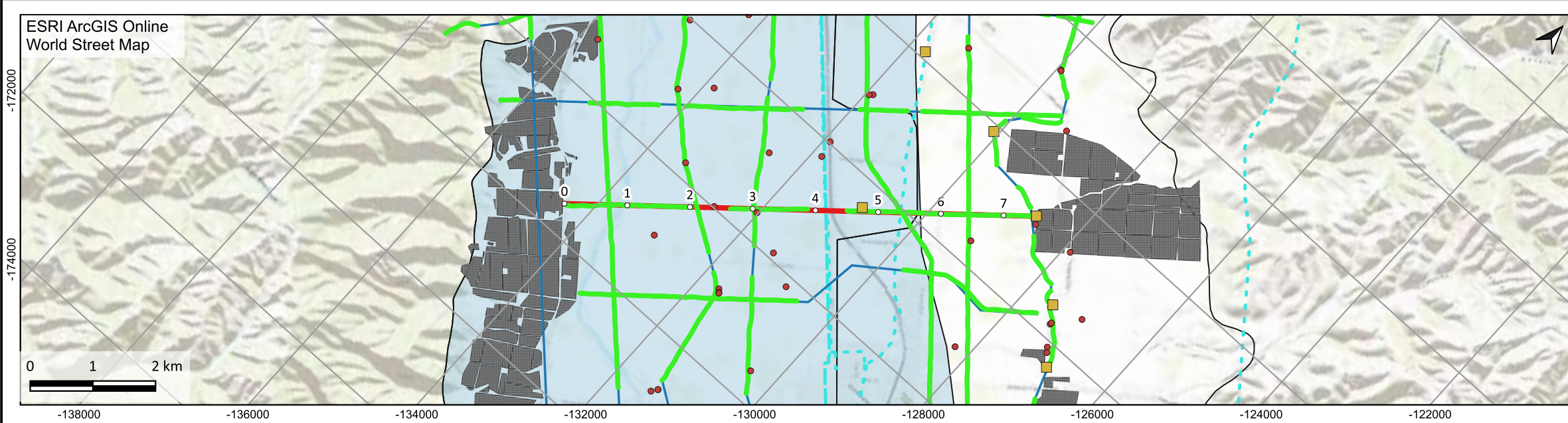
\*DOI = Depth of investigation

Lithology log	Resistivity log	Well completion report analysis

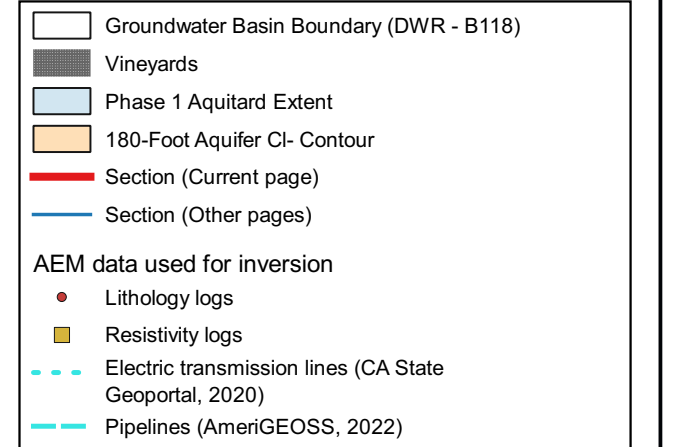
**Continuous conductor**

- Top of conductor
- Bottom of conductor
- Top of conductor (lower confidence)
- Bottom of conductor (lower confidence)

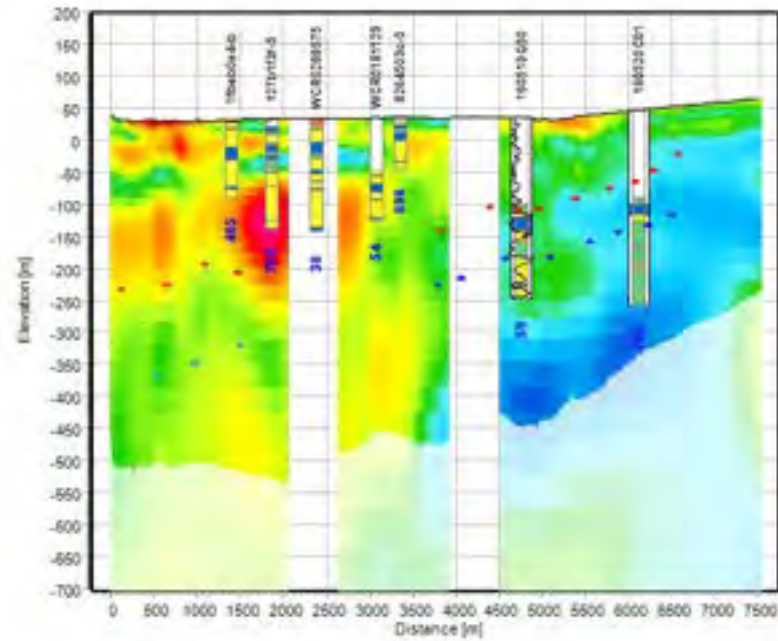




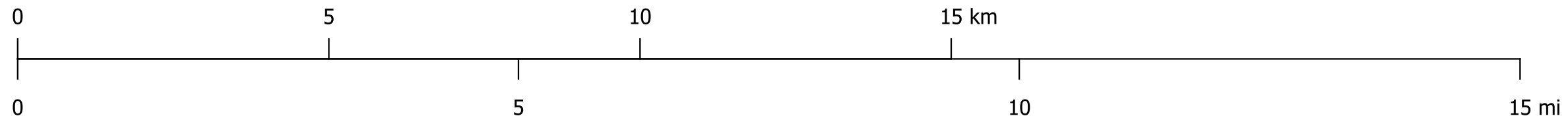
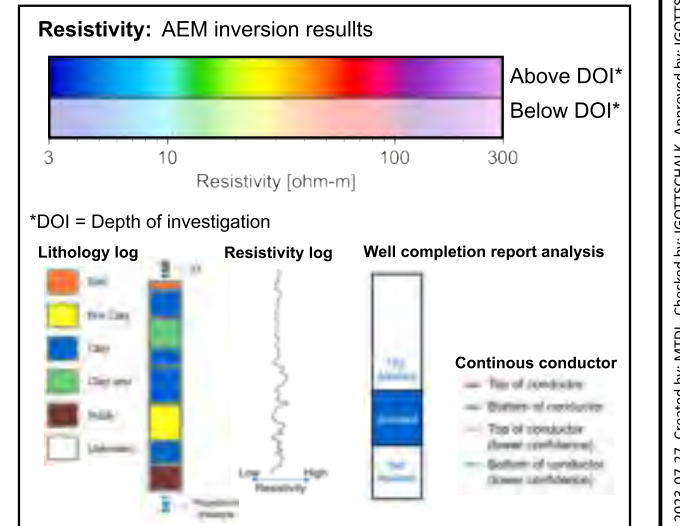
Legend for Maps

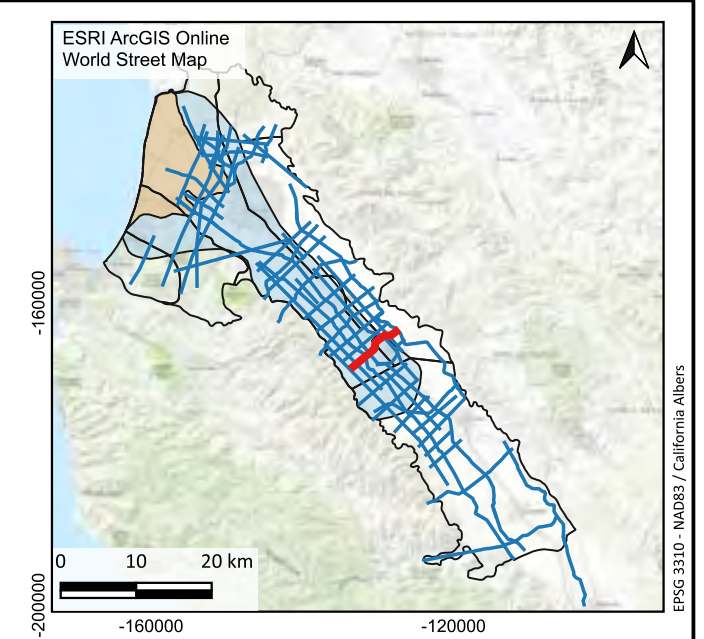
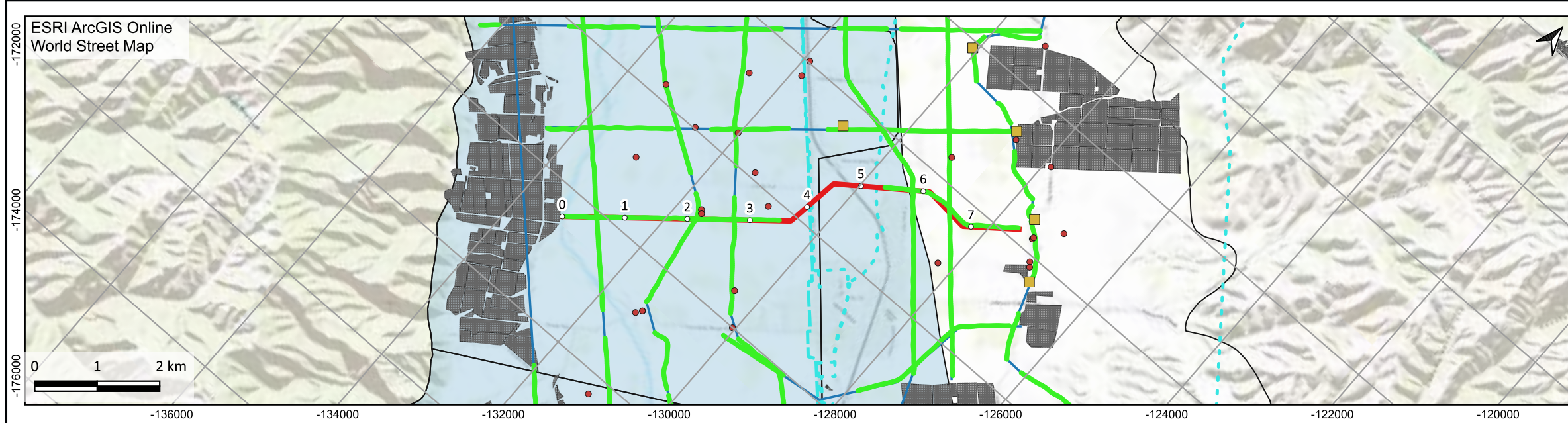


Smooth Model

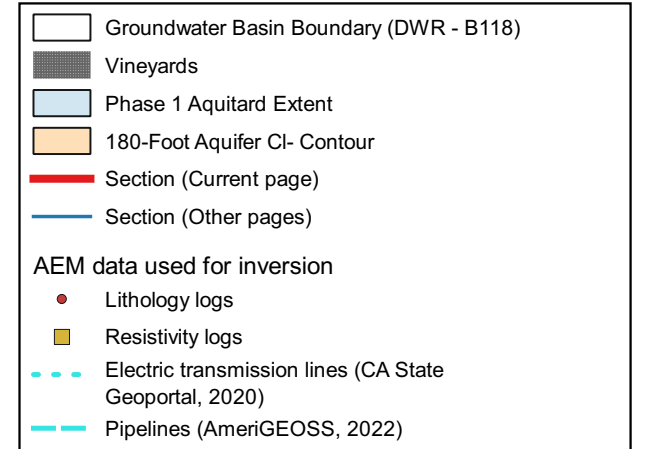


Legend for Model Sections

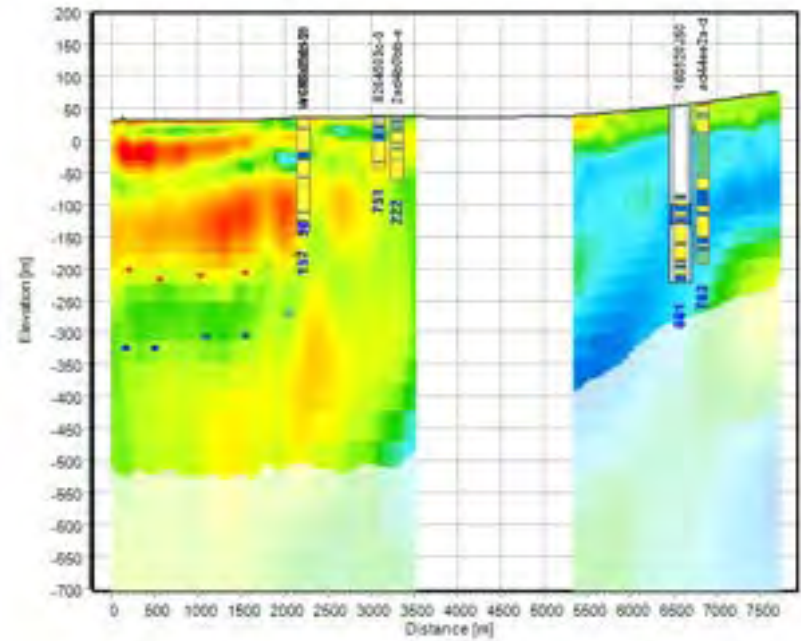




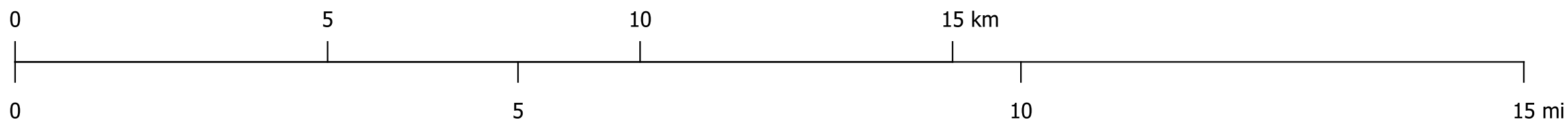
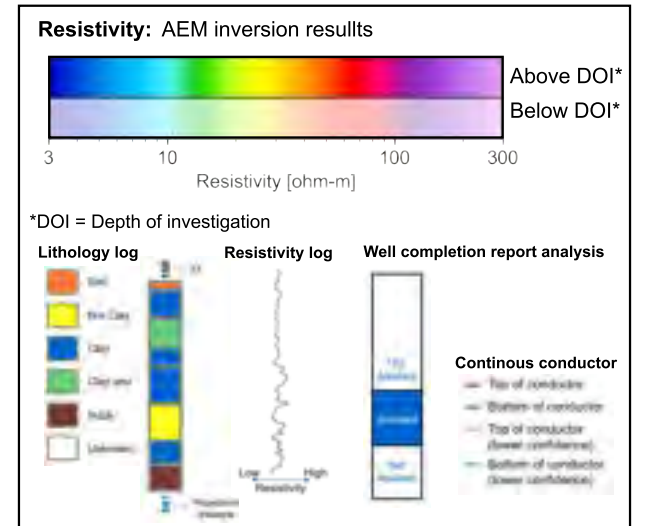
Legend for Maps

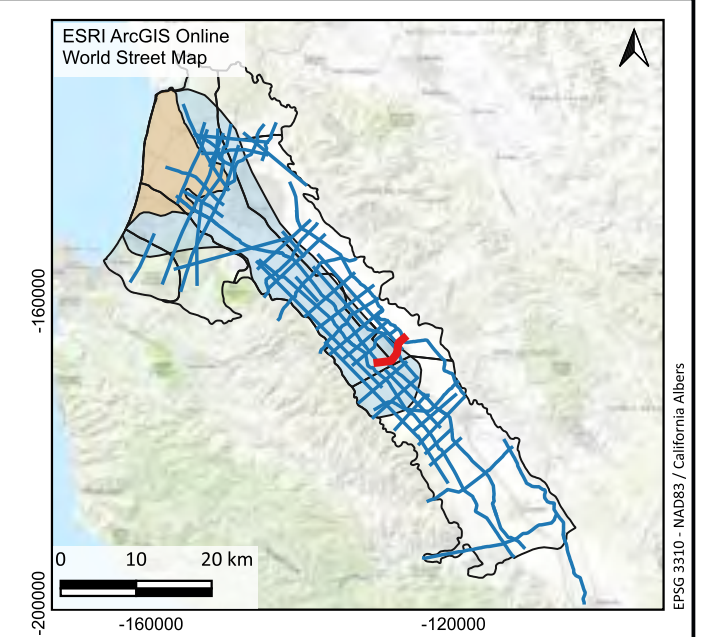
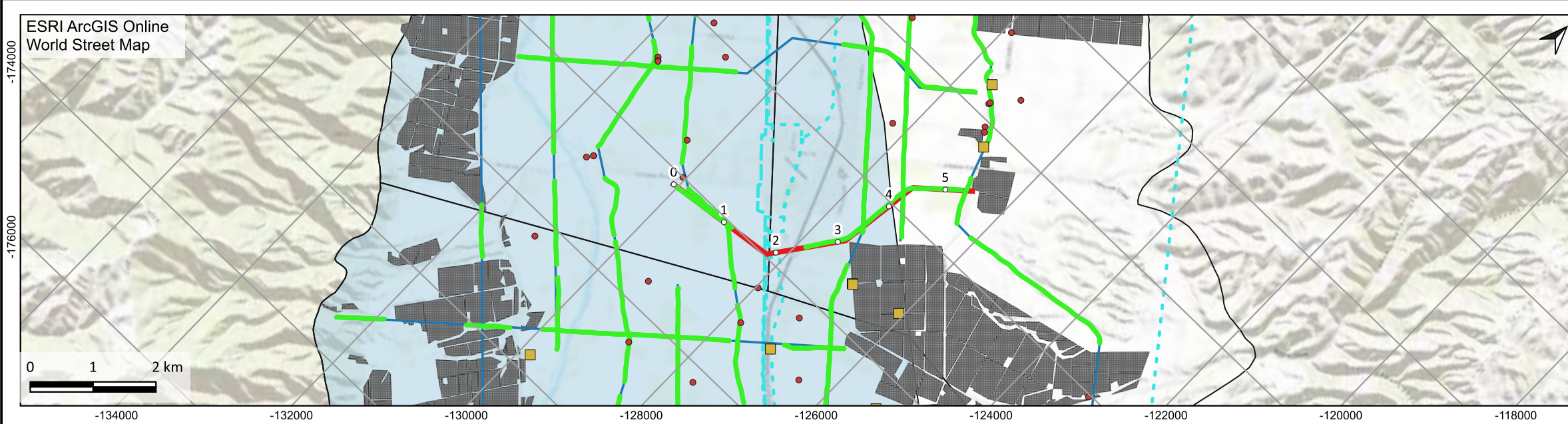


Smooth Model



Legend for Model Sections



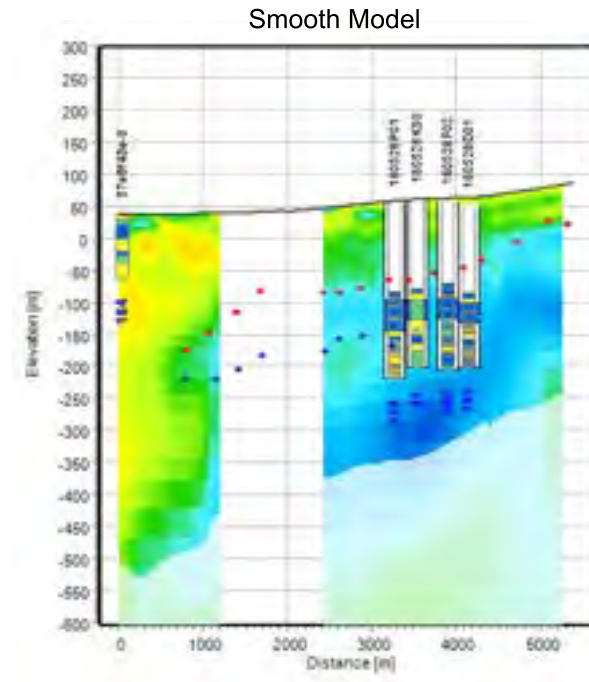


**Legend for Maps**

- Groundwater Basin Boundary (DWR - B118)
- Vineyards
- Phase 1 Aquitard Extent
- 180-Foot Aquifer CI- Contour
- Section (Current page)
- Section (Other pages)

**AEM data used for inversion**

- Lithology logs
- Resistivity logs
- Electric transmission lines (CA State Geoport, 2020)
- Pipelines (AmerGEOSS, 2022)



**Legend for Model Sections**

**Resistivity: AEM inversion results**

Above DOI\*  
Below DOI\*

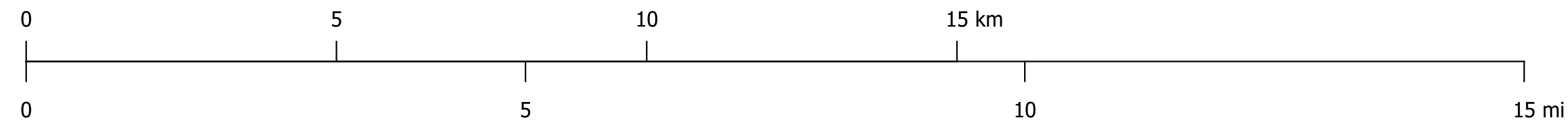
Resistivity [ohm-m]

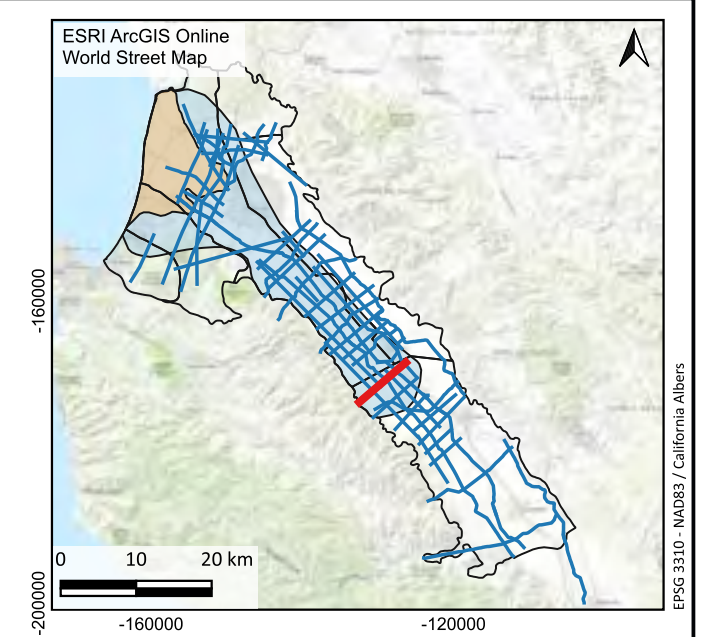
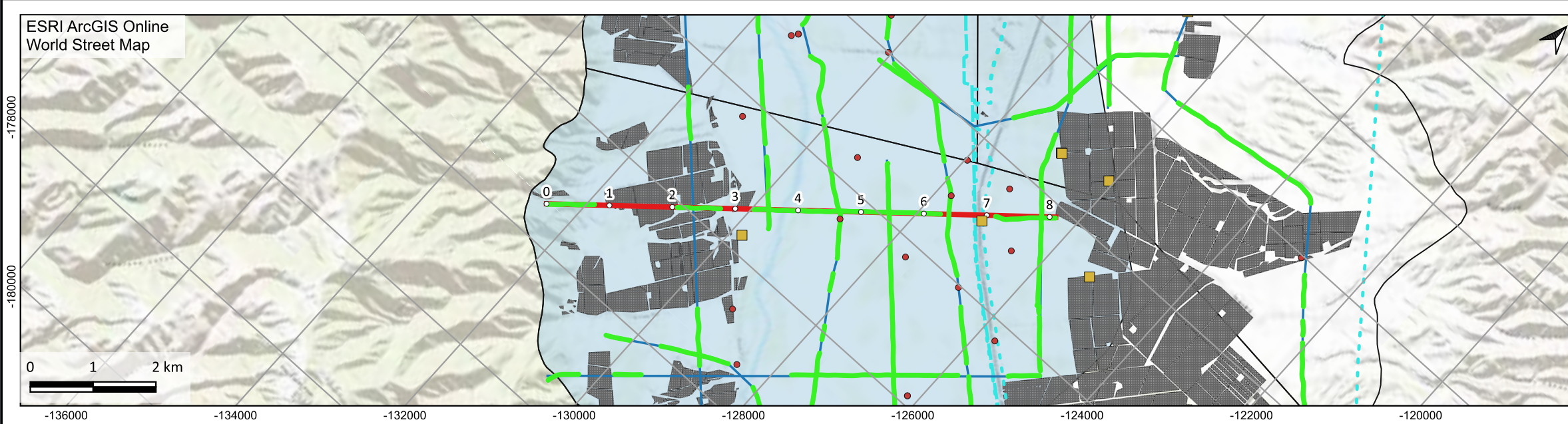
\*DOI = Depth of investigation

Lithology log	Resistivity log	Well completion report analysis
<ul style="list-style-type: none"> <li>Soil</li> <li>Fill Clay</li> <li>Clay</li> <li>Clay shale</li> <li>Silt</li> <li>Sandstone</li> </ul>		

**Continuous conductor**

- Top of conductor
- Bottom of conductor
- Top of conductor (lower confidence)
- Bottom of conductor (lower confidence)





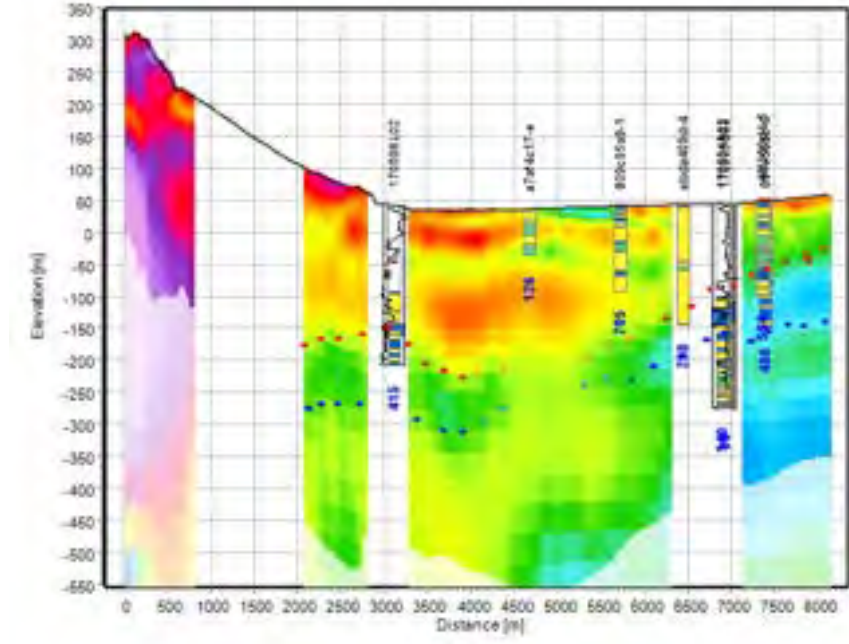
**Legend for Maps**

- Groundwater Basin Boundary (DWR - B118)
- Vineyards
- Phase 1 Aquitard Extent
- 180-Foot Aquifer CI- Contour
- Section (Current page)
- Section (Other pages)

**AEM data used for inversion**

- Lithology logs
- Resistivity logs
- Electric transmission lines (CA State Geoportals, 2020)
- Pipelines (AmeriGEOSS, 2022)

Smooth Model



**Legend for Model Sections**

**Resistivity: AEM inversion results**

Above DOI\*  
Below DOI\*

Resistivity [ohm-m]

\*DOI = Depth of investigation

**Lithology log**

- Sand
- Silt/Clay
- Clay
- Claystone
- Siltstone
- Limestone

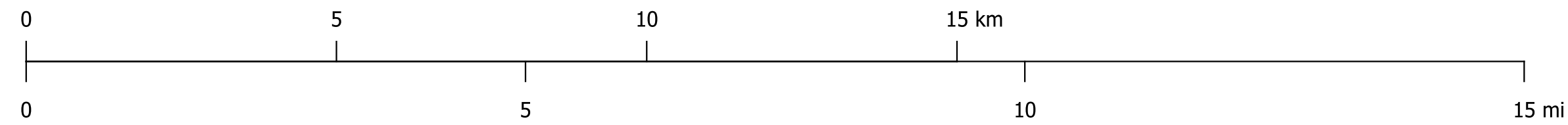
**Resistivity log**

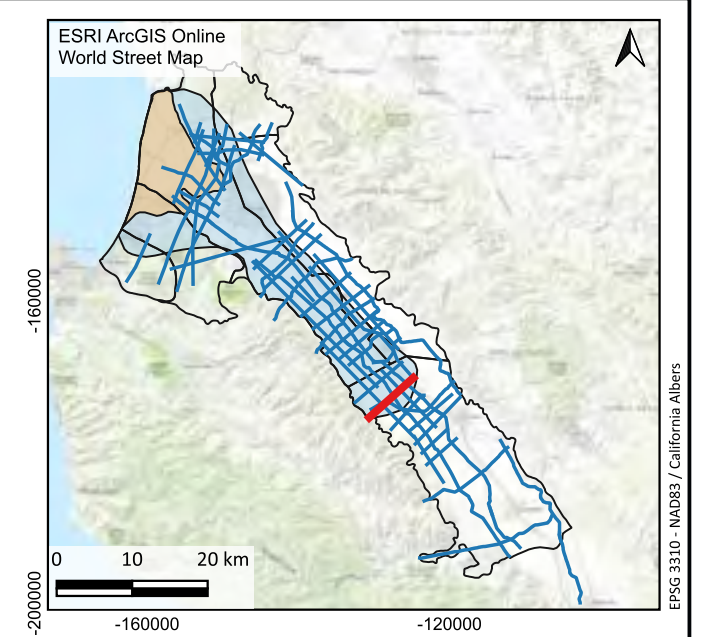
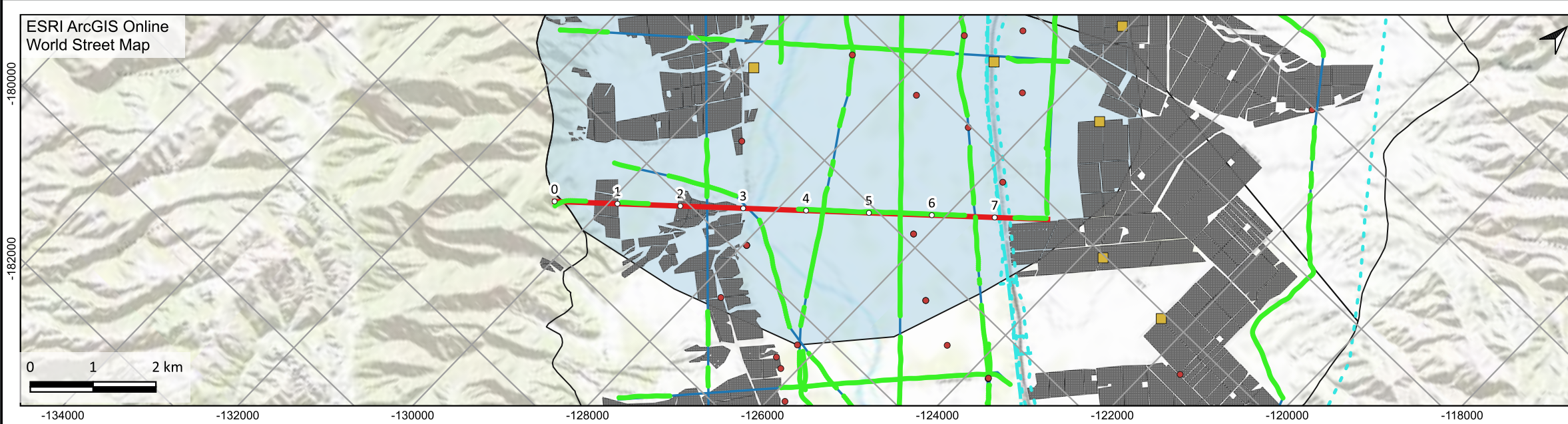
Log Resistivity

**Well completion report analysis**

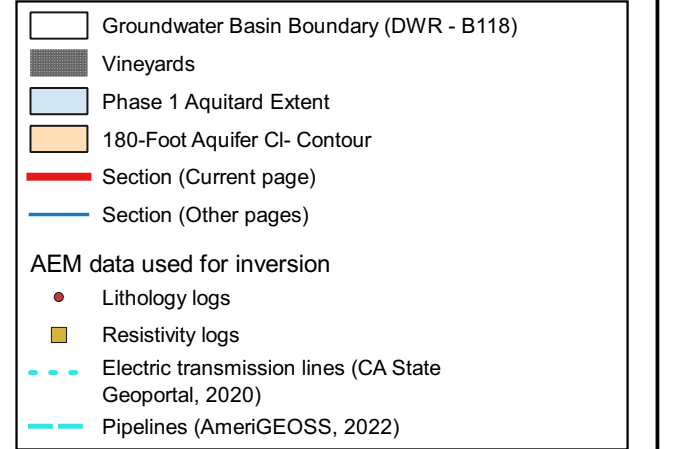
**Continuous conductor**

- Top of conductor
- Bottom of conductor
- Top of conductor (lower confidence)
- Bottom of conductor (lower confidence)

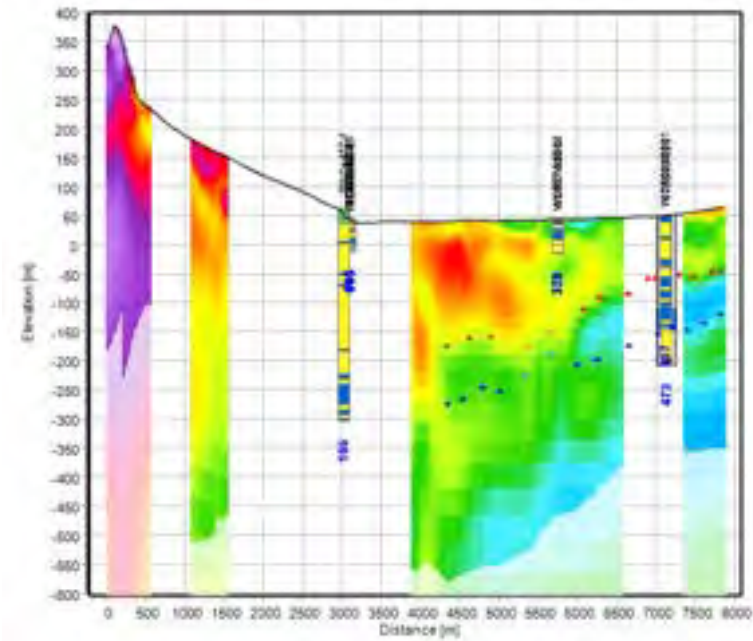




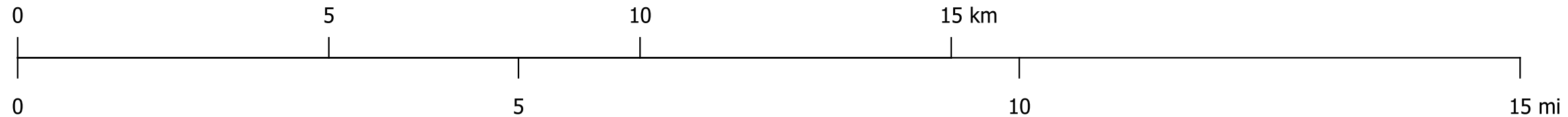
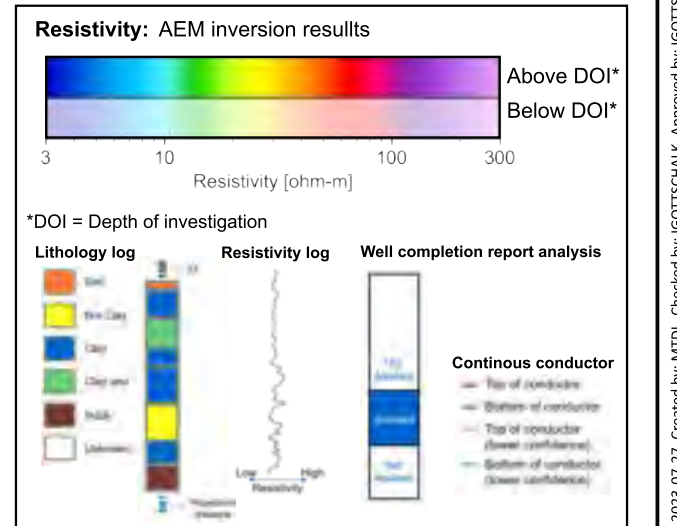
Legend for Maps

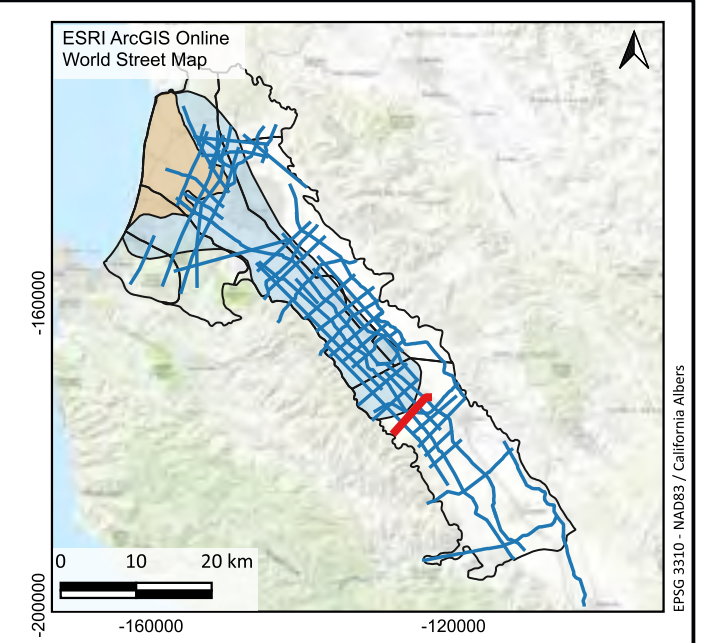
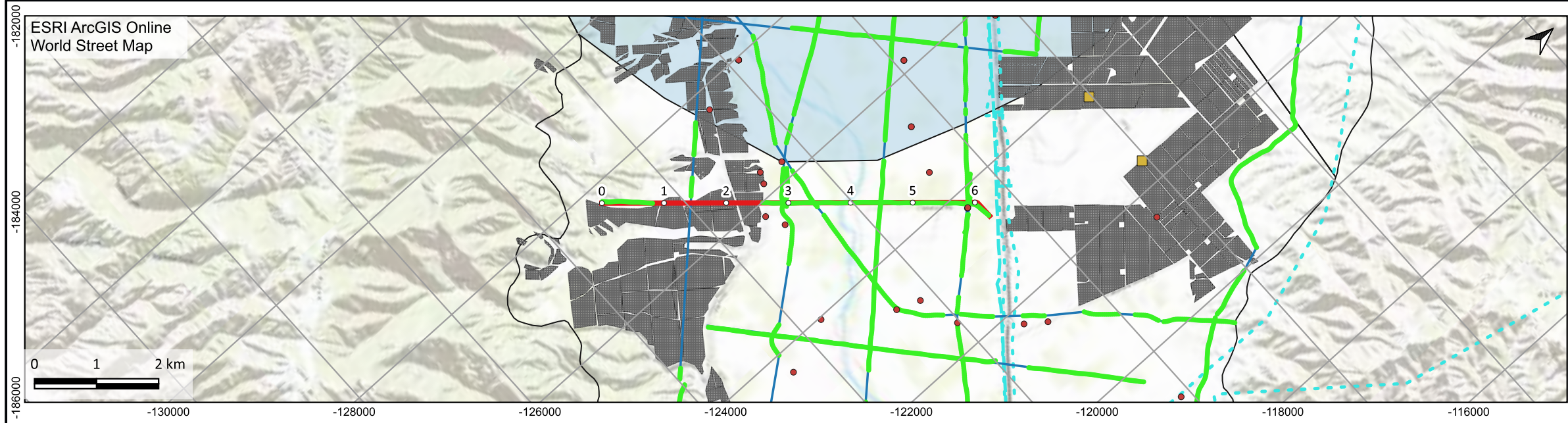


Smooth Model



Legend for Model Sections



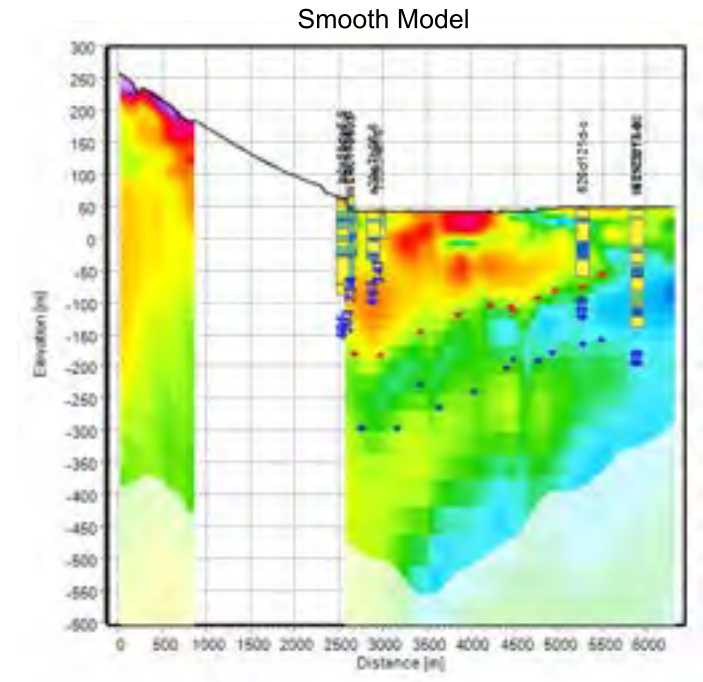


**Legend for Maps**

- Groundwater Basin Boundary (DWR - B118)
- Vineyards
- Phase 1 Aquitard Extent
- 180-Foot Aquifer CI- Contour
- Section (Current page)
- Section (Other pages)

**AEM data used for inversion**

- Lithology logs
- Resistivity logs
- Electric transmission lines (CA State Geoportal, 2020)
- Pipelines (AmeriGEOSS, 2022)



**Legend for Model Sections**

**Resistivity: AEM inversion results**

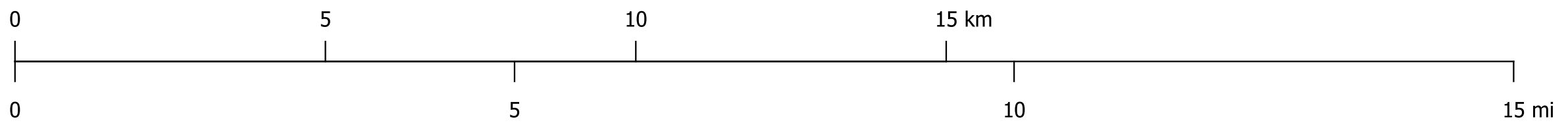
3      10      100      300  
Resistivity [ohm-m]

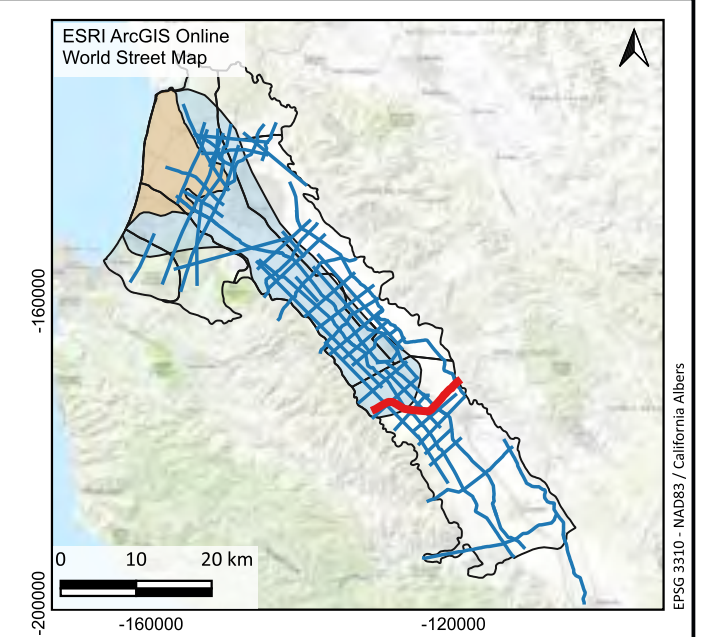
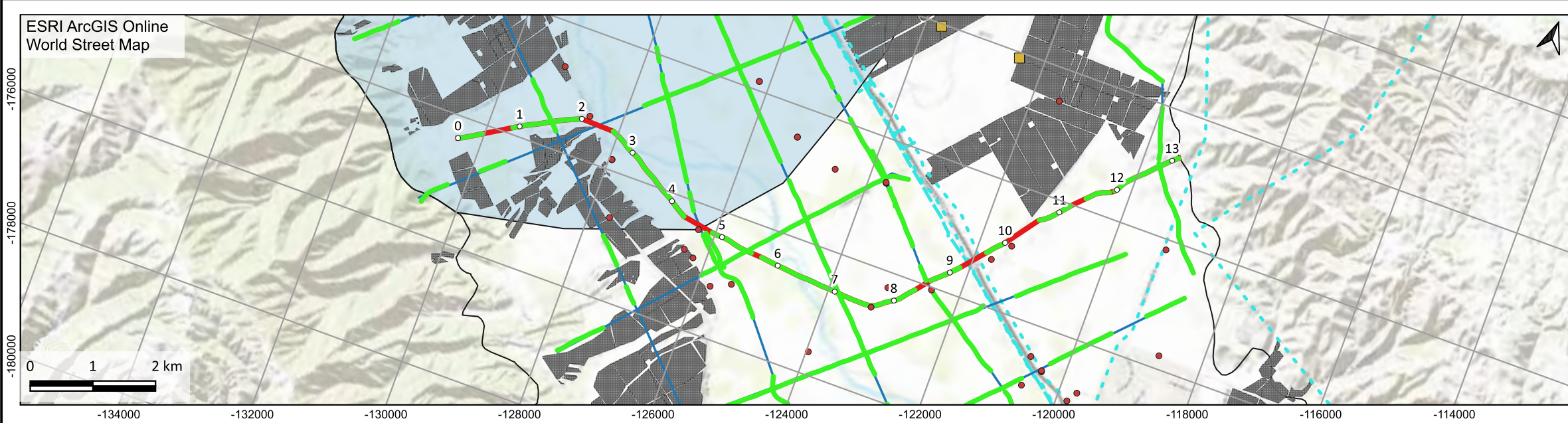
\*DOI = Depth of investigation

Lithology log	Resistivity log	Well completion report analysis

**Continuous conductor**

- Top of conductor
- Bottom of conductor
- Top of conductor (lower confidence)
- Bottom of conductor (lower confidence)





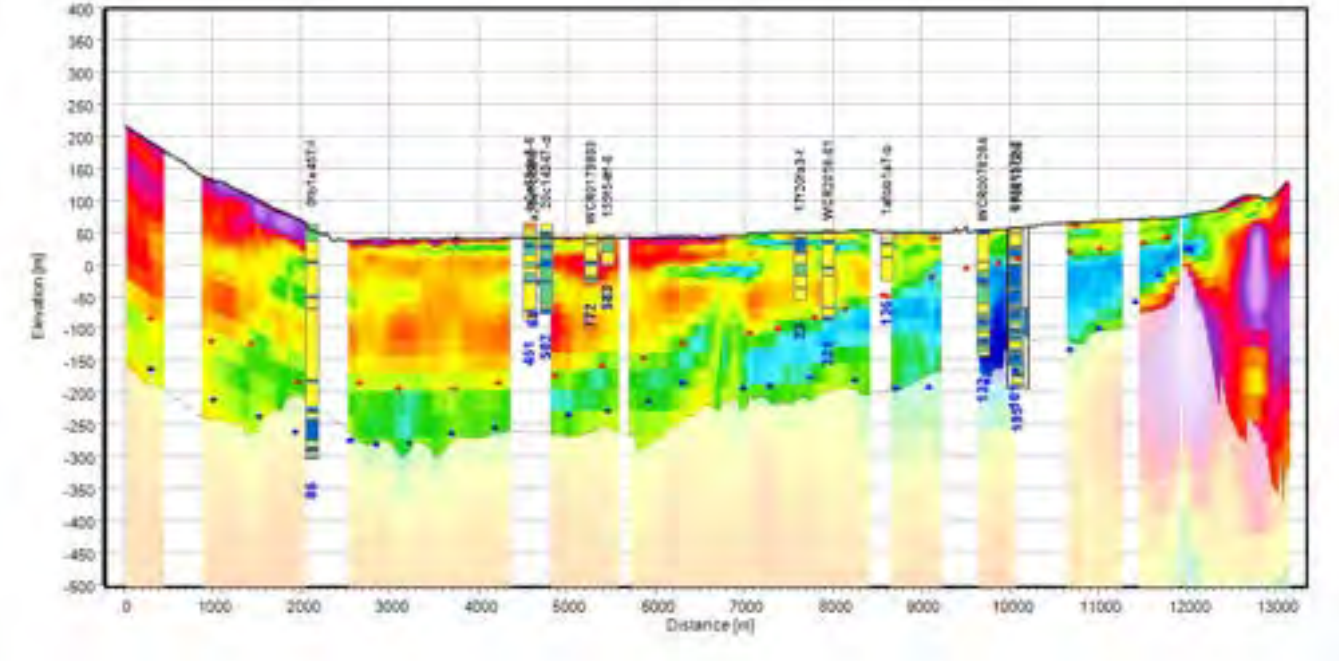
**Legend for Maps**

- Groundwater Basin Boundary (DWR - B118)
- Vineyards
- Phase 1 Aquitard Extent
- 180-Foot Aquifer CI- Contour
- Section (Current page)
- Section (Other pages)

**AEM data used for inversion**

- Lithology logs
- Resistivity logs
- Electric transmission lines (CA State Geoportal, 2020)
- Pipelines (AmeriGEOSS, 2022)

Smooth Model



**Legend for Model Sections**

**Resistivity: AEM inversion results**

3 10 100 300  
Resistivity [ohm-m]

\*DOI = Depth of investigation

**Lithology log**

- Sand
- Silt/Clay
- Clay
- Claystone
- Siltstone
- Lithology

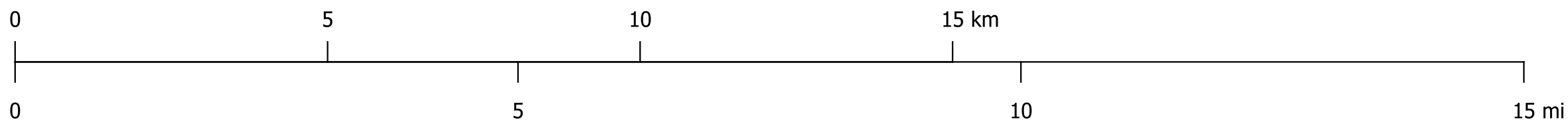
**Resistivity log**

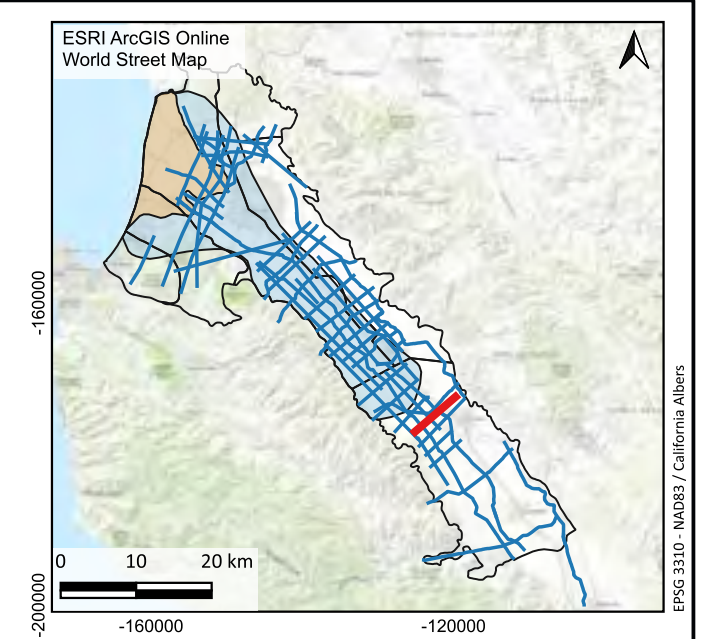
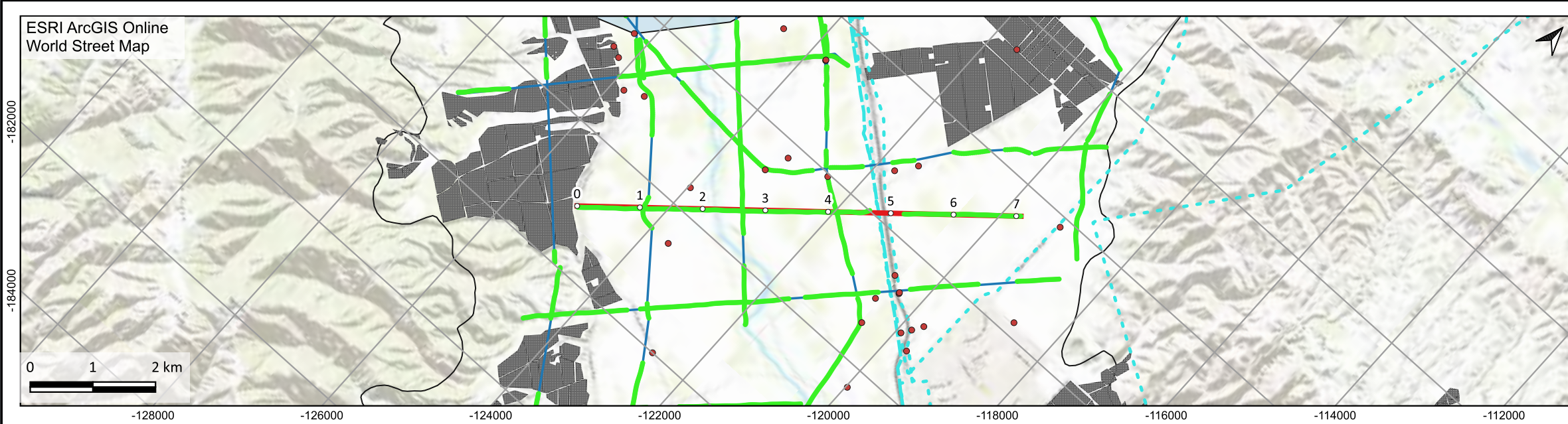
Log Resistivity High

**Well completion report analysis**

**Continuous conductor**

- Top of conductor
- Bottom of conductor
- Top of conductor (lower confidence)
- Bottom of conductor (lower confidence)



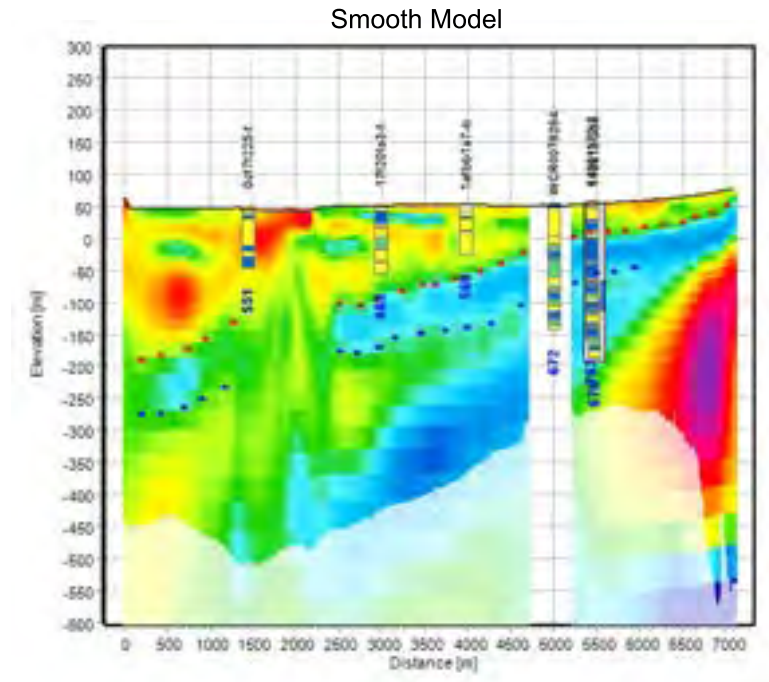


**Legend for Maps**

- Groundwater Basin Boundary (DWR - B118)
- Vineyards
- Phase 1 Aquitard Extent
- 180-Foot Aquifer CI- Contour
- Section (Current page)
- Section (Other pages)

**AEM data used for inversion**

- Lithology logs
- Resistivity logs
- Electric transmission lines (CA State Geoportal, 2020)
- Pipelines (AmeriGEOSS, 2022)



**Legend for Model Sections**

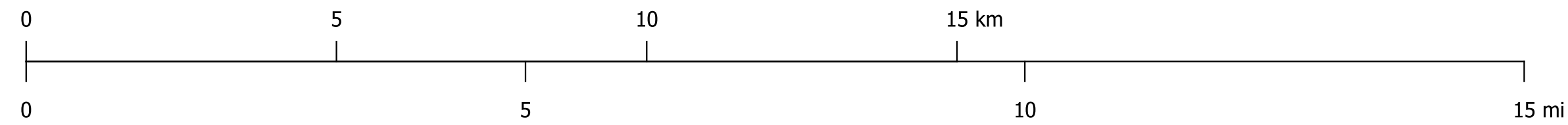
**Resistivity: AEM inversion results**

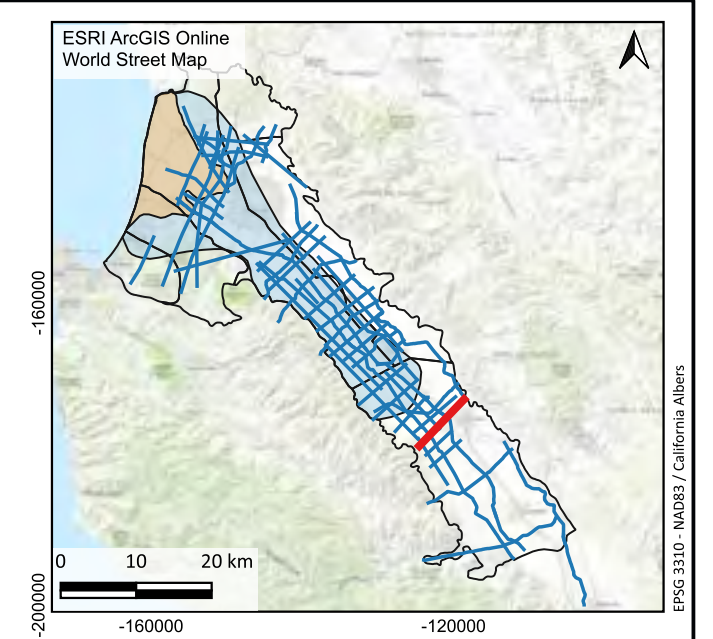
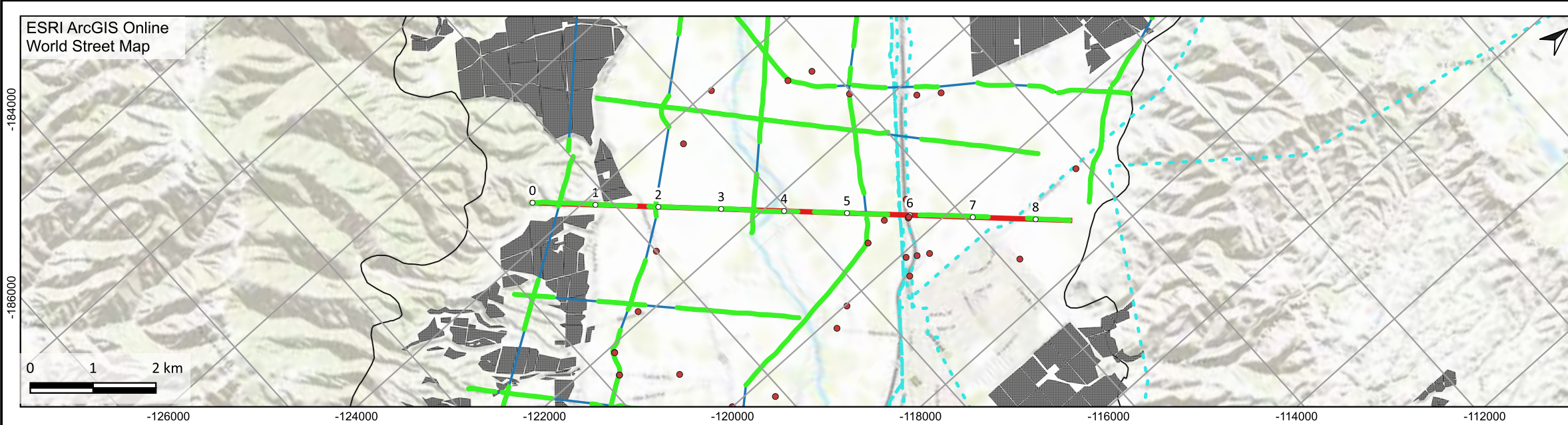
\*DOI = Depth of investigation

Lithology log	Resistivity log	Well completion report analysis

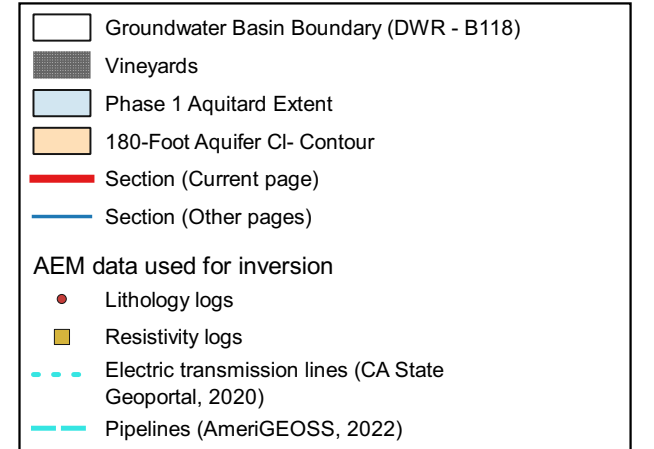
**Continuous conductor**

- Top of conductor
- Bottom of conductor
- Top of conductor (lower confidence)
- Bottom of conductor (lower confidence)

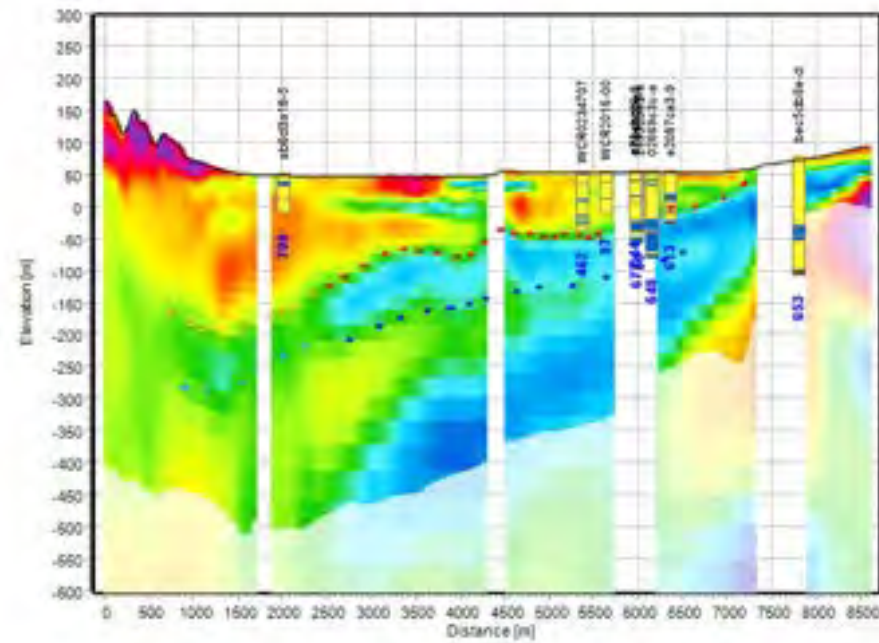




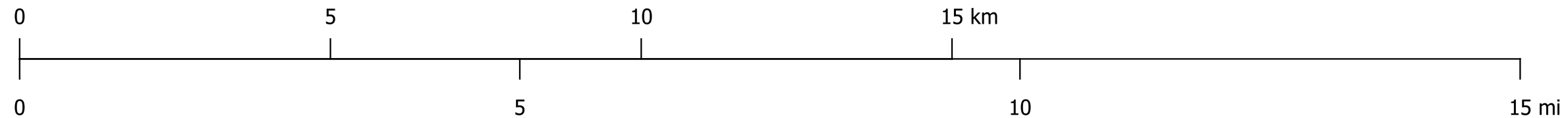
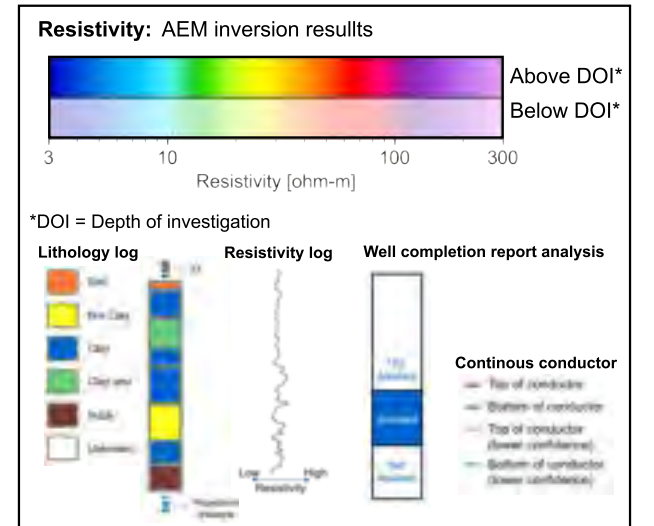
Legend for Maps

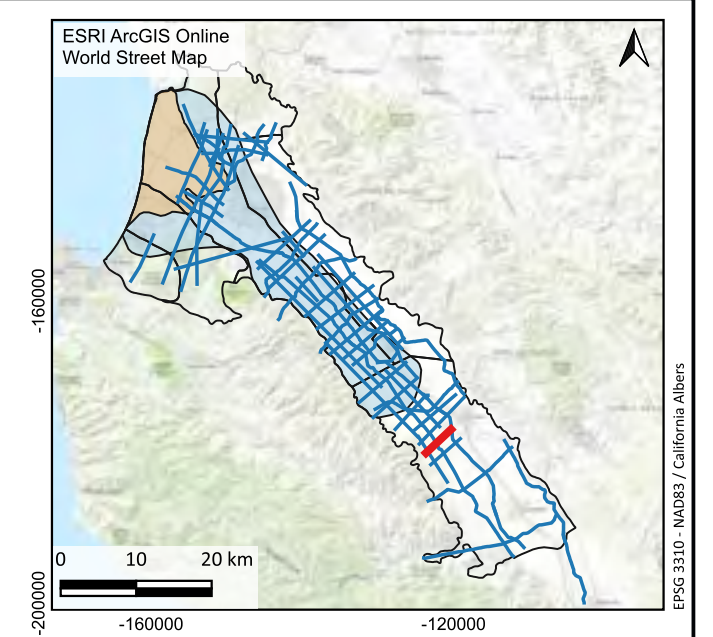
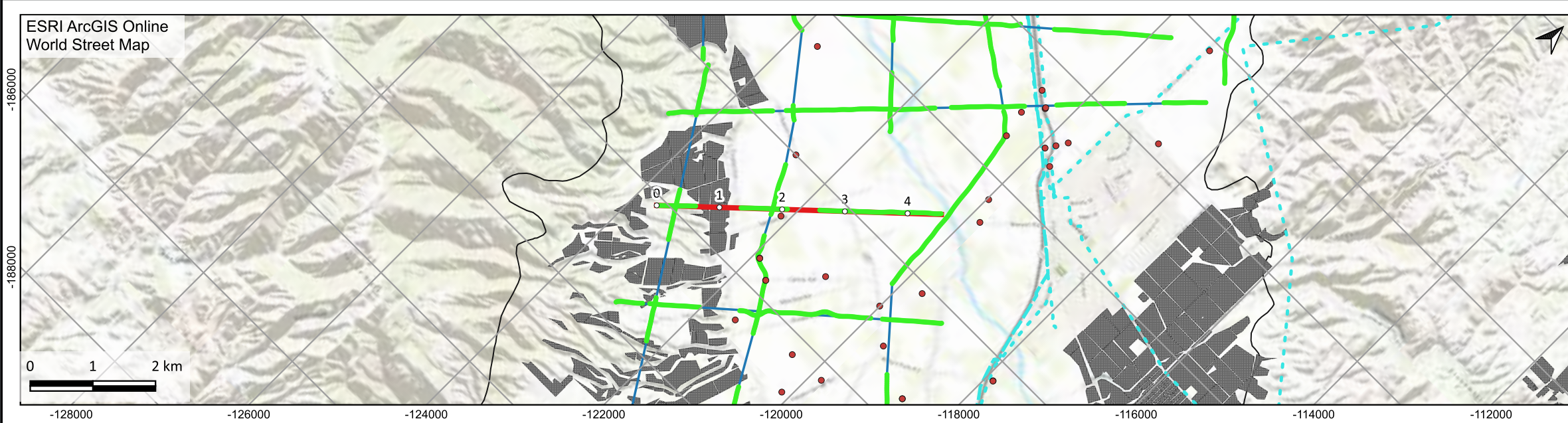


Smooth Model



Legend for Model Sections





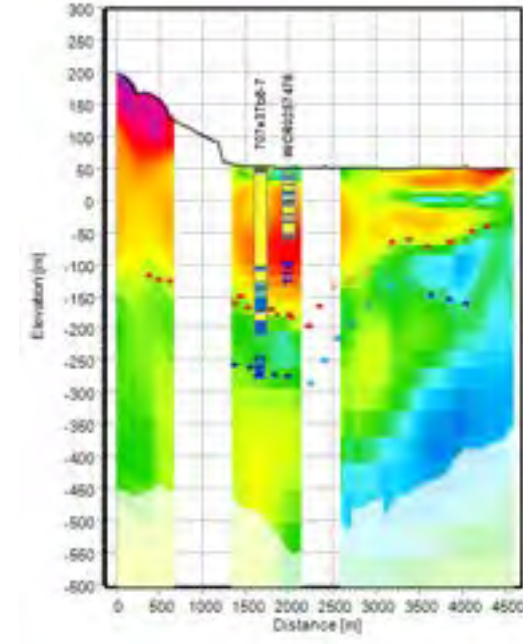
**Legend for Maps**

- Groundwater Basin Boundary (DWR - B118)
- Vineyards
- Phase 1 Aquitard Extent
- 180-Foot Aquifer CI- Contour
- Section (Current page)
- Section (Other pages)

**AEM data used for inversion**

- Lithology logs
- Resistivity logs
- Electric transmission lines (CA State Geoportal, 2020)
- Pipelines (AmeriGEOSS, 2022)

Smooth Model



**Legend for Model Sections**

**Resistivity: AEM inversion results**

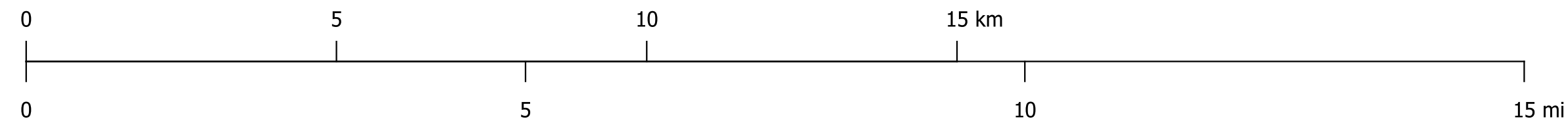
3 10 100 300  
Resistivity [ohm-m]

\*DOI = Depth of investigation

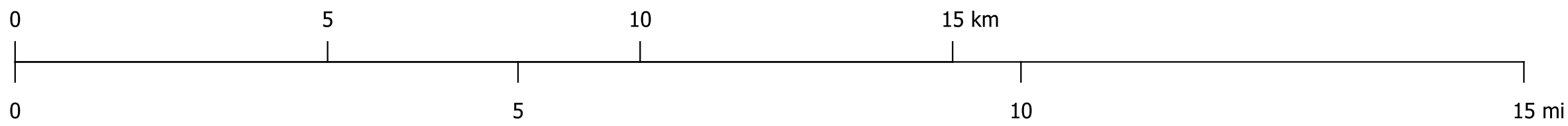
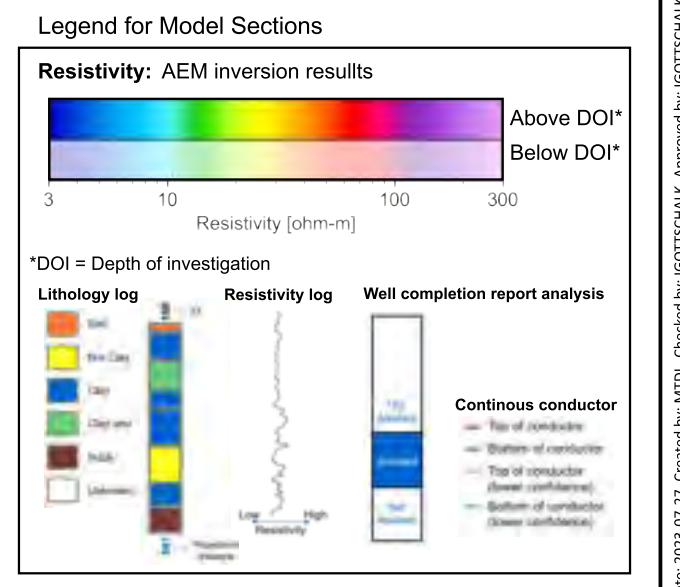
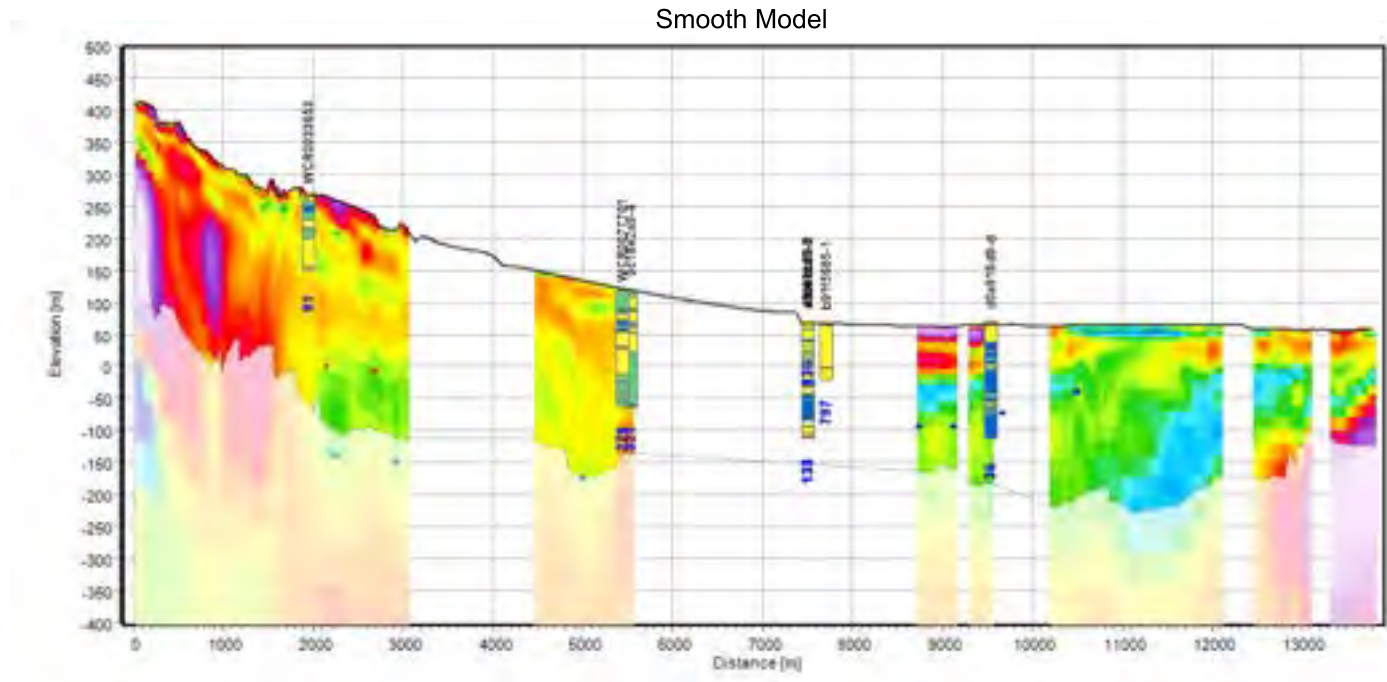
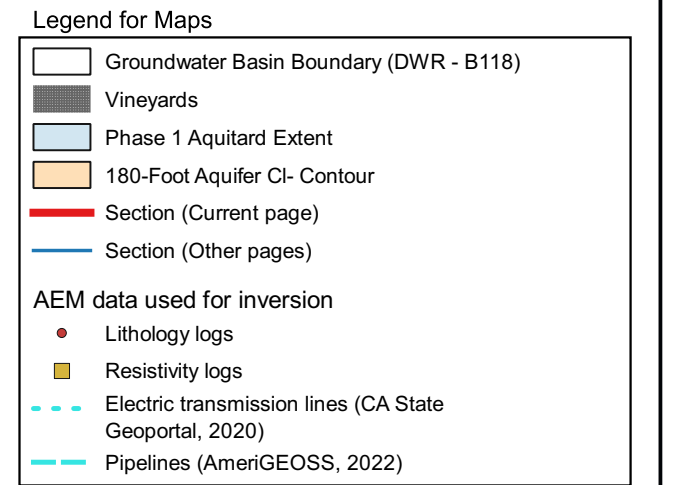
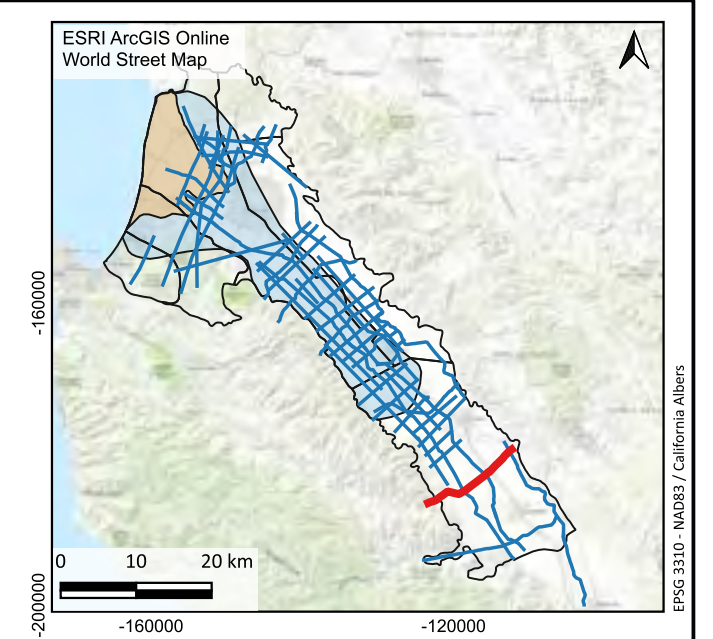
Lithology log	Resistivity log	Well completion report analysis
<ul style="list-style-type: none"> <li>Sand</li> <li>Silt Clay</li> <li>Clay</li> <li>Clay shale</li> <li>Siltstone</li> <li>Limestone</li> </ul>		

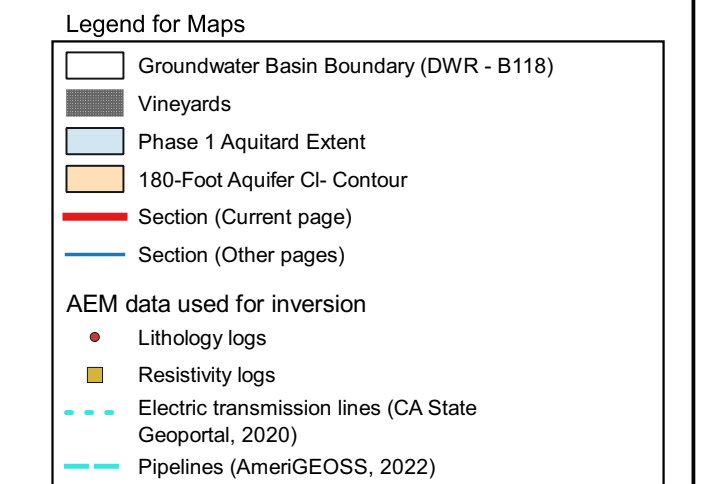
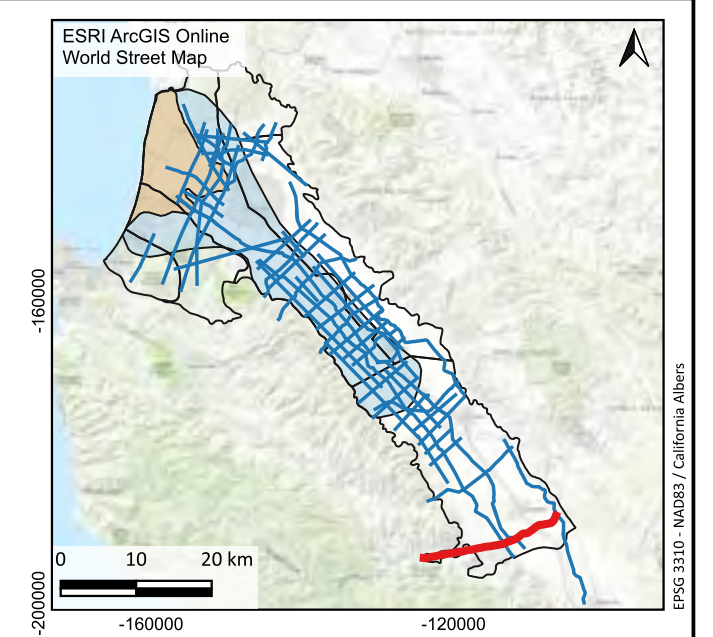
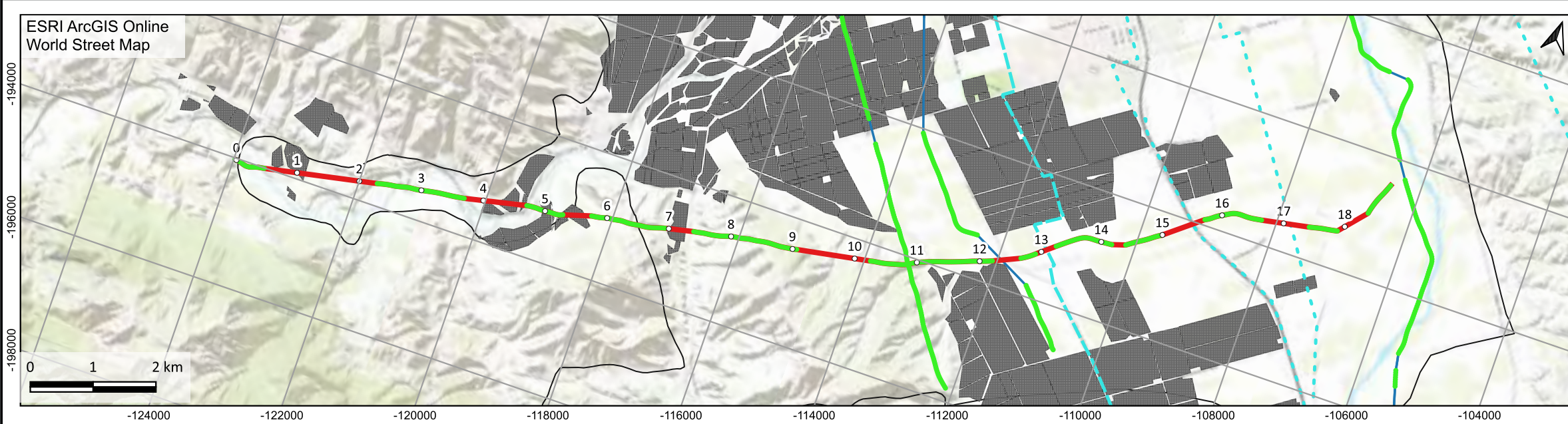
**Continuous conductor**

- Top of conductor
- Bottom of conductor
- Top of conductor (lower confidence)
- Bottom of conductor (lower confidence)

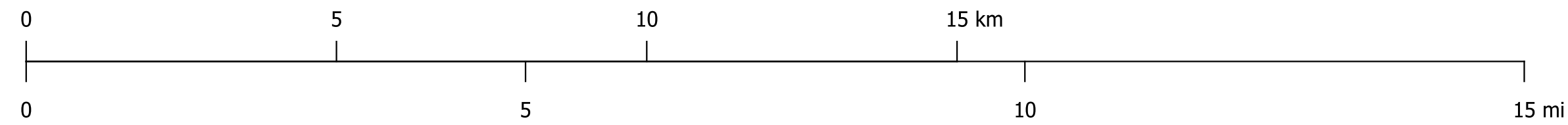
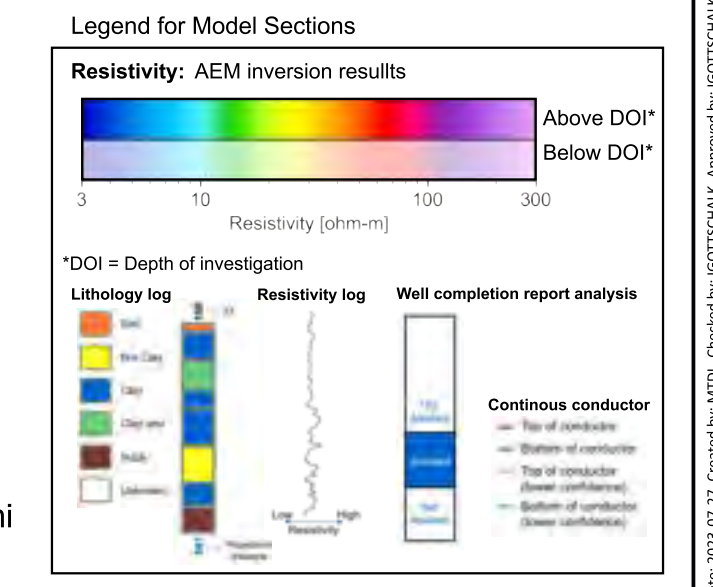
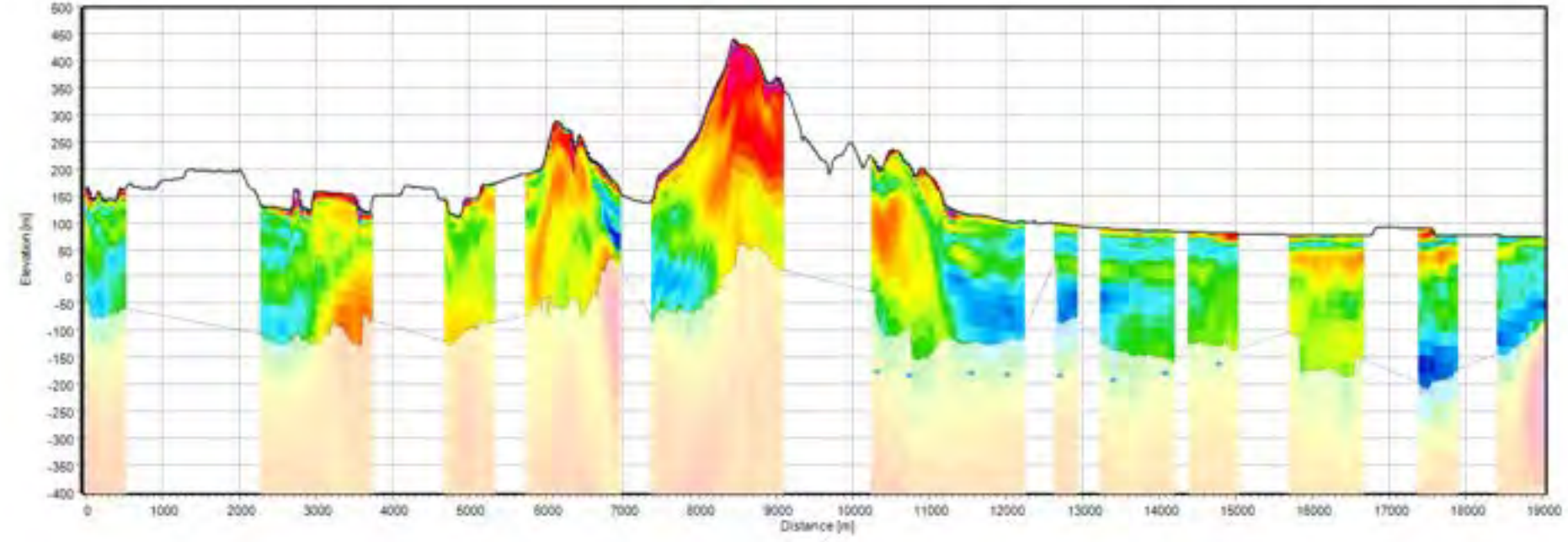


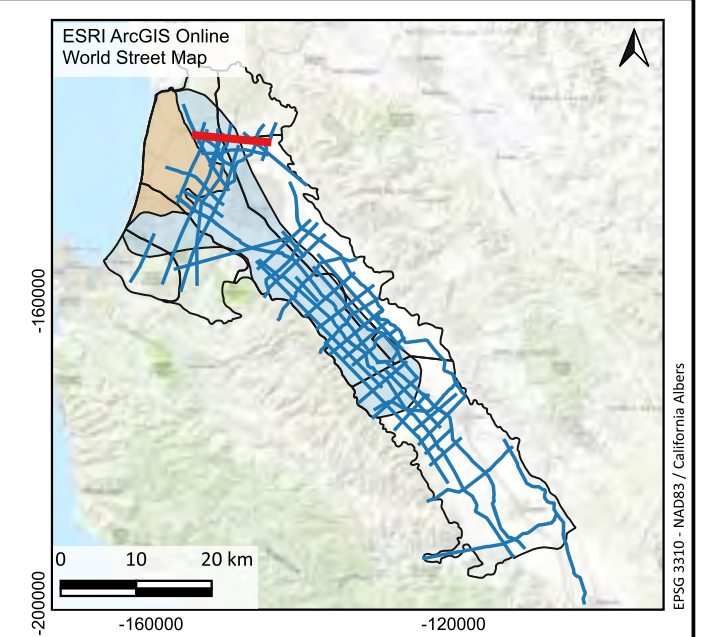
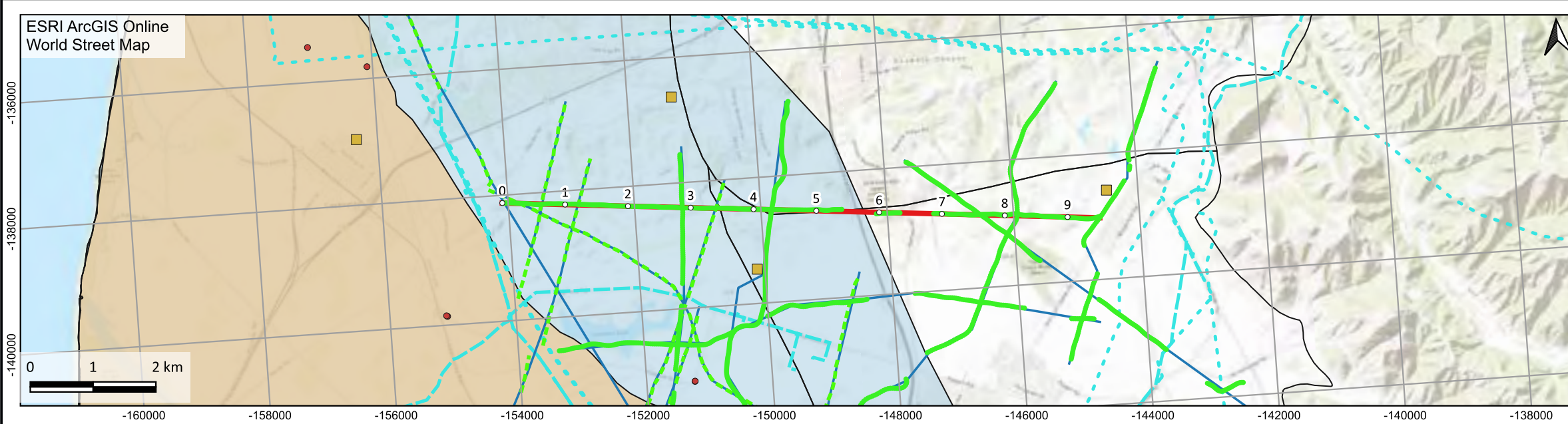






Smooth Model



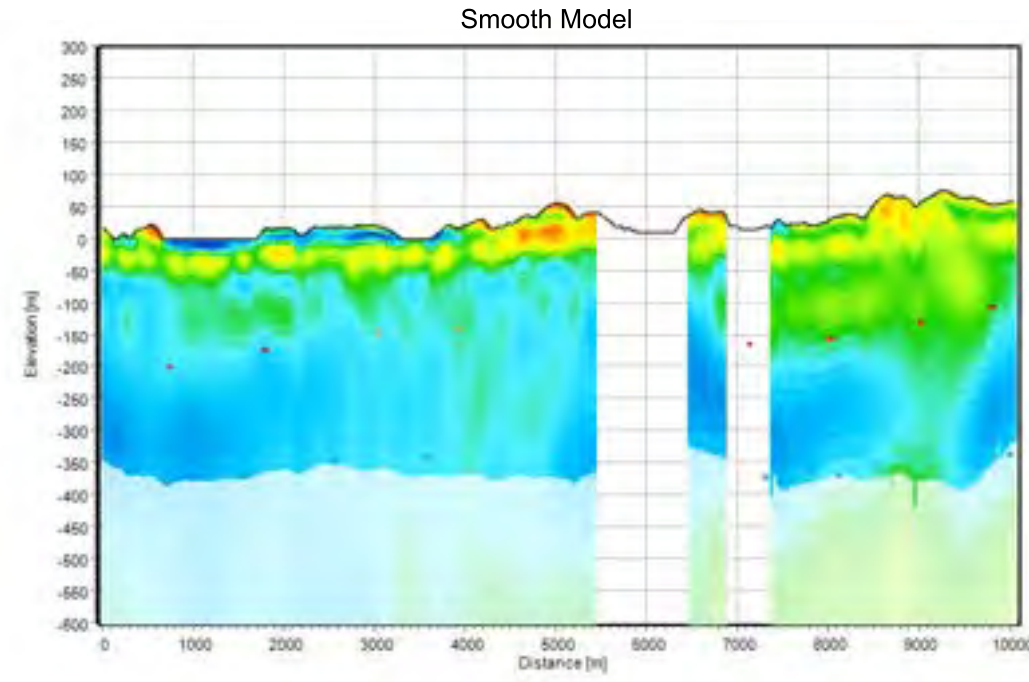


**Legend for Maps**

- Groundwater Basin Boundary (DWR - B118)
- Vineyards
- Phase 1 Aquitard Extent
- 180-Foot Aquifer CI- Contour
- Section (Current page)
- Section (Other pages)

**AEM data used for inversion**

- Lithology logs
- Resistivity logs
- Electric transmission lines (CA State Geoportal, 2020)
- Pipelines (AmeriGEOSS, 2022)



**Legend for Model Sections**

**Resistivity: AEM inversion results**

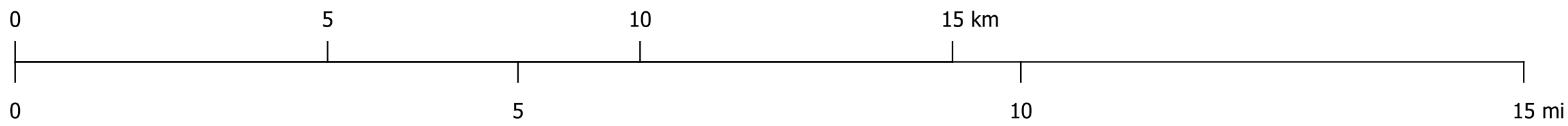
3      10      100      300  
Resistivity [ohm-m]

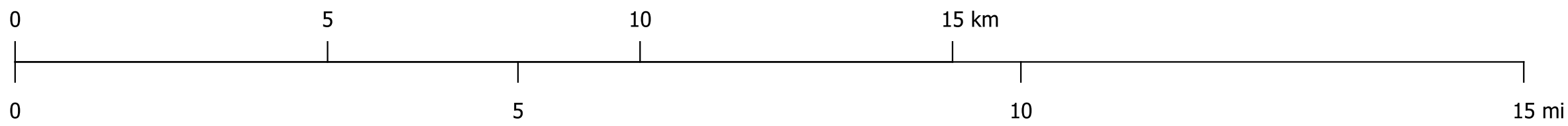
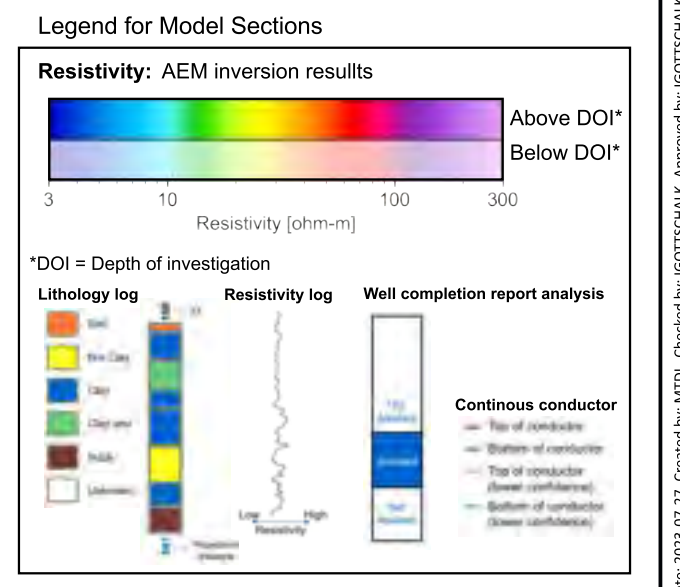
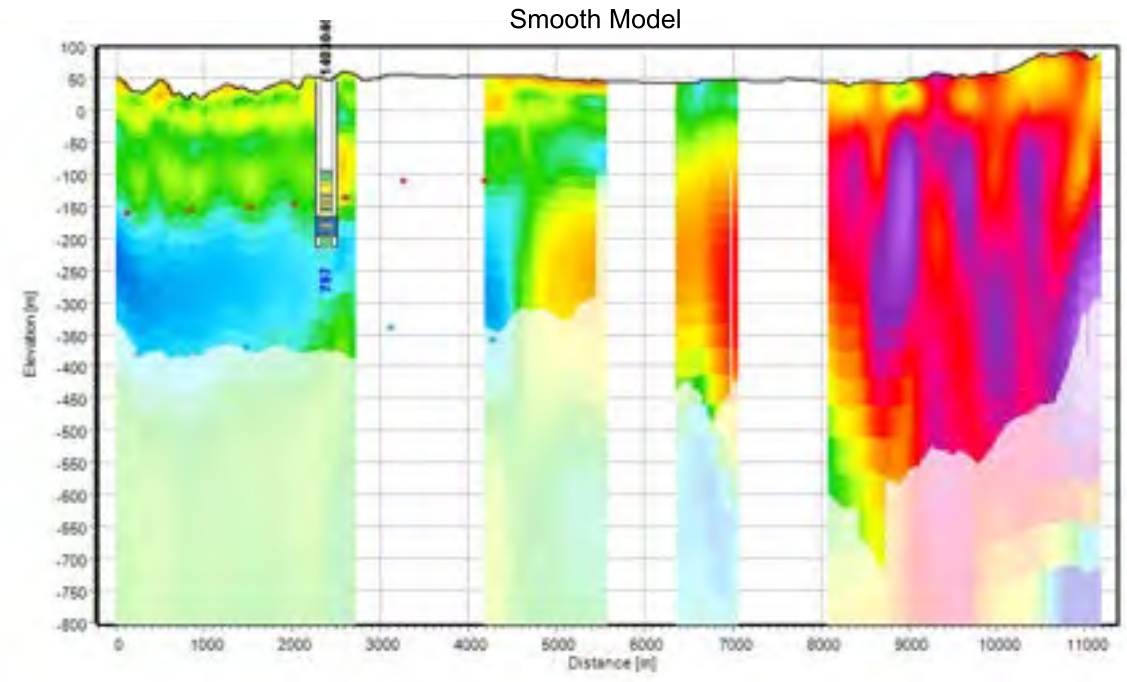
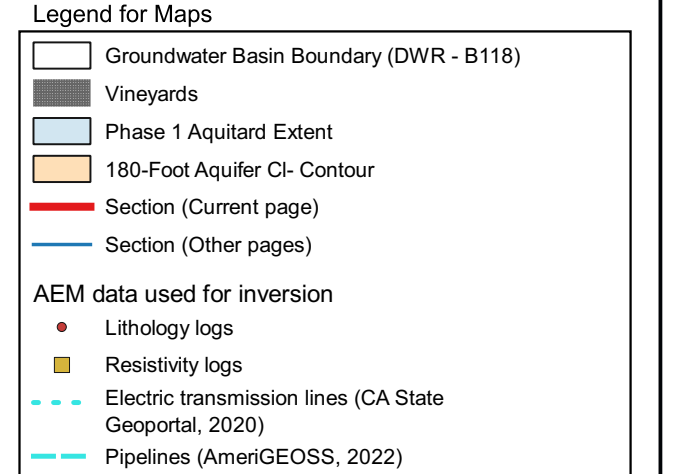
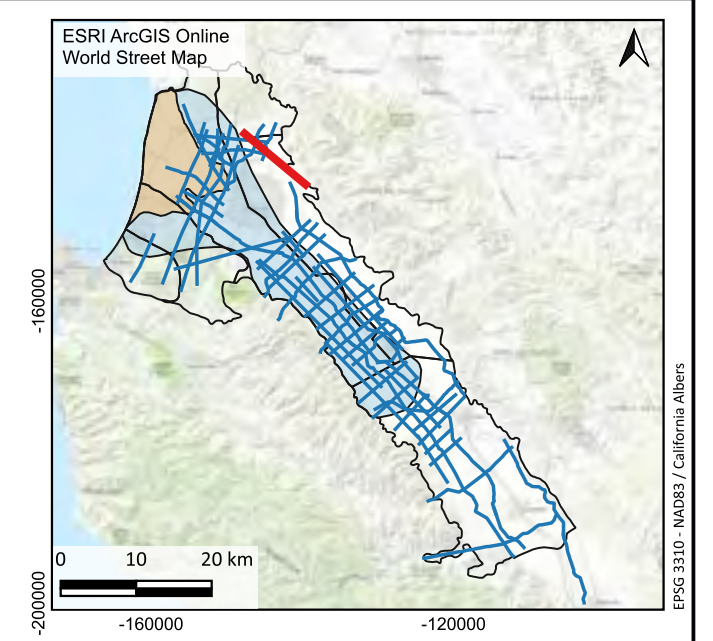
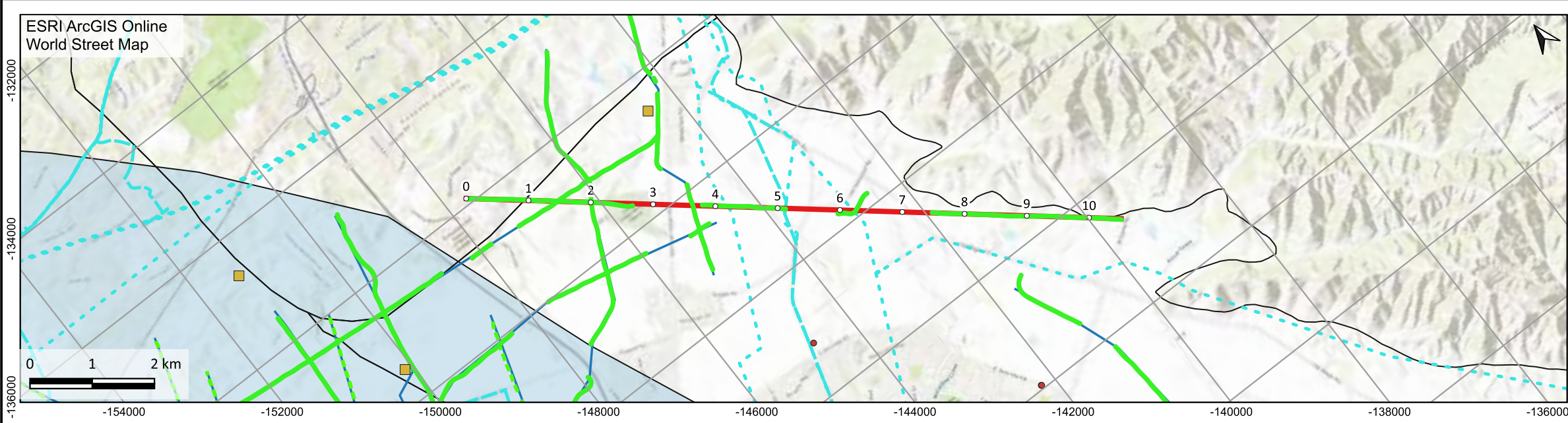
\*DOI = Depth of investigation

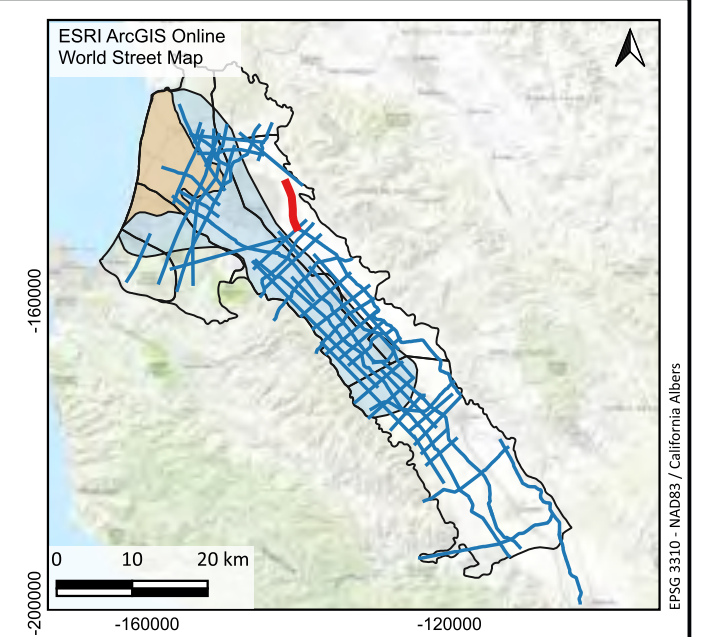
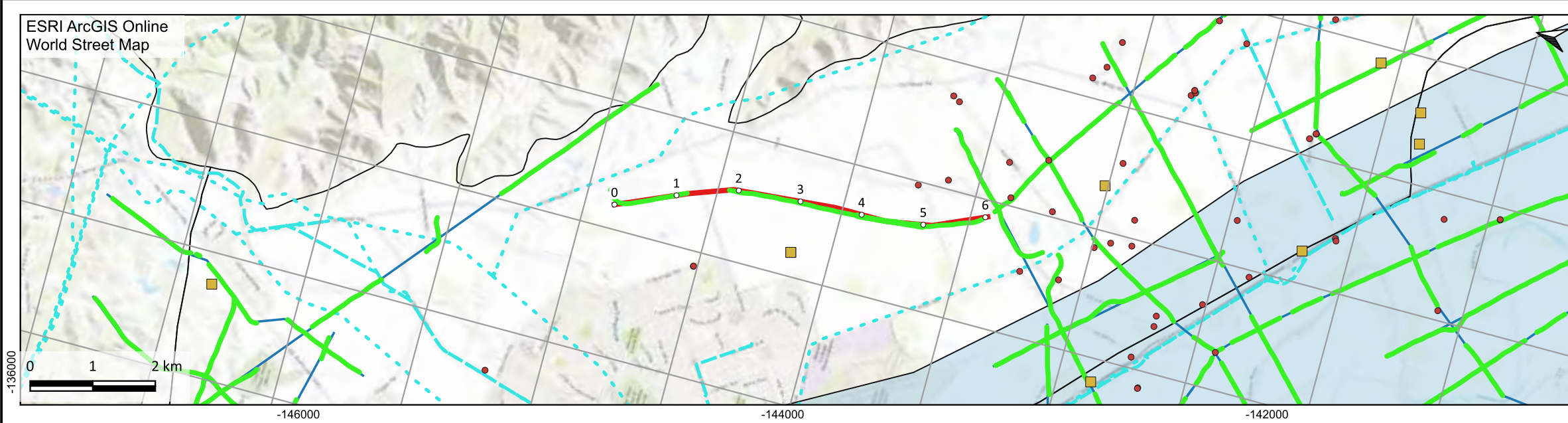
Lithology log	Resistivity log	Well completion report analysis

**Continuous conductor**

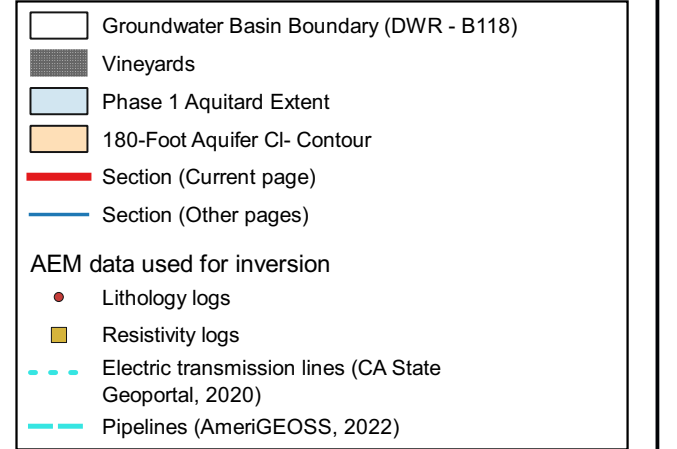
- Top of conductor
- Bottom of conductor
- Top of conductor (lower confidence)
- Bottom of conductor (lower confidence)



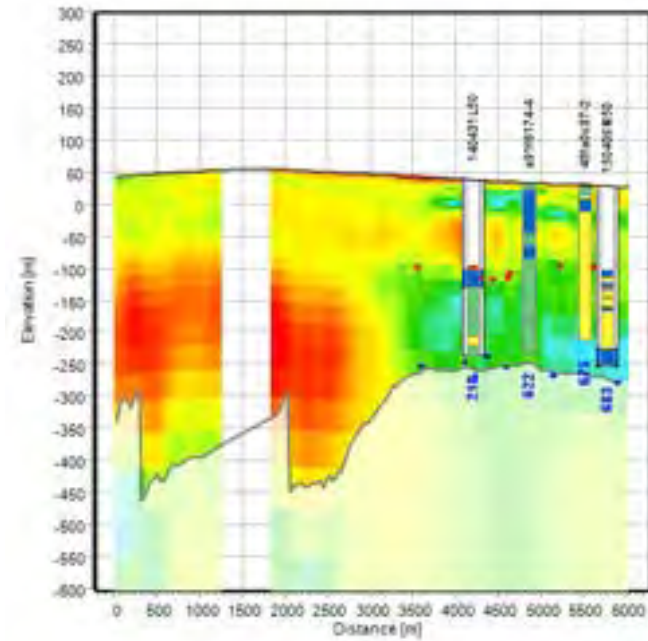




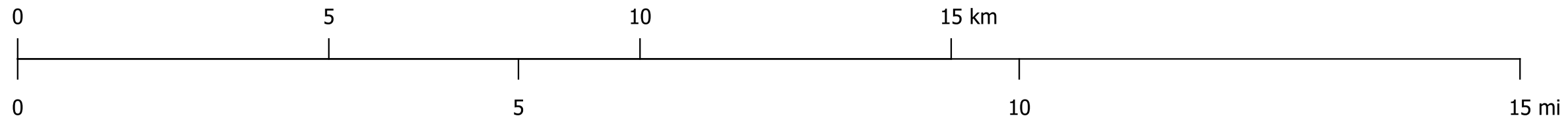
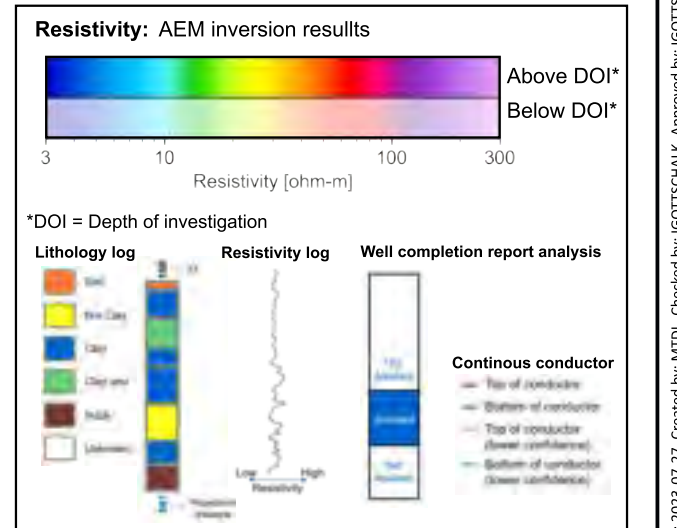
Legend for Maps

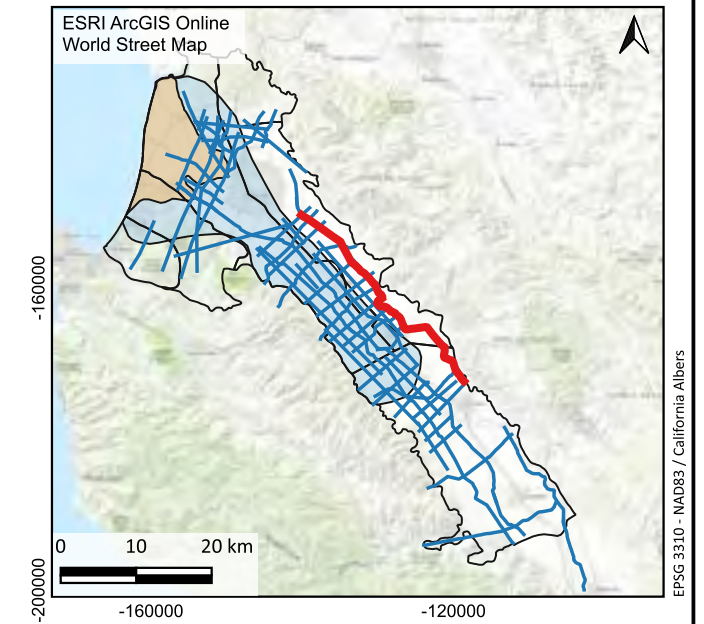
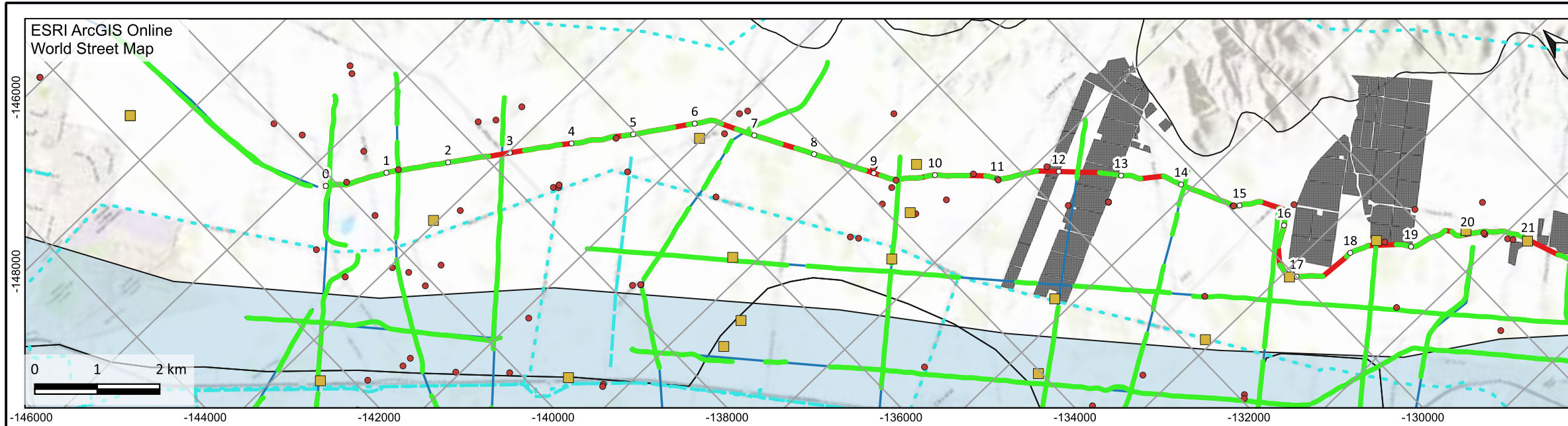


Smooth Model



Legend for Model Sections





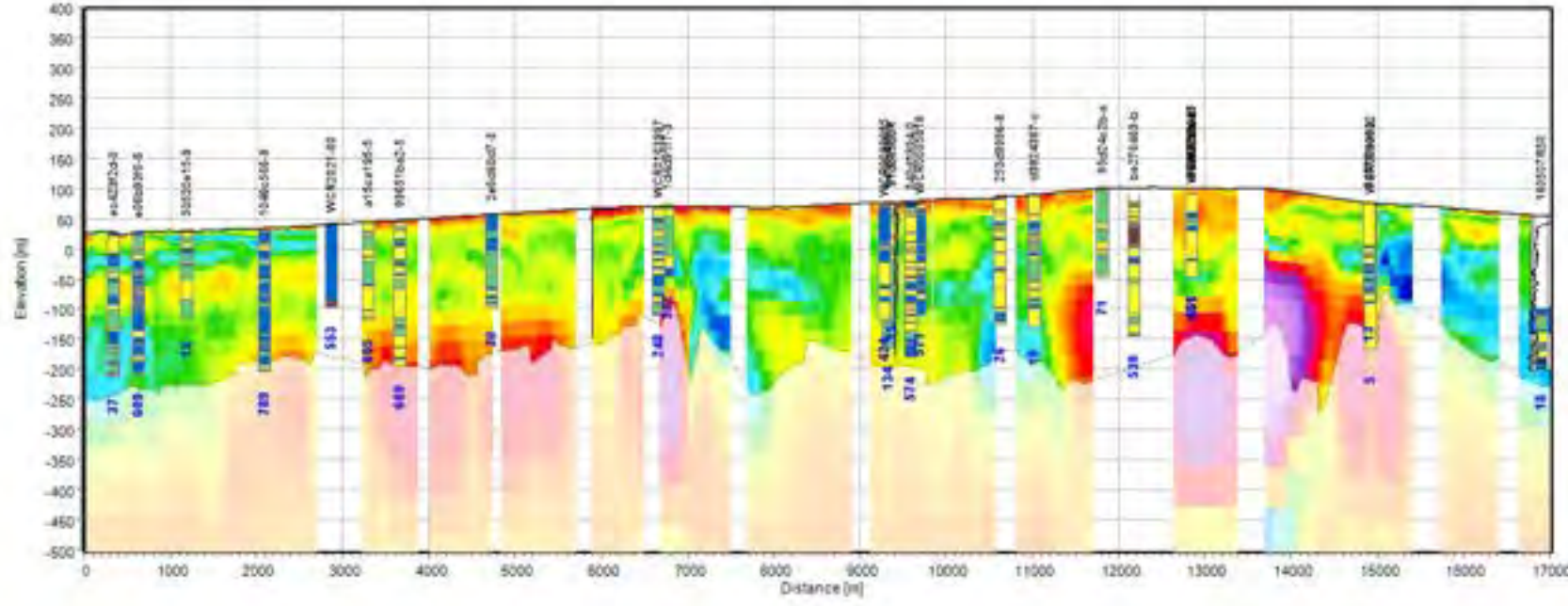
**Legend for Maps**

- Groundwater Basin Boundary (DWR - B118)
- Vineyards
- Phase 1 Aquitard Extent
- 180-Foot Aquifer CI- Contour
- Section (Current page)
- Section (Other pages)

**AEM data used for inversion**

- Lithology logs
- Resistivity logs
- Electric transmission lines (CA State Geoportals, 2020)
- Pipelines (AmerIGEISS, 2022)

Smooth Model



**Legend for Model Sections**

**Resistivity: AEM inversion results**

3 10 100 300  
Resistivity [ohm-m]

\*DOI = Depth of investigation

**Lithology log**

- Sand
- Fine Clay
- Clay
- Claystone
- Siltstone
- Limestone

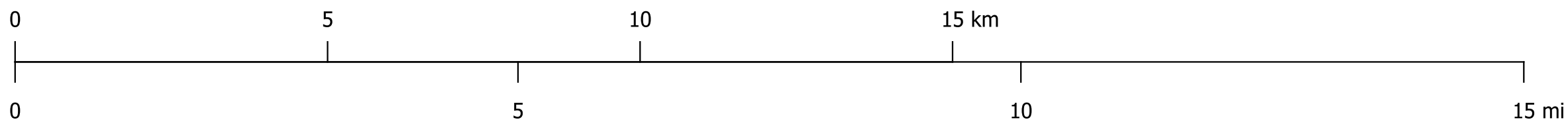
**Resistivity log**

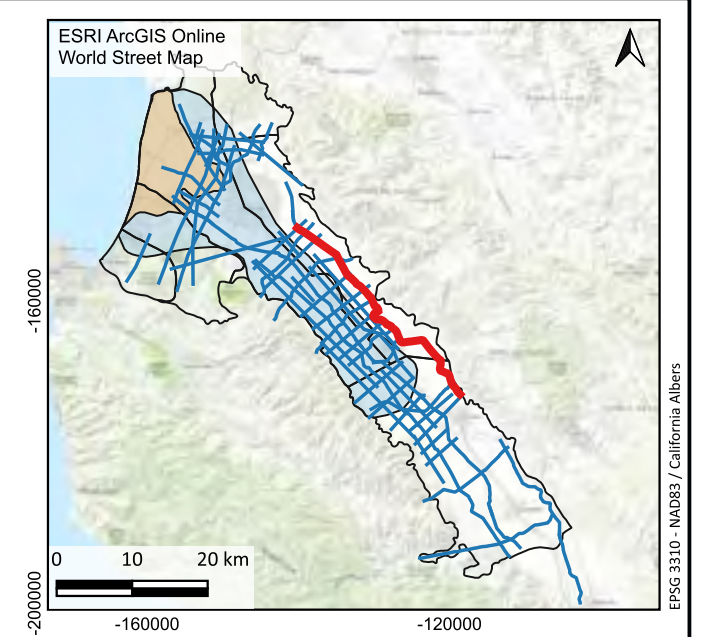
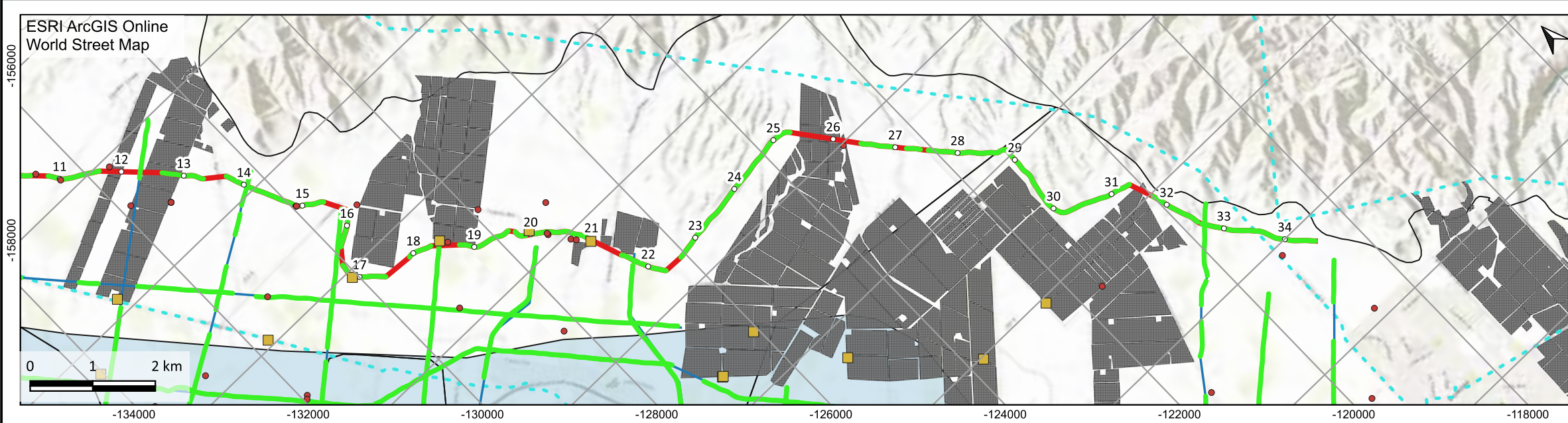
Log Resistivity

**Well completion report analysis**

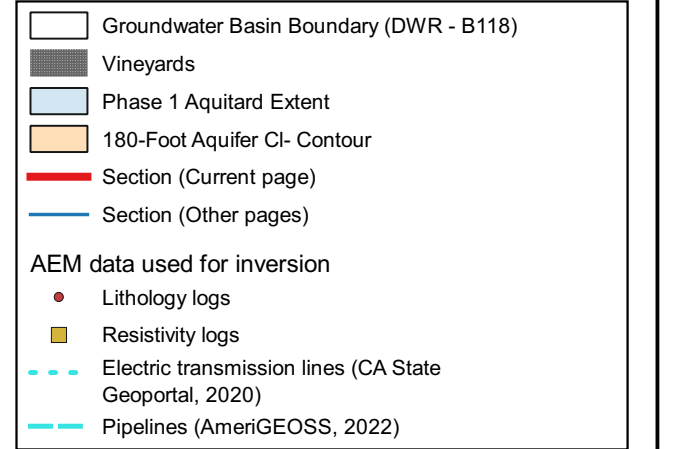
**Continuous conductor**

- Top of conductor
- Bottom of conductor
- Top of conductor (lower confidence)
- Bottom of conductor (lower confidence)

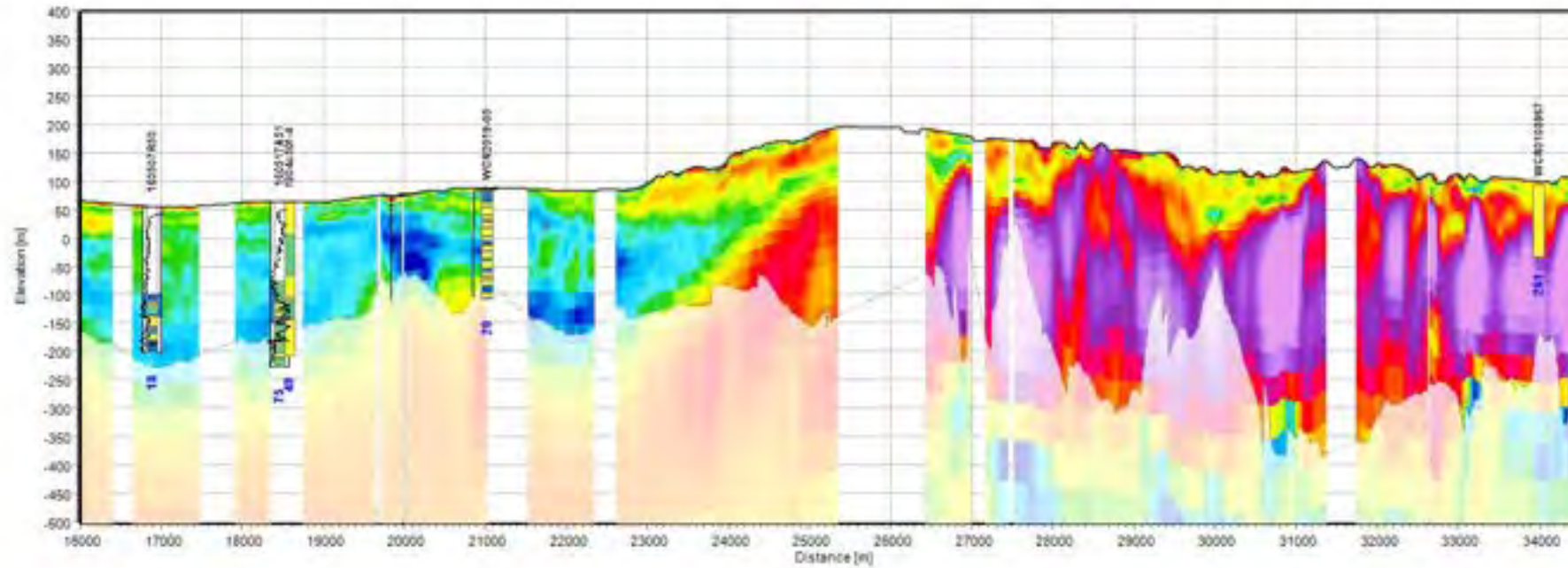




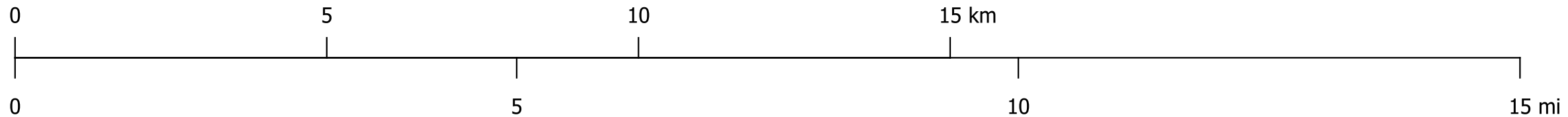
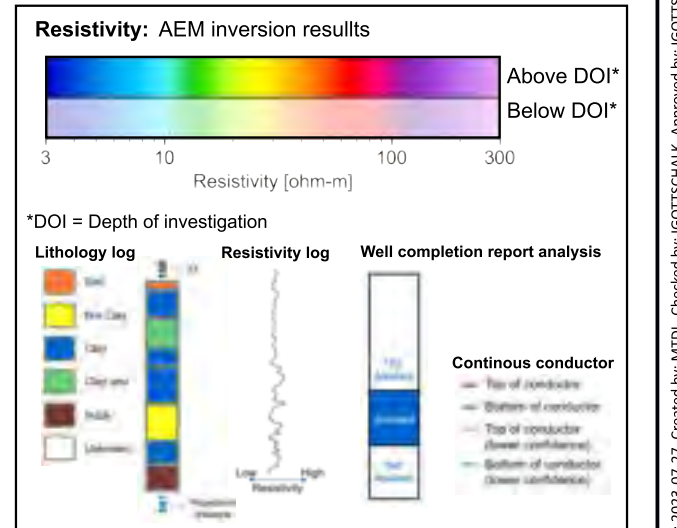
Legend for Maps

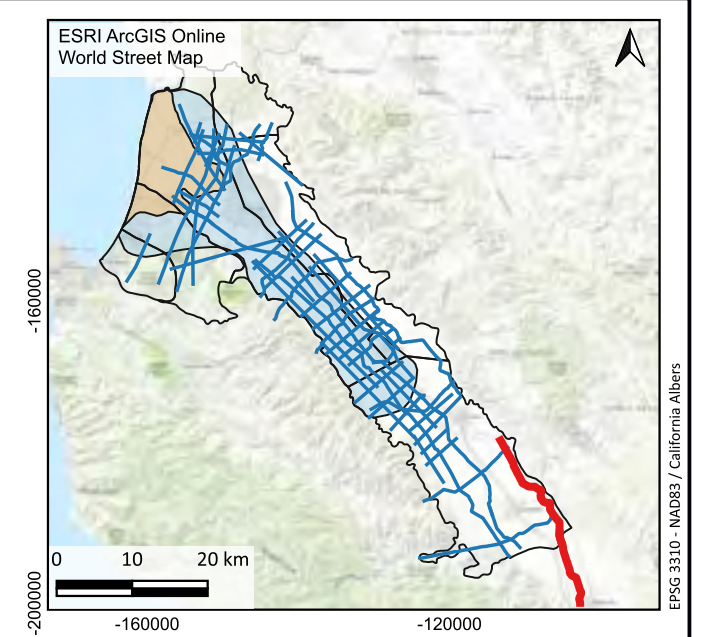
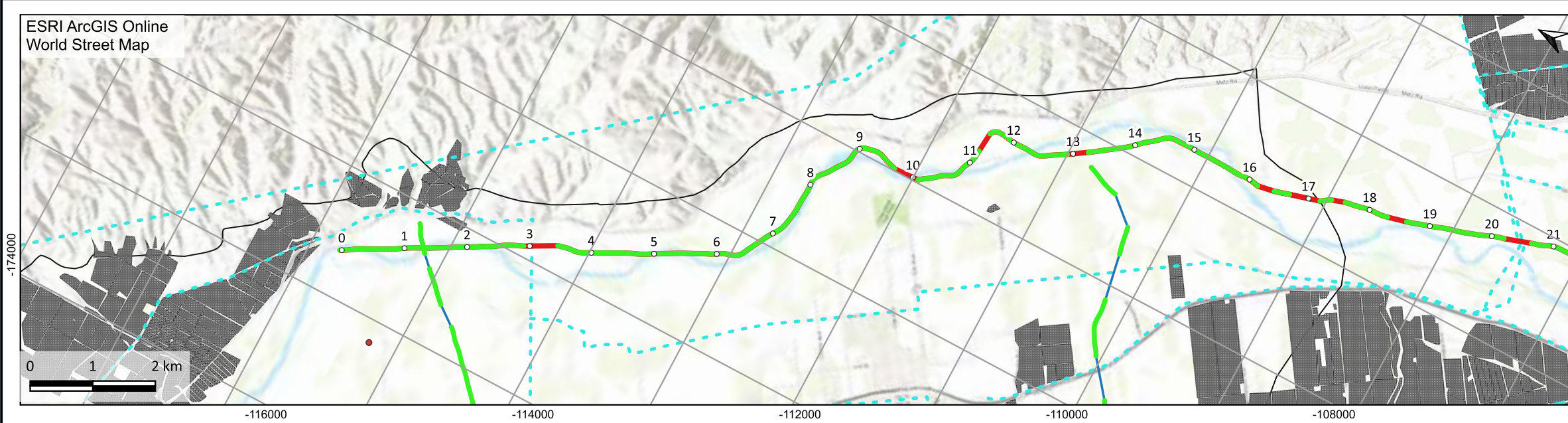


Smooth Model

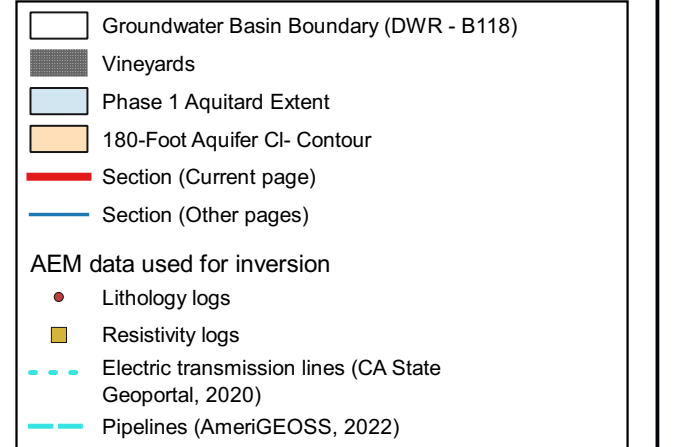


Legend for Model Sections

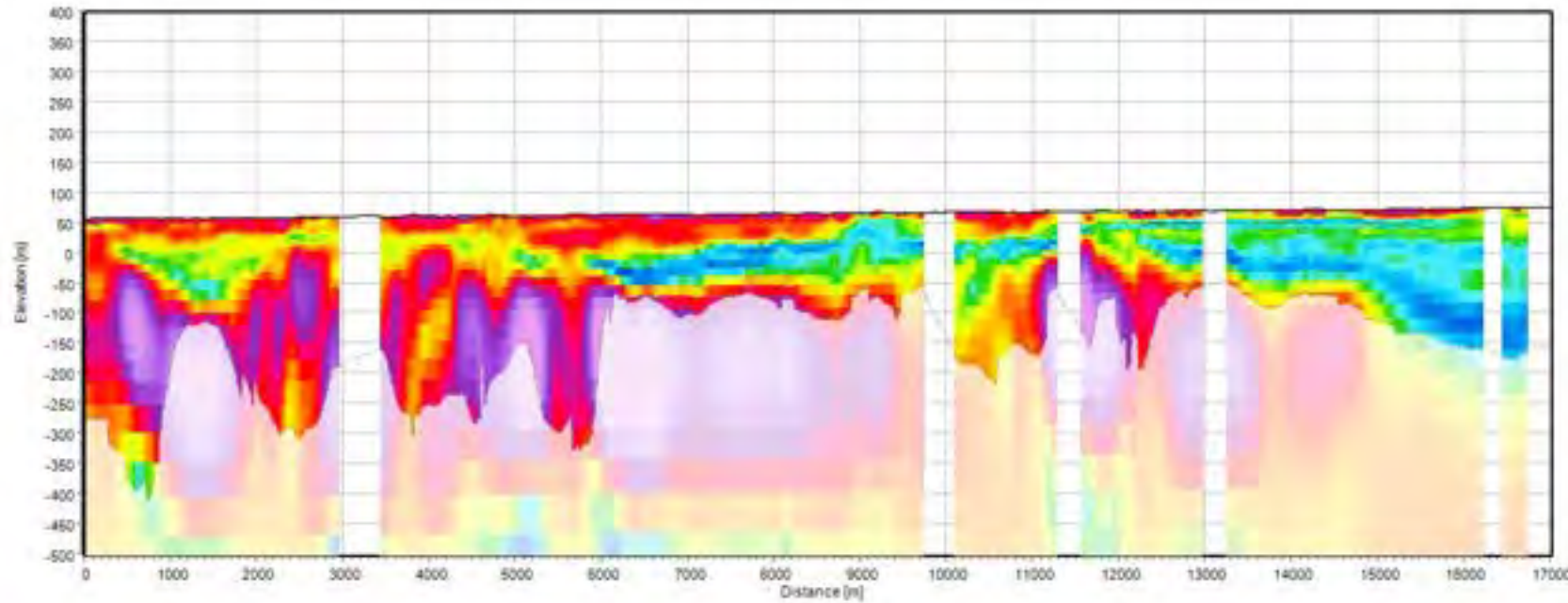




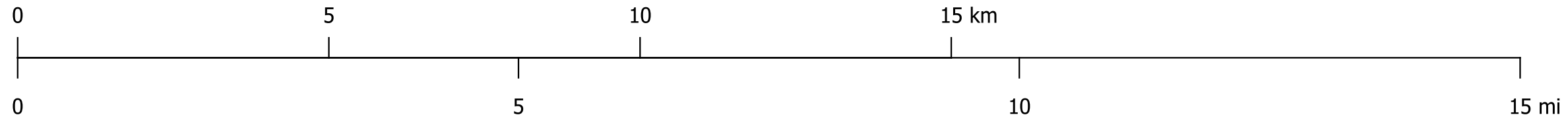
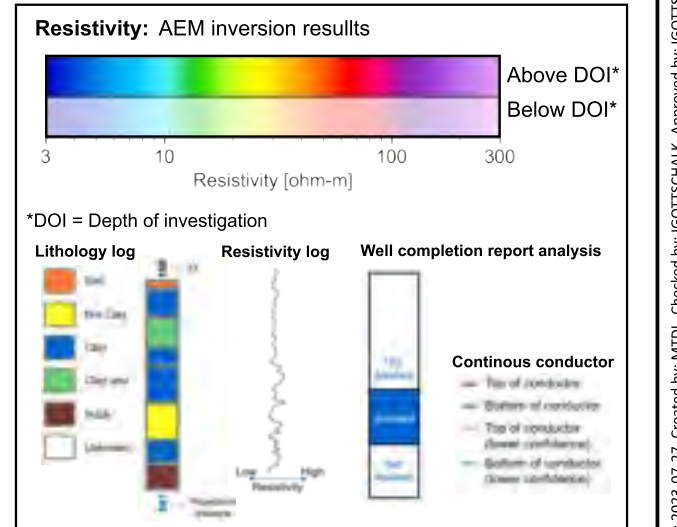
Legend for Maps

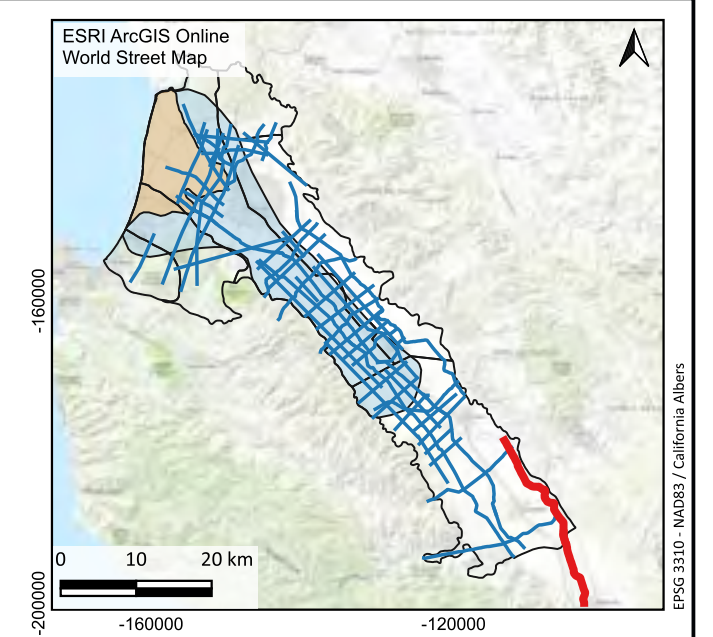
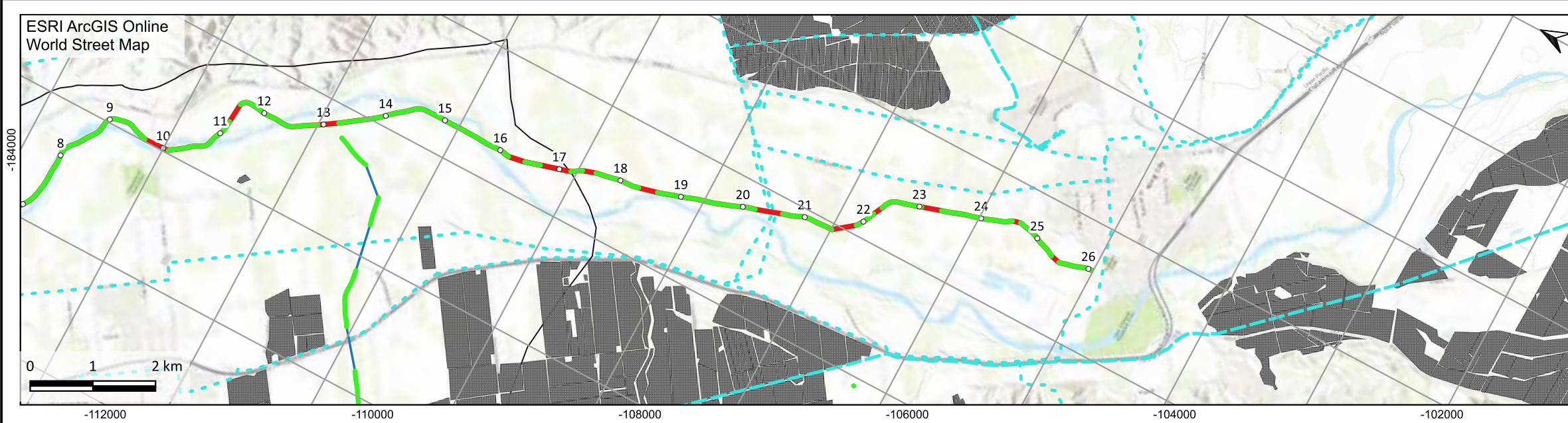


Smooth Model

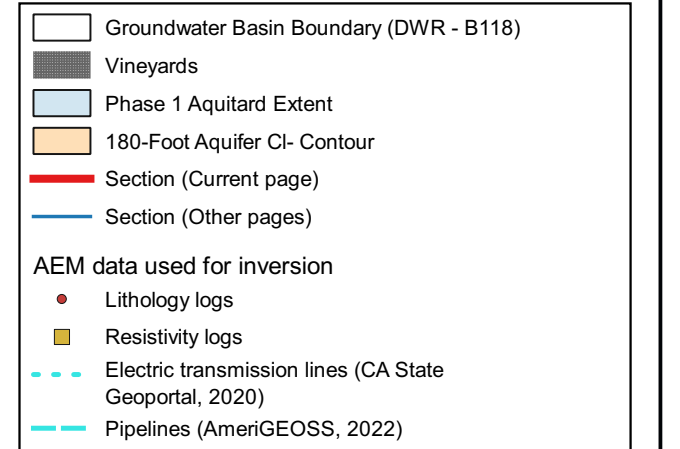


Legend for Model Sections

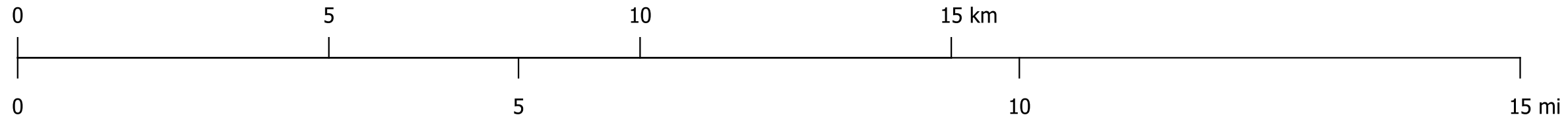
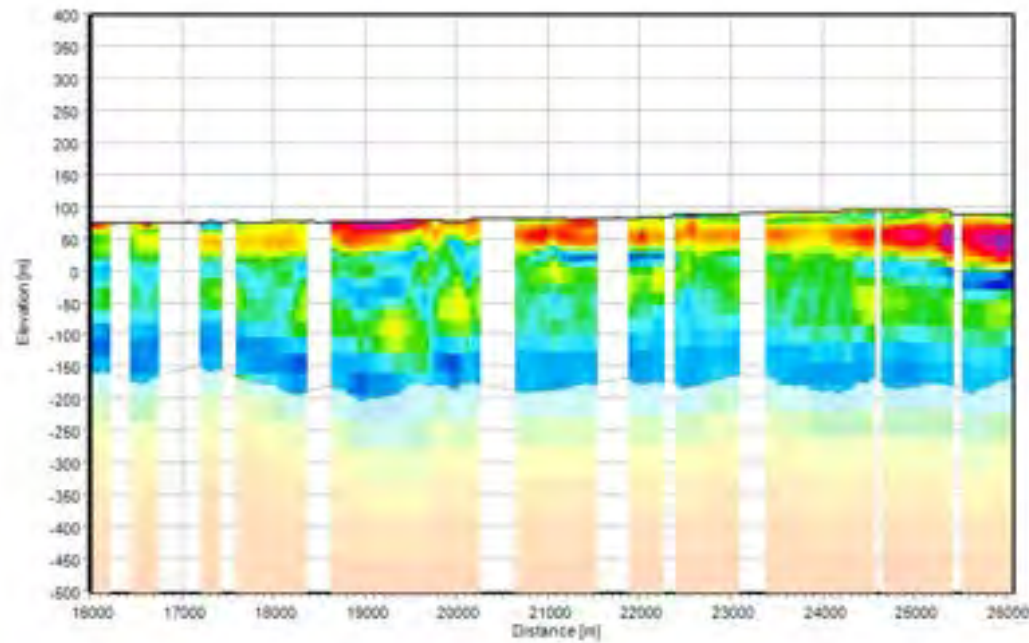




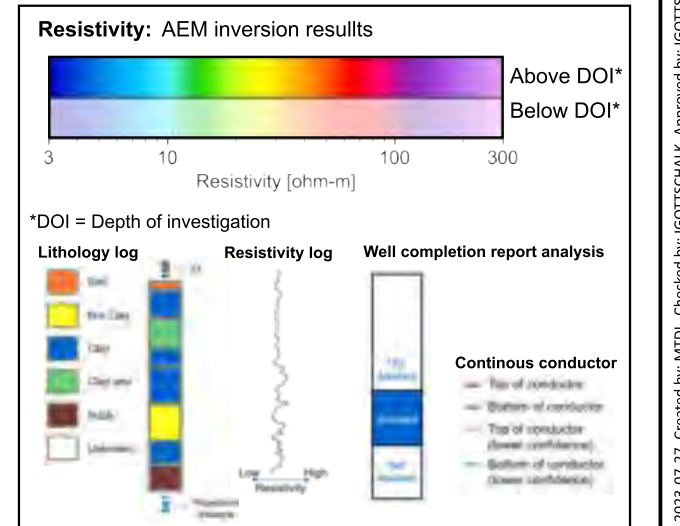
Legend for Maps

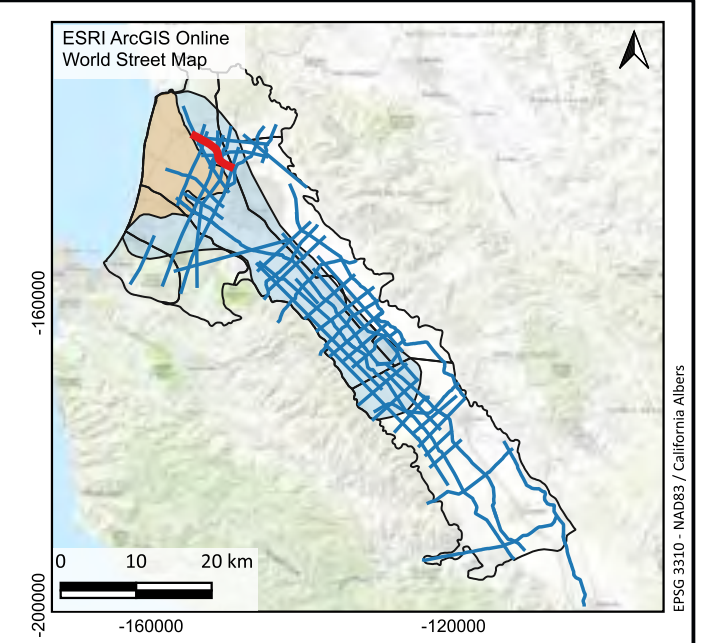
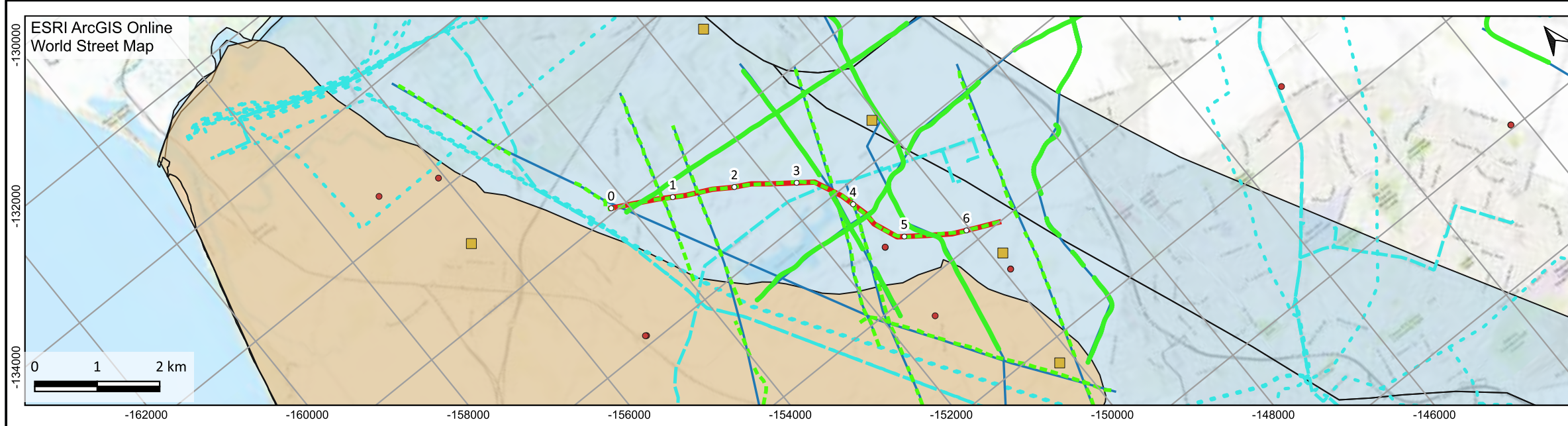


Smooth Model



Legend for Model Sections



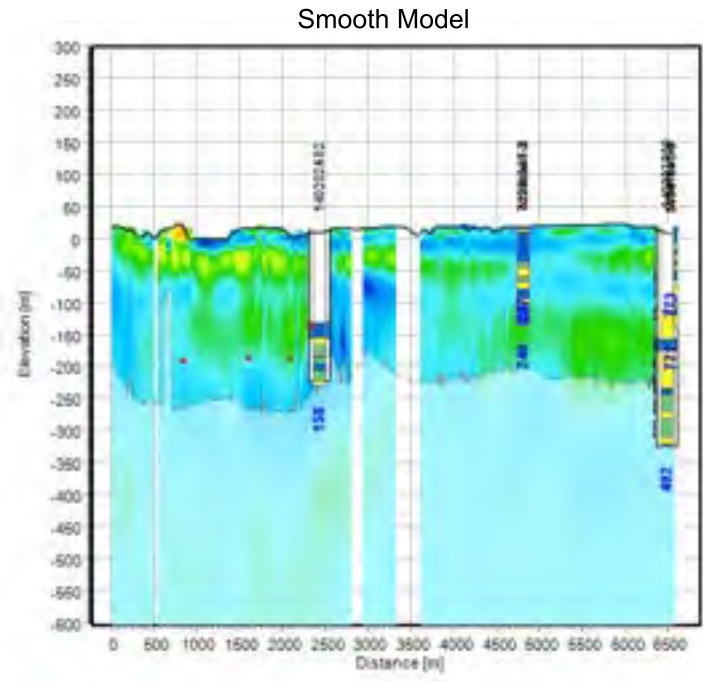


**Legend for Maps**

- Groundwater Basin Boundary (DWR - B118)
- Vineyards
- Phase 1 Aquitard Extent
- 180-Foot Aquifer CI- Contour
- Section (Current page)
- Section (Other pages)

**AEM data used for inversion**

- Lithology logs
- Resistivity logs
- Electric transmission lines (CA State Geoport, 2020)
- Pipelines (AmeriGEOSS, 2022)



**Legend for Model Sections**

**Resistivity: AEM inversion results**

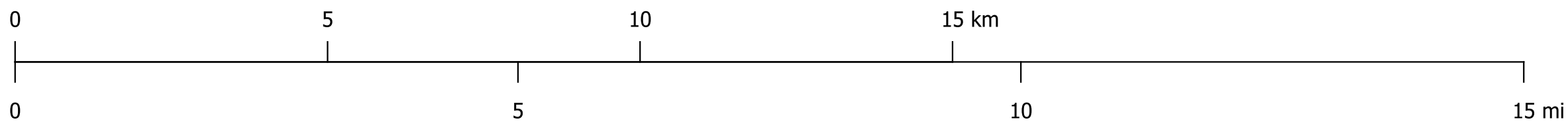
3      10      100      300  
Resistivity [ohm-m]

\*DOI = Depth of investigation

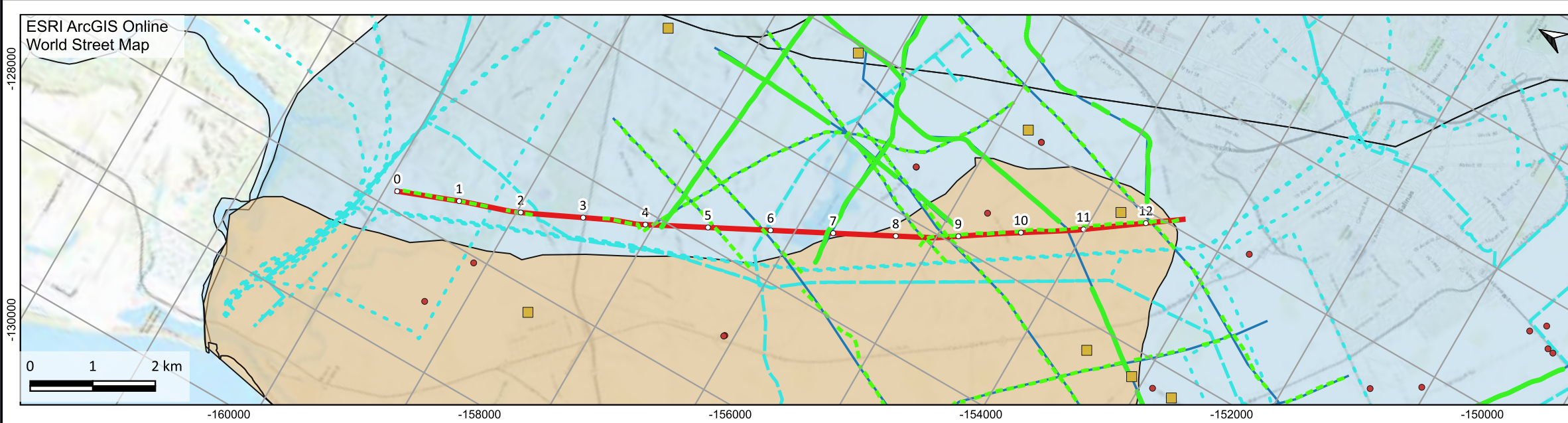
Lithology log	Resistivity log	Well completion report analysis
Sand		
Silt Clay		
Clay		
Clay shale		
Mudstone		
Limestone		

**Continuous conductor**

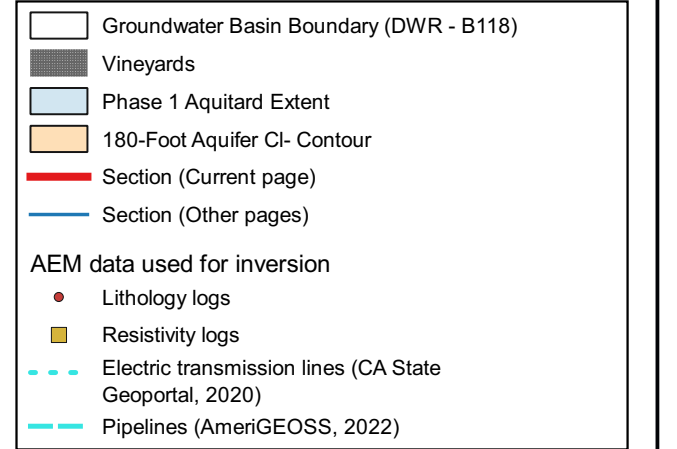
- Top of conductor
- Bottom of conductor
- Top of conductor (lower confidence)
- Bottom of conductor (lower confidence)



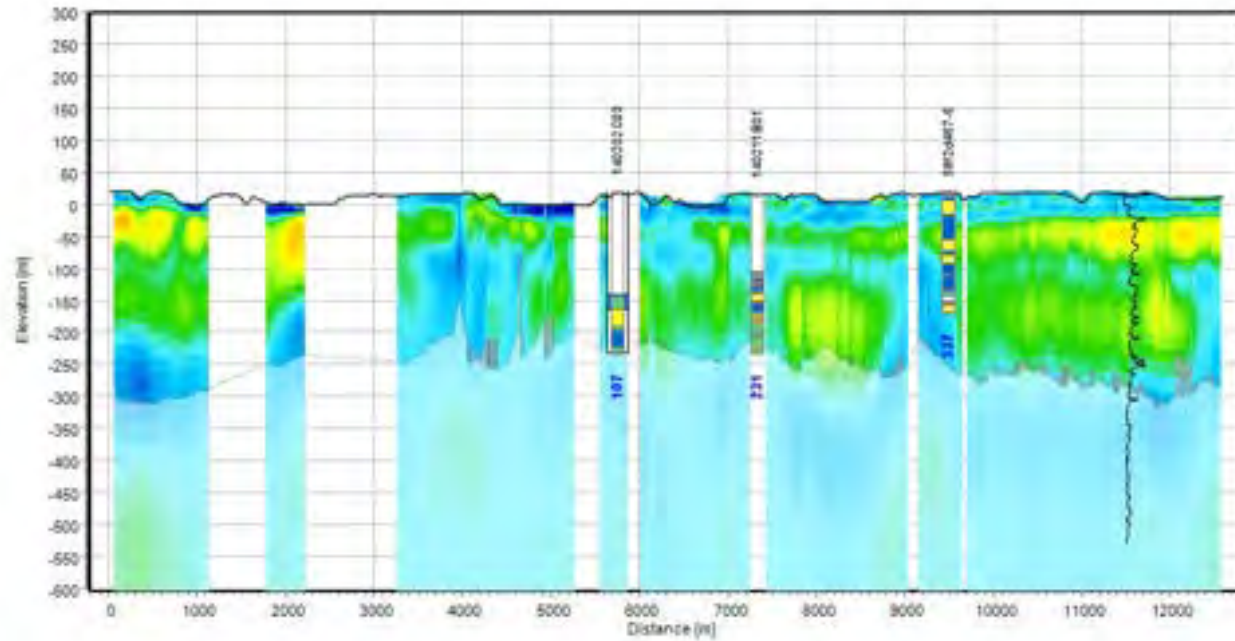




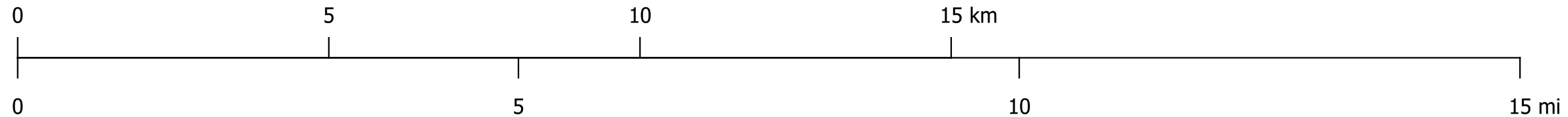
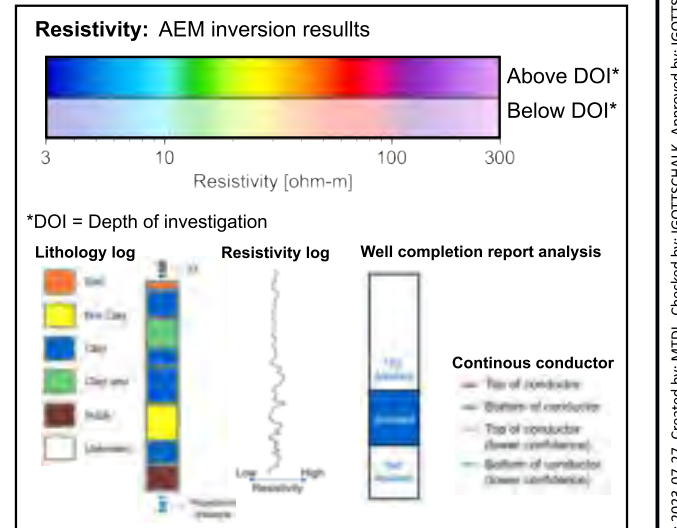
Legend for Maps

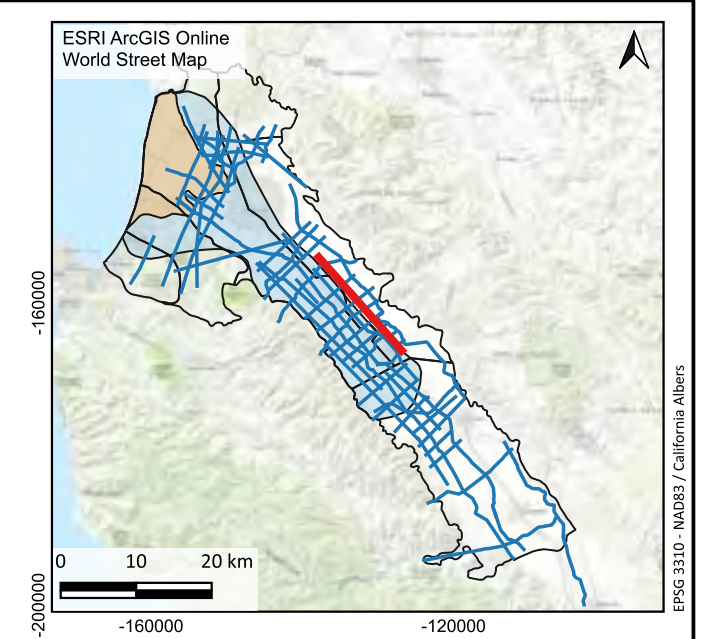
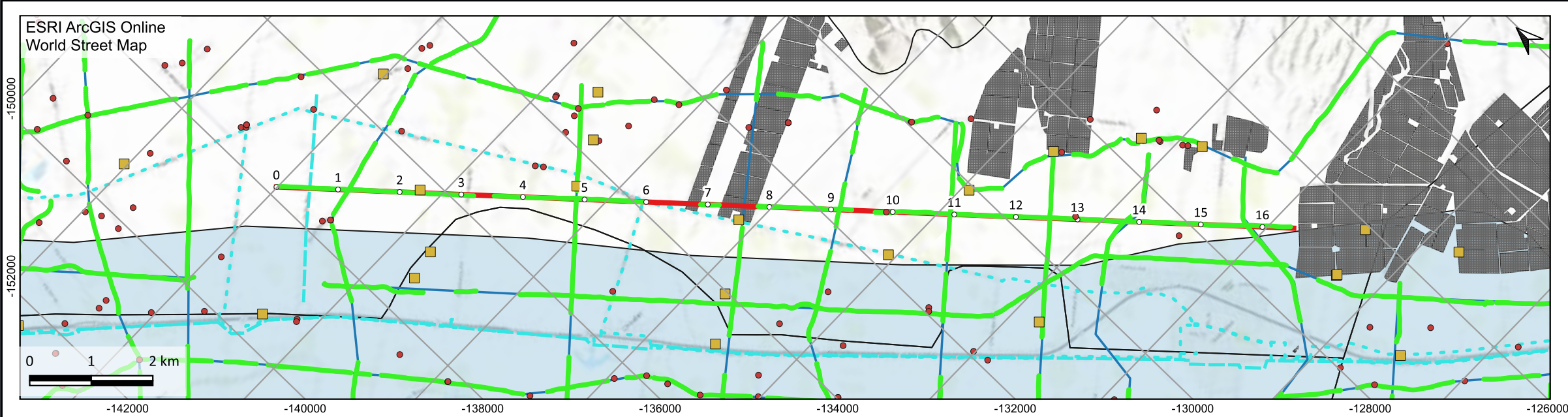


Smooth Model



Legend for Model Sections





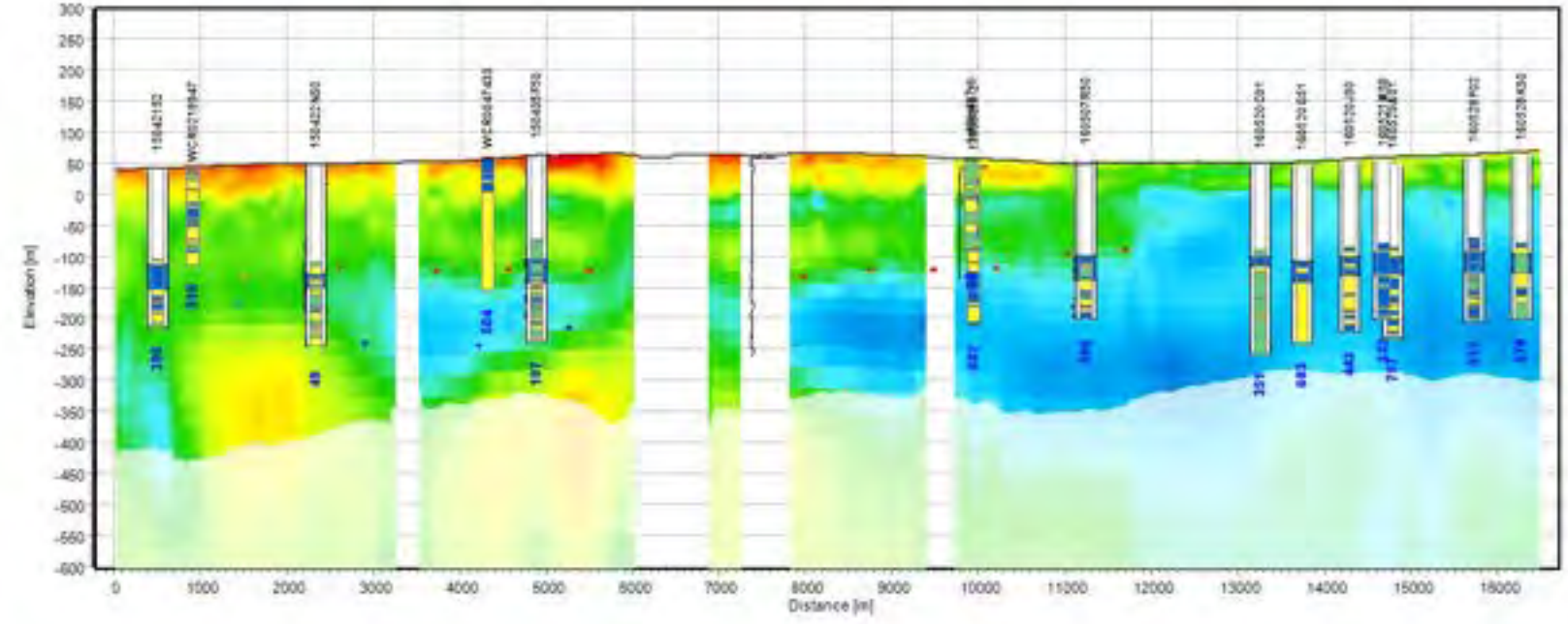
**Legend for Maps**

- Groundwater Basin Boundary (DWR - B118)
- Vineyards
- Phase 1 Aquitard Extent
- 180-Foot Aquifer CI- Contour
- Section (Current page)
- Section (Other pages)

**AEM data used for inversion**

- Lithology logs
- Resistivity logs
- Electric transmission lines (CA State Geoportals, 2020)
- Pipelines (AmeriGEOSS, 2022)

Smooth Model



**Legend for Model Sections**

**Resistivity: AEM inversion results**

3 10 100 300  
Resistivity [ohm-m]

\*DOI = Depth of investigation

**Lithology log**

- Soil
- Fine Clay
- Clay
- Clay shale
- Silt
- Sandstone

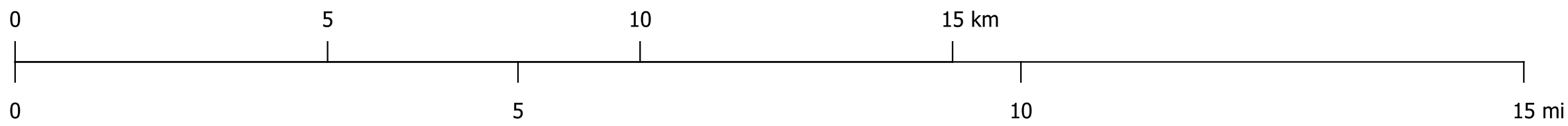
**Resistivity log**

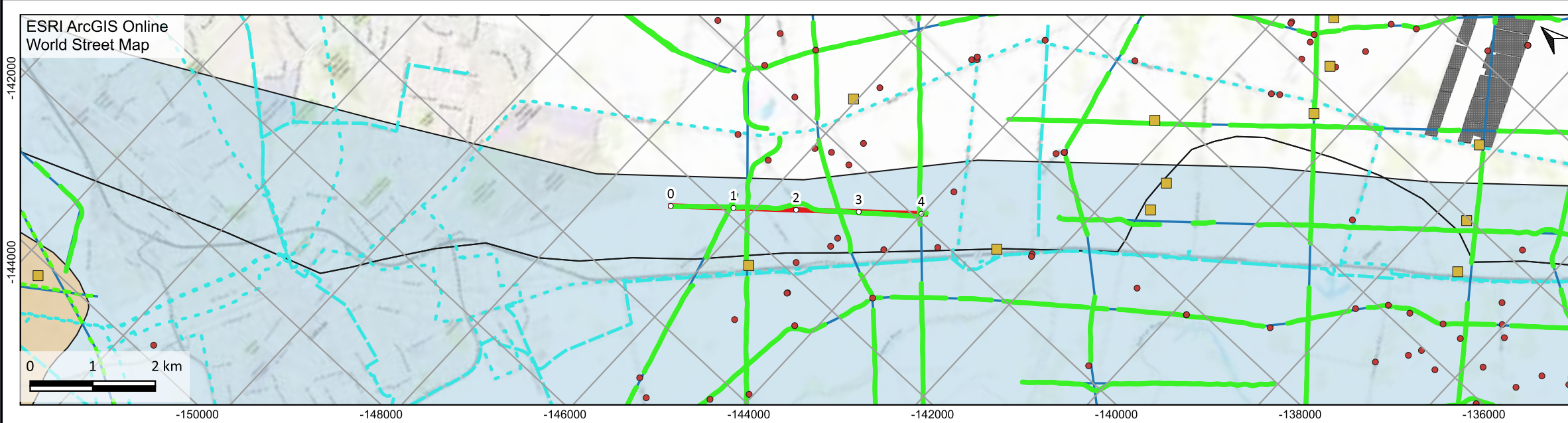
Log Resistivity

**Well completion report analysis**

**Continuous conductor**

- Top of conductor
- Bottom of conductor
- Top of conductor (lower confidence)
- Bottom of conductor (lower confidence)



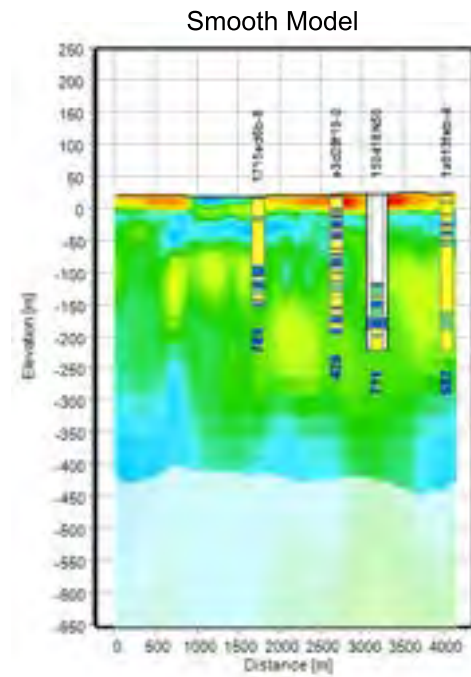


**Legend for Maps**

- Groundwater Basin Boundary (DWR - B118)
- Vineyards
- Phase 1 Aquitard Extent
- 180-Foot Aquifer CI- Contour
- Section (Current page)
- Section (Other pages)

**AEM data used for inversion**

- Lithology logs
- Resistivity logs
- Electric transmission lines (CA State Geportal, 2020)
- Pipelines (AmeriGEOSS, 2022)

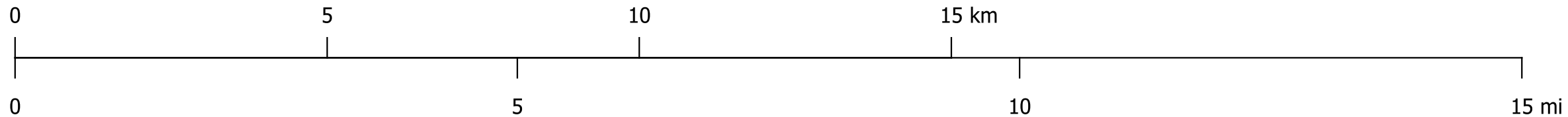


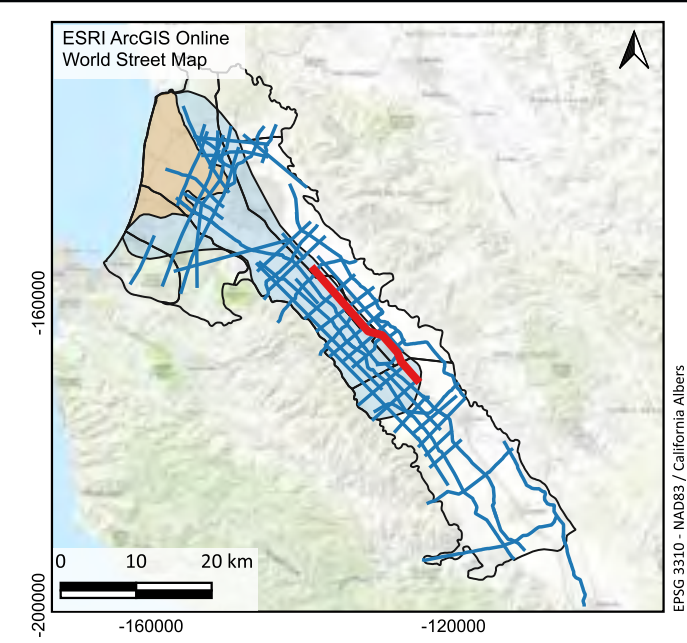
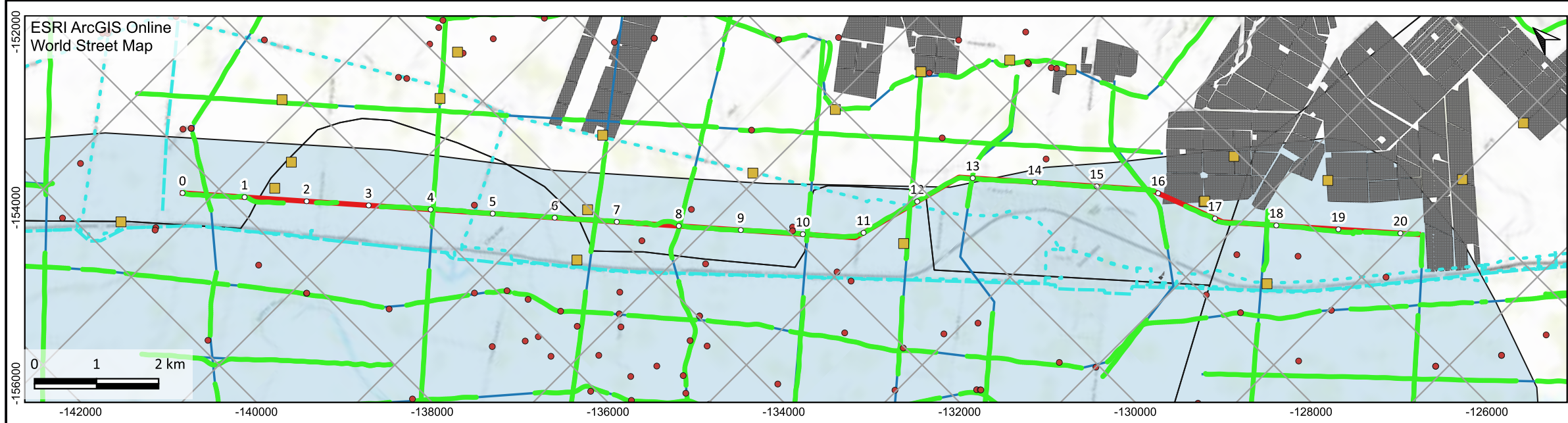
**Legend for Model Sections**

**Resistivity: AEM inversion results**

\*DOI = Depth of investigation

Lithology log	Resistivity log	Well completion report analysis
<ul style="list-style-type: none"> <li>Soil</li> <li>Site Clay</li> <li>Clay</li> <li>Clay shale</li> <li>Silt</li> <li>Sandstone</li> </ul>		<ul style="list-style-type: none"> <li>Continuous conductor</li> <li>Top of conductor</li> <li>Bottom of conductor</li> <li>Top of conductor (lower confidence)</li> <li>Bottom of conductor (lower confidence)</li> </ul>





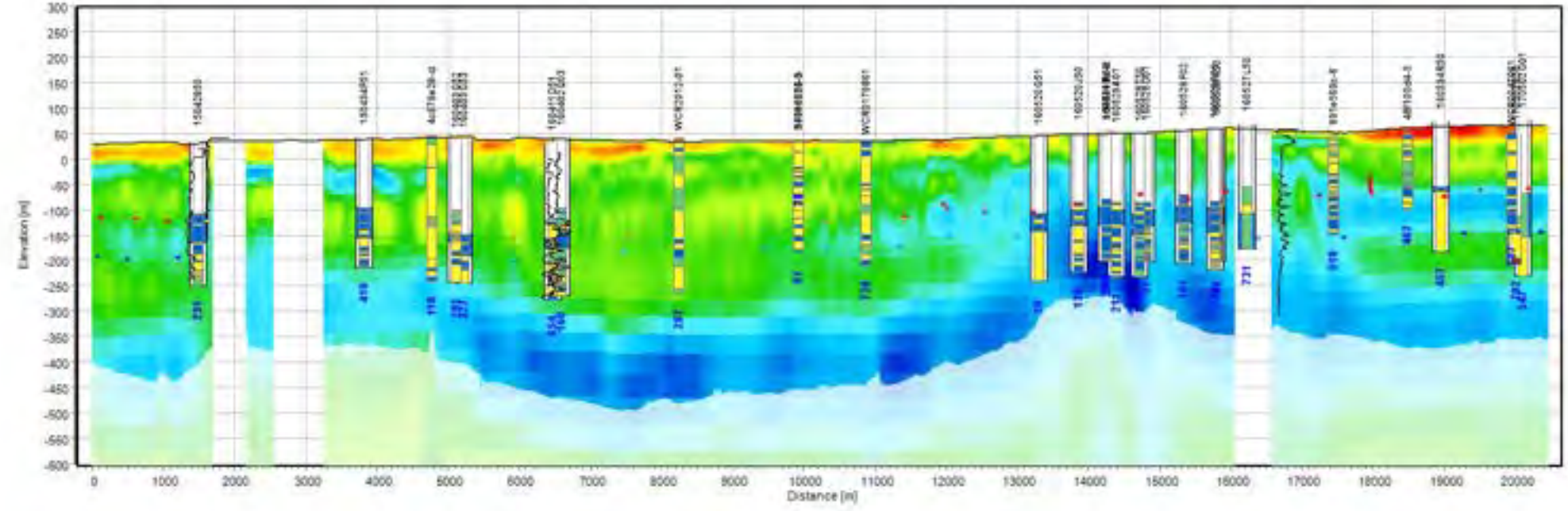
**Legend for Maps**

- Groundwater Basin Boundary (DWR - B118)
- Vineyards
- Phase 1 Aquitard Extent
- 180-Foot Aquifer CI- Contour
- Section (Current page)
- Section (Other pages)

**AEM data used for inversion**

- Lithology logs
- Resistivity logs
- Electric transmission lines (CA State Geoport, 2020)
- Pipelines (AmerGEOSS, 2022)

Smooth Model



**Legend for Model Sections**

**Resistivity: AEM inversion results**

3 10 100 300  
Resistivity [ohm-m]

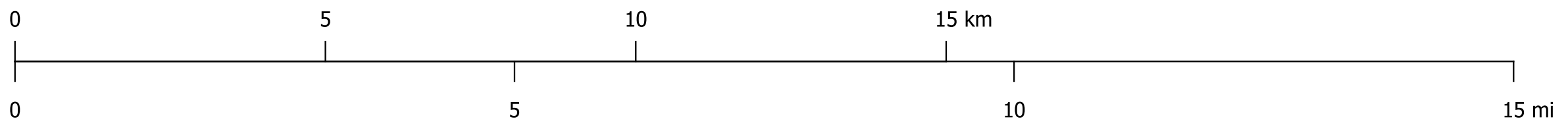
Above DOI\*  
Below DOI\*

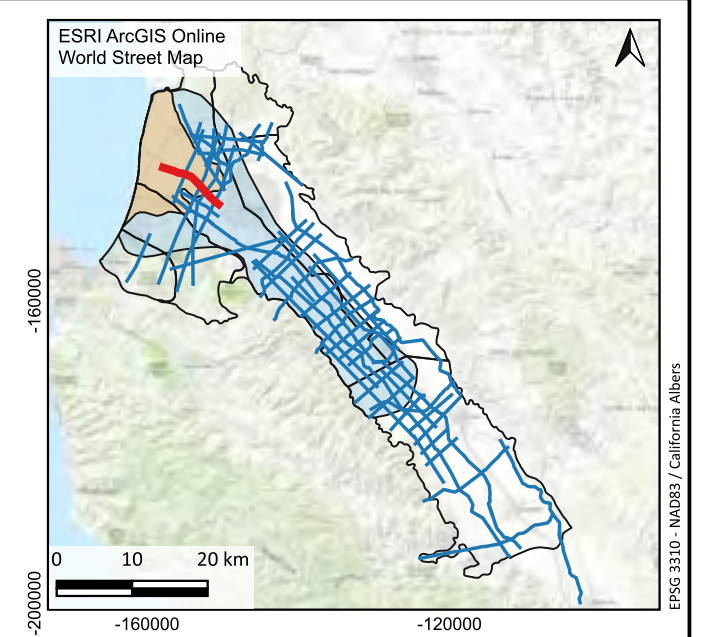
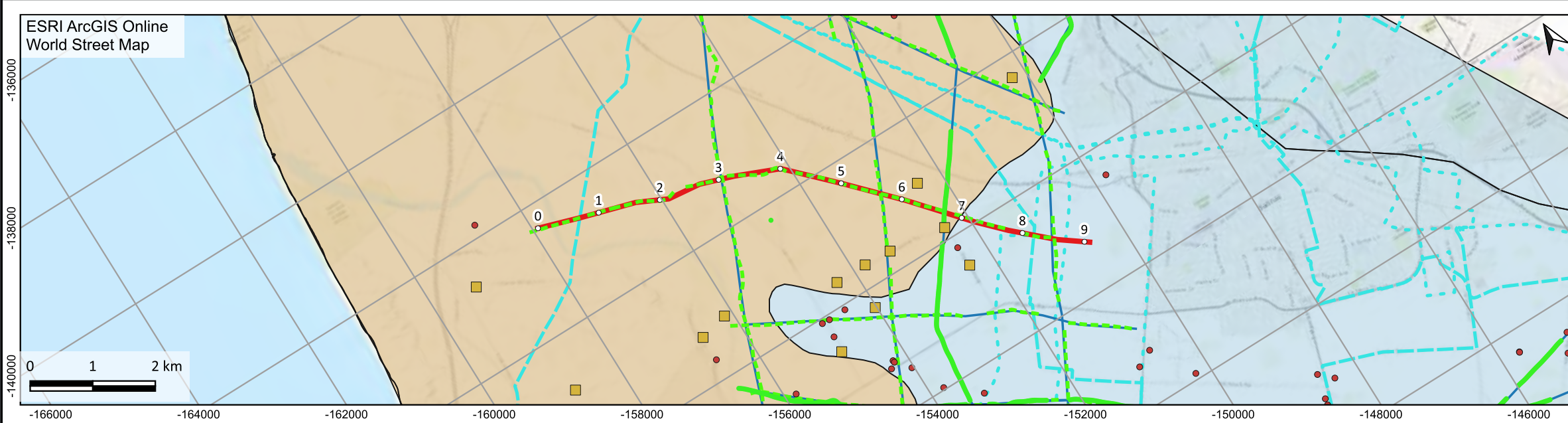
\*DOI = Depth of investigation

Lithology log	Resistivity log	Well completion report analysis
Soil		
Fine Clay		
Clay		
Clay shale		
Silt		
Lithology	Low Resistivity	High Resistivity

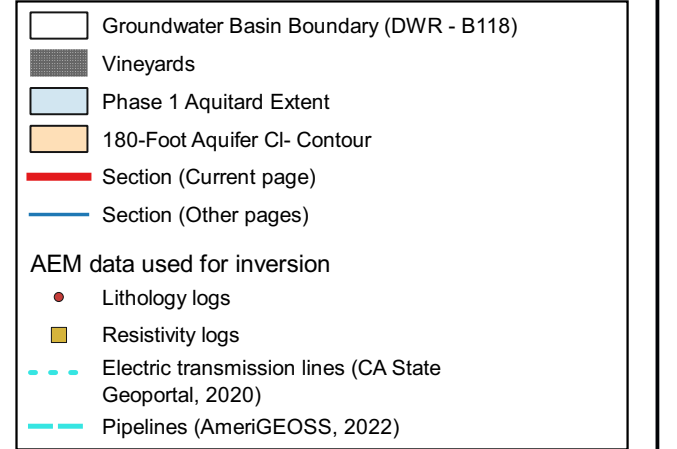
**Continuous conductor**

- Top of conductor
- Bottom of conductor
- Top of conductor (lower confidence)
- Bottom of conductor (lower confidence)

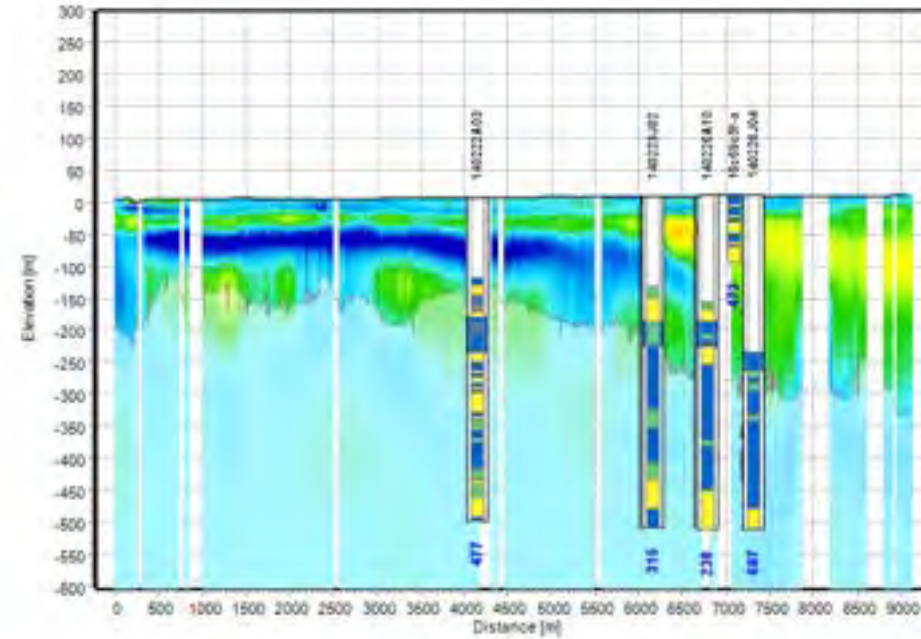




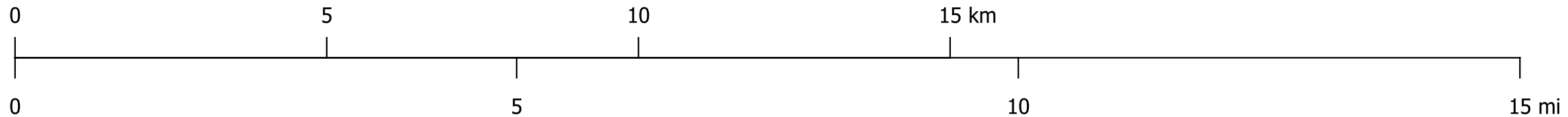
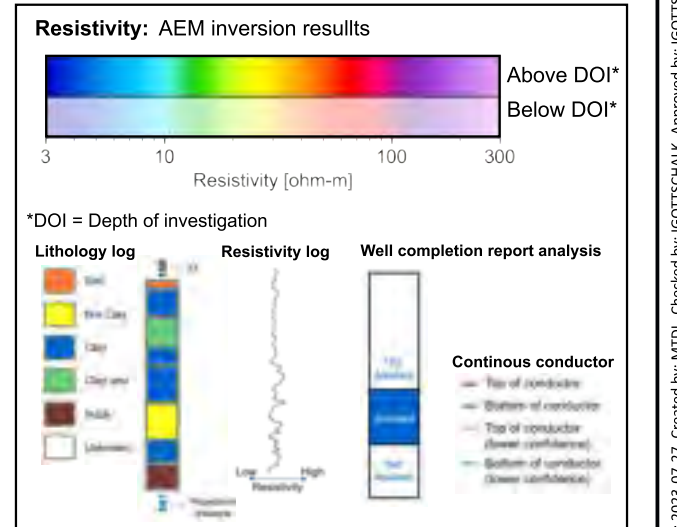
Legend for Maps

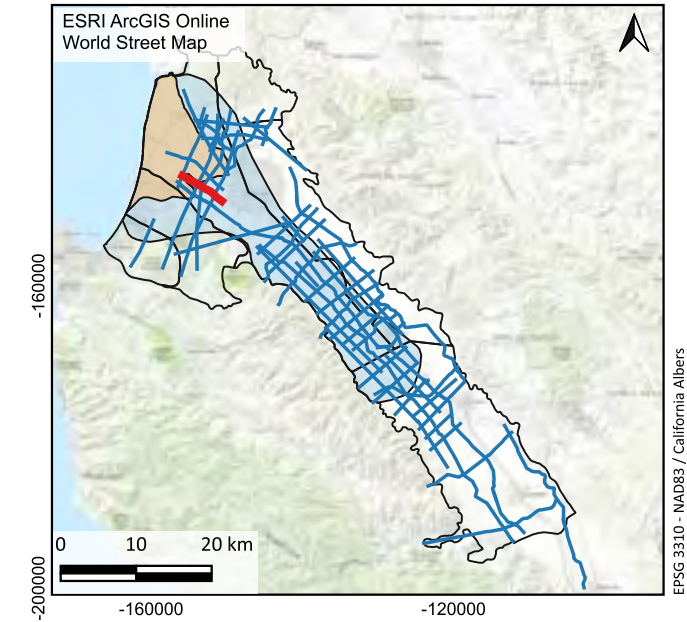
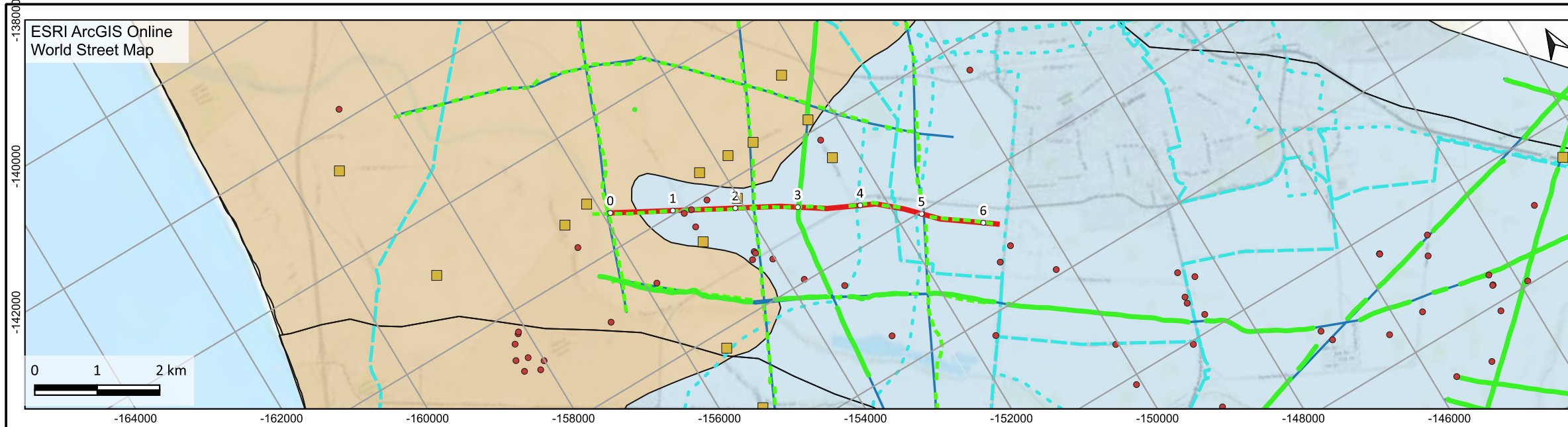


Smooth Model

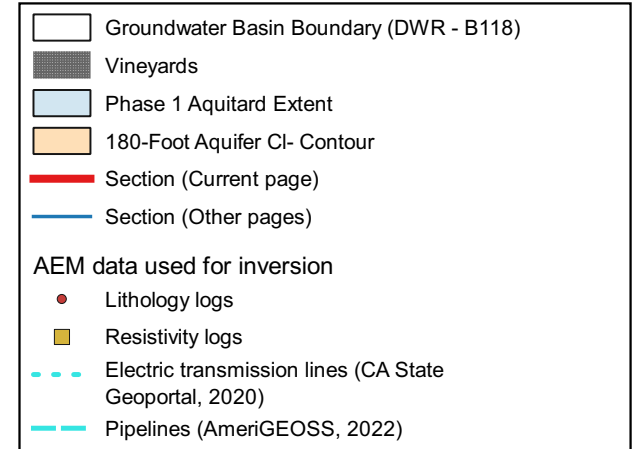


Legend for Model Sections

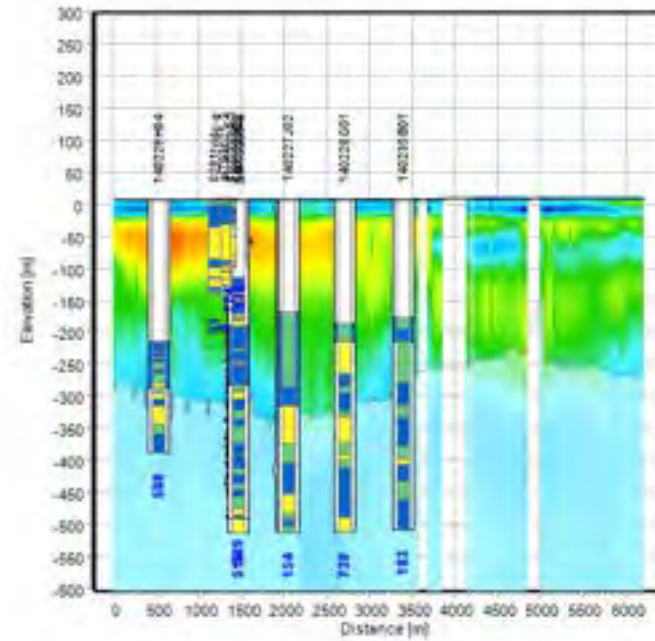




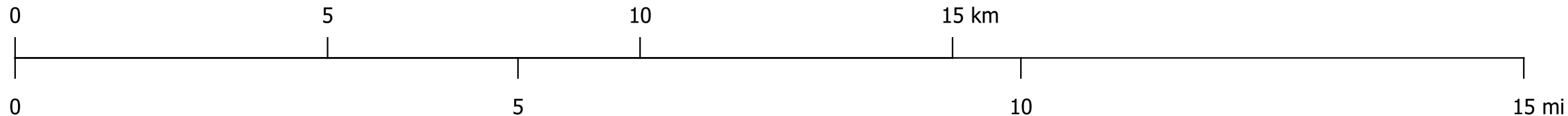
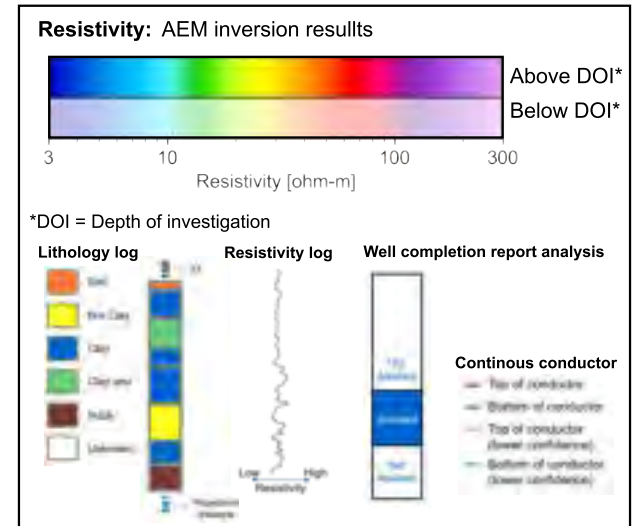
Legend for Maps

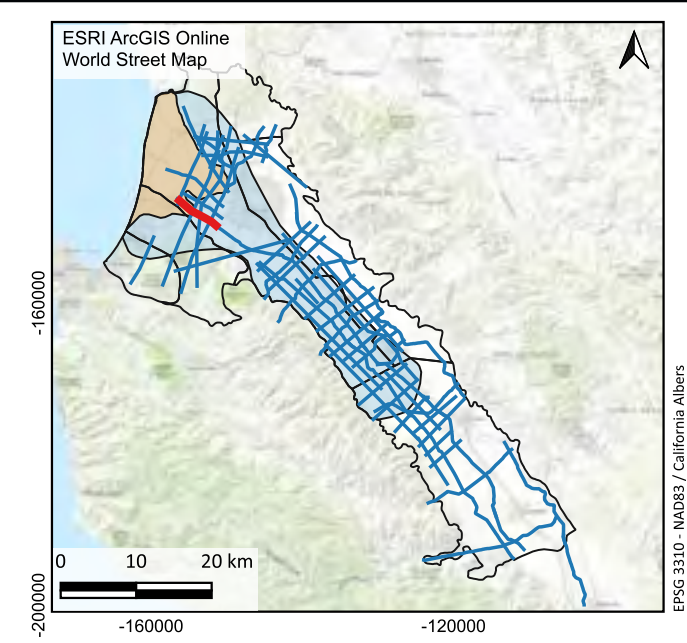
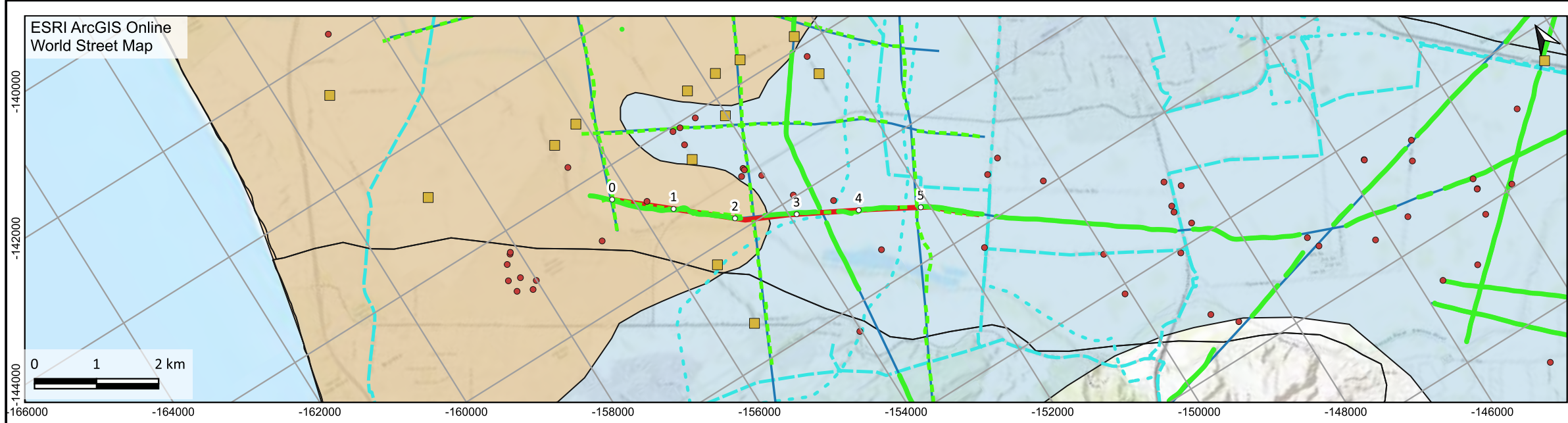


Smooth Model



Legend for Model Sections



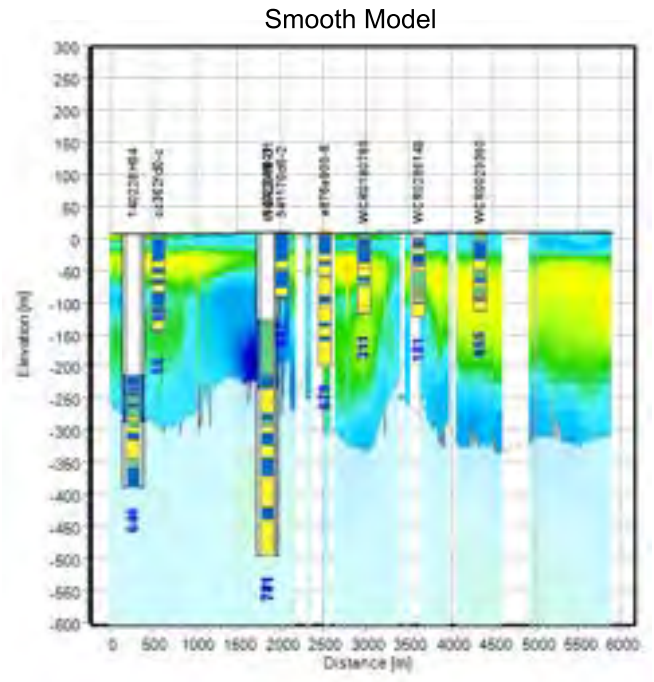


**Legend for Maps**

- Groundwater Basin Boundary (DWR - B118)
- Vineyards
- Phase 1 Aquitard Extent
- 180-Foot Aquifer CI- Contour
- Section (Current page)
- Section (Other pages)

**AEM data used for inversion**

- Lithology logs
- Resistivity logs
- Electric transmission lines (CA State Geoportals, 2020)
- Pipelines (AmeriGEOSS, 2022)



**Legend for Model Sections**

**Resistivity: AEM inversion results**

3      10      100      300  
Resistivity [ohm-m]

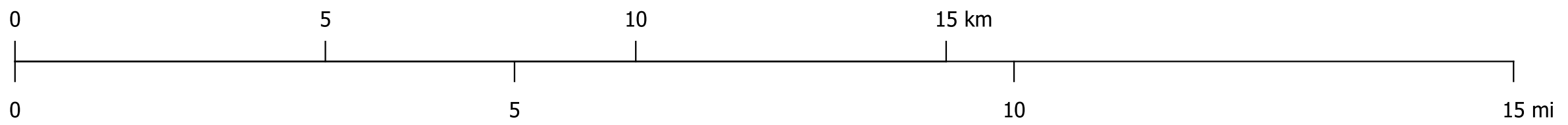
Above DOI\*  
Below DOI\*

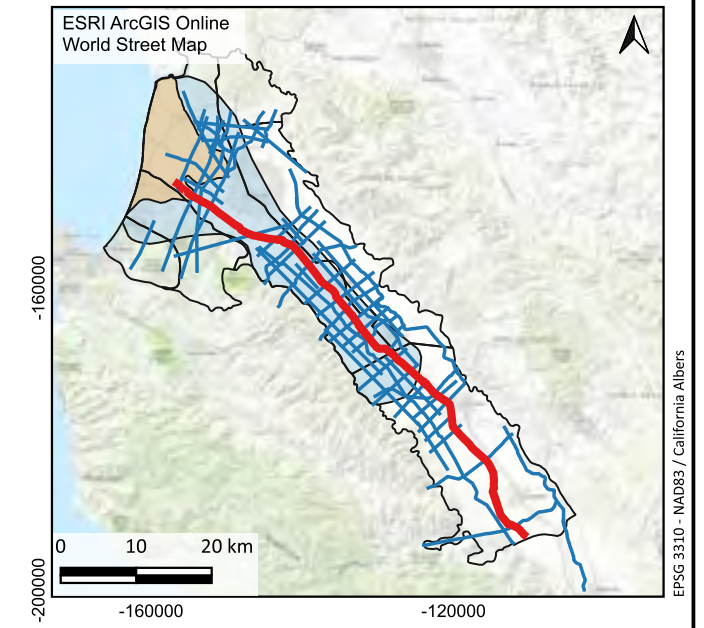
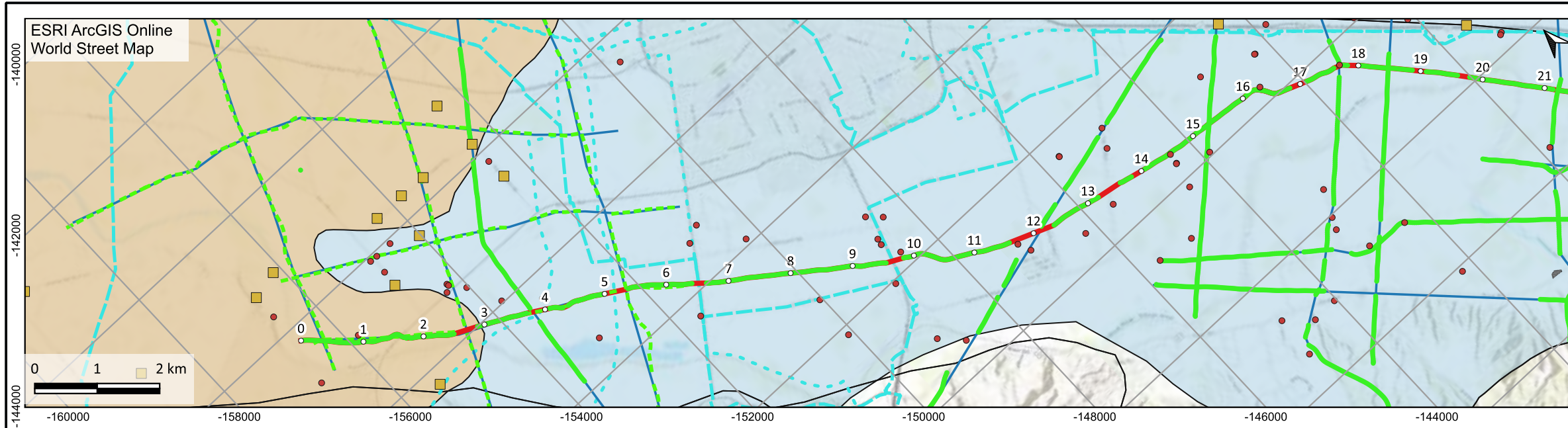
\*DOI = Depth of investigation

Lithology log	Resistivity log	Well completion report analysis
Sand		
Silt Clay		
Clay		
Clay shale		
Silt		
Lithology		

**Continuous conductor**

- Top of conductor
- Bottom of conductor
- Top of conductor (lower confidence)
- Bottom of conductor (lower confidence)





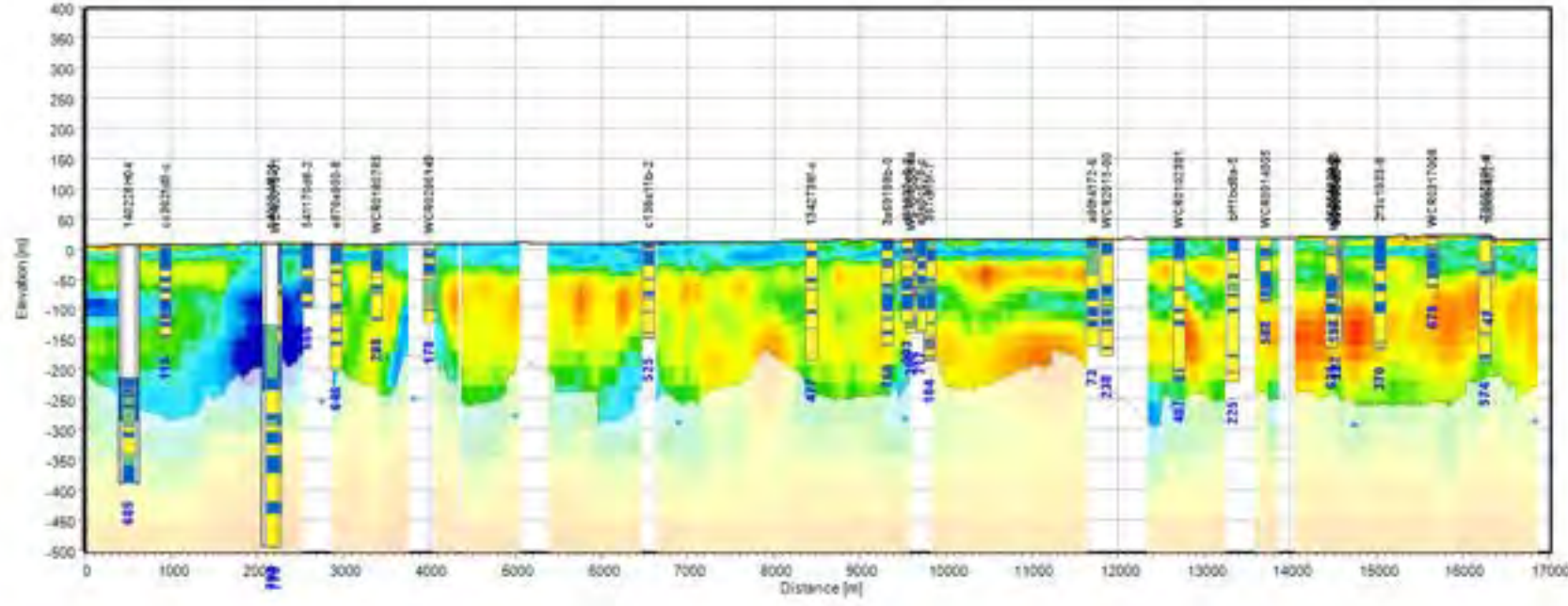
**Legend for Maps**

- Groundwater Basin Boundary (DWR - B118)
- Vineyards
- Phase 1 Aquitard Extent
- 180-Foot Aquifer CI- Contour
- Section (Current page)
- Section (Other pages)

**AEM data used for inversion**

- Lithology logs
- Resistivity logs
- Electric transmission lines (CA State Geoportals, 2020)
- Pipelines (AmeriGEOSS, 2022)

Smooth Model



**Legend for Model Sections**

**Resistivity: AEM inversion results**

3 10 100 300  
Resistivity [ohm-m]

\*DOI = Depth of investigation

**Lithology log**

- Sand
- Silt Clay
- Clay
- Clay shale
- Siltstone
- Limestone

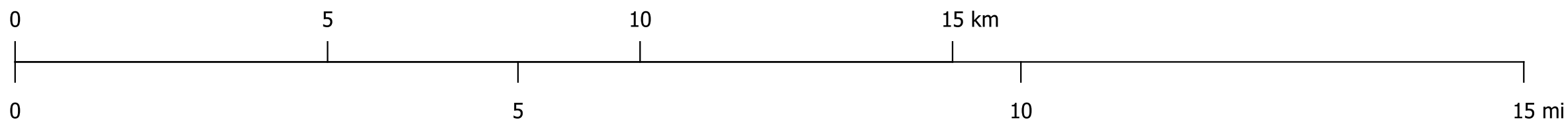
**Resistivity log**

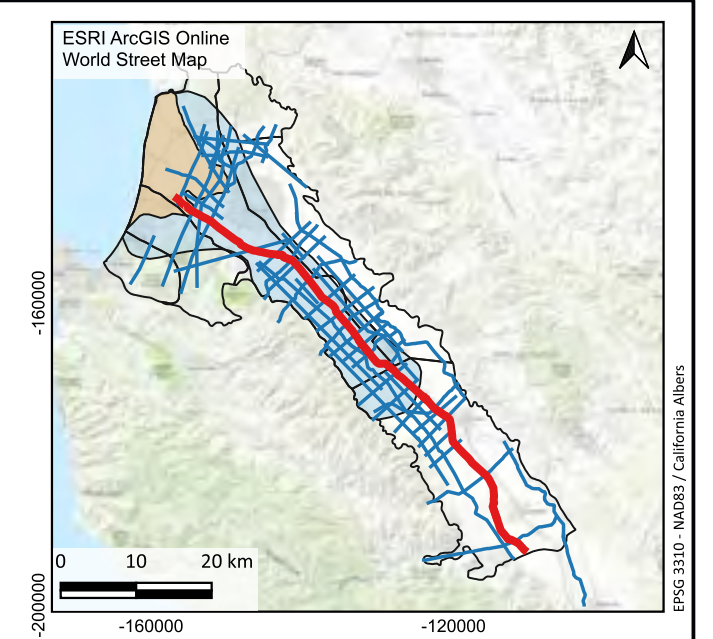
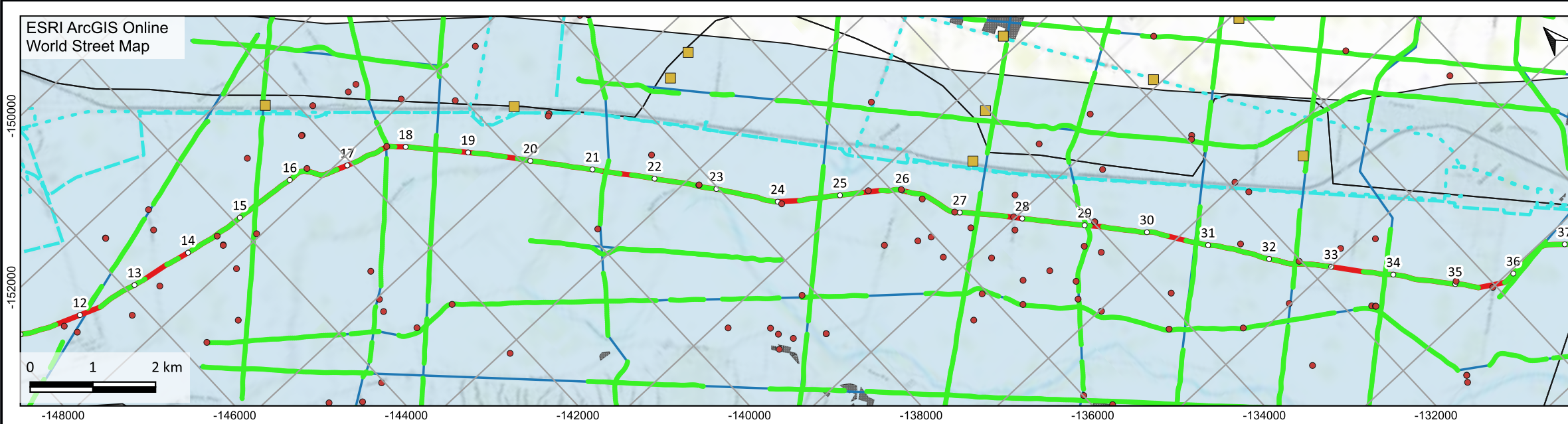
Log Resistivity High

**Well completion report analysis**

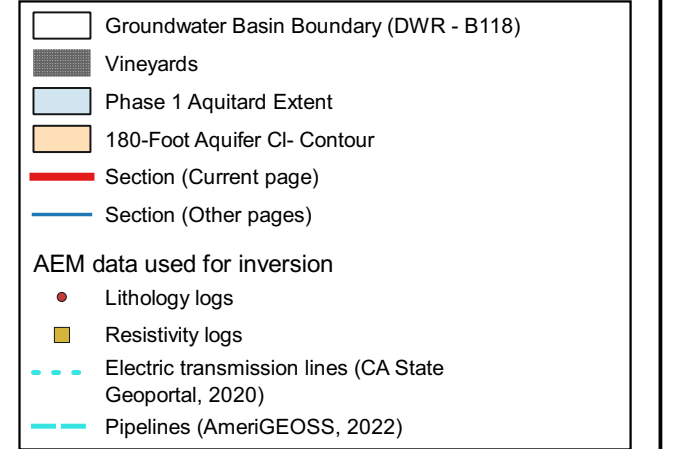
**Continuous conductor**

- Top of conductor
- Bottom of conductor
- Top of conductor (lower confidence)
- Bottom of conductor (lower confidence)

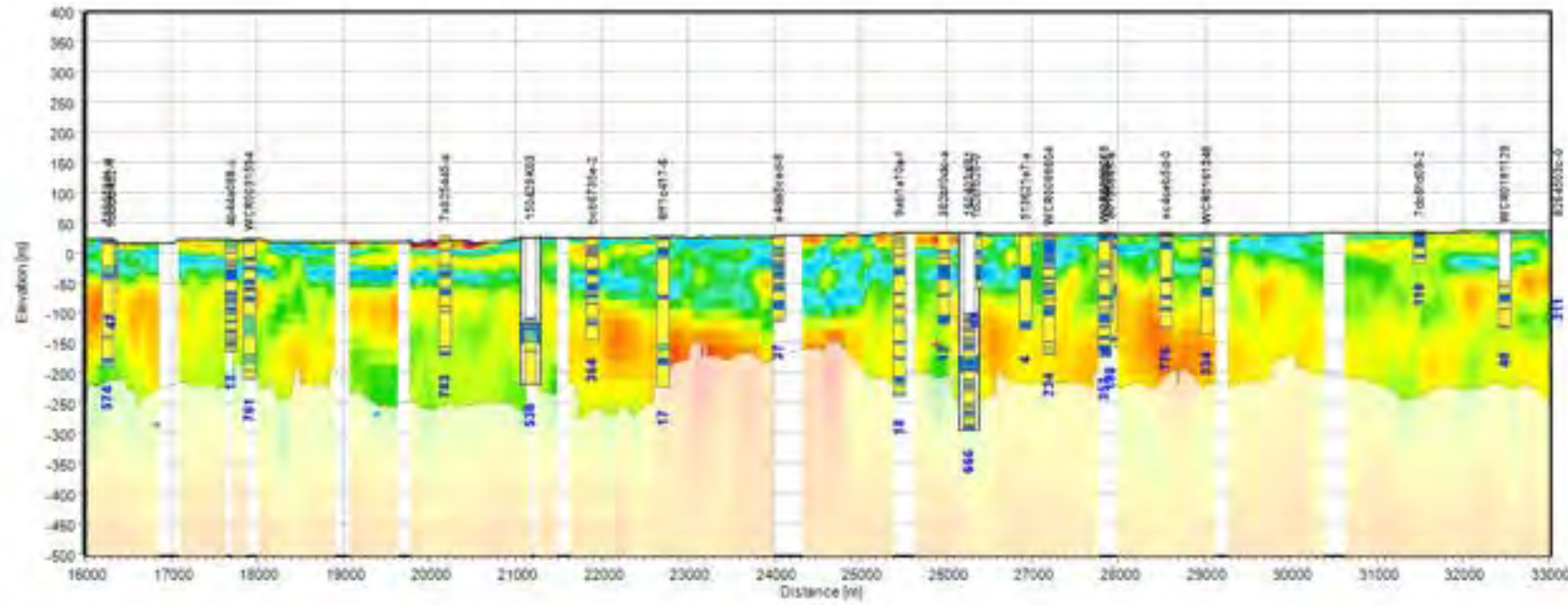




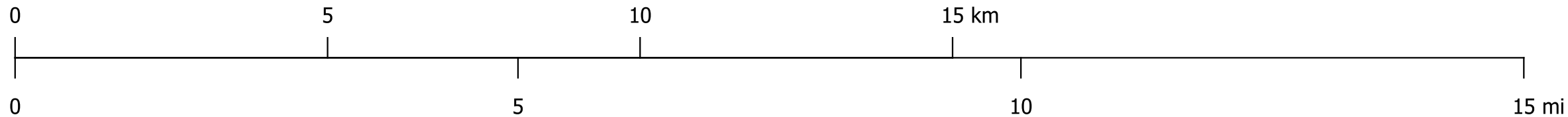
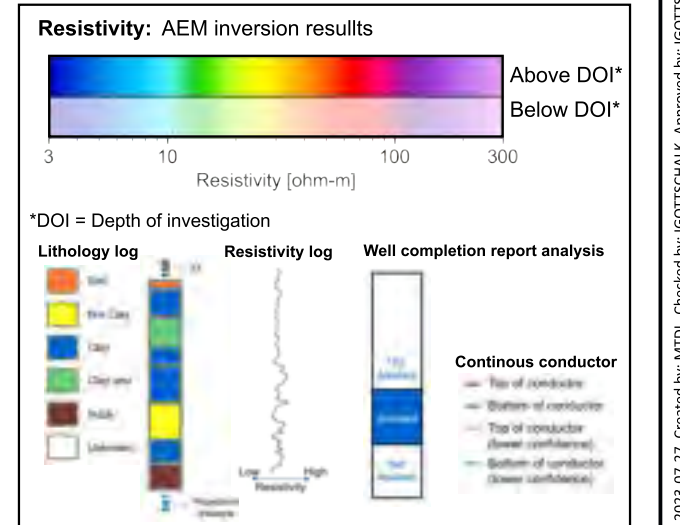
Legend for Maps

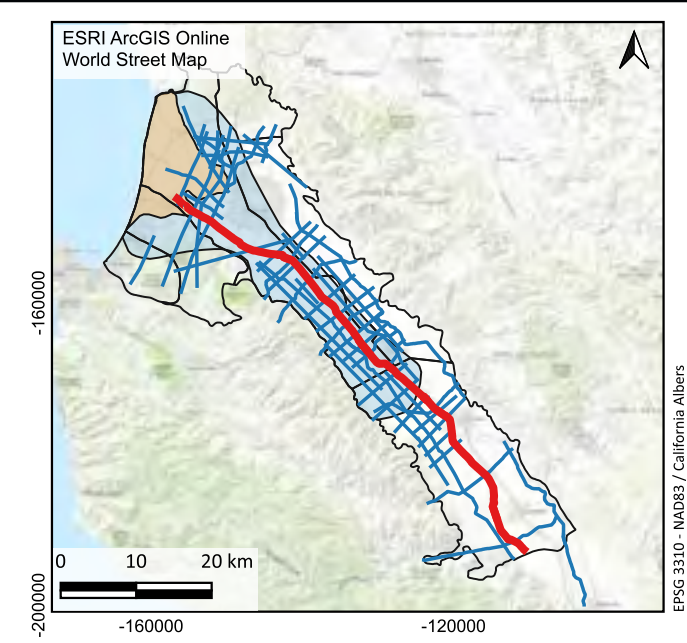
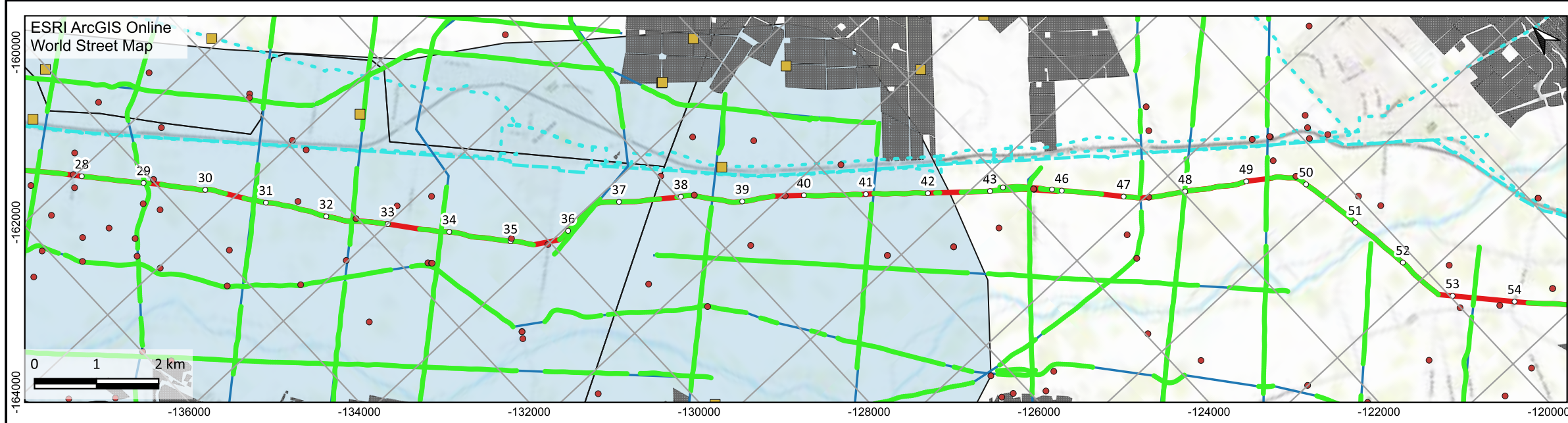


Smooth Model



Legend for Model Sections





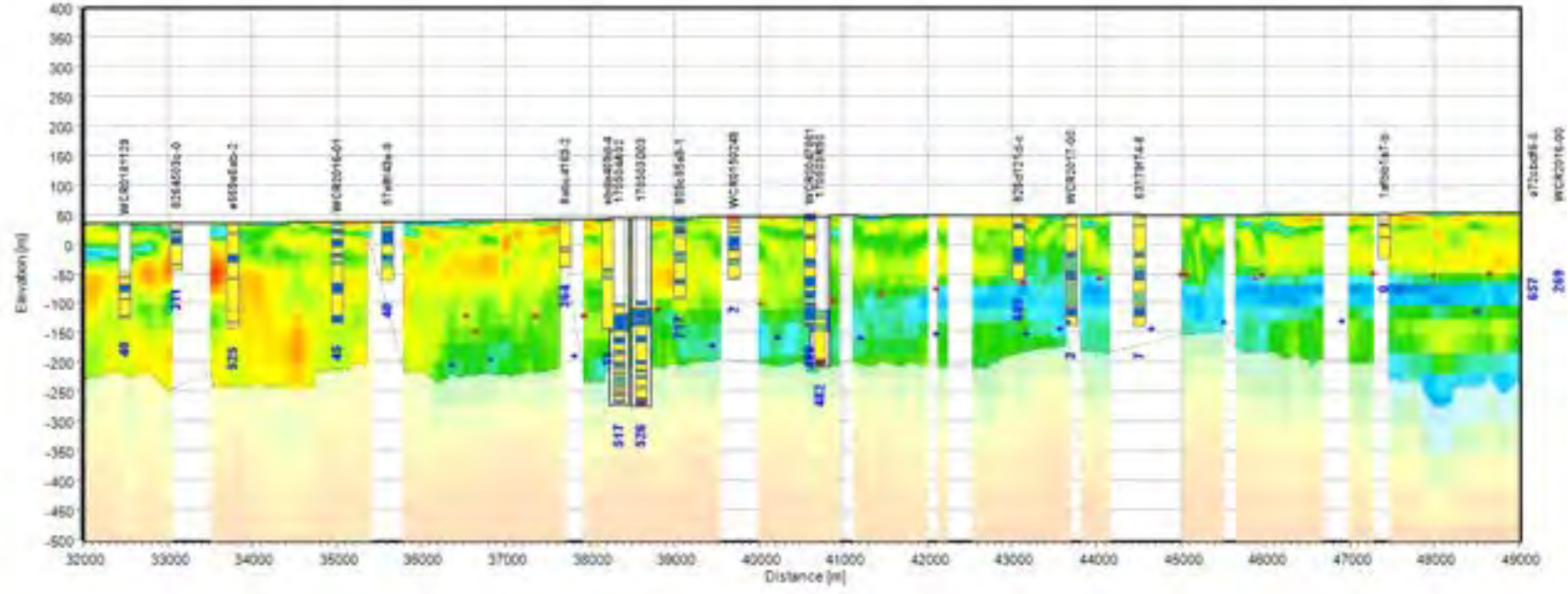
**Legend for Maps**

- Groundwater Basin Boundary (DWR - B118)
- Vineyards
- Phase 1 Aquitard Extent
- 180-Foot Aquifer CI- Contour
- Section (Current page)
- Section (Other pages)

**AEM data used for inversion**

- Lithology logs
- Resistivity logs
- Electric transmission lines (CA State Geoportals, 2020)
- Pipelines (AmeriGEOSS, 2022)

Smooth Model



**Legend for Model Sections**

**Resistivity: AEM inversion results**

3 10 100 300  
Resistivity [ohm-m]

\*DOI = Depth of investigation

**Lithology log**

- Sand
- Silt/Clay
- Clay
- Claystone
- Siltstone
- Lithology

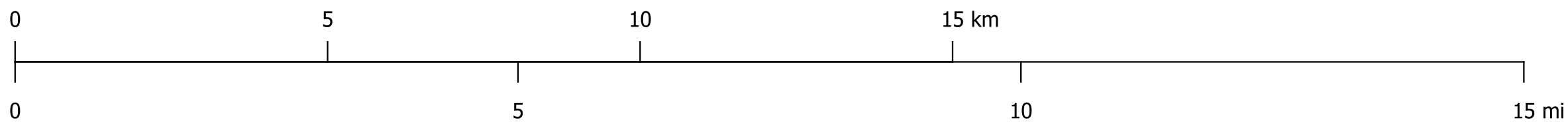
**Resistivity log**

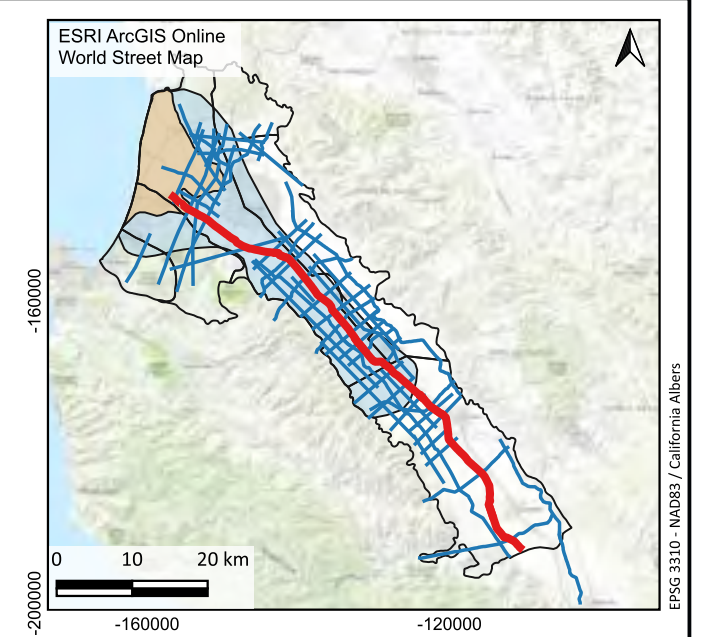
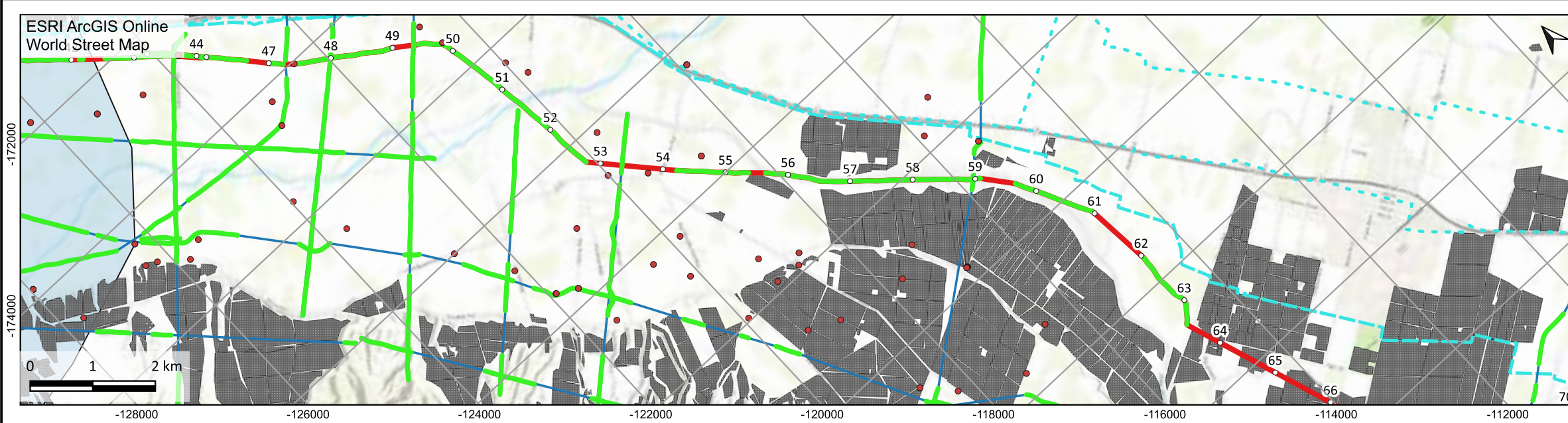
Log Resistivity

**Well completion report analysis**

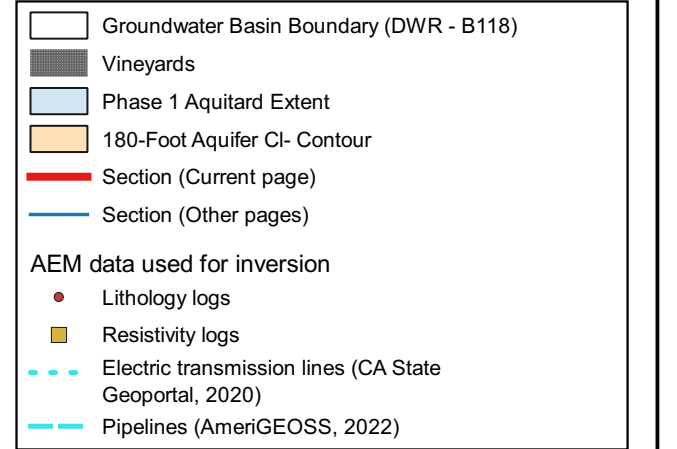
**Continuous conductor**

- Top of conductor
- Bottom of conductor
- Top of conductor (lower confidence)
- Bottom of conductor (lower confidence)

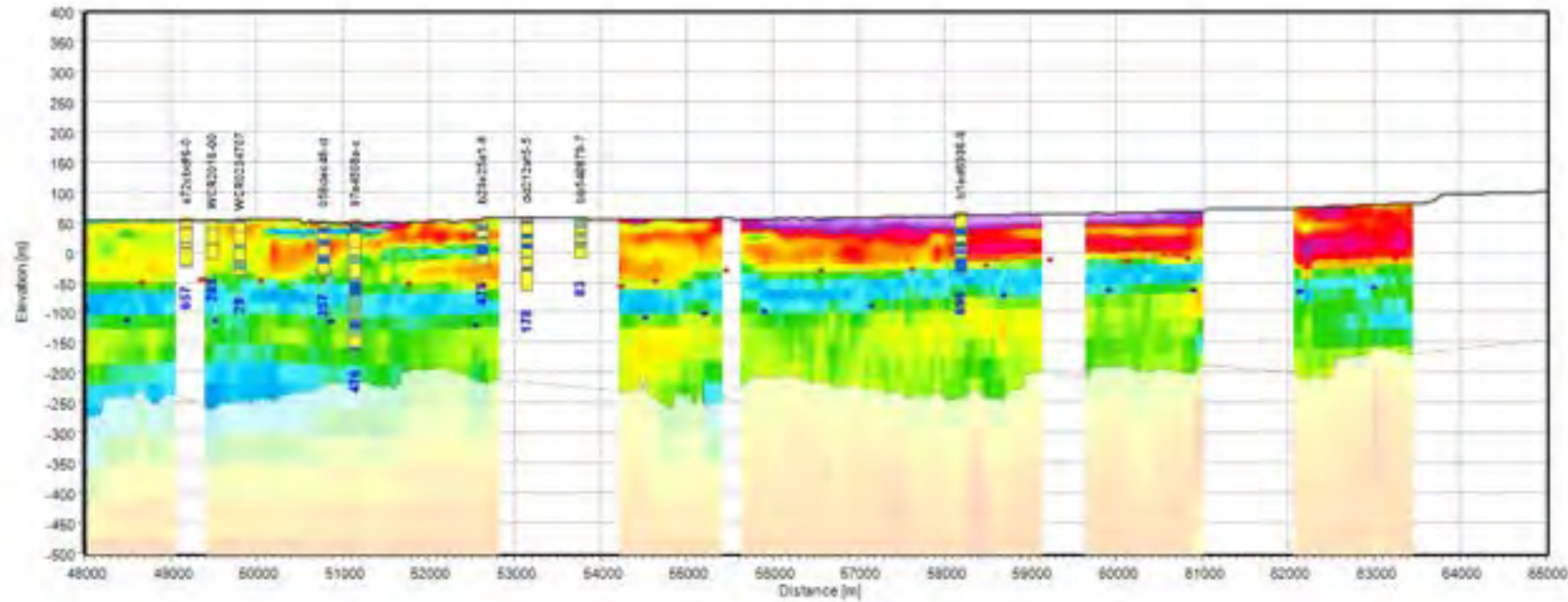




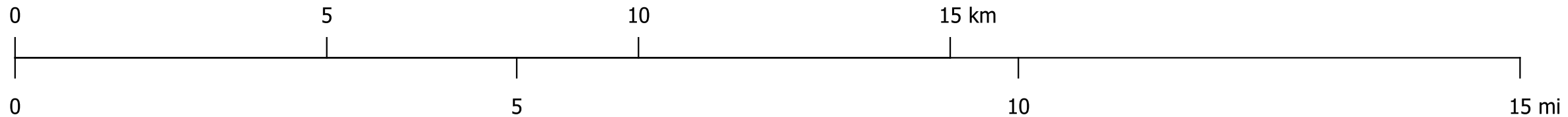
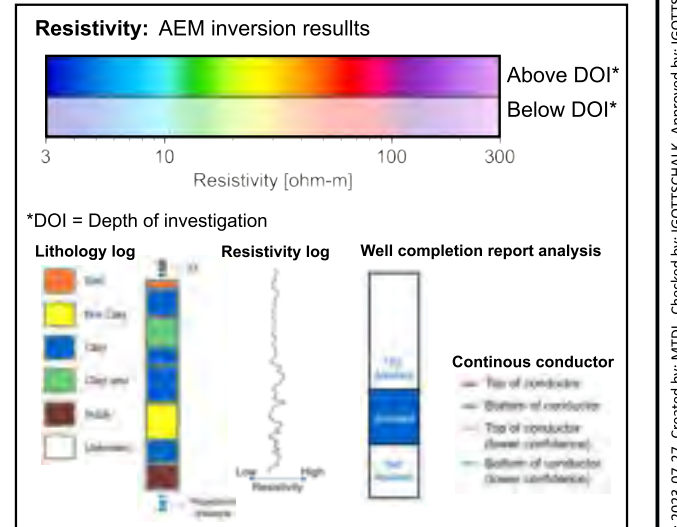
Legend for Maps

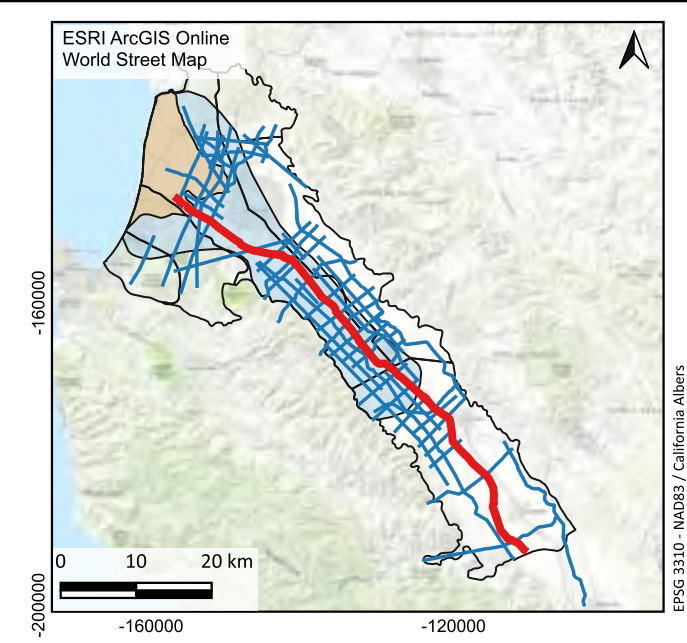
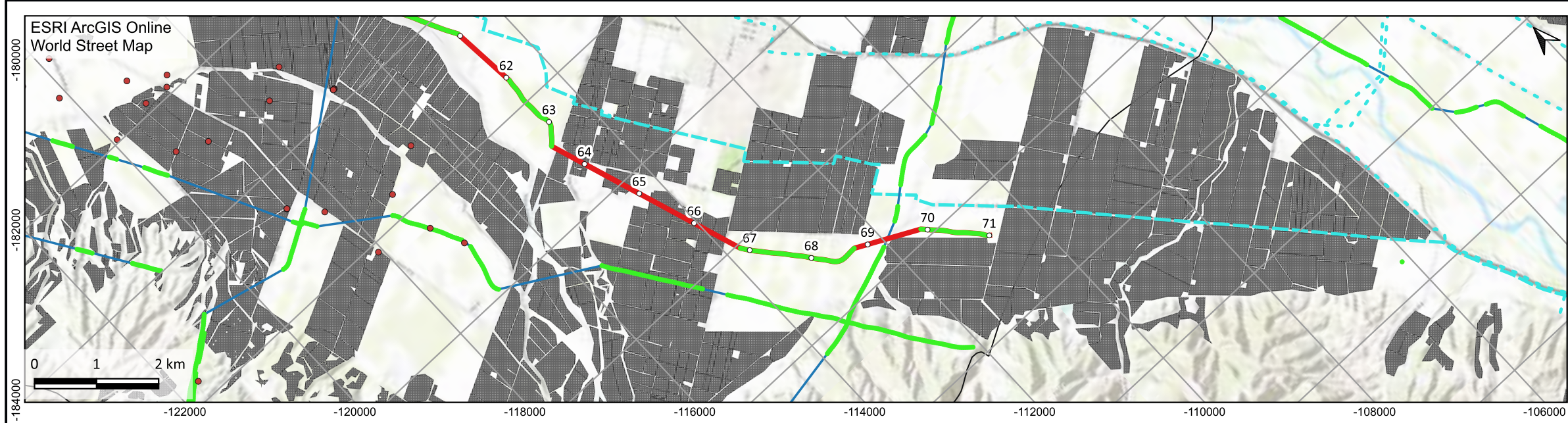


Smooth Model



Legend for Model Sections



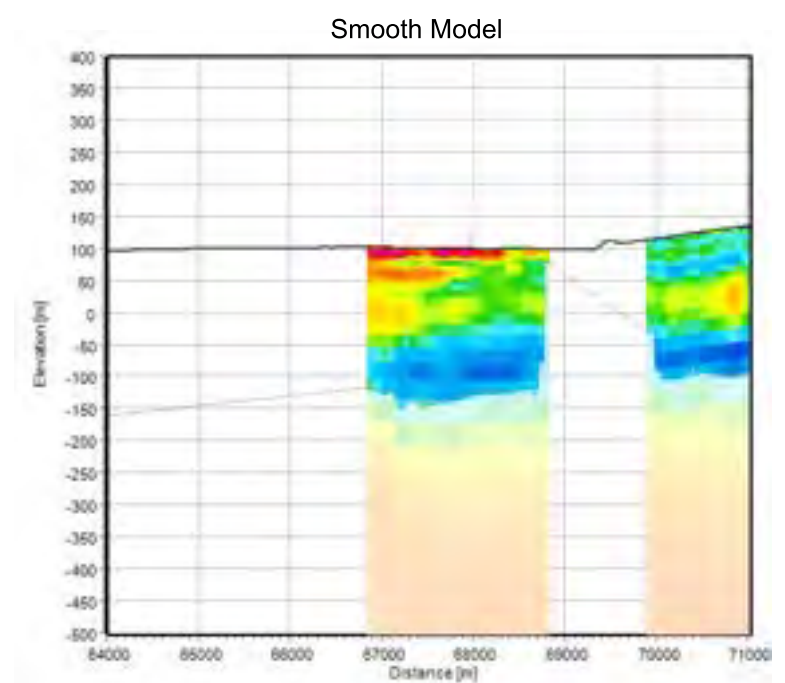


**Legend for Maps**

- Groundwater Basin Boundary (DWR - B118)
- Vineyards
- Phase 1 Aquitard Extent
- 180-Foot Aquifer CI- Contour
- Section (Current page)
- Section (Other pages)

**AEM data used for inversion**

- Lithology logs
- Resistivity logs
- Electric transmission lines (CA State Geoportal, 2020)
- Pipelines (AmeriGEOSS, 2022)



**Legend for Model Sections**

**Resistivity: AEM inversion results**

Above DOI\*  
Below DOI\*

Resistivity [ohm-m]

\*DOI = Depth of investigation

**Lithology log**

- Sand
- Thin Clay
- Clay
- Claystone
- Siltstone
- Lithology

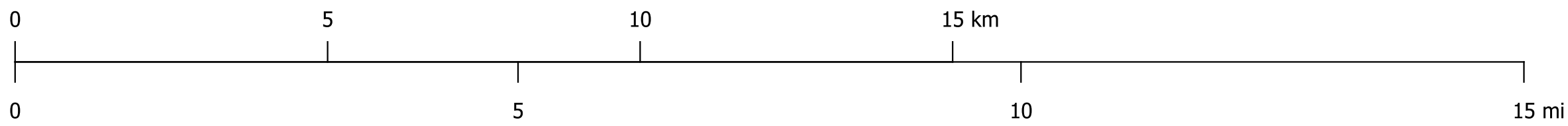
**Resistivity log**

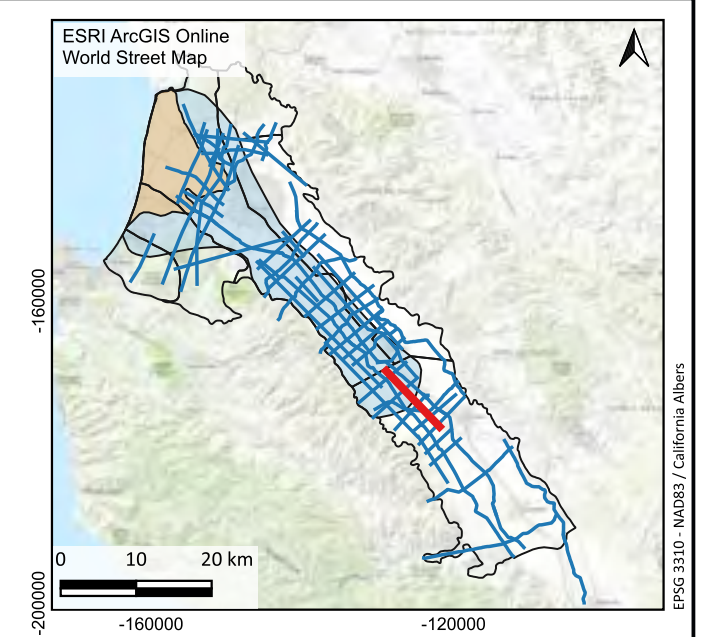
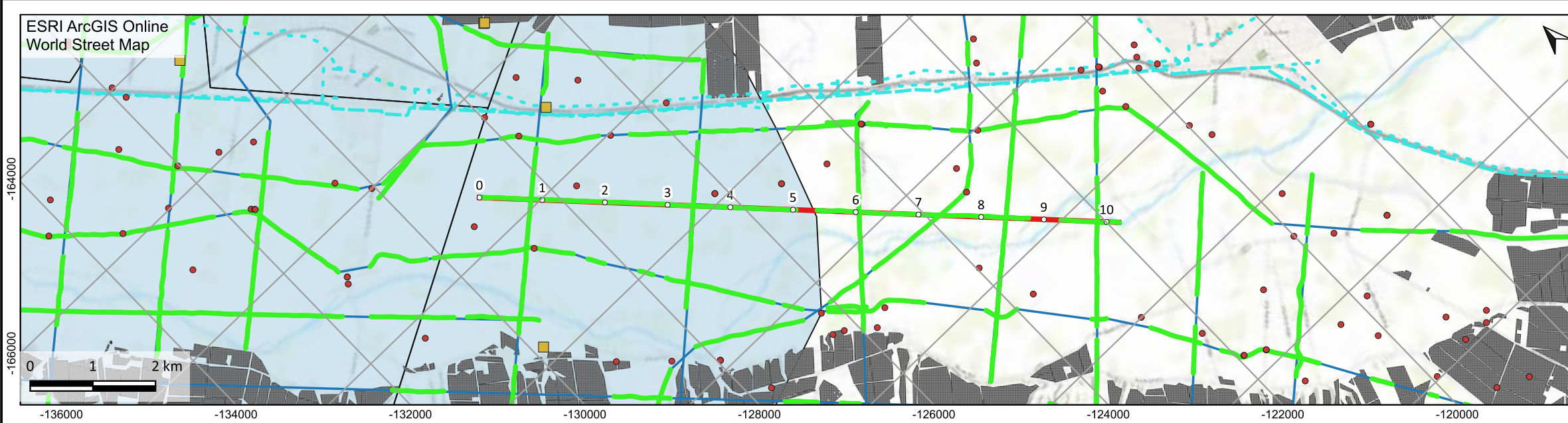
Log Resistivity

**Well completion report analysis**

**Continuous conductor**

- Top of conductor
- Bottom of conductor
- Top of conductor (lower confidence)
- Bottom of conductor (lower confidence)





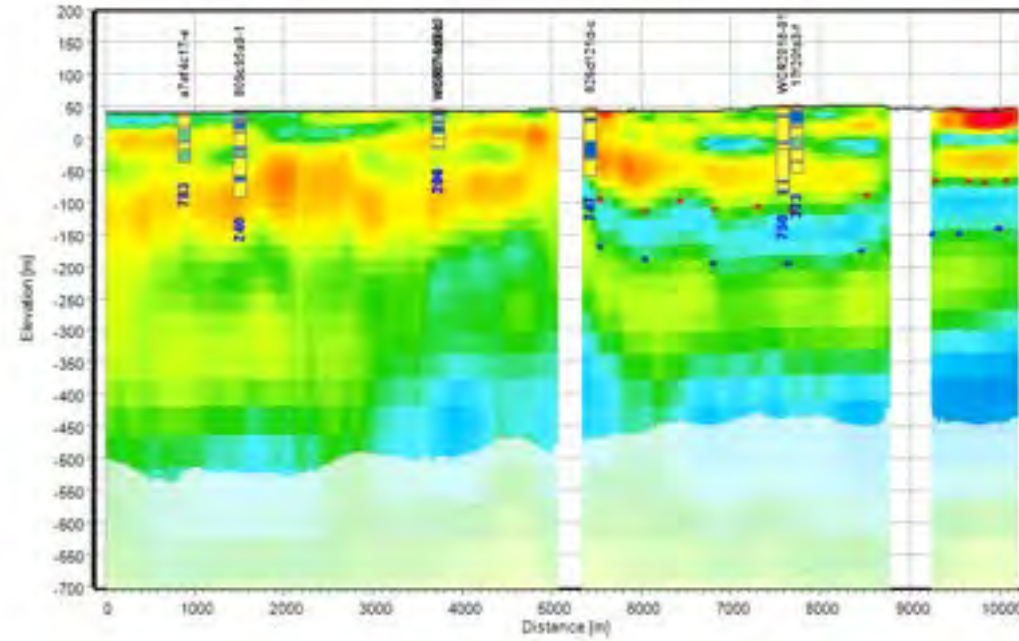
**Legend for Maps**

- Groundwater Basin Boundary (DWR - B118)
- Vineyards
- Phase 1 Aquitard Extent
- 180-Foot Aquifer CI- Contour
- Section (Current page)
- Section (Other pages)

**AEM data used for inversion**

- Lithology logs
- Resistivity logs
- Electric transmission lines (CA State Geportal, 2020)
- Pipelines (AmeriGEOSS, 2022)

Smooth Model



**Legend for Model Sections**

**Resistivity: AEM inversion results**

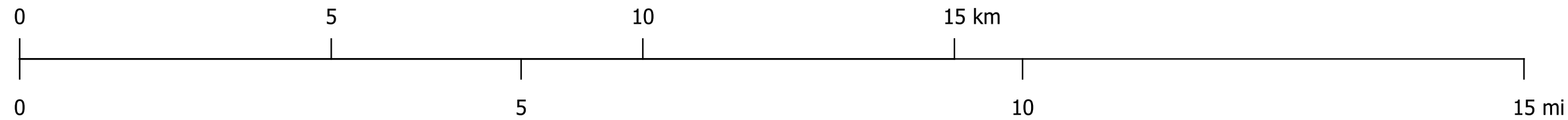
3 10 100 300  
Resistivity [ohm-m]

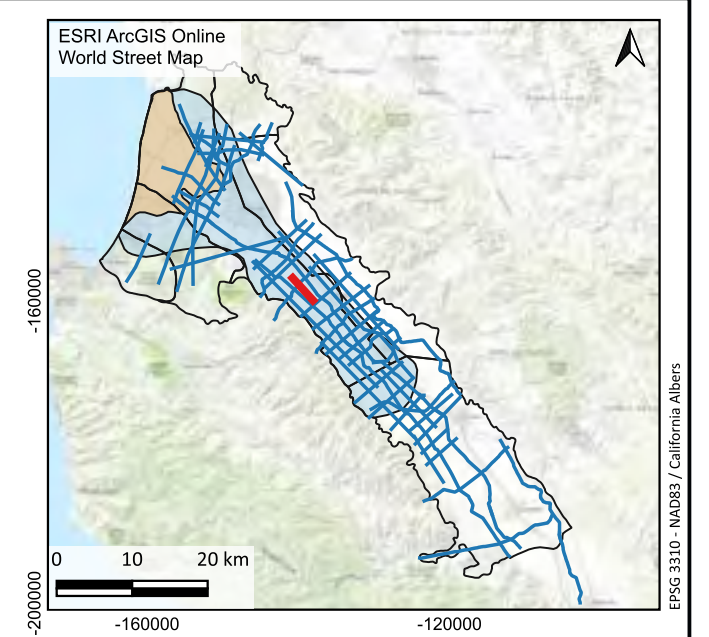
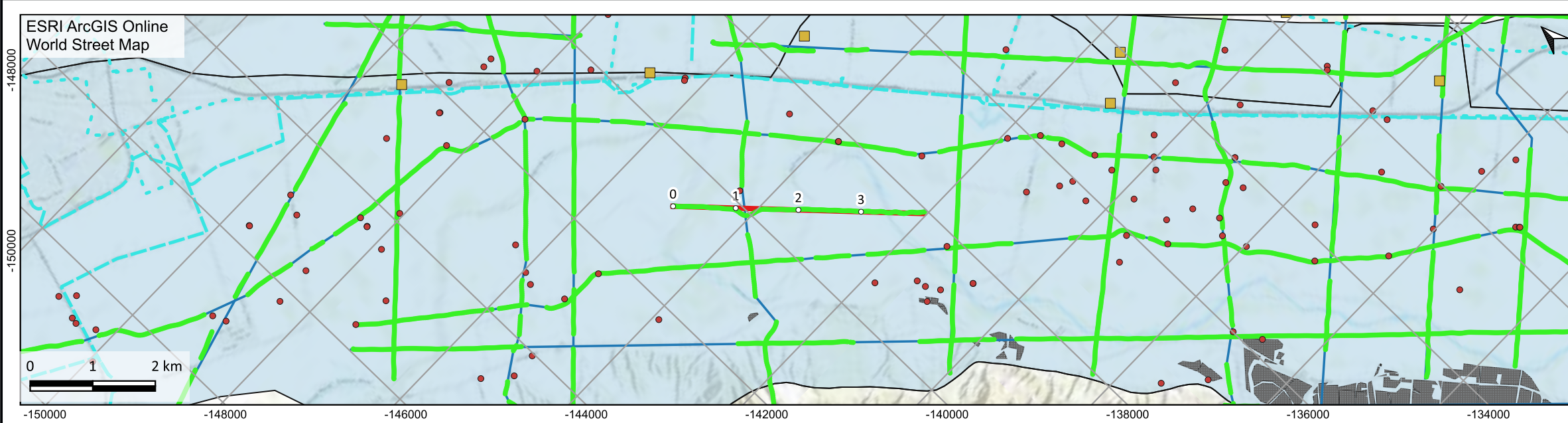
\*DOI = Depth of investigation

Lithology log	Resistivity log	Well completion report analysis
<ul style="list-style-type: none"> <li>Soil</li> <li>Site Clay</li> <li>Clay</li> <li>Clay shale</li> <li>Sand</li> <li>Siltstone</li> </ul>		

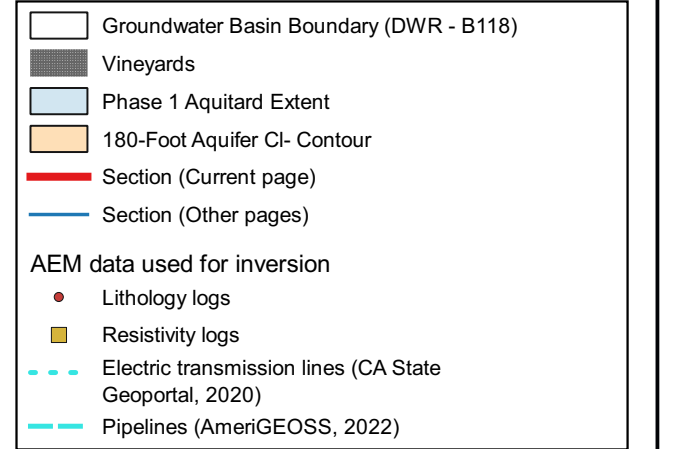
**Continuous conductor**

- Top of conductor
- Bottom of conductor
- Top of conductor (lower confidence)
- Bottom of conductor (lower confidence)

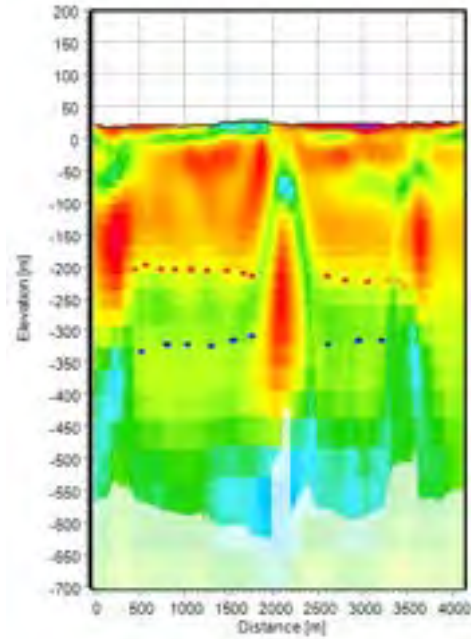




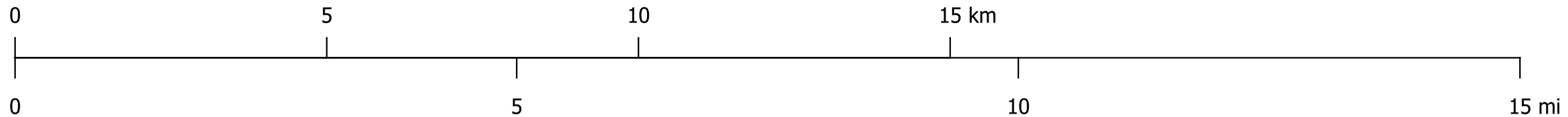
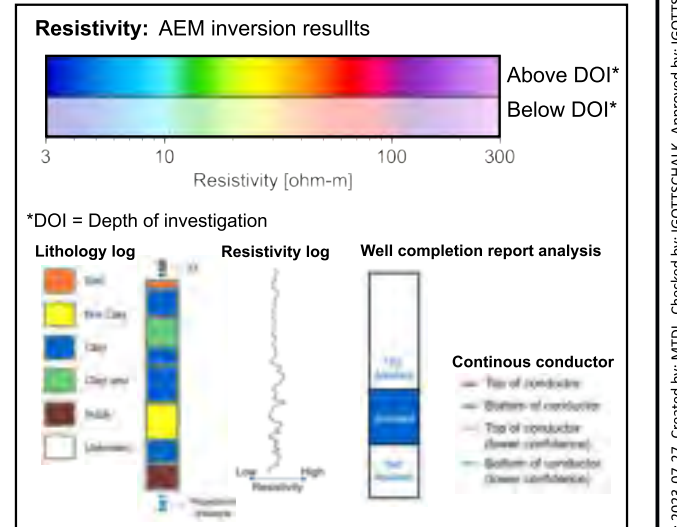
Legend for Maps

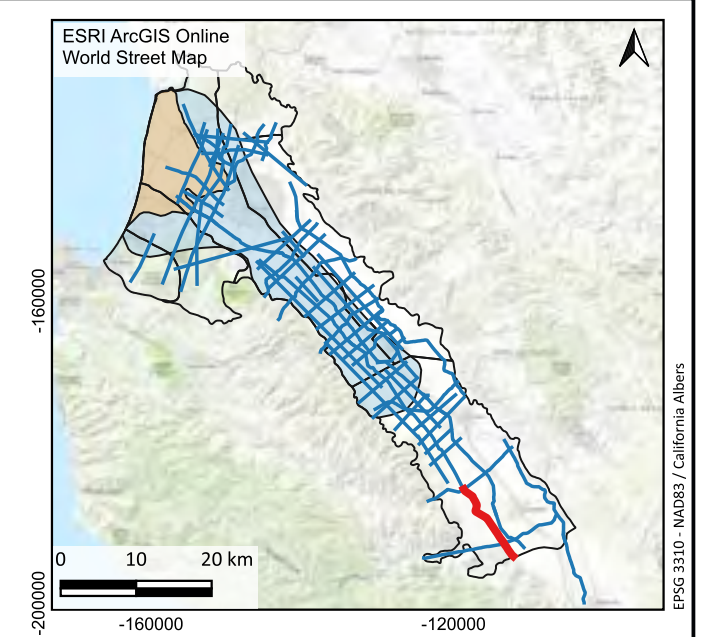


Smooth Model

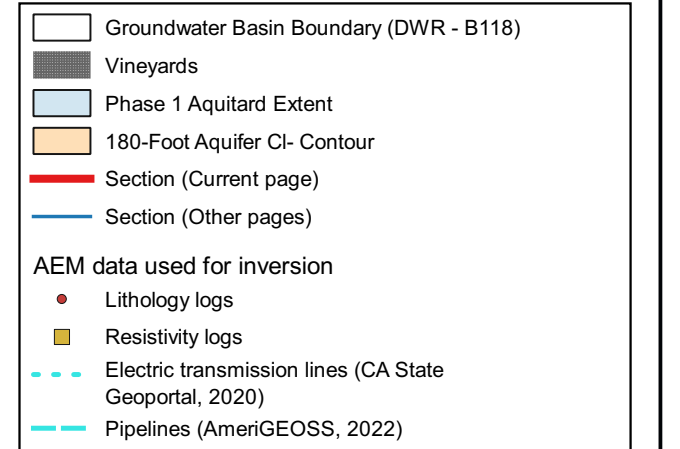


Legend for Model Sections

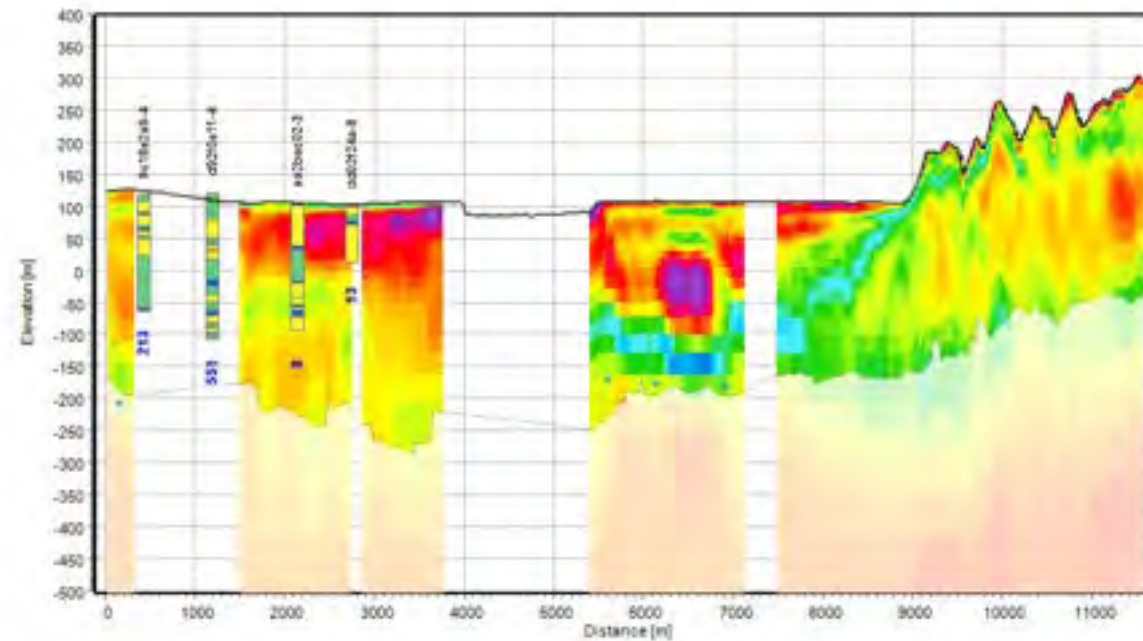




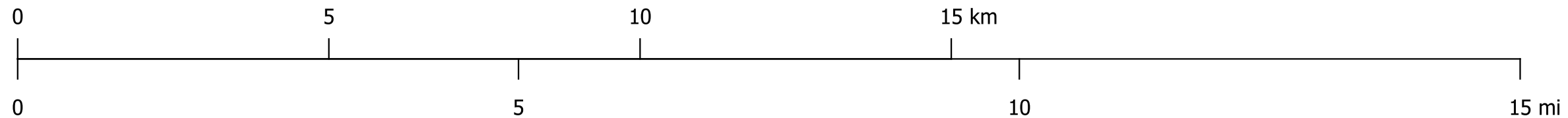
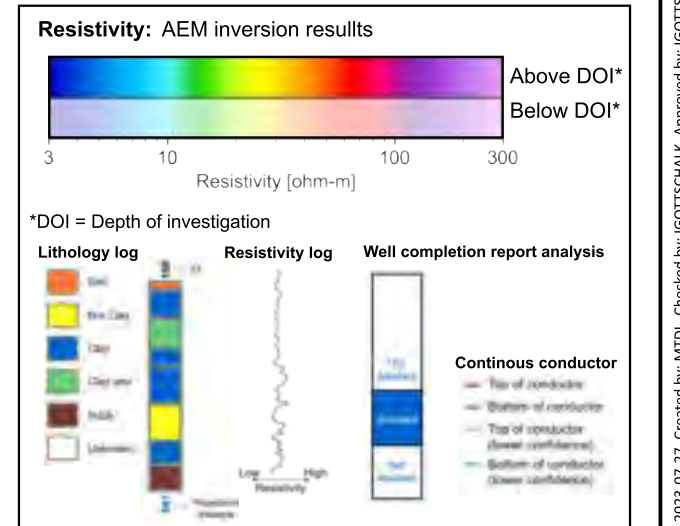
Legend for Maps

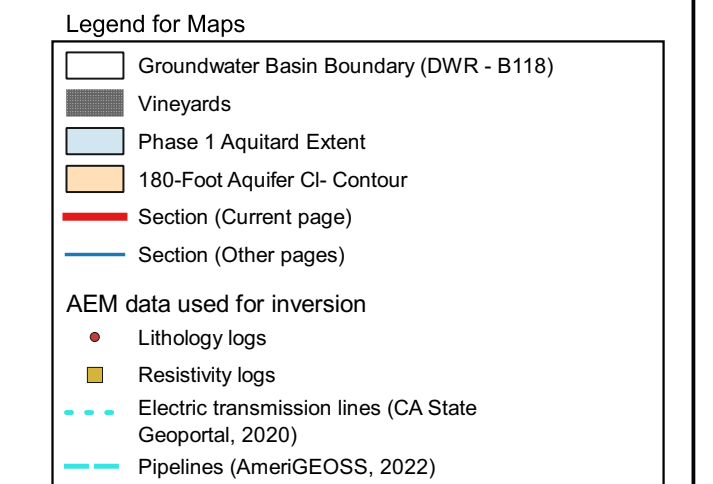
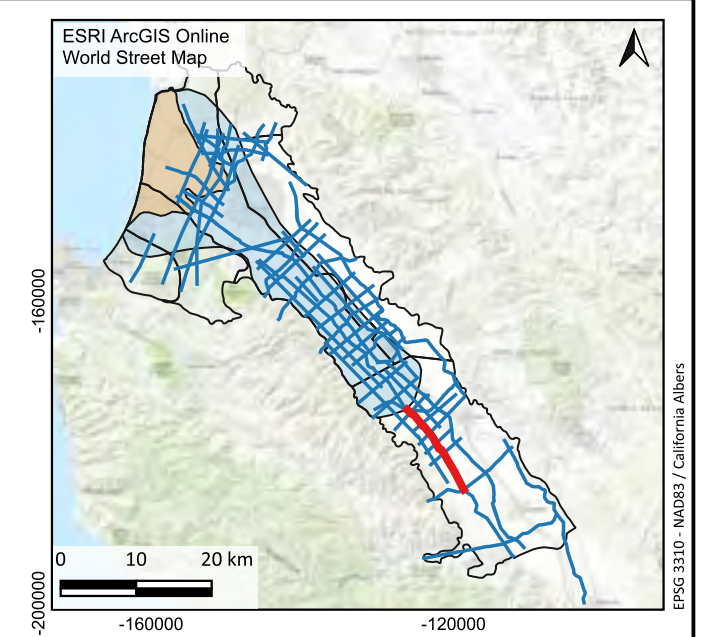
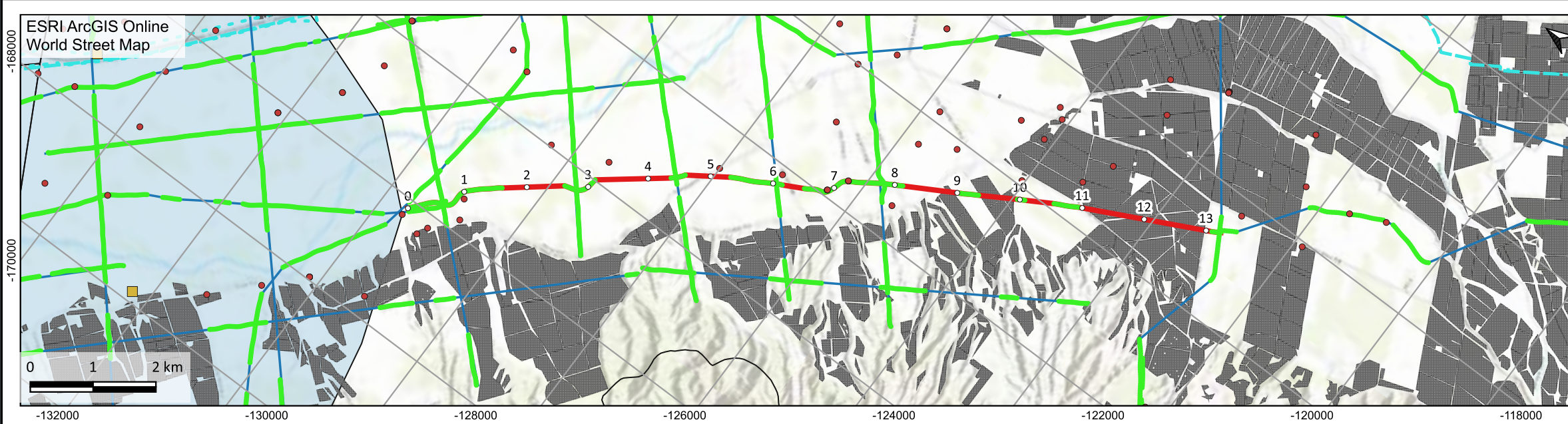


Smooth Model

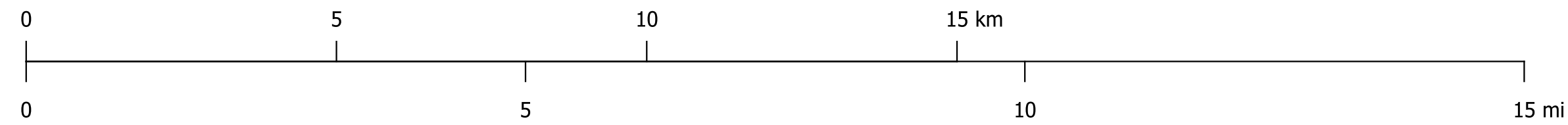
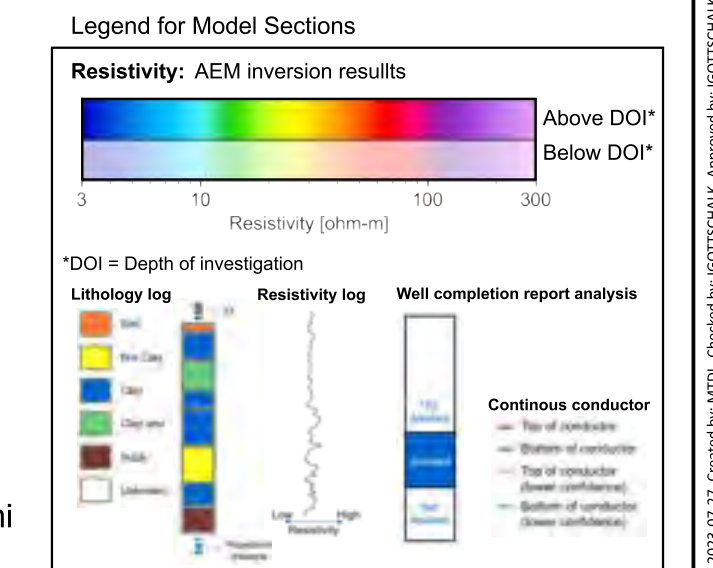
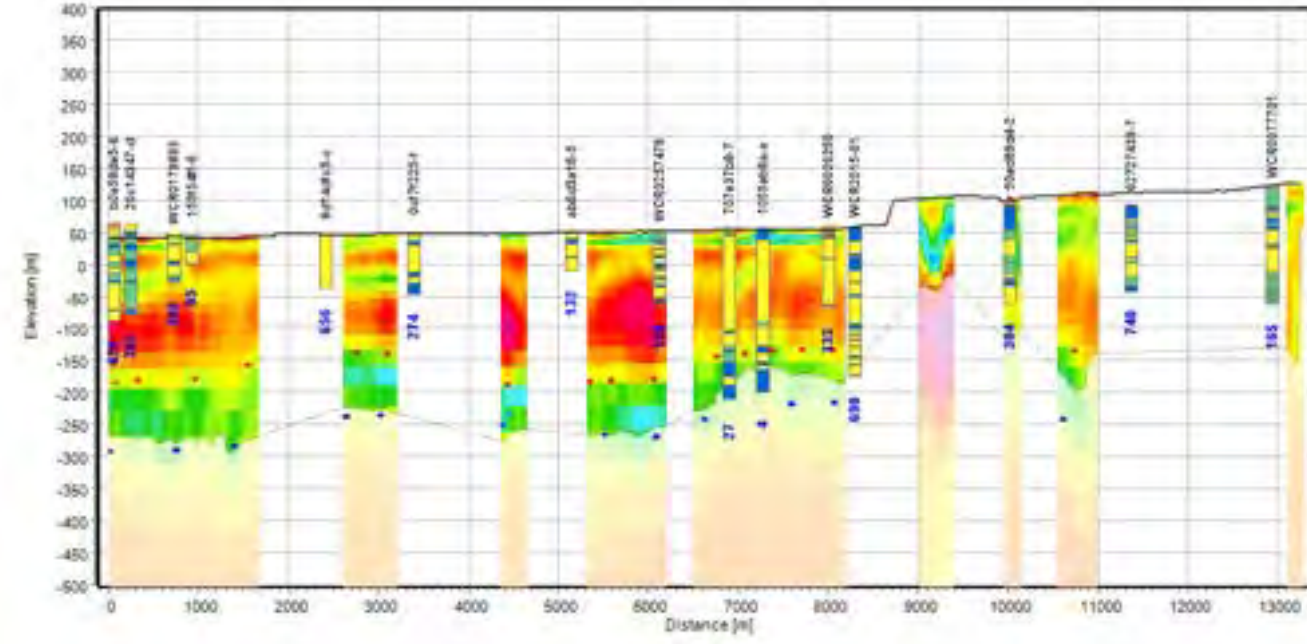


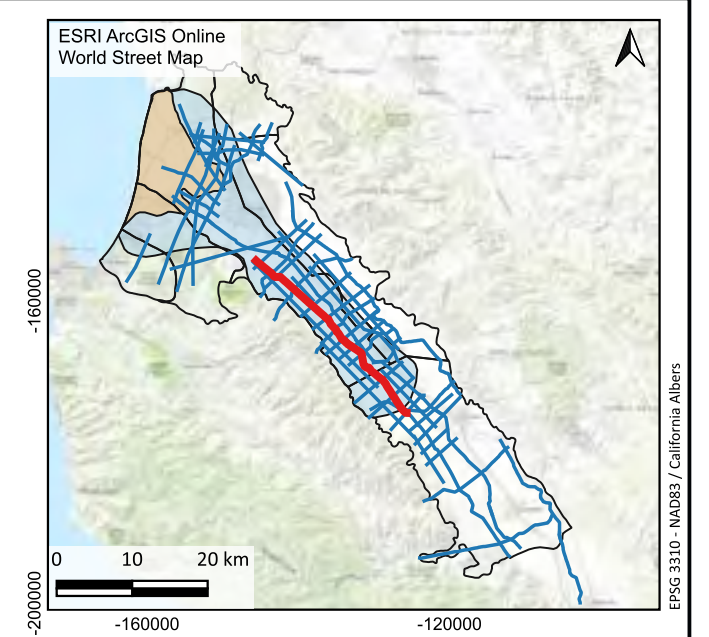
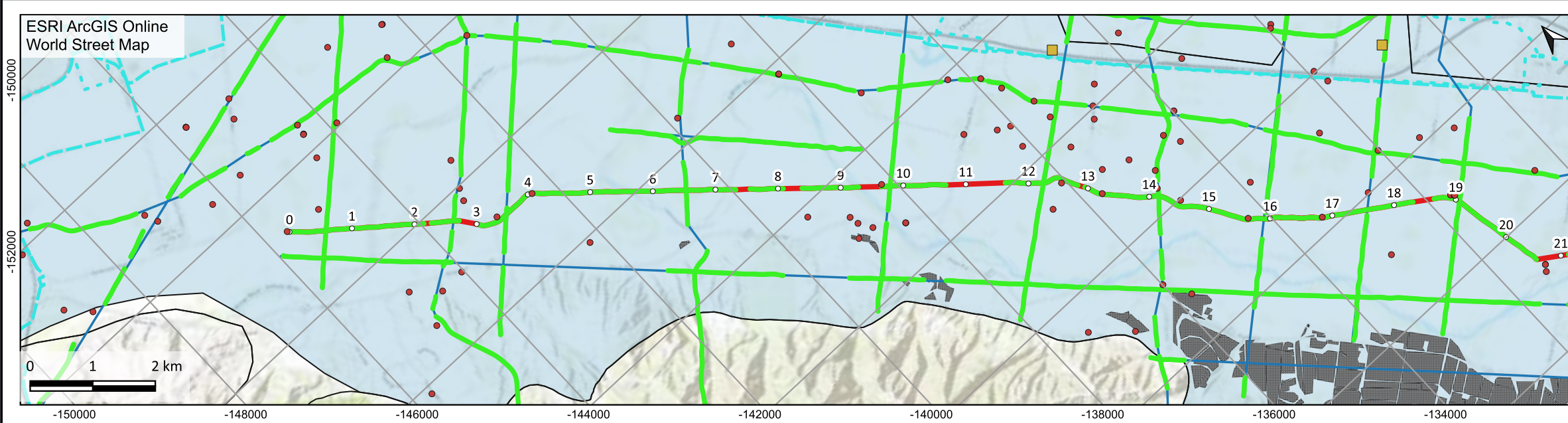
Legend for Model Sections



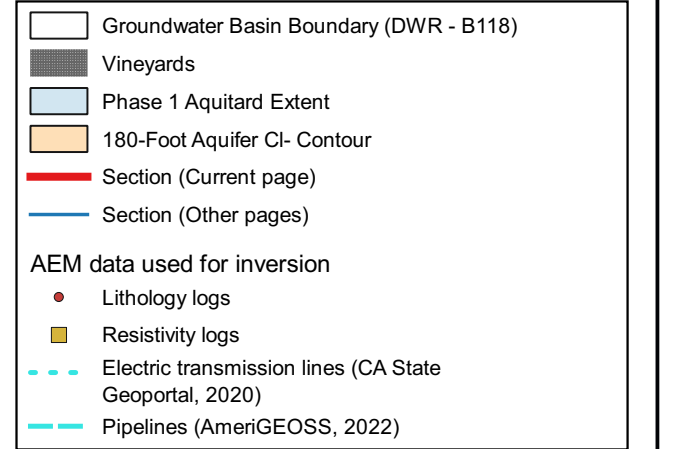


Smooth Model

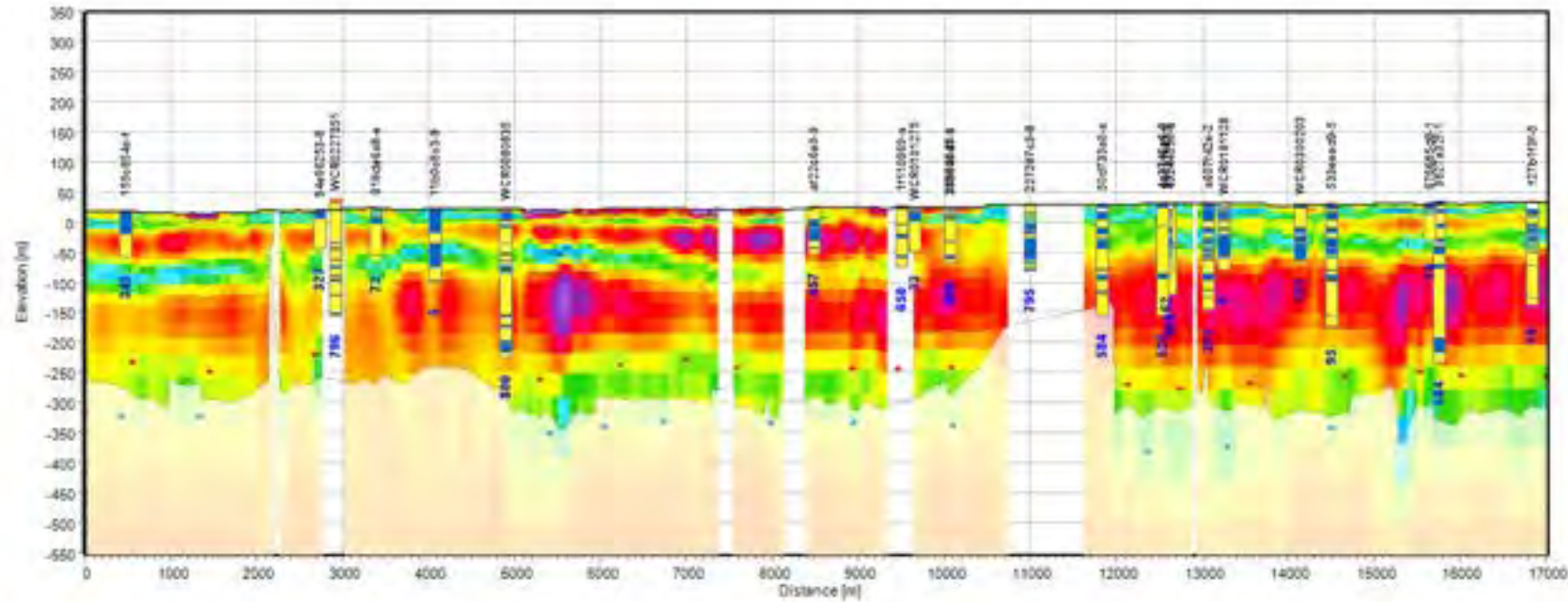




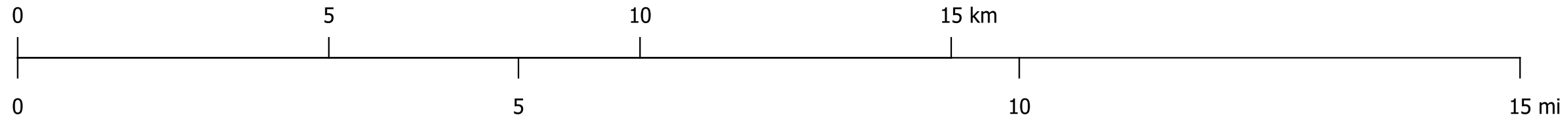
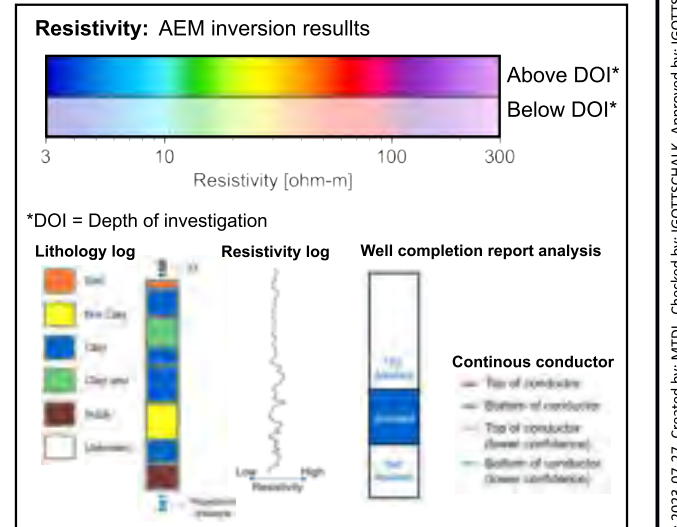
Legend for Maps

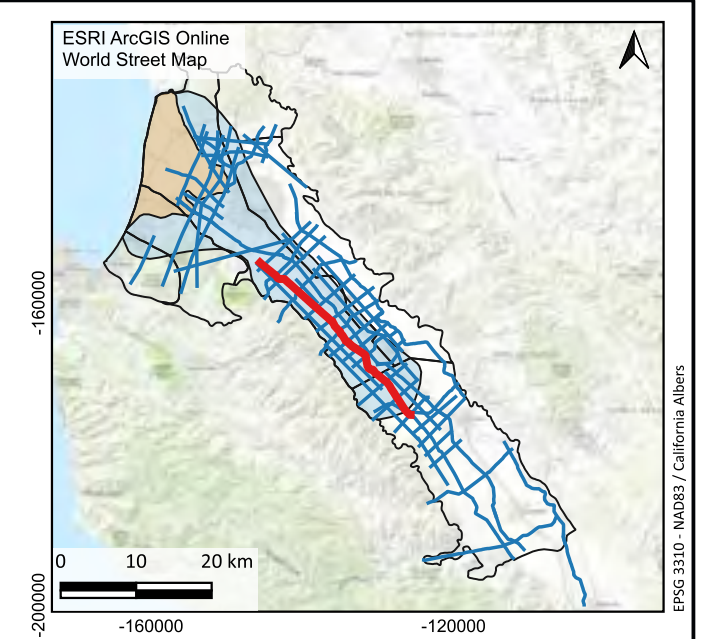
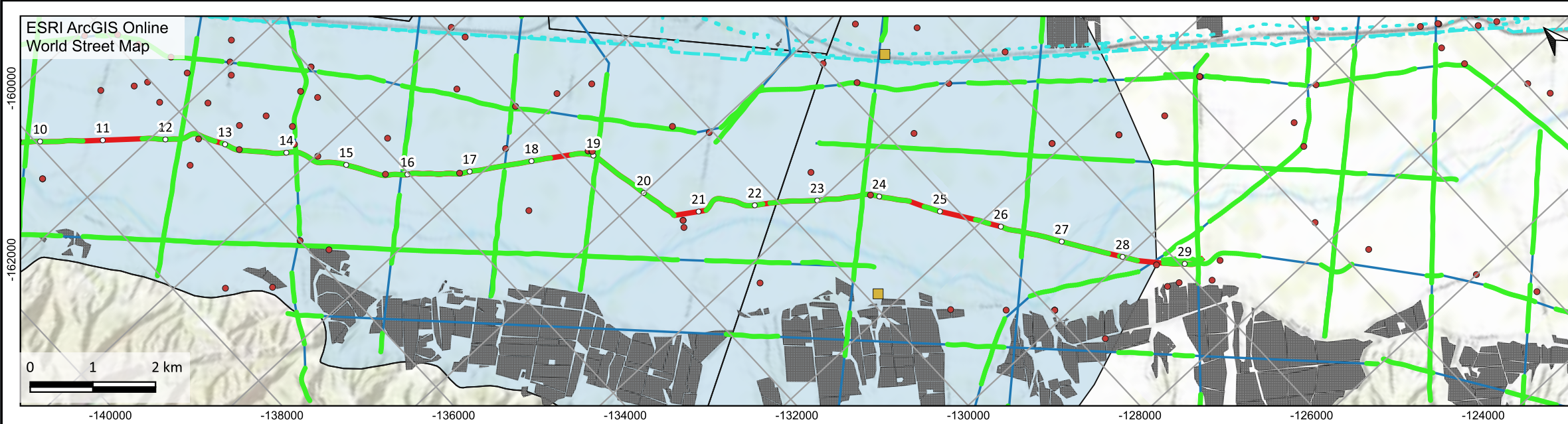


Smooth Model



Legend for Model Sections





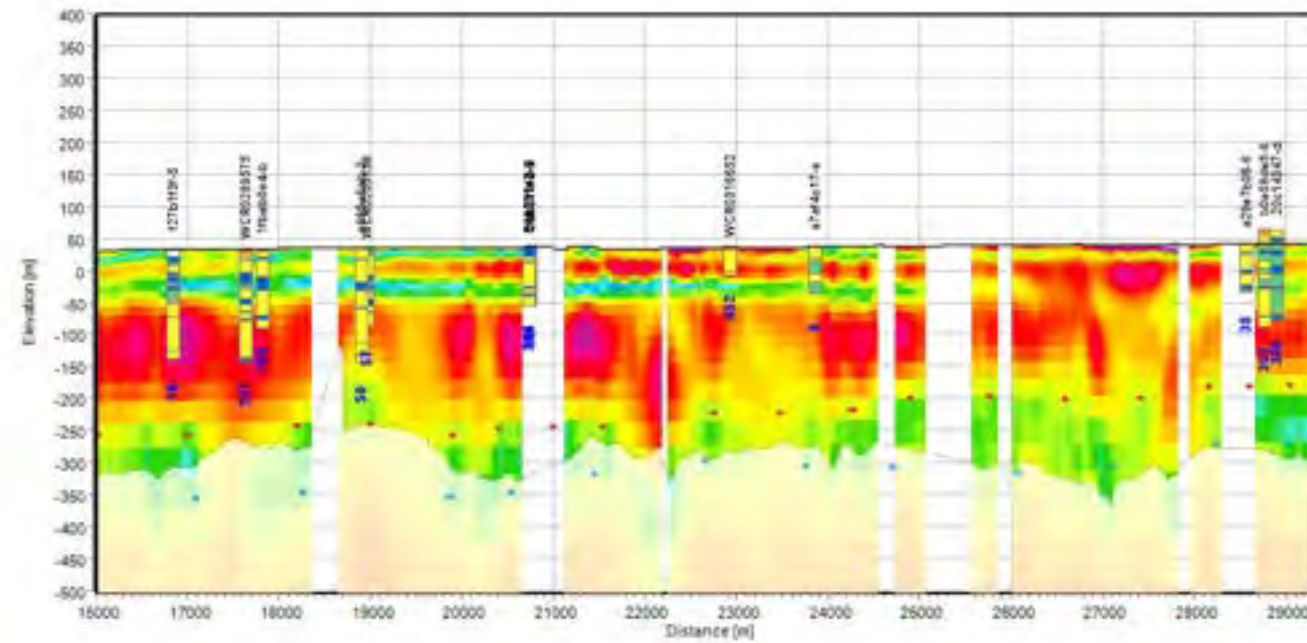
**Legend for Maps**

- Groundwater Basin Boundary (DWR - B118)
- Vineyards
- Phase 1 Aquitard Extent
- 180-Foot Aquifer CI- Contour
- Section (Current page)
- Section (Other pages)

**AEM data used for inversion**

- Lithology logs
- Resistivity logs
- Electric transmission lines (CA State Geoportals, 2020)
- Pipelines (AmeriGEOSS, 2022)

Smooth Model



**Legend for Model Sections**

**Resistivity: AEM inversion results**

Above DOI\*  
Below DOI\*

Resistivity [ohm-m]

\*DOI = Depth of investigation

**Lithology log**

- Sand
- Silt/Clay
- Clay
- Claystone
- Siltstone
- Limestone

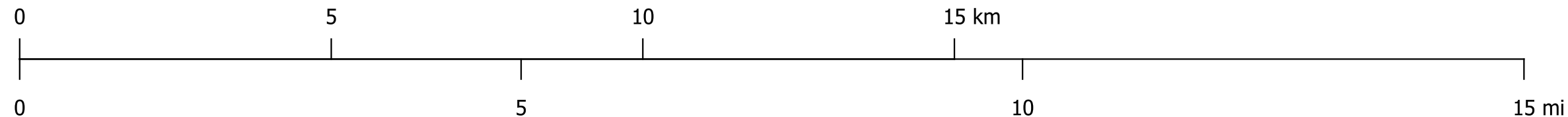
**Resistivity log**

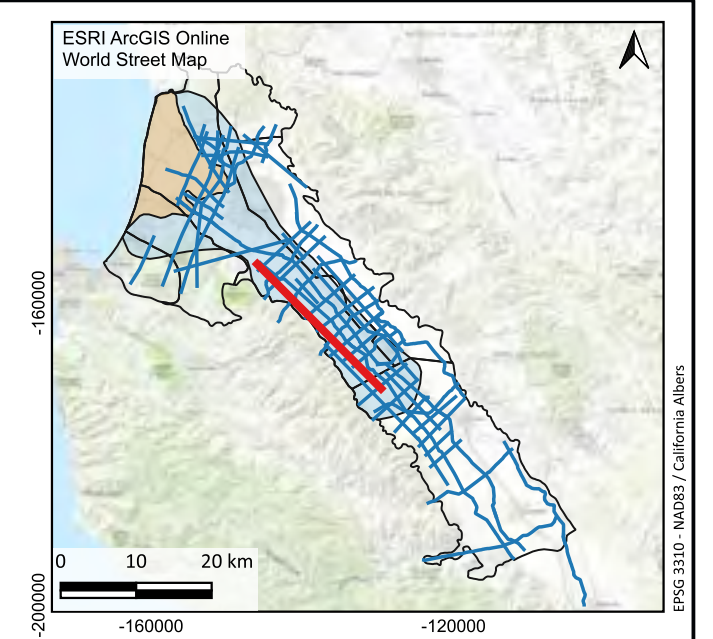
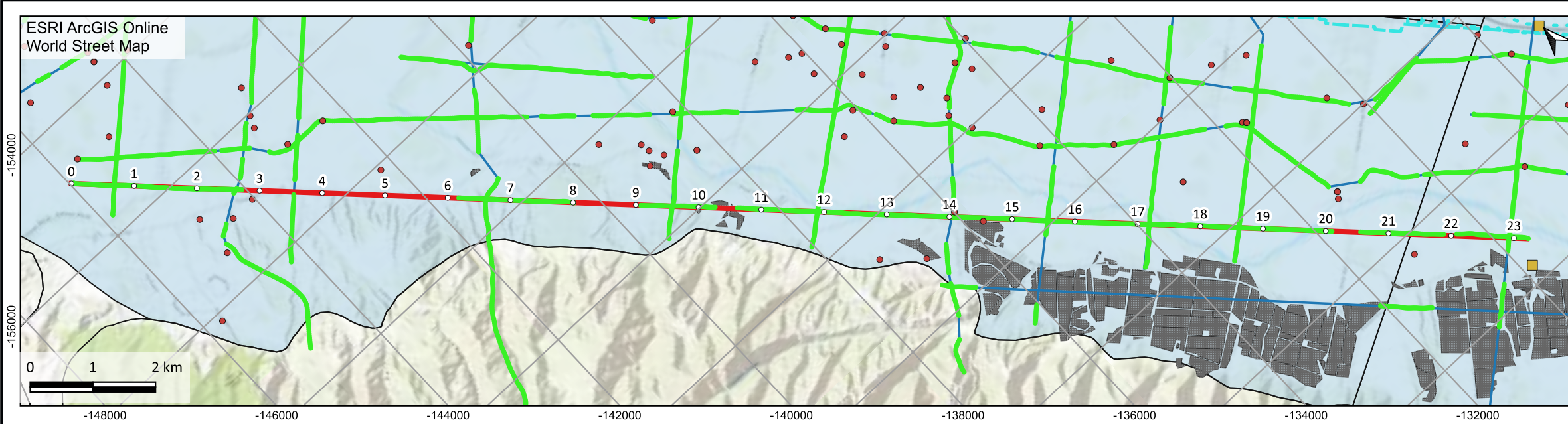
Log Resistivity High

**Well completion report analysis**

**Continuous conductor**

- Top of conductor
- Bottom of conductor
- Top of conductor (lower confidence)
- Bottom of conductor (lower confidence)





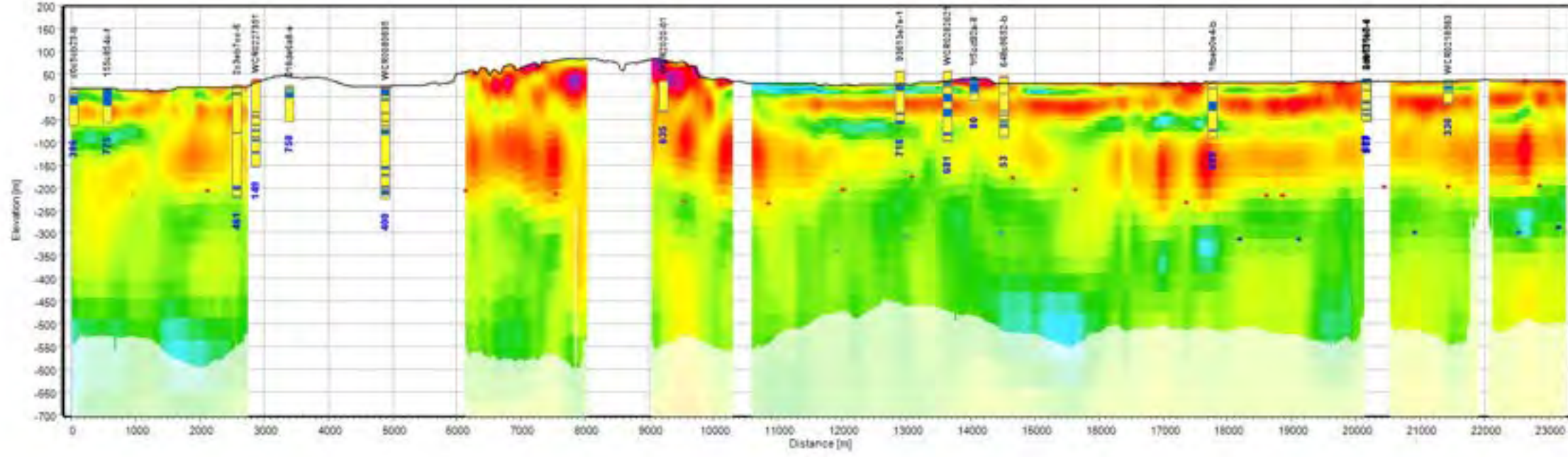
**Legend for Maps**

- Groundwater Basin Boundary (DWR - B118)
- Vineyards
- Phase 1 Aquitard Extent
- 180-Foot Aquifer CI- Contour
- Section (Current page)
- Section (Other pages)

**AEM data used for inversion**

- Lithology logs
- Resistivity logs
- Electric transmission lines (CA State Geoport, 2020)
- Pipelines (AmeriGEOSS, 2022)

Smooth Model



**Legend for Model Sections**

**Resistivity: AEM inversion results**

3 10 100 300  
Resistivity [ohm-m]

\*DOI = Depth of investigation

**Lithology log**

- Sand
- Silt/Clay
- Clay
- Claystone
- Siltstone
- Limestone

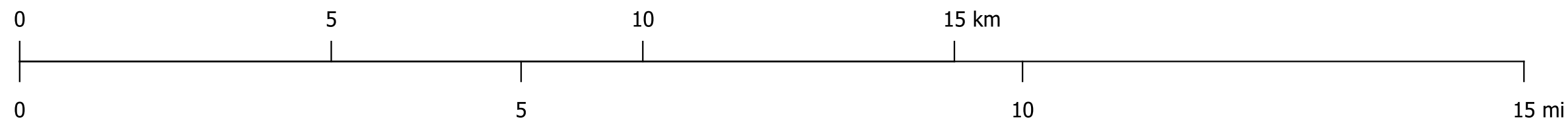
**Resistivity log**

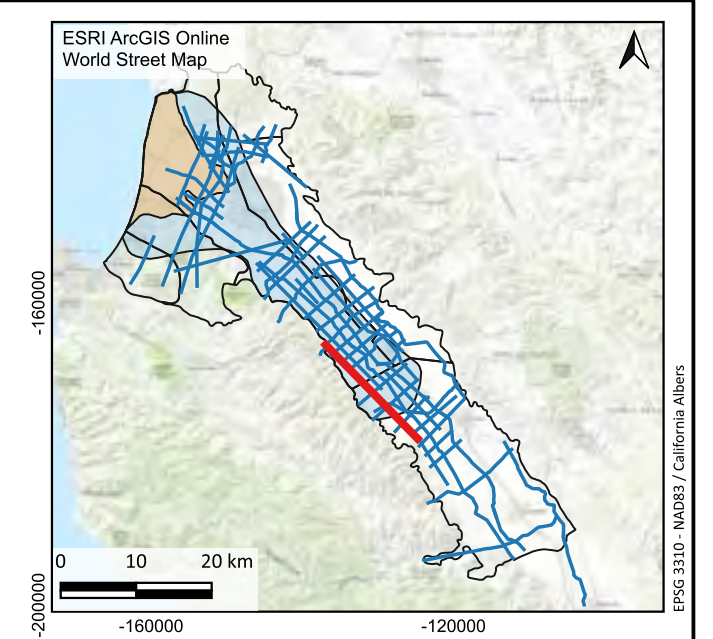
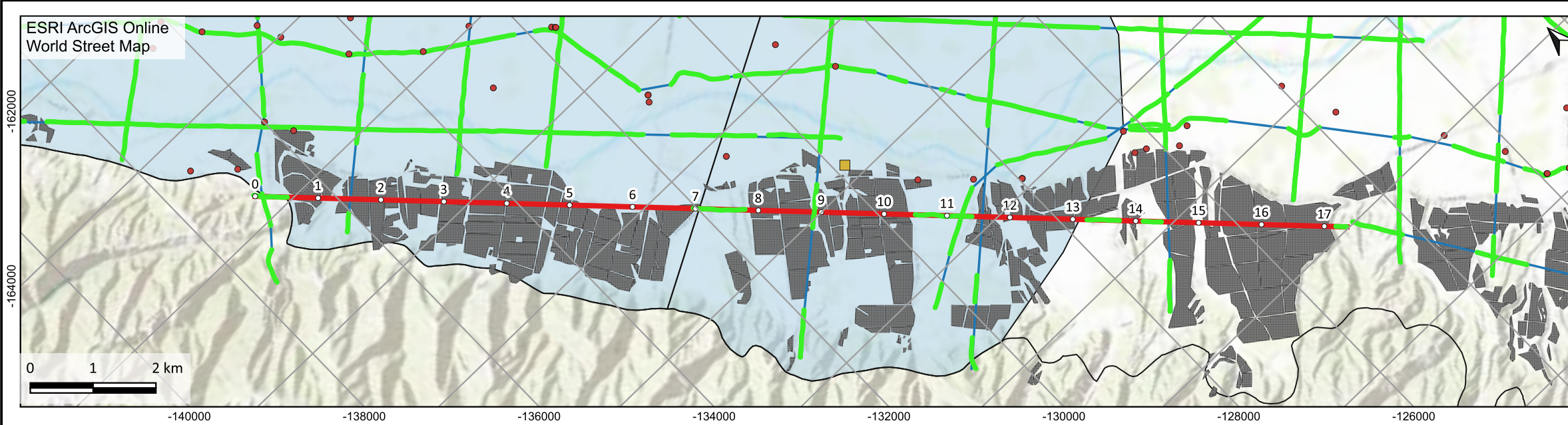
Log Resistivity

**Well completion report analysis**

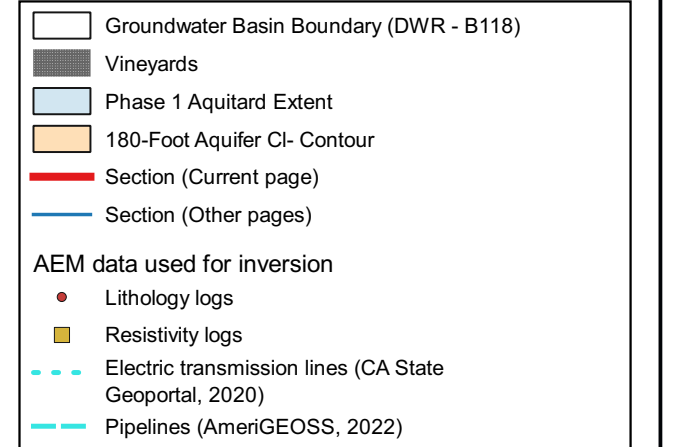
**Continuous conductor**

- Top of conductor
- Bottom of conductor
- Top of conductor (lower confidence)
- Bottom of conductor (lower confidence)

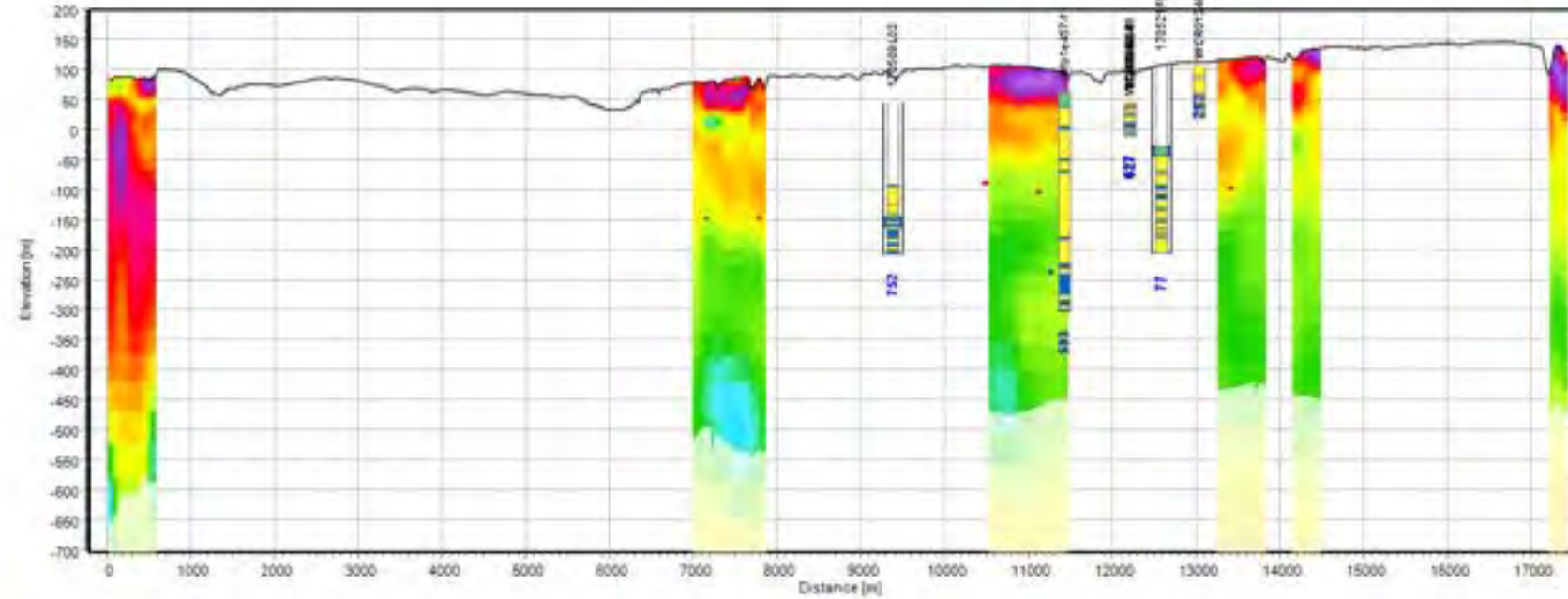




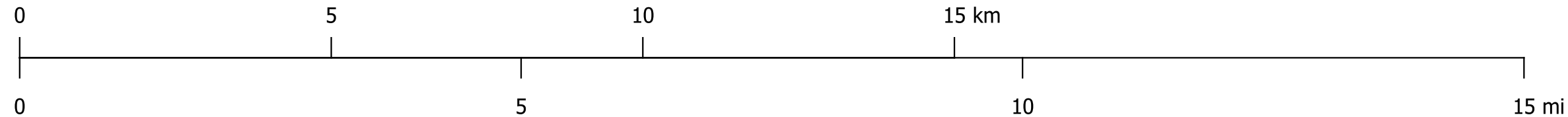
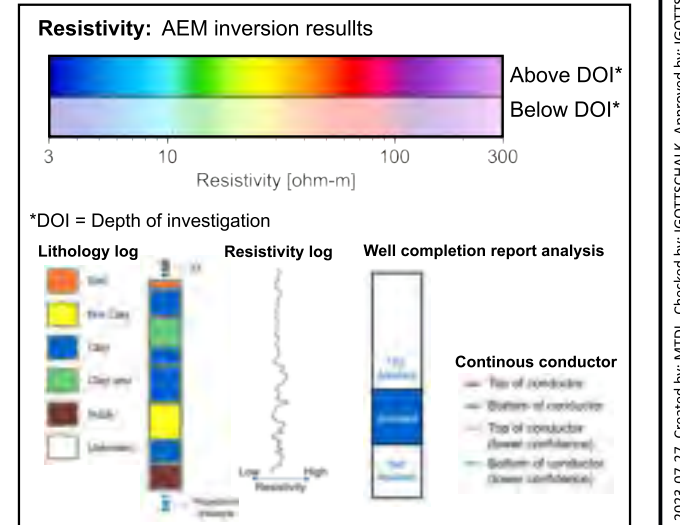
Legend for Maps

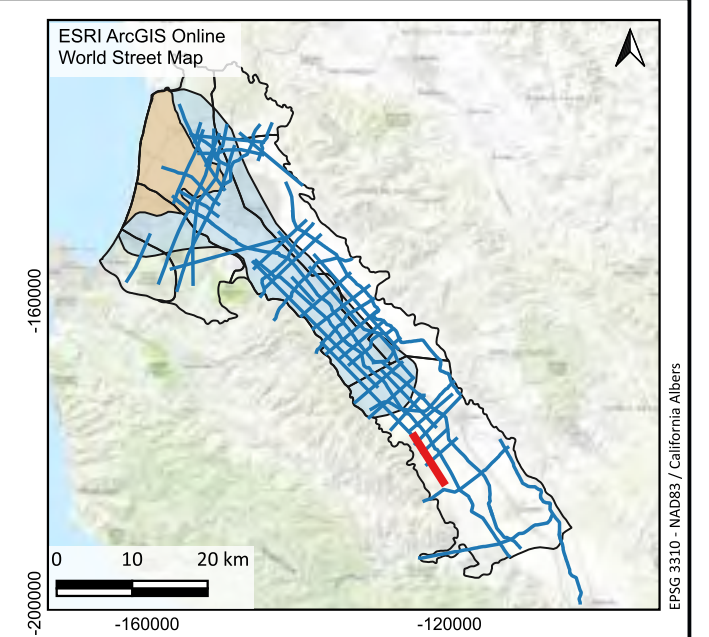
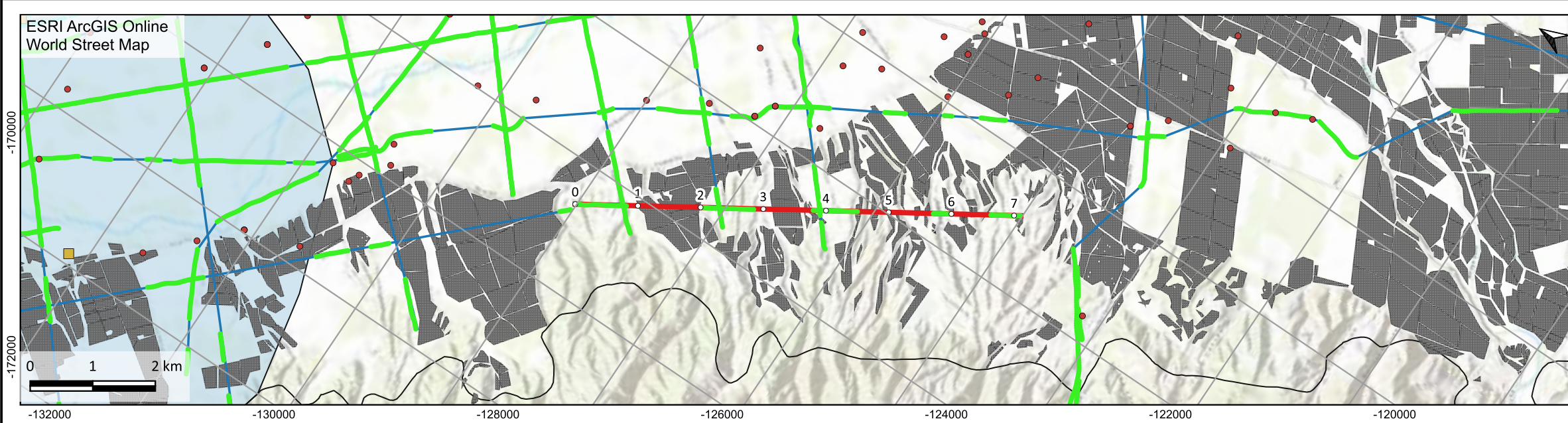


Smooth Model

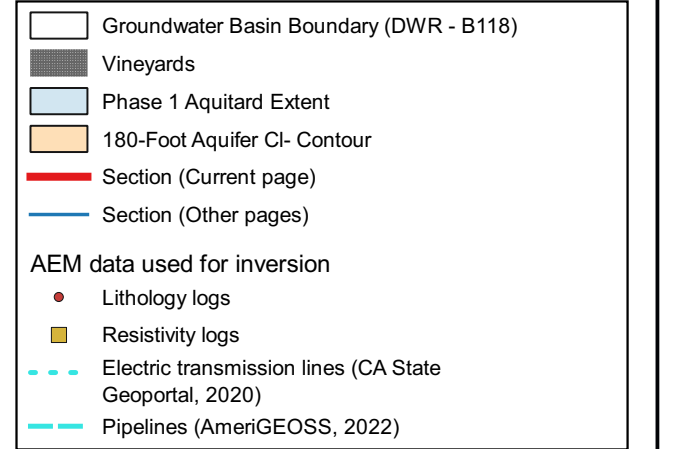


Legend for Model Sections

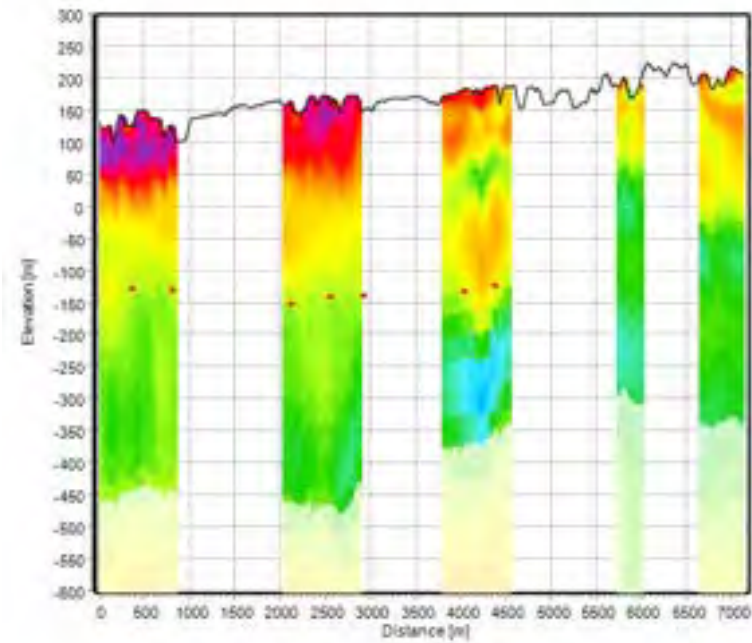




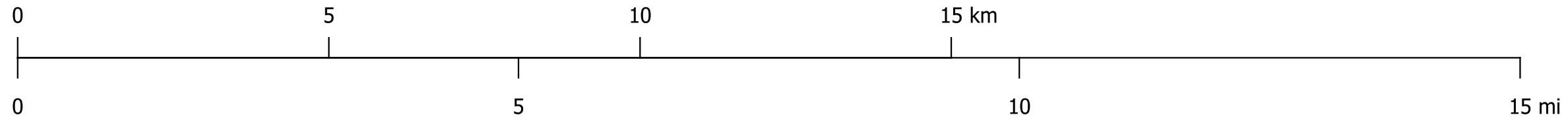
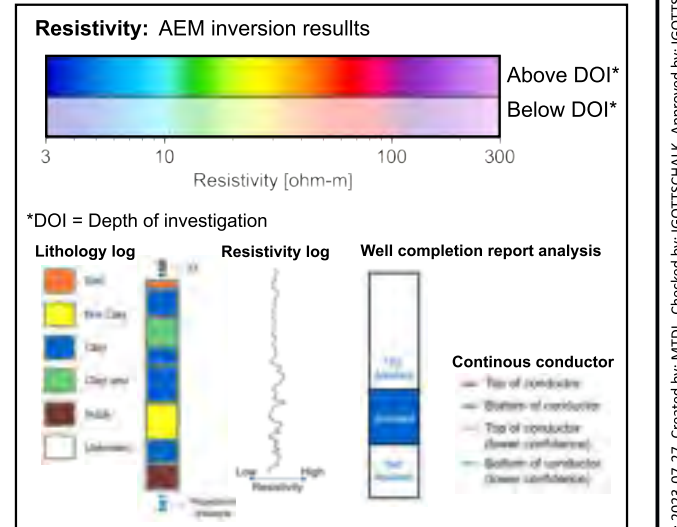
Legend for Maps



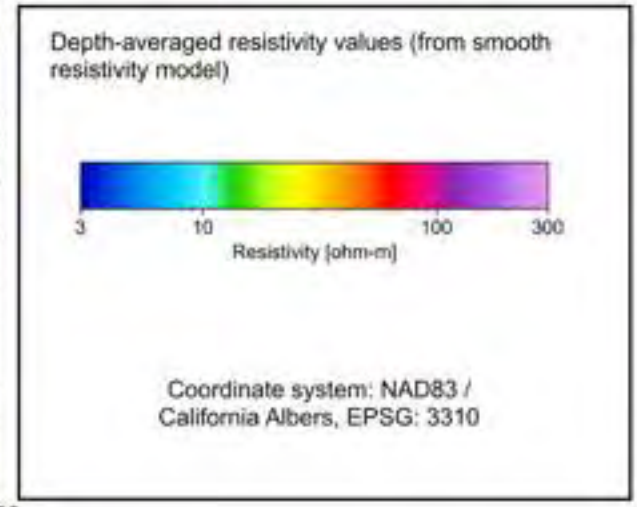
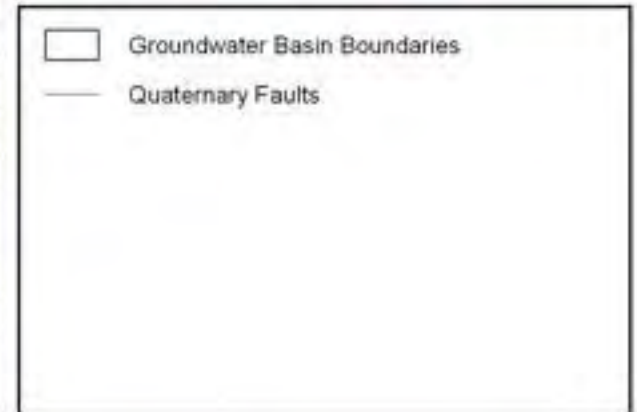
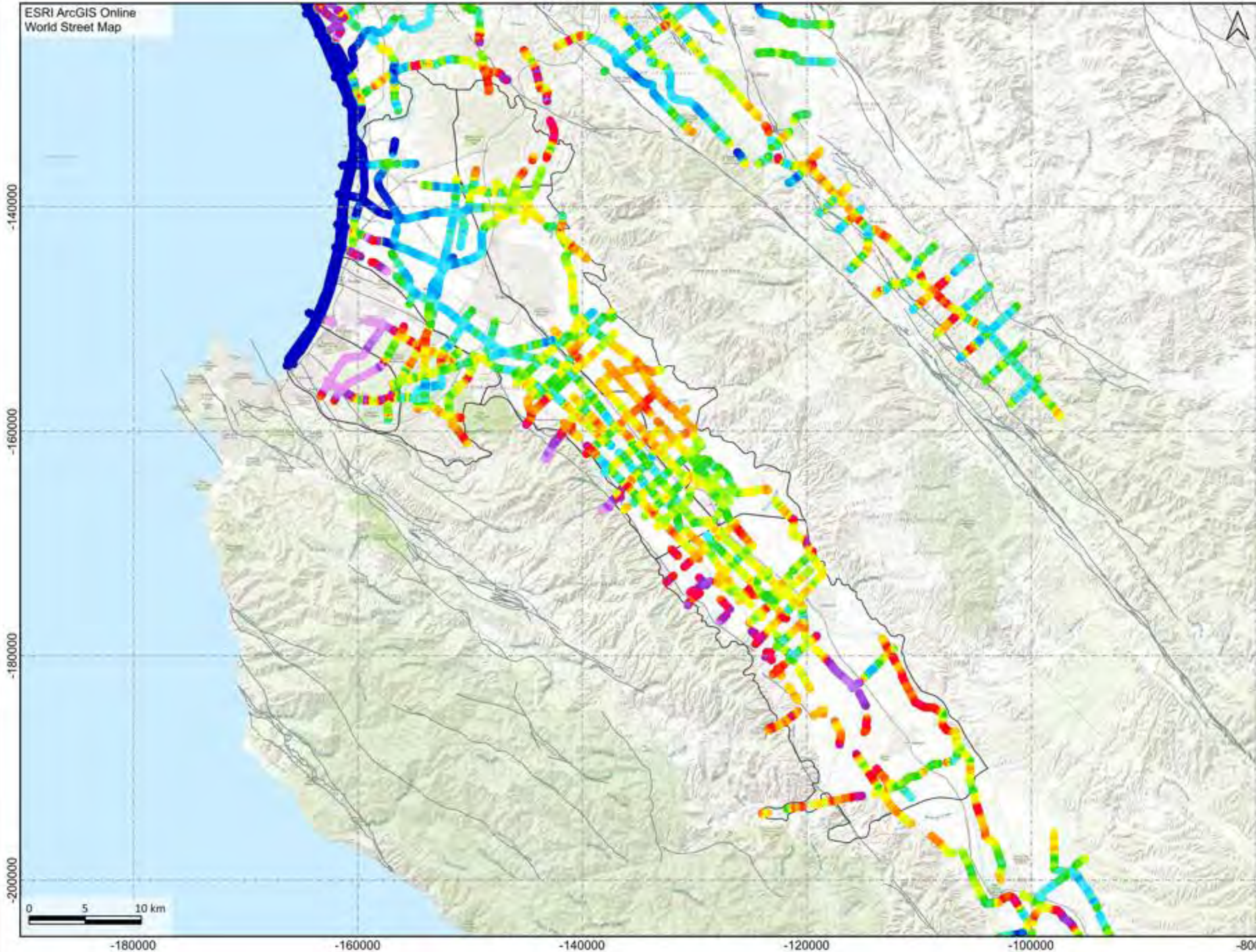
Smooth Model

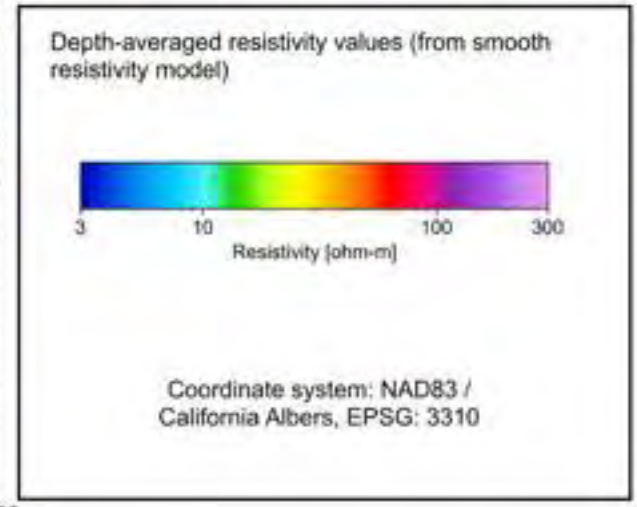
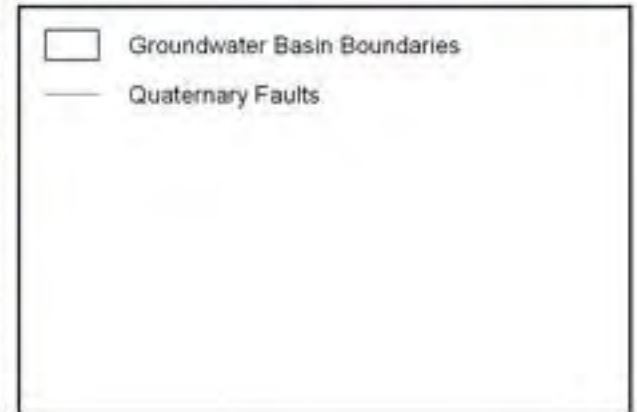
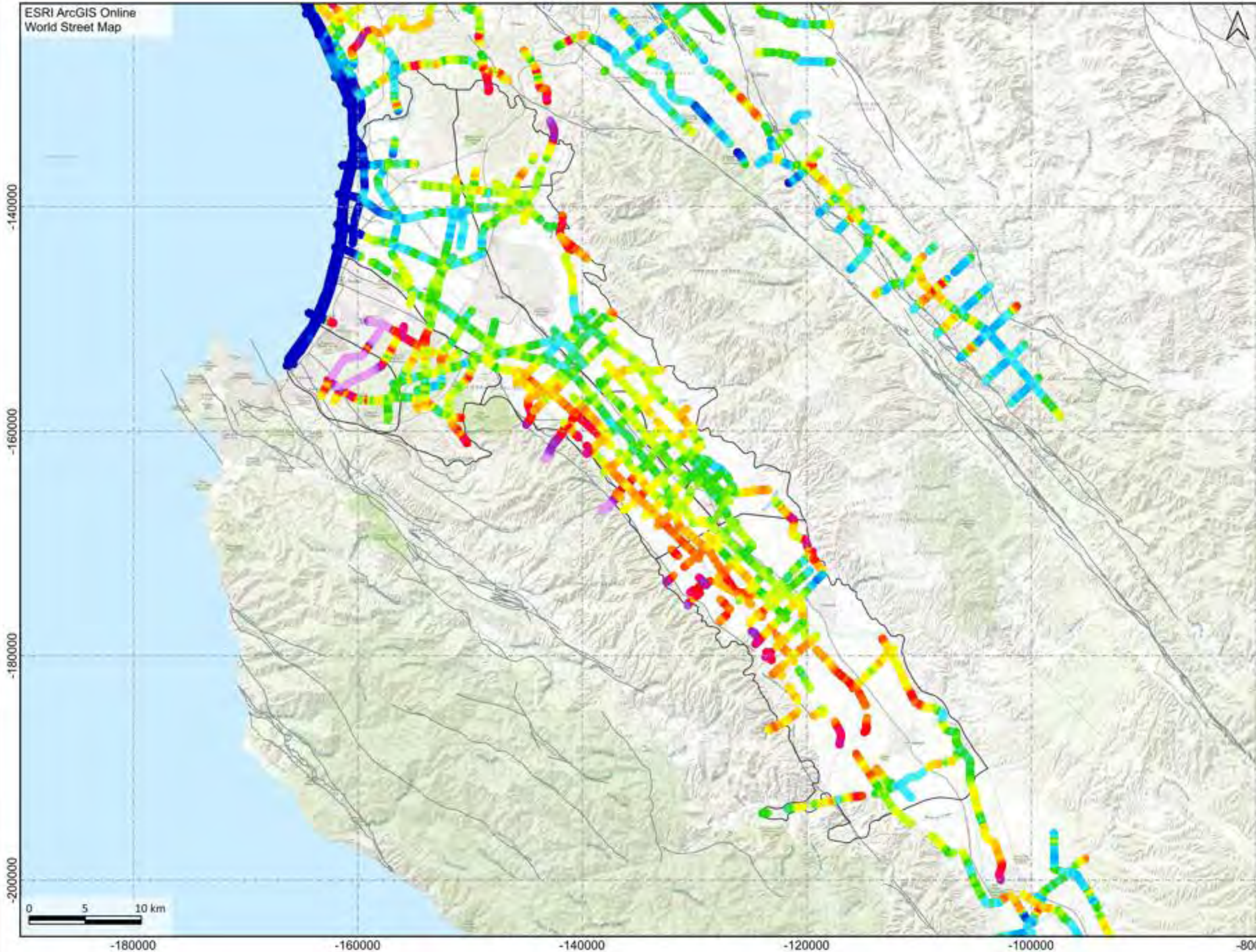


Legend for Model Sections



## Appendix 4 AEM Inversion Mean Resistivity Maps





Elevation Interval -150 to -100 m

AEM Mean Resistivity

